

**Synthesis and Biological Evaluation of
Imidazo[1,2-*b*]pyridazines as Inhibitors of *Mycobacterium
Tuberculosis***

A thesis submitted for the fulfilment of the degree of Doctor of Philosophy

By

Kyle D. Farrell

B. Sc. (Forensic and Analytical Science)(Honours)

Flinders University



Flinders
UNIVERSITY

College of Science and Engineering

16th August 2021

Declaration

I certify that this thesis does not incorporate without acknowledgment any material previously submitted for a degree or diploma in any university; and that to the best of my knowledge and belief it does not contain any material previously published or written by another person except where due reference is made in the text.

Kyle D. Farrell

24th February 2021

Acknowledgements

To begin, I would like to express my sincere gratitude to my supervisor at Flinders University, Associate Professor Michael Perkins, for being a great mentor. I always looked forward to our weekly meetings and felt energised by our discussions regarding this project. It has been a privilege gaining your insights and perspectives related to chemistry and problem solving. You have taught me invaluable lessons which I will utilise throughout the rest of my career. I would also like to send my gratitude to my supervisor at CSIRO, Dr Craig Francis, for going above and beyond with the amount of support you have provided to me throughout this project. Thank you for all your helpful and thorough feedback on this thesis, the monthly reports, and presentations; the motivational emails and comments scattered throughout your feedback; all your prompt replies via email when I needed assistance the most; and for all the times you flew from Melbourne to Adelaide for in person meetings. Although you were a whole state away, it felt as though your office was only down the corridor.

Additionally, I would like to thank Deborah A. Hughes from CSIRO for your previous work which served as a solid foundation for the synthetic protocols used within this thesis. I would also like to thank Robin Hanches, an intern at CSIRO, for the preparation of the 3-methoxy-6-(*N*-methylbenzylamino)2-phenylimidazo[1,2-*b*]pyridazine precursors and the “Q203/TB47 Hybrid” imidazo[1,2-*b*]pyridazine building blocks, **274**, **275** and **280**.

Thank you to Dr Craig Forsyth at Monash University for conducting X-ray Crystallography on compounds **195c**, **196c**, **197c**, **195g** and **197g** and to the members at the Centre for Drug Candidate Optimisation (CDCO) at the Monash Institute of Pharmaceutical Sciences (MIPS), Dr Susan Charman, Dr Andrew Powell, Dr Alison Thistlethwaite, Dr Michael Campbell, Caithlin White, and Dr Ei Lwin, for your work in determining the physicochemical and metabolic properties for the selected compounds described in Chapter 6. I would also like to thank and recognise members at Guangzhou Institutes of Biomedicine and Health (GIBH), Professor Tianyu Zhang, Yunxiang Tang, Zhengchao Tu, Yang Liu, and Yamin Gao, for all your critical biological work discussed in Chapters 5 and 6. Also, thank you to the Australian Government for the Australian Government Research Training Program Scholarship.

I would like to express a heartfelt thank you to my family, for all your unconditional love and support, for all your amazing cooking and for putting a roof above my head for the final year

of my PhD, without which I would have been unable to complete. Finally, I would like to express my deepest appreciation to my girlfriend Tess, for putting up with my stress and worry, for offering your spacious office to finish my thesis, and for your continued patience while I have gone through this process. I promise to reciprocate all the love and support you have provided me with throughout your PhD journey.

Presentation

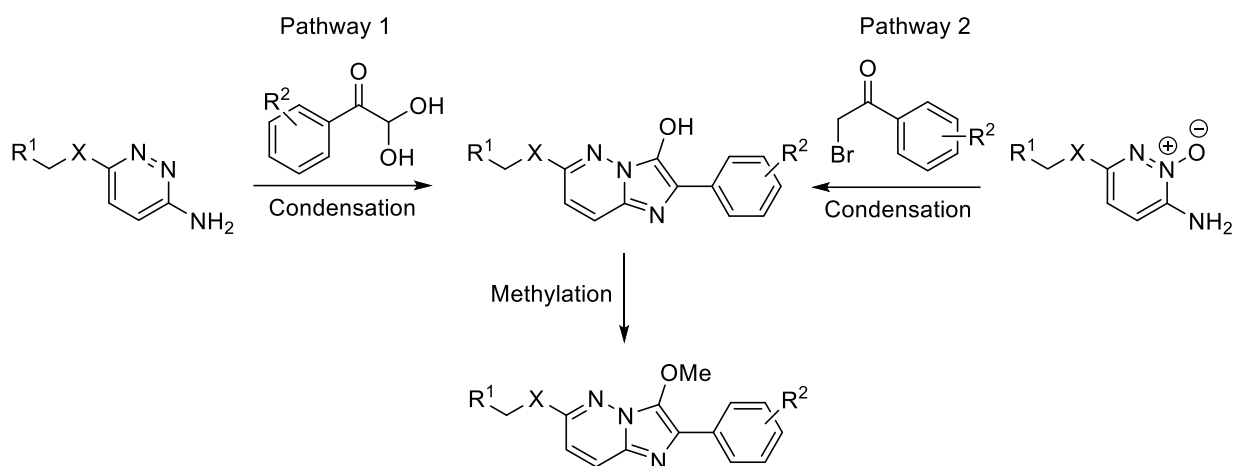
Drug Discovery for Tuberculosis

Poster presentation at the 24th RACI Organic Chemistry Conference, Perth, WA, 2018.

Thesis Summary

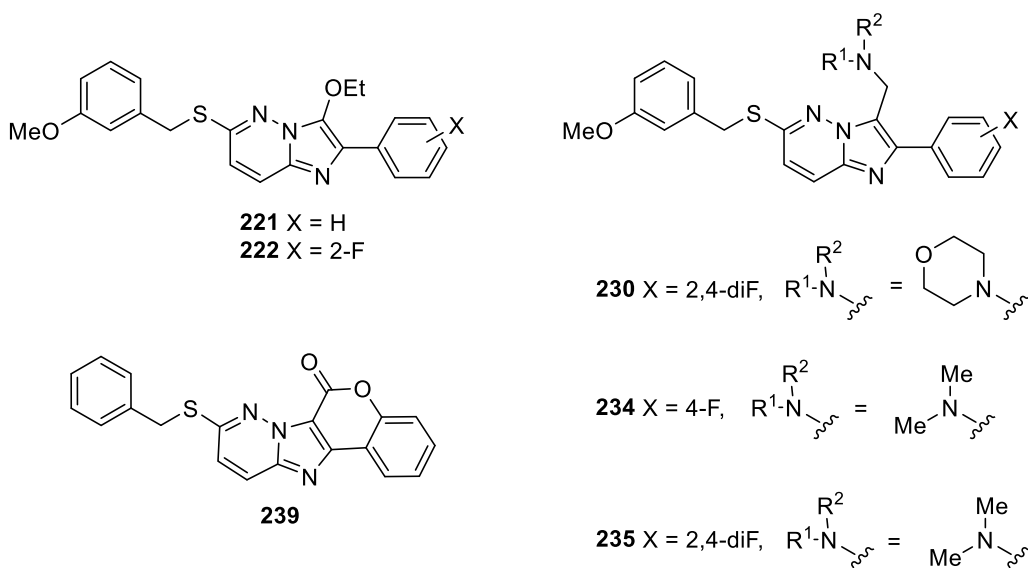
This thesis discusses the synthesis and biological evaluation of a library of imidazo[1,2-*b*]pyridazines as inhibitors of *Mycobacterium tuberculosis* (*Mtb*). Chapter 1 introduces the nature and impact of tuberculosis as well as the current methods used in treating the disease. Shortcomings of these methods, including a growing resistance to the drugs used in the current regimen, are highlighted. The drug discovery and development pipeline, a process which is used to find new antitubercular agents with the intention to alleviate these issues, is described. Compounds within the drug discovery and development pipeline, including Phase I clinical candidate Q203, are discussed. It is noted that Q203 possesses an imidazo[1,2-*a*]pyridine core structure which resembles the scaffold of interest, the imidazo[1,2-*b*]pyridazine. The antimycobacterial activity of these compounds became of interest after CSIRO (Commonwealth Science and Industrial Research Organisation) and GIBH (Guangzhou Institutes of Biomedicine and Health) screened 18,000 pre-existing CSIRO compounds against *Mtb* and discovered some to be highly active. High-throughput screening (HTS) results of a range of these imidazo[1,2-*b*]pyridazines from the CSIRO Compound Library are displayed and early structure-activity relationship (SAR) insights are discussed, providing the foundation for the design of the compounds synthesised in Chapter 2. Antitubercular imidazo[1,2-*b*]pyridazines were scarcely observed within the literature, which gave scope to claim intellectual property for these compounds and to move forward with this project.

Chapters 2 and 3 discuss the syntheses of a range of imidazo[1,2-*b*]pyridazines for screening against *Mtb*. Chapter 2 focuses on two synthetic pathways which converge at the condensation product, 2-phenylimidazo[1,2-*b*]pyridazin-3-ol, which can be methylated to form the desired 3-methoxy-2-phenylimidazo[1,2-*b*]pyridazine. Side-products discovered along these synthetic pathways are structurally elucidated and mechanisms for their production are proposed.



*Overview of the synthetic pathways used to synthesise 3-methoxy-2-phenylimidazo[1,2-*b*]pyridazines*

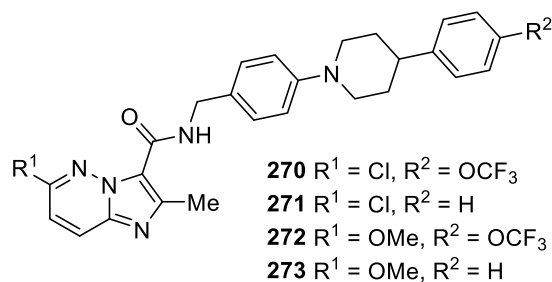
Chapter 3 discusses the syntheses of imidazo[1,2-*b*]pyridazines with other C3 substituents other than a methoxy moiety to probe this position for SARs. The compounds synthesised in this chapter include 3-ethoxy- (**221** and **222**), 3-dialkylaminomethyl- (**230**, **234** and **235**) and 3-carboxylate(lactone)- (**239**) substituted-imidazo[1,2-*b*]pyridazines shown below.



*The structures of 3-ethoxy- (**221** and **222**), 3-dialkylaminomethyl- (**230**, **234** and **235**) and 3-carboxylate(lactone)-substituted (**239**) imidazo[1,2-*b*]pyridazines*

Chapter 4 discusses the attempts made to scaffold hop from an imidazo[1,2-*b*]pyridazine to an imidazo[2,1-*b*][1,3,4]thiadiazole core structure, in hope of finding a potent bioisostere to

inhibit *Mtb*. Furthermore, hybridisation of Q203 and TB47 (a GIBH compound structurally similar to Q203 with comparable potency against *Mtb* but contains a pyrazolo[1,5-*a*]pyridine core structure) and a scaffold hop to the imidazo[1,2-*b*]pyridazine led to the successful syntheses of “Q203/TB47 hybrid” imidazo[1,2-*b*]pyridazines **270** – **273**.



*The structures of “Q203/TB47 hybrid” imidazo[1,2-*b*]pyridazines **270** – **273***

SARs of the imidazo[1,2-*b*]pyridazines synthesised in Chapters 2, 3 and 4 are discussed in Chapter 5 on the basis of their *in vitro* antimycobacterial activities against *Mtb* and *Mm* (*Mycobacterium marinum*). The IC₅₀ and MIC values of imidazo[1,2-*b*]pyridazines from the CSIRO library were also evaluated to gather further SAR data. Five compounds displaying highly potent *in vitro* activity were evaluated in a mouse *in vivo* study conducted at GIBH, discussed in Chapter 6. However, all five compounds exhibited no *in vivo* activity. Four of these compounds were evaluated for their physicochemical and metabolic properties at the CDCO at MIPS which provided reasons for their lack of *in vivo* activity.

In Chapter 7, conclusions from the work described in Chapters 2 - 6 are presented, followed by a discussion of future directions. Chapter 8 contains the experimental protocols for the compounds synthesised. The appendices are divided into two sections where Section 1 contains the NMR spectra, LC-MS and HRMS chromatograms/spectra for compounds tested against *Mtb* and Section 2 contains the NMR and HRMS spectra for miscellaneous compounds, mostly side-products, described throughout this thesis.

Abbreviations

Below is a list of abbreviations used throughout this thesis with their corresponding standard names.

Abbreviation	Standard Name
~	Approximately
°C	Degrees Celcius
<	Less than
>	Greater than
≥	Greater than or equal to
2D	Two dimensional
3D	Three dimensional
Å	Angstrom
ADME	Absorption Distribution Metabolism Excretion
Almu	<i>Autoluminescent Mycobacterium ulcerans</i>
AlRv	Autoluminescent <i>Mtb</i> H37Rv
APCI	Atmospheric-pressure chemical ionisation
API	Atmospheric-pressure ionisation
Arom.	Aromatic
ATP	Adenosine triphosphate
BBr ₃	Boron tribromide
BEH	Ethylene Bridged Hybrid
Br	Bromo
C ₁₈	Octadecylsilane
CCl ₄	Carbon tetrachloride
CDCl ₃	Deuterated chloroform
CDCO	Centre for Drug Candidate Optimisation
CF ₃	Trifluoromethyl
CFU	Colony-forming units
CH ₂ NH ₂ COR	Methyl-amide
CH ₂ NMe ₂	Methyl-dimethylamine
CH ₂ S	Dimethyl sulfide
CH ₃	Methyl
Cl _{blood}	Hepatic blood clearance
Cl _{int, in vitro}	<i>In vitro</i> intrinsic clearance
Cl _{int, in vivo}	<i>In vivo</i> intrinsic clearance
clogD	Calculated distribution coefficient
clogP	Calculated partition coefficient
CMC-Na	Carboxymethylcellulose-sodium
CN	Nitrile
CO	Carbon monoxide
COSY	Correlation Spectroscopy
CSIRO	Commonwealth Scientific and Industrial Research Organisation
CuI	Copper (I) iodide
CYP450	Cytochrome P450
DOTS	Directly observed treatment, short-course

d	Doublet
DCC	<i>N,N</i> -Dicyclohexylcarbodiimide
DCM	Dichloromethane
dd	Doublet of doublets
DIPEA	<i>N,N</i> -Diisopropylethylamine
DME	Dimethoxyethane
DMF	Dimethyl formamide
DMSO	Dimethyl sulfoxide
DMSO- <i>d</i> ₆	Deuterated dimethyl sulfoxide
DNA	Deoxyribonucleic acid
DSA-ToF	Direct Sample Analysis/Time-of-Flight
dt	Doublet of triplets
EBA	Early bactericidal activity
EDC	1-Ethyl-3-(3-dimethylaminopropyl)carbodiimide
EDG	Electron donating group
E _H	Hepatic extraction ratio
EMB	Ethambutol
ES	Electrospray
Ether	Diethyl ether
Etl	Ethyl iodide
EtOH	Ethanol
FDA	Food and Drug Administration
Fe ^{III} -TAML	Iron (III) tetraamido macrocycle
FRB	Free rotating bonds
Fsp ³	sp ³ carbons/total carbon count
FTMS	Fourier Transform Ion Cyclotron Resonance Mass Spectrometry
g	Grams
GIBH	Guangzhou Institutes of Biomedicine and Health
glogD	Distribution coefficient estimation using chromatography
gmol ⁻¹	Grams per mole
h	Hour
H	Hydrogen
H ₂	Hydrogen gas
H ₂ O	Water
H ₂ SO ₄	Sulfuric acid
Halo	Halogen
HBA	Hydrogen bond acceptors
HBD	Hydrogen bond donors
HBr	Hydrogen bromide
HCl	Hydrochloric acid
HDMS	High Definition Mass Spectrometry
HI	Hydrogen iodide
HMBC	Heteronuclear Multiple-Bond Correlation
HMQC	Heteronuclear Multiple-Quantum Correlation
HOBt	Hydroxybenzotriazole
HOSu	<i>N</i> -Hydroxysuccinimide
HPLC	High-pressure Liquid Chromatography

HRMS	High-resolution mass spectrometry
HTS	High-throughput screening
Hz	Hertz
I	Iodo
IC ₅₀	Half-maximal inhibitory concentration
INH	Isoniazid
IPA	Imidazo[1,2- <i>a</i>]pyridine amide
<i>J</i>	Coupling constant
K ₂ CO ₃	Potassium carbonate
KMnO ₄	Potassium permanganate
kPa	Kilopascal
kV	Kilovolts
LC-MS	Liquid chromatography-mass spectrometry
LiOH	Lithium hydroxide
logP	Partition coefficient
m	Multiplet
M	Molar
m/z	Mass to charge ratio
MCF-7	Michigan Cancer Foundation-7
MDCK-MDR1	Madin-Darby Canine Kidney-Multi-Drug Resistance Gene cells
MDR-TB	Multidrug-resistant tuberculosis
Me	Methyl
MeCN	Acetonitrile
Mel	Methyl iodide
MeO	Methoxy
MeOH	Methanol
mg	Milligrams
mg/kg	Milligrams per kilogram
mg/mL	Milligrams per millilitre
MHz	Megahertz
MIC	Minimum inhibitory concentration
min	Minutes
MIPS	Monash Institute of Pharmaceutical Sciences
mL/min	Millilitres per minute
<i>Mm</i>	<i>Mycobacterium marinum</i>
mm	Millimetres
MsOH	Methanesulfonic acid
<i>Mtb</i>	<i>Mycobacterium tuberculosis</i>
<i>Mu</i>	<i>Mycobacterium ulcerans</i>
MW	Molecular weight
N ₂	Nitrogen gas
N ₃	Azide
NaBr	Sodium bromide
NADPH	Nicotinamide Adenine Dinucleotide Phosphate Hydrogen
NaH	Sodium hydride
NaHCO ₃	Sodium bicarbonate
NaOH	Sodium hydroxide

NaOMe	Sodium methoxide
NBS	<i>N</i> -bromosuccinimide
nM	Nanomolar
nm	Nanometres
OCF ₃	Trifluoromethoxy
OCH ₂ CH ₂ OMe	Ethoxymethoxy
OCH ₃	Methoxy
OEt	Ethoxy
⁻ OH	Hydroxide
ORTEP	Oak Ridge Thermal Ellipsoid Plot
Ph	Phenyl
pH	Potential of hydrogen
PhD	Doctor of Philosophy
PhO	Phenoxy
PhS	Phenylthio
PIDA	Phenyliodine (III) diacetate
PK	Pharmacokinetics
pKa	Negative log of the acid dissociation constant
Pks13	Polyketide synthase 13
ppm	Parts per million
PSA	Polar surface area
pTsOH	Para-toluenesulfonic acid
PZA	Pyrazinamide
q	Quartet
QC	Quality Control
QDa	Quadruple Dalton
Ra	Avirulent
RFB	Rifabutin
RLU	Relative light units
RMP	Rifampicin
RNA	Ribonucleic acid
rRNA	Ribosomal ribonucleic acid
rt	Room temperature
Rv	Virulent
s	Singlet
SAR	Structure-activity relationship
SeO ₂	Selenium dioxide
STR	Streptomycin
t	Triplet
T _{1/2}	Half-life
TB	Tuberculosis
TBAB	Tetrabutylammonium bromide
td	Triplet of doublets
TDR-TB	Totally drug-resistant tuberculosis
TEA	Triethylamine
TFAA	Trifluoroacetic anhydride
TGA	Therapeutic Goods Administration

THF	Tetrahydrofuran
TMS-Cl	Trimethylsilyl chloride
tt	Triplet of triplets
UHP	Urea hydrogen peroxide
UPLC	Ultra performance liquid chromatography
USA	United States of America
V	Volts
WHO	World Health Organisation
XDR-TB	Extensively drug-resistant tuberculosis
α	Alpha
β	Beta
δ	Chemical shift
$\mu\text{g/mL}$	Micrograms per millilitre
μM	Micromolar
μm	Micrometres

Table of contents

Declaration.....	ii
Acknowledgements.....	iii
Presentation.....	v
Thesis Summary	vi
Abbreviations.....	ix
Chapter 1. Introduction – Drug Discovery for Tuberculosis.....	1
Chapter 1 Summary	2
1.1 The nature and impact of tuberculosis.....	3
1.2 The current methods in treating tuberculosis	4
1.3 Drug discovery and development pipeline	7
1.4 Promising drug candidates.....	9
1.4.1 Oxazolidinones.....	9
1.4.2 Diarylquinolines	10
1.4.3 Nitroimidazoles	11
1.4.4 Rifamycins	12
1.4.5 Ethylenediamines.....	13
1.4.6 Fluoroquinolones	13
1.5 The discovery of Q203	14
1.6 Q203 mode of action	15
1.7 Related structures to Q203.....	16
1.7.1 Pyrazolo[1,5- <i>a</i>]pyridine-3-carboxamides.....	17
1.7.2 Imidazo[1,2- <i>a</i>]pyridine-8-carboxamides.....	18
1.7.3 Imidazo[1,2- <i>a</i>]pyridine-2-carboxamides.....	18
1.7.4 <i>N</i> -(2-Phenoxyethyl)imidazo[1,2- <i>a</i>]pyridine-3-carboxamides	19
1.7.5 Anagrams and other analogues of Zolpidem.....	20
1.7.6 Imidazo[1,2- <i>a</i>]pyridine amide-cinnamamide hybrids.....	22
1.8 Imidazo[1,2- <i>b</i>]pyridazines and screening of the CSIRO Compound Library	24
1.9 Conclusions	28
Chapter 2. 3-Methoxyimidazo[1,2- <i>b</i>]pyridazine Syntheses.....	29
Chapter 2 Summary	30
2.1 Synthetic Pathway 1 – 6-substituted-pyridazine-3-amines and phenylglyoxals	31
2.1.1 6-Aminopyridazine-3-thiol alkylations.....	33
2.1.2 Phenylglyoxal monohydrate syntheses	39
2.1.3 Attempted syntheses of heteroaryl glyoxals	43

2.1.4 Imidazo[1,2- <i>b</i>]pyridazin-3-ol syntheses.....	47
2.1.5 3-Methoxyimidazo[1,2- <i>b</i>]pyridazine syntheses.....	53
2.1.6 3-Methoxy-6-((3-methoxybenzyl)sulfonyl)-2-phenylimidazo[1,2- <i>b</i>]pyridazine syntheses .	64
2.2 Synthetic Pathway 2 – 3-substituted-6-aminopyridazine-1-oxides and phenacyl bromides	74
2.3 Attempted syntheses of 6-amino-3-((3-methoxybenzyl)(methyl)amino)pyridazine 1-oxide.....	84
2.4 Conclusions	90
Chapter 3. Other 3-substituted Imidazo[1,2- <i>b</i>]pyridazine Syntheses.....	92
Chapter 3 Summary	93
3.1 3-Ethoxy-imidazo[1,2- <i>b</i>]pyridazine syntheses	94
3.2 3-Dialkylaminomethyl-imidazo[1,2- <i>b</i>]pyridazines	94
3.3 3-Carboxylate(lactone)-substituted imidazo[1,2- <i>b</i>]pyridazine synthesis	101
3.4 Conclusions	107
Chapter 4. Scaffold Hopping	108
Chapter 4 Summary	109
4.1 Scaffold Hopping.....	110
4.2 Antitubercular activity of imidazo[2,1- <i>b</i>][1,3,4]thiadiazoles	110
4.3 Attempted syntheses of 5-hydroxyimidazo[2,1- <i>b</i>][1,3,4]thia(oxa)diazoles	114
4.4 Q203/TB47 imidazo[1,2- <i>b</i>]pyridazine hybrids	120
4.5 Conclusions	131
Chapter 5. <i>In Vitro</i> Evaluation	132
Chapter 5 Summary	133
5.1 Structure Activity Relationships (SARs) of imidazo[1,2- <i>b</i>]pyridazines against Mtb and Mm ...	134
5.2 Conclusions	158
Chapter 6. <i>In Vivo</i> Evaluation	160
Chapter 6 Summary	161
6.1 In vivo method, results, and analysis for imidazo[1,2- <i>b</i>]pyridazine 64	162
6.2 In vivo results and analysis of 65 , 17 , 190b and 190d	164
6.3 Physicochemical Evaluation	169
6.4 Metabolic Evaluation	173
6.5 Conclusions	178
Chapter 7. Conclusions and Future Directions	179
7.1 3-Methoxy-2-phenylimidazo[1,2- <i>b</i>]pyridazines.....	180
7.2 Other 3-substituted imidazo[1,2- <i>b</i>]pyridazines.....	180
7.3 Scaffold hop from the imidazo[1,2- <i>b</i>]pyridazine	181
7.4 In vivo study conclusions	182

7.5 Future Directions	182
Chapter 8	185
8.1 General experimental procedures	186
8.2 General procedure for the syntheses of 6-(substituted)methylthio-3-amino-pyridazines	188
8.3 General procedure for the syntheses of phenylglyoxal monohydrates	194
8.4 General procedure for the syntheses of imidazo[1,2- <i>b</i>]pyridazin-3-ols	196
8.5 General procedure for the syntheses of 3-methoxyimidazo[1,2- <i>b</i>]pyridazines	204
8.6 Procedures for the synthesis of 2-(2-Fluorophenyl)-3-methoxy-6-((3-methoxybenzyl)thio)imidazo[1,2- <i>b</i>]pyridazine 17	221
8.7 General procedure for the syntheses of 3-methoxy-6-((3-methoxybenzyl)sulfonyl)imidazo[1,2- <i>b</i>]pyridazines	223
8.8 General procedure for the syntheses of 3-ethoxy-imidazo[1,2- <i>b</i>]pyridazines	225
8.9 General procedure for the syntheses of 6-((3-methoxybenzyl)thio)imidazo[1,2- <i>b</i>]pyridazines	227
8.10 Procedures for the syntheses of 3-Dialkylaminomethyl-imidazo[1,2- <i>b</i>]pyridazines	229
8.11 Procedures for the synthesis of 9-Benzylthio-6 <i>H</i> -chromeno[4',3':4,5]imidazo[1,2- <i>b</i>]pyridazin-6-one 234	232
8.12 Procedures for attempted syntheses of imidazo[2,1- <i>b</i>][1,3,4]thia(oxa)diazoles	235
8.13 Procedures for the syntheses of ethyl 2-methylimidazo[1,2- <i>b</i>]pyridazine-3-carboxylates 272 and 273	237
8.14 General procedure for the syntheses of 2-methylimidazo[1,2- <i>b</i>]pyridazine-3-carboxylic acids	238
8.15 General procedure for the syntheses of 2-methyl- <i>N</i> -(4-(4-phenylpiperidin-1-yl)benzyl)imidazo[1,2- <i>b</i>]pyridazine-3-carboxamides	240
8.16 Decomposition studies of 6-(<i>N</i> -methylbenzylamino)-2-phenylimidazo[1,2- <i>b</i>]pyridazines	243
References	245
Appendices	254
Section 1: NMR spectra, LC-MS and HRMS chromatograms/spectra for compounds tested against Mtb	255
Section 2: NMR and HRMS spectra for miscellaneous compounds	401

Chapter 1.
Introduction –
Drug Discovery for Tuberculosis

Chapter 1 Summary

Chapter 1 provides background information on tuberculosis and the current methods in treating the disease. The drug discovery and development pipeline and highly active compounds against *Mycobacterium tuberculosis* reported in the literature, discovered via this process, are described. Among these compounds is the Phase I clinical candidate Q203 which possesses an imidazo[1,2-*a*]pyridine core structure that highly resembles the imidazo[1,2-*b*]pyridazine ring system – the scaffold of main focus in this thesis. High-throughput screening results from a set of imidazo[1,2-*b*]pyridazine derivatives from the CSIRO Compound Library are summarized and early structure-activity relationship insights are discussed. A brief summary of bioactive imidazo[1,2-*b*]pyridazine derivatives reported in the literature is provided.

1.1 The nature and impact of tuberculosis

Tuberculosis (TB) is an infectious disease caused mainly by *Mycobacterium tuberculosis* (*Mtb*) among other *Mycobacteria* that are a part of the *Mycobacterium Tuberculosis* Complex such as *M. africanum*, *M. bovis*, *M. caprae*, *M. canettii*, *M. microti*, and *M. pinnipedii*.^{1,2} It mainly affects the lungs (pulmonary TB) or in 5-10% cases it can affect other parts of the body termed extrapulmonary TB.^{1,3} This infectious disease is spread via an infected person sneezing or coughing and a healthy individual inhaling the respiratory fluids and consequently becoming infected.⁴ For *Mtb*, bacilli are carried in small droplets that are inhaled into the healthy person's lungs.^{4,5} After infection, the disease occurs in two stages; latent and active.⁶ In the first stage (latent) the infected individual shows no signs or symptoms and can persist as asymptomatic for many years.⁶ An estimated 2 billion people have latent TB and are at risk of activation of the disease.^{2,7} When the host's immune system becomes weakened (such as the host obtaining HIV) the bacteria begin replicating causing symptoms such as coughing, chest pain, fatigue, weight loss and ultimately death if left untreated.⁶

Tuberculosis is one of the most prevalent diseases worldwide claiming a life every 20s among those who suffer from active TB.⁸ World Health Organisation (WHO) surveys estimate that close to 2 million deaths occur every year and that there are approximately 8 million new cases annually.⁶ These cases are so prevalent as that it has been estimated that one in every three individuals worldwide has been exposed to or infected by *Mtb*.^{6,5} Although TB is mostly found in developing countries such as Africa and Southeast Asia, industrialised nations are also at risk due to the increase in drug-resistant TB, global travel and immigration.^{9,10} Due to this pandemic claiming a great number of lives, new drugs are urgently required in order to treat TB effectively.

1.2 The current methods in treating tuberculosis

Currently, the standard chemotherapy recommended by WHO is a 6 month regimen called DOTS (directly observed treatment, short-course) involving an initial two months phase with four drugs isoniazid (INH), rifampicin (RMP), pyrazinamide (PZA) and ethambutol (EMB) followed by four months of INH and RMP (continuation phase).^{1,10} In the DOTS program, health workers are employed to observe the intake of medication by the patient to ensure patient compliance.¹ This program is the recommended therapy for all TB patients since a cure rate of about 95% is achieved.^{1,5,11,12} These drugs along with streptomycin (STR) and rifabutin (RFB) are termed first-line drugs as they are known to have high anti-tubercular efficacy, bactericidal action and relatively low toxicity (Figure 1.1).¹

However, increasingly in recent times, resistant cases have emerged, termed MDR-TB (multi-drug resistant tuberculosis), in which the cure rates of the DOTS regimen fall to 50% therefore requiring a different regimen.¹ MDR-TB is resistant to isoniazid and rifampicin which are the most potent first line drugs.^{1,13} As a result, different second- and third-line drugs are required.⁴ Second-line drugs have lower efficacy and higher toxicity in comparison to first-line drugs and include ethionamide, prothionamide, *p*-aminosalicylic acid, cycloserine, kanamycin, amikacin, levofloxacin, ciprofloxacin, moxifloxacin, gatifloxacin, capreomycin, viomycin and enviomycin (Figure 1.2).^{1,14,15} In addition to MDR-TB, cases of XDR-TB (extensively drug resistant) have emerged, which are similar to MDR-TB but cannot be treated with the most potent second-line drugs such as fluoroquinolone.^{1,13} TDR-TB (totally drug resistant) strains also have emerged and these cases are resistant to a wider range of drugs in comparison to MDR/XDR-TB.¹³ There are also third-line drugs that have undefined roles in which their efficacy has not been properly established.¹ These include clarithromycin, linezolid, thioacetazone, and an analogue of clofazimine (Figure 1.3).^{1,15} Due to the existence of MDR- and XDR-TB and the issues associated with second- and third-line drugs, new drugs are urgently required.¹

Chapter 1

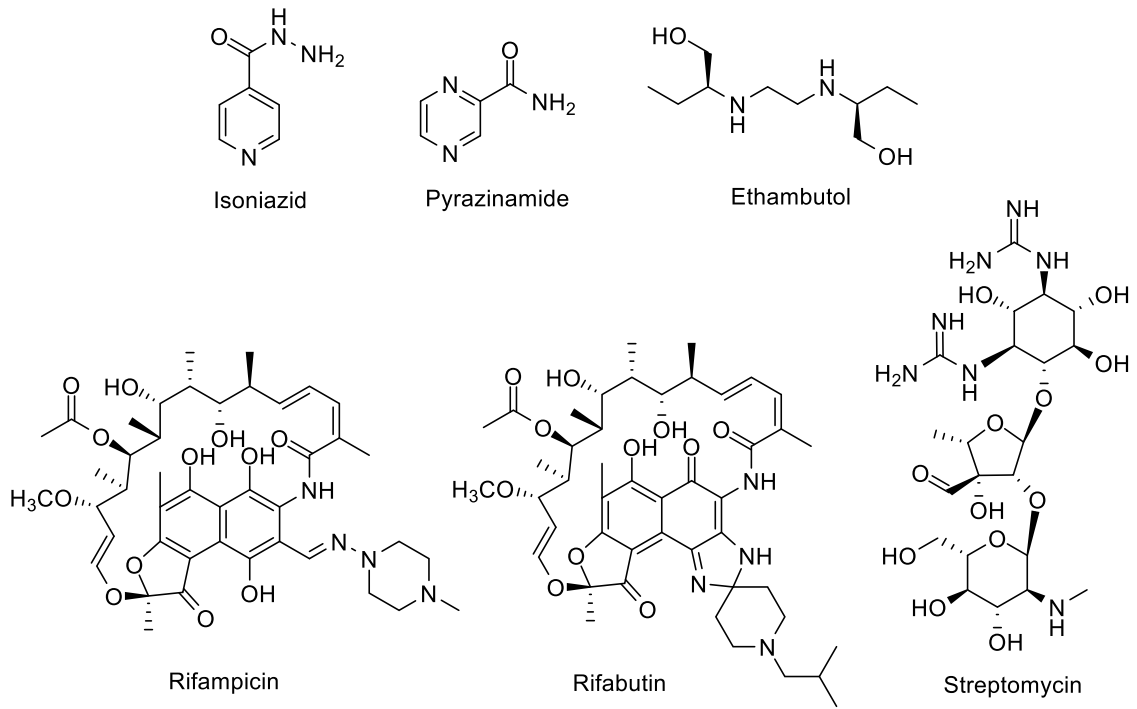


Figure 1.1: Structures of first-line drugs

Chapter 1

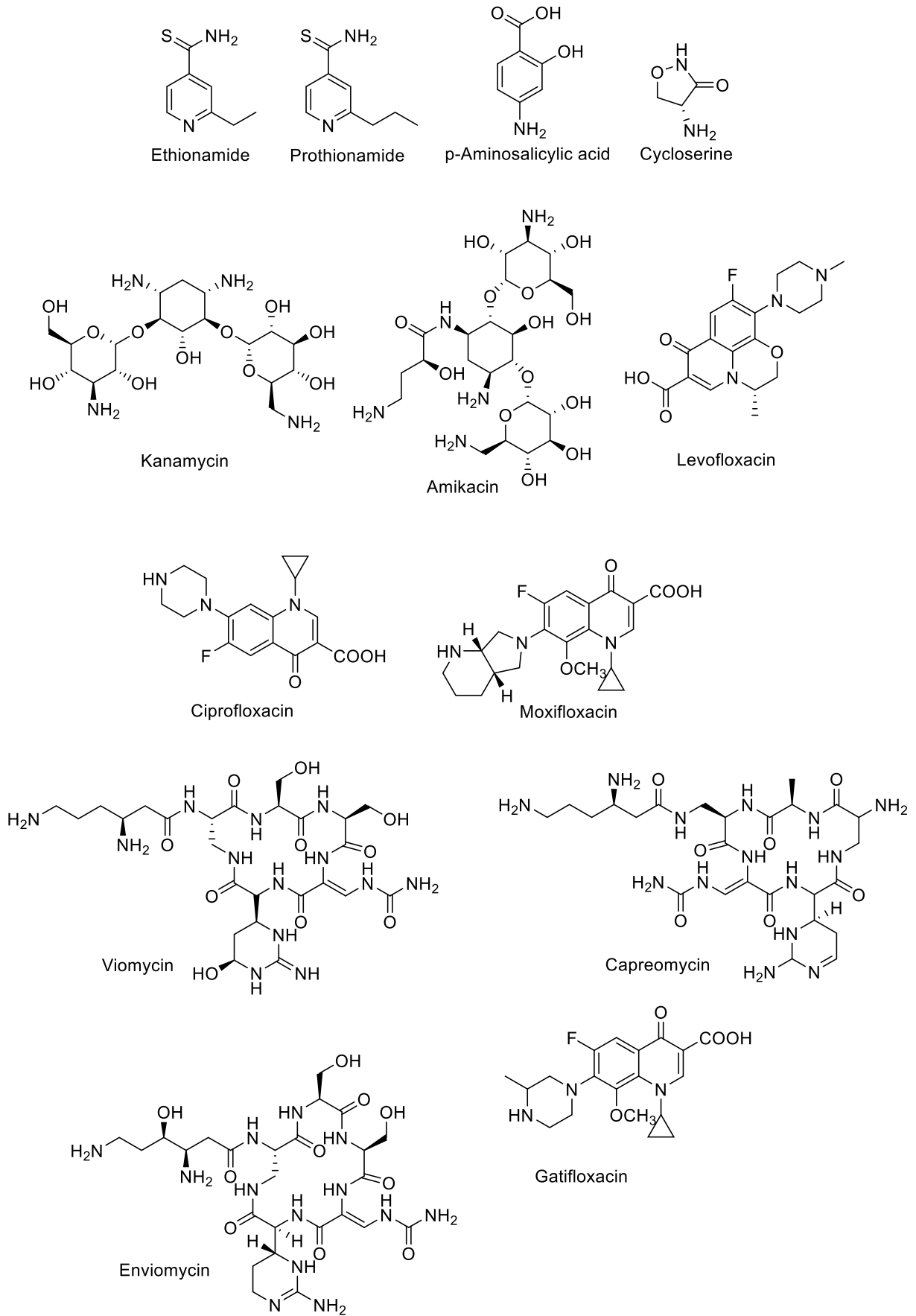


Figure 1.2: Structures of second-line drugs

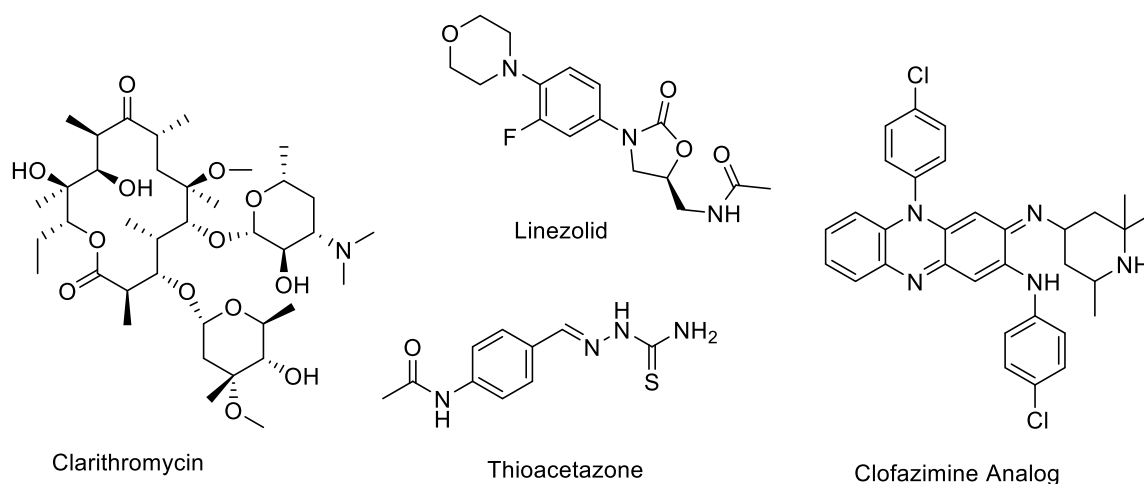


Figure 1.3: Structures of third-line drugs

The long duration times of the standard chemotherapies is a major issue leading to an increased chance of non-compliance by patients, which in turn leads to drug resistance.^{1,16} Long duration times of the chemotherapy are required due to the regimen being biphasic in its killing of the disease.^{1,17} The bacteria population is heterogeneous in nature in terms of some being slow growing, others growing rapidly, and some growing sporadically.^{1,17} Consequently, the rapid growing bacilli are eliminated first during the bactericidal phase while the slow growing bacilli are killed later in the therapy which is the sterilizing phase.^{1,17} As a result, different drugs are used in the different stages of the chemotherapy in order to eliminate the specific bacilli prolonging the chemotherapy.

1.3 Drug discovery and development pipeline

In order to combat this persistent disease, potential drug compounds are progressed through a generally accepted drug-discovery and development pipeline methodology (Figure 1.4).⁴ The first phase of drug discovery is the hit-to-lead process in which thousands of drug-candidates are tested via a high throughput screen (HTS) against *M. tuberculosis*.⁴ This process is essentially discovering lead compounds that could possibly be effective against TB. The next stage is lead-optimisation in which the structure of the lead compound is systematically altered in order to increase the activity against *Mtb*.⁴ This stage is essentially an iterative feedback loop involving chemical synthesis, evaluation of biological screening

Chapter 1

results, and refinement of chemical structures, in order to establish Structure Activity Relationships (SAR) enabling the eventual identification of a favoured compound as a potential development candidate.

In the second stage of the “pipeline” is the preclinical research. This part of the process tests the toxicity of the compound via *in vitro* and *in vivo* assays.¹⁸ These studies provide detailed information on the dosing and toxicity levels and enables a decision on whether the compound should be tested on people.¹⁸

The third stage of the “pipeline” is the clinical research, in which there are four phases.¹⁸ In phase I, the compound is tested on 20 to 100 healthy human volunteers or volunteers with the disease/condition in order to determine its safety and the correct dosage.¹⁸ Approximately 70% of drugs move to phase II.¹⁸ In phase II, the compound is tested on several hundred people with the disease or condition in order to determine its efficacy and potential side effects.¹⁸ Approximately 33% of drugs move to the next phase.¹⁸ In phase III, the compound is tested on 300 to 3,000 volunteers who have the disease or condition in order to measure the compound’s efficacy against existing treatments and for monitoring adverse reactions.¹⁸ Approximately 25-30% of drugs move to the next phase.¹⁸ In Phase IV the drug is tested on several thousand volunteers who have the disease/condition in order to confirm its safety and efficacy.¹⁸

Once the compound has passed the clinical trials the company that developed the compound can submit an application to the relevant government authority (e.g. FDA in the case of USA, TGA in Australia) to market the drug.¹⁸ The government authority then reviews all of the clinical data and a decision is made whether or not to approve the application.¹⁸

REMOVED DUE TO COPYRIGHT RESTRICTION

Figure 1.4: Drug Discovery and Development-Timeline. Reproduced from <https://www.aravalipharma.com/drug-discovery/>

1.4 Promising drug candidates

Due to the many issues involved with the current drugs used to treat tuberculosis, new TB drugs are required to solve the issues such as MDR/XDR-TB and the long duration times of the current chemotherapy regimen. The probability of a compound successfully passing through the drug discovery pipeline to being government approved is low, as outlined above. At the present time there are only a few compounds that are in clinical trials. Some of these compounds belong to the structural classes of oxazolidinones, diarylquinolines, nitroimidazoles, rifamycin and ethylenediamines.¹

Following are some compound classes currently under evaluation in clinical trials.

1.4.1 Oxazolidinones

Oxazolidinones have been shown to be active against tubercle bacilli *in vitro* and *in vivo*.^{1,19,20} Their activity is the result of inhibiting protein synthesis by binding to 23S rRNA of the 50S ribosomal subunit.¹ Specifically, there are 3 compounds in this class that are currently in phase II clinical trials; sutezolid (PNU-100480), linezolid and AZD5847 (Figure 1.5).¹ Linezolid

(the lead antimicrobial compound out of these three) has been shown to be effective against MDR-TB in combination with other drugs.¹ After prolonged use, however, linezolid can become toxic.¹ To limit the neurotoxic effects, the optimal dosage of this drug is still under investigation.¹

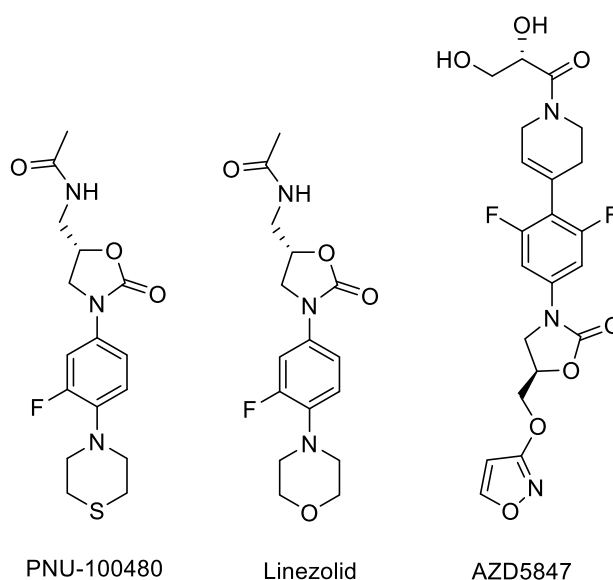


Figure 1.5: Oxazolidinones in phase II clinical trials for treatment of TB

PNU-100480 is currently being developed for susceptible and drug-resistant TB while AZD5847 is about to go through phase IIb studies.^{1,21}

1.4.2 Diarylquinolines

TMC207 or Bedaquiline (Figure 1.6) was the first novel tuberculosis drug to be FDA approved in over 40 years in 2012.²² TMC207 has been shown to be the most active diarylquinoline compound through *in vivo* studies.¹ This high activity can be attributed to its effect on the *atpE* gene that codes for the c subunit of ATP synthase of *M. tuberculosis*.^{1,23} The fact that it affects the *atpE* gene can be advantageous since the human proteins encoded by *atpE* are not similar to the mycobacterial proteins encoded by this gene.¹ Therefore TMC207 is unlikely to affect the human host.¹

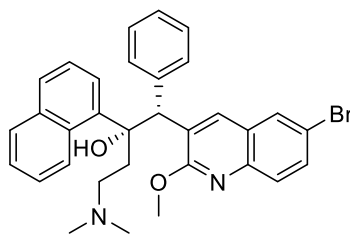


Figure 1.6: Structure of the diarylquinoline, TMC207

Other useful features of this compound include a long half-life and good absorption without any observed toxicity, strong bactericidal and sterilizing properties and no cross-resistance to first-line drugs.^{1,23,24} Bedaquiline, now sold under the brand name Sirturo®, is part of a combination therapy for MDR-TB.²⁵

1.4.3 Nitroimidazoles

Within the nitroimidazole class are PA-824 (a nitroimidazo-oxazine) and OPC67683 (a nitroimidazo-oxazole) (Figure 1.7).¹ These anti-TB compounds are referred to as prodrugs since they are activated by nitroreduction within the cell.^{1,26,27} This nitroreduction produces many reactive species that inhibit protein and lipid biosynthesis within the mycobacterial cell.^{1,26,27,28} Additionally, these compounds have been shown to reduce the time of sterilization when used in combination with Rifampicin and Isoniazid.^{1,26,29,30,31} As a result, these compounds could reduce the overall time of chemotherapy. PA-824 has shown successful phase I results and is currently in phase II clinical trials.¹ It appears to be specific in nature since it is ineffective against a wide-range of gram-positive/negative bacteria and has considerable activity against drug-resistant clinical isolates.¹ Additionally, it does not interact with anti-HIV drugs and therefore can be prescribed to patients on antiretroviral therapy.¹ OPC67683 is further advanced in the phase III clinical trials and exhibits promising characteristics based on phase IIb clinical data.¹

Chapter 1

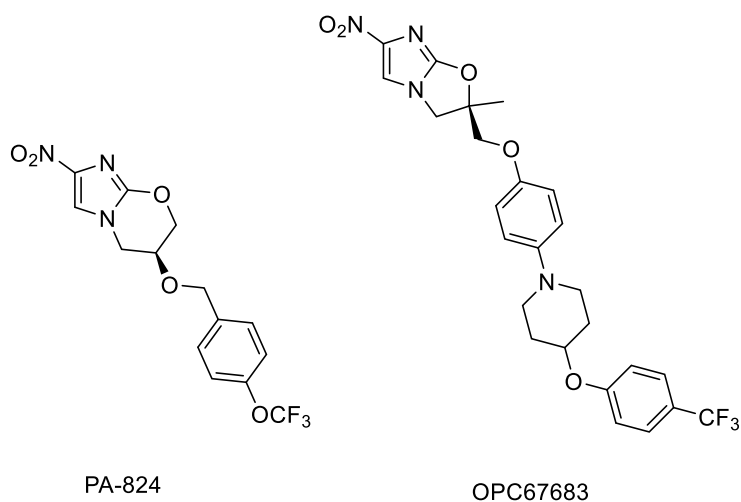


Figure 1.7: Structures of the nitroimidazoles, PA-824 and OPC67683

1.4.4 Rifamycins

Among the first-line rifamycins, such as rifabutin and rifampicin, a relatively new rifamycin, rifampentine could potentially join these compounds in first-line TB treatment (Figure 1.8).¹ These compounds are known to inhibit DNA-dependent RNA polymerase which is required for RNA synthesis.¹ Rifampentine was registered in 1998 and was approved by the FDA for treatment of TB.¹ It has been shown to have the same activity against *M. tuberculosis* as rifampicin which is promising since this first-line drug has shortened the overall time of TB chemotherapy treatment.¹ It is expected that if the dose of rifampentine is increased, the duration of chemotherapy will be reduced.^{1,32} This has caused a renewed interest in the compound's safety, PK properties and efficacy at these higher doses.³³ Rifampentine is presently undergoing phase II/III clinical trials.¹

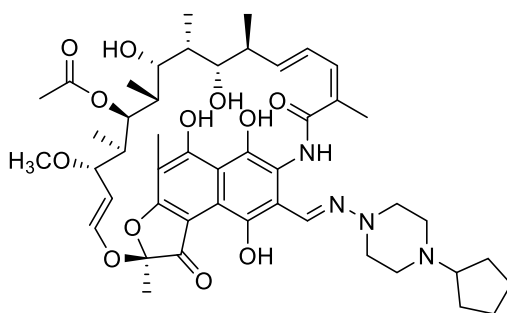


Figure 1.8: Structure of rifampentine

1.4.5 Ethylenediamines

After screening many analogues of the first-line drug ethambutol, SQ109 was discovered (Figure 1.9).¹ It was found to have significant activity against susceptible strains of TB as well as isoniazid-ethambutol and rifamycin resistant strains under *in vitro* conditions.^{1,34} Additionally, SQ109 can act effectively in conjunction with isoniazid and rifampicin and therefore could potentially be used in combinational therapy with these first line drugs.^{1,35} The mechanism of action is not fully understood at this time. Since SQ109 is active against ethambutol resistant strains the mechanism of action likely differs to that of ethambutol.^{1,34} Currently SQ109 is in a phase IIa Early Bactericidal Activity (EBA) study after showing promising results in the phase I clinical trials.¹

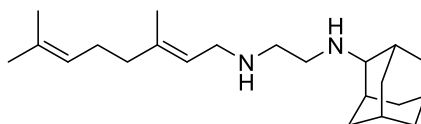


Figure 1.9: The structure of the ethylenediamine, SQ109

1.4.6 Fluoroquinolones

Within the fluoroquinolone class are two compounds which recently passed phase III clinical trials; gatifloxacin and moxifloxacin (Figure 1.10).¹ They are categorized as second-line drugs for tuberculosis and are known to inhibit the DNA gyrase.¹ The phase III trials involved a 4 month regimen for the treatment of drug-susceptible TB.¹ These two compounds were used as substitutes for the first-line drugs, ethambutol and isoniazid.¹ It was found that isoniazid could only be replaced by moxifloxacin and ethambutol could be replaced by both moxifloxacin and gatifloxacin.¹ As a result, these compounds could be used if a patient has isoniazid- and ethambutol-susceptible TB.

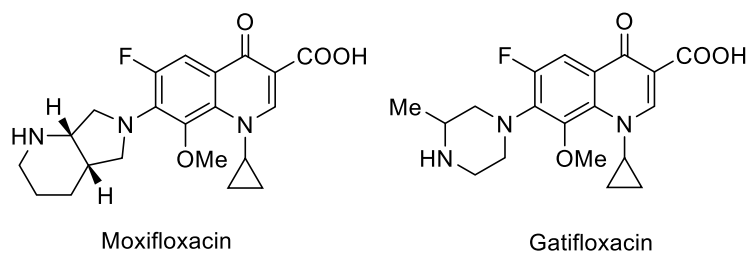


Figure 1.10: The structures the fluoroquinolones, moxifloxacin and gatifloxacin

1.5 The discovery of Q203

Another compound class within the TB drug discovery and development pipeline is the imidazo[1,2-*a*]pyridine amide (IPA). The phase I clinical candidate Q203 (Figure 1.11)³⁶ belongs to this class.³⁷ Q203 was discovered by screening 121,156 compounds from various commercial chemical libraries using a phenotypic high-content screening technology in infected macrophages.³⁷

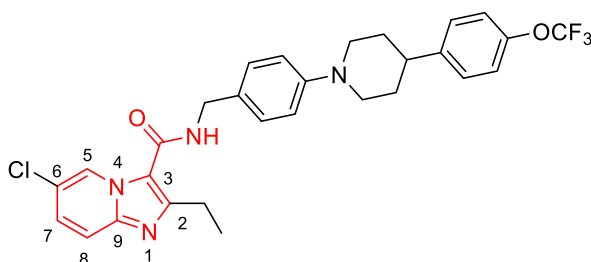


Figure 1.11: Structure of Q203, with IPA highlighted in red

Two IPAs, IPA01 and IPA02 were selected for study since both of these compounds were active against *Mtb* in the low micromolar range (Figure 1.12).³⁷ Consequently, these scaffolds were further engineered in the lead-optimization phase.³⁷ The synthesis and evaluation of 477 derivatives led to the optimized IPA Q203.³⁷ The carboxamide with the *N*-benzylic group in the 3-position of Q203 was found to be critical for its anti-tubercular activity in comparison to other amide or amine linker chains.³⁸ Attached to the *N*-benzylic amide group is a three ring system which enhanced anti-mycobacterial activity as well as solubility in cell environments.³⁸ A chloro substituent in the 6-position was found to improve anti-

mycobacterial activity and metabolic stability.³⁸ An ethyl group was also desirable since smaller alkyl groups, such as methyl and ethyl showed better activity than longer and bulkier groups such as propyl and isopropyl,³⁸ the larger bulkier groups may disturb the positioning of the carboxamide.³⁸ The ethyl was preferred compared to the methyl since the potency against intracellular mycobacteria was increased by 30-fold when an analogue containing an ethyl was used instead of the methyl.³⁸ The MIC₅₀ value of Q203 was 2.7 nM in the culture broth and 0.28 nM inside macrophages of the strain *Mtb* H37Rv.³⁷ Additionally, the inhibitory ability of Q203 was specific to *Mtb* and it was active against MDR/XDR clinical isolates.³⁷ As a result, Q203 must have a different mode of action to rifampicin and isoniazid since these first-level drugs are inactive against MDR/XDR-TB.³⁷

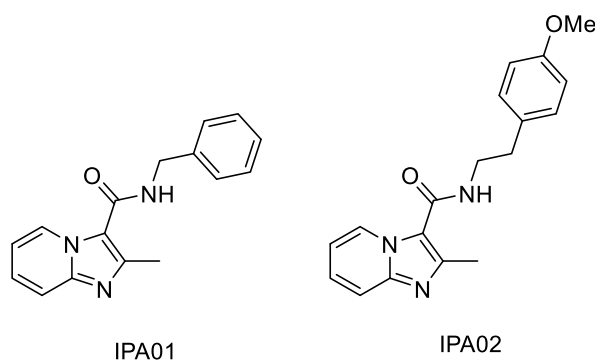


Figure 1.12: Structures of IPA01 and IPA02

1.6 Q203 mode of action

It has been found that Q203, and other IPA analogues such as **1** - **4** (Figure 1.13) inhibit the cytochrome *b* subunit of the cytochrome *bc*₁ complex encoded by the *qcrB* gene.^{37,39} The cytochrome *bc*₁ complex is located in the inner mitochondrial membrane and is a part of the electron transport chain.⁴⁰ Its specific purpose is to transfer electrons from ubiquinol to cytochrome *c* which is referred to as the Q-cycle.^{40,41}

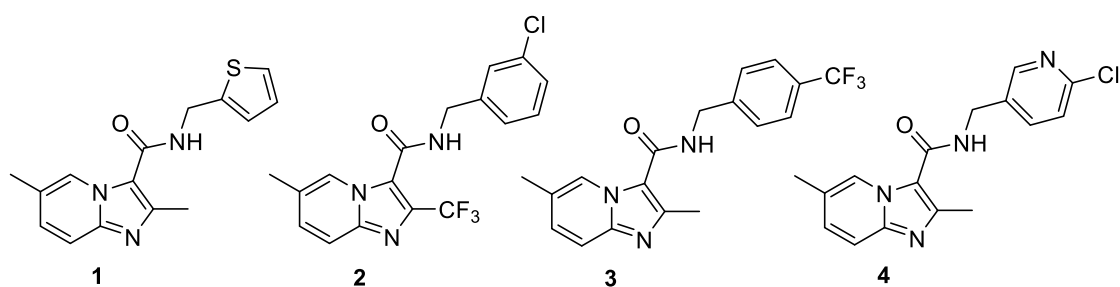


Figure 1.13: Structures of the IPAs 1 - 4

The cytochrome bc_1 complex is composed of three main components; cytochrome c_1 (which contains 1 heme group), cytochrome b (which contains 2 heme groups) and the Rieske centre (which contains a 2Fe-2S group).^{39,40} Specifically, cytochrome b recycles electrons in order to continue transferring electrons from ubiquinol to cytochrome c .⁴⁰ This overall process uses the electron transport to synthesise ATP.^{40,39} It was found that the b subunit is most likely the primary target (among other possible targets) of Q203 since there was a rapid inhibition of ATP synthesis at low concentration of Q203.³⁷ Due to the novelty of the target as a major component of the electron transport chain there is considerable promise for IPA compounds in the treatment of both active and latent phase mycobacterial infection.³⁹ Interestingly, latent infections have shown to be susceptible to inhibitors of the electron transport chain.⁴⁰

1.7 Related structures to Q203

Many other structures related to imidazo[1,2-*a*]pyridines and to specifically Q203 have been explored for their anti-tubercular activity. This section will describe various antitubercular imidazo[1,2-*a*]pyridines and close analogues that have been reported in the literature. The core structures of these derivatives are closely related to the imidazo[1,2-*b*]pyridazine template which is the main focus of this PhD project. Imidazo[1,2-*b*]pyridazines will be thoroughly discussed in subsequent sections and chapters.

1.7.1 Pyrazolo[1,5-*a*]pyridine-3-carboxamides

Pyrazolo[1,5-*a*]pyridine-3-carboxamides were also investigated for their anti-tubercular activity.⁴² After evaluating the SAR of these pyrazolo[1,5-*a*]pyridine-3-carboxamides it was found that TB47 (Figure 1.14) was the most potent against H37Rv *Mtb* (MIC = 11.1 nM).⁴² It can be seen that TB47 is very similar in structure to Q203 (Figure 1.11). Both compounds include the same carboxamide substituent at C3 as well as an alkyl group at C2 of the pyrazolo[1,5-*a*]pyridine ring system.⁴² The SAR suggested that a long hydrophobic chain at C3 was most appropriate for increased potency against *Mtb*.⁴² Additionally, a substitution at C5 on the pyridine ring was optimal in comparison to the 4-, 6-, or 7-position.⁴² A large hydrophobic substituent at C5 was detrimental to the compounds' activity whereas methyl, ethyl, methoxy and chloro groups were suitable substituents.⁴² At C2, small hydrophobic groups such as methyl, ethyl or cyclopropyl were superior to being unsubstituted or phenyl substituted.⁴²

TB47 was found to be active against both drug sensitive and resistant *Mtb* strains.⁴² Additionally, TB47 showed promising results in an infected mouse model, which revealed activity against H37Rv *Mtb in vivo* and the compound was well-tolerated with no mortality.⁴² As a result, TB47 could be a lead compound for further anti-TB drug discovery.⁴² Furthermore, TB47 was found to be highly bactericidal against *Mycobacterium ulcerans* (*Mu*) and was found to reduce the bacterial burden by more than 2.5 log₁₀ colony-forming units (CFU) in mouse footpads compared to the WHO recommended treatment regimen.⁴³

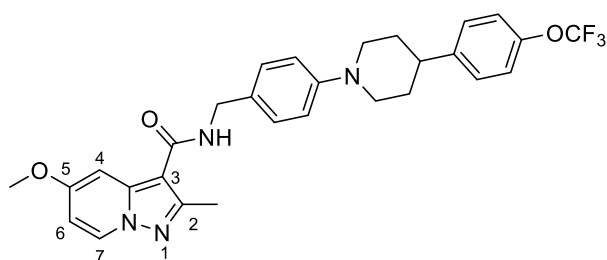


Figure 1.14: The structure of the pyrazolo[1,5-*a*]pyridine-3-carboxamide, TB47

1.7.2 Imidazo[1,2-*a*]pyridine-8-carboxamides

A study of the SARs of imidazo[1,2-*a*]pyridine-8-carboxamides identified structure **5** (Figure 1.15) as a lead compound for further progression (MIC = 0.25 $\mu\text{g}/\text{mL}$).⁴⁴ It was found that the C8 primary amide, a hydrogen bond donor, positioned on ring A enhanced the compound's activity against *Mtb*.⁴⁴ Additionally, it was found that for strong activity there should be no other substituents on ring B and that ring C should be a 3-substituted aryl ring.⁴⁴ The compound was also found to have negligible cytotoxicity, since it had no effect on the A549 cell line at 100 μM , and high selectivity for *Mtb* compared to gram positive/negative pathogens.⁴⁴ However, its low aqueous solubility, most likely due to its high lipophilicity and the planarity of the scaffold, could be improved.⁴⁴

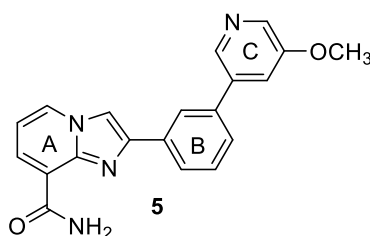


Figure 1.15: The structure of the imidazo[1,2-*a*]pyridine-8-carboxamide **5**

1.7.3 Imidazo[1,2-*a*]pyridine-2-carboxamides

In light of the recent success of the imidazopyridine amides (IPAs), especially Q203, anti-tubercular studies were also conducted with imidazo[1,2-*a*]pyridine-2-carboxamides.³ Compounds **6**, **7** and **8** (Figure 1.16) all exhibited low MIC values (6.25 $\mu\text{g}/\text{mL}$) against *Mtb* H37Rv.³ SAR studies revealed that the presence of hydrophobic substituents for R¹ and R² increased the anti-mycobacterial potency.³ The overall hydrophobic nature of these compounds may have allowed them to penetrate the cell wall of the mycobacterium.³ Molecular docking studies indicated that the long-chain enyl-acyl carrier protein reductase (InhA) may be the target of these imidazo[1,2-*a*]pyridine-2-carboxamides.³ Additionally, the *in vitro* toxicity of these molecules was low when tested against the Human Kidney Cell-line 293-T (HEK-293T) making them qualified lead compounds for optimization.³

Chapter 1

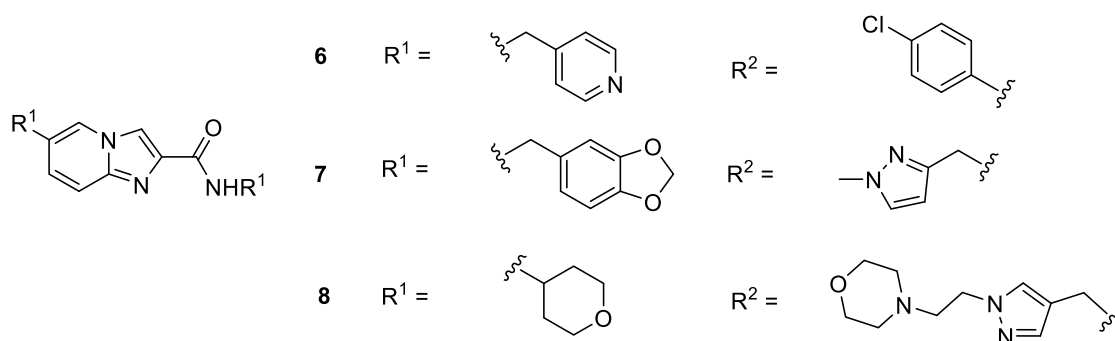


Figure 1.16: The structures of the imidazo[1,2-a]pyridine-2-carboxamides **6**, **7** and **8**

1.7.4 *N*-(2-Phenoxyethyl)imidazo[1,2-a]pyridine-3-carboxamides

The SAR studies of IPAs, in particular Q203 and ND-09759 (ND-09759 is in pre-clinical trials), (Figure 1.17) which both target the cytochrome *b* subunit of the cytochrome *bc*₁ complex, revealed that the carboxamide linker with the *N*-benzylic group is critical for anti-tubercular activity.⁴⁵ These two compounds were subjected to peripheral modification in which DNB1 was taken into consideration (Figure 1.18).⁴⁵ DNB1 displayed high activity against *Mtb* including XDR strains and targets DprE1/DprE2.⁴⁵ Therefore, the *N*-2-phenoxyethyl moiety in DNB1 was used for the peripheral modification of Q203 and ND-09759 resulting in structure **9**.⁴⁵

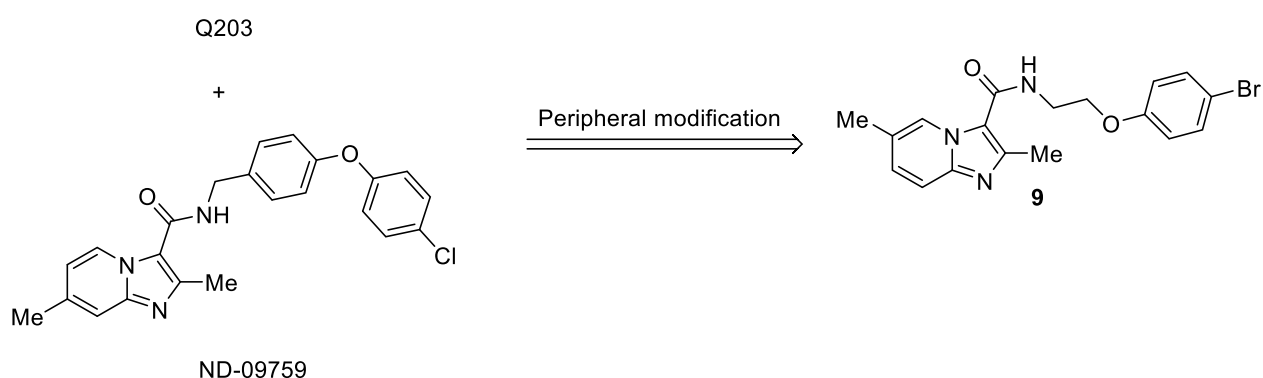


Figure 1.17: Peripheral modification of Q203 and ND-09759 resulting in **9**

Chapter 1

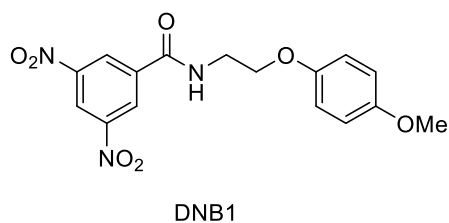


Figure 1.18: Structure of DNB1

After the SAR analysis and evaluation of its selectivity, safety and PK properties, compound **9** was found to be a promising lead compound for further optimisation.⁴⁵ The SAR analysis demonstrated that 2,6-dimethyl IPAs are much more potent than 2,7-dimethyl IPAs.⁴⁵ Additionally, the presence of electron-donating groups or a halogen atom on the benzene ring was generally preferred over electron-withdrawing groups or a bulkier phenyl group.⁴⁵ Seven of the *N*-(2-phenoxyethyl)imidazo[1,2-*a*]pyridine-3-carboxamides exhibited high activity against both drug susceptible- and MDR-TB (which were resistant against isoniazid and rifampicin).⁴⁵ Interestingly, none of the compounds that were tested were active against Gram-negative and Gram-positive strains which demonstrates their high selectivity for TB.⁴⁵

1.7.5 Anagrams and other analogues of Zolpidem

Zolpidem (Figure 1.19, **10**) is an approved drug for the treatment of insomnia.⁸ Coincidentally, it has a very similar structure to anti-tubercular imidazo[1,2-*a*]pyridine-3-carboxamides.⁸ Zolpidem was screened against *Mtb* H37Rv and was found to have a MIC value of 10 μ M; a relatively low activity when compared to other imidazo[1,2-*a*]pyridine-3-carboxamides.⁸ Therefore through chemical syntheses the structure of Zolpidem was altered generating different Zolpidem anagrams (Figure 1.19) as well as different analogues of the sedative.⁸

Chapter 1

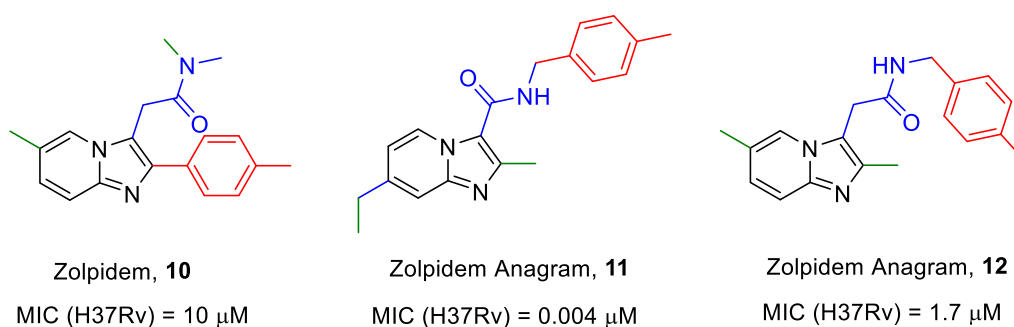


Figure 1.19: Structure of Zolpidem **10** and Zolpidem anagrams **11** and **12**

The alteration of Zolpidem to different isomers as well as other analogues drastically improved its anti-tubercular activity. For example, Zolpidem anagram **11** had an MIC (H37Rv) = 0.004 μ M and Zolpidem anagram, **12** had an MIC (H37Rv) = 1.7 μ M (Figure 1.19).⁸ *N*-benzylic amide **11** had the highest activity series of 3-substituted compounds tested (imidazo[1,2-*a*]pyridine-3-carboxamides, imidazo[1,2-*a*]pyridine-3-oxoacetamides, and imidazo[1,2-*a*]pyridine-3-acetamides) (Figure 1.20).⁸ It was found that the 3-carboxamides generally showed the highest activity with MIC values being 2-3 times lower than the oxoacetamide and acetamide series.⁸ Interestingly, steric bulk at the 2-position did not have an effect on the activity of the 3-carboxamides and the 3-acetamide series while this was not the case for the 3-oxoacetamide series.⁸ Additionally, it was found for all three series that benzyl amides were more effective than *N,N*-dimethyl amides and that secondary amides showed reduced activity against *Mtb*, suggesting that a hydrogen bond donor is required.⁸

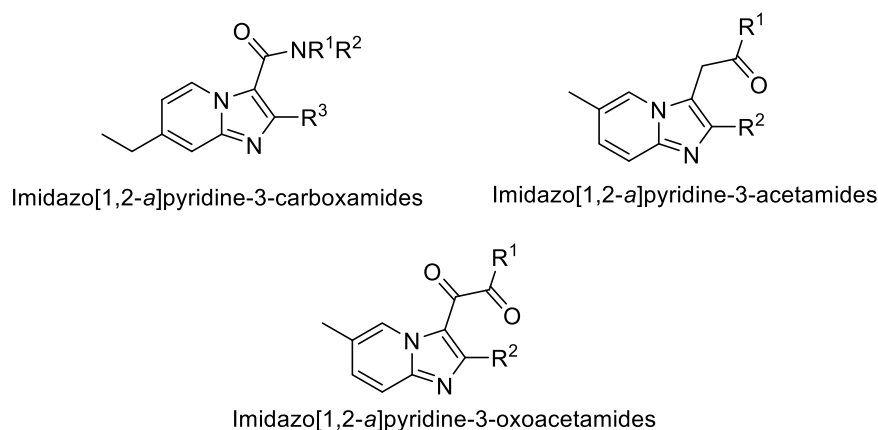


Figure 1.20: General structures of the imidazo[1,2-a]pyridine-3-carboxamides, imidazo[1,2-a]pyridine-3-oxoacetamides, and imidazo[1,2-a]pyridine-3-acetamides

The activity of *N*-benzylic amides **11** and **12** against drug-resistant, MDR-TB and XDR-TB was also evaluated and **11** had an MIC of <0.03 μ M for most clinical strains.⁸ Specifically, **11** did not show any observable toxicity to VERO cells and in human cell lines (HeLa, PC-3 and MCF-7).⁸ Additionally, it was found that **11** targeted the *bc*₁ complex similarly to Q203.⁸ These results suggest that further modification of the imidazo[1,2-*a*]pyridine template may lead to enhanced potency against *Mtb*.⁸

1.7.6 Imidazo[1,2-*a*]pyridine amide-cinnamamide hybrids

IPA derivatives containing an *N*-(2-phenoxy)ethyl or an *N*-(2-phenylamino)ethyl moiety such as IMB-1502 (Figure 1.21) have been observed to have nanomolar potency against *Mtb* H37Rv and MDR-TB strains.³⁶ Cinnamic acid was shown to exhibit anti-tubercular properties and can act synergistically with isoniazid, rifamycin and other anti-tubercular agents³⁶ and psioniamide (Figure 1.21) is cinnamamide natural product that displays anti-tubercular activity.³⁶ Therefore, it was hypothesised that the molecular hybridization of IMB-1502 and psioniamide might further enhance the IPAs' potency against *Mtb* (Figure 1.21).³⁶

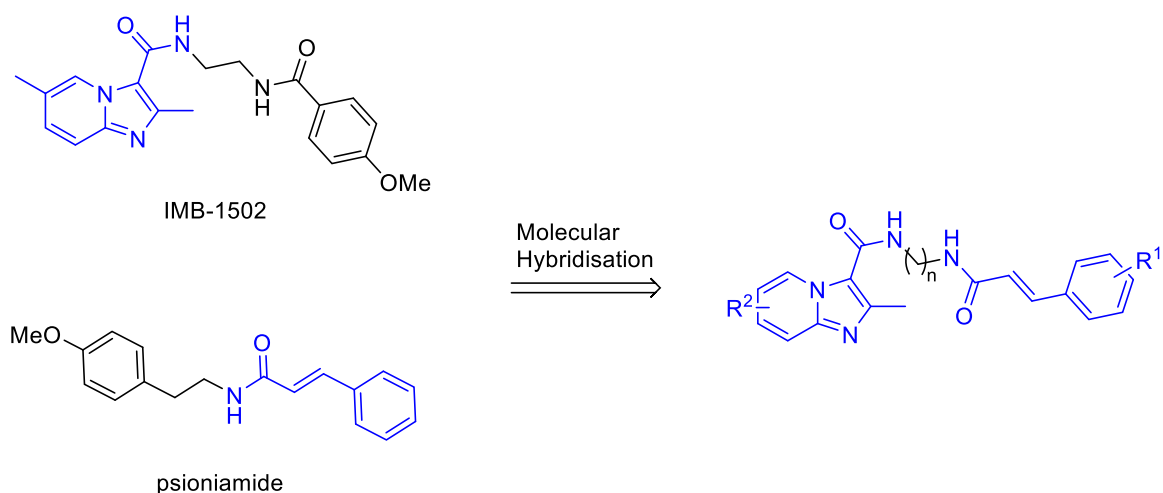


Figure 1.21: Molecular Hybridisation of IMB-1502 and psioniamide

It was found through analysis of SARs that a methyl group at C6 of the IPA moiety (R^2 , Figure 1.21) afforded enhanced activity compared to the 7-methyl analogue.³⁶ Hybrids with an ethyl linker ($n=2$, Figure 1.21) were also compared to hybrids with a propyl linker ($n=3$, Figure 1.21); the derivatives containing the ethyl linker seemed to have superior activity.³⁶ Additionally, electron withdrawing groups such as 4- CF_3 and 4- OCF_3 at R^1 afforded enhanced anti-tubercular activity. Compounds **13** and **14** had the lowest MIC value of 4 $\mu\text{g/mL}$ (Figure 1.22).³⁶

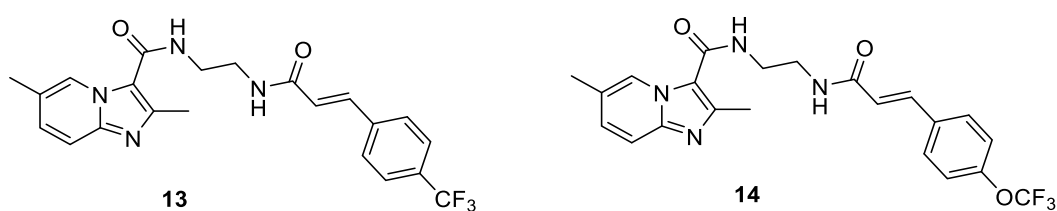


Figure 1.22: Structures of **13** and **14**

1.8 Imidazo[1,2-*b*]pyridazines and screening of the CSIRO Compound Library

Clearly, there are many imidazo[1,2-*a*]pyridines and related derivatives reported to have high anti-tubercular activity. Another closely related compound class are the imidazo[1,2-*b*]pyridazines (Figure 1.23), examples of which have shown antitubercular activity. Notably, this core structure has a nitrogen instead of a carbon at position 5 when being compared to the imidazo[1,2-*a*]pyridine. CSIRO (Commonwealth Science and Industrial Research Organisation) and GIBH (Guangzhou Institutes of Biomedicine and Health) discovered the activity of these compounds after GIBH screened 18,000 pre-existing CSIRO compounds against *Mtb*. More than 200 imidazo[1,2-*b*]pyridazine derivatives were screened by GIBH and 7 of these compounds were found to be active (defined as >50% inhibition at 10 μ M). A stable and virulent strain of autoluminescent *Mtb* H37Rv (AIRv) was used to detect and measure the bioluminescence of the bacteria using relative light unit readings (RLU). The RLU readings correlate with the population of bacteria allowing to calculate the inhibition of *Mtb*.

In terms of the initial SAR it was found that a methoxy at C3 was preferable due to 6 out of 7 of the most active compounds in this class having this moiety (Figure 1.23). All except one of these derivatives also had a benzyl substituent at C6 with either a sulfur, oxygen or nitrogen linking heteroatom. All 7 compounds had a phenyl ring at C2. Compounds **15**, **16**, **17** and **18** (Figure 1.23) displayed >95 % inhibition and were selected as lead compounds. Importantly, these structures have not been reported to inhibit *Mtb*, allowing the possibility for CSIRO to secure the available intellectual property.

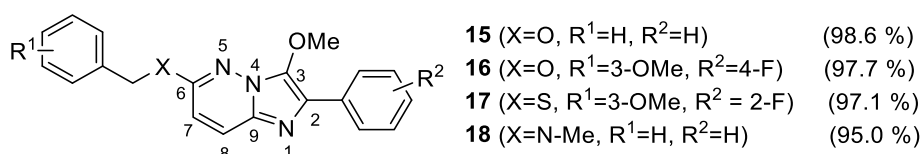


Figure 1.23: Structures of CSIRO imidazo[1,2-*b*]pyridazines with percent growth inhibitions at 10 μ M

Chapter 1

The inventors of the clinical candidate Q203, Institute Pasteur Korea, patented⁴⁶ the imidazo[1,2-*a*]pyridine and several related core structures. Interestingly and importantly, despite claiming structures with heteroatoms at any of positions 6, 7, and 8, structures with nitrogen at position 5 (Figure 1.24), such as the imidazo[1,2-*b*]pyridazine structures of interest in this project, were not claimed. This was significant in terms of scope to secure available intellectual property and freedom to operate in proceeding with this project.

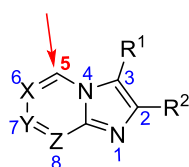


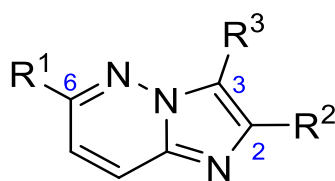
Figure 1.24: General core structures claimed in Institute Pasteur Korea patent.

Many different derivatives of imidazo[1,2-*b*]pyridazine from the CSIRO Compound Library were tested and their MIC values against *Mtb* were determined by GIBH. Table 1.1 below displays a selection of the range of compounds, including compounds **15** – **67**, tested from May 2016 – January 2018 (note: Table 1.1 does not include every compound tested, but illustrates the variety of substituents used for R¹, R² and R³). In assays performed between May and September of 2016, the derivatives **15**, **16**, **17**, **18** and **19** showed very promising activity, but some variability in the assay and weaker results were observed in November 2016 which is the reason for the large MIC and IC₅₀ ranges in some cases. Later results confirmed the strong *in vitro* activity of these and close analogues.

The derivatives **53** to **56**, **58**, and **64** to **66** also showed promising results. Notably, these compounds share similar functional groups with a methoxy-substituted benzyl group at C6, a methoxy at C3 and a halogen substituted or non-substituted phenyl ring at C2. Specifically, compound **64** showed excellent MIC values (≤ 0.625 $\mu\text{g/mL}$) (Table 1.1). The close fluoro analogue **65** also showed this MIC value in one assay.

Chapter 1

Table 1.1: Overview of selected imidazo[1,2-b]pyridazine compound Mtb screening results from GIBH, May 2016 – January 2018



(1000 x $\mu\text{g/mL}$)/M.W. = μM

Compound no.	R^1	R^2	R^3	IC_{50} (μM) range	MIC ($\mu\text{g/mL}$) range
15	BnO	Ph	OMe	0.11	1 - 10
16	3-MeO-BnO	4-F-Ph	OMe	0.65 – 32.9	25
17	3-MeO-BnS	2-F-Ph	OMe	0.32 - 0.40	0.25 - 50
18	BnNMe	Ph	OMe	0.72 – 1.15	1 - 4
19	BnS	Ph	OMe	0.04 -35.9	1 - 10
20	BnS	Ph	OEt		25
21	MeS	2-naph	OMe	>30	
22	H	$\text{CH}_2\text{CH}_2\text{Ph}$	CH_2NHCOMe	>30	
23	^nPrS	3,4,5-tri-MeO-Ph	H	>30	
24	MeS	3,4-di-Me-Ph	H	>30	
25	3- NO_2 -BnS	Bn	OMe	11.0	>100
26	4-Me-BnS	Bn	OMe	12.4 -33.3	100
27	PhS	Ph	OMe	>30 – 37.5	50
28	EtS	Ph	OMe	15.3 – 43.8	50
29	F	4-F-Ph	OMe	>30	>100
30	Cl	3-thienyl	OMe	6.58 – 94.1	50
31	2-MeO-PhS	Ph	OMe	1.26	>100
32	3-Me-PhS	Ph	OMe	25 – 72.0	100
33	4-Me ₂ N-PhS	Ph	OMe	13.4-132.8	100
34	2-MeO-PhO	4-Et-Ph	OMe	>30	>100
35	2-MeO-PhO	4-F-Ph	OMe	5.73	>100
36	2-MeS-PhO	4-F-Ph	OMe	12.4	>100
37	MeS	3-MeO-Ph	OMe	7.96	
38	PhO	Me	OMe	>30	
39	4-MeO-PhO	$\text{CH}_2\text{CH}_2\text{Ph}$	OMe	>30 – 33.3	25
40	EtS	3,4-O CH_2O -Ph	CH_2NHCOPh	>30	

Chapter 1

41	EtO	4-Cl-Ph	CH ₂ NHCOPh	>30	
42	MeOCH ₂ CH ₂ O	Ph	CH ₂ NHCOPh	>30	
43	MeO	4-Cl-Ph	CH ₂ N ⁺ Me ₃ F ⁻	>30	
44	BnS	Ph	CH ₂ NMe ₂	1.92 – 10.7	2 – 8
45	3,4-OCH ₂ O- BnNH	3,4-OCH ₂ O-Ph	H	28.2	
46	Me	4-Me-Ph	CH ₂ SMe	>30	>100
47	BnO	Ph	Cl	60	20-100
48	BnO	Ph	CN	>100	>100
49	BnO	Ph	Me		>100
50	3-MeO-BnS	3,4-di-MeO- Ph	OMe	>30	>100
51	BnO	4-MeO-Ph	OMe	5.89	
52	2-Cl-BnS	Ph	OMe	1.83	>100
53	3-MeO-BnNH	Ph	OMe		5
54	3-MeO-BnNH	2-F-Ph	OMe		5
55	3-MeO-BnNH	4-F-Ph	OMe		10
56	2-MeO-BnNH	4-Me-Ph	OMe		10
57	2-Cl-BnNH	4-Cl-Ph	OMe	29.4	
58	3-MeO-BnNH	4-Me-Ph	OMe	1.7 – 2.4	5
59	3-MeO-BnNH	4-CF ₃ -Ph	OMe	2.9 - >30	5
60	BnNMe	3-NH ₂ -Ph	OMe	3.28 - ≤17.4	12.5
61	BnNMe	3-F-Ph	OMe	4.70 – 17.2	25
62	2-MeO-PhO	4-MeO-Ph	OMe	>30 – 33.1	100
63	3-MeO-BnO	4-F-Ph	OH	68.4	50
64	3-MeO-BnS	Ph	OMe		≤0.625
65	3-MeO-BnS	4-F-Ph	OMe		≤0.625 - 5
66	3-MeO-BnS	2,4-di-F-Ph	OMe		≤6.25
67	3-MeO-BnS	Ph	OEtOMe		12.5

The imidazo[1,2-*b*]pyridazine scaffold has appeared in the literature for the inhibition of parasites such as *Plasmodium* species which cause malaria^{47,48,49} and *Haemonchus contortus*⁵⁰ but the use of such compounds for the inhibition of *Mtb* has scarcely been explored. Garret C. Moraski *et al.* investigated the antitubercular activity of a library of different 5,6-fused

bicyclic heteroaromatic compounds, including imidazo[1,2-*b*]pyridazine **68** (Figure 1.25).⁵¹ Imidazo[1,2-*b*]pyridazine **68** only exhibited moderate activity against *Mtb*.⁵¹ However, the C2, C3 and C6 substituents in **68** are vastly different to the substituents observed in the aforementioned potent imidazo[1,2-*b*]pyridazines **15**, **16**, **17** and **18** (Figure 1.23).⁵¹ The rarity and high activity of these imidazo[1,2-*b*]pyridazines encouraged further investigations into their antitubercular activity. The syntheses of imidazo[1,2-*b*]pyridazines **15**, **16**, **17** and **18** (and other imidazo[1,2-*b*]pyridazines) and their interaction with benzodiazepine receptors were reported in a body of seminal work by Barlin *et al.*^{52,53,54,55}

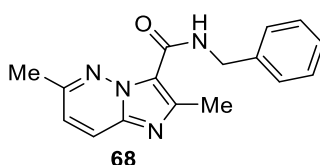


Figure 1.25: Structure of *N*-benzyl-2,6-dimethylimidazo[1,2-*b*]pyridazine-3-carboxamide **68**

1.9 Conclusions

The recent collaboration between CSIRO and GIBH in China identified a number of related and strongly antimycobacterial imidazo[1,2-*b*]pyridazine hit compounds by high throughput screening (HTS). These promising compounds are rare in the literature, providing scope for development and intellectual property. Closely related core structures such as the imidazo[1,2-*a*]pyridine and associated anti-tubercular activity have been reported in the literature, but relevant patents do not claim the imidazo[1,2-*b*]pyridazine template.

This project focuses on the hit-to-lead and lead-optimisation phase of the drug discovery process and essentially involves the systematic structural modification of these compounds synthetically to increase the activity against *Mycobacterium tuberculosis*. A key aspect of the project is the establishment of detailed SARs via an iterative feedback loop between compound design and synthesis (Flinders/CSIRO) and GIBH biological screening results. The most promising lead compounds will be evaluated, at GIBH, in further *in vitro* and *in vivo* tests for pharmacokinetics and toxicity with an overarching aim to identify one or more candidates for possible development.

Chapter 2.
3-Methoxyimidazo[1,2-*b*]pyridazine
Syntheses

Chapter 2 Summary

Chapter 2 discusses two synthetic pathways for the syntheses of 3-methoxy-2-phenylimidazo[1,2-*b*]pyridazines which are based on literature precedent,^{50,55} with some modifications/improvements. Pathway 1 involves the reactions of 6-substituted-pyridazine-3-amines with various phenylglyoxals to prepare a library of 6-benzylthio- (and related) 3-methoxy-2-phenylimidazo[1,2-*b*]pyridazines. The discovery of interesting side-products along this synthetic pathway is noted. Complications were encountered when attempting to synthesise 2-(2-fluorophenyl)-3-methoxy-6-((3-methoxybenzyl)thio)imidazo[1,2-*b*]pyridazine (**17**) using Pathway 1 which prompted the employment of Pathway 2. Pathway 2 involves the reactions of 6-substituted-3-aminopyridazine-1-oxides with phenacyl bromides and afforded seven 3-methoxy-6-(*N*-methylbenzylamino)-2-phenylimidazo[1,2-*b*]pyridazines. The characterisation and mechanism for the synthesis of side-products at the final step is discussed.

2.1 Synthetic Pathway 1 – 6-substituted-pyridazine-3-amines and phenylglyoxals

In order to synthesise a library of 6-benzylthio-3-methoxy-2-phenylimidazo[1,2-*b*]pyridazines and related compounds, Pathway 1 was followed (Scheme 2.1). A decision was made to synthesise 6-benzylthio-3-methoxy-2-phenylimidazo[1,2-*b*]pyridazines instead of 6-benzyloxy-3-methoxy-2-phenylimidazo[1,2-*b*]pyridazines due to easier synthetic access to the thio compounds. 6-Benzyloxy-3-methoxy-2-phenylimidazo[1,2-*b*]pyridazines, a building block for 6-benzyloxy-3-methoxy-2-phenylimidazo[1,2-*b*]pyridazines, have proven to be difficult to synthesise; usually harsh conditions are required for substitution of 6-chloropyridazin-3-amine with benzyl alcohol and the process is complicated by formation of bis-benzylated side-products⁵² (Deborah A. Hughes, CSIRO, 2017). This can be explained at least in part by the lower nucleophilicity of alcohols or alkoxides compared to corresponding thiols or thiolates.

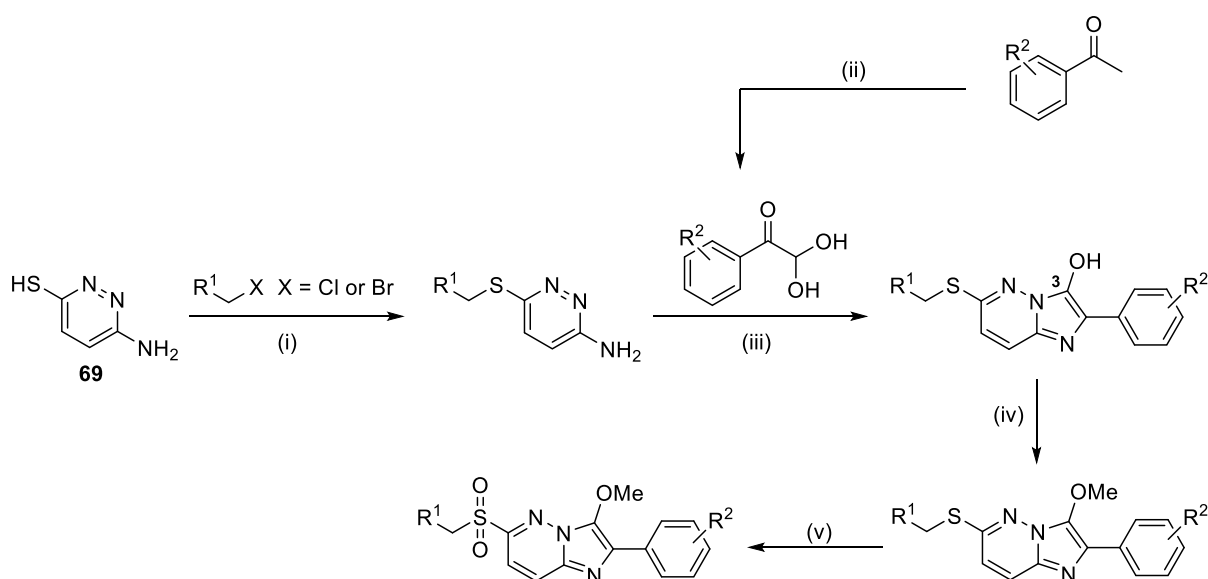
However, rather than starting with odorous thiols, it was found to be convenient to prepare the required amino-pyridazine building blocks via *S*-alkylation of 6-aminopyridazine-3-thiol (**69**) with a variety of bromo- or chloro-methyl derivatives (Scheme 2.1, i) where R¹ was a substituted phenyl group, a heterocycle, ester or morpholine amide group (Table 2.1). Sodium hydroxide in water was generally used; but in some cases, a 1,4-dioxane/THF/water mixture or THF/water mixture was required to enhance the miscibility of the alkylating agent. In some instances, potassium carbonate, a non-nucleophilic base, was used in DMF to avoid undesired side reactions.

Phenyl groups as R¹ were desired since previous SAR data revealed these moieties generally enhanced the compounds' activity as discussed in the Introduction. Replacing this phenyl group with a heterocycle was also desirable since heterocyclic compounds can behave as bioisosteres to phenyl rings,⁵⁶ and replacing the phenyl group with a heterocycle not only expands the chemical space of the imidazo[1,2-*b*]pyridazines providing further SAR data, but also increases their "drug-likeness"⁵⁷ by lowering their logP value and increasing their polar surface area and aqueous solubility. Such modifications of these chemical properties can improve the drugs' pharmacokinetics including absorption, distribution, metabolism and excretion (ADME).⁵⁷

A variety of phenylglyoxal monohydrate derivatives were synthesised from corresponding acetophenones by oxidation with HBr, DMSO and water (Scheme 2.1, ii).⁵⁸ Mixtures of the *S*-alkylated pyridazine derivatives with various phenylglyoxal monohydrates in 1,4-dioxane were heated at reflux to effect a condensation reaction to form the desired imidazo[1,2-*b*]pyridazin-3-ols. As discovered by Deborah A. Hughes (CSIRO, 2017), higher yields were obtained when catalytic HCl in 1,4-dioxane or aqueous 1,4-dioxane⁵⁹ were utilised compared with Barlin's conditions (HCl in EtOH).⁵⁵

O-Methylation of the hydroxyl at C3 of the imidazo[1,2-*b*]pyridazine ring with DMF, NaH and MeI produced the desired 3-methoxy-6-methylthio-imidazo[1,2-*b*]pyridazines (Scheme 2.1, iv). Furthermore, oxidation of the thioether to the sulfone was achieved with urea hydrogen peroxide and trifluoroacetic anhydride in acetonitrile for a few cases (Scheme 2.1, v).⁶⁰

This chapter discusses the different derivatives synthesised using Pathway 1 and the discovery of some interesting side-products.



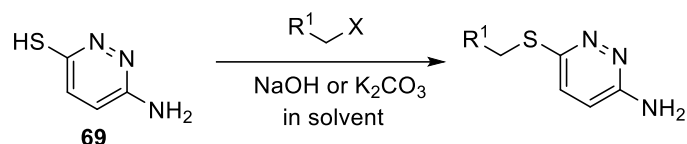
Scheme 2.1 - Reagents and conditions for Pathway 1: (i) NaOH or K₂CO₃ in solvent; (ii) HBr/H₂O/DMSO, 55 °C; (iii) HCl, H₂O/1,4-dioxane, reflux; (iv) DMF, NaH, MeI; (v) UHP, TFAA, MeCN.

2.1.1 6-Aminopyridazine-3-thiol alkylations

Table 2.1 summarises the S-alkylation reactions of **69** using a range of alkylating agents (**70-80**) and sodium hydroxide or potassium carbonate as the base to afford products **81-92** (Scheme 2.2). A low yield of 7 % for 6-((4-methoxybenzyl)thio)pyridazin-3-amine (**82**) (Entry 2, Table 2.1) was obtained after **82** was isolated via column chromatography. Many other side-products eluted from the column providing reason for the low yield of **82**. The low yield, in part, could be due to **82** undergoing side-reactions since N2 of the pyridazine ring has nucleophilic character which was corroborated from Deborah A. Hughes' discovery in 2017 after conducting this reaction under similar conditions; the isolation of a bis-benzylated pyridazine, 2-(4-methoxybenzyl)-6-((4-methoxybenzyl)thio)pyridazin-3(2*H*)-imine (**93**) (Figure 2.1). This may also be the reason for the low yield observed for the synthesis of 6-(benzylthio)pyridazin-3-amine (**81**) (Entry 1, Table 2.1). Avoiding this side reaction by using a less electrophilic alkylating agent such as benzyl chloride (instead of benzyl bromide) might improve the yield of **81**.

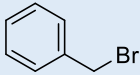
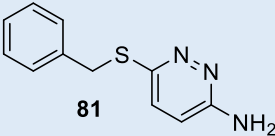
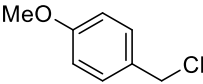
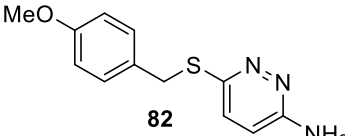
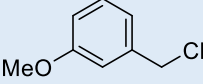
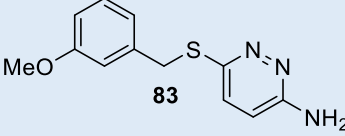
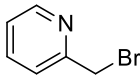
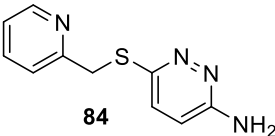
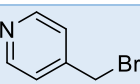
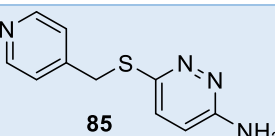
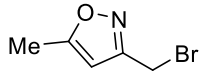
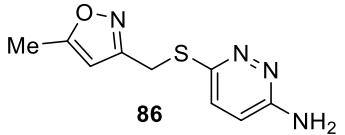
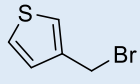
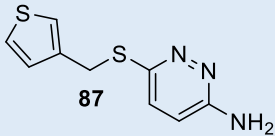
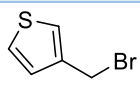
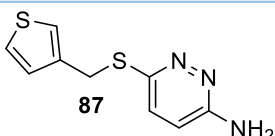
The reactions described in Entries 3 (an adaption of a protocol reported by Barlin *et al.*⁵³ – Deborah A. Hughes, CSIRO, 2017) and 4-6 proceeded in moderate to high yields of 40 – 95 % (Table 2.1). An improved yield was observed for the synthesis of 6-((thiophen-3-ylmethyl)thio)pyridazin-3-amine (**87**) after modification of the reaction conditions - the alkylating agent, 3-(bromomethyl)thiophene (**76**), was much more miscible in DMF (Entry 8) compared to aqueous 1,4-dioxane/THF (Entry 7).

Chapter 2



Scheme 2.2

Table 2.1: Syntheses of 6-([substituted]methylthio)pyridazin-3-amines

Entry	Alkylating agent ($\text{R}^1\text{-CH}_2\text{-X}$)	Reaction conditions	Product structure	Yield (%)
1	 70	K_2CO_3 , DMF	 81	11
2	 71	0.5 M NaOH	 82	7
3	 72	0.5 M NaOH	 83	45
4	$\text{HBr} \cdot$  73	1 M NaOH	 84	40
5	$\text{HBr} \cdot$  74	1 M NaOH	 85	70
6	 75	$\text{H}_2\text{O}/\text{THF}$ 0.5 M NaOH	 86	95
7	 76	1,4-dioxane/THF/ H_2O 1 M NaOH	 87	47
8	 76	K_2CO_3 , DMF	 87	60

Chapter 2

9		1 M NaOH		17
10		0.8 M NaOH in THF/H ₂ O		24
11		K ₂ CO ₃ , DMF		23
12		1 M NaOH		69
13		K ₂ CO ₃ , DMF		37
14		1 M NaOH		68
15		1 M NaOH		-
16		K ₂ CO ₃ , DMF		79

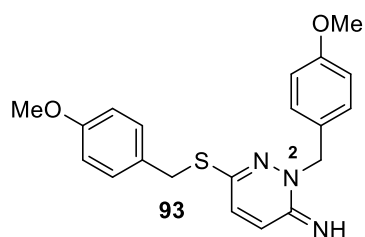


Figure 2.1: 2-(4-methoxybenzyl)-6-((4-methoxybenzyl)thio)pyridazin-3(2H)-imine (**93**)

Chapter 2

For the synthesis of 6-(((1*H*-benzo[*d*]imidazol-2-yl)methyl)thio)pyridazin-3-amine (**88**) a low yield of 17 % was achieved (Entry 9, Table 2.1). This was attributed to the incomplete consumption of **69** (37 % recovery) and the low purity of the 2-(chloromethyl)-1*H*-benzo[*d*]imidazole **77** (commercial) starting material. THF was employed as a cosolvent in a similar reaction (Entry 10) but 48 % of **69** along with a low yield of **88** was obtained. When the conditions were changed to DMF and potassium carbonate (Entry 11), it appeared that the reaction almost went to completion, by analysis of the crude ¹H NMR spectrum and via TLC analysis. However, difficulties were experienced during purification resulting in a poor yield of **88**.

To synthesise ethyl 2-((6-aminopyridazin-3-yl)thio)acetate (**90**), 6-aminopyridazine-3-thiol and ethyl bromoacetate (**79**) were subjected to the standard conditions of sodium hydroxide in water at ambient temperature (Entry 12, Table 2.1). This, however, resulted in base hydrolysis of the ethyl ester resulting in the synthesis of 2-((6-aminopyridazin-3-yl)thio)acetic acid (**89**) (Entry 12, Table 2.1). Although this compound was not desired at the time, acid **89** was still used as a precursor for the synthesis of an imidazo[1,2-*b*]pyridazine derivative discussed under the heading “2.1.4 Imidazo[1,2-*b*]pyridazin-3-ol syntheses”. To avoid base hydrolysis of the ethyl ester, K₂CO₃ (a non-nucleophilic base) was used instead of NaOH, which resulted in the synthesis of **90** in 37 % yield (Entry 13, Table 2.1).

The final alkylation attempted was the synthesis of 6-(prop-2-yn-1-ylthio)pyridazine-3-amine (**92**) (Entry 15, Table 2.1). After the reaction mixture was stirred overnight, only 35 mg of material was extracted from the reaction mixture using ethyl acetate, even though 500 mg of **69** was used. The bulk of the material remained in the aqueous phase. After 8 days the water in the aqueous phase evaporated revealing a dark brown crystalline solid. This dark brown crystalline solid was identified as 3-methyl-6-amino-thiazolo[3,2-*b*]pyridazin-4-ium salt (**94** or **95**) via ¹H (Figure 2.2), ¹³C (Figure 2.3), COSY, HSCQ and HMBC NMR spectroscopy (refer to Section 2 of the Appendices for the 2D NMR spectroscopic data). Table 2.2 lists the assigned chemical shifts in the NMR spectra of **94** as well as COSY and HMBC correlations. The ionic nature of **94** explains its high solubility in water. Notably, an extra peak at 1.66 ppm was observed in Figure 2.2 and an extra 2 peaks were observed at 24.88 ppm and 175.18 ppm in Figure 2.3. It was found the peak at 1.66 ppm correlates to the peak at 24.88 ppm via HMQC and to the peak at 175.18 ppm via HMBC. Additionally, these peaks did not correlate to any

of the other chemical shifts indicating it was a separate compound. An acetate counter ion is consistent with these NMR spectroscopic data.

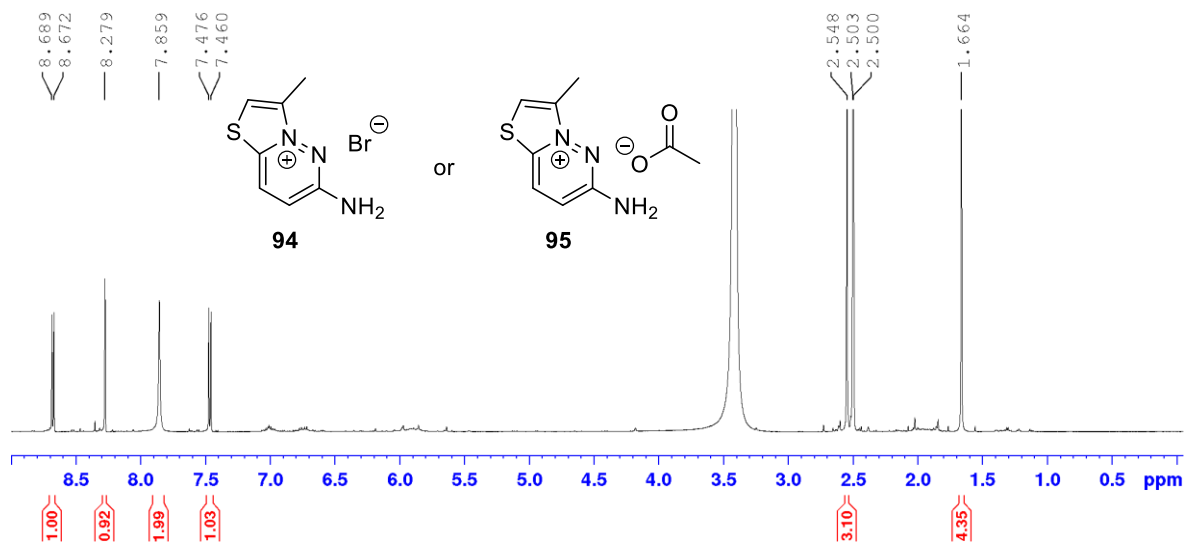


Figure 2.2: ¹H NMR spectrum of **94** or **95** in CDCl₃

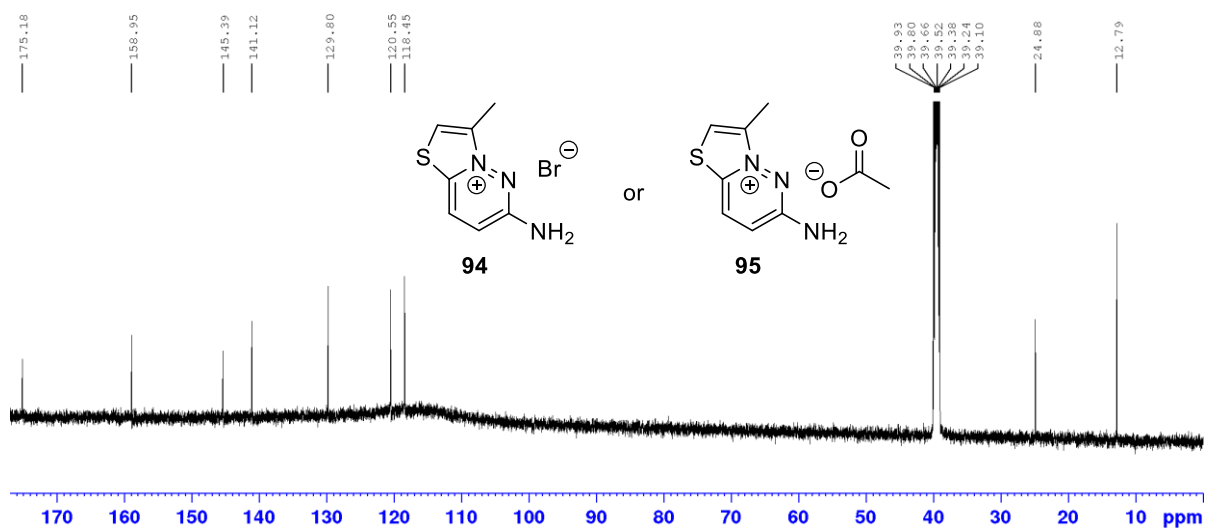
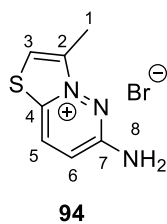


Figure 2.3: ¹³C NMR spectrum of **94** or **95** in CDCl₃

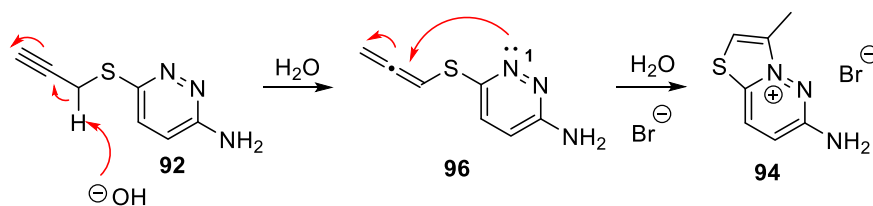
Chapter 2

Table 2.2: ^{13}C , ^1H and 2D NMR spectroscopic data from **94**



Atom Number	^{13}C (ppm)	^1H (ppm)	COSY atom correlation	HMBC atom correlation (^{13}C to ^1H)
1	12.79	2.54	3	3
2	141.12	-	-	1,3
3	120.54	8.27	1	1
4	145.39	-	-	3,5,6
5	129.80	8.68	6	6
6	118.44	7.47	5	8
7	158.95	-	-	5,6
8	-	7.85	-	-

To obtain **92**, potassium carbonate in DMF was used (Entry 16, Table 2.1) to avoid the unwarranted side-reaction proposed in Scheme 2.3 where deprotonation of the methylene forms an electrophilic allene group in intermediate **96**. Under these conditions, *S*-propargyl derivative **92** was obtained in 79 % yield.

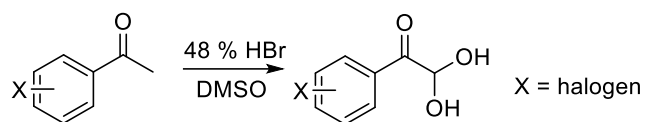


Scheme 2.3: Proposed mechanism for the synthesis of **94**

2.1.2 Phenylglyoxal monohydrate syntheses

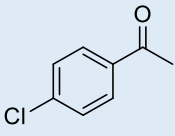
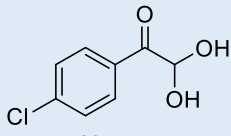
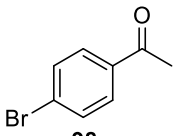
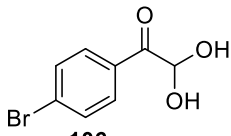
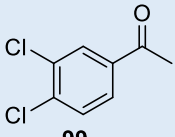
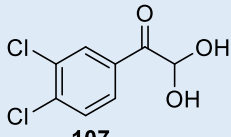
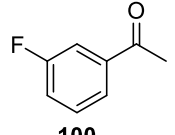
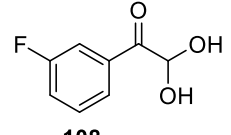
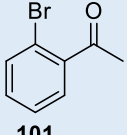
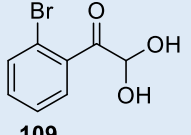
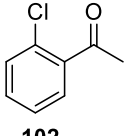
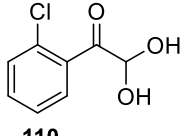
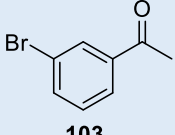
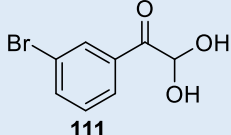
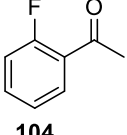
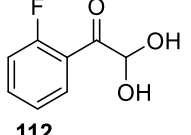
Various halo-substituted acetophenones (**97-104**) were stirred with 48 % HBr in DMSO at 55 °C to synthesise phenylglyoxal monohydrate derivatives **105-112** (Scheme 2.4, Table 2.3) according to a literature procedure.⁵⁸ Phenylglyoxal monohydrates **113 - 115** (Figure 2.4) were commercially bought. The yields of 4'-chlorophenylglyoxal monohydrate (**105**) and 4'-bromophenylglyoxal monohydrate (**106**) were moderate while the yields of 3',4'-dichlorophenylglyoxal monohydrate (**107**) and 3'-fluorophenylglyoxal monohydrate (**108**) were low. The poor yield for **107** may be attributed to the reaction not going to completion. Thus, this was monitored by TLC and the starting material was not completely consumed after 27 hours. Similarly, for Entry 4 3'-fluoroacetophenone (**100**) was not completely consumed within 17 hours. Attempted syntheses of 2'-bromo (**109**) and 2'-chlorophenylglyoxal monohydrate (**110**) using these conditions were ineffective, due to the formation of many undesired side-products. The attempted synthesis of 3'-bromophenylglyoxal monohydrate (**111**) was unsuccessful and 3'-bromomandelic acid (**116**) (Figure 2.5) was isolated instead (19 % yield), evidenced by ¹H (Figure 2.5), ¹³C, COSY, HMQC and HMBC NMR spectroscopic data (refer to Section 2 of the Appendices for the NMR spectroscopic data). Such rearrangements are known to occur under acid conditions.⁵⁸

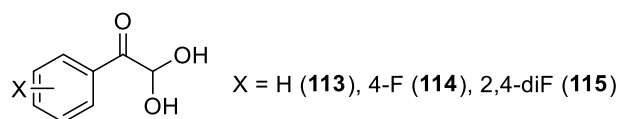
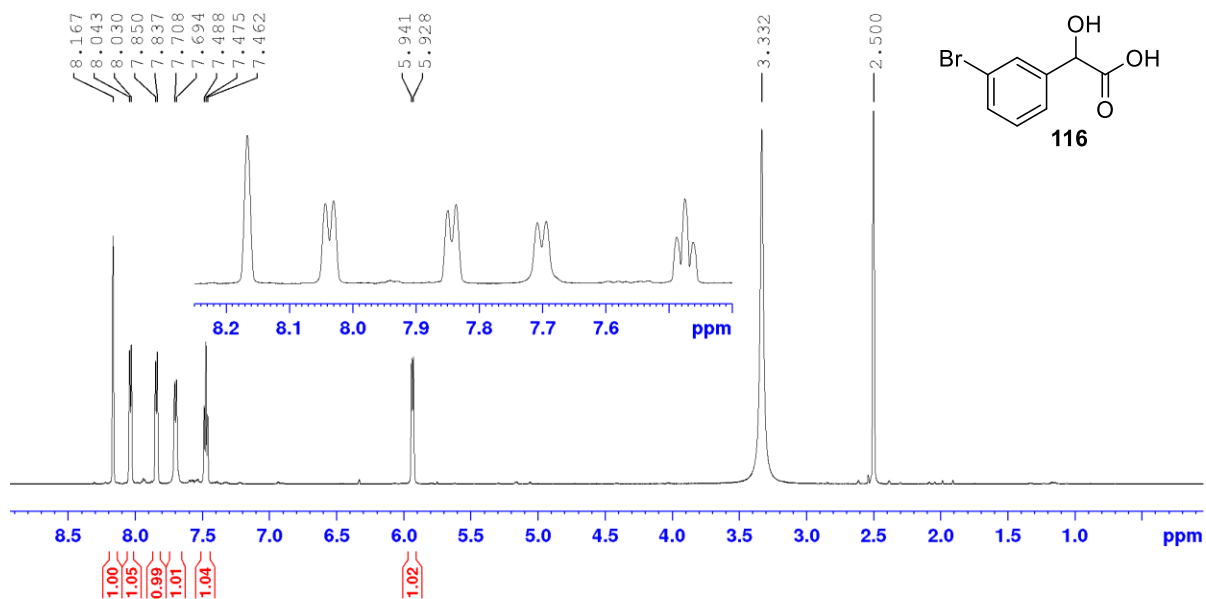
Chapter 2



Scheme 2.4

Table 2.3: Syntheses of halo-substituted phenylglyoxal monohydrates

Entry	Substrate structure	Product structure	Yield (%)
1	 97	 105	50
2	 98	 106	43
3	 99	 107	12
4	 100	 108	4
5	 101	 109	-
6	 102	 110	-
7	 103	 111	-
8	 104	 112	-

Figure 2.4: Phenylglyoxal monohydrates **113** – **115**Figure 2.5: ^1H NMR spectrum of **116** in $\text{DMSO-}d_6$

An attempted preparation of 2'-fluorophenylglyoxal monohydrate (**112**) resulted in a large amount of unreacted starting material remaining after the reaction mixture was stirred for 17 hours. The desired product appeared to be present in the crude mixture by ^1H NMR spectroscopic analysis but purification proved to be difficult due to the presence of a complex mixture of side-products, which prompted the search for new reaction conditions. Acetophenone **104** was heated at reflux with selenium dioxide in 1,4-dioxane for 17.5 hours.⁶¹ The aldehyde derivative seemed to be present by analysis of the crude ^1H NMR spectrum which included a singlet at 9.68 ppm. An attempted conversion of the aldehyde to the hydrate derivative involved the addition of boiling water to the crude mixture and hot filtration. The filtrate was extracted with ethyl acetate, and the extract was dried with sodium sulfate and concentrated under vacuum, revealing a yellow oil. However, analysis of the ^1H NMR

Chapter 2

spectrum of the crude material revealed a complex mixture plus a large amount of unreacted starting material. Therefore, this was not pursued any further.

Acetophenone **104** was stirred with NaBr in DMSO and heated to 85 °C.⁶² When 85 °C was reached, H₂SO₄ was added and bubbles began to form, indicating that the by-product dimethyl sulfide had formed.^{62,63} The stirred mixture was heated to 115 °C for 30 minutes.^{63,63} From the ¹H NMR spectrum of the crude product it appeared that all starting material was consumed and a significant amount of the aldehyde derivative was produced, as indicated by a singlet at 9.68 ppm. Water was added to the crude mixture and the whole was heated at reflux for 30 minutes in an attempt to convert the aldehyde into the hydrate.⁶³ The desired product was not observed in the crude mixture by ¹H NMR spectroscopy.

To produce corresponding 2-fluorophenylimidazo[1,2-*b*]pyridazine **17**, 2-fluorophenacyl bromide **117** (Figure 2.6) was used as an alternative substrate to **112**, and is further discussed under “2.2 Synthetic Pathway 2 – 3-substituted-6-aminopyridazine-1-oxides and phenacyl bromides”.

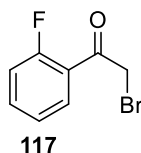


Figure 2.6: 2-Fluorophenacyl bromide (**117**)

2.1.3 Attempted syntheses of heteroarylglyoxals

With an aim of introducing further structural diversity at C2 of the imidazo[1,2-*b*]pyridazine template, the synthesis of heteroarylglyoxals was also attempted (Scheme 2.5). These experiments, summarised in Table 2.4, proved to be ineffective.



Scheme 2.5

Table 2.4: Attempted syntheses of heteroarylglyoxals

Entry number	HetAryl	Conditions
1		48 % HBr in DMSO
2		48 % HBr in DMSO
3		48 % HBr in DMSO
4		CuCl ₂ ·H ₂ O in DMSO
5		CuCl ₂ ·H ₂ O in DMSO
6		SeO ₂ in H ₂ O/dioxane reflux
7		SeO ₂ in H ₂ O/dioxane reflux
8		SeO ₂ in H ₂ O/dioxane reflux
9		SeO ₂ in H ₂ O/dioxane reflux

Initially the HBr/H₂O/DMSO conditions⁵⁸ were employed. In Entry 1, the desired products (the aldehyde and the hydrate) were produced but in the presence of impurities. Chromatographic purification of the crude product was unsuccessful (the components all streaked down the column), so the crude material was taken to the next step of the reaction pathway, resulting in the formation of a complex mixture.

For Entry 2, the crude ¹H NMR spectrum revealed mostly the recovery of starting material. Unknown side-products were also observed, but not the desired product. For Entry 3, only an unknown side-product was isolated. As a result, 48 % HBr in DMSO was deemed ineffective for the synthesis of heteroarylaldehydes.

An alternative oxidant, cupric chloride hydrate in DMSO⁶⁴, was also ineffective; no reaction occurred for 4-acetylpyridine (Entry 4) and with 2-acetylpyrazine (Entry 5) a low yield of a complex crude mixture was obtained.

Selenium dioxide in aqueous dioxane has been utilised to oxidise acetophenones to phenylglyoxals.⁶¹ Using these conditions, 4-acetylpyridine (Entry 6) was converted to isonicotinic acid (**118**) in 66 % yield (Figure 2.7 and 2.8 for ¹H and ¹³C NMR spectra, respectively) indicating oxidative cleavage had occurred.

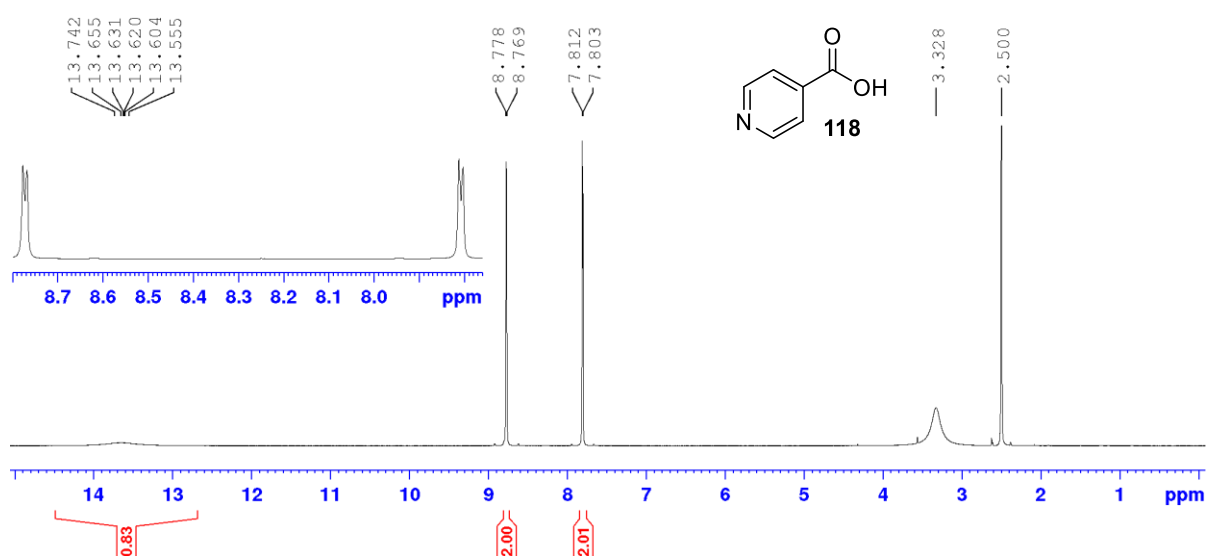


Figure 2.7: ¹H NMR spectrum of **118** in DMSO-*d*₆

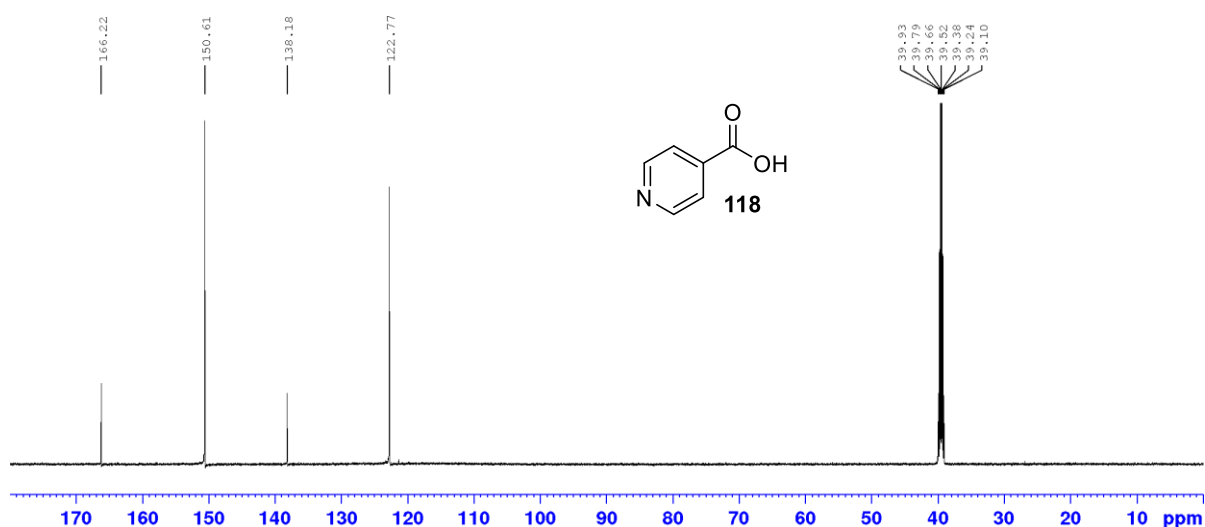


Figure 2.8: ^{13}C NMR spectrum of **118** in $\text{DMSO-}d_6$

Treatment of 2-acetylthiophene with SeO_2 (Entry 7) resulted in the major product being identified as 2-hydroxy-2-(thien-2-yl)acetic acid (**119**, Figure 2.9) by ^1H NMR spectroscopy. Starting material and low amounts of desired product were present. Notably, **119** has been synthesized previously using 2-acetylthiophene, selenium dioxide and aqueous dioxane.⁶⁵ However, Amberlyst 26 was used to catalyse the synthesis of these α -hydroxy-arylacetic acids.⁶⁵ SeO_2 treatment of 2-chloro-5-acetylthiophene (Entry 8) proceeded similarly to Entry 7; hydroxy(5-chloro-thien-2-yl)acetic acid (**120**, Figure 2.9) was the major product along with a minor proportion of desired product. Due to the small amounts of the desired products observed in their respective crude mixtures, purification was not attempted. Interestingly, this phenomenon was observed for the attempted synthesis of **111** using 48 % HBr in DMSO (Table 2.3, Entry 7), suggesting that the production of α -hydroxy-aryl acetic acids is a significant reaction pathway under various oxidation conditions.

For Entry 9, 27 % of starting material was recovered and an unknown side-product was observed.

Chapter 2

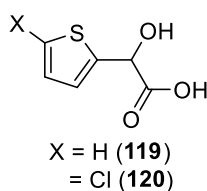


Figure 2.9: Structures of 2-hydroxy-2-(thien-2-yl)acetic acid (**119**) and hydroxy(5-chloro-thien-2-yl)acetic acid (**120**)

It has been reported previously that *N*-heterocyclic methyl ketones cannot be effectively converted to the corresponding glyoxal under these conditions.⁶⁶ For example, 2-acetylpyridine and 2-acetamidoacetophenone were oxidised to their corresponding glyoxylic acids **121** and **122** (Figure 2.10).⁶⁶ Although such products were not observed in our study (Entries 6 to 9), perhaps the corresponding α -hydroxy-arylacetic acids and glyoxylic acids were intermediates to carboxylic acid derivatives, including carboxylic acid **118** which was observed in Entry 6.⁶⁶

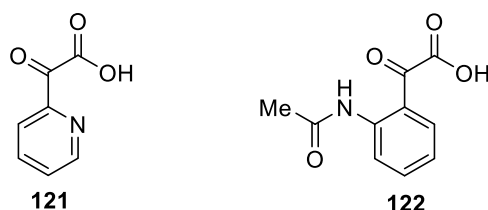
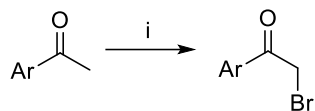


Figure 2.10: Structures of glyoxylic acids **121** and **122**

The attempted heteroaryl glyoxal syntheses using the above conditions were unsuccessful. However for future work, bromomethyl hetero(aryl) ketones could be used as alternative imidazo[1,2-*b*]pyridazine precursors. These precursors can be synthesized conveniently from aromatic methyl ketones and phenyltrimethylammonium tribromide in THF (Scheme 2.6).⁶⁷ The use of phenacyl bromides in synthesizing imidazo[1,2-*b*]pyridazines is shown within this chapter under the heading, “2.2 Synthetic Pathway 2 – 3-substituted-6-aminopyridazine-1-oxides and phenacyl bromides” and later in Chapter 3 under the heading, “3.2 3-Dialkylaminomethyl-imidazo[1,2-*b*]pyridazines”.

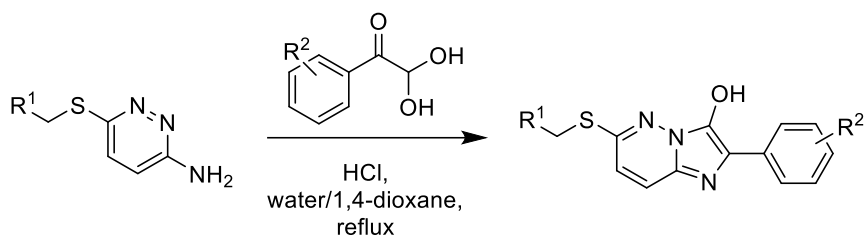


Scheme 2.6: Reagents and conditions: i) phenyltrimethylammonium tribromide, THF, 0 °C to rt, 2.5 – 16 h, 28 % - 100 %⁶⁷

2.1.4 Imidazo[1,2-*b*]pyridazin-3-ol syntheses

Most imidazo[1,2-*b*]pyridazin-3-ol preparations, conducted as outlined in Scheme 2.7 and Table 2.5, worked well, affording moderate to high product yields for compounds **123-139** (56 % - 95 %) except for Entries 18 and 19, which will be discussed below.

Chapter 2

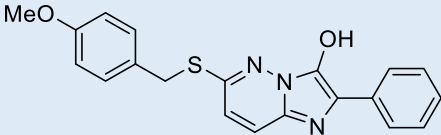
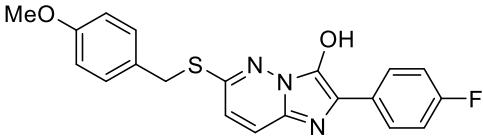
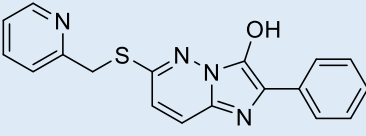
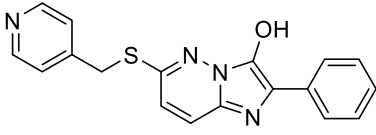
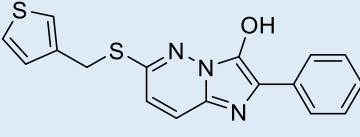
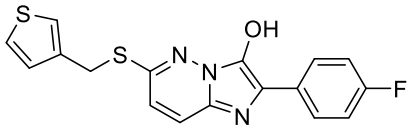
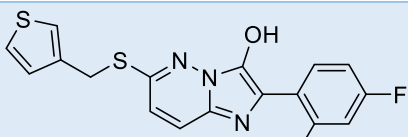
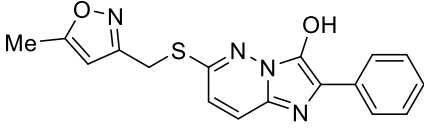
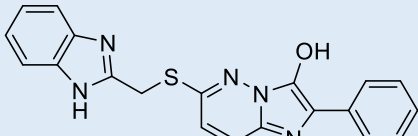


Scheme 2.7

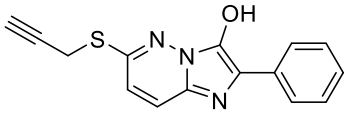
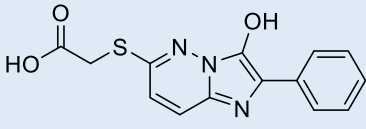
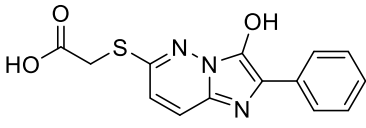
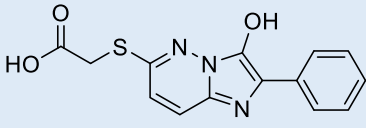
Table 2.5: Syntheses of imidazo[1,2-b]pyridazin-3-ols

Entry	Product structure	Yield (%)
1	<p style="text-align: center;">123</p>	87
2	<p style="text-align: center;">124</p>	80
3	<p style="text-align: center;">125</p>	75
4	<p style="text-align: center;">126</p>	72
5	<p style="text-align: center;">127</p>	70
6	<p style="text-align: center;">128</p>	93

Chapter 2

7	 <p>129</p>	65
8	 <p>130</p>	66
9	 <p>131</p>	86
10	 <p>132</p>	95
11	 <p>133</p>	86
12	 <p>134</p>	62
13	 <p>135</p>	76
14	 <p>136</p>	56
15	 <p>137</p>	79

Chapter 2

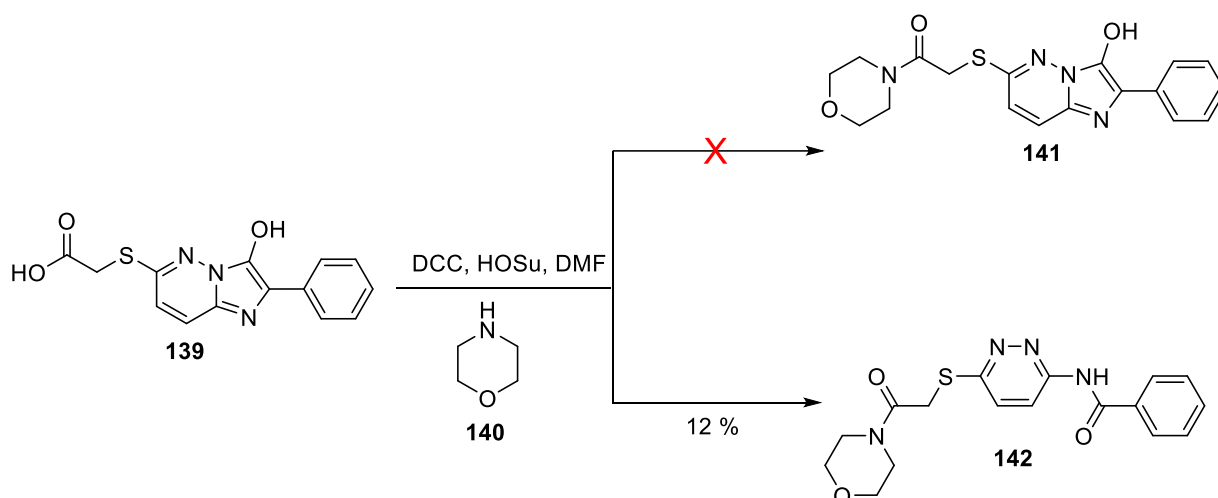
16	 138	84
17 ^a	 139	62
18 ^b	 139	64
19 ^c	 139	69

For Entry 18, instead of producing the desired product, the ethyl ester of **90** was hydrolysed under acidic conditions, affording carboxylic acid **139** in a yield of 64 %, which was similar to that from the reaction where it was the desired product (Entry 17). For Entry 19, the amide moiety of **91** was hydrolysed, also producing carboxylic acid **139** in a yield of 69 %. Interestingly, hydrolysis of 2-((6-aminopyridazin-3-yl)thio)-1-morpholinoethanone (**91**) (Table 2.1, Entry 14) had not occurred in an alkaline medium. Amide coupling was attempted between morpholine (**140**) and **139** using DCC and HOSu (*N*-hydroxysuccinimide) in DMF in order to synthesise 2-phenyl-*N*-(6-((2-morpholino-2-oxoethyl)thio)imidazo[1,2-*b*]pyridazin-3-ol (**141**) (Scheme 2.8). The crude ¹H NMR spectrum revealed a complex mixture, which was chromatographed using a solvent gradient of 5 - 30 % ether/DCM. The desired product was not observed and instead *N*-(6-((2-morpholino-2-oxoethyl)thio)pyridazin-3-yl)benzamide (**142**), resulting from cleavage of the imidazole moiety, was isolated in 12 % yield (Scheme 2.8) (refer to Section 1 of the Appendices for the NMR spectroscopic and LC-MS data). Cleavage of the imidazole moiety occurred on several occasions under a range of conditions and will be discussed in more detail under section 2.2.

^a 2-((6-Aminopyridazin-3-yl)thio)acetic acid (**89**) was used as the pyridazine substrate.

^b Ethyl 2-((6-aminopyridazin-3-yl)thio)acetate (**90**) was used as the pyridazine substrate.

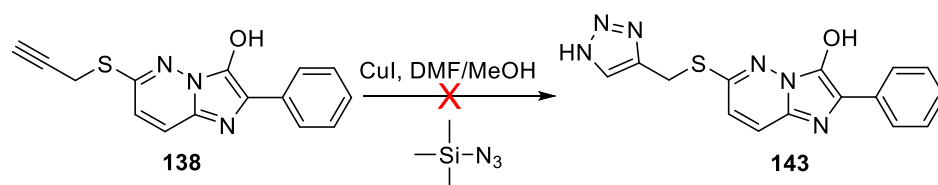
^c 2-((6-Aminopyridazin-3-yl)thio)-1-morpholinoethan-1-one (**91**) was used as the pyridazine substrate.



Scheme 2.8: Synthesis of *N*-(6-((2-morpholino-2-oxoethyl)thio)pyridazin-3-yl)benzamide (**142**)

To avoid amide bond hydrolysis as in Entry 19 (Table 2.5), methane sulfonic acid was used instead of HCl to exclude water from the reaction mixture. However, these conditions produced a low yield of a complex mixture; therefore this approach was not pursued any further.

2-Phenyl-6-(2-propynylthio)imidazo[1,2-*b*]pyridazin-3-ol (**138**) was prepared as a synthetic precursor to 6-(((1*H*-1,2,3-triazol-4-yl)methyl)thio)-2-phenylimidazo[1,2-*b*]pyridazin-3-ol (**143**) via a copper-catalysed [3+2] cycloaddition of the alkyne moiety with trimethylsilyl azide in a DMF/MeOH mixture (Scheme 2.9).⁶⁸ After the reaction mixture was heated at 100 °C for 16.5 hours, THF was added to the cooled mixture at 0 °C resulting in the precipitation of a black solid which was collected via vacuum filtration.



Scheme 2.9: Attempted synthesis of 6-(((1*H*-1,2,3-triazol-4-yl)methyl)thio)-2-phenylimidazo[1,2-*b*]pyridazin-3-ol (**143**)

Chapter 2

The filtrate was extracted with ethyl acetate and the extract was washed with water, dried with sodium sulfate and concentrated under vacuum. A black residue appeared to be a complex mixture by ^1H NMR spectroscopic analysis. The desired product was not present, as indicated by the absence of a CH_2S signal.

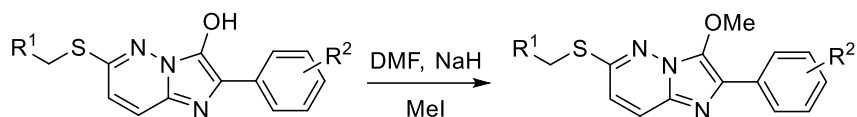
Only 39 mg of organic material was obtained when 100 mg of starting material (**138**) was used. It was thought the 3-hydroxyl substituent on the imidazo[1,2-*b*]pyridazine ring would confer hydrophilicity and lead to loss of material in the aqueous phase. Therefore, changing the order of the synthetic steps was considered. *O*-Methylation of the *S*-propargyl compound **135** would increase lipophilicity. Subsequent conversion of the alkyne to the triazole would ideally increase the amount of crude material extracted into the organic phase. Further details for this synthetic pathway are discussed below.

The ^{13}C NMR spectroscopic data for the imidazo[1,2-*b*]pyridazine-3-ols in Table 2.5 were not obtained due to a lack of intensity of the peaks. However, the structures for the 3-methoxyimidazo[1,2-*b*]pyridazines described below were supported by ^{13}C NMR spectroscopic data which indirectly corroborates the structures of the 3-hydroxyl precursors in Table 2.5.

2.1.5 3-Methoxyimidazo[1,2-*b*]pyridazine syntheses

The *O*-methylation reactions affording the 3-methoxyimidazo[1,2-*b*]pyridazines (**64-66** and **144-160**) generally proceeded well, in yields typically between 30 % and 80 % (Scheme 2.10, Table 2.6). This procedure was discovered by Deborah A. Hughes at CSIRO in 2017 and was an adaption of a protocol reported by Guildford *et al.*⁶⁹ This method, which used methyl iodide, was a safer alternative to Barlin *et al.*'s diazomethane methylation methods.^{70,71} These 3-methoxyimidazo[1,2-*b*]pyridazines generally shared characteristic ¹H NMR spectroscopic signals including two pyridazine CH signals (7.69-7.61 ppm and 6.86-6.77 ppm with *J* = 9.3-9.4 Hz), methylene group signals (4.01-4.80 ppm) and the 3-methoxy signal (3.99-4.15 ppm). Interestingly, fine doublets for the 3-methoxy carbon were observed in the ¹³C NMR spectra when compounds contained a fluorine substitution on the ortho position of the 2-phenyl ring (⁶*J*). These compounds include 3-methoxyimidazo[1,2-*b*]pyridazines **66** and **151**. This phenomenon was observed for other compounds bearing a 3-methoxy and 2-fluoro- or 2,4-difluoro-phenyl group (refer to Chapters 8.5, 8.6 and 8.7 and Appendices section 1).

Chapter 2

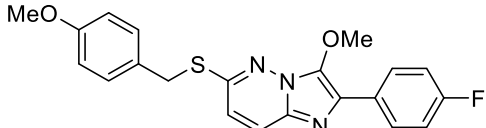
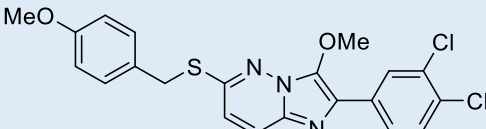
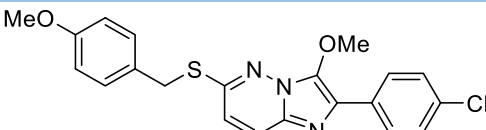
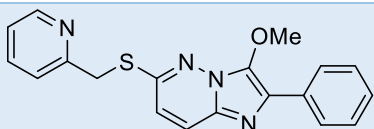
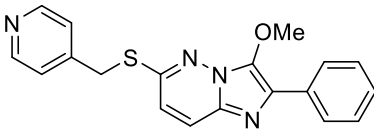
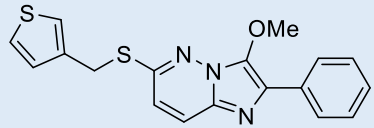
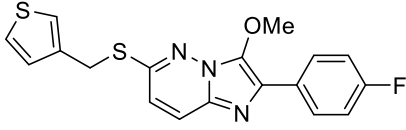
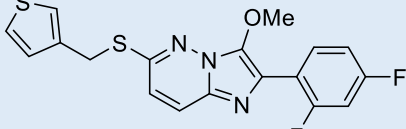
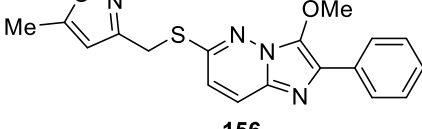


Scheme 2.10

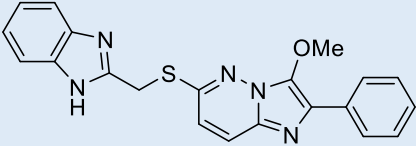
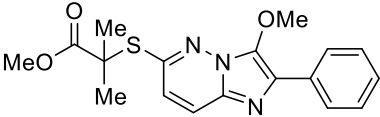
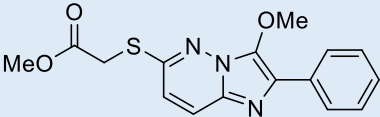
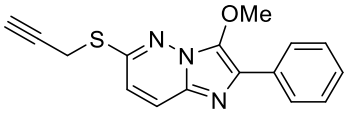
Table 2.6: Syntheses of 3-methoxy-2-phenyl-6-((substituted)methylthio)imidazo[1,2-*b*]pyridazines

Entry	Desired product structure	Yield (%)
1	<p style="text-align: center;">64</p>	31
2	<p style="text-align: center;">65</p>	79
3	<p style="text-align: center;">66</p>	78
4	<p style="text-align: center;">144</p>	75
5	<p style="text-align: center;">145</p>	42
6	<p style="text-align: center;">146</p>	30
7	<p style="text-align: center;">147</p>	80

Chapter 2

8	 <p>148</p>	78
9	 <p>149</p>	66
10	 <p>150</p>	23 (impure)
11	 <p>151</p>	52
12	 <p>152</p>	27
13	 <p>153</p>	54
14	 <p>154</p>	74
15	 <p>155</p>	46
16	 <p>156</p>	57

Chapter 2

17	 <p style="text-align: center;">157</p>	-
18 ^d	 <p style="text-align: center;">158</p>	17
19 ^e	 <p style="text-align: center;">159</p>	-
20	 <p style="text-align: center;">160</p>	-

Side-products were observed for some of the reactions in Table 2.6 above (Entries 7, 8 and 10). These compounds all had very similar ¹H NMR spectra and were discovered to have analogous structures as shown in Figure 2.11 (more details for the discovery of structural elucidation of these compounds are discussed below under section 2.2). The structures were corroborated by High Resolution Mass Spectrometry Atmospheric-pressure chemical ionisation (HRMS-APCI) (refer to Section 2 of the Appendices for the NMR spectroscopic and HRMS data).

^d 6 equivalents of methyl iodide used.

^e 2 equivalents of methyl iodide used.

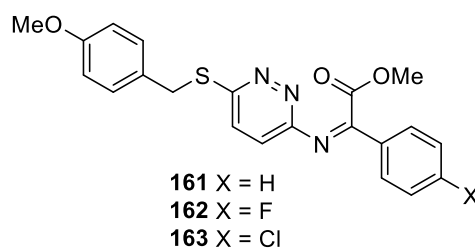


Figure 2.11: Methyl ester side products **161**, **162** and **163** observed in Entries 7, 8 and 10 in Table 2.6, respectively

Another side-product observed in Entry 12 of Table 2.6 was 3-methoxy-6-(methylthio)-2-phenylimidazo[1,2-*b*]pyridazine (**164**) (Figure 2.12) in <5 % yield (impure sample). The structure of this side-product was determined via ^1H NMR spectroscopy; the *S*-methyl and methoxy moieties were responsible for two singlets, integrated for three hydrogen atoms, at 2.67 ppm and 4.17 ppm, respectively and the benzyl peaks were absent while the imidazo[1,2-*b*]pyridazine and 2-phenyl signals remained. Additionally, this ^1H NMR spectrum was consistent with the NMR spectroscopic data Barlin *et al* obtained for this compound.⁷¹ It should be noted there were slight chemical shift differences, presumably caused by the different spectral radiofrequencies used – Barlin *et al* used 90 MHz⁷¹ while we used 600 MHz. Methylthio **164** was not observed for any other *O*-methylation shown in Table 2.6 which prompted the thought that the 4-pyridine moiety may influence the decomposition. Precursor compound 2-phenyl-6-((pyridin-4-ylmethyl)thio)imidazo[1,2-*b*]pyridazin-3-ol (**132**) may have actually been hydrochloride salt **165** (produced from the previous reaction) since the HCl-containing reaction mixture was not neutralised - the 3.39 ppm peak in the ^1H NMR spectrum of precursor **165** (Figure 2.13) may be attributable to the pyridinium ion, which could activate the reaction to produce **164**.

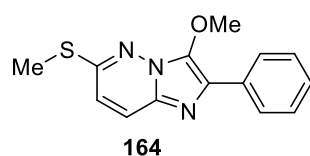


Figure 2.12: 3-methoxy-6-(methylthio)-2-phenylimidazo[1,2-*b*]pyridazine (**164**)

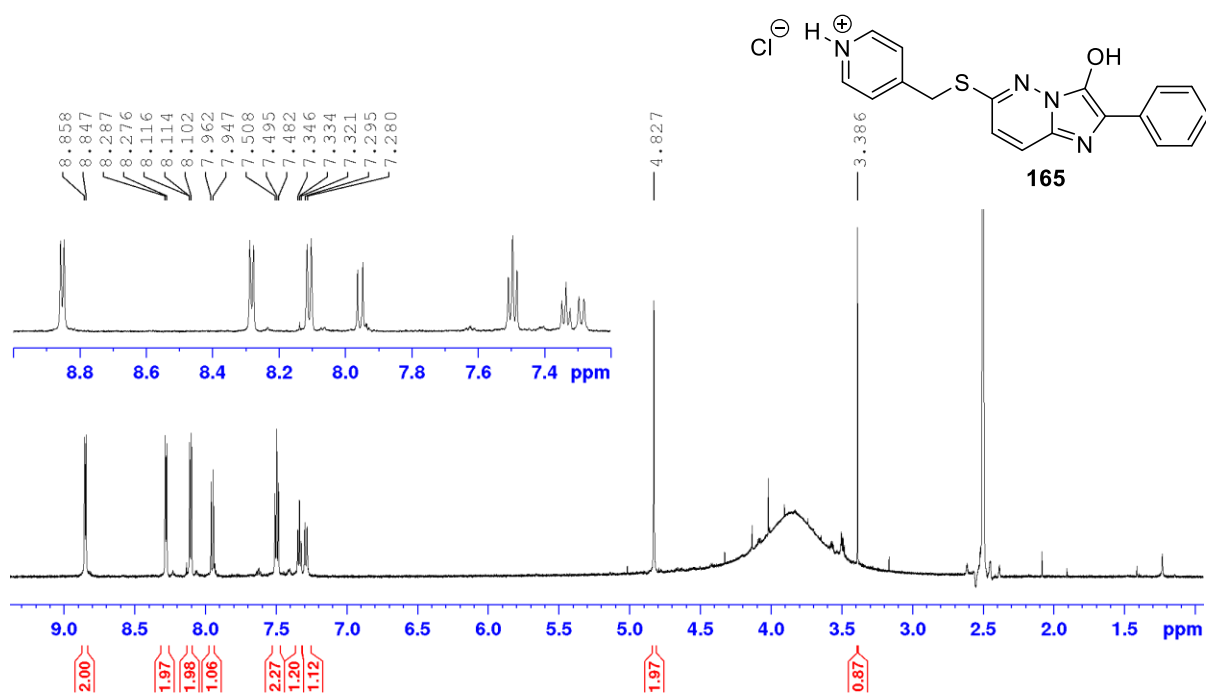
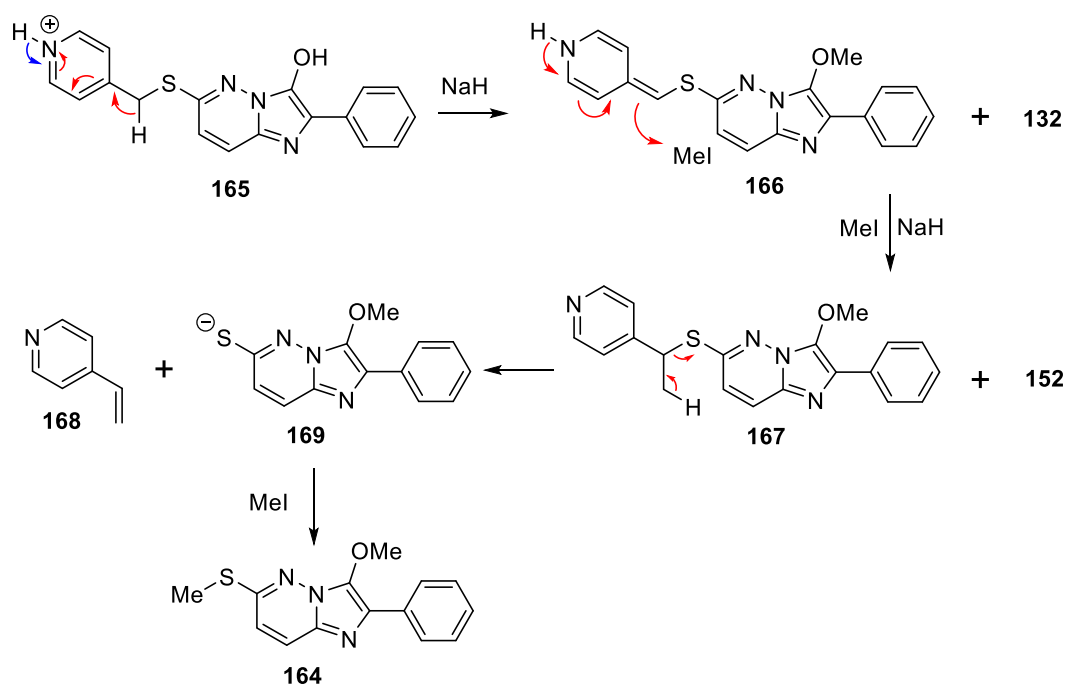


Figure 2.13: ^1H NMR spectrum of hydrochloride salt **165**

A proposed mechanism for the synthesis of **164** is shown in Scheme 2.11. Sodium hydride can either deprotonate the hydrogen atom on the pyridinium moiety of **165** reforming 3-hydroxyl derivative **132** (blue arrow) (which can be methylated to form the desired product **152**) or quaternisation of the pyridyl moiety may increase the acidity of the methylene hydrogen atoms, resulting in the production of **166** (red arrows). The deprotonated methylene now bearing a formal negative charge can nucleophilically attack methyl iodide resulting in **167**. Deprotonation of the methyl hydrogen and cleavage of the carbon-sulfur bond produces 4-vinylpyridine **168** and thiolate **169**. Methylation of the thiolate affords methylthio derivative **164**.



Scheme 2.11: Proposed mechanism for the synthesis of **164**

Some reactions in Table 2.6 required different conditions due to complications using DMF, NaH and MeI. For example, in Entry 17, **170** (which provides indirect evidence for the mechanism proposed in Scheme 2.11) and **171** (Figure 2.14) were produced instead of 6-(((1*H*-benzo[*d*]imidazol-2-yl)methyl)thio)-3-methoxy-2-phenylimidazo[1,2-*b*]pyridazine (**157**). Separation of these compounds via column chromatography was difficult and only **170** (trimethylated product) was recovered in poor purity. Potassium carbonate was used instead of sodium hydride in order to reduce the strength of the base to avoid methylating the CH₂ group and only the mono- and di-methylated imidazo[1,2-*b*]pyridazines were observed (Scheme 2.12). The bis-methylated compound **171** was purified via column chromatography (15 %). The monomethylated product **157** eluted afterwards with impurities present (6 % impure).

Chapter 2

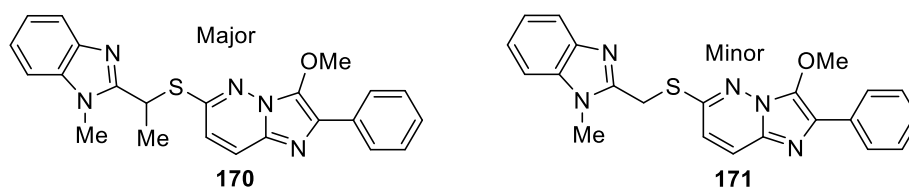
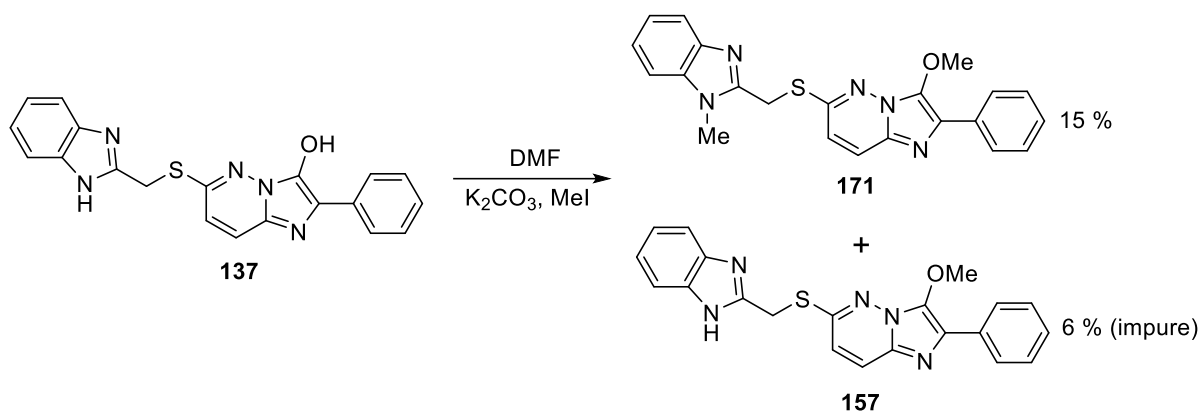


Figure 2.14: Structures of **170** and **171**

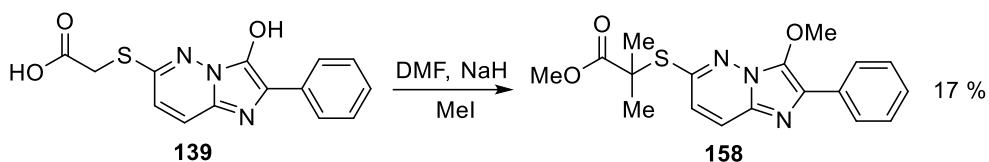


Scheme 2.12: Synthesis of **171** and **157**

An unusual tetra-methylation of carboxylic acid **139** (Entry 18) was thought to have occurred due to the poor solubility of **139** in DMF. Two equivalents of methyl-iodide were used in the reaction, and it was expected that only methylation of the hydroxyl and carboxylate groups would occur (**159**, Entry 19). However, only the tetra-methylated product (**158**) was isolated in low yield. It was believed that once methylation of **139** occurred it was more soluble in the DMF allowing further methylation to afford the tetra-methylated compound. Consequently, this would leave a large proportion of unreacted **139**. The mass recovery from this reaction was poor.

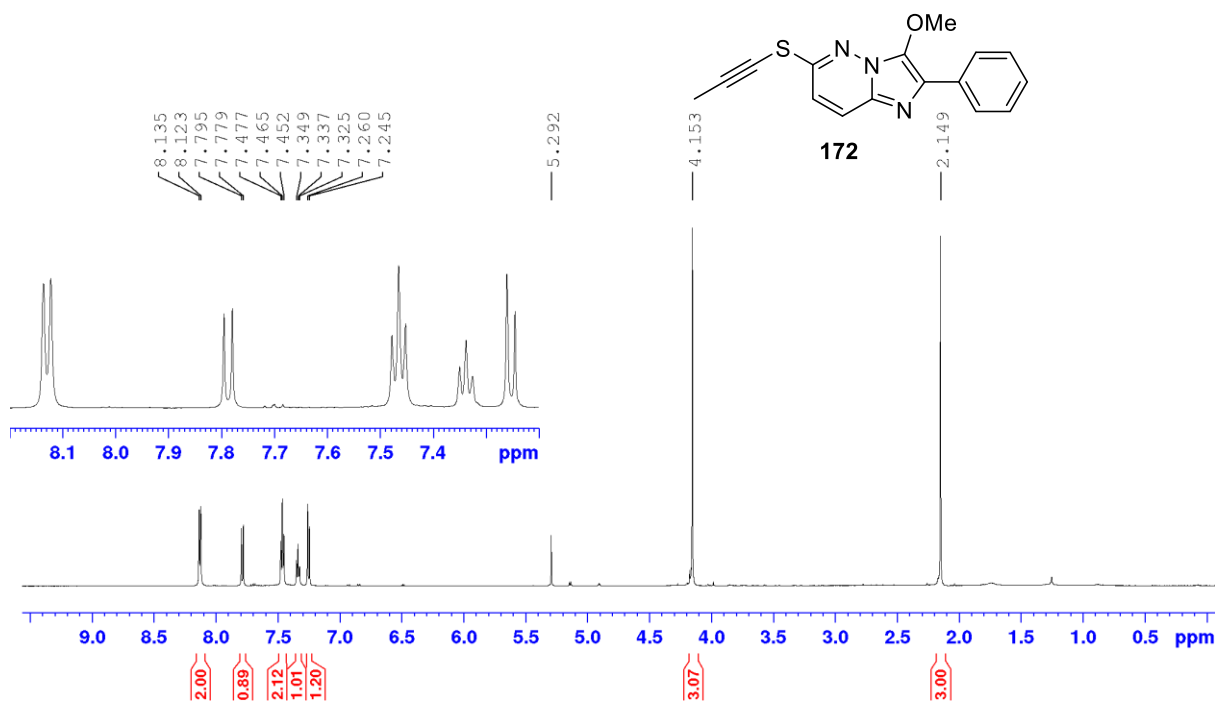
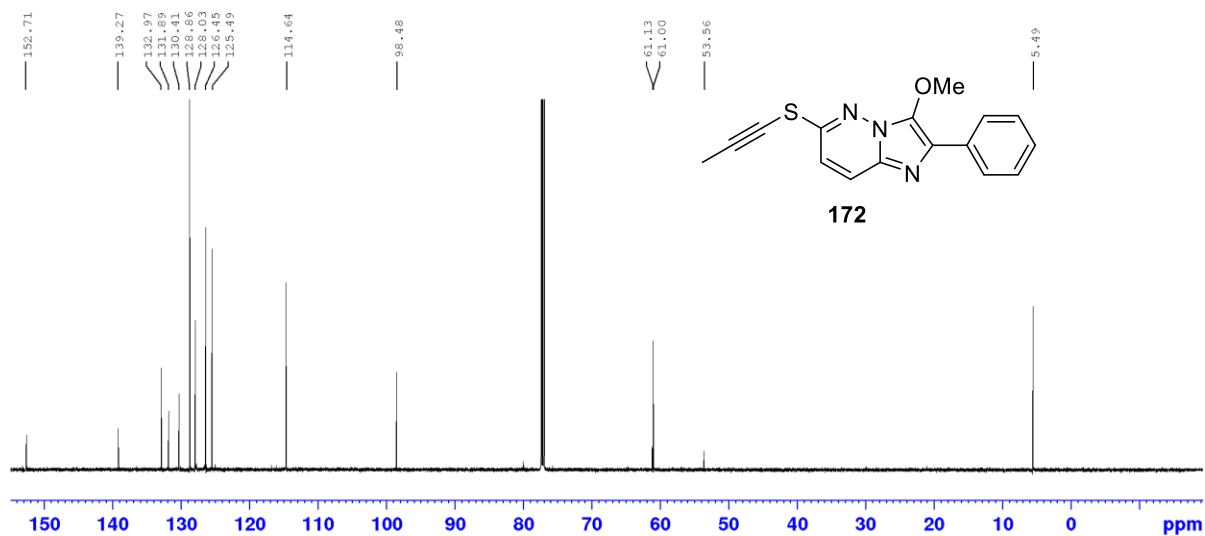
The use of six equivalents of methyl iodide in a similar reaction resulted in an increased mass recovery and allowing a simpler purification, providing **158** in 17 % yield (Entry 18, Scheme 2.13).

Chapter 2



Scheme 2.13: Synthesis of **158** with six equivalents of methyl iodide

Methylation of **138** (Entry 20) afforded 2-phenyl-3-methoxy-6-(1-propynylthio)imidazo[1,2-*b*]pyridazine (**172**) (Figure 2.15 for ^1H NMR spectrum, and Figure 2.16 for ^{13}C NMR spectrum). In the ^1H NMR spectrum the phenyl signals (8.13 ppm, 7.46 ppm, 7.33 ppm), the two imidazo[1,2-*b*]pyridazine signals (7.79 ppm and 7.24 ppm) and the methoxy signal (4.15 ppm) were present plus a methyl peak at 2.14 ppm. There were no signals attributable to the terminal alkyne hydrogen atom or the CH_2S moiety.

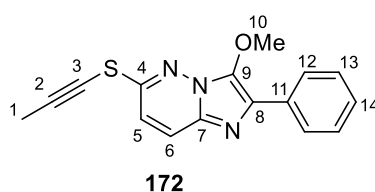
Figure 2.15: ¹H NMR spectrum of compound **172** in CDCl₃Figure 2.16: ¹³C NMR spectrum of compound **172** in CDCl₃

HRMS (APCI) provided a $[M+H]^+ = 296.0855$ (refer to Section 2 of the Appendices for the HRMS data). The formula C₁₆H₁₄N₃OS⁺ has a $m/z = 296.0853$. Accordingly, the formula for the green solid was most likely to be C₁₆H₁₃N₃OS matching the chemical formula for **172**. Analysis of 2D NMR spectroscopic data provided further evidence that the compound was **172** (Table 2.7)

Chapter 2

(refer to Section 2 of the Appendices for the NMR spectroscopic data). However, an unusual HMBC 5-bond correlation was observed between the hydrogen on carbon atom 1 and carbon atom 4. Such HMBC 5-bond correlations have been reported for purines,⁷² 4,4-dimethylantracen-1,9,10(4*H*)-trione, ethyl crotonate and the *Z*-isomer of 3-(4-oxo-4*H*-chromen-3-yl)-acrylic acid ethyl ester.⁷³ The 400 x 100 MHz pulse frequency used for this HMBC experiment appears to allow a correlation between hydrogen 1 and carbon 4 of **172**.

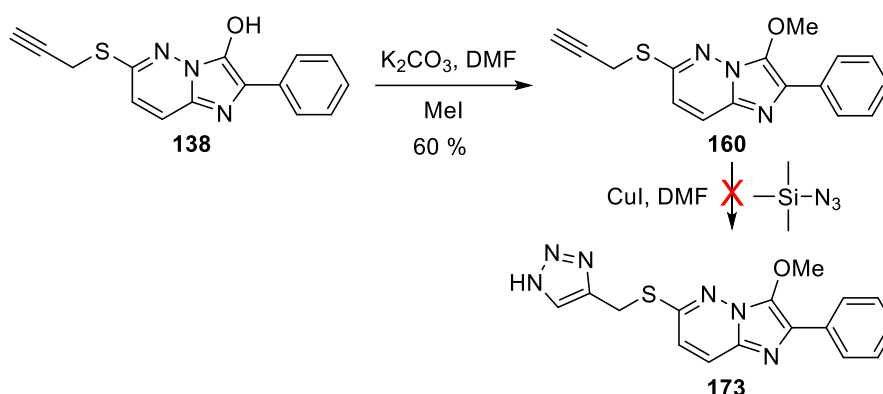
Table 2.7: ¹³C, ¹H and 2D NMR spectroscopic data from **172**



Atom number	¹³ C (ppm)	¹ H (ppm)	COSY atom correlations	HMBC atom correlations
1	5.49	2.15	-	2, 3, 4
2	61.03	-	-	1
3	98.48	-	-	1
4	152.71	-	-	1, 5
5	125.49	7.79	6	4, 7
6	114.64	7.24	5	7
7	131.89	-	-	5
8	130.41	-	-	12
9	139.27	-	-	10
10	61.00	4.15	-	9
11	132.97	-	-	13
12	126.45	8.13	13	8, 14
13	128.86	7.46	12, 14	11, 14
14	128.03	7.33	13	12, 13

The use of potassium carbonate (a weaker base than sodium hydride) was proposed for the *O*-methylation of **138** to avoid the alkyne migration observed in **172** (Scheme 2.14). Sodium hydride was confirmed to be the cause of the alkyne migration, since 3-methoxy-2-phenyl-6-(2-propynylthio)imidazo[1,2-*b*]pyridazine (**160**) was produced in 60 % yield under the conditions outlined in Scheme 2.14.

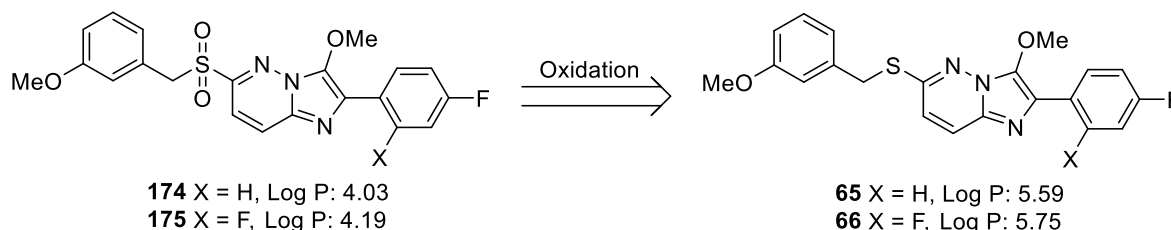
Alkyne **160** was heated at 105 °C with cuprous iodide and trimethylsilyl azide in DMF under a nitrogen atmosphere for 18.5 hours (Scheme 2.14) aiming to affect a cycloaddition reaction to produce triazole **173**. The ¹H NMR spectrum of the crude material indicated a complex mixture. It was unclear if the desired product was present.



Scheme 2.14: Attempted synthesis of 6-(((1H-1,2,3-triazol-4-yl)methyl)thio)-3-methoxy-2-phenylimidazo[1,2-b]pyridazine (**173**)

2.1.6 3-Methoxy-6-((3-methoxybenzyl)sulfonyl)-2-phenylimidazo[1,2-b]pyridazine syntheses

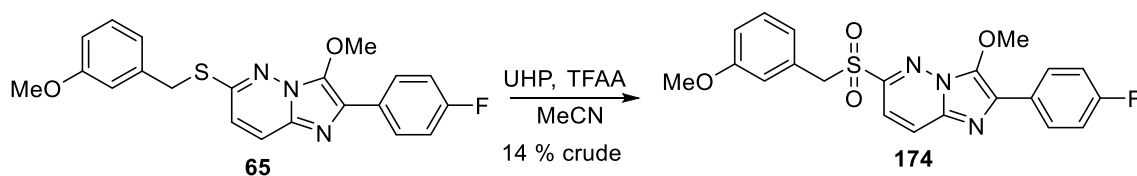
We sought to oxidise the thioether moiety of representative compounds 2-(4-fluorophenyl)-3-methoxy-6-((3-methoxybenzyl)thio)imidazo[1,2-*b*]pyridazine (**65**) and 2-(2,4-difluorophenyl)-3-methoxy-6-((3-methoxybenzyl)thio)imidazo[1,2-*b*]pyridazine (**66**), to the corresponding sulfones (which were considered to be likely metabolites) to observe the effect on the compounds' antitubercular activity and to lower their log P value (Scheme 2.15).



Scheme 2.15: Oxidation of **65** and **66** to **174** and **175**, respectively

Chapter 2

An oxidation procedure was adapted from a protocol reported by Stéphane Caron *et al.*⁶⁰ Thioether **65** was stirred with urea hydrogen peroxide and trifluoroacetic anhydride in acetonitrile at room temperature for 55 minutes and quenched with 1 M sodium bisulfite, which resulted in the synthesis of 2-(4-fluorophenyl)-3-methoxy-6-((3-methoxybenzyl)sulfonyl)imidazo[1,2-*b*]pyridazine (**174**) (Scheme 2.16). In the ¹H NMR spectrum, all signals belonging to the starting material were present but were slightly shifted (Figure 2.17). TLC analysis indicated the reaction went to completion within the first 5 minutes but was stirred for a further 50 minutes. The many side-products observed in the ¹H NMR spectrum of the extract of the filtrate suggested the prolonged reaction time resulted in decomposition of either the desired product or the starting material.



Scheme 2.16: Synthesis of **174**

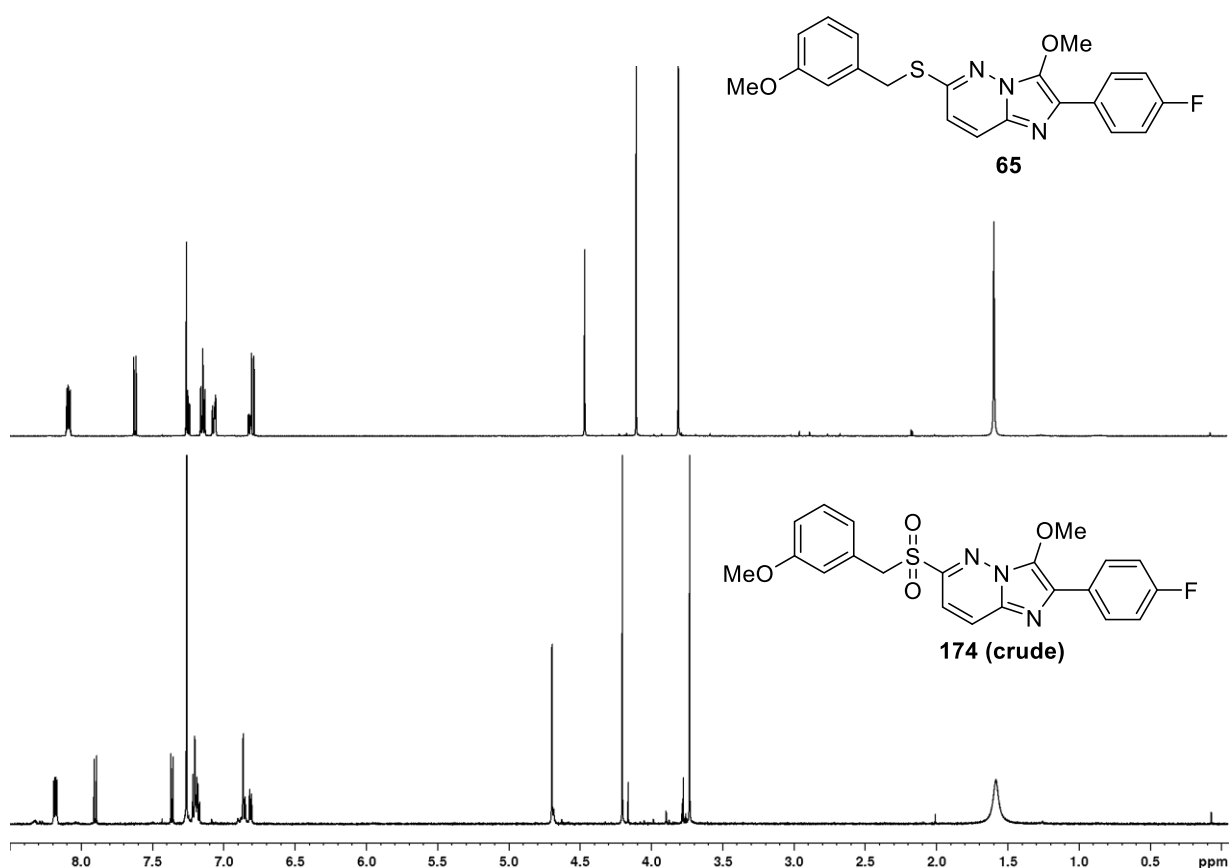
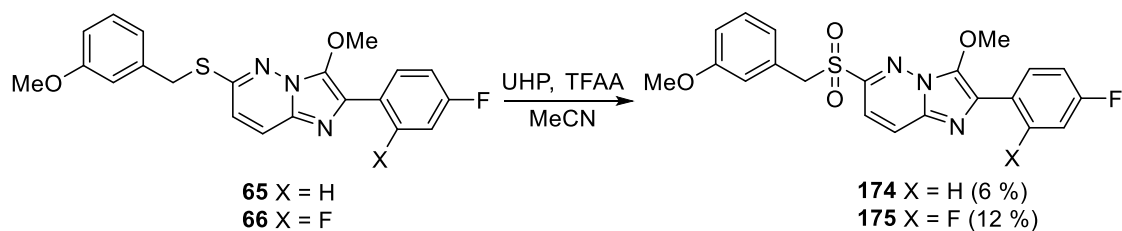


Figure 2.17: Overlay of ¹H NMR spectra of **65** and crude product **174**

To minimise the decomposition and increase the yield of **174**, the reaction was stirred for 12 minutes rather than 55 minutes (Scheme 2.17). However, the formation of a complex mixture was observed by ¹H NMR spectroscopy, indicating the oxidative decomposition process occurs rapidly. Chromatographic purification using DCM as the mobile phase provided impure sulfone **174**. Recrystallisation from a DCM/ether mixture (1:5) resulted in a pure sample of the sulfone **174** (6 % yield), the structure of which was confirmed by LC-MS.

Additionally, 2 side-products eluted from the column before **174** and ¹H, ¹³C, COSY, HSQC and HMBC NMR spectra were used to identify their structures. The compound which eluted first was found to be the known compound, methyl 2-(4-fluorophenyl)-2-oxoacetate (**176**) (Figure 2.18, Figure 2.19 and Table 2.8). The NMR spectroscopic data obtained for this compound was consistent with the literature NMR spectroscopic data.^{74,75} The α -oxoester **176** was obtained in 13 % yield and the proposed mechanism of formation is shown in Scheme 2.18. It

was unknown whether decomposition of starting material **65** and/or oxidation product **174** was responsible for the formation of this ester side-product.



Scheme 2.17: Syntheses of **174** and **175**

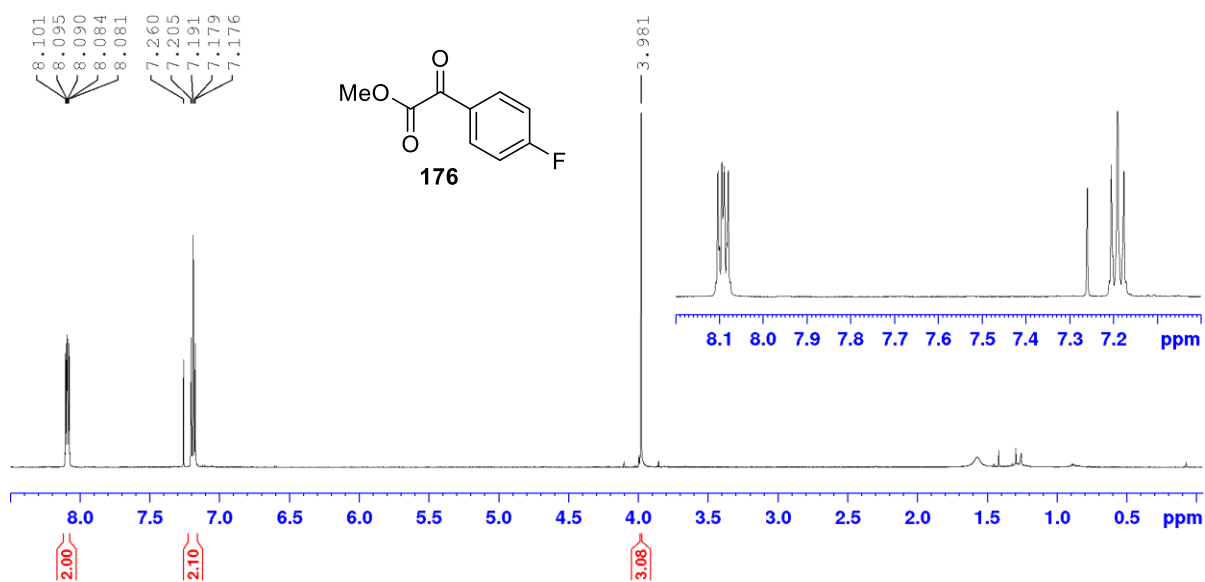


Figure 2.18: ^1H NMR spectrum of side-product **176** in CDCl_3

Chapter 2

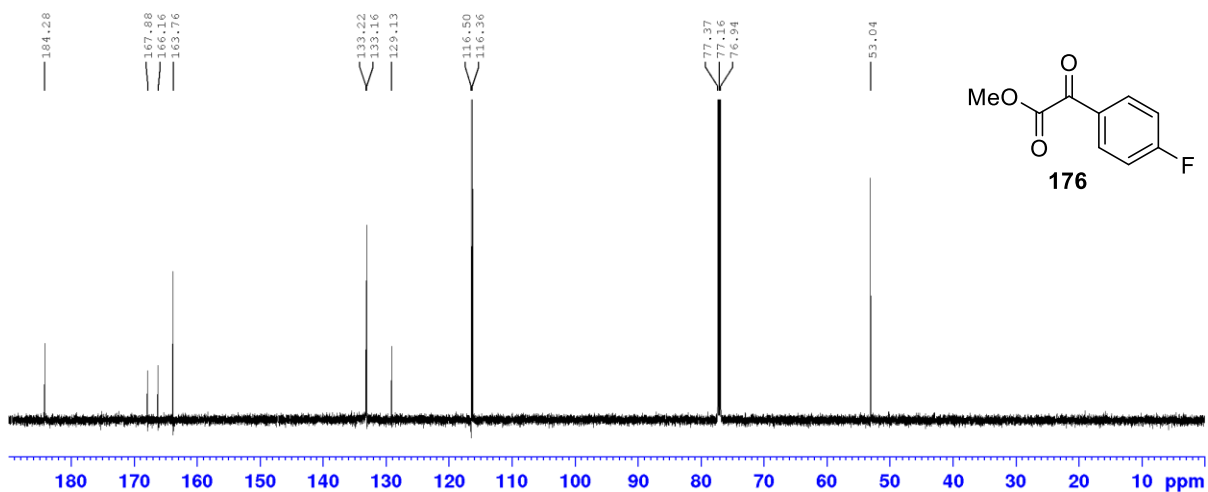
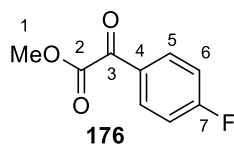
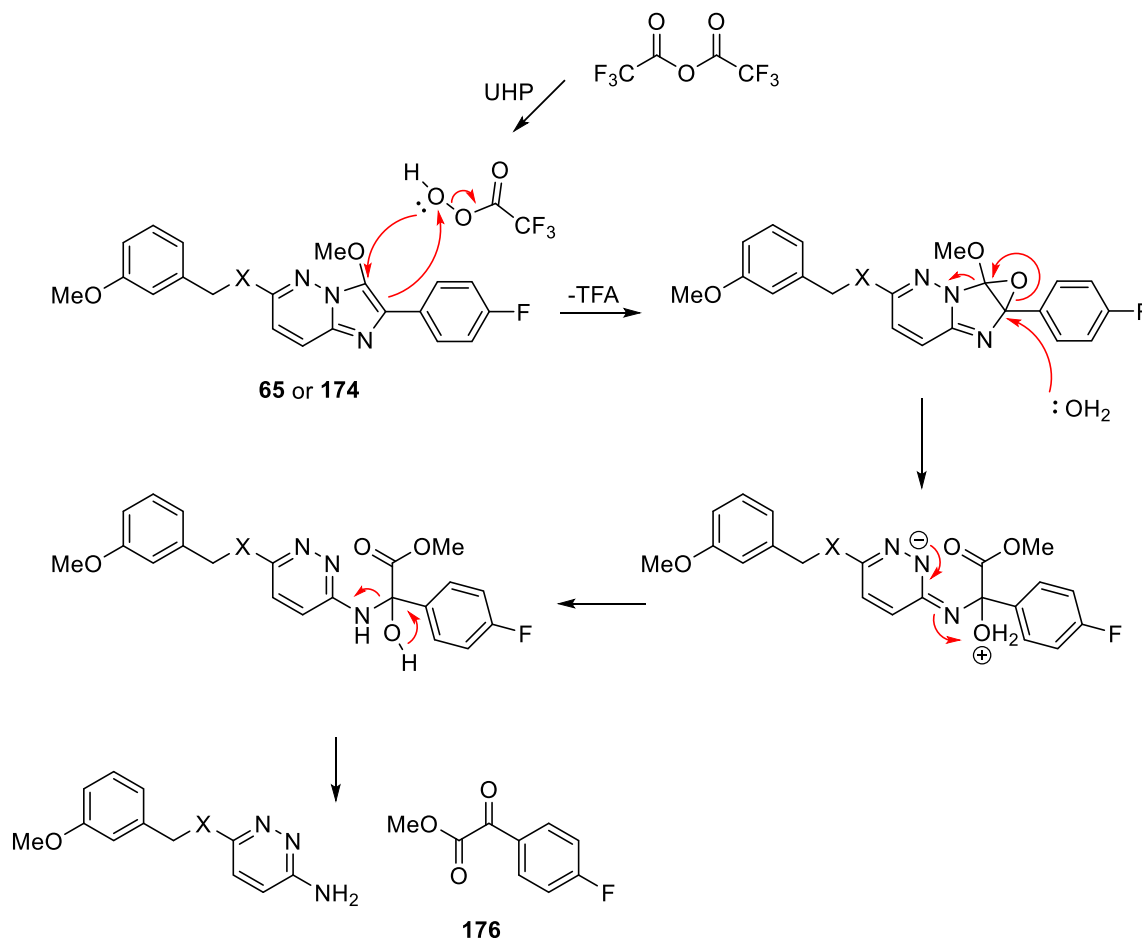


Figure 2.19: ^{13}C NMR spectrum of side-product **176** in CDCl_3

Table 2.8: ^{13}C , ^1H and 2D NMR spectroscopic data from **176**



Atom #	^{13}C (ppm)	^1H (ppm)	COSY (ppm)	HMBC ^{13}C to ^1H (ppm)
1	53.04	3.97	-	-
2	163.76	-	-	3.97
3	184.27	-	-	8.09
4	129.13	-	-	7.18
5	116.43	8.09	7.18	8.09
6	133.19	7.18	8.09	-
7	167.02	-	-	8.09, 7.18



Scheme 2.18: Proposed mechanism for the synthesis of **176** where X = S or SO₂

The second side-product that eluted from the column was determined to be 6-(4-fluorobenzamido)-3-((3-methoxybenzyl)sulfonyl)pyridazine 1-oxide (**177**) which was supported by ¹H (Figure 2.20), ¹³C (Figure 2.21), COSY, HMQC and HMBC NMR spectra (Table 2.9) and HRMS (APCI) (refer to Section 2 of the Appendices for these data). Benzamide **177** was believed to contain a sulfone rather than a thioether linkage due to the chemical shift of the adjacent CH₂ group in the ¹H NMR spectrum (4.67 ppm) resembling the CH₂ chemical shift in the ¹H NMR spectrum of **174** (4.69 ppm) which is considerably downfield from the CH₂ chemical shift of the starting material **65** (4.46 ppm). This structure was supported by HRMS (APCI) since an [M+H]⁺ = 418.0855 peak was found which corresponds to C₁₉H₁₇FN₃O₅S⁺ (calculated [M+H]⁺ = 418.0868). N1, in preference to N2 on the pyridazine ring, was believed to be oxidised since N1 on the pyridazine ring is generally more oxidisable than N2.⁷⁶ An [M+H]⁺ = 402.0920 peak with lower intensity was also found which corresponds to C₁₉H₁₇FN₃O₄S⁺ (calculated [M-O+H]⁺ = 402.0919); benzamide **177** without the oxide moiety.

This compound was likely to form during vaporisation/ionisation.⁷⁷ The largest peak (459.1135) is unknown but could be the result of decomposition/adduct formation of benzamide **177** during ionisation. Benzamide **177** was obtained in 2 % yield. The proposed mechanism shown in Scheme 2.19 has the same mechanistic steps in Scheme 2.24 under section 2.2 (further details of this mechanism are discussed below). However, the major difference between these pathways was the *N*-demethylation shown in Scheme 2.19 due to the presence of hydrogen peroxide. Notably, Do Pham *et al* have reported the *N*-demethylation of tropane alkaloids using hydrogen peroxide and a Fe^{III}-TAML catalyst.⁷⁸ Although no metal catalyst was present under these conditions, oxidation of **178** and loss of formaldehyde from **179** could result in the formation of **180**, which can be oxidised to *N*-oxide **177** (Scheme 2.19).

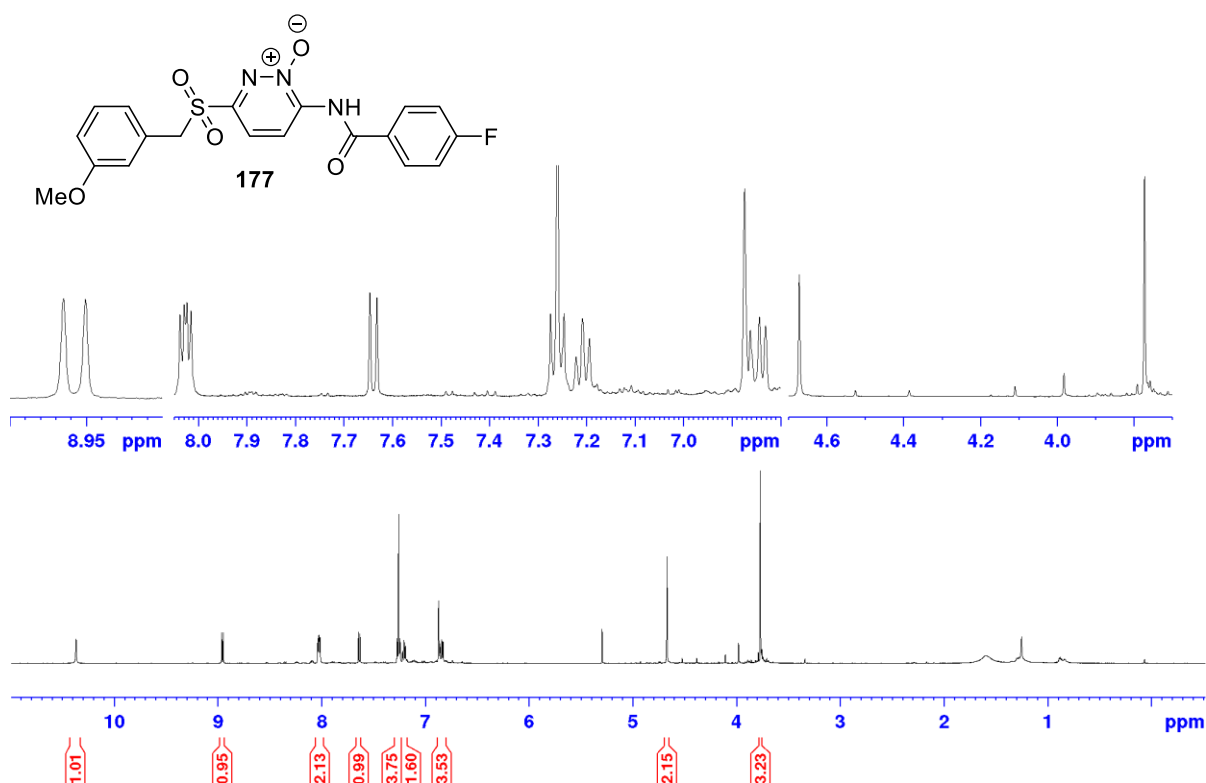


Figure 2.20: ¹H NMR spectrum of **177** in CDCl₃

Chapter 2

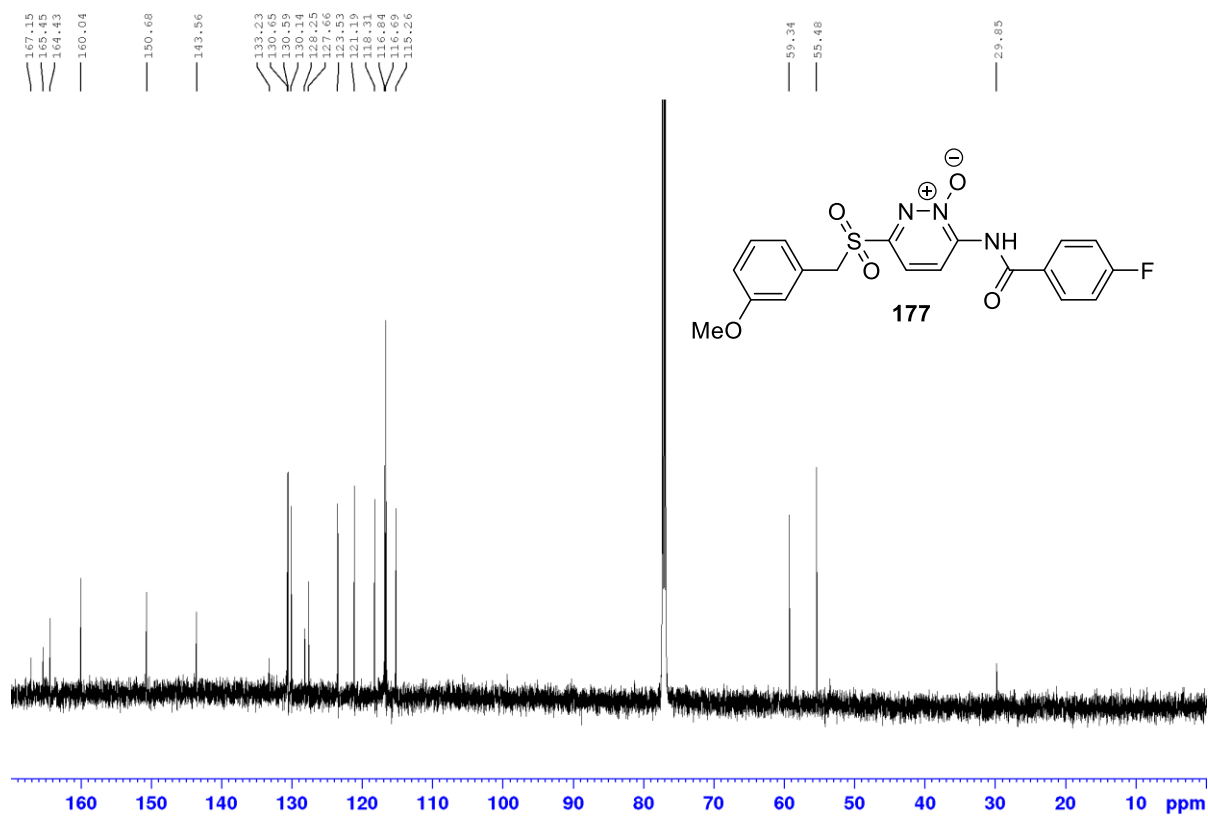
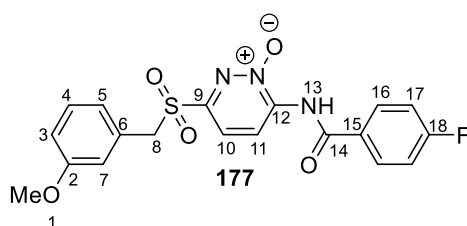


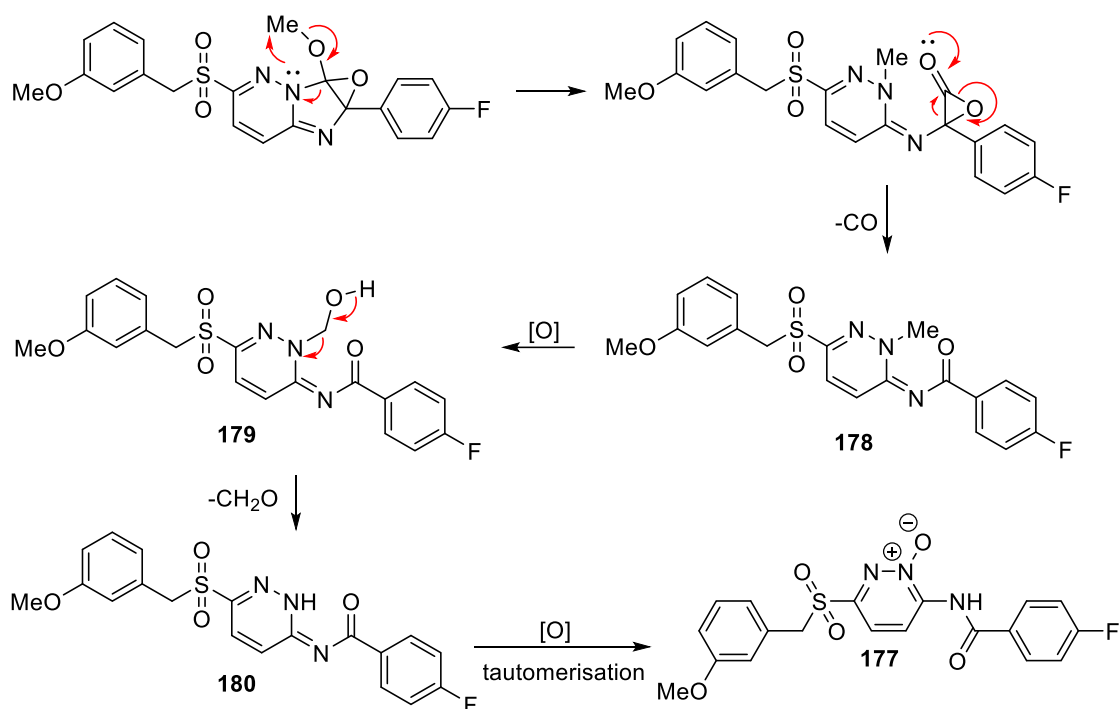
Figure 2.21: ^{13}C NMR spectrum of **177** in CDCl_3

Chapter 2

Table 2.9: ^{13}C , ^1H and 2D NMR spectroscopic data from **177**



Atom #	^{13}C (ppm)	^1H (ppm)	COSY atom correlations (ppm)	HMBC ^{13}C to ^1H atom correlations (ppm)
1	55.48	3.77	-	-
2	160.04	-	-	1, 4
3	115.26	6.86	4	5, 7
4	130.14	7.20	3, 5	-
5	123.53	6.83	4, 8	8
6	127.66	-	-	4, 8
7	116.69	6.87	8	8
8	59.34	4.67	5, 7	5, 7
9	150.68	-	-	10 or 11
10	118.31 or 121.19	7.64 or 8.96	11	13
11	118.31 or 121.19	7.64 or 8.96	10	13
12	143.56	-	-	10 or 11, 13
13	-	10.36	-	14
14	164.43	-	-	16
15	128.25	-	-	17
16	130.62	8.02	17	-
17	116.84	7.26	16	-
18	167.30	-	-	16, 17



Scheme 2.19: Proposed mechanism for the synthesis of **177**

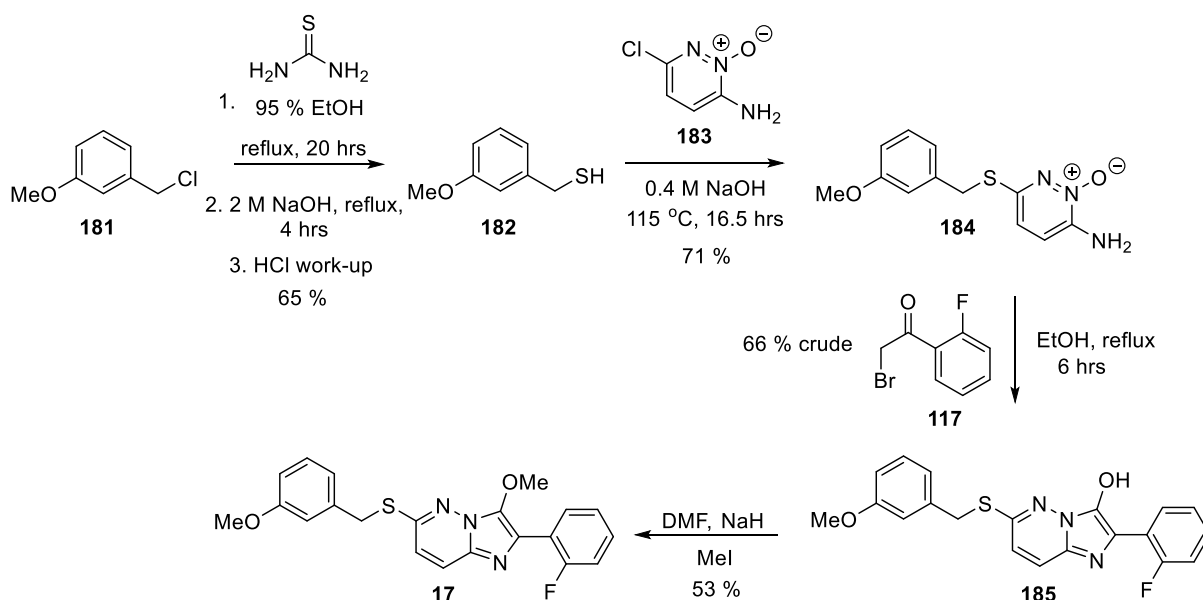
The difluoro compound **66** was treated with the UHP-TFAA oxidation conditions for 10 minutes to oxidise the thioether to the sulfone (Scheme 2.17). The reaction went to completion and the formation of a complex crude mixture was observed by ^1H NMR spectroscopy. The crude material was chromatographed and elution with DCM afforded 2-(2,4-difluorophenyl)-3-methoxy-6-(3-methoxybenzylsulfonyl)imidazo[1,2-*b*]pyridazine (**175**) in 12 % yield.

The complete consumption of the starting material and the formation of a complex mixture leading to a low product yield (observed in the syntheses of **174** and **175**) suggests that these 6-((3-methoxybenzyl)thio(sulfonyl))imidazo[1,2-*b*]pyridazines are generally vulnerable to this particular set of oxidative conditions.

2.2 Synthetic Pathway 2 – 3-substituted-6-aminopyridazine-1-oxides and phenacyl bromides

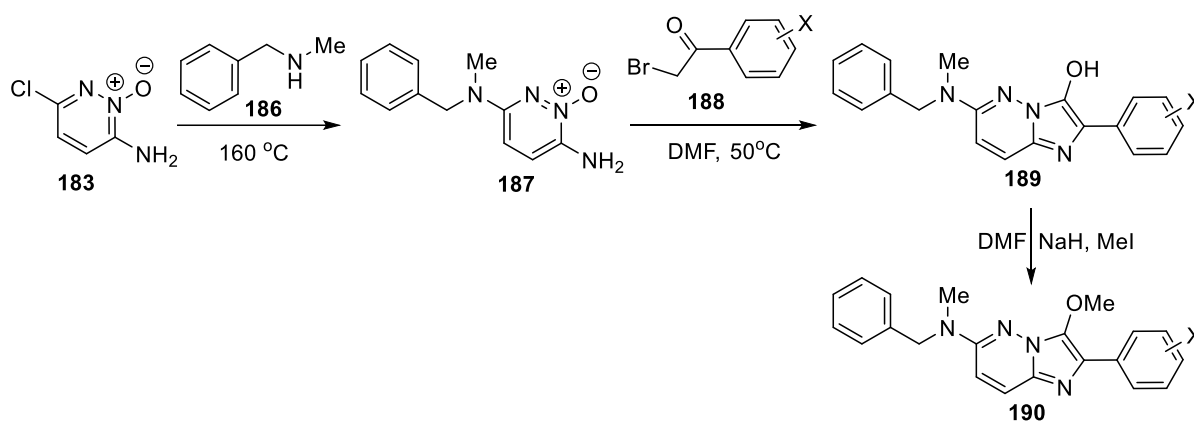
Due to the difficulties experienced in synthesizing 2-fluorophenylglyoxal monohydrate (**112**) a new synthetic pathway not requiring a phenylglyoxal derivative was sought and established. The alternative route outlined in Scheme 2.20 started with thiourea being heated at reflux with 3-methoxybenzyl chloride (**181**) in ethanol for 20 hours.⁷⁹ After the addition of sodium hydroxide, 3-methoxybenzyl thiol (**182**) was produced (65 %).⁷⁹ Thiol **182** was stirred with 6-amino-3-chloropyridazine-1-oxide (**183**) in 0.4 M NaOH at 115 °C in a sealed reaction vessel for 16.5 hours, affording 6-amino-3-((3-methoxybenzyl)thio)pyridazine-1-oxide (**184**) in 71 % yield.⁷⁹ A mixture of amine **184** and 2'-fluorophenacyl bromide (**117**) in ethanol was heated at reflux for 6 hours, producing 2-(2-fluorophenyl)-6-((3-methoxybenzyl)thio)imidazo[1,2-*b*]pyridazin-3-ol (**185**) in 66 % crude yield.⁷⁹

O-Methylation of **185** using sodium hydride and methyl iodide in DMF under a nitrogen atmosphere produced a crude product, which was recrystallized from an ether : hexane (4 : 5) mixture, affording **17** as a golden solid.



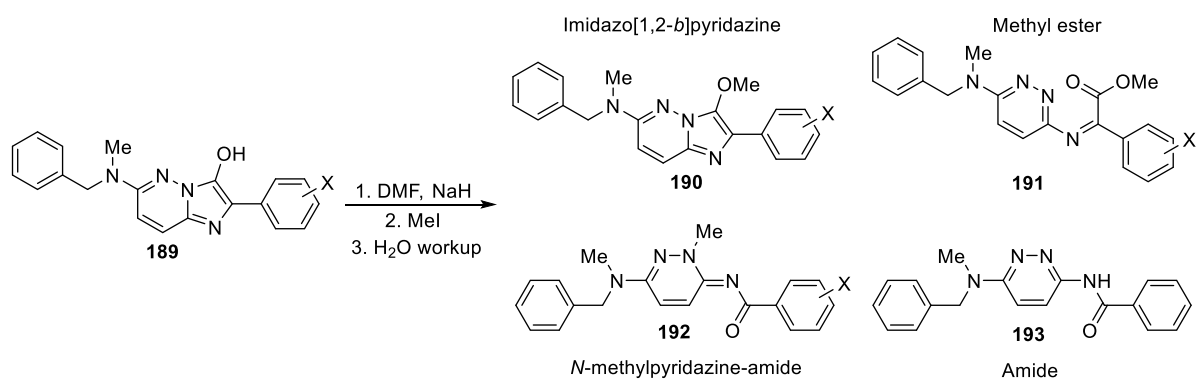
Scheme 2.20: Pathway 2 to synthesis **17**

6-Amino-3-chloropyridazine 1-oxide (**183**) was also utilised as a building block to synthesise imidazo[1,2-*b*]pyridazines with a 6-*N*-methyl linker group instead of a 6-*S* linker group, as outlined in Scheme 2.21. Robin Henches (CSIRO student, 2018) prepared the required hydroxyl precursors by heating 6-amino-3-chloropyridazine 1-oxide (**183**) with *N*-methylbenzylamine (**186**) in a sealed reaction vessel at 160 °C to produce 6-amino-3-(benzyl(methyl)amino)pyridazine 1-oxide (**187**), samples of which were subsequently stirred with different halogen substituted phenacyl bromides (**188**) in DMF at 50 °C to produce the desired 6-(*N*-methylbenzylamino)-2-phenylimidazo[1,2-*b*]pyridazin-3-ols (**189a-g**). These hydroxyl-substituted precursors were *O*-methylated as described previously to provide 3-methoxy-6-(*N*-methylbenzylamino)-2-phenylimidazo[1,2-*b*]pyridazines (**18, 190b-g**). Yields of these reactions were between 30 % and 60 % (Scheme 2.22, Table 2.10).



Scheme 2.21: Synthesis of 3-methoxy-6-(*N*-methylbenzylamino)-2-phenylimidazo[1,2-*b*]pyridazines (**190**)

Chapter 2



Scheme 2.22

Table 2.10: Syntheses of 3-methoxy-6-(*N*-methylbenzylamino)-2-phenylimidazo[1,2-*b*]pyridazines and side-products

Entry	Notation (a-g)	X	Yield of 190 (%)	Yield of 191 (%)	Yield of 192 (%)	Yield of 193 (%)
1	a	H	37	7	2	7
2	b	2-F	41	-	4	-
3	c	4-F	48	3	12	-
4	d	2,4-diF	60	-	-	-
5	e	4-Br	31	5	-	-
6	f	4-Cl	57	-	-	-
7	g	4-CF ₃	37	1	20	-

Low yields of side products (**191 - 193**) for many of the reactions in Table 2.10 were observed (Scheme 2.22). These side-products exhibited very similar ¹H NMR spectra to the desired

Chapter 2

products; all aromatic peaks, the benzylic peak and the two methyl peaks were present (only the chemical shifts were different). For example, Figure 2.22 displays an overlay of the ^1H NMR spectra for compounds observed in the reaction where $\text{R}^1 = \text{H}$ in Table 2.10, Entry 1. Minor impurities were present in some of these samples including residual DCM.

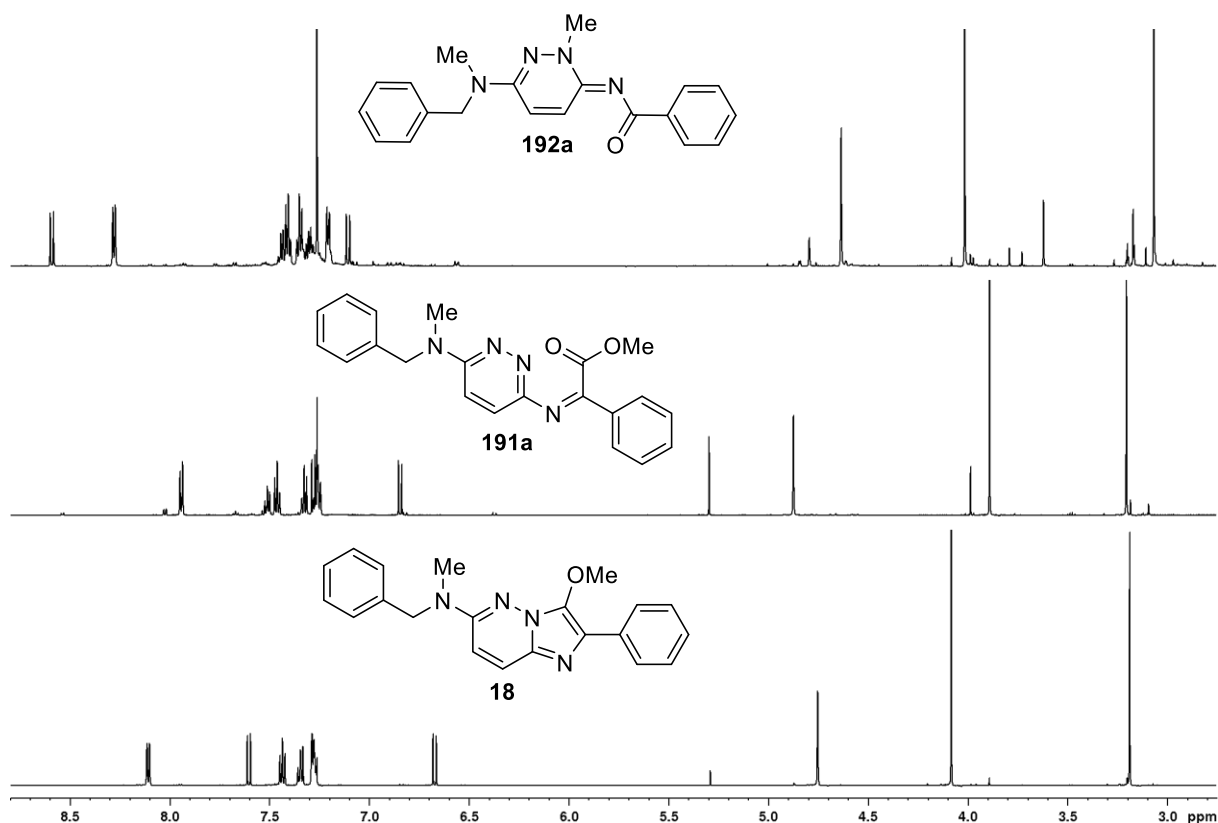


Figure 2.22: Overlay of ^1H NMR spectra of compounds observed from the reaction where $\text{R}^1 = \text{H}$ (Table 2.10, Entry 1)

Further characterization was required to determine which spectrum belonged to the desired product and which spectrum belonged to each side-product. To elucidate the structures of these compounds, three products synthesised from the reaction where $\text{R}^1 = 4\text{-F}$ (Table 2.10, Entry 3) and two products from the reaction where $\text{R}^1 = 4\text{-CF}_3$ (Table 2.10, Entry 7) were crystallised from ether and washed with petrol containing a few drops of ether. The crystals

Chapter 2

were sent to Dr. Craig Forsyth of Monash University (2018) to determine their structures via X-ray Crystallography (Figure 2.23 and 2.24).

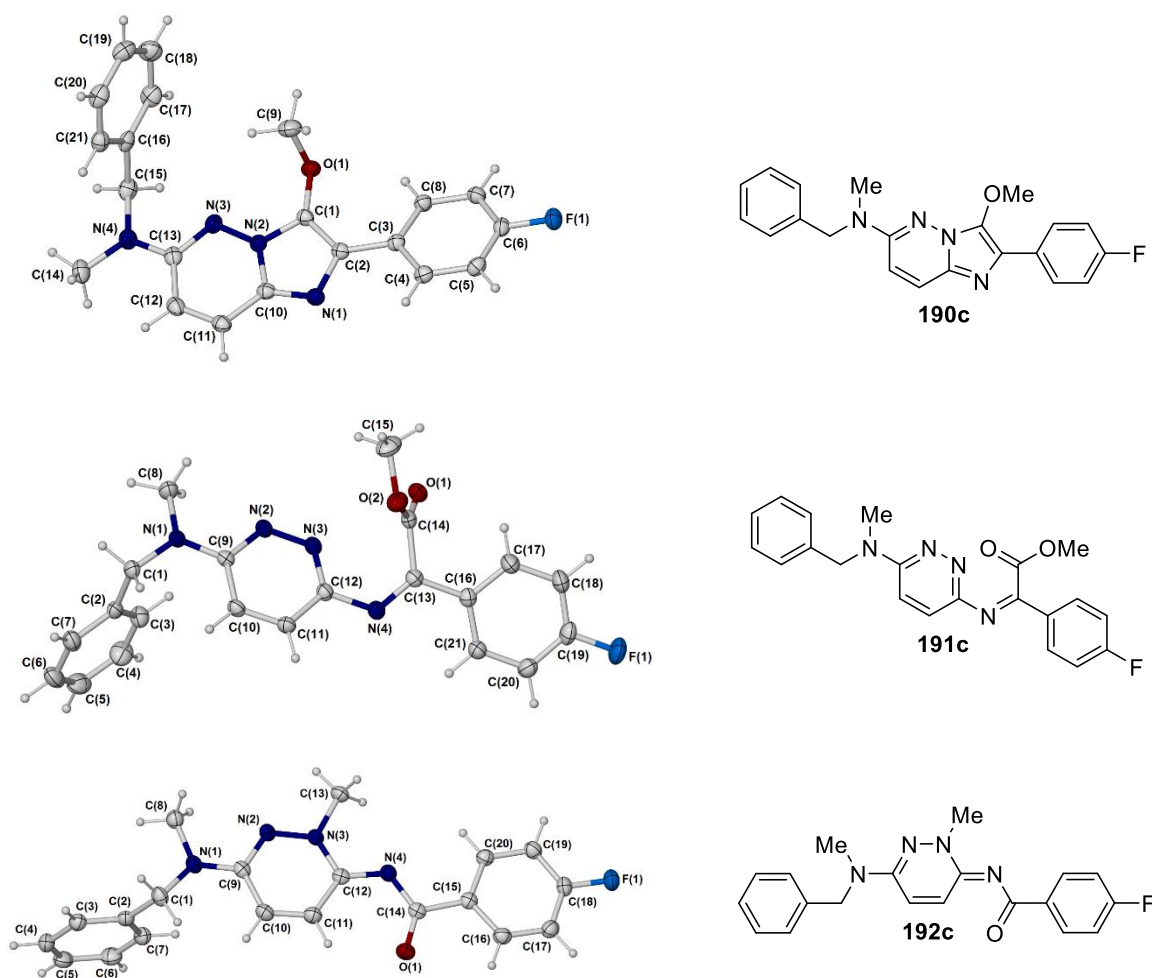


Figure 2.23: ORTEP diagrams of the desired product and side products when $R^1 = 4\text{-F}$ (Table 2.10, Entry 3)

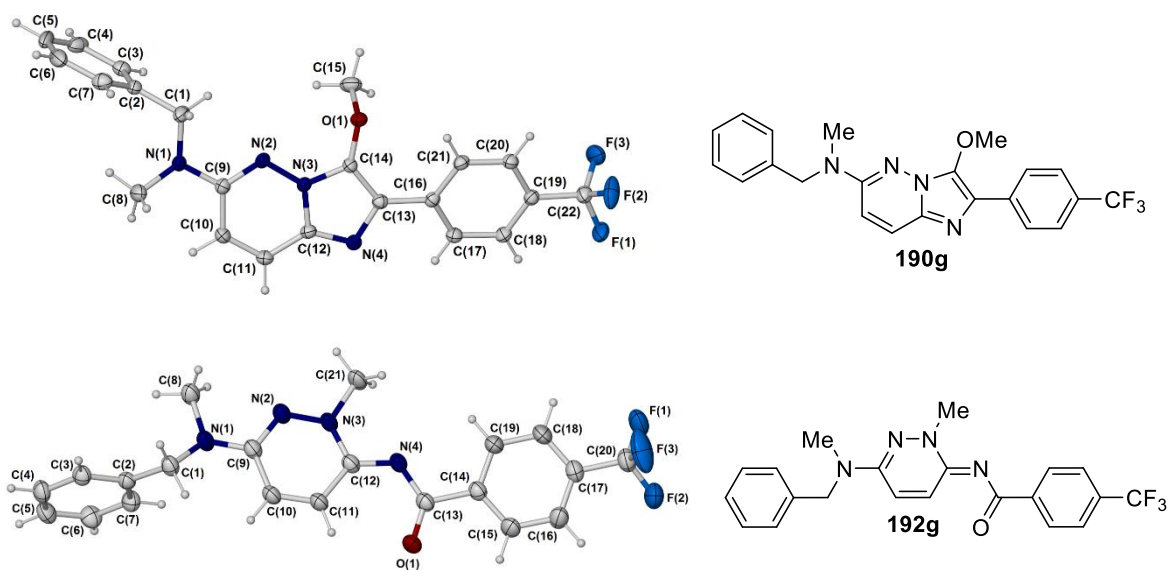


Figure 2.24: ORTEP diagrams of the desired product and side products when $R^1 = 4\text{-CF}_3$
(Table 2.10, Entry 7)

The structures of the other side-products from the remaining reactions in Table 2.10 were determined by a comparison of their ^1H NMR spectra with the spectra of **191c**, **192c** and **192g**. A key characteristic of the ^1H NMR spectra of *N*-methylpyridazine amides **192c** and **192g** was one of the hydrogens on the imidazo[1,2-*b*]pyridazine core structure being significantly further downfield than any signals in the spectra of the other products. Ester **191c** was distinguished from *N*-methylpyridazine amides **192c** and **192g** since the ortho hydrogens on the substituted phenyl ring of **191c** are furthest downfield. Either one of these patterns were observed for all the side-products that were obtained. Therefore, by comparing the ^1H NMR spectra and observing this pattern, the structure of all side-products observed in Table 2.10 were assigned. LC-MS and HRMS data also supported the identity of these structures. Refer to Section 1 and 2 of the Appendices for these ^1H NMR spectroscopic, LC-MS and HRMS data.

The structure of “Amide” side product **193a** (Table 2.10, Entry 1) was determined via ^1H , ^{13}C , COSY, HSQC and HMBC NMR spectroscopy. The HRMS (APCI) spectrum found $[\text{M}+\text{H}^+] = 319.1553$, corresponding to $\text{C}_{19}\text{H}_{19}\text{N}_4\text{O}$ (calculated $[\text{M}+\text{H}]^+ = 319.1554$). Refer to Section 2 of the Appendices for the ^1H NMR spectroscopic and HRMS data.

Chapter 2

The formation of these side-products involved cleavage of the imidazole moiety in either the starting material or the product. In one of the side-products a methyl ester was formed and for the other side-product *N*-methylation of the pyridazine ring occurred along with an amide formation. It was hypothesized that decomposition of the desired product led to the formation of these side-products. This hypothesis was developed based on the formation of the methyl ester side-product. Notably, an extra oxygen atom was inserted into the structure. The only other oxygen containing compound that was introduced into the reaction mixture was water during the work-up of the reaction. It was considered unlikely that the starting material would decompose during the work-up of the reaction forming the carboxylic acid and subsequently become methylated by methyl iodide forming the methyl ester. Under these conditions it is likely that methyl iodide would be quenched by water forming methanol. Instead, it was believed the desired product was decomposed under basic, aqueous conditions.

To test this hypothesis, a control reaction was conducted where 3-methoxy-6-(*N*-methylbenzylamino)-2-(4-(trifluoromethyl)phenyl)imidazo[1,2-*b*]pyridazine (**190g**) was re-subjected to the conditions of its formation. A ~91 % of **190g** was recovered; the *N*-methylpyridazine-amide or methyl ester side-products were observed but at a much lower concentration relative to the reaction conducted in Table 2.10 (Entry 7).

This result suggests that the starting material must be reacting via a different pathway to form these side-products. It was thought that the DMF in the reactions conducted in Table 2.10 may have contained a trace amount of water, resulting in the production of these side-products. The reaction in Entry 7 of Table 2.10 was repeated but with freshly distilled DMF. A ¹H NMR spectra overlay of the crude material from both reactions is shown in Figure 2.25. The bottom ¹H NMR spectrum is the crude product of **190g** which was synthesised with freshly distilled DMF while the top ¹H NMR spectrum is the crude product from the reaction conducted in Entry 7 of Table 2.10. The bottom spectrum appears to be of higher purity than the top spectrum, indicating that the greater water content in the DMF may be causing these side-reactions. Additionally, the peaks that are labelled in the top spectrum belong to *N*-methylpyridazine-amide **192g**. Note, methyl ester **191g** was present in both spectra, but at very low concentrations. *N*-methylpyridazine-amide **192g** was present in the bottom spectrum but only at a very low concentration.

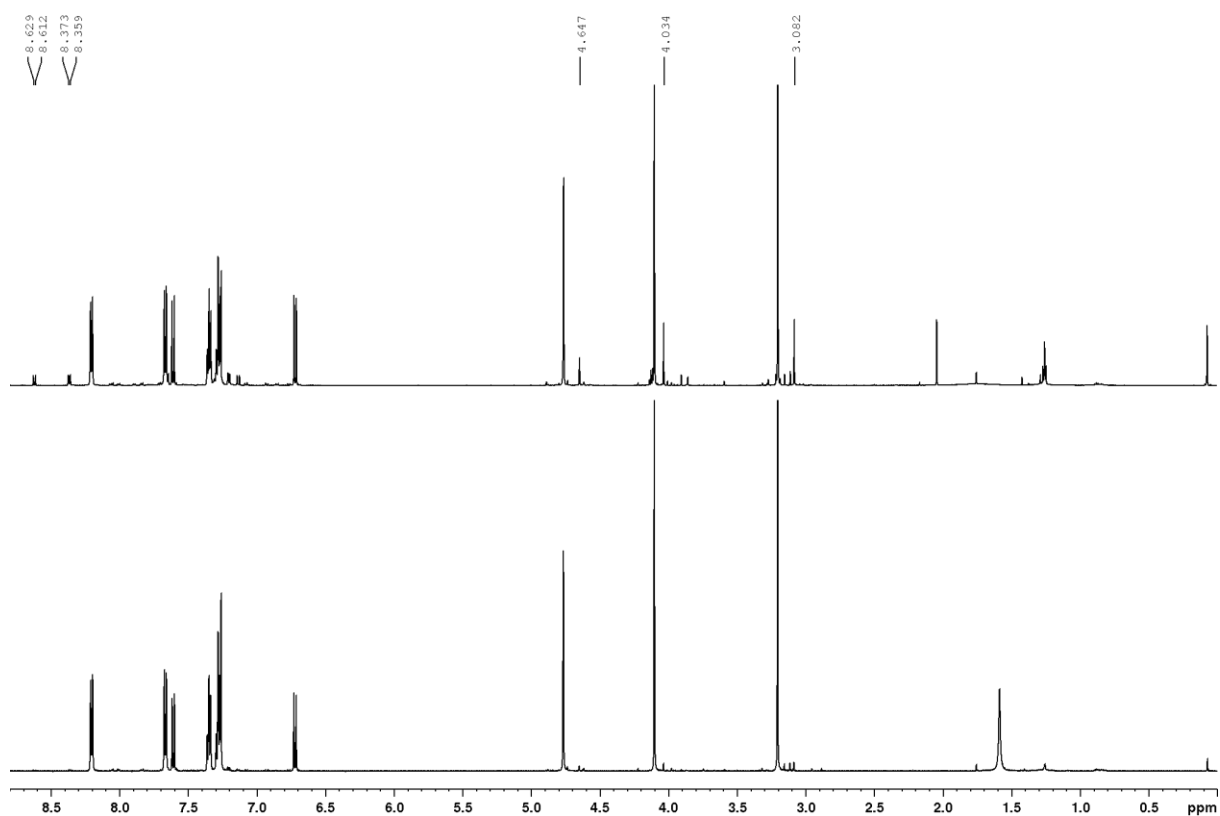
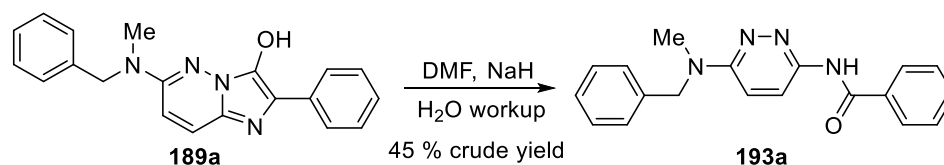


Figure 2.25: Overlay of ^1H NMR spectra of crude **190g**

Separately, the mechanism for the synthesis of amide **193a** was investigated. It was considered likely that this compound was also formed from a side-reaction beginning with the starting material since it was not methylated. 3-Hydroxyimidazopyridazine **189a** was stirred with sodium hydride in DMF for 40 minutes and then quenched with water, resulting in the formation of **193a** with a crude yield of 45 % (Scheme 2.23), directly supporting the hypothesis that the starting material was undergoing these side-reactions. The structure of compound **193a** is similar to compound **192a** but not methylated, indicating that **193a** may be a precursor to *N*-methyl compound **192a**.

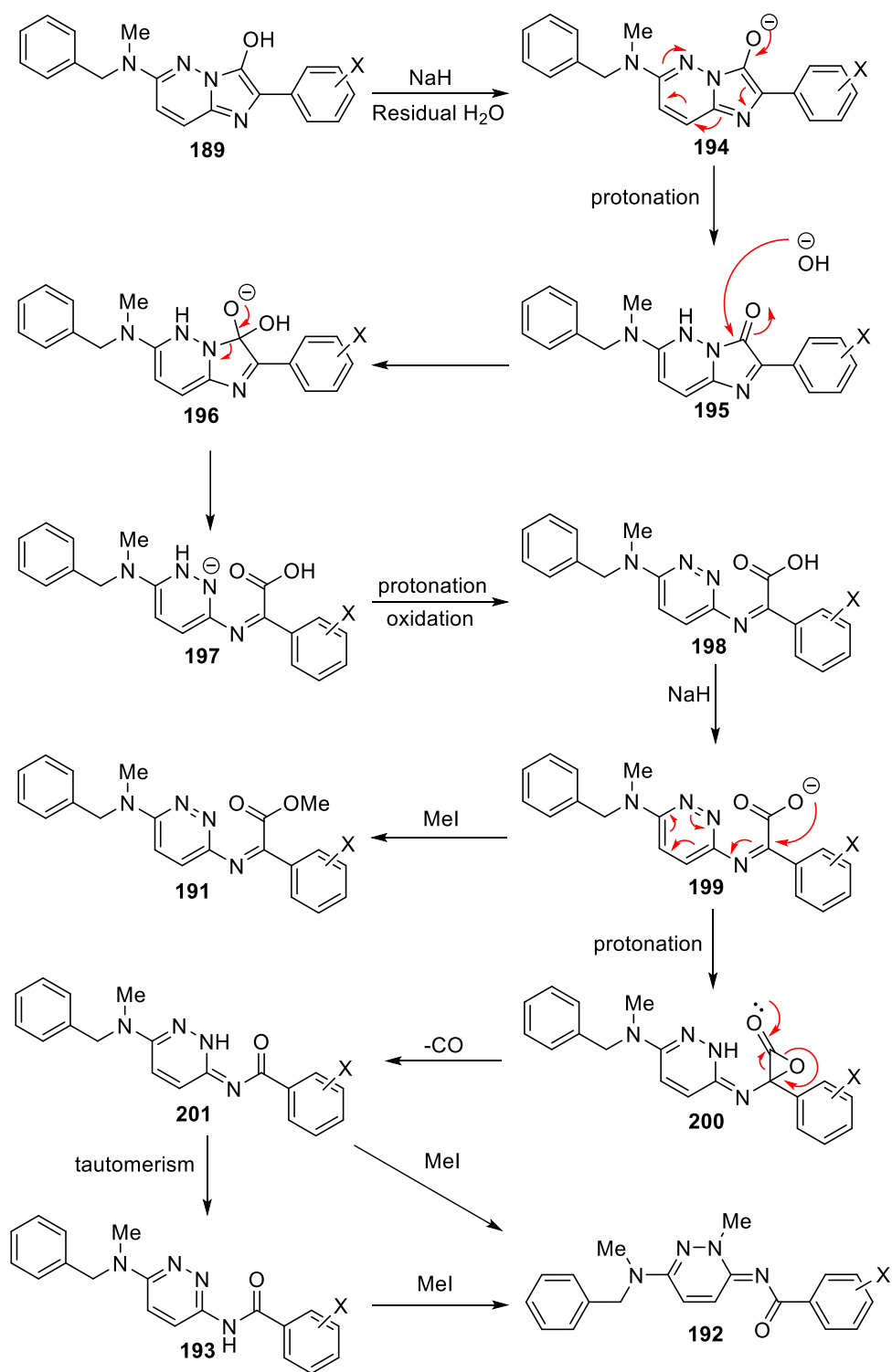
Chapter 2



Scheme 2.23: Synthesis of **193a**

The 3-methoxy group in **190g** (and generally for all imidazo[1,2-*b*]pyridazines) may stabilise the core structure relative to the 3-hydroxyl moiety. Under basic conditions the hydroxyl of **189** can be deprotonated and the resulting anion appears capable of reacting via multiple pathways leading to unstable intermediates as shown for **194** in the proposed mechanism for the formation of these side-products (Scheme 2.24). Protonation of **194** by residual water and hydration of **195** under basic conditions could result in cleavage of the imidazole moiety in **196** forming **197**. Protonation and oxidation of **197** restores the aromaticity of the pyridazine ring, producing carboxylic acid **198** - the oxidant could possibly be dissolved oxygen. Deprotonation of **198** forms carboxylate **199** which could be methylated to afford product **191**. Alternatively, **199** could undergo an intramolecular reaction where the carboxylate attacks the carbon of the "imine" producing lactone intermediate **200**. It appears that carboxylic acid **199** would be unstable under these basic conditions which provides an answer as to why **199** was never isolated. Decarbonylation of strained lactone **200** and tautomerism of **201** leads to the amide product **193** which could be methylated to form the *N*-methylpyridazine amide product **192**. The presumably more thermodynamically stable *E* isomer was isolated.

Chapter 2

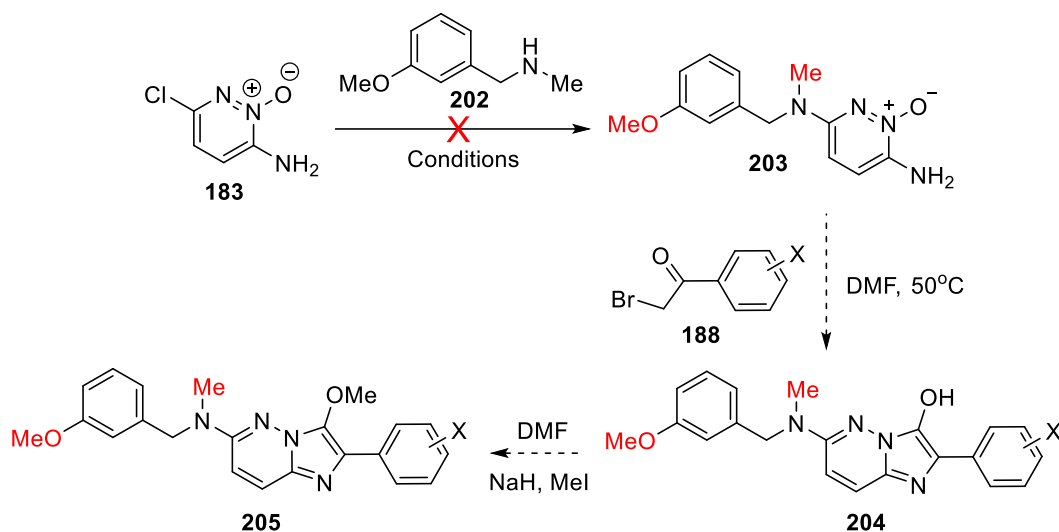


Scheme 2.24: Mechanism for the formations of the methyl ester, amide, and N-methylpyridazine amide side-products

2.3 Attempted syntheses of 6-amino-3-((3-methoxybenzyl)(methyl)amino)pyridazine 1-oxide

The 3-methoxy substituent on the 6-benzyl moiety of the 2-phenyl-3-methoxy-6-((3-methoxybenzyl)thio)imidazo[1,2-*b*]pyridazines generally enhanced the compounds' activity (refer to Chapter 5). Therefore, we sought to introduce this substituent to the 6-benzylamino group of the 3-methoxy-6-(*N*-methylbenzylamino)-2-phenylimidazo[1,2-*b*]pyridazines **190**.

In order to install the 3-methoxy group in the 6-(*N*-methylbenzylamino) group, a nucleophilic aromatic substitution reaction between 6-amino-3-chloropyridazine 1-oxide (**183**) and 1-(3-methoxyphenyl)-*N*-methylmethanamine (**202**) was required to produce 6-amino-3-((3-methoxybenzyl)(methyl)amino)pyridazine 1-oxide (**203**) (Scheme 2.25). Ideally, the conditions used for the synthesis of **187** (Scheme 2.21) could be replicated for the synthesis of **203** (Scheme 2.25). Amine **186** (Scheme 2.21) was used as both solvent and substrate since it was a cheap starting material; the 3-methoxy derivative **202** was more expensive. Consequently, it made economic sense to use **202** only in (near) stoichiometric amounts. This prompted a search for new reaction conditions.

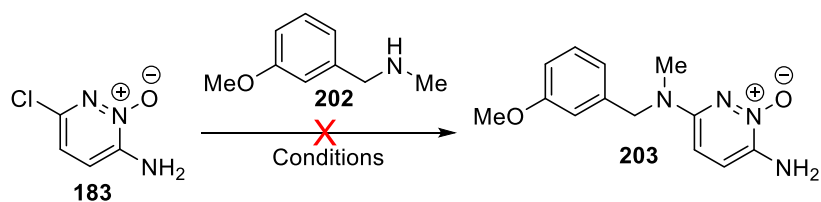


Scheme 2.25: Synthetic pathway for 3-methoxy-6-((3-methoxybenzyl)(methyl)amino)-2-phenylimidazo[1,2-*b*]pyridazines **205**

Chapter 2

Six sets of reaction conditions were trialled in attempts to synthesise **203** but all trials were unsuccessful (Scheme 2.26, Table 2.11). For Entry 1, a mixture of **183** and **202** was heated at 130 °C in 1.2 M NaOH solution in a sealed reaction vessel for 17 hours. 83 % of **202** was recovered and the desired product was not observed. For Entry 2, pyridine was employed both as a solvent and a base. A small amount of water was also added to improve the solubility of **183**. The reaction mixture was heated at reflux for a total of 17 hours. Pyridazine **183** (71 %) precipitated from solution indicating the reaction failed. For Entry 3, a mixture of **183** and **202** was heated at 135 °C in DMF in a sealed reaction vessel for 17 hours but the desired product was not observed. Instead, 37 % of **183** was recovered and *N*-(3-methoxybenzyl)-*N*-methylformamide (**206**) was produced (30 %). At this high temperature and pressure the carbonyl group of DMF was susceptible to nucleophilic attack by the amine of **202** resulting in the production of formamide **206**. The ¹H NMR spectrum (Figure 2.26) and the ¹³C NMR spectrum (Figure 2.27) of **206** each show 2 sets of signals, presumably due to the delocalisation of the electrons in the formamide bond and the presence of the *cis*-oid and *trans*-oid forms.

Chapter 2



Scheme 2.26

Table 2.11: Attempted syntheses of **203**

Entry	Conditions	Recovery of 183 (pyridazine) (%)	Recovery of 202 (amine) (%)	Yield of 203 (%)	Side-product structure and yield
1	1.5 eq of 207 , 1.2 M NaOH, 130 °C, sealed reaction vessel, 17 hrs	-	83	0	None
2	1.3 eq of 207 , aqueous pyridine, reflux, 17 hrs	71	-	0	None
3	1.5 eq of 207 , DMF, 135 °C, sealed reaction vessel, 17 h	37	-	0	 30 % 206
4	1.5 eq of 207 , DMSO, 125 °C, 5 mins, 150 W, microwave	-	77 (impure)	0	None
5	1.5 eq of 207 , water, 125 °C, 10 mins, 150 W, microwave	33	84	0	None
6	1.5 eq of 207 , 1.1 NaOH, 170 °C, 30 mins, 150 W, microwave	0	100	0	 207

Chapter 2

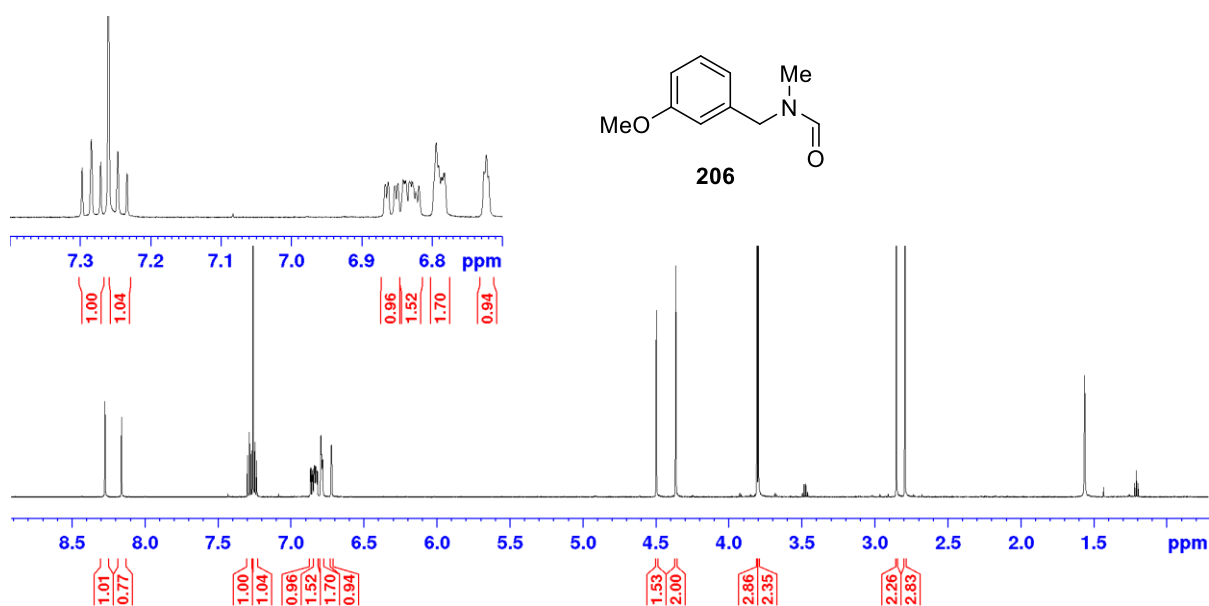


Figure 2.26: ^1H NMR spectrum of **206** in CDCl_3

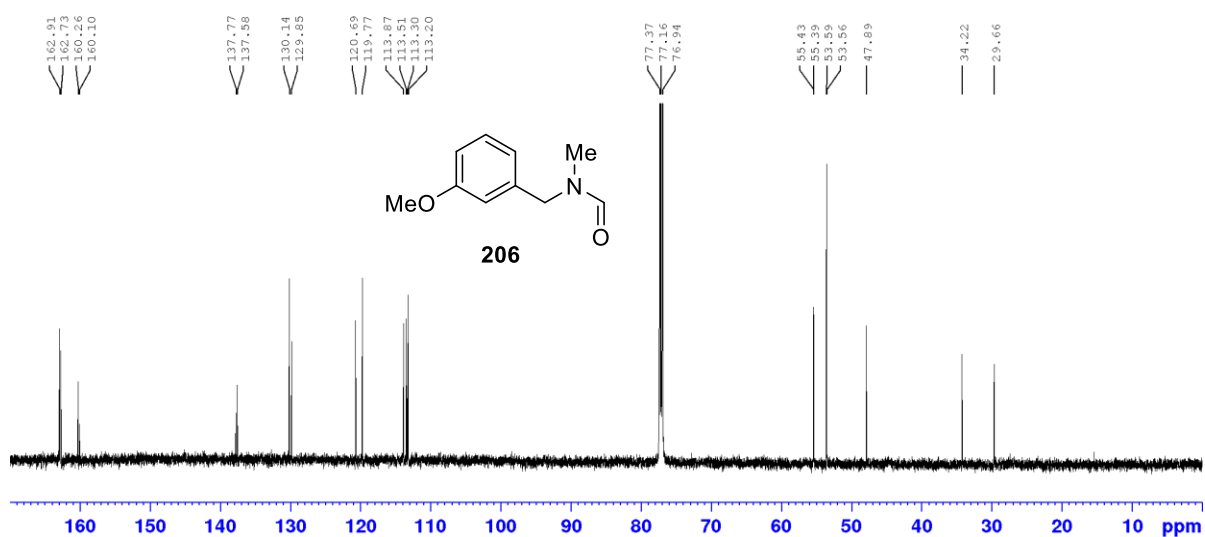
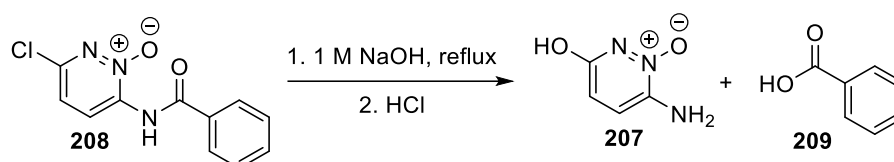


Figure 2.27: ^{13}C NMR spectrum of **206** in CDCl_3

For Entries 4-6 a microwave reactor was utilized. For Entry 4 a mixture of the two reactants was heated in DMSO at 125 °C at 150 W for 5 minutes. No desired product was observed and 77 % of impure **202** was recovered. This method was repeated but water was used as the solvent and the reaction was heated for 10 minutes but recovery of both starting materials was observed (Table 2.11, Entry 5). These results suggested that a base was necessary to deprotonate the amine to increase its nucleophilicity. For Entry 6, the mixture of reactants in

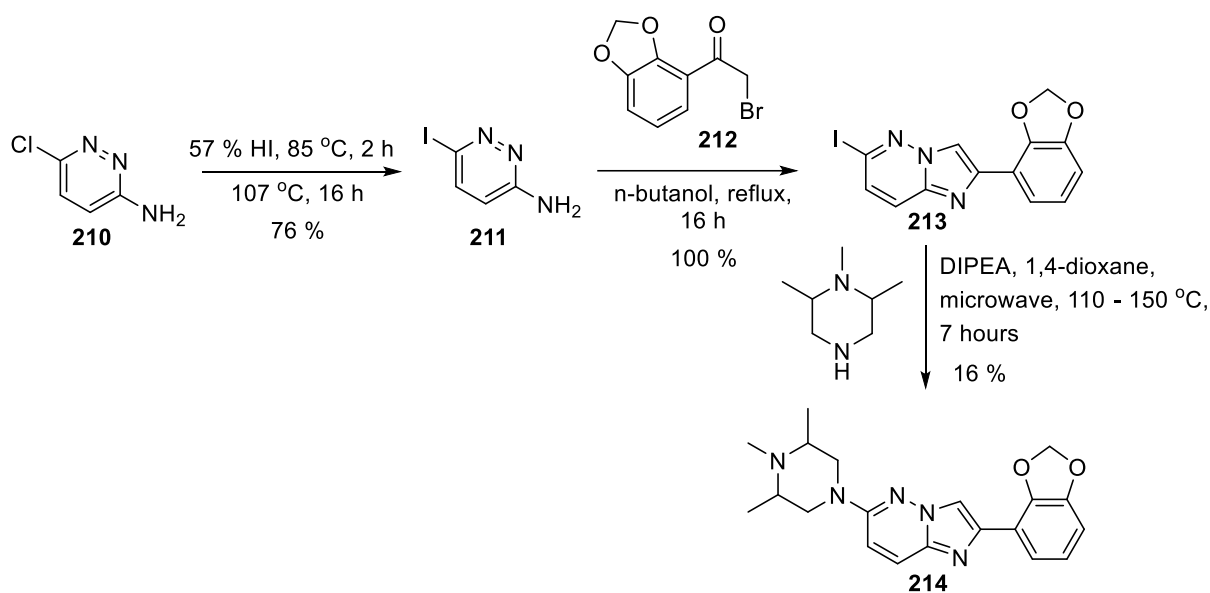
Chapter 2

1.1 M NaOH solution was heated at 170 °C and 150 W for 30 minutes. However, 100 % of **202** was recovered while **183** underwent a side-reaction with sodium hydroxide producing the 6-hydroxy-pyridazin-2-amine derivative **207**. A yield of **207** was not recorded since difficulties were encountered when attempting to dry **207** due to its high solubility in water. This compound has been produced previously by Barlin *et al*⁸⁰ (Scheme 2.27), where *N*-(6-Chloro-2-oxo-pyridazin-3-yl)benzamide (**208**) was heated with 1 M sodium hydroxide resulting in base hydrolysis of the amide bond and aromatic substitution with hydroxide. Acidification afforded both **207** and benzoic acid (**209**). Accordingly, sodium hydroxide solution was not a suitable solvent since the hydroxide displacement of the chloride in **183** was a significant side reaction. Although hydroxypyridazine **207** was not observed in Entry 1 of Table 2.11, it may have been produced but remained in the aqueous phase due to its high solubility.



Scheme 2.27: Synthesis of **207**⁸⁰

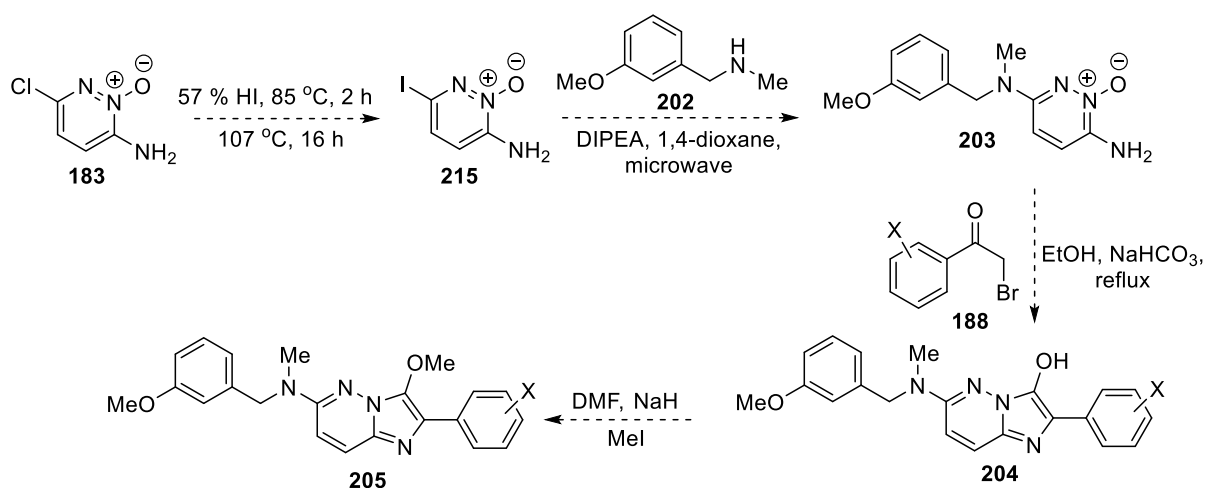
The *N*-oxide moiety of **183** reduces the amount of electron density at the carbon bearing the chloride, thereby activating the site for nucleophilic aromatic substitution. However, **183** was not sufficiently electrophilic to undergo nucleophilic aromatic substitution with **202**. Other methods to increase the electrophilicity of this carbon include substituting the chloride for an iodide.⁶⁷ For example, others have reported that heating **210** in 57 % HI at 85 °C for 2 hours and subsequently at 107 °C for 16 hours provided **211** in 76 % yield (Scheme 2.28).⁶⁷ After a condensation reaction with phenacyl bromide **212** to produce imidazo[1,2-*b*]pyridazine **213**, a microwave heated mixture of 1,2,6-trimethylpiperazine and DIPEA in 1,4-dioxane at 110 – 150 °C for 7 hours afforded **214** in a yield of 16 %.⁶⁷



Scheme 2.28: Synthetic method for the 6-aminoimidazo[1,2-*b*]pyridazine **214**

Alternatively, *N*-oxide **183** could replace **210** as the substrate in the first step of Scheme 2.28 producing 6-amino-3-iodopyridazine 1-oxide (**215**) (Scheme 2.29). It was considered likely that C3 of the pyridazine ring of iodopyridazine *N*-oxide **215** would be more electrophilic than **183** and **211** due to both the presence of the iodide leaving group and the *N*-oxide electron withdrawing effect, and therefore less strenuous conditions would be required when conducting the nucleophilic aromatic substitution between **215** and benzylic amine **202** (Scheme 2.29). Ideally, this would result in a higher yield of **203** which can be used to produce **204** in the condensation reaction with **188** followed with *O*-methylation to produce **205** (Scheme 2.29).

It was found (see Chapter 6) that 3-methoxy-6-(*N*-methylbenzylamino)-2-phenylimidazo[1,2-*b*]pyridazines (**190b** and **190d**) and 3-methoxy-6-((3-methoxybenzyl)thio)-2-phenylimidazo[1,2-*b*]pyridazines (**64** and **65**) were readily metabolized when incubated with mouse liver microsomes. Due to the structural similarities **190b**, **190d**, **64** and **65** have with 3-methoxy-6-((3-methoxybenzyl)(methyl)amino)-2-phenylimidazo[1,2-*b*]pyridazines (**205**), the syntheses of these compounds were no longer considered as high priority since it was believed that **205** would also be metabolised readily.

Scheme 2.29: Proposed synthetic pathway for **205**

2.4 Conclusions

Pathways 1 and 2 are alternative synthetic routes to 3-methoxy-2-phenylimidazo[1,2-*b*]pyridazines. The section describing Pathway 1, involving the key condensation reaction between 6-substituted-pyridazine-3-amines and phenylglyoxals, details the many different building blocks synthesised which were used to prepare a library of 3-methoxy-6-(substituted)methylthio-imidazo[1,2-*b*]pyridazines. The final products synthesised (Table 2.6) were obtained in a range of yields between 17 % and 80 %. Oxidation of thioether to sulfone in **65** and **66** produced **174** and **175**, respectively. Many side-products were observed throughout this synthetic pathway. Methyl ester side-products **161**, **162** and **163** were observed when attempting to form the corresponding methoxy derivatives. Cleavage of the benzyl group of **165** producing **164** was also observed. Finally, isolation of **176** and **177** revealed cleavage of the imidazo[1,2-*b*]pyridazine core structure under oxidative conditions. The formation of these side-products sheds light on the instability of some of these imidazo[1,2-*b*]pyridazine derivatives, and may provide some insight into the compounds' metabolic instability *in vivo*.

Pathway 2, involving the condensation reaction between 3-substituted-6-aminopyridazine-1-oxides and phenacyl bromides, was used successfully as an alternative synthetic route to **17** since complications were encountered in Pathway 1 when attempting to synthesise phenylglyoxal derivative **112**.

Pathway 2 was also employed to synthesise 6-(*N*-methylbenzylamino)-2-phenylimidazo[1,2-*b*]pyridazin-3-ols (**189**) which were *O*-methylated to obtain seven 3-methoxy-6-(*N*-methylbenzylamino)-2-phenylimidazo[1,2-*b*]pyridazines (**190**) with a range of yields between 31 % and 60 %. Side-products with similar ¹H NMR spectra to the desired products prompted further characterization of all compounds synthesised at this step. The structures of these side products were established from X-ray crystallography (Dr. Craig Forsyth, Monash University), NMR spectroscopy and mass spectral data as the methyl esters (**191**), *N*-methylpyridazine-amides (**192**), and the amides (**193**) (Table 2.10). Control reactions were employed to assist in determining the mechanism for the synthesis of these side-products which led to the proposed mechanism outlined in Scheme 2.24. Attempts at synthesising the building block **203** for 3-methoxy-6-((3-methoxybenzyl)(methyl)amino)-2-phenylimidazo[1,2-*b*]pyridazines (**205**) were also described but all failed.

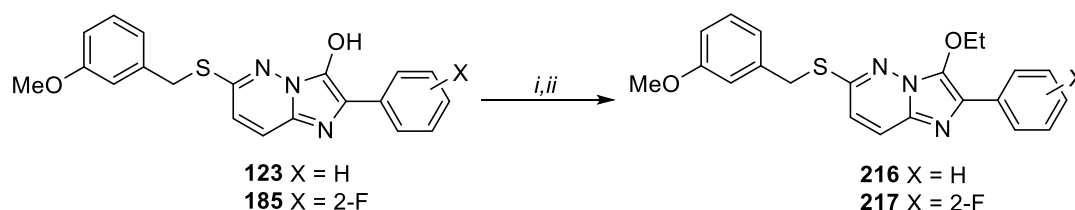
Chapter 3.
Other 3-substituted Imidazo[1,2-*b*]pyridazine
Syntheses

Chapter 3 Summary

Chapter 3 discusses the syntheses of imidazo[1,2-*b*]pyridazines with substituents other than a methoxy group installed at C3 to gather more SAR data and to perhaps enhance their metabolic stability. The desired products include 3-ethoxy-, 3-dialkylaminomethyl- and 3-carboxylate(lactone)-substituted imidazo[1,2-*b*]pyridazines.

3.1 3-Ethoxy-imidazo[1,2-*b*]pyridazine syntheses

Although the 3-methoxy moiety on the imidazo[1,2-*b*]pyridazine is clearly associated with antimycobacterial activity (as discussed in Chapter 5), different substituents were installed at this location in order to gather further SAR data. To probe SAR around the 3-methoxy-substituent, initially some 3-ethoxy-imidazo[1,2-*b*]pyridazines (**216** and **217**) were synthesised since the 3-ethoxy moiety differs to the 3-methoxy by only 1 carbon unit. These compounds were chosen for this modification since analogous 3-methoxy derivatives **64** and **17** showed potent antimycobacterial activity (Chapter 5). *O*-Ethylation of the 3-hydroxyl group of imidazo[1,2-*b*]pyridazines **123** and **185** was achieved using the conditions described below in Scheme 3.1. 3-Ethoxy-6-((3-methoxybenzyl)thio)-2-phenylimidazo[1,2-*b*]pyridazine (**216**) and 3-ethoxy-2-(2-fluorophenyl)-6-((3-methoxybenzyl)thio)imidazo[1,2-*b*]pyridazine (**217**) were produced in 75 % and 76 % yield, respectively. These compounds possessed highly similar NMR data to their analogous 3-methoxy derivatives except for the presence of the 3-ethoxy peaks. In the ¹³C NMR spectrum of compound **217**, coupling between the 2-fluorophenyl group and the methylene unit of the 3-ethoxy moiety (⁶*J*) was observed (refer to Chapter 8.8 and Appendices section 1).



Scheme 3.1: i) **123**, DMF, K₂CO₃, TBAB, EtI, N₂ atmosphere, rt, 17.5 h, 75 %; ii) **185**, DMF, K₂CO₃, EtI, N₂ atmosphere, rt, 17 h, 76 %.

3.2 3-Dialkylaminomethyl-imidazo[1,2-*b*]pyridazines

During the initial high-throughput screening of CSIRO library compounds against *Mtb* in 2016, 1-(6-benzylthio-2-phenylimidazo[1,2-*b*]pyridazin-3-yl)-*N,N*-dimethylmethanamine (**44**) was found to have comparable activity to 6-benzylthio-3-methoxy-2-phenylimidazo[1,2-*b*]pyridazine (**19**) (Figure 3.1). The only difference between the two structures is the moiety

at C3 of the imidazo[1,2-*b*]pyridazine ring system. Since both of these C3 substituents on the imidazo[1,2-*b*]pyridazine appear to enhance the compounds' activity, it was thought likely that the presence of a heteroatom in the C3 substituent was important.

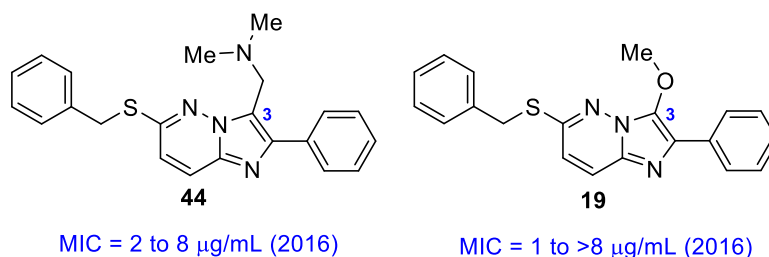
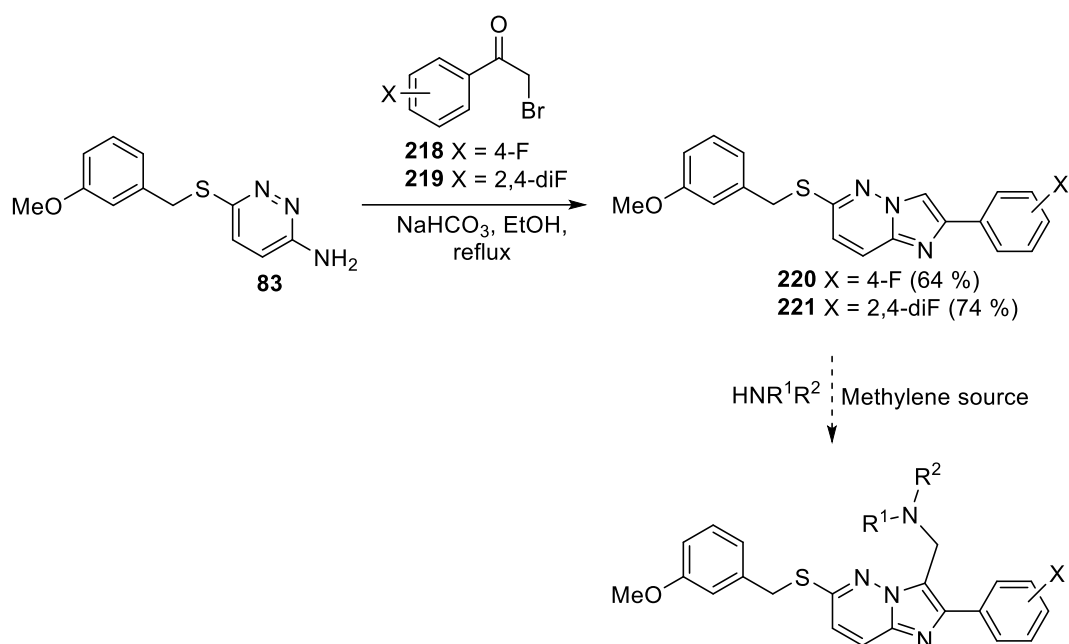


Figure 3.1: Structures of **44** and **19**

Earlier SAR studies in this work showed that 6-(3-methoxybenzylthio), 2-(2-fluorophenyl) and 2-(2,4-difluorophenyl) groups on the imidazo[1,2-*b*]pyridazine core enhanced activity against *Mtb* (refer to Chapter 5); therefore, including these moieties in target structures seemed logical in the pursuit of highly active compounds.

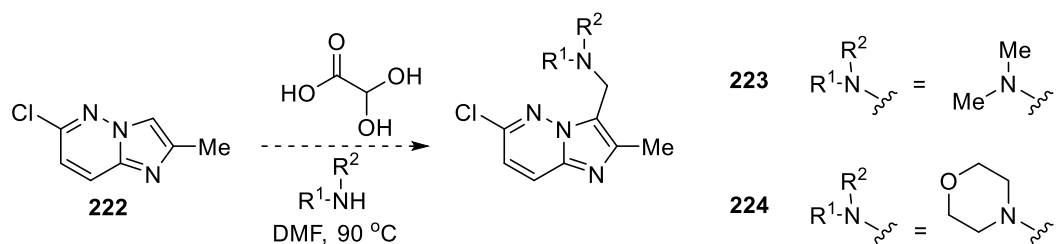
In order to synthesise the required precursors for the 3-dialkylaminomethyl-imidazo[1,2-*b*]pyridazines, mixtures of 6-((3-methoxybenzyl)thio)pyridazin-3-amine (**83**) with each of 4-fluorophenacyl bromide (**218**) and 2,4-difluorophenacyl bromide (**219**) and sodium bicarbonate in ethanol were heated at reflux to produce 2-(4-fluorophenyl)-6-((3-methoxybenzyl)thio)imidazo[1,2-*b*]pyridazine (**220**) (60 %) and 2-(2,4-difluorophenyl)-6-((3-methoxybenzyl)thio)imidazo[1,2-*b*]pyridazine (**221**) (74 %), respectively (Scheme 3.2).⁸¹ The next step was to treat these precursors with a secondary amine and a methylene source under Mannich-type conditions to yield different 3-dialkylaminomethyl-imidazo[1,2-*b*]pyridazines (Scheme 3.2). Barlin *et al* typically used heated mixtures of ethanolic dialkylamine, aqueous formaldehyde (or paraformaldehyde) and acetic acid to synthesise these derivatives but new reaction conditions were sought since long reaction times (up to 60 hours) and poor yields were observed.⁸¹



Scheme 3.2: General synthetic pathway to 3-dialkylaminomethylimidazo[1,2-*b*]pyridazines

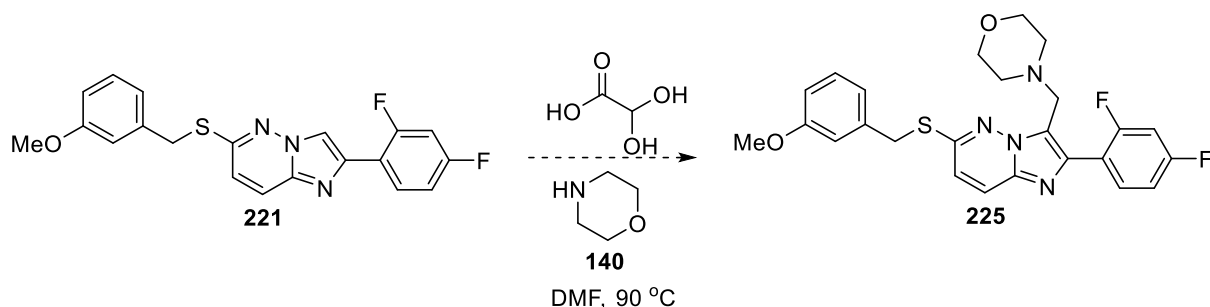
Before attempting the 3-aminomethylations with valuable compounds **220** and **221**, 6-chloro-2-methylimidazo[1,2-*b*]pyridazine (**222**) was used as a model compound (Scheme 3.3) to establish appropriate conditions. “Mannich-like” conditions were employed in order to aminomethylate C3 of the imidazo[1,2-*b*]pyridazine ring, using glyoxylic acid monohydrate as a methylene source (Scheme 3.3).⁸² Dimethylamine was used as the amine source and the reaction mixture was heated at 90 °C in DMF for 17.5 hours in a sealed reaction vessel. However, only starting material was recovered. It was reasoned that dimethylamine may have mainly been in the headspace due to its low boiling point.

A similar experiment with morpholine instead of dimethylamine resulted in a similar outcome, which suggested the low boiling point of the dimethylamine in the earlier experiment was not the sole reason for its failure (Scheme 3.3). Perhaps the specific electronic properties of **222** are not suited for this reaction.



Scheme 3.3: Attempted syntheses of 1-(6-chloro-2-methylimidazo[1,2-*b*]pyridazin-3-yl)-*N,N*-dimethylmethanamine (**223**) and 4-((6-chloro-2-methylimidazo[1,2-*b*]pyridazin-3-yl)methyl)morpholine (**224**)

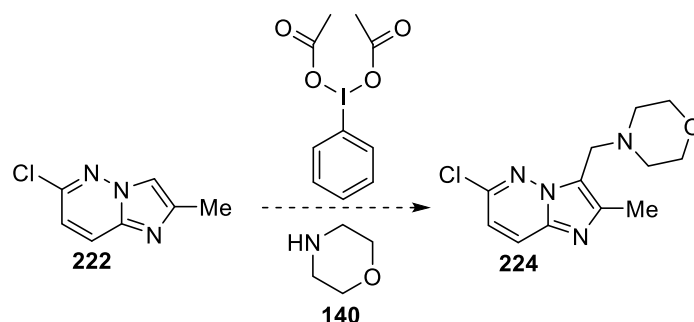
A similar experiment in which the 6-benzylthio derivative **221** instead of 6-chloro compound **222** was used (Scheme 3.4), resulted, once again, in only starting material being recovered. These results suggest that the electronic properties of imidazo[1,2-*b*]pyridazine derivatives **221** and **222** were not suitable for these “Mannich-like” conditions.



Scheme 3.4: Attempted synthesis of 4-((2-(2,4-difluorophenyl)-6-((3-methoxybenzyl)thio)imidazo[1,2-*b*]pyridazin-3-yl)methyl)morpholine (**225**)

Attention was turned to another method to aminomethylate the imidazo[1,2-*b*]pyridazine ring. Mondal *et al* reported the aminomethylation of imidazo-fused heterocycles with morpholine (**140**) using phenyliodine (III) diacetate (PIDA) and no solvent.⁸³ The imidazo-fused heterocyclic substrates included imidazopyridines, benzoimidazothiazoles, indolizines and indoles.⁸³ Additionally, neat conditions were found to be necessary since use of solvents such as 1,4-dioxane lead to direct amination rather than aminomethylation.^{83,84} This method was trialled on imidazo[1,2-*b*]pyridazine **222**, which was stirred with PIDA in morpholine (**140**) for

20 minutes at room temperature under a nitrogen atmosphere (Scheme 3.5). When PIDA was added to the mixture, a rapid reaction was observed and the reaction mixture solidified. After an aqueous/extractive workup, only starting material was isolated. It was thought that other material remained in the aqueous phase. Therefore, THF was added to the aqueous phase to azeotropically remove the water. The solvent mixture was removed under vacuum affording morpholin-4-ium acetate (**226**) as yellow crystals (Figure 3.2 for ^1H NMR spectrum),⁸⁵ indicating PIDA and the morpholine (**140**) were consumed in an unwanted side-reaction.



Scheme 3.5: Attempted synthesis of 4-((6-chloro-2-methylimidazo[1,2-b]pyridazin-3-yl)methyl)morpholine (**224**)

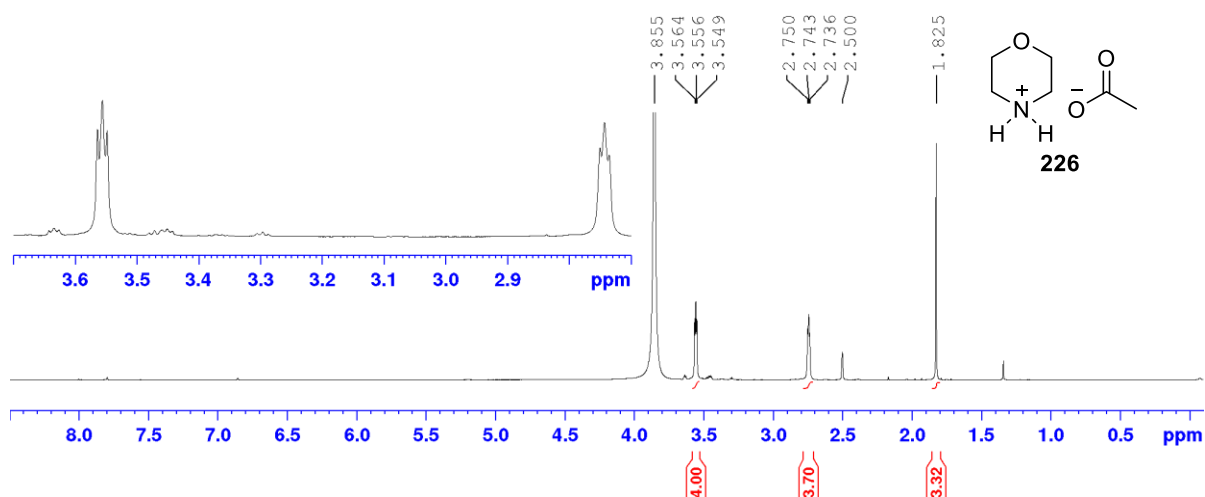
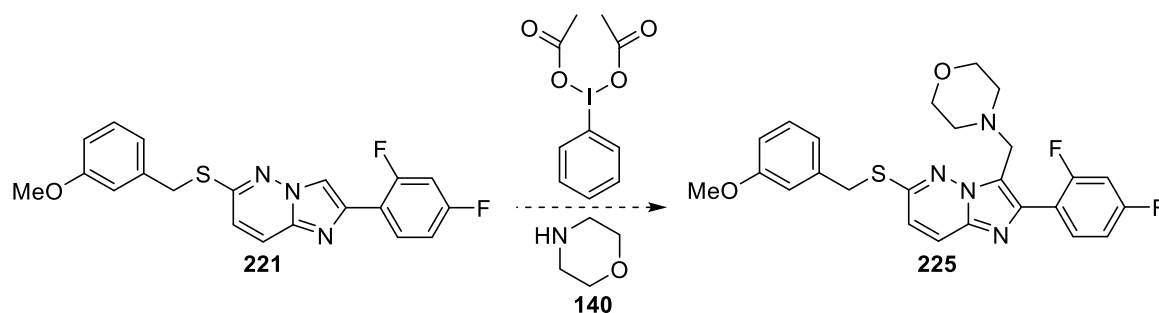


Figure 3.2: ^1H NMR spectrum of morpholin-4-ium acetate (**226**) in $\text{DMSO-}d_6$

Synthesis of 4-((2-(2,4-difluorophenyl)-6-((3-methoxybenzyl)thio)imidazo[1,2-*b*]pyridazin-3-yl)methyl)morpholine (**225**) was attempted using these same conditions except 8.9 equivalents of morpholine (**140**) was used instead of 2 (Scheme 3.6).⁸³ The extra equivalents were utilised in order to solubilize all substrates for the entire reaction time. Compound **221** dissolved in morpholine after the stirred and heated mixture reached 50 °C. The reaction mixture was cooled to room temperature (20 °C) and PIDA was added. After the reaction mixture was stirred for 70 minutes, ethyl acetate and water were added. The aqueous phase was extracted with ethyl acetate, and the combined organic phase was washed with water, dried with sodium sulfate and concentrated under vacuum. Only starting material **221** was recovered (79 %), indicating these reaction conditions are not appropriate for aminomethylation of imidazo[1,2-*b*]pyridazines.



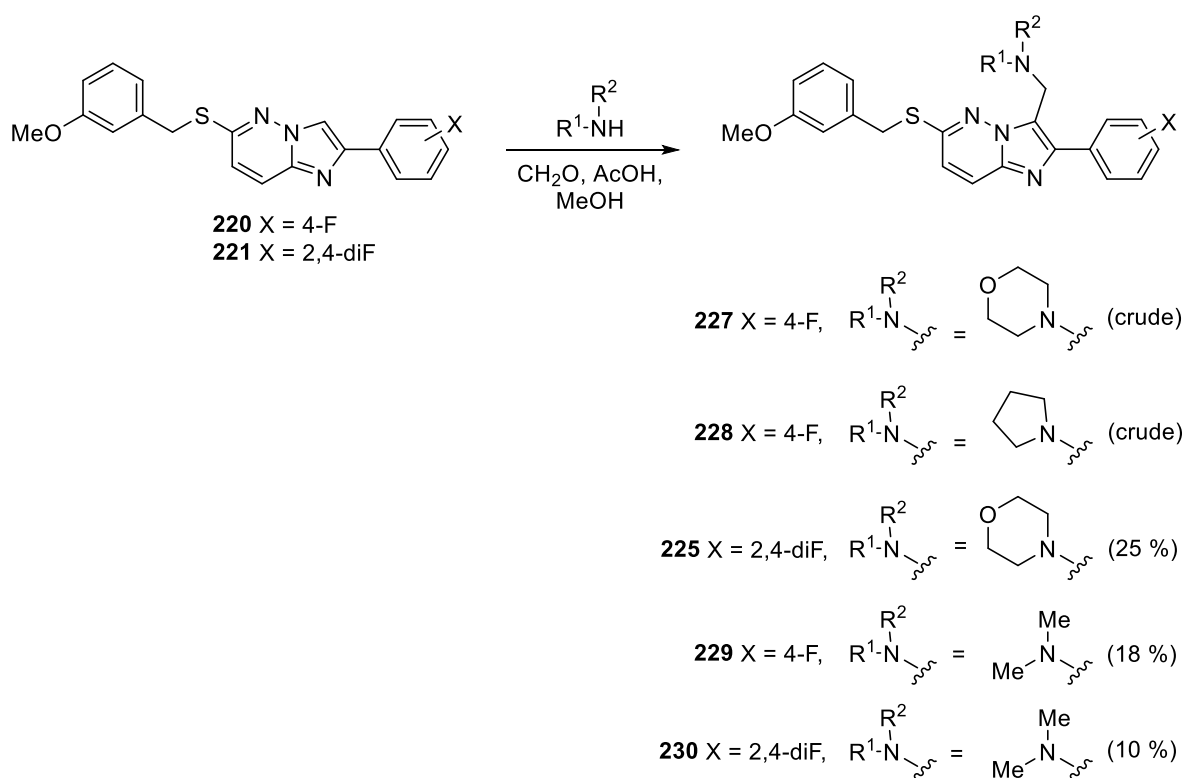
Scheme 3.6: Attempted synthesis of 4-((2-(2,4-difluorophenyl)-6-((3-methoxybenzyl)thio)imidazo[1,2-*b*]pyridazin-3-yl)methyl)morpholine (**225**)

Attention was turned to classic Mannich chemistry to synthesise these 3-aminomethyl-imidazo[1,2-*b*]pyridazines. As previously mentioned Barlin *et al* established Mannich conditions, but with low yields and long reaction times.⁸¹ In order to reduce this reaction time and increase the yields, we sought alternative conditions. It was found that imidazo[2,1-*b*][1,3,4]thiadiazoles could be aminomethylated at C3 using methanol as the solvent and acetic acid as a catalyst.⁸⁶ These reactions took only 8 hours (compared to 60 hours) and proceeded in high yields.^{81,86} Therefore, these reaction conditions were applied to imidazo[1,2-*b*]pyridazines **220** and **221** (Scheme 3.7).

The syntheses of 4-((2-(4-fluorophenyl)-6-((3-methoxybenzyl)thio)imidazo[1,2-*b*]pyridazin-3-yl)methyl)morpholine (**227**), 2-(4-fluorophenyl)-6-((3-methoxybenzyl)thio)-3-(pyrrolidin-1-

ylmethyl)imidazo[1,2-*b*]pyridazine (**228**) and 4-((2-(2,4-difluorophenyl)-6-((3-methoxybenzyl)thio)imidazo[1,2-*b*]pyridazin-3-yl)methyl)morpholine (**225**), described in Scheme 3.7, all went to completion, according to TLC analysis, indicating methanol may facilitate the reaction. The ^1H NMR spectrum of the crude product in the synthesis of **227** revealed that the desired product was the major component, indicated by the absence of the 3-*H* signal and the appearance of the 3-dialkylamino methyl signals. Purification via trituration with ether/hexane (2:5 x 2) was unsuccessful. The same issue was encountered with the purification of **228** (Scheme 3.7). However, these experiments proved that the conditions outlined in Scheme 3.7 were effective for amino-methylation of C3 on the imidazo[1,2-*b*]pyridazine ring system.

Although purification of **227** and **228** was not trivial, **225** was more easily purified and isolated with a yield of 25 % (Scheme 3.7). The crude material from this reaction was a lot cleaner than the crude material from the syntheses of **227** and **228**, allowing for a simpler purification.



Scheme 3.7: Mannich syntheses of 3-dialkylaminomethyl imidazo[1,2-*b*]pyridazines

With appropriate reaction conditions established, C3-aminomethylations with dimethyl amine were attempted. For the synthesis of 1-(2-(4-fluorophenyl)-6-((3-methoxybenzyl)thio)imidazo[1,2-*b*]pyridazin-3-yl)-*N,N*-dimethylmethanamine (**229**) (Scheme 3.7), the reaction mixture was stirred at room temperature for 1.5 hours and heated at reflux for 17.25 hours. The reaction appeared to go to completion, by TLC and ¹H NMR spectroscopic analysis. The crude material was chromatographed using a solvent gradient of 0 - 1 % MeOH/DCM affording a high purity sample of **229**.

Finally, these Mannich conditions were applied to dimethylaminomethylation of 2-(2,4-difluorophenyl) derivative **221** (Scheme 3.7). The reaction mixture was heated at reflux and stirred at room temperature intermittently for 48 hours. Further portions of formalin, dimethyl amine solution and acetic acid were added during the cooler periods to provide more of the iminium ion intermediate. Even after two days, the reaction did not go to completion. Both the desired product (major) and the starting material (minor) were present. This reaction may have not gone to completion simply because it was too dilute. Although the Mannich reaction leading to **230** did not go to completion, a sample of **230** was purified via column chromatography and recrystallisation from an ether/hexane mixture. The long-range coupling phenomenon (⁵*J*) between the ortho-fluorine and the methylene unit of the 3-dialkylaminomethyl group was observed with each of compounds **225** and **230**.

3.3 3-Carboxylate(lactone)-substituted imidazo[1,2-*b*]pyridazine synthesis

A 2018 report described a range of benzofurans and coumestans with antitubercular activity, including 5-hydroxy-4-((4-methylpiperidin-1-yl)methyl)-2-phenylbenzofuran-3-carboxylate (**231**) and 8-hydroxy-7-(piperidin-1-ylmethyl)-6*H*-benzofuro[3,2-*c*]chromen-6-one (**232**) (Figure 3.3).⁸⁷ The majority of the benzofurans had an ethyl ester at C3 of the benzofuran core.⁸⁷ One compound which showed promising activity was benzofuran **231** with a MIC (H37Rv) value of 1 µg/mL (Figure 3.3).⁸⁷ However, it was thought the ethyl ester may have been a metabolic target by endogenous esterases which would reduce its activity.⁸⁷

This reduction in activity was likely since 5-hydroxy-4-((4-methylpiperidin-1-yl)methyl)-2-phenylbenzofuran-3-carboxylic acid (**233**) had a MIC (H37Rv) value of >64 µg/mL (Figure 3.4).⁸⁷ The 3-carboxylate ester was believed to be a metabolic liability,⁸⁷ which was supported when **231** was shown to be inactive in the (mouse) serum inhibition titration (SIT) assay.⁸⁷

In order to overcome this possible metabolic issue, converting the benzofuran **231** to the coumestan **232** was envisioned (Figure 3.3).⁸⁷ The coumestan is the tetracyclic ring system containing a benzofuran, a phenyl ring and a lactone.⁸⁷ Coumestans are common moieties seen in a range of bioactive natural products which provided further motivation to synthesise these derivatives.⁸⁷ A particularly active coumestan was 8-hydroxy-7-(piperidin-1-ylmethyl)-6*H*-benzofuro[3,2-*c*]chromen-6-one (**232**) showing a MIC (H37Rv) value of 0.125 – 0.25 µg/mL; a 4-8 fold increase in activity compared to **231**.⁸⁷ Not only did the activity increase, but also its metabolic stability, since it was orally bioactive in the SIT assay.⁸⁷

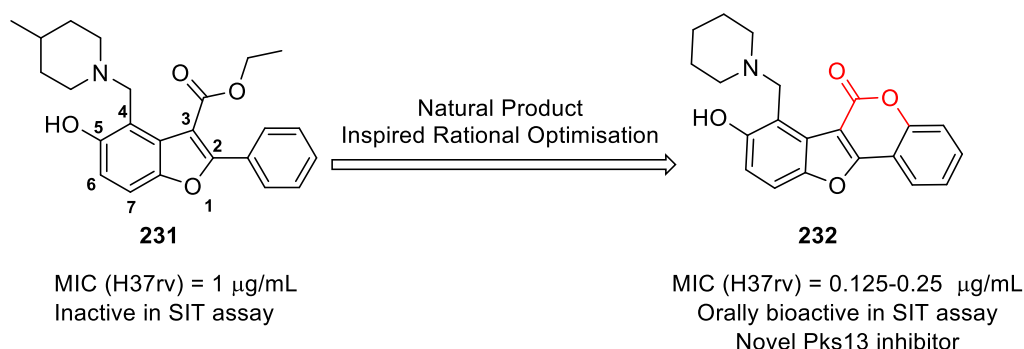


Figure 3.3: Natural product inspired rational optimization of ethyl 5-hydroxy-4-((4-methylpiperidin-1-yl)methyl)-2-phenylbenzofuran-3-carboxylate (**231**) to 8-hydroxy-7-(piperidin-1-ylmethyl)-6*H*-benzofuro[3,2-*c*]chromen-6-one (**232**)⁸⁷

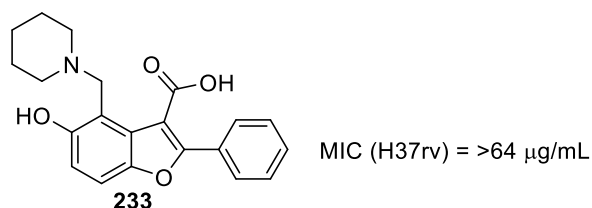


Figure 3.4: Structure of 5-hydroxy-2-phenyl-4-(piperidin-1-ylmethyl)benzofuran-3-carboxylic acid (**233**)⁸⁷

The structure of benzofuran was observed to have the same basic, planar geometry as the core imidazo[1,2-*b*]pyridazine system; a 6 membered ring fused with a 5 membered ring. Additionally, both structures can have functional groups installed at the C2 and C3 position of their respective 5 membered rings (Figure 3.5). For example, coumestan **232** has the chromeno/lactone type moiety (in blue) fused at the C2 and C3 position of the benzofuran ring forming the coumestan (Figure 3.5), whereas imidazo[1,2-*b*]pyridazine **19** has a phenyl group installed at the C2 position and a methoxy at the C3 position (Figure 3.5). Molecular hybridization of these two compounds can afford the structure 9-benzylthio-6*H*-chromeno[4',3':4,5]imidazo[1,2-*b*]pyridazine-6-one (**234**) where the 2-phenyl and 3-methoxy groups in **19** can be replaced by the chromeno/lactone type moiety (in blue) (Figure 3.5). Such structures were considered in an effort to enhance the antitubercular activity of the imidazo[1,2-*b*]pyridazine compounds, since the chromeno/lactone moiety enhanced activity in the reported benzofuran series (**232**).⁸⁷ The installation of the fused chromeno/lactone type moiety maintains an oxygen heteroatom in the C3-substituent and may also enhance the metabolic stability of the compound. It is likely that a particular mechanism of metabolism is demethylation of the methoxy group and glucuronidation of the liberated hydroxyl group, since for example, this is a major metabolic pathway of berberine in rats.⁸⁸ Not only may replacement of the methoxy group with a lactone moiety enhance stability, but it also lowers clogP value from 5.56 in **19** to 5.00 for **234** (ChemDraw Prime) (Figure 3.5). Reduction in clogP was a desirable property change since **64**, **65**, **190b** and **190d** all had solubility issues in aqueous media (refer to Chapter 6).

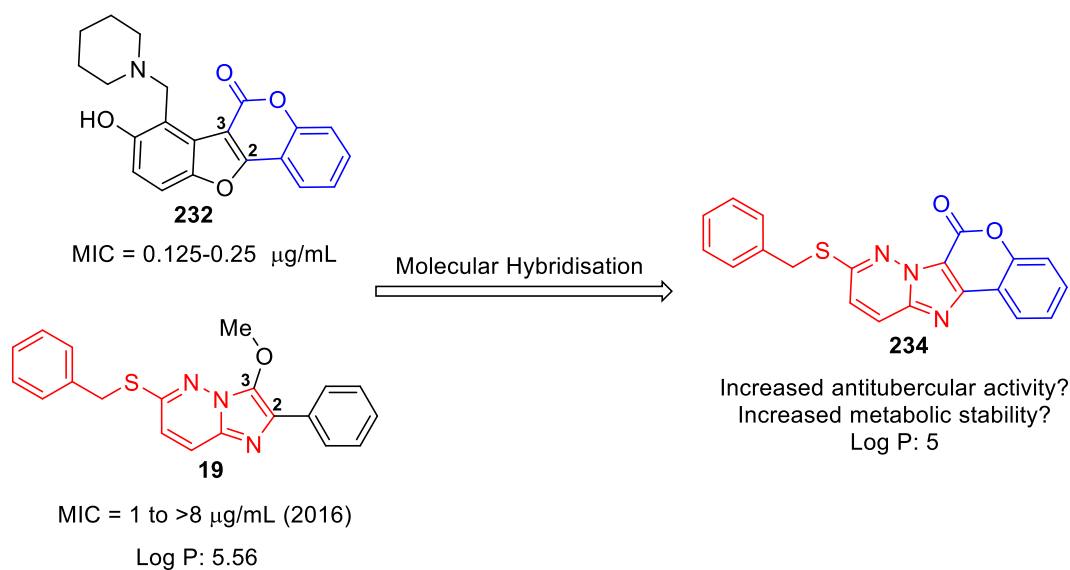
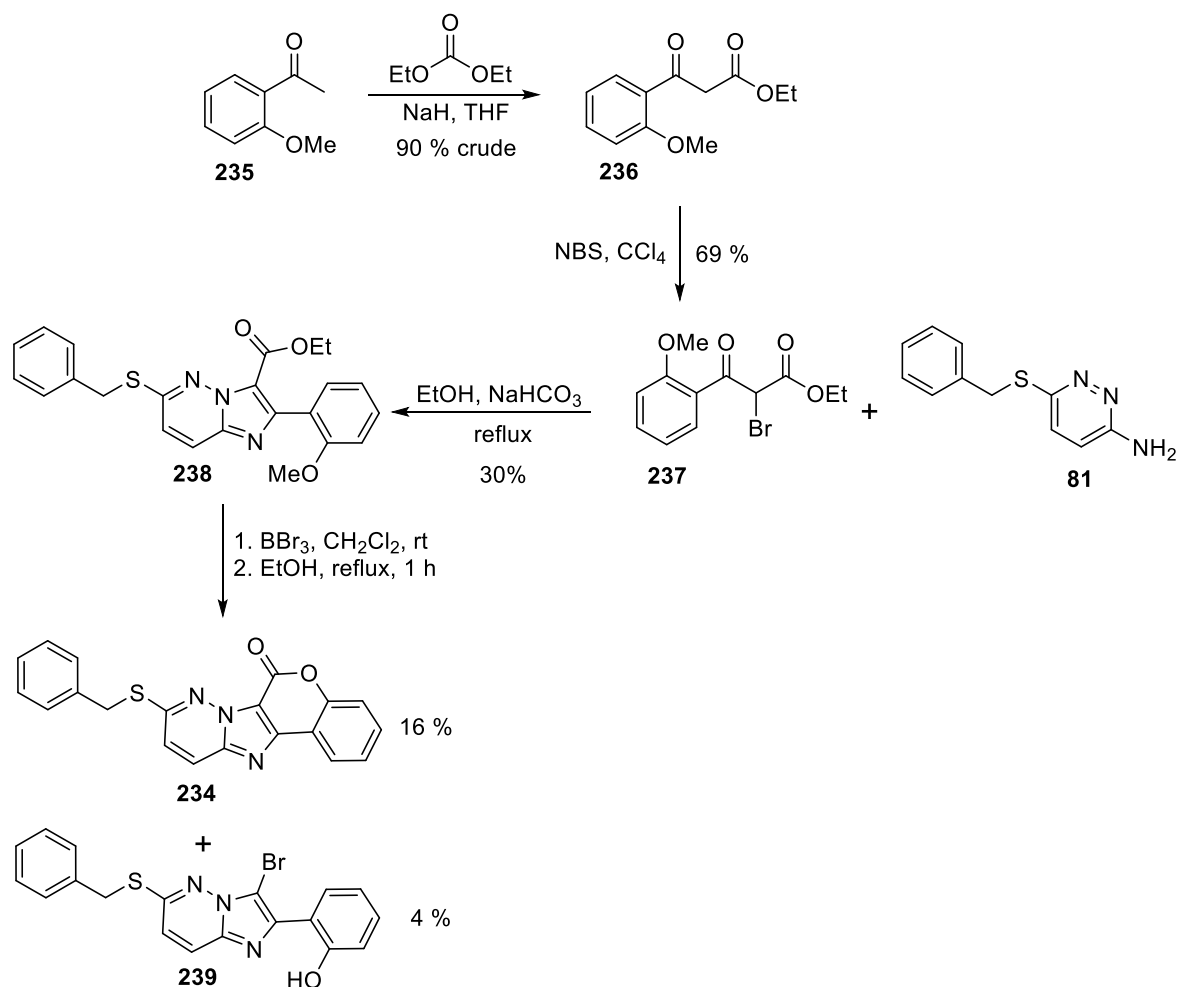


Figure 3.5: Molecular hybridization of **232** and **19** to afford **234**

The synthetic pathway to lactone **234** is outlined in Scheme 3.8. 2-Methoxyacetophenone (**235**) and diethyl carbonate underwent a Claisen condensation reaction using sodium hydride in THF to obtain ethyl 3-(2-methoxyphenyl)-3-oxopropanoate (**236**) in 90 % crude yield (Scheme 3.8).⁸⁹ Bromination of the α -carbon of the β -keto ester using NBS in carbon tetrachloride afforded ethyl 2-bromo-3-(2-methoxyphenyl)-3-oxopropanoate (**237**) in 69 % yield.⁹⁰ The number of equivalents of NBS was increased from an initial 1.2 equivalents to 2.4 equivalents to obtain the 69 % yield. When 1.2 equivalents were used, the reaction did not go to completion since starting material **236** was observed in the ^1H NMR spectrum of the crude material.

A mixture of bromoketone **237**, 6-(benzylthio)pyridazin-3-amine (**81**), and sodium bicarbonate in ethanol was heated at reflux, producing ethyl 6-benzylthio-2-(2-methoxyphenyl)imidazo[1,2-*b*]pyridazine-3-carboxylate (**238**). Treatment of **238** with boron tribromide in dichloromethane at room temperature followed by heating in ethanol at reflux afforded the cyclised product, **234** in 16 % yield (Scheme 3.8), after column chromatography. Elution of a side-product was also observed (Figure 3.6 for ^1H NMR spectrum and Figure 3.7 for ^{13}C NMR spectrum). The structure was assigned as 2-(6-benzylthio-3-bromoimidazo[1,2-*b*]pyridazin-2-yl)phenol (**239**) via 2D NMR spectroscopy (Table 3.1) and LC-MS analyses (refer to Section 1 of the Appendices for the NMR spectroscopic and LC-MS data). This side-product

was also sent for screening against *Mtb*. A clear spectroscopic difference between lactone **234** and side-product **239** was the presence of the *o*-hydroxyl signal (12.13 ppm) in the ^1H NMR spectrum of side-product **239**.



Scheme 3.8: Synthetic pathway for 9-benzylthio-6H-chromeno[4',3':4,5]imidazo[1,2-b]pyridazine-6-one (**234**)

Chapter 3

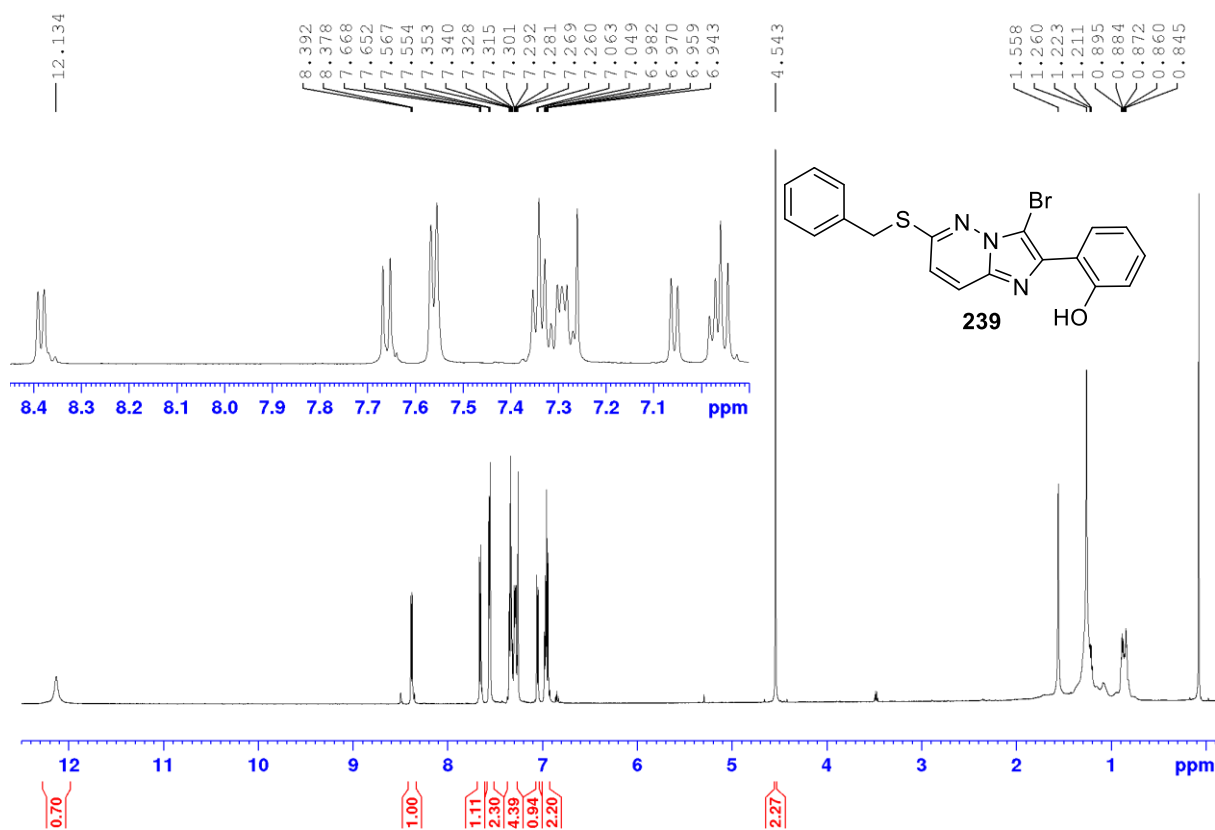


Figure 3.6: ¹H NMR spectrum of **239** in CDCl₃

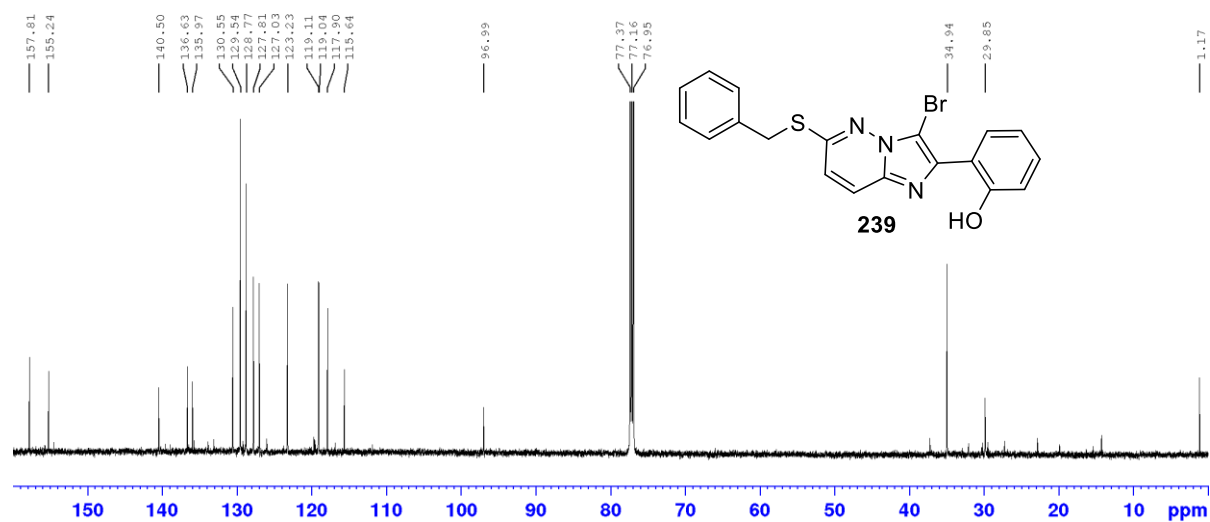
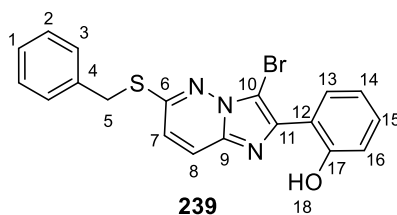


Figure 3.7: ¹³C NMR spectrum of **239** in CDCl₃

Note, the ^1H and ^{13}C NMR spectroscopic chemical shifts in red font in Table 3.1 correlate to one another via HMQC if they are in the same row.

Table 3.1: ^{13}C , ^1H and 2D NMR spectroscopic data from **239**



Atom number	^{13}C (ppm)	^1H (ppm)	COSY atom correlations	HMBC atom correlations (^{13}C to ^1H)
1	127.81	7.29	-	3
2	128.77	7.33	3	2
3	129.54	7.56	2	1, 3, 5
4	136.63	-	-	2, 5
5	34.94	4.54	-	3
6	155.24	-	-	5, 7, 8
7	119.11	6.95	8	9
8	123.23	7.67	7	6
9	135.97	-	-	7, 8
10	96.99	-	-	-
11	140.50	-	-	13 or 16
12	115.64	-	-	13 or 16; 14 or 15
13	127.03 or 117.90	8.39 or 7.06	14 or 15	14 or 15
14	130.55 or 119.04	7.30 or 6.97	13 or 16	13 or 16
15	130.55 or 119.04	7.30 or 6.97	13 or 16	13 or 16
16	127.03 or 117.90	8.39 or 7.06	14 or 15	14 or 15
17	157.81	-	-	13 or 16; 14 or 15
18	-	12.14	-	-

3.4 Conclusions

The syntheses of a range of 3-ethoxy-, 3-aminomethyl- and 3-carboxylate (lactone)-substituted imidazo[1,2-*b*]pyridazines were achieved. Two 3-ethoxy-imidazo[1,2-*b*]pyridazines, **216** and **217**, were synthesised via *O*-ethylation of **123** and **185** with 75 % and 76 % yields, respectively. Three 3-dialkylaminomethyl-imidazo[1,2-*b*]pyridazines, **225**, **229**, **230** were produced in 25 %, 18 % and 10 % yields respectively, using classic Mannich chemistry conditions.^{81,86} Finally, 9-benzylthio-6*H*-chromeno[4',3':4,5]imidazo[1,2-*b*]pyridazine-6-one (**234**) was synthesised via a concise four-step process.

Chapter 4.

Scaffold Hopping

Chapter 4 Summary

Chapter 4 discusses the concept of scaffold hopping and how it can be applied to the imidazo[1,2-*b*]pyridazine core structure in the context of the present work. Specifically, a scaffold hop from an imidazo[1,2-*b*]pyridazine to an imidazo[2,1-*b*][1,3,4]thiadiazole core was proposed. Syntheses of imidazo[2,1-*b*][1,3,4]thiadiazole derivatives with similar substituents to those on the imidazo[1,2-*b*]pyridazines discussed in Chapter 2 were explored. We envisaged that molecular hybridisation between the known antimycobacterial compounds Q203 and TB47⁹¹ and the imidazo[1,2-*b*]pyridazines described in the present work might lead, via a scaffold hop, to highly potent compounds. This chapter discusses the syntheses of 4 different “Q203/TB47 hybrid” imidazo[1,2-*b*]pyridazines.

4.1 Scaffold Hopping

The process of scaffold hopping involves replacing scaffolds (or core structures) in compounds shown to have relevant biological activity with other similar molecular scaffolds.^{92,93} These alternative molecular scaffolds are identified by bioisosteric replacements of the original core structure with the intention to maintain similar geometry and functionality while improving certain properties.^{92,93} Properties that can be improved via scaffold hopping include binding affinity, lipophilicity, polarity, toxicity, and intellectual property rights, such as structural novelty.⁹³

As a result of the initial promising results from the imidazo[1,2-*b*]pyridazines, it was thought that scaffold hops to the imidazo[2,1-*b*][1,3,4]thiadiazole (**240**) and imidazo[2,1-*b*][1,3,4]oxadiazole template would be worthy of investigation (Figure 4.1). The only difference between these bicyclic scaffolds was the replacement of the pyridazine moiety in the imidazo[1,2-*b*]pyridazine by a 1,3,4-thiadiazole or a 1,3,4-oxadiazole. Furthermore, the sulfur or oxygen atom in the imidazo[2,1-*b*][1,3,4]thia(oxa)diazole can be thought of as a replacement for the carbon to carbon double bond between C7 and C8 in the imidazo[1,2-*b*]pyridazine system. This subtly changes the overall shape, size and electronics of the scaffolds. These modifications to the imidazo[1,2-*b*]pyridazine structure may improve the compounds' activity against *Mtb* by, for example, improving binding affinity.⁹³

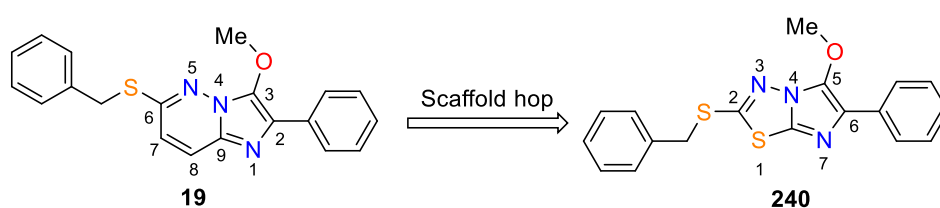


Figure 4.1: Scaffold hop example from an imidazo[1,2-*b*]pyridazine to an imidazo[2,1-*b*][1,3,4]thiadiazole

4.2 Antitubercular activity of imidazo[2,1-*b*][1,3,4]thiadiazoles

Encouragingly, derivatives of the imidazo[2,1-*b*][1,3,4]thiadiazole core structure have appeared in the literature for being anti-tubercular as well as antibacterial, antifungal,

leishmanicidal, herbicidal, anticancer, anthelmintic, anticonvulsant, analgesic, antiinflammatory, antipyretic, local anaesthetic, cardiotoxic and diuretic.⁹⁴ Scope for intellectual property still exists since the benzyl, methoxy and the phenyl substituents at C2, C5 and C6 respectively, preferred in the present work, have not been reported in the literature. There is, however, an array of other imidazo[2,1-*b*][1,3,4]thiadiazoles that have antitubercular activity in the literature.

For example, 5-dialkylaminomethyl and 5-formyl imidazo[2,1-*b*][1,3,4]thiadiazoles **241**, **242**, **243** and **244** were found to have excellent *in vitro* activity against *Mtb* (Figure 4.2).⁹⁵ Notably, these compounds are structurally similar to the 3-dialkylaminomethyl-imidazo[1,2-*b*]pyridazines **225**, **227**, **228** described in the previous chapter.

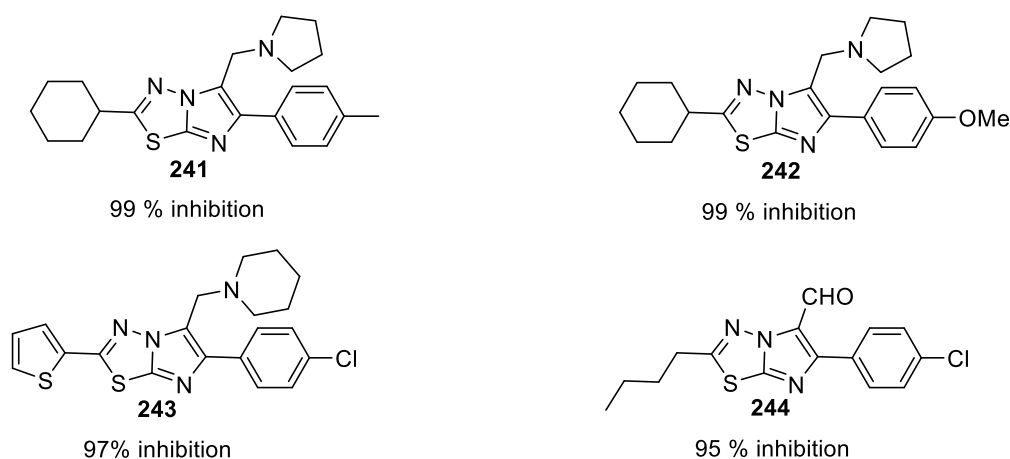


Figure 4.2: % inhibition of *Mtb* H37Rv at 6.25 µg/mL from imidazo[2,1-*b*][1,3,4]thiadiazole derivatives **241**, **242**, **243** and **244**

The 2-substituted-5,6-diarylsubstituted imidazo[2,1-*b*][1,3,4]thiadiazoles **245** and **246** (Figure 4.3) bearing aminosulfonyl or trifluoromethyl groups at C2, respectively, were found to have very high activity against *Mtb* (MIC = 1.25 µg/mL).⁹⁶ These derivatives were also tested for cytotoxicity and the results revealed that these compounds have anti-tubercular activity at non-cytotoxic concentrations.⁹⁶ Specifically, **245** and **246** showed IC₅₀ values of 246.6 µM and 147.3 µM respectively against a mammalian Vero cell line.

Chapter 4

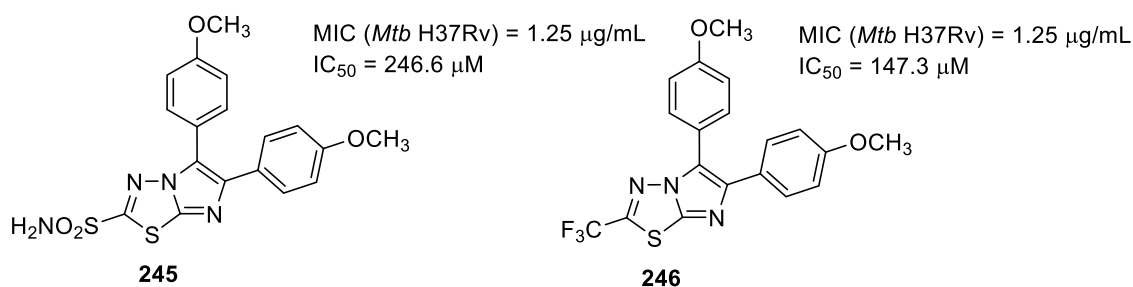


Figure 4.3: Structures, MIC values and IC₅₀ values of **245** and **246**

The clinical candidate SQ109, which was discussed in Chapter 1, bears a pendant adamantane moiety.⁹⁷ Due to the recent success of the imidazo[2,1-*b*][1,3,4]thiadiazoles, hybridization of this core structure with an adamantanyl ring was employed (Figure 4.4).⁹⁷ The adamantanyl ring is thought to increase the lipophilicity of the compound which may allow the compound to inhibit targets on the lipid-rich cell mycobacterium cell surface.⁹⁷

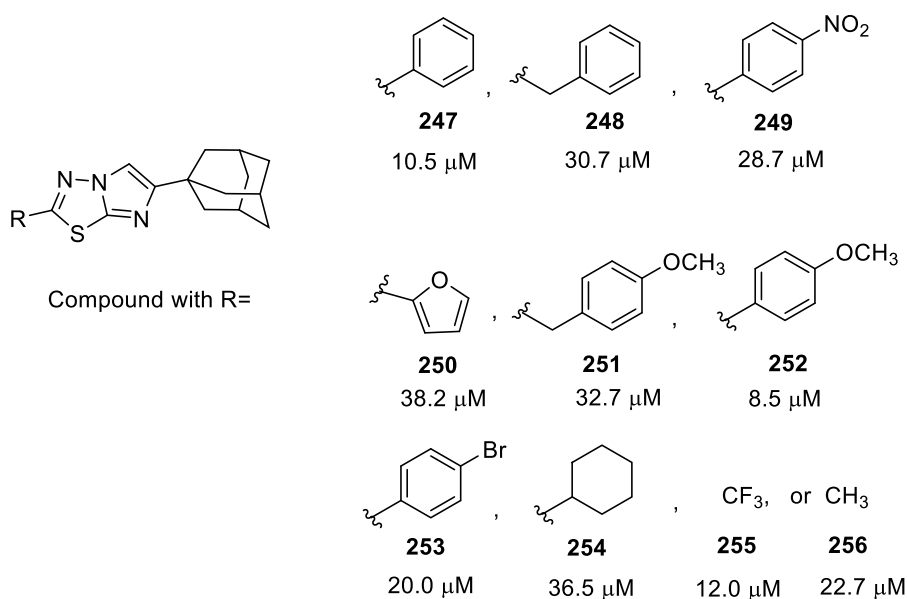


Figure 4.4: Adamantyl-imidazo[2,1-*b*][1,3,4]thiadiazole derivatives with respective MIC values against *Mtb* H37Rv

Ten compounds (**247-256**) were tested against *Mtb* H37Rv and it was found that the benzylic substituents (**248** and **251**) reduced activity when compared to phenyl substituents (**247** and **252**).⁹⁷ Furthermore, electron-donating groups such as the 4-methoxy substituent (**252**) on the phenyl ring were superior compared to electron withdrawing groups such as nitro (**249**)

and bromine (**253**).⁹⁷ The trifluoromethyl substituent was also preferable (**255**).⁹⁷ Overall, it was found that **252** had the highest activity against *Mtb*.⁹⁷ Interestingly, these compounds may target sterol 14 α -demethylase (CYP51) which was supported by *in silico* analysis as well as experimental activity of **252** in this system.⁹⁷

Imidazo[2,1-*b*][1,3,4]thiadiazole bearing triazole-containing groups were also found to have activity against *Mtb* (Figure 4.5).⁹⁸

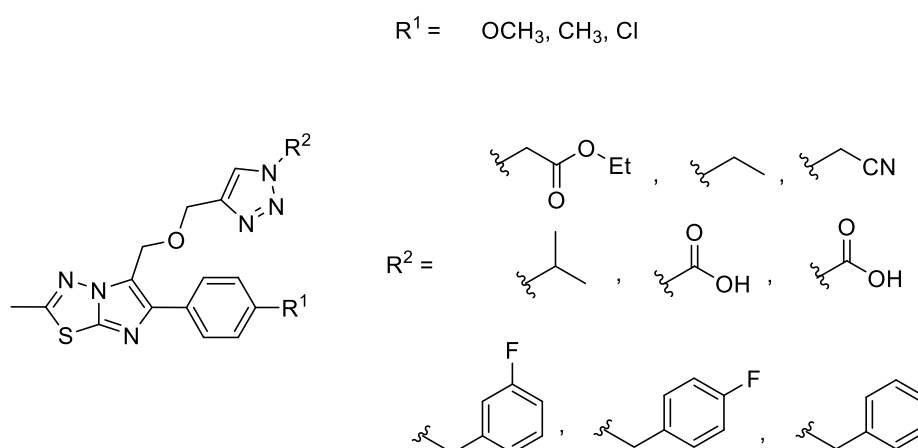


Figure 4.5: Triazole-methoxymethyl imidazo[2,1-*b*][1,3,4]thiadiazole derivatives

In terms of the SAR the methoxy and the chloro substituent for R^1 were generally preferable compared to the methyl.⁹⁸ All methyl substituted derivatives displayed MIC values greater than or equal to 25 $\mu\text{g}/\text{mL}$ while the methoxy and chloro substituted derivatives displayed MIC values in the range 3.125 - 12.5 $\mu\text{g}/\text{mL}$.⁹⁸ Furthermore, the ethyl and benzyl substituents for R^2 showed superior MIC values.⁹⁸ Consequently, **257** and **258** (Figure 4.6) displayed the highest activity against *Mtb* (3.125 $\mu\text{g}/\text{mL}$) which was equivalent to ethambutol.⁹⁸ The derivatives displaying a MIC value less than or equal to 12.5 $\mu\text{g}/\text{mL}$ were also tested for their cytotoxicity revealing they were active against *Mtb* at non-cytotoxic concentrations.⁹⁸

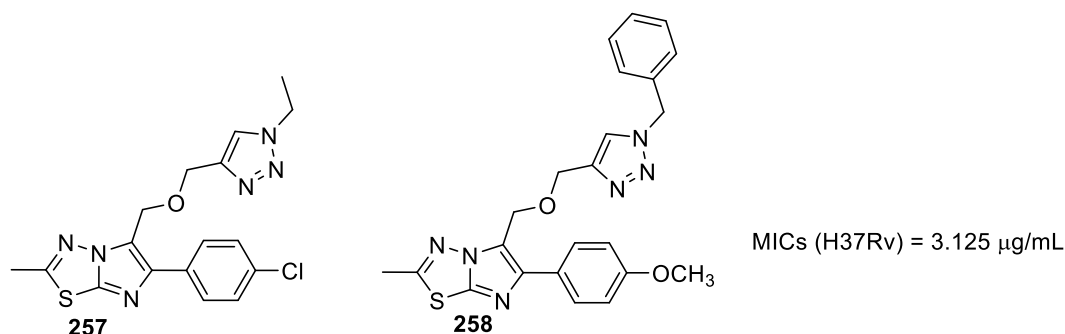


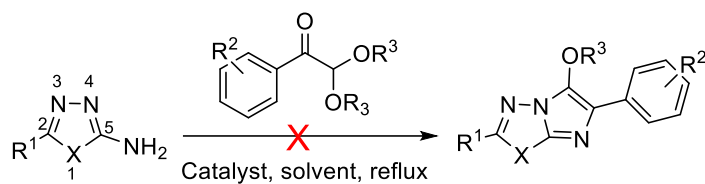
Figure 4.6: Structures of **257** and **258** with MIC values

The abundance of imidazo[2,1-*b*][1,3,4]thiadiazole derivatives having anti-tubercular activity within the literature encouraged the proposed scaffold hop from the imidazo[1,2-*b*]pyridazine to the imidazo[2,1-*b*][1,3,4]thiadiazole ring system.

4.3 Attempted syntheses of 5-hydroxyimidazo[2,1-*b*][1,3,4]thia(oxa)diazoles

A number of attempts to synthesise 5-hydroxyimidazo[2,1-*b*][1,3,4]thiadiazole and 5-hydroxyimidazo[2,1-*b*][1,3,4]oxadiazole derivatives all failed (Scheme 4.1, Table 4.1). Most experiments outlined in Table 4.1 (which utilised amino-diazoles which were synthesised and extracted from the CSIRO Library) targeted imidazo[2,1-*b*][1,3,4]thia(oxa)diazol-5-ols. The 5-hydroxyl moiety was required for *O*-methylation. A methoxy group in this position replicates the active 3-methoxyimidazo[1,2-*b*]pyridazines discussed in Chapters 2 and 5. For Entries 1 and 2, HCl and ethanol were used since they worked well in similar syntheses of imidazo[1,2-*b*]pyridazines. However, 2-benzylthio-5-ethoxy-6-phenylimidazo[2,1-*b*][1,3,4]thiadiazole (**259**) and 5-ethoxy-2,6-diphenylimidazo[2,1-*b*][1,3,4]thiadiazole (**260**) (Figure 4.7) were produced instead in impure form and in very low yields (2 % and 3 % respectively) (refer to Section 2 of the Appendices for the NMR spectroscopic and HRMS data). There was insufficient sample of **259** and **260** for testing against *Mtb*.

Chapter 4



Scheme 4.1

Table 4.1: Attempted syntheses of imidazo[2,1-b][1,3,4]thia(oxa)diazoles

Entry	R ¹	R ²	R ³	X	Catalyst	Solvent
1	Benzylthio	H	H	S	HCl	EtOH
2	Phenyl	H	H	S	HCl	EtOH
3	Propyl	H	H	S	HCl	EtOH
4	Benzylthio	H	H	S	MsOH	MeCN
5	Benzylthio	H	H	S	pTsOH	MeCN
6	Benzylthio	H	H	S	HCl	20 % H ₂ O/dioxane
7	Benzylthio	4-Cl	H	S	HCl	20 % H ₂ O/dioxane
8	2-Cl-phenyl	H	H	O	HCl	20 % H ₂ O/dioxane
9	Benzylthio	H	H	S	NaOMe	MeOH
10	Benzylthio	H	Me	S	HCl	MeOH
11	Benzylthio	H	Me	S	HCl	20 % H ₂ O/dioxane

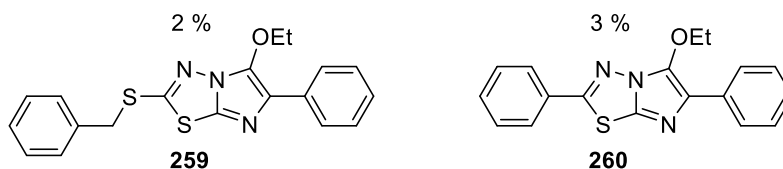
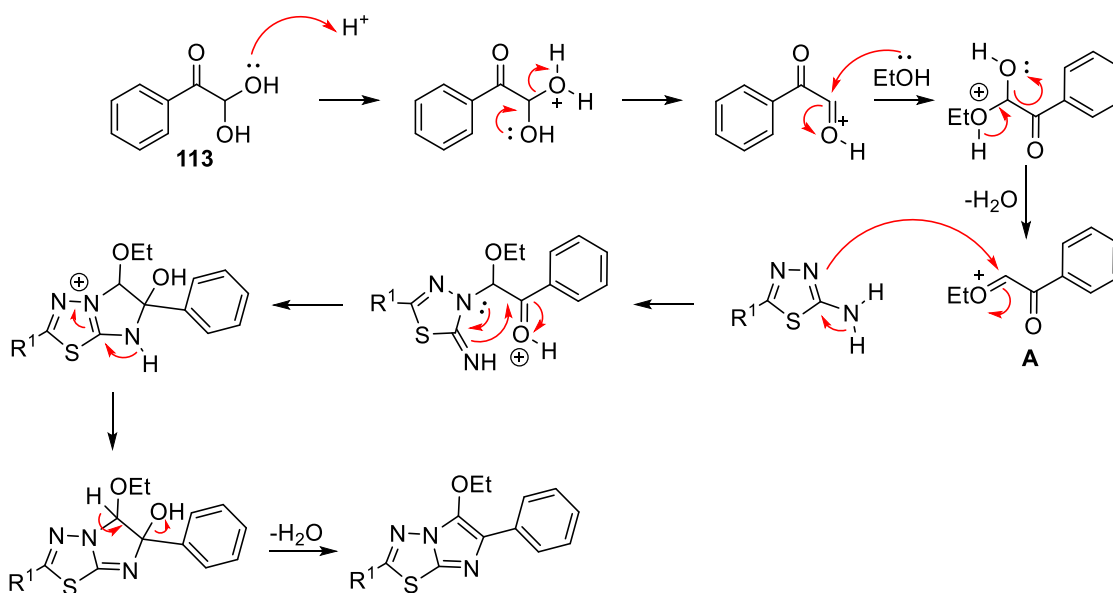


Figure 4.7: Structures and yields of **259** and **260** from Entries 1 and 2 respectively

A mechanism for formation of **259** and **260** was proposed (Scheme 4.2) in which ethanol was involved in producing the hemiacetal (or acetal) which reacts with the thiadiazole via nucleophilic attack at the α -carbon of intermediate A.



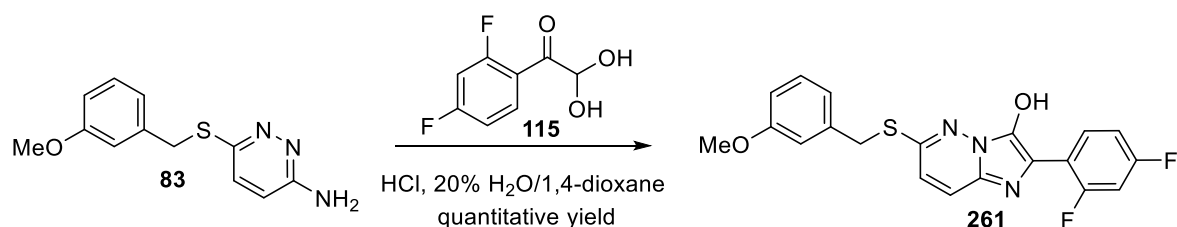
Scheme 4.2: Proposed mechanism for the side reactions of Entries 1 and 2, Table 4.1

In Entry 3 ($R^1 = \text{propyl}$), neither the desired product nor the 5-ethoxy species was isolated. In Entries 4 and 5 the solvent was changed to acetonitrile and the catalyst was changed to the organic acids MsOH and pTsoH, respectively. Changing the solvent to acetonitrile would preclude the involvement of ethanol in the reaction. The change from an aqueous acid to organic acids was employed to observe their effects on the reaction. For Entry 4, the ^1H NMR spectrum of the crude product indicated the recovery of both starting materials. For Entry 5, it was not obvious what was produced from the ^1H NMR spectrum of the crude product and

no clear indications of the desired product were present; therefore, purification was not pursued.

It was found by Yueting Lu *et al* that imidazo[1,2-*a*]pyridines could be synthesized using aqueous dioxane in the presence of HCl.⁵⁹ A quantitative yield of 2-(2,4-difluorophenyl)-6-((3-methoxybenzyl)thio)imidazo[1,2-*b*]pyridazin-ol (**261**) using 20 % H₂O/1,4-dioxane in the presence of HCl showed that these conditions can provide high yields of imidazo[1,2-*b*]pyridazines (Deborah A. Hughes, CSIRO, 2017) (Scheme 4.3). These conditions were trialled for the syntheses of imidazo[2,1-*b*][1,3,4]thiadiazole derivatives in Entries 6 and 7 but also failed to produce the desired product. Entry 6 was attempted twice; once for 5.5 hours and another for 7 days. Even after 7 days the thiadiazole starting material remained present. These conditions were repeated using 4'-chlorophenylglyoxal monohydrate (Entry 7). It was thought that the chloro group in the para position of the 6-phenyl ring may activate the phenylglyoxal monohydrate species through inductive effects. This reaction, using 1.2 equivalents of 4-chlorophenylglyoxal monohydrate, was monitored via TLC for 5 days; however, the thiadiazole starting material was not consumed.

It was clear, though somewhat surprising, that the 2-amino[1,3,4]thiadiazole starting materials were not as reactive as the 3-aminopyridazine starting materials in reactions with phenylglyoxal monohydrates. It was thought that replacing the sulfur in the thiadiazole ring with oxygen (therefore using an oxadiazole starting material instead) could possibly increase the nucleophilicity of this aromatic ring due to the subtle change in electronics. However, the slight change in electronics of this aromatic ring failed to result in reaction with phenylglyoxal monohydrate to produce the desired product (Entry 8).



Scheme 4.3: Synthesis of 2-(2,4-difluorophenyl)-6-((3-methoxybenzyl)thio)imidazo[1,2-*b*]pyridazin-ol (**261**)

As a result of the failed attempts at synthesizing the imidazo[2,1-*b*][1,3,4]thiadiazoles under acidic conditions, use of basic conditions was briefly investigated. It was thought that the acid might be protonating the thiadiazole starting material's ring nitrogen (N3), reducing its nucleophilicity. Therefore, the proposed reaction in Entry 9, using thiadiazole **262**, glyoxal **113** and sodium methoxide in methanol, was conducted under a nitrogen atmosphere for 22 hours. A peak at 8.51 ppm as well as peaks in the aromatic region were present in the ¹H NMR spectrum of the crude product (Figure 4.8). A control experiment involving phenylglyoxal monohydrate and sodium methoxide in methanol resulted in decomposition of phenylglyoxal monohydrate, according to analysis of the ¹H NMR spectrum of the crude product (Figure 4.8). Notably, there was an extra set of aromatic peaks at 7.36 ppm, 7.20 ppm, and 7.11 ppm in the control ¹H NMR spectrum (Figure 4.8). In the control reaction it was found from analysing the 2D NMR spectroscopic data that the peak at 8.50 ppm correlated to a carbonyl peak at 166.53 ppm (HMQC), attributable to an aldehyde. These were the only peaks belonging to the aldehyde since no correlations were observed in the HMBC; consequently, this compound was identified as sodium formate (not formic acid since the sodium methoxide was not quenched). Additionally, there were 3 other compounds present which all contained a phenyl moiety each with an unknown substituent. It was concluded that a combination of sodium methoxide and phenylglyoxal monohydrate was not a suitable set of conditions for the synthesis of 5-hydroxyimidazo[2,1-*b*][1,3,4]thiadiazoles.

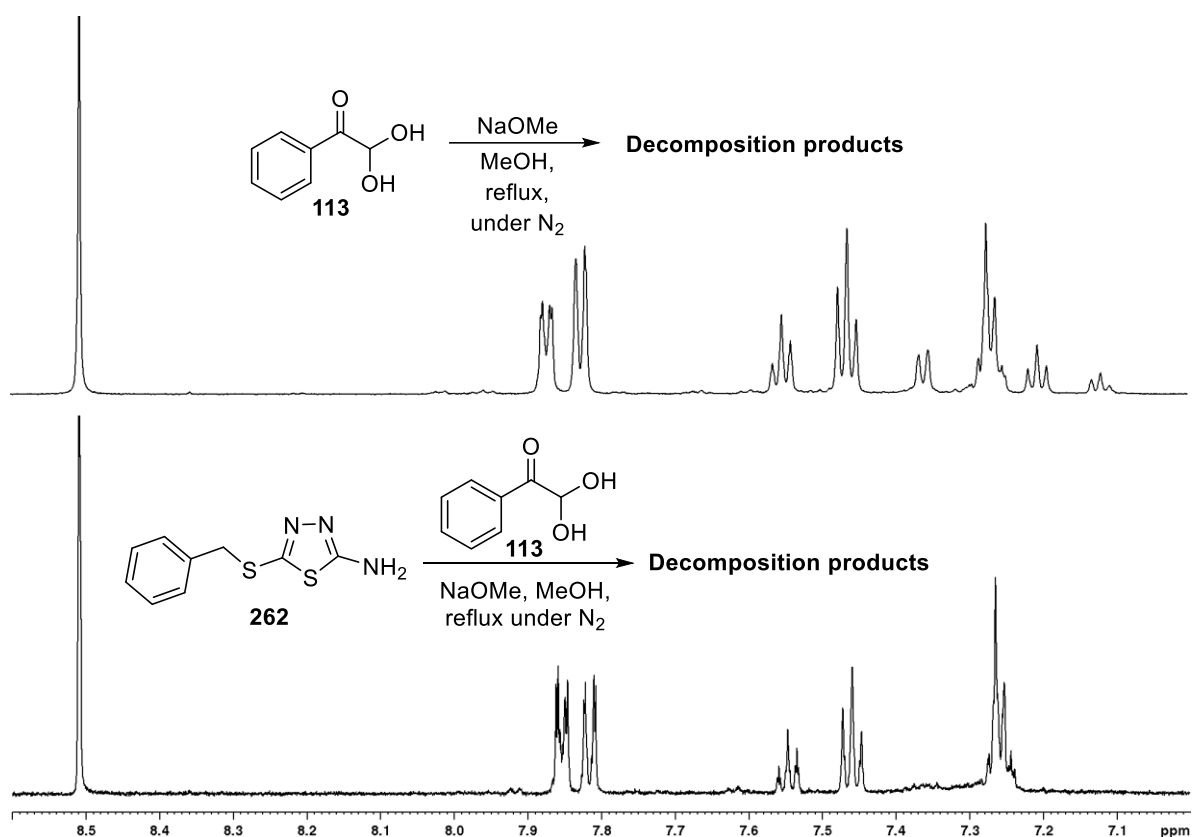
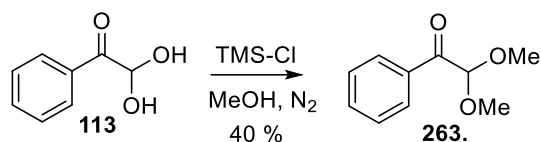


Figure 4.8: ¹H NMR spectral comparisons of Entry 9 from Table 4.1 and control reaction between phenylglyoxal monohydrate (**113**) and sodium methoxide in methanol in DMSO-d₆

Phenylglyoxal monohydrate was converted to the corresponding dimethyl acetal (**263**, Scheme 4.4)⁹⁹ and used in Entry 10 and 11, aiming to obtain the 5-methoxy species directly, skipping the final *O*-methylation step. The syntheses of **259** and **260** provided the idea for this reaction as it was originally thought that phenylglyoxal diethyl acetal may have been a key intermediate to these side-products. However, only starting materials were recovered in Entry 10 and 11. Consequently, the hemiacetal instead of the acetal as proposed in Scheme 4.2 could be a key intermediate for the syntheses of **259** and **260**.



Scheme 4.4: Conversion of phenylglyoxal monohydrate (**113**) to phenylglyoxal dimethyl acetal (**263**) using trimethylsilyl chloride and methanol

4.4 Q203/TB47 imidazo[1,2-*b*]pyridazine hybrids

As discussed in Chapter 1, the recently reported antimycobacterial compound, TB47, was identified via a scaffold hop from the imidazo[1,2-*a*]pyridine core structure of the clinical candidate Q203 to a pyrazolo[1,5-*a*]pyridine scaffold (Figure 4.9).^{43,91} Other structural changes between Q203 and TB47 include the 2-ethyl group for a 2-methyl group and a 6-chloro group for a 6-methoxy group.⁹¹ The MIC values of both compounds are similar.⁹¹ TB47 also exhibited high activity against multi-drug resistant strains and showed significant *in vivo* activity.⁹¹

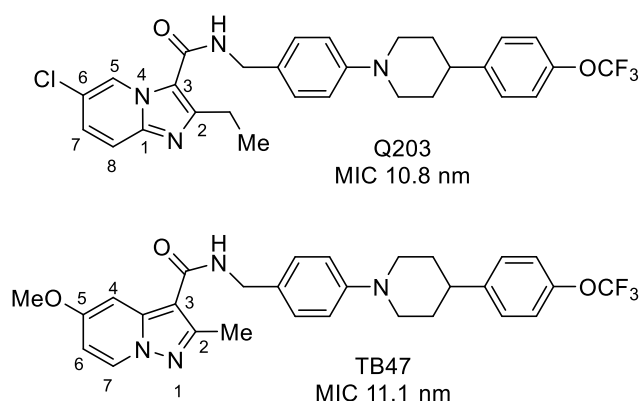
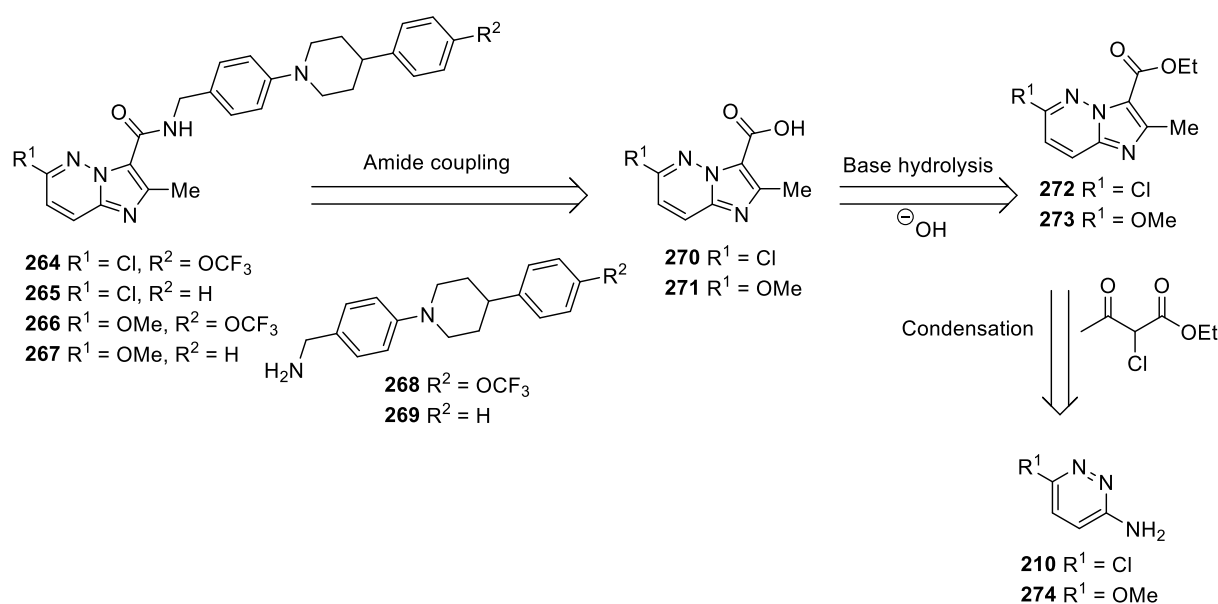


Figure 4.9: Structures of Q203 and TB47

The core scaffolds of imidazo[1,2-*a*]pyridine Q203 and pyrazolo[1,5-*a*]pyridine TB47 are very similar in structure and geometry to the imidazo[1,2-*b*]pyridazine system. All core structures consist of a 6 membered heteroaromatic ring fused with a 5 membered heteroaromatic ring containing two nitrogen atoms. Both Q203 and TB47 have 2 nitrogen heteroatoms in their

core structure but the position of the nitrogen atom at N4 in Q203 has shifted in TB47 (Figure 4.9). The imidazo[1,2-*b*]pyridazine core structure contains 3 nitrogen atoms; a nitrogen replaces the carbon atom of C5 in the imidazo[1,2-*a*]pyridine in Q203. Due to these structural similarities, molecular hybridization between Q203 and TB47 and a scaffold hop to the imidazo[1,2-*b*]pyridazine could possibly lead to compounds with antimycobacterial activity.

The retrosynthetic pathway for 4 different imidazo[1,2-*b*]pyridazine analogues of Q203/TB47 (**264**, **265**, **266** and **267**) is shown in Scheme 4.5. Such imidazo[1,2-*b*]pyridazines could be obtained via amide coupling of amines **268** and **269** with 2-methylimidazo[1,2-*b*]pyridazine-3-carboxylic acids **270** and **271**. Carboxylic acids **270** and **271** could be synthesised via base hydrolysis of ethyl 2-methylimidazo[1,2-*b*]pyridazine-3-carboxylates **272** and **273**. A condensation cyclisation reaction between pyridazines **210** and **274** with ethyl 2-chloroacetoacetate would produce the desired imidazo[1,2-*b*]pyridazine core structure.

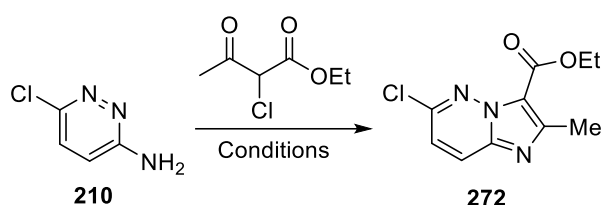


Scheme 4.5: Retrosynthesis of Q203/TB47 imidazo[1,2-*b*]pyridazine hybrids **264**, **265**, **266** and **267**

In order to synthesise ethyl 6-chloro-2-methylimidazo[1,2-*b*]pyridazine-3-carboxylate (**272**) (Scheme 4.6), a mixture of 6-chloropyridazin-3-amine (**210**) and ethyl 2-chloroacetoacetate in DME in the presence of sodium bicarbonate was heated at reflux for 51 hours (Entry 1, Table 4.2). The ¹H NMR spectrum of the crude product revealed the presence of **210** and the

absence of ethyl 2-chloroacetoacetate indicating ethyl 2-chloroacetoacetate decomposed under these conditions.

For Entry 2, a similar procedure using ethanol instead of DME as the solvent was employed and the reaction went for 18 hours. The reaction mixture was heated at reflux for 2 hours before adding the sodium bicarbonate. Analysis of the ^1H NMR spectrum of the crude product indicated that the reaction did not go to completion; aminopyridazine **210** along with desired product **272** were present in a ratio of 3:1, while ethyl 2-chloroacetoacetate was not present. Therefore, some of ethyl 2-chloroacetoacetate decomposed which prevented a complete reaction. Since **272** was present at low concentration in the complex crude mixture (by ^1H NMR spectroscopy), purification was not conducted. New reaction conditions were sought.



Scheme 4.6

Table 4.2: Synthetic protocols for ethyl 6-chloro-2-methylimidazo[1,2-b]pyridazine-3-carboxylic acid (**272**)

Entry	Conditions	Yield of 278 (%)
1	NaHCO ₃ , DME, reflux, 51 h	-
2	NaHCO ₃ , EtOH, reflux, 18 h	-
3	EtOH, reflux, 34 h	28
4	EtOH, reflux, 21 h	21

In Entry 3, a mixture of **210** and ethyl 2-chloroacetoacetate was heated at reflux in ethanol without sodium bicarbonate for 34 hours. Analysis of the ^1H NMR spectrum of the crude material revealed that the desired product was formed amongst side-products at lower concentration. Additionally, both starting materials were present indicating the reaction did not go to completion. The crude mixture was chromatographed using 10 – 20 % ether/DCM

eluting **272** in the presence of a minor impurity (~28 % yield) (Figure 4.10). The minor impurity was assigned as 1-(6-chloro-2-hydroxyimidazo[1,2-*b*]pyridazine-3-yl)ethanone (**275**) due to the two aromatic peaks at 8.05 ppm and 7.06 ppm and the methyl peak at 2.52 ppm (Figure 4.10). A proposed mechanism is shown in Scheme 4.7.

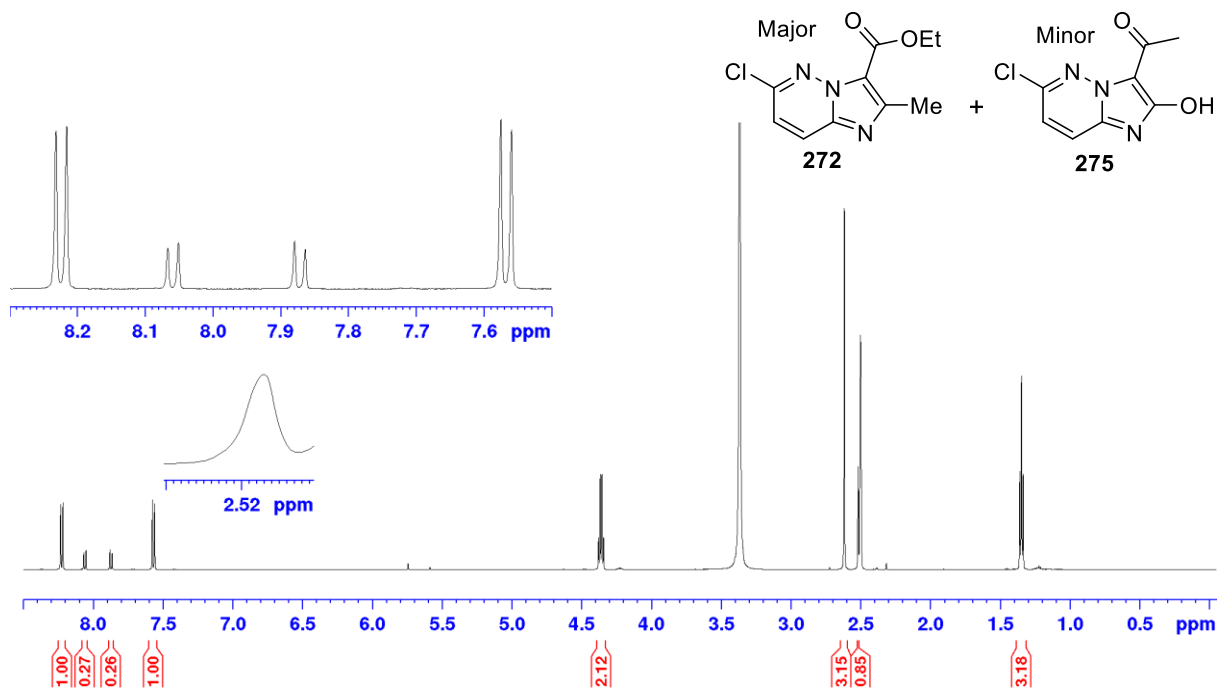
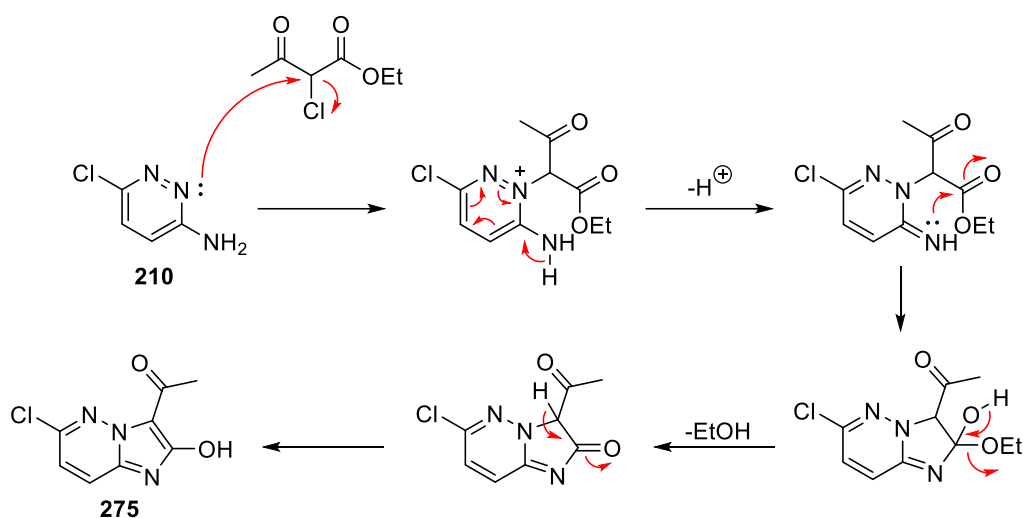


Figure 4.10: ^1H NMR spectrum of **272** and **275** in $\text{DMSO-}d_6$



Scheme 4.7: Proposed mechanism for the synthesis of **275**

Two other side-products eluted from the column. One compound was found to be 6-chloro-2-methylimidazo[1,2-*b*]pyridazine **222** (6 % yield) as evidenced by ^1H (Figure 4.11), ^{13}C (Figure 4.12), COSY, HMQC and HMBC NMR spectroscopic data (Table 4.3). Note: for atom numbers 2 and 3 the ^1H NMR spectroscopic chemical shifts coloured in red correlate to the ^{13}C NMR spectroscopic chemical shifts coloured in red via HMQC. The structure of **222** was corroborated by HRMS (APCI); $[\text{M}+\text{H}]^+ = 168.0320$ ($\text{C}_7\text{H}_7\text{ClN}_3^+$ required 168.0323) (refer to Section 2 of the Appendices for the NMR spectroscopic and HRMS data). Compound **222** is likely to be the product of partial hydrolysis and subsequent decarboxylation of **272** after being heated for a prolonged amount of time in the presence of atmospheric moisture.

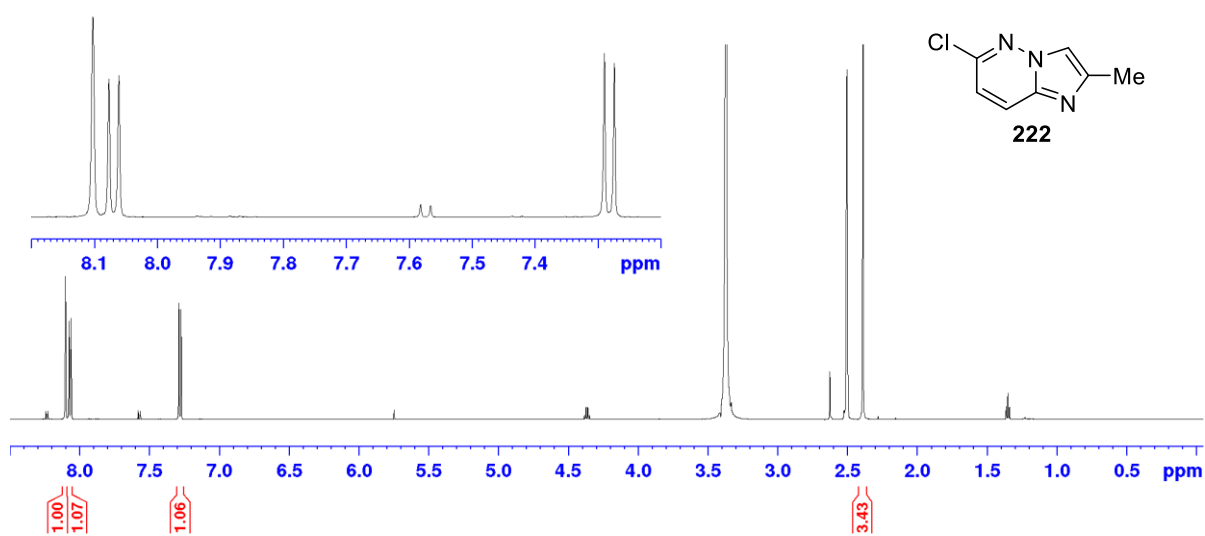
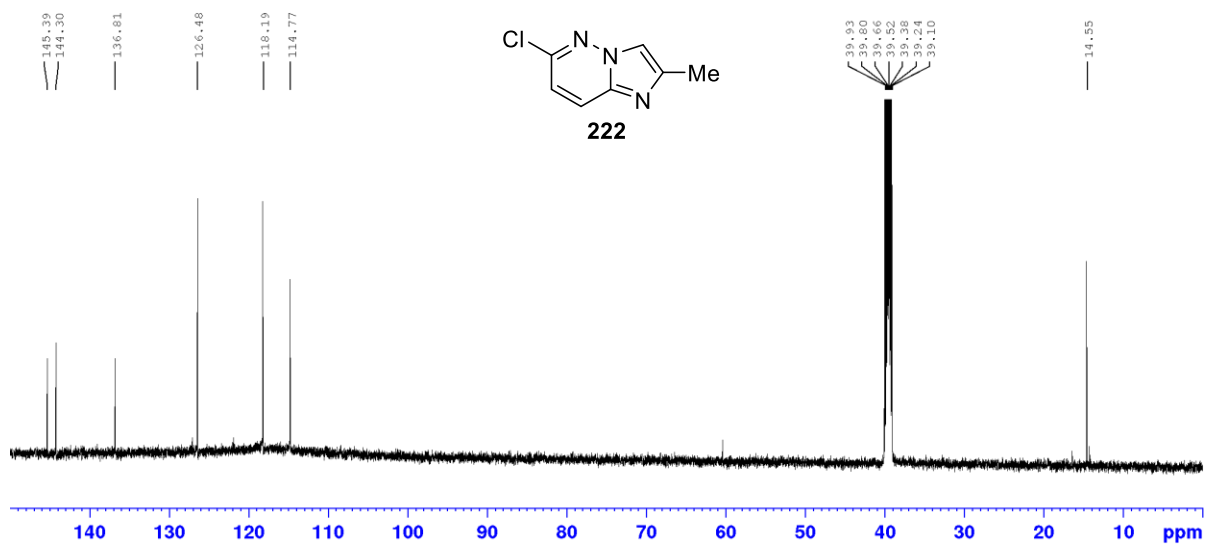
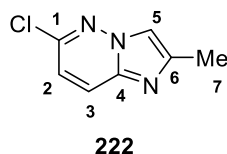
Figure 4.11: ^1H NMR spectrum of **222** in DMSO-d_6 Figure 4.12: ^{13}C NMR spectrum of **222** in DMSO-d_6

Table 4.3: ^{13}C , ^1H and 2D NMR spectroscopic data of **222**

Atom number	^{13}C chemical shift (ppm)	^1H chemical shift (ppm)	COSY atom correlations	HMBC atom correlations
1	136.87	-	-	2 or 3
2	118.07 or 126.46	7.29 or 8.07	3	-
3	118.07 or 126.46	7.29 or 8.07	2	-
4	145.36	-	-	2 or 3
5	114.73	8.10	-	7
6	144.24	-	-	5, 7
7	14.55	2.38	-	-

The other isolated compound (0.2 % yield) was unusual as it appeared to contain two ethyl esters with the same chemical environment according to the ^1H NMR spectrum (Figure 4.13). ^{13}C NMR (Figure 4.14), COSY, HMQC, and HMBC 2D NMR spectroscopic data provided further structural information about the molecule (refer to Section 2 of the Appendices for the 2D NMR spectroscopic data). After analysis of the NMR spectroscopic data the compound was assigned as diethyl 2-((6-chloropyridazin-3-yl)amino)-2-methylmalonate (**276**) (Table 4.4). The mechanism for the synthesis of this minor side-product is unknown, however, it is suspected that it may have been produced via an $\text{S}_{\text{N}}1$ reaction involving **210** and a malonate impurity in the ethyl 2-chloroacetoacetate starting material.

Chapter 4

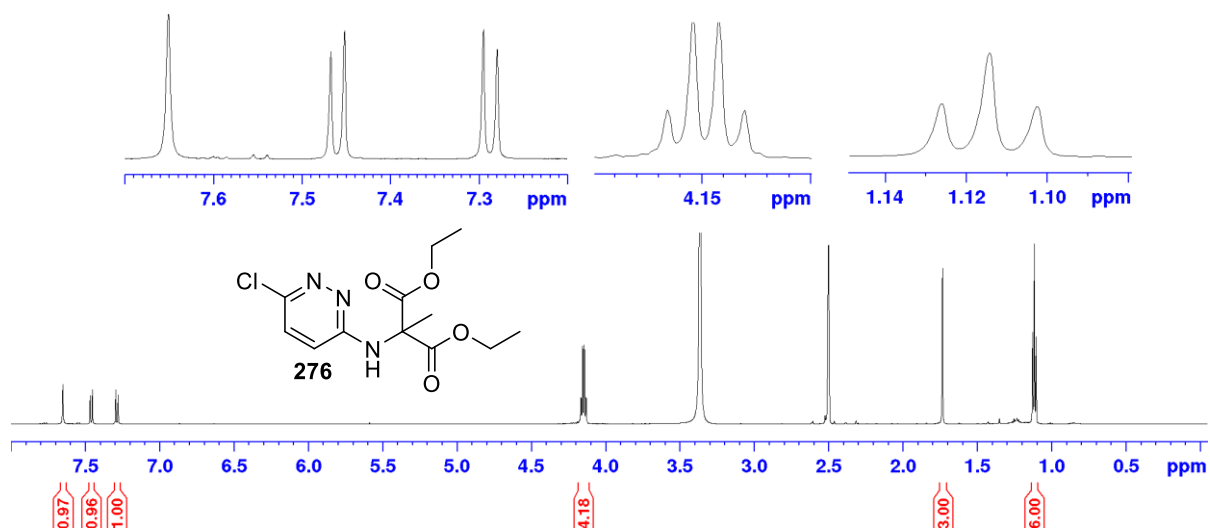


Figure 4.13: ^1H NMR spectrum of **276** in $\text{DMSO-}d_6$

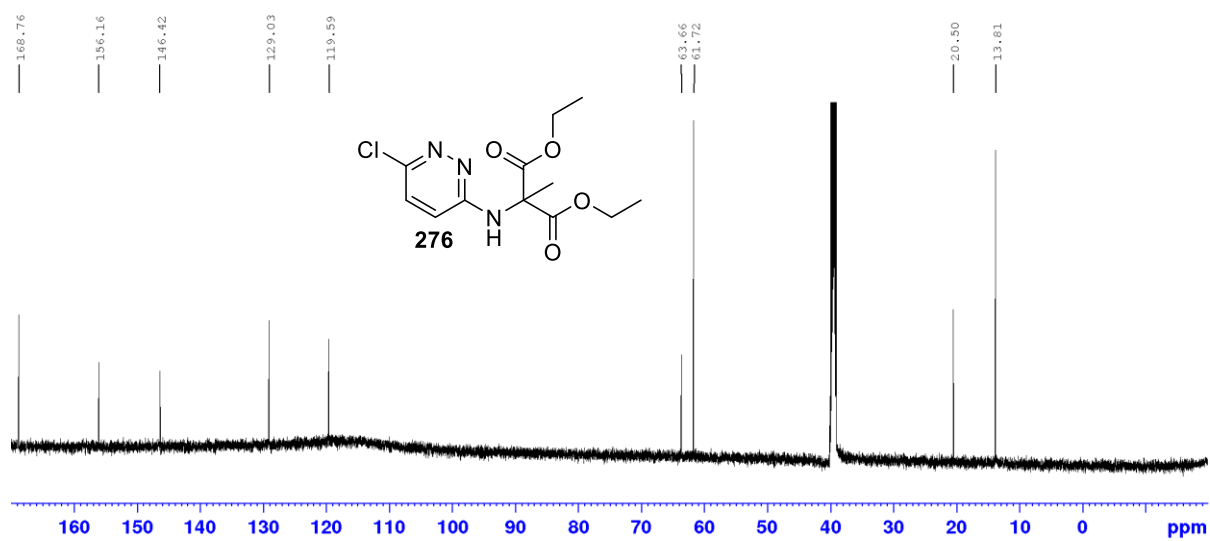
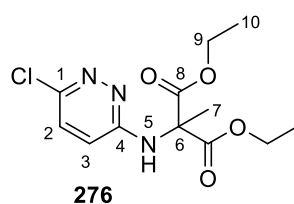


Figure 4.14: ^{13}C NMR spectrum of **276** in $\text{DMSO-}d_6$

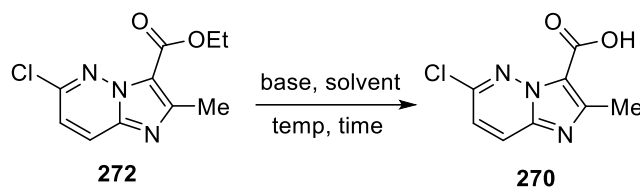
Chapter 4

Table 4.4: ^{13}C , ^1H and 2D NMR spectroscopic data from **276**



Atom #	^{13}C (ppm)	^1H (ppm)	COSY atom correlation	HMBC atom correlation (^{13}C to ^1H)
1	146.24	-	-	2 or 3
2	119.59 or 129.03	7.29 or 7.46	3	5
3	119.59 or 129.03	7.29 or 7.46	2	5
4	156.15	-	-	5; 2 or 3
5	-	7.65	-	-
6	63.66	-	-	5, 7
7	20.50	1.73	-	5
8	168.72	-	-	5, 9, 7
9	61.72	4.15	10	10
10	13.80	1.11	9	9

Saponification of the ethyl ester of **272** (Scheme 4.8) was achieved after some experimentation (Table 4.5). Initially, ester **272** was stirred with lithium hydroxide monohydrate in aqueous ethanol for 16.5 hours at room temperature (Entry 1). An 82 % recovery of starting ester **272** indicated that these reaction conditions were insufficient.



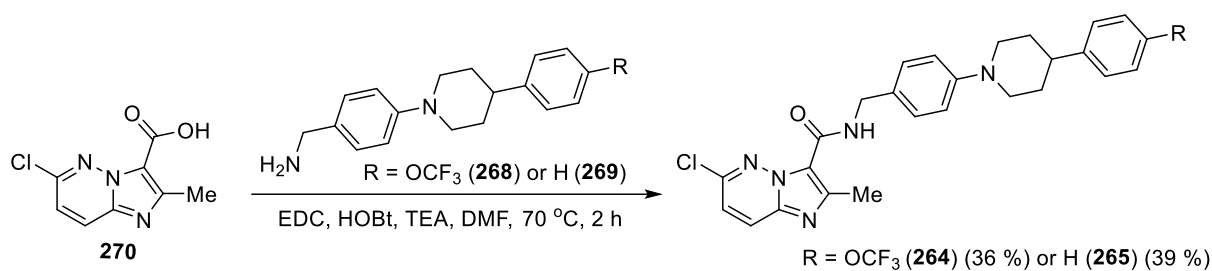
Schemed 4.8

Table 4.5: Synthetic protocols for 6-chloro-2-methylimidazo[1,2-*b*]pyridazine-3-carboxylic acid (**270**)

Entry	Base	Solvent	Temperature (°C)	Time (h)	Yield (%)
1	LiOH.H ₂ O	~33 % H ₂ O/EtOH	RT	16.5	-
2	NaOH	50% H ₂ O/EtOH	60	17.5	57

The alternative conditions involving sodium hydroxide was used as the base and a 50 % H₂O/EtOH mixture as the solvent system (Entry 2, Table 4.5) resulted in the synthesis of the imidazo[1,2-*b*]pyridazine carboxylic acid **270** with a yield of 57 %. The improved outcome of this reaction is thought to be due to the increased solubility of the sodium hydroxide in the solvent system.

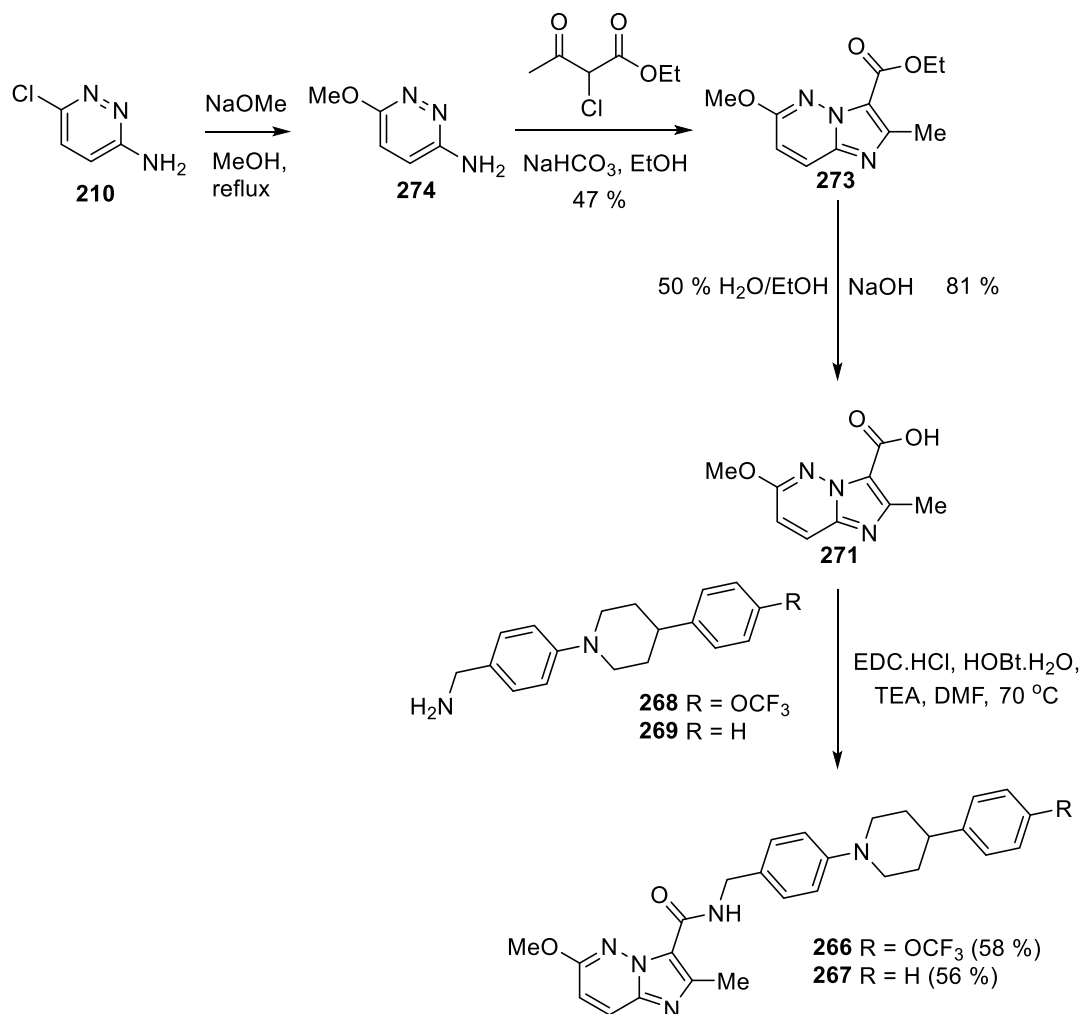
The EDC/HOBt-mediated coupling reactions of acid **270** with each of amines **268** and **269** (each prepared by Robin Henches) afforded Q203/TB47 analogues **264** and **265** in yields of 36 % and 39 %, respectively (Scheme 4.9). In the ¹H NMR spectra, the presence of a broad singlet at 8.69 ppm and a doublet at 4.68 ppm (*J* = 5.6 Hz), attributable to the amide hydrogen atom and methylene group, respectively, indicated successful amide coupling (refer to Chapter 8.15 and Appendices section 1).



Scheme 4.9: Synthesis of Q203/TB47 imidazo[1,2-*b*]pyridazines **264** and **265**

Inspired by the biological activity of TB47, the 6-Cl group in the imidazo[1,2-*b*]pyridazine ring systems of **264** and **265** was replaced with a 6-OMe group.⁹¹ In order to install the 6-OMe group on the 6-methoxyimidazo[1,2-*b*]pyridazine-3-carboxylate precursor (**273**), Robin Henches (CSIRO, 2018) heated 6-chloropyridazine-3-amine (**210**) with sodium methoxide in methanol at reflux to produce 6-methoxypyridazine-3-amine (**274**) (Scheme 4.10), according to a literature procedure.¹⁰⁰

The remainder of the synthetic pathway was analogous to that used for the synthesis of 6-chloroimidazo[1,2-*b*]pyridazine-3-carboxamides **264** and **265** (Scheme 4.10). Ethyl 2-methyl-6-methoxyimidazo[1,2-*b*]pyridazine-3-carboxylate (**273**) was synthesised (47 % yield) by heating **274** with ethyl 2-chloroacetoacetate in ethanol at reflux. After 4 hours, sodium bicarbonate was added and the reaction mixture was heated at reflux for a further 2.5 hours to drive the reaction to completion. Interestingly, the crude material was a lot cleaner in comparison to the crude material from the analogous reaction with the 6-Cl substrate (Entry 3 of Table 4.2). For Entry 3 in Table 4.2 more side-products were formed and the reaction did not go to completion after 34 hours. In the synthesis of **273**, the reaction went to completion within 6.5 hours and with very few side-products. The electron-donating effect of the 6-methoxy group appeared to activate the pyridazine ring to undergo the desired reaction. Base hydrolysis of the ethyl ester of **273** using sodium hydroxide in aqueous ethanol produced **271** in 81 % yield. Subsequent EDC.HCl/HOBT.H₂O amide coupling of **271** to each of amines **268** and **269** produced carboxamides **266** (58 %) and **267** (56 %), respectively. Similarly, to compounds **264** and **265**, formation of the amide bond in carboxamides **266** and **267** was inferred due to the presence of a broad singlet at 8.75-8.76 ppm (amide hydrogen atom) and a doublet at 4.61 ppm ($J = 4.6$ - 4.7 Hz) (methylene group) in the ¹H NMR spectra.



Scheme 4.10: Synthetic pathway for Q203/TB47 imidazo[1,2-*b*]pyridazines **266** and **267**

4.5 Conclusions

Despite their close similarity to imidazo[1,2-*b*]pyridazin-3-ols, the efforts to synthesise similar imidazo[2,1-*b*][1,3,4]thiadiazol-5-ols or imidazo[2,1-*b*][1,3,4]oxadiazol-5-ols were unsuccessful, after an investigation of a range of conditions. It appeared that the 2-amino[1,3,4]thiadiazole and 2-amino[1,3,4]oxadiazole starting materials were not sufficiently strong bis-nucleophiles to condense with phenylglyoxal monohydrate derivatives.

Four imidazo[1,2-*b*]pyridazine analogues of the known antitubercular compounds Q203 and TB47, carboxamides **264**, **265**, **266** and **267**, were synthesised via a convenient and efficient general protocol.

Chapter 5.
***In Vitro* Evaluation**

Chapter 5 Summary

Chapter 5 describes the *in vitro* antimycobacterial activity against *Mycobacterium tuberculosis* (*Mtb*) and *Mycobacterium marinum* (*Mm*) and the structure-activity-relationships (SARs) of the imidazo[1,2-*b*]pyridazines that were discussed in Chapters 2, 3 and 4. Selected imidazo[1,2-*b*]pyridazines from the CSIRO library were also evaluated for their inhibition of *Mtb* and *Mm*.

5.1 Structure Activity Relationships (SARs) of imidazo[1,2-*b*]pyridazines against *Mtb* and *Mm*

Mm was used as a surrogate for *Mycobacterium ulcerans* (*Mu*) and is 99.6 % identical in genome DNA to *Mu*.¹⁰¹ *Mm* is used instead of *Mu* since *Mm* replicates at a much higher rate and rarely causes disease in humans.¹⁰¹ A stable and virulent autoluminescent *Mtb* H37Rv (AIRv) and an autoluminescent reporter of *Mu* (Almu) were used. Feng Yang et al,¹⁰² Tianyu Zhang et al¹⁰³ and Goverdhan Surineni¹⁰⁴ describe the bioassay/detection methods used for this chapter. Rifampicin (RIF) was used as a positive control and carboxymethyl cellulose sodium (CMC-Na) was used as a negative control. For this Chapter, if a compound is coloured in black, that compound was synthesised in the work described in Chapters 2, 3 or 4. If a compound structure is coloured in dark blue, that compound was extracted from the CSIRO library or/and synthesised by Deborah A. Hughes (2016-2017). Additionally, if a compound is referred to as inactive, its MIC is ≥ 100 $\mu\text{g}/\text{mL}$. All imidazo[1,2-*b*]pyridazines synthesised in this PhD work (and CSIRO library compounds used for confirmatory testing) were required to pass a Quality Control (QC) process before being submitted for testing. To pass QC, the compound sample required a purity greater than or equal to 90 % (by ^1H NMR spectroscopy and LC-MS analysis). However, compounds in the original High Throughput Screening (HTS) campaign were not subjected to these Quality Control measures (these compounds have their IC₅₀ and MIC values in Table 5.1 coloured in grey). Some of these compounds (mostly those with apparent biological activity) had their purity checked via ^1H NMR spectroscopy and LC-MS analysis after the original HTS campaign. The IC₅₀ and MIC values of these compounds are coloured in purple if their purity was between 85 – 90 %, light blue if their purity was between 80 – 85 %, orange if the compound was not subjected to LC-MS but their ^1H NMR spectrum and LR-MS chromatogram indicated high purity and red if the compound failed the QC measures, in Table 5.1, Table 5.2, and Table 5.3 below.

More than 200 imidazo[1,2-*b*]pyridazine derivatives from the CSIRO library were screened against *Mtb* in a HTS campaign in 2016 and these results enabled some early SARs to be established (Figure 5.1). Generally, imidazo[1,2-*b*]pyridazines with various phenyl units at C2, a methoxy group at C3 and various benzyl units with a heteroatom linker (O, S, or N) at C6 were of interest. Table 5.1 below shows a selection of variously substituted imidazo[1,2-*b*]pyridazines in the CSIRO library that were screened against *Mtb* and *Mm* and generally

differ in structure to the most active derivatives. These imidazo[1,2-*b*]pyridazines were generally weakly active or inactive with some exceptions. For example, imidazo[1,2-*b*]pyridazines **25** and **26** (Entries 2 and 3) possessed a benzyl unit, rather than a phenyl moiety, at C2 of the imidazo[1,2-*b*]pyridazine ring system and had weak to no activity.

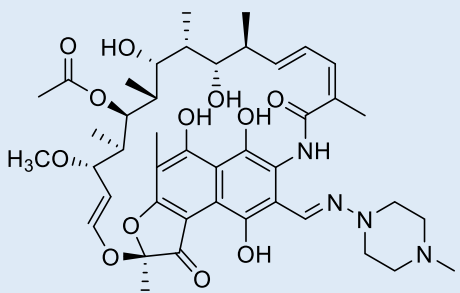
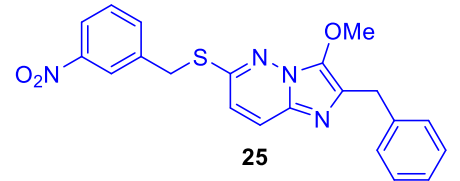
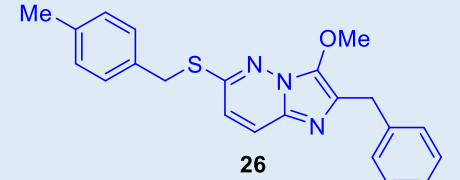
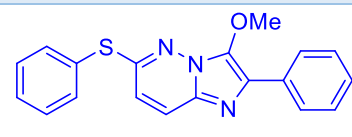
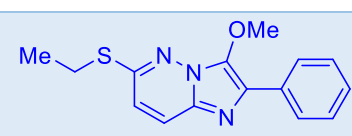
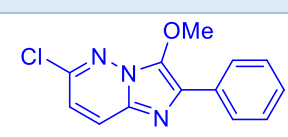
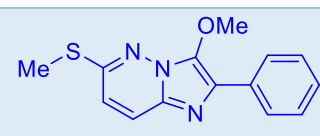
The activities of imidazo[1,2-*b*]pyridazines **27**, **28**, **277** and **164** (Entries 4 to 7) demonstrate the importance of the 6-benzyl unit (refer to imidazo[1,2-*b*]pyridazines **64**, **147**, **15** and **19** in Table 5.2 in Entries 2, 15, 20 and 21, respectively, and **18** and **53** in Table 5.3 in Entries 2 and 12, respectively) since truncation of this moiety generally results in weaker activity. For example, compounds **27**, **28** and **277** (Entries 4 to 6), possessing a 6-phenylthio, a 6-ethylthio and a 6-chloro respectively, showed weak to no activity. The 6-methylthio compound **164** (Entry 7) showed moderate activity (MIC = 4 – 5 µg/mL against *Mtb*) but this was weaker than activities of imidazo[1,2-*b*]pyridazines with a benzyl moiety linked by a heteroatom (O, S or *N*-Me) at C6. It appears that a distal aromatic moiety connected to C6 of the imidazo[1,2-*b*]pyridazine core via a flexible two atom linker facilitates activity, as demonstrated by **64** and **19** (Table 5.2, Entries 2 and 21). Bulky aromatic groups closer to the imidazo[1,2-*b*]pyridazine core, such as the 6-phenylthio in **27** (Entry 4), have the opposite effect. Additionally, similar results to **277** (Entry 6) were seen with other imidazo[1,2-*b*]pyridazines possessing halogens at C6 (**29** and **30**, Entries 8 and 9).

Further corroborating the importance of the benzyl moiety linked to C6, other imidazo[1,2-*b*]pyridazines possessing 6-phenylthio or 6-phenyloxy groups with different substitutions on the aromatic ring resulted in a loss of activity (**31** to **36** and **278**, Entries 10 to 16). 6-Methylthio derivative **37** (Entry 17) showed lower activity than the 6-benzylthio derivatives. Replacing the 2-phenyl moiety with alkyl groups such as a 2-methyl group while keeping the 6-benzyloxy substituent (**38**, Entry 18) did not improve the activity against *Mtb*. Only moderate activity was observed when an aromatic group was attached via two carbon units to the C2 position of the imidazo[1,2-*b*]pyridazine ring system (**39**, Entry 19); similar to 2-benzyl derivatives **25** and **26** (Entries 2 and 3).

Changing the 3-methoxy group to a 3-(acetoamidomethyl) (**279**, Entry 20), a 3-(benzamidomethyl) (**40** – **42**, Entries 21 to 23) or a 3-*N,N,N*-trimethylmethanaminium moiety (**43**, Entry 24) also resulted in a loss of activity, providing evidence for the importance of the

3-methoxy substituent. The installation of a dimethylaminomethyl group at C3 (**280**, **44**, Entries 25 and 26) resulted in relatively high antimycobacterial activity. The activity of 3-dimethylaminomethyl derivative **44** in Entry 26 (as discussed in Chapter 3) inspired the synthesis of **225**, **229** and **230** (Table 5.4, Entries 18 to 20); SARs involving these two compounds are discussed below. Activity was only observed for specific derivatives possessing (smaller) 3-dimethylaminomethyl groups. The 3-unsubstituted **45** (Entry 27) or 3-methylthiomethyl derivative **46** (Entry 28) lacked activity. Deborah A. Hughes (2017) further probed C3 SARs by synthesising compounds **47**, **281** and **282** (Entries 29 to 31) and testing their antimycobacterial activity. 6-Benzyloxy-3-*halo*-2-phenylimidazo[1,2-*b*]pyridazine derivatives generally resulted in poorer activity against *Mtb*. No activity was also observed if these halogens were replaced with a nitrile (**48**, Entry 32). In one experiment, 6-benzyloxy-3-methyl-2-phenylimidazo[1,2-*b*]pyridazine **49** (Entry 33) exhibited an MIC of 0.5 µg/mL against *Mtb* but was inactive (>100 µg/mL) in two other 2 experiments. These results appear to reinforce the finding that a methoxy group at C3 of the imidazo[1,2-*b*]pyridazine is associated with strong antimycobacterial activity.

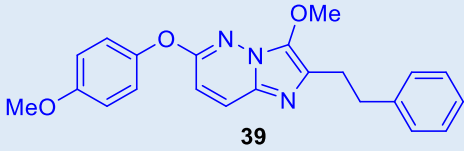
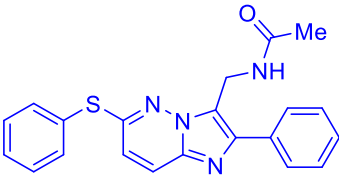
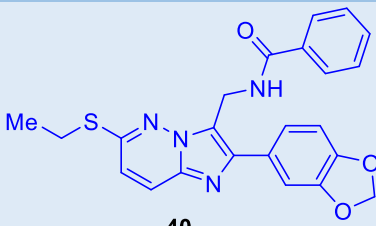
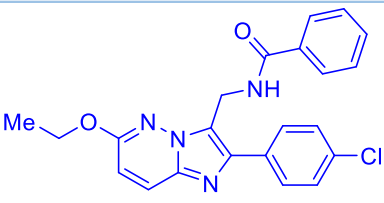
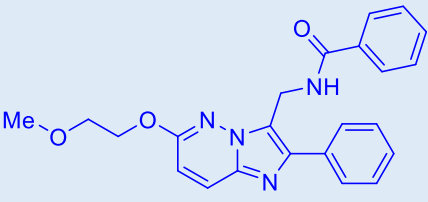
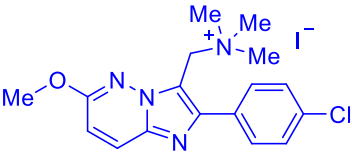
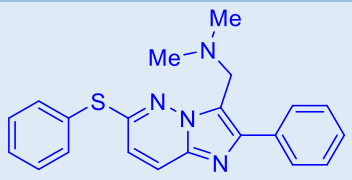
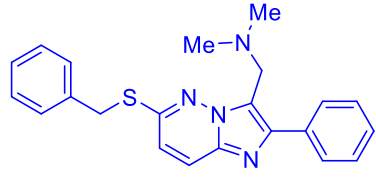
Table 5.1: Imidazo[1,2-b]pyridazines from CSIRO Library - IC_{50} values against *Mtb* and MIC values against *Mtb* and *Mm*

Entry	Structure	IC_{50} range (μ M) against <i>Mtb</i>	MIC range (μ g/mL) against <i>Mtb</i>	MIC range (μ g/mL) against <i>Mm</i>
1	 <p>RIF</p>	-	0.06 – 0.25	0.2
2	 <p>25</p>	11.0	>100	-
3	 <p>26</p>	12.4 – 33.3	5 - 100	10
4	 <p>27</p>	12.5 – 37.5	50	-
5	 <p>28</p>	12.5 – 43.8	50	-
6	 <p>277</p>	2.05 – 96.3	100	-
7	 <p>164</p>	3.69 – 10.6	4 - 5	10

Chapter 5

8	 29	>30	>100	-
9	 30	6.58 – 94.1	50	-
10	 31	1.26	100	100
11	 278	>30	>100	>100
12	 32	25 – 72	100	-
13	 33	13.4 – 132.8	100	-
14	 34	>30	>100	-
15	 35	5.73	>100	>100
16	 36	12.4	>100	-
17	 37	7.96	-	-
18	 38	>30	-	-

Chapter 5

19	 <p style="text-align: center;">39</p>	12.5 – 33.3	20 - 25	10
20	 <p style="text-align: center;">279</p>	>30	>100	>100
21	 <p style="text-align: center;">40</p>	>30	-	-
22	 <p style="text-align: center;">41</p>	>30	-	-
23	 <p style="text-align: center;">42</p>	>30	-	-
24	 <p style="text-align: center;">43</p>	>30	-	-
25	 <p style="text-align: center;">280</p>	3.98	-	-
26	 <p style="text-align: center;">44</p>	1.92 – 10.7	2 - 8	5

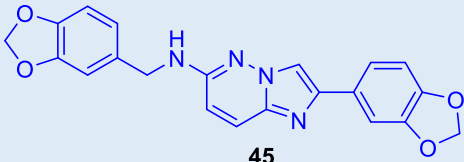
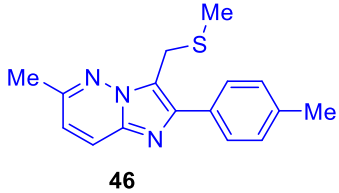
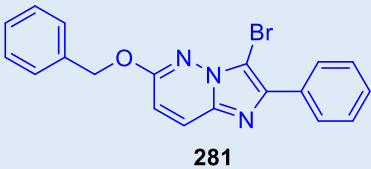
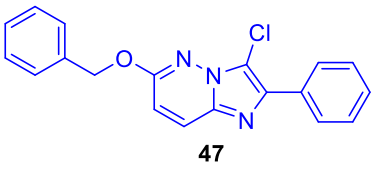
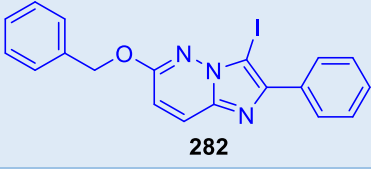
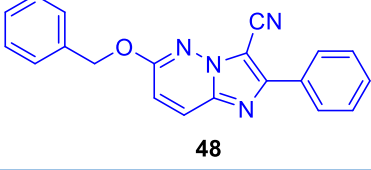
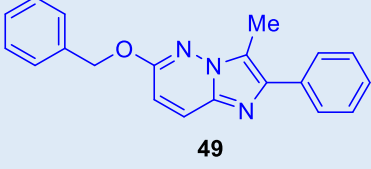
27	 45	28.2	-	-
28	 46	>30	>100	-
29	 281	>100	>100	>100
30	 47	60	20 - 100	-
31	 282	>100	>100	>100
32	 48	>100	>100	>100
33	 49	-	0.5 - 100	0.25 - 100

Figure 5.1 below shows the general initial SAR analysis of the imidazo[1,2-*b*]pyridazine derivatives tested and includes moieties that enhance activity such as various phenyl units at C2, a methoxy group at C3 and various benzyl units with a specific heteroatom linker (O, S or *N*-Me). The MIC values of generally more active compounds and closely structurally related derivatives are shown in Tables 5.2, 5.3 and 5.4. The MIC values of Q203/TB47 hybrid imidazo[1,2-*b*]pyridazines and pyridazine side-products are shown in Tables 5.5 and 5.6. The SARs of these compounds are discussed below.

Chapter 5

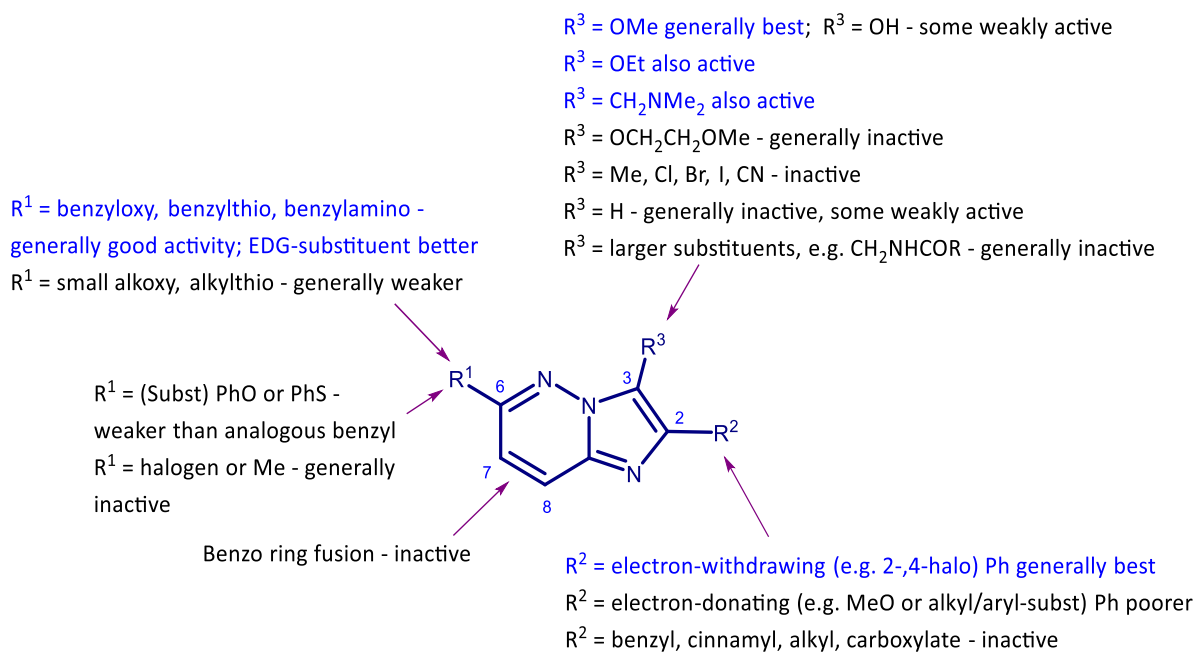
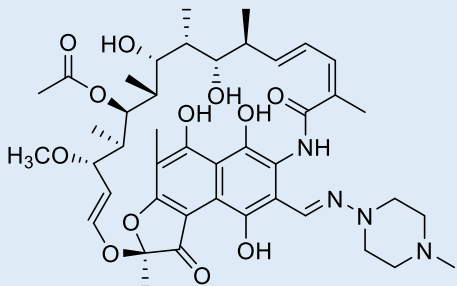
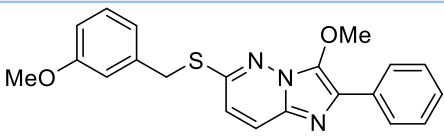
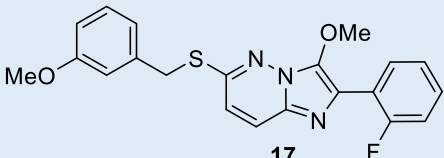
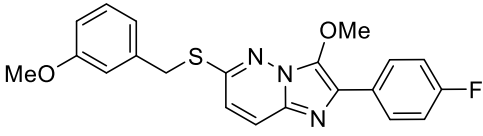
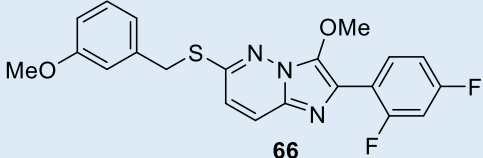
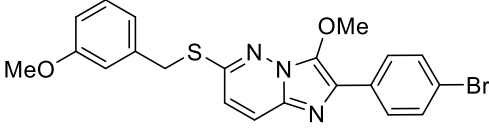
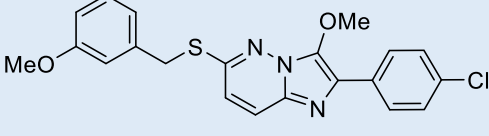


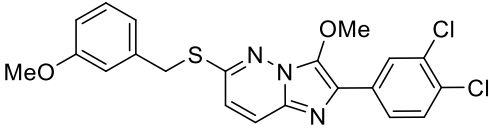
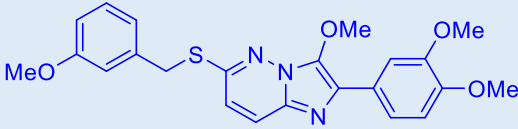
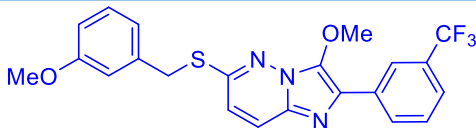
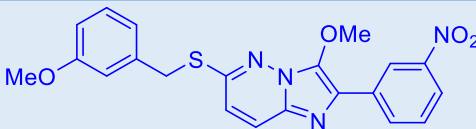
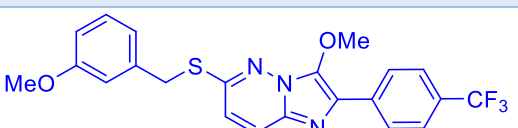
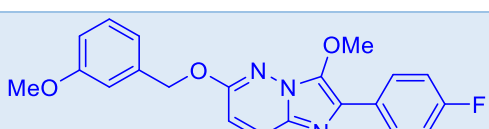
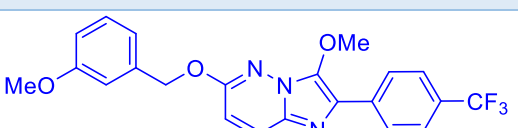
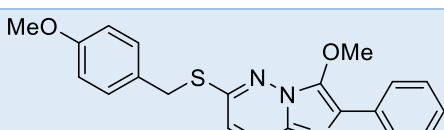
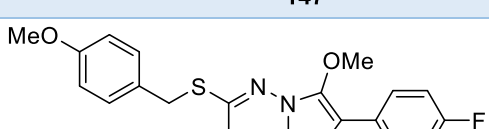
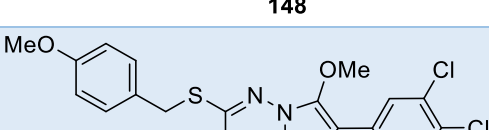
Figure 5.1: Initial SAR Analysis, after screening of CSIRO library compounds

Chapter 5

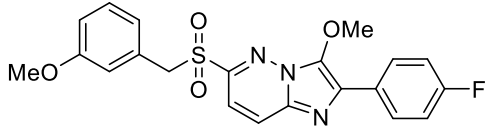
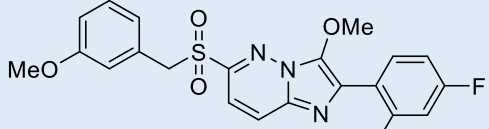
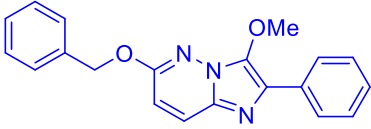
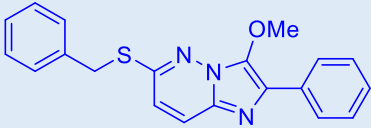
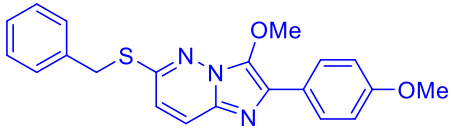
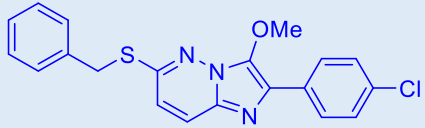

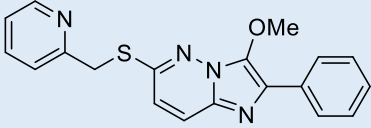
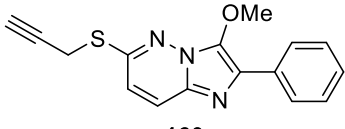
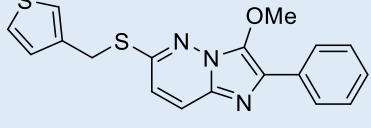
Table 5.2: 6-(substituted)thio- and 6-(substituted)oxy-Imidazo[1,2-b]pyridazine MIC values against *Mtb* and *Mm*

Entry	Structure	MICs ($\mu\text{g/mL}$) against <i>Mtb</i>	MICs ($\mu\text{g/mL}$) against <i>Mm</i>
1	 <p>RIF</p>	0.06 – 0.25	0.2
2	 <p>64</p>	≤ 0.625	1
3	 <p>17</p>	0.25 - 50	0.06
4	 <p>65</p>	0.25 - 5	0.25 - 0.5
5	 <p>66</p>	6.25 - 20	0.5 - 5
6	 <p>144</p>	5	5
7	 <p>145</p>	4	1.25

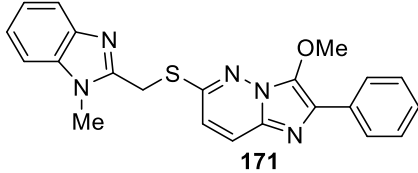
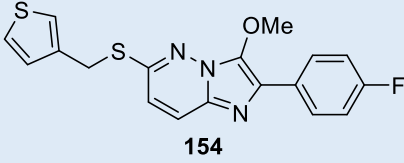
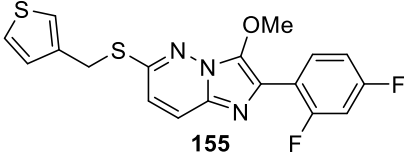
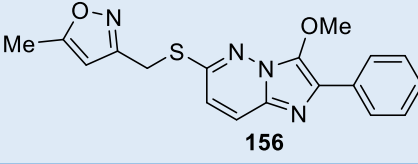
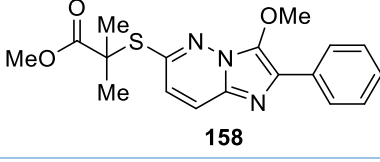
Chapter 5

8	 <p>146</p>	>100	>100
9	 <p>34</p>	>30 - 100	>100
10	 <p>283</p>	>100	-
11	 <p>284</p>	>100	>100
12	 <p>285</p>	>100	>100
13	 <p>16</p>	1 - 25	-
14	 <p>286</p>	>100	>100
15	 <p>147</p>	2	2 - 100
16	 <p>148</p>	2.5	5
17	 <p>149</p>	>100	>100

Chapter 5

18	 <p>174</p>	100	100
19	 <p>175</p>	100	100
20	 <p>15</p>	1 - 10	0.25 - 0.5
21	 <p>19</p>	0.5 - 10	0.25
22	 <p>287</p>	1 - 100	0.5
23	 <p>288</p>	1 - 100	1
24	 <p>52</p>	2.5 - 100	1.25
25	 <p>151</p>	2	1
26	 <p>160</p>	2.5	5
27	 <p>153</p>	0.25	0.5

Chapter 5

28	 171	10	100
29	 154	10	2
30	 155	4	1
31	 156	100	100
32	 158	10 - 100	10 - 100

3-Methoxyimidazo[1,2-*b*]pyridazines **17**, **34**, **64** – **66**, **144** – **146**, **283** – **285** which include some of the most potent compounds identified in this study, have a 6-(3-methoxybenzyl)thio group with various substitutions on the 2-phenyl ring (Table 5.2, Entries 1 – 12). On the C2-phenyl substituent, no substitution resulted in an MIC of ≤ 0.625 $\mu\text{g}/\text{mL}$ against *Mtb* (**64**, Entry 2) and a 2-fluoro (**17**, Entry 3) or a 4-fluoro substitution (**65**, Entry 4), in certain evaluations, resulted in similarly strong antimycobacterial activities against *Mtb* (0.25 $\mu\text{g}/\text{mL}$) and *Mm* (0.06 $\mu\text{g}/\text{mL}$ and 0.25 $\mu\text{g}/\text{mL}$, respectively). Strong activity was also observed when fluorine atoms were introduced at the 2- and 4-positions of the 2-phenyl moiety, such as in compound **66** (Entry 5, 6.25 - 20 $\mu\text{g}/\text{mL}$ against *Mtb*), or if other halogens, such as bromine and chlorine, were introduced to the para- position of the 2-phenyl group, as in compounds **144** and **145** (Entries 6 to 7), respectively. However, complete loss of activity was observed when two chlorine or methoxy groups were introduced in the 3- and 4-positions of the 2-phenyl group, as in compounds **146** and **34** (Entries 8 and 9), respectively. Furthermore, if a single trifluoromethyl (**283**, Entry 10) or nitro group (**284**, Entry 11) was substituted at the 3-position of the 2-phenyl

ring, the compound became inactive. It appears that substitutions at the 3-position or the 3,4-positions of the 2-phenyl ring of 3-methoxy-6-((3-methoxybenzyl)thio)imidazo[1,2-*b*]pyridazines result in a loss of activity. The 2-(4-trifluoromethylphenyl)-substituted derivative **285** (Entry 12) was inactive, in contrast to **65**, containing a 2-(4-fluorophenyl) moiety, which showed relatively high activity. A similar observation was made with 6-((3-methoxybenzyl)oxy)imidazo[1,2-*b*]pyridazines **16** and **286** (Entries 13 and 14).

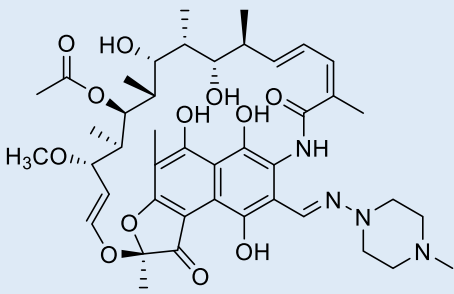
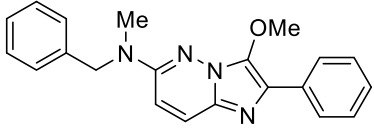
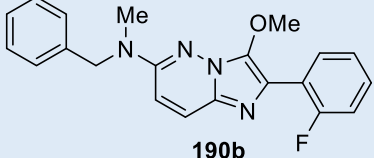
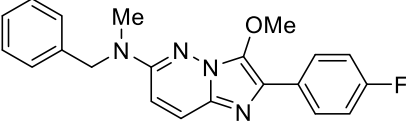
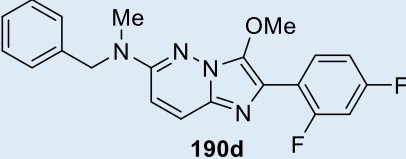
Comparisons of **147** (Entry 15) to **64** and **148** (Entry 16) to **65**, suggest that the 6-(3-methoxybenzyl)thio moiety increases activity subtly but consistently more than the 6-(4-methoxybenzyl)thio moiety. The lack of activity exhibited by compound **149** (Entry 17) was believed to be caused by the 2-(3,4-dichlorophenyl) group. This result was corroborated by the inactivity of 6-(3-methoxybenzyl)thio derivative **146**, also possessing the 2-(3,4-dichlorophenyl) moiety. Oxidation of the thioether in the 6-(3-methoxybenzyl)thio group to the corresponding sulfone resulted in a loss of activity, as demonstrated by sulfones **174** and **175** (Entries 18 and 19).

6-Benzoyloxy derivative **15** (Entry 20) and 6-benzylthio analogue **19** (Entry 21), exhibited similar MIC values against *Mtb*, indicating that the linker heteroatom can be interchanged between oxygen and sulfur without adverse effect. This finding is corroborated by the assay results from compounds **65** and **16** which also possess a 6-(3-methoxybenzyl)thio group and a 6-(3-methoxybenzyl)oxy group, respectively. Compounds **287** (Entry 22) and **288** (Entry 23) both contain a 6-benzylthio substituent but different substitutions on the 2-phenyl ring; the 4-methoxyphenyl **287**, and the 4-chlorophenyl derivative **288** had comparable activities against *Mtb*. A comparison between the activities of 6-(2-chlorobenzyl)thio derivative **52** (Entry 24) and 6-(3-methoxybenzyl)thio analogue **64**, indicated that the 6-(3-methoxybenzyl)thio substitution pattern increased the potency of the imidazo[1,2-*b*]pyridazine ring system more than the 6-(2-chlorobenzyl)thio group in **52**.

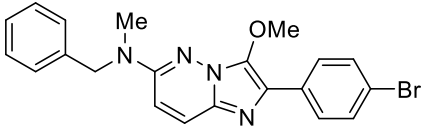
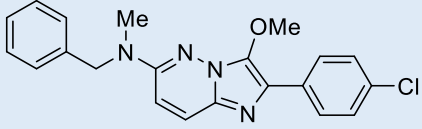
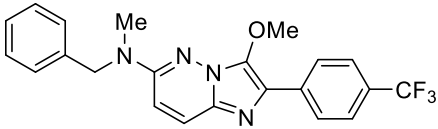
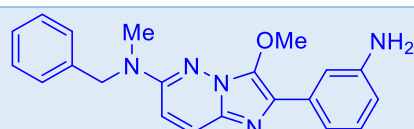
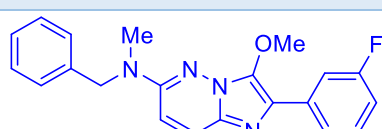
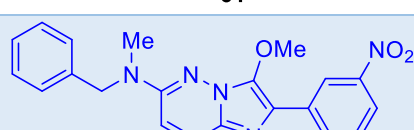
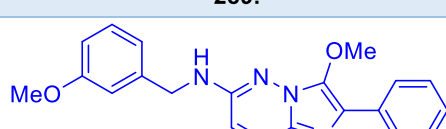
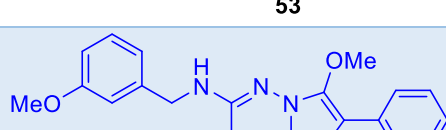
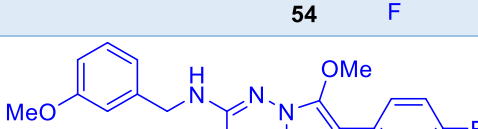
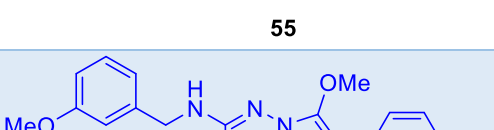
The antimycobacterial activities of 6-*heterocyclic*-methylthio-3-methoxyimidazo[1,2-*b*]pyridazines and related compounds were also analysed. Pyridylmethylthio derivative **151** (Entry 25) and compound **160** (Entry 26) possessing an *S*-propargyl group (intended to be a triazole precursor) both showed moderately high activities (MIC = 2 µg/mL and 2.5 µg/mL against *Mtb* respectively) whereas **153** (Entry 27) with a 3-thienyl group showed a greater

activity (0.25 $\mu\text{g}/\text{mL}$). A slight loss in activity was observed when the 3-thienyl group in **153** was replaced with a 2-(1-methyl-1*H*-benzo[*d*]imidazole) moiety in **171** (Entry 28, MIC = 10 $\mu\text{g}/\text{mL}$). This activity was maintained with 3-thienyl compounds **154** (Entry 29) and **155** (Entry 30). However, unlike the other 6-*heterocyclic*-imidazo[1,2-*b*]pyridazines, 3-(5-methylisoxazole) **156** (Entry 31) was not active. Methyl ester **158** (Entry 32) also showed a lack of inhibition against *Mtb* and *Mm*.

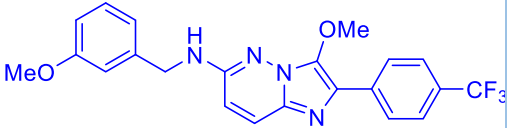
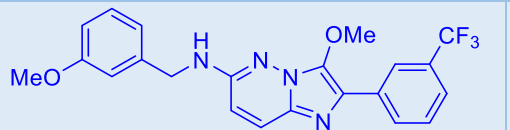
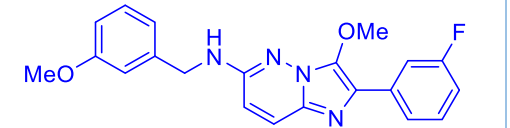
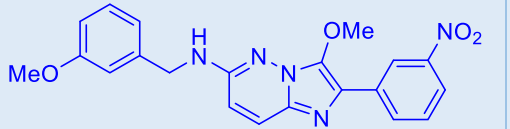
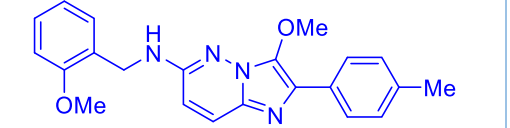
Table 5.3: 6-Benzylamino-imidazo[1,2-*b*]pyridazine MIC values against *Mtb* and *Mm*

Entry	Structure	MICs ($\mu\text{g}/\text{mL}$) against <i>Mtb</i>	MICs ($\mu\text{g}/\text{mL}$) against <i>Mm</i>
1	 <p style="text-align: center;">RIF</p>	0.06 – 0.25	0.2
2	 <p style="text-align: center;">18</p>	1 - 4	0.5
3	 <p style="text-align: center;">190b</p>	0.25	0.25
4	 <p style="text-align: center;">190c</p>	0.5	0.5
5	 <p style="text-align: center;">190d</p>	0.25	0.25

Chapter 5

6	 <p>190e</p>	2.5	5
7	 <p>190f</p>	2.5	2.5
8	 <p>190g</p>	2.5	5
9	 <p>60</p>	12.5 - 20	5
10	 <p>61</p>	2.5 - 25	1.25
11	 <p>289.</p>	>100	>100
12	 <p>53</p>	2.5 - 5	2.5
13	 <p>54</p>	2.5 - 5	2.5
14	 <p>55</p>	2.5 - 10	5
15	 <p>58</p>	2.5 - 5	5

Chapter 5

16	 59	5 - 20	10
17	 290	10 - 100	4
18	 291	20 - 100	10
19	 292	20 - 100	>100
20	 56	5 - 10	10

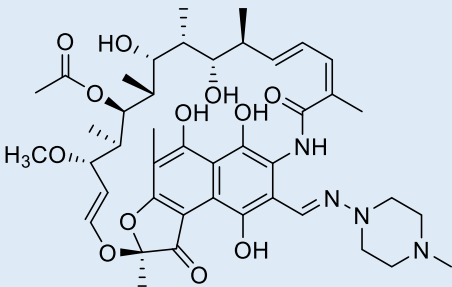
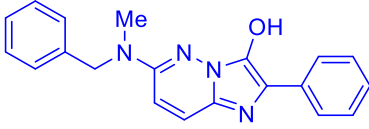
Substitutions on the 2-phenyl ring of 3-methoxy-6-(*N*-methylbenzylamino)-2-phenylimidazo[1,2-*b*]pyridazines were also analysed (Table 5.3). Compounds **18** and **190b** to **190g** (Entries 2 to 8), mostly containing halo-substituted C2-phenyl substituents, exhibited relatively high activity. Specifically, C2 fluorophenyl derivatives **190b** (Entry 3) and **190d** (Entry 5) exhibited superior MIC values at 0.25 $\mu\text{g}/\text{mL}$ for *Mtb* and *Mm*. Similar derivatives **195c** (Entry 4) with the 2-(4-fluorophenyl) and **18** (Entry 2) with the unsubstituted phenyl ring showed high activities (MIC = 0.5 $\mu\text{g}/\text{mL}$ and 1 - 4 $\mu\text{g}/\text{mL}$, respectively). Activity was slightly reduced when the phenyl ring was substituted with a 4-bromo- (**190e**, Entry 6), 4-chloro- (**190f**, Entry 7) or a 4-trifluoromethyl-substituent (**190g**, Entry 8). Moreover, fluorine substitution in the 2-position, the 4-position, or both the 2- and 4-positions appeared to enhance the antitubercular activity. However, compounds **60** (Entry 9), **61** (Entry 10) and **289** (Entry 11) having a 3-amino, a 3-fluoro or a 3-nitro group were generally less active suggesting that, in general, substitution on the 3-position of the 2-phenyl ring is deleterious. A similar SAR pattern was observed with the previously discussed 3-methoxy-6-((3-

methoxybenzyl)thio)-2-phenylimidazo[1,2-*b*]pyridazines in Table 5.2 in Entries 2 to 12 (**17**, **34**, **64 – 66**, **144 – 146**, **283 – 284**).

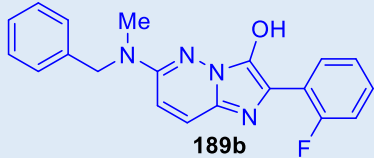
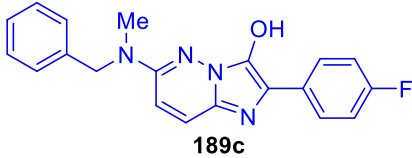
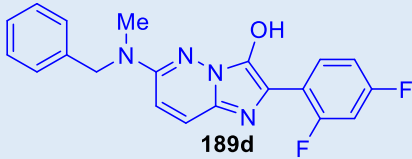
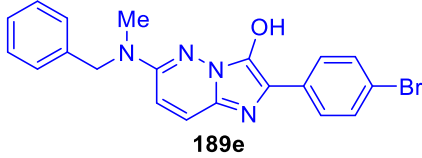
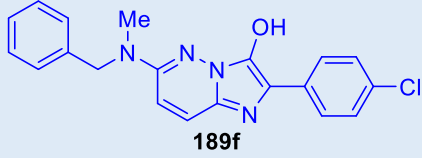
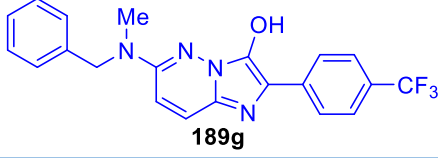
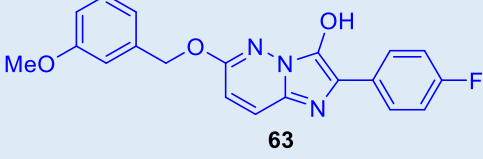
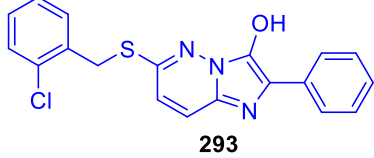
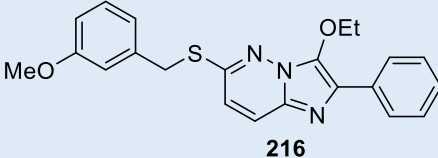
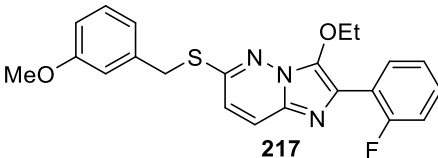
Generally, the 3-methoxy-6-(*N*-methylbenzylamino)-2-phenylimidazo[1,2-*b*]pyridazines (**18** and **190b** to **190g**) were more active than the 3-methoxy-6-((3-methoxybenzyl)thio)-phenylimidazo[1,2-*b*]pyridazines (**17**, **64 – 66**, **144**, **145** and **285**), indicating the 6-benzyl(methyl)amino substituent increases the inhibitory activity of the imidazo[1,2-*b*]pyridazine more than the 6-(3-methoxybenzyl)thio substituent.

The MIC results for a series of closely related 3-methoxy-6-(methoxy)benzylamino-2-phenylimidazo[1,2-*b*]pyridazines (**53 – 56**, **58**, **59**, **290 – 292**, Entries 12 to 19 in Table 5.3) from the CSIRO library were also consistent with the SAR pattern described above, but generally slightly less potent than the corresponding *N*-methyl analogues (**18** and **190b** to **190g**). For this group of compounds, having a non-substituted, 2-fluoro-substituted or a 4-fluoro-substituted C2 phenyl group, resulted in relatively high activity against *Mtb* (generally 2.5 – 5 µg/mL). A considerable loss in activity was observed when various groups were installed in the 3-position of the 2-phenyl ring.

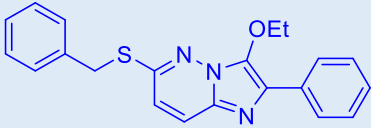
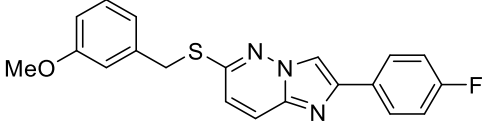
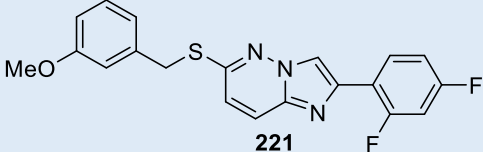
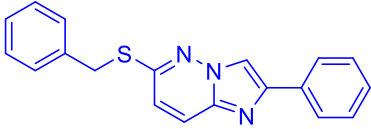
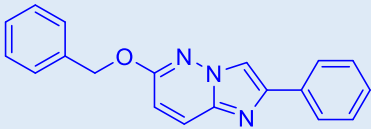
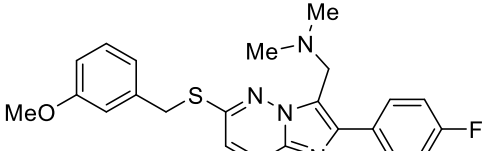
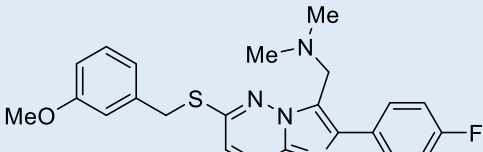
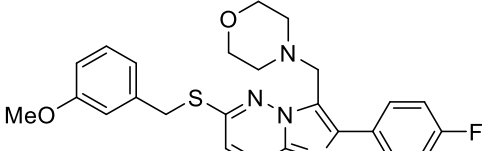
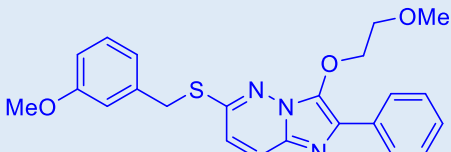
Table 5.4: Other 3-substituted-imidazo[1,2-*b*]pyridazine MIC values against *Mtb* and *Mm*

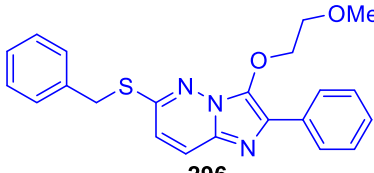
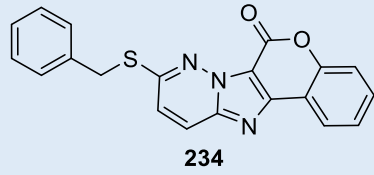
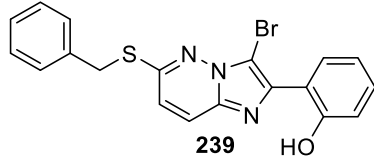
Entry	Structure	MICs (µg/mL) against <i>Mtb</i>	MICs (µg/mL) against <i>Mm</i>
1	 <p>RIF</p>	0.06 – 0.25	0.2
2	 <p>189a</p>	100	>100

Chapter 5

3	 <p>189b</p>	50	100
4	 <p>189c</p>	50	50
5	 <p>189d</p>	100	>100
6	 <p>189e</p>	100	>100
7	 <p>189f</p>	100	>100
8	 <p>189g</p>	>100	100
9	 <p>63</p>	6.25 - 50	25
10	 <p>293</p>	50	100
11	 <p>216</p>	1	0.5
12	 <p>217</p>	1.25	1.25

Chapter 5

13	 <p style="text-align: center;">20</p>	1-25	25
14	 <p style="text-align: center;">220</p>	10	1
15	 <p style="text-align: center;">221</p>	100	100
16	 <p style="text-align: center;">294</p>	>100	>100
17	 <p style="text-align: center;">295</p>	100	>100
18	 <p style="text-align: center;">229</p>	10	20
19	 <p style="text-align: center;">230</p>	100	100
20	 <p style="text-align: center;">225</p>	100	100
21	 <p style="text-align: center;">67</p>	12.5	50

22	 296	~100	25
22	 234	100	100
23	 239	100	100

Imidazo[1,2-*b*]pyridazin-3-ols **189a** to **189g** (Table 5.4, Entries 2 to 8), the precursors to the aforementioned 3-methoxyimidazo[1,2-*b*]pyridazines **18** and **190b** to **190g** (Table 5.3, Entries 2 to 8), showed very low to no activity. Comparisons between these compounds demonstrate the importance of the 3-methoxy moiety in the inhibition of *Mtb* and *Mm*. Compounds **63** and **293** (Table 5.4, Entries 9 and 10) possessing the 3-hydroxyl moiety also displayed low activity.

The activities of other 3-substituted imidazo[1,2-*b*]pyridazines were explored (Table 5.4). Compounds **216** (Entry 11), **217** (Entry 12) and **20** (Entry 13) with 3-ethoxy groups showed high activities with MIC values of around 1–1.25 $\mu\text{g}/\text{mL}$ against *Mtb* and *Mm*. However, in comparison to their respective, direct 3-methoxy analogues, **64** (≤ 0.625 $\mu\text{g}/\text{mL}$), **17** (0.25 – 50 $\mu\text{g}/\text{mL}$) and **19** (0.5 – 10 $\mu\text{g}/\text{mL}$) (Table 5.2 in Entries 2, 3 and 21, respectively), the 3-methoxy derivatives generally showed higher activity. For compounds unsubstituted at C3, for example, **220** (Entry 14) and **221** (Entry 15), **294** (Entry 16) and **295** (Entry 17), generally weak to no activity was observed. Notably, for the 3-unsubstituted-imidazo[1,2-*b*]pyridazines, the 2-(4-fluorophenyl) derivative **220** showed a greater activity than the 2-(2,4-difluorophenyl) derivative **221**, which was consistent with **65** and **66** (Table 5.2 in Entries 4 and 5, respectively). Similar comparative results were drawn between the 3-dialkylaminomethyl derivatives **229** (10 $\mu\text{g}/\text{mL}$), **230** (100 $\mu\text{g}/\text{mL}$) and **225** (100 $\mu\text{g}/\text{mL}$) (Entries 18 to 20) and 3-methoxy derivatives **65** and **66**. Introduction of 2-methoxyethoxy groups at C3 of the

imidazo[1,2-*b*]pyridazine ring system resulted in moderate activity (**67**, 12.5 µg/mL against *Mtb*, Entry 21) to no activity (**296**, ~100 µg/mL against *Mtb*, Entry 22); further confirming the importance of the 3-methoxy group, perhaps partly due to its relatively small size. Additionally, the incorporation of a 3-methoxy group on the C6 benzylthio substituent of **67** expectedly enhanced activity against *Mtb* and *Mm* (compared to **296**).

There is an apparent discrepancy in relative MIC values for imidazo[1,2-*b*]pyridazines with a 2-(4-fluorophenyl) or 2-(2,4-difluorophenyl) moiety (**65/66** (Table 5.2 in Entries 4 and 5, respectively), **220/221** (Table 5.4 in Entries 14 and 15, respectively) and **229/230** (Table 5.4 in Entries 18 and 19, respectively) versus **154/155** (Table 5.2 in Entries 29 and 30, respectively) and **190c/190d** (Table 5.3 in Entries 4 and 5, respectively). The relative activities of 2-(4-fluorophenyl) or 2-(2,4-difluorophenyl) substituted imidazo[1,2-*b*]pyridazines seemed to depend on the 6-substitution of the core ring system. 2-(4-Fluorophenyl)-6-((3-methoxybenzyl)thio)imidazo[1,2-*b*]pyridazines (**65**, **220**, **229**) were more active than 2-(2,4-difluorophenyl)-6-((3-methoxybenzyl)thio)imidazo[1,2-*b*]pyridazines (**66**, **221**, **230**). However, for imidazo[1,2-*b*]pyridazines without the 6-((3-methoxybenzyl)thio) group, 2-(2,4-difluorophenyl)imidazo[1,2-*b*]pyridazines (**155**, **190d**) were more active than 2-(4-fluorophenyl)imidazo[1,2-*b*]pyridazines (**154**, **195c**). These imidazo[1,2-*b*]pyridazines possessed either the 6-(thiophen-3-ylmethyl)thio or the 6-*N*-methylbenzylamino moiety. These results suggest that the activity depends on the combination of moieties at C2 and C6 of the imidazo[1,2-*b*]pyridazine ring system. Specific C2/C6 combinations may influence the overall electronic properties of the molecules, which consequently may have an impact on activity against *Mtb* and *Mm*. Additionally, specific substituents may alter the preferred molecular conformers which can directly affect binding ability with the target. The differences in activities of **285** and **286** (Table 5.2 in Entries 12 and 14, respectively) compared to **190g** and **59** (Table 5.3 in Entries 8 and 16, respectively) might also reflect specific electronic properties and/or different conformational isomers conferred by the C6 linker (oxo, thio, amino, or (methyl)amino) on the of the imidazo[1,2-*b*]pyridazine ring system.

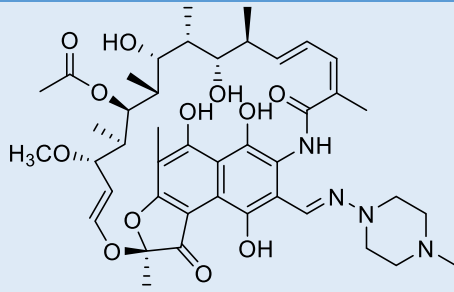
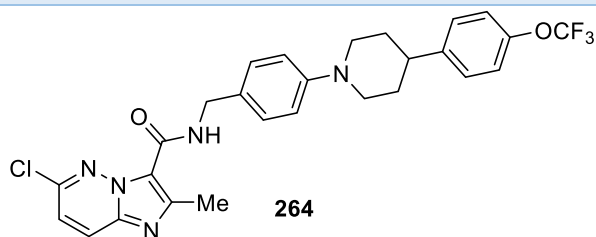
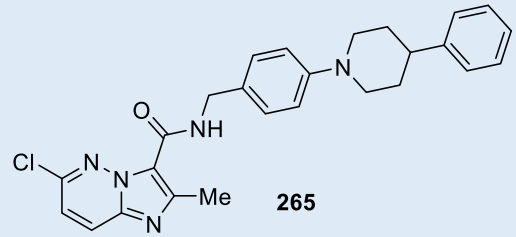
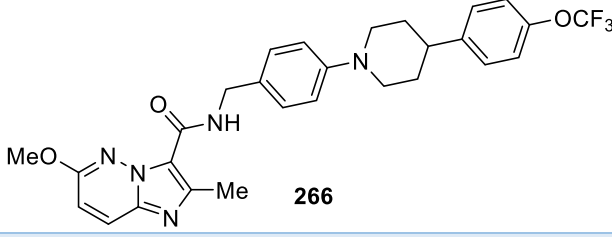
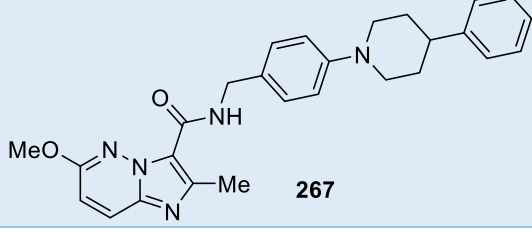
Lactone **234** and side-product **239** showed no activity against *Mtb* and *Mm* (Table 5.4 in Entries 22 and 23, respectively). Similarly, and disappointingly, no activity was observed for the Q203/TB47 imidazo[1,2-*b*]pyridazine hybrids **264**, **265**, **266** and **267** (Table 5.5). Apparently, lactone **234** was not able to inhibit Pks13, an enzyme involved in the biosynthesis

Chapter 5

of mycolic acid which was targeted by coumestans.^{87,105} Furthermore, Q203/TB47 imidazo[1,2-*b*]pyridazines were not able to inhibit QcrB, the target of Q203 and TB47.^{37,38} This latter finding in particular highlights that even an apparently subtle change to the core structure, such as introducing an extra nitrogen heteroatom, can have a dramatic effect on the compound's antimycobacterial activity.

Chapter 5

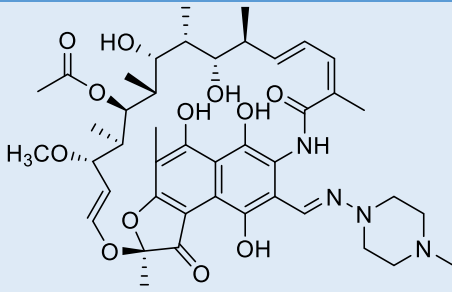
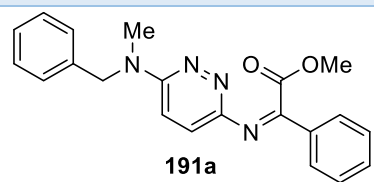
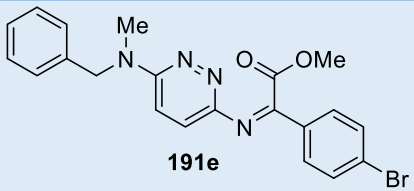
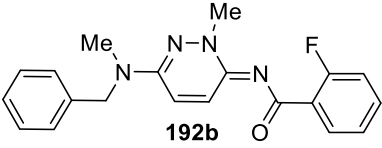
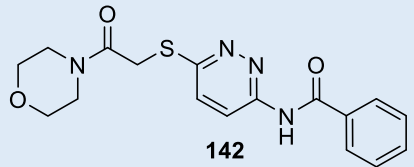
Table 5.5: Q203/TB47 hybrid imidazo[1,2-b]pyridazine MIC values against *Mtb* and *Mm*

Entry	Structure	MICs (µg/mL) against <i>Mtb</i>	MICs (µg/mL) against <i>Mm</i>
1	 <p style="text-align: center;">RIF</p>	0.06 – 0.25	0.2
2	 <p style="text-align: center;">264</p>	100	100
3	 <p style="text-align: center;">265</p>	100	100
4	 <p style="text-align: center;">266</p>	100	100
5	 <p style="text-align: center;">267</p>	100	100

Chapter 5

The pyridazine side-products that were synthesised during the work described in Chapter 2 were also evaluated for their *in vitro* inhibition of *Mtb* and *Mm* (Table 5.6). However, all compounds were inactive, highlighting the importance of the intact 3-methoxyimidazo[1,2-*b*]pyridazine ring system.

Table 5.6: Pyridazine side-product MIC values against *Mtb* and *Mm*

Entry	Structure	MICs ($\mu\text{g/mL}$) against <i>Mtb</i>	MICs ($\mu\text{g/mL}$) against <i>Mm</i>
1	 RIF	0.06 – 0.25	0.2
2	 191a	>100	>100
3	 191e	>100	>100
4	 192b	100	10-100
5	 142	>100	>100

5.2 Conclusions

The SARs described within this chapter allowed for the identification of particular substituents on the imidazo[1,2-*b*]pyridazine core structure that generally resulted in enhanced inhibition of *Mtb* and *Mm*. Such substituents include a phenyl, a 2-fluorophenyl, a 4-fluorophenyl and a 2,4-difluorophenyl at C2; a methoxy at C3; and a 3-(methoxybenzyl)thio and a 6-*N*-methylbenzylamino at C6. Compounds which possessed these moieties and exhibited superior activity (0.25 – 0.625 $\mu\text{g/mL}$) include **17**, **64**, **65**, **190b** and **190d** (Figure 5.2).

Chapter 5

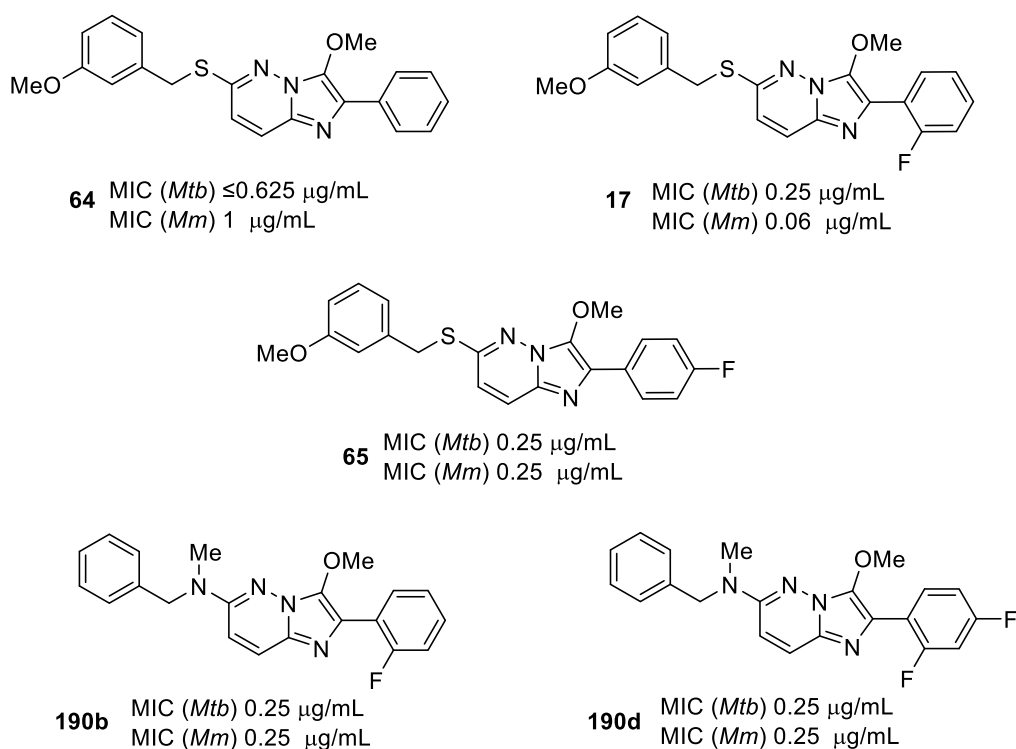


Figure 5.2: *In vitro* antimycobacterial activity of compounds **17**, **64**, **65**, **190b** and **190d**

Consequently, these five compounds were selected for an *in vivo* (mouse) study which sought to confirm activity *in vivo* in the hope to identify new lead compounds for further development. The results from the mouse study, along with the results from a physicochemical and metabolic evaluation of the compounds, will be discussed in the next chapter.

Chapter 6.
***In Vivo* Evaluation**

Chapter 6 Summary

The discovery of strong *in vitro* activity for imidazo[1,2-*b*]pyridazines **17**, **64**, **65**, **190b** and **190d**, discussed in Chapter 5, prompted a mouse *in vivo* study conducted at GIBH. In addition, the physicochemical and metabolic properties of **64**, **65**, **190b** and **190d** were evaluated at the Centre for Drug Candidate Optimisation (CDCO) at the Monash Institute of Pharmaceutical Sciences (MIPS). Evaluation of the compounds' *in vivo* antitubercular activity in mice, and their physicochemical and metabolic properties are discussed within this chapter.

6.1 *In vivo* method, results, and analysis for imidazo[1,2-*b*]pyridazine

64

Mice were infected with autoluminescent *Mtb* H37Ra via intravenous injection. The bioluminescence was detected and measured in relative light unit (RLU) readings. The RLU readings correlate with the population of bacteria residing within the mice. Mice with similar RLU readings (on day 0) were allocated into groups of four and each group was administered a particular agent – carboxymethyl cellulose sodium (CMC-Na) as a negative control, rifampicin (RIF) (10 mg/kg) as a positive control and imidazo[1,2-*b*]pyridazine (300 mg/kg). Treatment of the agent was administered once daily via oral gavage for a total of 5 days (days 1 to 5) while RLU readings were detected on days 2, 4 and 5. Similar methods were used for imidazo[1,2-*b*]pyridazines **17**, **65**, **190b** and **190d**.

Figure 6.1 shows a bar graph of the mean \log_{10} RLU count in the lungs of the different groups of mice at day 5 in addition to the mean \log_{10} RLU count of their lungs at day 0. The CMC-Na, group, as expected, showed an increase in growth of *Mtb* from day 0 to day 5 and rifampicin acted as a bactericidal agent between day 0 and day 5. Compound **64** appeared to have no obvious activity against *Mtb* since no clear change in the RLU count was detected from day 0 to day 5. The same conclusions were drawn from Figure 6.2 which shows the mean \log_{10} RLU count in the spleens of the different groups of mice.

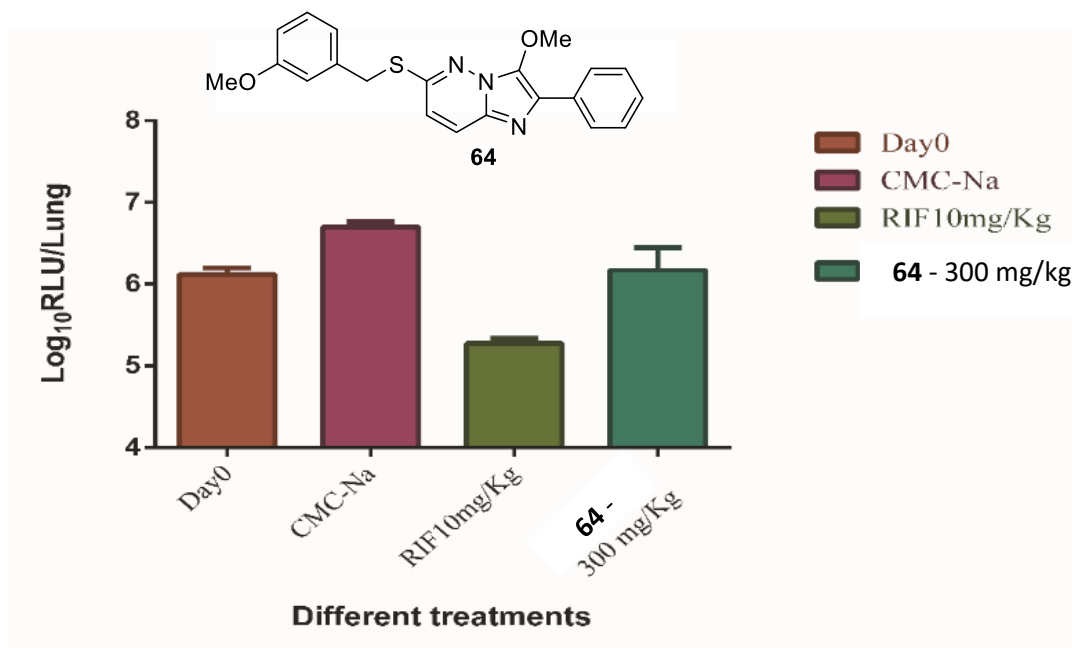


Figure 6.1: Mean RLU count (\pm SD) from the lung of mice treated with CMC-Na (negative control), rifampicin (positive control) and imidazo[1,2-b]pyridazine **64** at 300 mg/kg after 6 days.

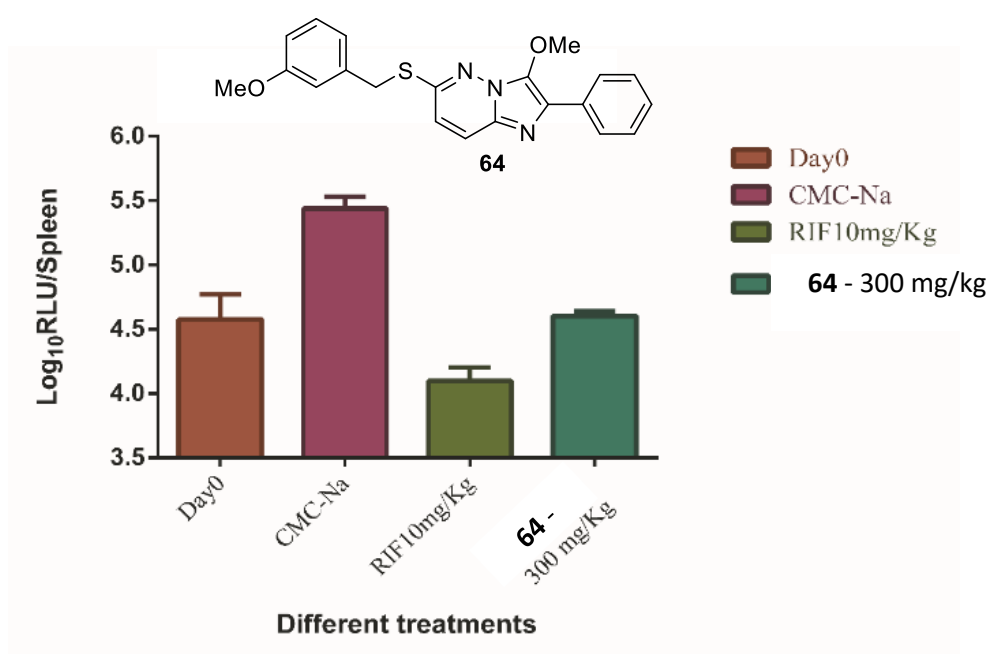


Figure 6.2: Mean RLU count (\pm SD) from the spleen of mice treated with CMC-Na (negative control), rifampicin (positive control) and imidazo[1,2-b]pyridazine **64** at 300 mg/kg after 6 days.

The ratio of the RLU readings of day n to day 0 from the chest of live mice were plotted against the number of days post initial treatment (Figure 6.3). These kinetic curves corroborated the finding that compound **64** had no antitubercular activity since the population of bacteria in the chest of mice treated with **64** were consistently greater than the population of bacteria in the negative control group (CMC-Na). Additionally, in a cytotoxicity assay of **64** using MDCK-MDR1 cells (a non-small Lung cancer cell line), evaluated by the 3-(4,5-dimethylthiazol-2-yl)-2,5-diphenyltetrazolium bromide (MTT) dye assay,¹⁰⁶ compound **64** was found to be non-toxic; it showed an $IC_{50} > 100 \mu\text{g/mL}$.

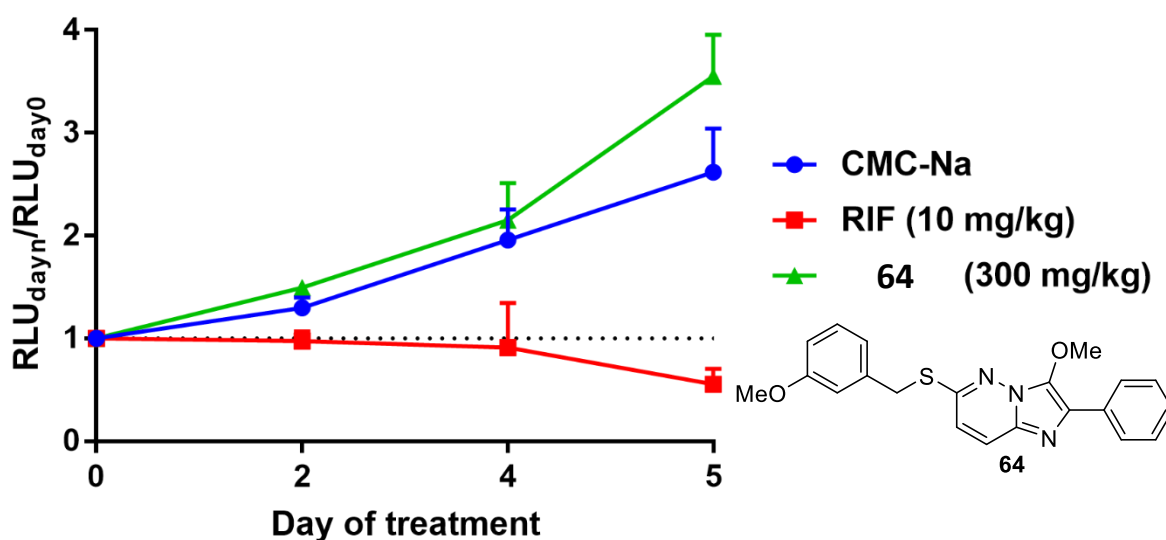


Figure 6.3: Kinetic curves of RLU_s from the chest of live mice treated with CMC-Na (negative control), rifampicin (positive control) and imidazo[1,2-*b*]pyridazine **64** at 300 mg/kg.

6.2 *In vivo* results and analysis of **65**, **17**, **190b** and **190d**

The kinetic curves for the 2-(4-fluorophenyl)imidazo[1,2-*b*]pyridazine **65** at different concentrations alongside the curves for CMC-Na and rifampicin are displayed in Figure 6.4. The kinetic curves of **65** at 30 mg/kg, 100 mg/kg and 300 mg/kg closely resemble the kinetic curve of the negative control, CMC-Na, suggesting no *in vivo* activity. Additionally, these kinetic curves show a lack of resemblance to the positive control, rifampicin, which appears to be acting as a bacteriostatic agent. Notably, this appears to be inconsistent with rifampicin

acting as a bactericidal agent in the experiments summarised in Figures 6.1, 6.2 and 6.3 and is likely due to the differences in the amounts of bacteria being injected on the days of infection. The status of the *Mtb* strains or the biology of the mice can also affect the agent's activity.

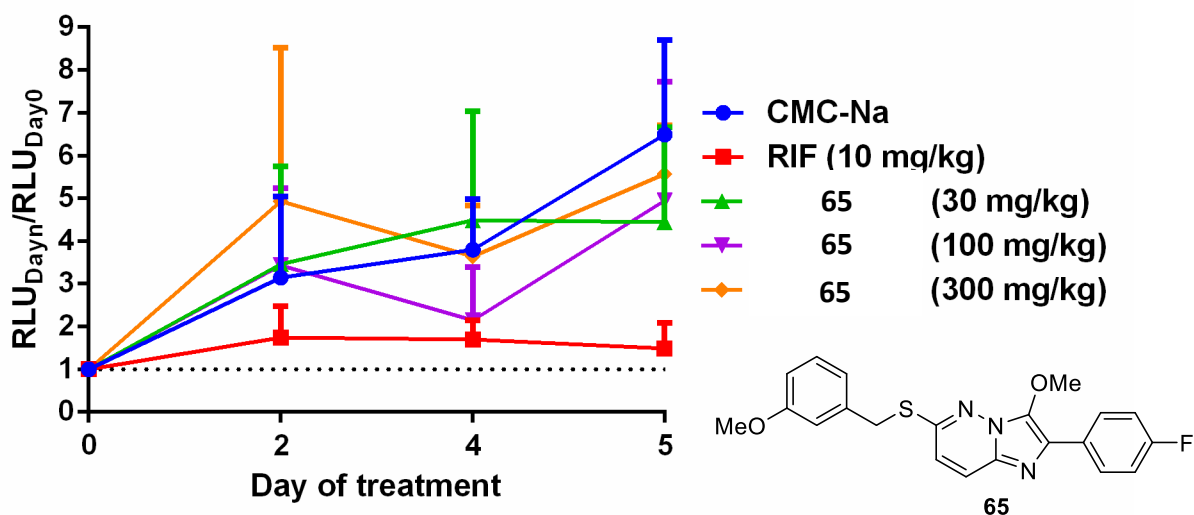


Figure 6.4: Kinetic curves of RLUs from the chest of live mice treated with CMC-Na (negative control), rifampicin (positive control) and imidazo[1,2-b]pyridazine **65** at different concentrations.

P-values were also calculated between CMC-Na and the different concentrations of **65** (Table 6.1). The P-value between CMC-Na and rifampicin was found to be 0.1123 and could be referred to as the significance level. The P-value for all concentrations of **65** were not near this value which indicates there was no significant difference between the activity of **65** and the activity of the positive control, CMC-Na. Therefore, it can be concluded that **65** showed no obvious antitubercular activity.

Table 6.1: The P-value between CMC-Na (positive control) and rifampicin (negative control) and the P-value between CMC-Na and **65** at different concentrations

Test group	P-value
Rifampicin	0.1123
65 (30 mg/kg)	0.8574
65 (100 mg/kg)	0.6246
65 (300 mg/kg)	0.9124

Similar observations and conclusions were made for **17** (Figure 6.5, Table 6.2), **190b** (Figure 6.6, Table 6.3) and **190d** (Figure 6.7, Table 6.4). The most likely explanations to account for the lack of *in vivo* activity the imidazo[1,2-*b*]pyridazines exhibited are poor bioavailability or a very short metabolic half-life. To address these issues, **64**, **65**, **190b** and **190d** were sent to the CDCO at MIPS to evaluate their physicochemical properties and metabolic half-life.

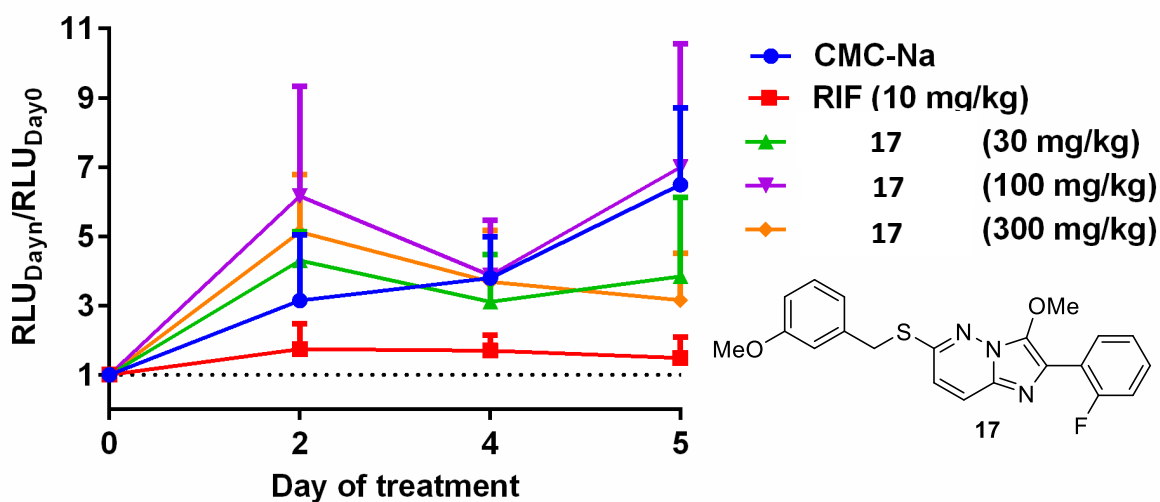


Figure 6.5: Kinetic curves of RLUs from the chest of live mice treated with CMC-Na (negative control), rifampicin (positive control) and imidazo[1,2-*b*]pyridazine **17** at different concentrations.

Table 6.2: The P-value between CMC-Na (positive control) and rifampicin (negative control) and the P-value between CMC-Na and **17** at different concentrations

Test group	P-value
Rifampicin	0.1123
17 (30 mg/kg)	0.6985
17 (100 mg/kg)	0.6268
17 (300 mg/kg)	0.8055

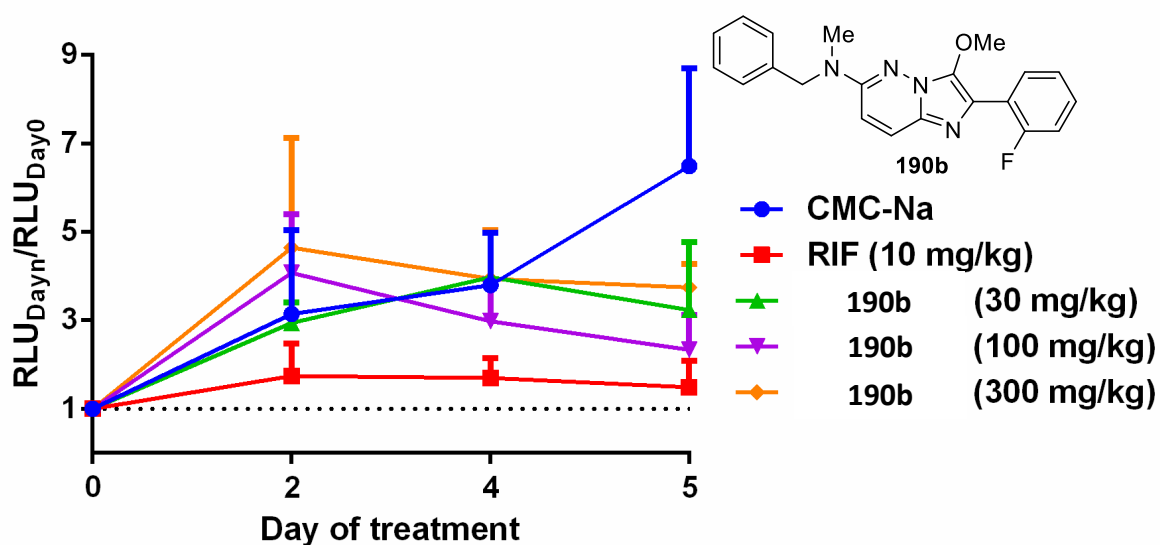


Figure 6.6: Kinetic curves of RLUs from the chest of live mice treated with CMC-Na (negative control), rifampicin (positive control) and imidazo[1,2-b]pyridazine **190b** at different concentrations.

Table 6.3: The P-value between CMC-Na (positive control) and rifampicin (negative control) and the P-value between CMC-Na and **190b** at different concentrations

Test group	P-value
Rifampicin	0.1123
195b (30 mg/kg)	0.5495
195b (100 mg/kg)	0.4658
195b (300 mg/kg)	0.8480

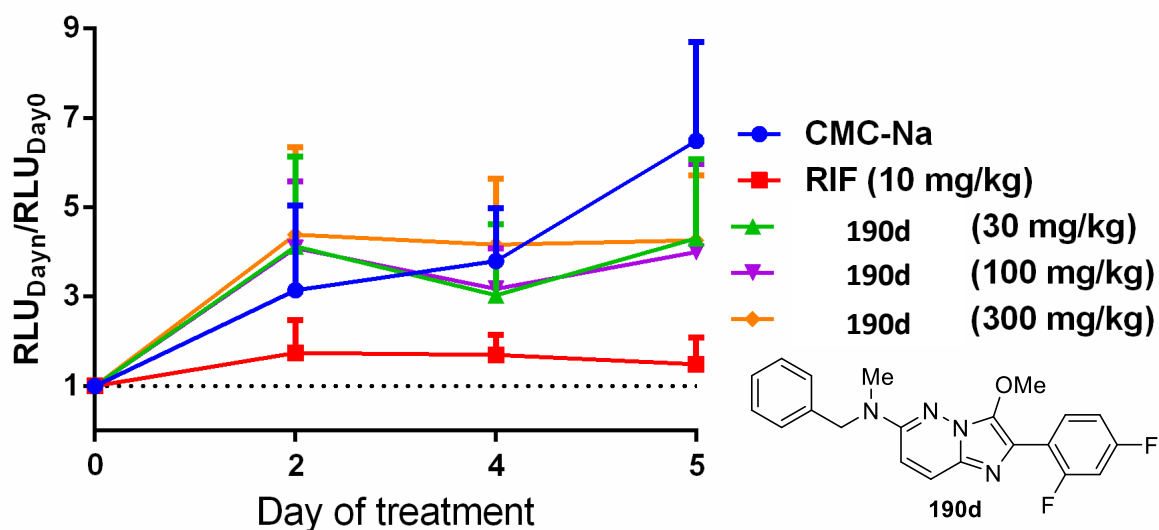


Figure 6.7: Kinetic curves of RLUs from the chest of live mice treated with CMC-Na (negative control), rifampicin (positive control) and imidazo[1,2-b]pyridazine **190d** at different concentrations.

Table 6.4: The P-value between CMC-Na (positive control) and rifampicin (negative control) and the P-value between CMC-Na and **190d** at different concentrations

Test group	P-value
Rifampicin	0.1123
190d (30 mg/kg)	0.7297
190d (100 mg/kg)	0.6993
190d (300 mg/kg)	0.9148

6.3 Physicochemical Evaluation

A range of physicochemical properties relevant to evaluation of drug-likeness and likely oral absorption characteristics of imidazo[1,2-*b*]pyridazines **64**, **65**, **190b** and **190d** were calculated at CDCO-MIPS using the ChemAxon chemistry cartridge via JChem for Excel software (version 16.4.11). The parameters calculated are shown in Table 6.5. These parameters were compared to generally preferred ranges based on absorption, distribution, metabolism and excretion (ADME) literature from key industry and academic sources.^{107,108,109,110}

The imidazo[1,2-*b*]pyridazines in Table 6.5 all had appropriate molecular weights (MW) since they were <500 gmol⁻¹. All imidazo[1,2-*b*]pyridazines were found to have appropriate predicted membrane permeabilities since their calculated polar surface areas (PSA) at pH 7.4 were <140 Å². PSA at pH 7.4 inversely correlates with membrane permeability. The number of hydrogen bond donors (HBD) and acceptors (HBA) indicates the compounds' capacity to hydrogen bond, which is also inversely related to membrane permeability. No compound possessed an HBD while all consisted of 4 HBAs which were within the ideal range (HBDs should be <5 while HBAs should be <10). The HBAs in imidazo[1,2-*b*]pyridazines **64** and **65** were thought to be the 3-methoxy on the benzyl ring, the 3-methoxy on the imidazo[1,2-*b*]pyridazine ring system, and N1 and N5 of the imidazo[1,2-*b*]pyridazine ring system (Figure 6.8). N4 was not regarded as a HBA since its lone pair would contribute to the aromaticity of the imidazo[1,2-*b*]pyridazine ring system. These HBAs were observed in **190b** and **190d** except the 3-methoxy on the benzyl ring was exchanged for the *N*-methyl linker group at C6 of the imidazo[1,2-*b*]pyridazine ring system (Figure 6.8).

The number of free rotating bonds (FRB) is a measure of the conformational flexibility of a molecule. Imidazo[1,2-*b*]pyridazines **64** and **65** consist of 6 FRBs while **190b** and **190d** possess 5 due to the absence of the 3-methoxy group on the benzyl moiety (Figure 6.8). The number of aromatic rings (Arom. Rings) is also related to the molecule's flexibility and each of the four compounds possessed 4 such rings (Figure 6.8). Consequently, these imidazo[1,2-*b*]pyridazines may not have an appropriate amount of flexibility since <4 aromatic rings is considered ideal. The fraction of the sp³ carbons to the total number of carbons (Fsp³) represents the complexity of the molecule's 3D structure. The four imidazo[1,2-*b*]pyridazines

were calculated to have F_{sp^3} values of 0.14 which is less than the preferred F_{sp^3} value (>0.3), indicating a lack of three-dimensional complexity.

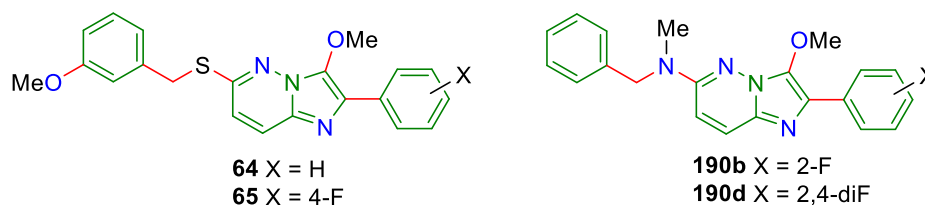


Figure 6.8: The structures of **64**, **65**, **190b** and **190d** displaying their hydrogen bond donors (blue), free rotating bonds (red), and aromatic rings (green)

Their predicted pK_a values were also calculated to develop a greater understanding of the molecule's solubility and permeability - only physiological relevant pK_a values were provided in Table 6.5 ($0 < pK_a < 12$). Compounds **64** and **65** have a basic pK_a of 1.6 while **190b** and **190d** have a basic pK_a of 2.4. The basic pK_a values signify the acidity of the conjugate acids of the basic sites of the molecule. Therefore, the conjugate acids of **64** and **65** are stronger than the conjugate acids of **190b** and **190d** by almost 10-fold. It was thought **190b** and **190d** would be more basic than **64** and **65** due to the presence of the tertiary amine and consequently would form more stable (weaker) conjugate acids. Additionally, no acidic sites at physiological pH were present in the compounds' structures; the methylene unit may have some acidity but its pK_a is likely greater than 12. The partition coefficient of the neutral structure (cLogP) reflects the compounds' lipophilicity while the distribution coefficient (cLogD) reflects their partitioning properties while ionised at pH 7.4 - cLogP and cLogD values of <5 are deemed to be drug-like characteristics. However, the imidazo[1,2-*b*]pyridazines presented in Table 6.5 all have cLogP and cLogD >5 indicating high lipophilicity.

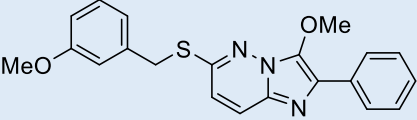
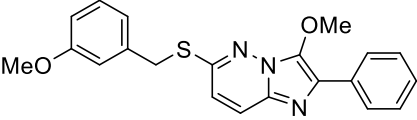
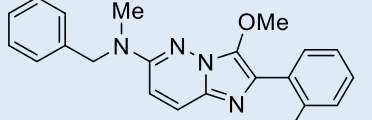
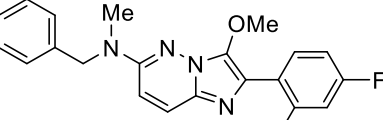
The remaining parameters in Table 6.5 (gLogD at pH 7.4, solubility at pH 2 and solubility at pH 6.5) were measured experimentally. The Distribution Coefficient Estimation using Chromatography (gLogD) was estimated for compounds **64**, **65**, **190b** and **190d** by comparing their chromatographic retention times against a series of standard compounds with known partition coefficient values at pH 7.4. The method used was a modified version of Lombardo's

Chapter 6

HPLC based protocol.¹¹¹ Consistent with the cLogP values, all imidazo[1,2-*b*]pyridazines in Table 6.5 possessed gLogD values >4, corroborating high lipophilicity.

Kinetic Solubility Estimations (Sol at pH 2.0 and 6.5) of the imidazo[1,2-*b*]pyridazines were also determined in acidic and neutral media. Each compound was dissolved in DMSO and spiked into either a 0.01 M HCl solution (approximately pH 2.0) or into a pH 6.5 phosphate buffer solution with the final DMSO concentration being 1 %. After 30 minutes the samples were analysed via Nephelometry to determine a solubility range, using a method reported by Bevan and Lloyd.¹¹² The results showed that thioether compounds **64** and **65** had poor solubilities at pH 2 and 6.5 indicating they do not possess an appropriate level of hydrophilicity. Amines **190b** and **190d**, while lacking solubility at pH 6.5, demonstrated markedly higher solubility in acidic media, presumably due to the increased basicity of the *N*-methylamino linker group at C6 of the imidazo[1,2-*b*]pyridazine ring system.

Table 6.5: Physicochemical evaluation of imidazo[1,2-b]pyridazines **64**, **65**, **190b** and **190d**:

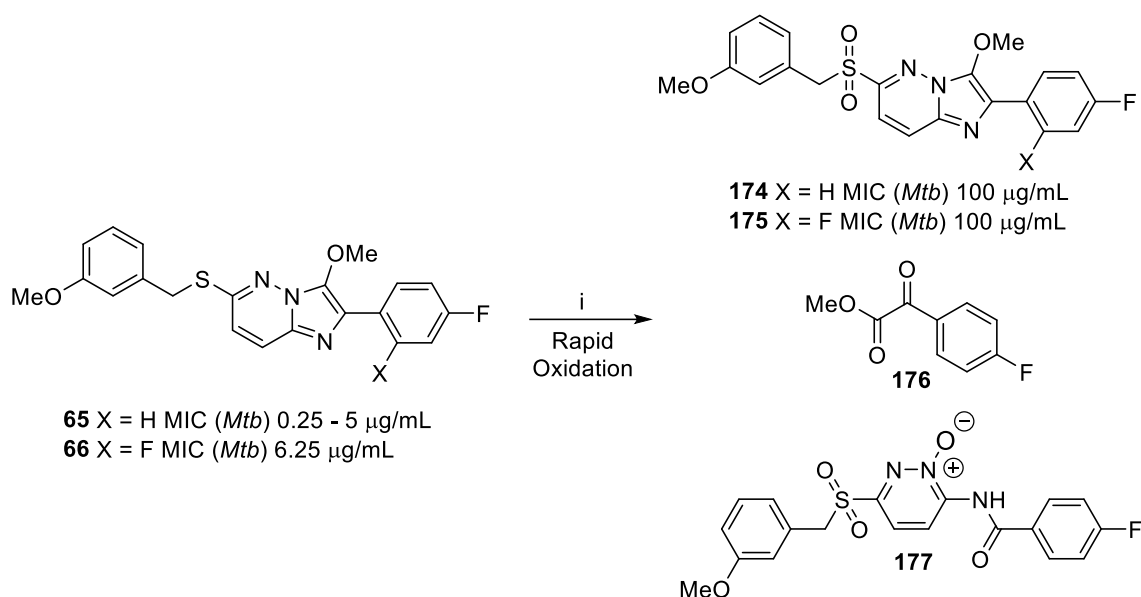
Structure	MW (g ^{mol} ⁻¹)	PSA (Å ²)	HBD	HB A	FRB	Arom. Rings	Fsp ³	Predicted pKa (0 - 12 only)	cLogP	cLog D at pH 7.4	gLogD at pH 7.4	Sol at pH 2 (µg/m L)	Sol at pH 6.5 (µg/m L)
 <p>64</p>	377.46	48.7	0	4	6	4	0.14	Basic: 1.6 Acidic: none	5.3	5.3	4.8	3.1 - 6.3	<1.6
 <p>65</p>	395.45	48.7	0	4	6	4	0.14	Basic: 1.6 Acidic: none	5.4	5.4	4.9	1.6 - 3.1	<1.6
 <p>190b</p>	362.41	42.7	0	4	5	4	0.14	Basic: 2.4 Acidic: none	5.2	5.2	4.5	25-50	<1.6
 <p>190d</p>	380.4	42.7	0	4	5	4	0.14	Basic: 2.4 Acidic: none	5.3	5.3	4.6	25-50	<1.6

6.4 Metabolic Evaluation

The metabolic stabilities of imidazo[1,2-*b*]pyridazines **64**, **65**, **190b** and **190d** were evaluated by incubating the compounds at a concentration of 1 μ M in liver microsomes (supplied by XenoTech, lot 1910002) at 37 °C with a protein concentration of 0.4 mg/mL. An NADPH-regenerating system, serving as a source of electrons for P450 oxidative reactions, was added to initiate the metabolic reaction. Over a 60-minute period, samples of the metabolic reaction mixture were quenched intermittently by the addition of acetonitrile with diazepam as an internal standard. Control samples containing no NADPH were also monitored and were quenched at 2 minutes, 30 minutes, and 60 minutes to determine if degradation occurred without the cofactor.

The experimental and calculated results for each compound are shown below in Table 6.6. Imidazo[1,2-*b*]pyridazines **64** and **65**, both containing a 3-methoxy-benzylthio group attached to C6 of the imidazo[1,2-*b*]pyridazine ring system, exhibited the same metabolic results. Both compounds had a half-life of <2 minutes which translates to an *in vitro* intrinsic clearance ($Cl_{int, in vitro}$) value of >866 μ L/min/mg protein. Species scaling from Ring *et al*¹¹³ were used to convert the $Cl_{int, in vitro}$ to the *in vivo* intrinsic clearance values ($Cl_{int, in vivo}$). The *in vivo* intrinsic clearance ($Cl_{int, in vivo}$) represents the ability of the liver to remove compounds by all pathways without flow limitations.¹¹⁴ Both **64** and **65** showed high $Cl_{int, in vivo}$ values at >2235 mL/min/kg indicating both compounds were readily metabolised in the liver. The hepatic blood clearance (Cl_{blood}) and hepatic extraction ratio (E_H) were calculated using the well stirred model of hepatic extraction in each species, according to the “*in vitro* $T_{1/2}$ ” approach.¹¹⁵ Cl_{blood} can be defined as the volume of blood perfusing the liver that is cleared of the compound per unit time¹¹⁴ while E_H is the ratio of the hepatic blood clearance to the hepatic blood flow.¹¹⁶ Both **64** and **65** were calculated to have Cl_{blood} values of >113 mL/min/kg which corresponds to E_H values of >0.94. This E_H value was then used to classify compounds as having low (<0.3), high (0.7-0.94) or very high (>0.94) hepatic extraction ratios. As a result, **64** and **65** had very high E_H values and therefore were rapidly metabolised. Imidazo[1,2-*b*]pyridazine **190b** and **190d** were also readily metabolised, although more slowly than the aforementioned compounds. Specifically, **190b** exhibited an E_H value of 0.90 (a high hepatic extraction ratio) while **190d** exhibited a slightly lower but still categorically high E_H value of 0.82.

It was believed NADPH-dependent oxidative metabolic pathways occurred in preference to other metabolic routes including conjugation, reduction and hydrolysis since non-NADPH-mediated degradation was insignificant in the microsome control samples. Since all of the imidazo[1,2-*b*]pyridazines in Table 6.5 exhibited high to very high E_H values, rapid metabolic degradation is believed to be key reason for their lack of *in vivo* activity against *Mtb*. In Chapter 2 (2.1.6 3-Methoxy-6-((3-methoxybenzyl)sulfonyl)-2-phenylimidazo[1,2-*b*]pyridazine syntheses) rapid oxidation of the thioether to the sulfone in **65** and **66** was observed using urea hydrogen peroxide and trifluoroacetic anhydride in acetonitrile (Scheme 6.1). This was consistent with the rapid metabolic rate of **64** and **65** indicating the thioether moiety was a likely target for oxidative metabolism. If the potential sulfone metabolites of **64** and **65** were not excreted from the host and were bioavailable to *Mtb*, no inhibitory effect would be observed since the sulfone derivatives **174** and **175** had no *in vitro* activity (Scheme 6.1). Furthermore, compounds **176** and **177** were produced within 12 minutes when **65** was treated under oxidative conditions (Scheme 6.1). Consequently, significant cleavage of the imidazo[1,2-*b*]pyridazine ring system can result under these conditions in a short amount of time. The proposed mechanisms for **176** and **177** under section 2.1.6 suggests the C=C double bond in the imidazole ring is likely to be susceptible to oxidation and thereby an oxidative metabolic target.



Scheme 6.1: Rapid oxidation of **65** and **66** (and the *in vitro* MIC values of **65**, **66**, **174-177**) using i) urea hydrogen peroxide and trifluoroacetic anhydride in acetonitrile

In addition to the thioether and olefin oxidative metabolic pathways, oxidative debenzylation, and arene oxidation are possible mechanisms of metabolism for imidazo[1,2-*b*]pyridazines **64**, **65**, **190b** and **190d**. These modes of metabolism have been reported in the literature. For example, PAC-1 - an *o*-hydroxy-*N*-acylhydrazone that induces apoptosis in cancer which is susceptible to metabolic degradation, shares moieties with the aforementioned imidazo[1,2-*b*]pyridazines (benzyl, olefin and aromatic moieties).¹¹⁷ Three major metabolic pathways for PAC-1 were found to be olefin oxidation, oxidative debenzylation and arene oxidation¹¹⁷ – which may be occurring with our imidazo[1,2-*b*]pyridazines. As discussed in Chapter 3 (3.3 3-Carboxylate(lactone)-substituted imidazo[1,2-*b*]pyridazine synthesis), demethylation of the methoxy group and glucuronidation of the liberated hydroxyl group may be an additional major metabolic pathway.⁸⁸ *N*-Demethylation, another common metabolic pathway, could also occur for imidazo[1,2-*b*]pyridazines **190b** and **190d**.^{118,119,120}

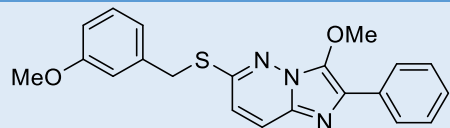
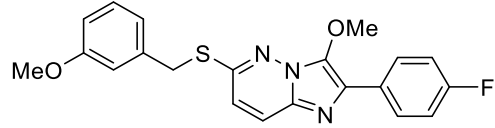
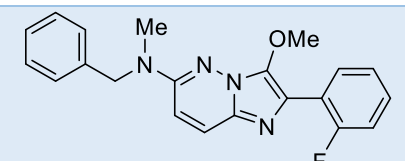
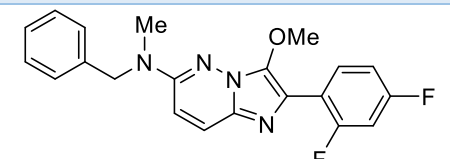
The rapid oxidation of the thioether to the sulfone in **65** and **66** may account for the higher rates of metabolic degradation of **64** and **65** in contrast to **190b** and **190d**. However, **190b** and **190d** have other likely metabolically labile sites, specified previously, which may explain their high hepatic extraction ratios. Interestingly, **190d** was less susceptible to metabolism than **190b**, presumably due the additional fluoro group in the para position of the 2-phenyl

Chapter 6

ring. Introduction of fluorine groups to form aryl fluorides have previously improved metabolic stability by blocking undesired metabolic arene oxidation.^{117,121}

Furthermore, the high lipophilic nature of these compounds, may have an impact on their metabolic stability since it has been found that the higher the log D value of a CYP450 substrate, the greater its intrinsic clearance.¹²² Lipophilic compounds are thought to be rapidly metabolised since the binding sites of CYP450s are considered lipophilic in nature.¹²² Decreasing the lipophilicity of the imidazo[1,2-*b*]pyridazines may lower their intrinsic clearance.¹²³ However, without addressing the discussed metabolic vulnerabilities, the compounds' half-lives are unlikely to be extended.¹²³

Table 6.6: Metabolic evaluations of imidazo[1,2-b]pyridazines **64**, **65**, **190b** and **190d**

Compound number	Structure	T _{1/2} (min)	Cl _{int, in vitro} (μL/min/mg/protein)	Predicted Cl _{int, in vivo} (mL/min/kg)	Predicted Cl _{blood} (mL/min/kg)	Predicted E _H	Clearance Classification
64		<2	>866	>2235	>113	>0.94	Very high
65		<2	>866	>2235	>113	>0.94	Very high
190b		4	405	1044	108	0.90	High
190d		8	215	554	99	0.82	High

6.5 Conclusions

Although imidazo[1,2-*b*]pyridazines **17**, **64**, **65**, **190b** and **190d** were found to be highly active against *Mtb* *in vitro*, no obvious *in vivo* activity was observed in mice. Evaluation of the physicochemical properties of imidazo[1,2-*b*]pyridazines **64**, **65**, **190b** and **190d** revealed they have molecular weight, polar surface area, and hydrogen bond donor and acceptor values within the generally acceptable ranges for membrane permeability and good oral absorption characteristics. However, they all exhibited poor solubility in neutral aqueous media consistent with their high lipophilicities (glogD at pH 7.4 >4). Their poor solubility and high lipophilicities arise from all compounds consisting of four aromatic rings and low Fsp³ values. Amine-containing derivatives **190b** and **190d**, however, exhibited greater solubility in acidic media, presumably due to the basicity of the *N*-methylamino moiety. However, their poor metabolic stability appears to be the key reason for their lack of *in vivo* activity against *Mtb*; benzylthio derivatives **64** and **65** had hepatic clearance classifications categorised as “very high” (E_H = >0.94), while benzylamino derivatives **190b** and **190d** were categorised as “high” (E_H = 0.90 and 0.82, respectively).

Chapter 7.

Conclusions and Future Directions

7.1 3-Methoxy-2-phenylimidazo[1,2-*b*]pyridazines

Chapter 2 describes two synthetic pathways used to synthesise a library of 3-methoxy-2-phenylimidazo[1,2-*b*]pyridazines, which included the most active imidazo[1,2-*b*]pyridazines against *Mtb in vitro* (Figure 7.1) identified in this study. SARs discussed in Chapter 5 identified particular substituents which generally enhanced the antimycobacterial activity of the imidazo[1,2-*b*]pyridazine. Such moieties include a phenyl, a 2-fluorophenyl, a 4-fluorophenyl and a 2,4-difluorophenyl at C2; a methoxy at C3; and a 3-(methoxybenzyl)thio and an *N*-methylbenzylamino at C6. Compounds bearing these substituents and which exhibited superior antimycobacterial activity (0.25 – 0.625 µg/mL) include **17**, **64**, **65**, **190b** and **190d** (Figure 5.2).

7.2 Other 3-substituted imidazo[1,2-*b*]pyridazines

In the work described in Chapter 3, other 3-substituted imidazo[1,2-*b*]pyridazines were synthesised to probe C3 SARs. The syntheses of two 3-ethoxy-imidazo[1,2-*b*]pyridazines, **216** and **217**; three 3-dialkylaminomethyl-imidazo[1,2-*b*]pyridazines, **225**, **229** and **230**; and 3-carboxylate (lactone) **234** imidazo[1,2-*b*]pyridazines were described within this chapter. In Chapter 5 it was described that both the 3-ethoxy-imidazo[1,2-*b*]pyridazines, **216** and **217** exhibited relatively high *in vitro* antitubercular activity with MIC values of 1 µg/mL and 1.25 µg/mL, respectively (Figure 7.2). No activity was observed for 3-dialkylaminomethyl derivatives **225** and **230** while moderate activity (10 µg/mL against *Mtb*) was observed for **229**. Finally no activity was observed when a carboxylate (lactone) was installed at C3 of the imidazo[1,2-*b*]pyridazine ring system indicating this compound was unable to inhibit Pks13, the target of the coumestans.⁸⁷ The general lack of antimycobacterial activity of these compounds demonstrated the importance of the 3-methoxy moiety.

Chapter 7

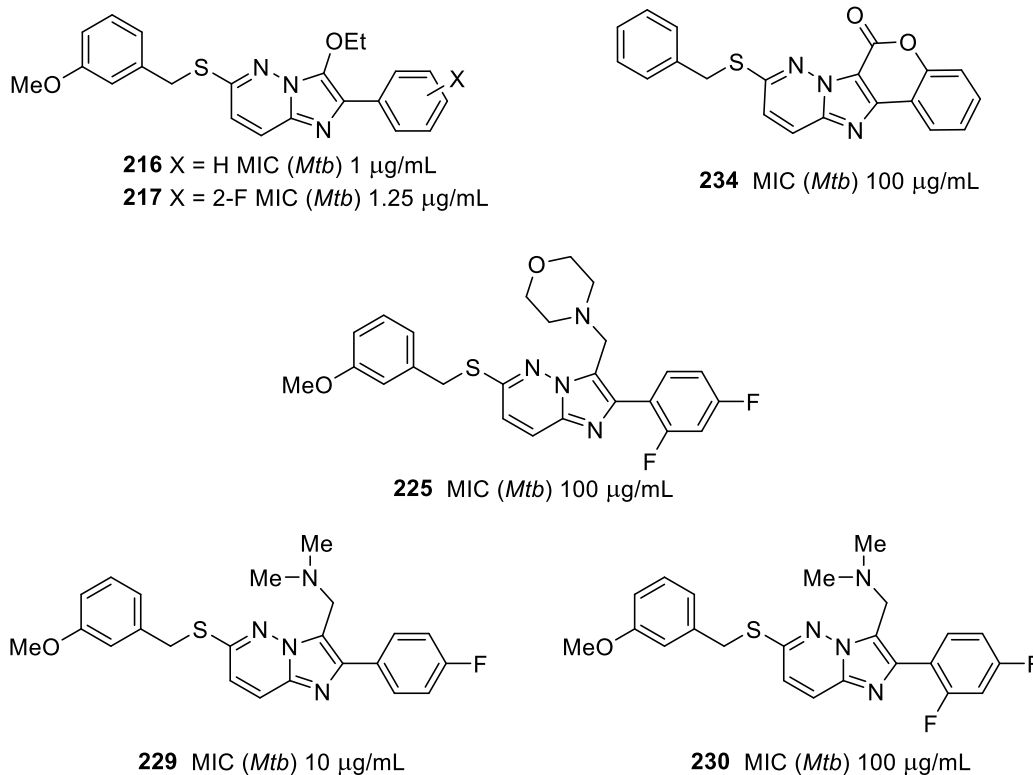


Figure 7.2: Antitubercular activity of other 3-substituted imidazo[1,2-*b*]pyridazines

7.3 Scaffold hop from the imidazo[1,2-*b*]pyridazine

Chapter 4 discussed the concept of scaffold hopping and how it was applied to the imidazo[1,2-*b*]pyridazine derivatives in this study. Imidazo[2,1-*b*][1,3,4]thiadiazole and imidazo[2,1-*b*][1,3,4]oxadiazole derivatives were targeted for synthesis since their core scaffolds shared structural similarities to the imidazo[1,2-*b*]pyridazine system, with subtle modifications. It was postulated that these structural changes might lead to improved antimycobacterial activity. However, the syntheses of imidazo[2,1-*b*][1,3,4]thiadiazol-5-ols and imidazo[2,1-*b*][1,3,4]oxadiazol-5-ols were unsuccessful, after an investigation of a range of conditions. It appeared that the 2-amino[1,3,4]thiadiazole and 2-amino[1,3,4]oxadiazole starting materials were not sufficiently reactive bis-nucleophiles to condense with phenylglyoxal monohydrate derivatives.

Hybridisation of known antitubercular compounds Q203^{38,37} and TB47^{43,91} and a scaffold hop to the imidazo[1,2-*b*]pyridazine was successful after carboxamides **264**, **265**, **266** and **267** were synthesised. However, as described in Chapter 5, no activity was observed for the Q203/TB47 imidazo[1,2-*b*]pyridazine hybrids suggesting these compounds were not able to inhibit QcrB.^{38,37,43}

7.4 *In vivo* study conclusions

Imidazo[1,2-*b*]pyridazines **17**, **64**, **65**, **190b** and **190d**, having the most potent *in vitro* activity, were selected for an *in vivo* mouse study (described in Chapter 6) but exhibited no *in vivo* activity against *Mtb*. After evaluating their metabolic stability using liver microsomes/NADPH, it was found the four compounds, **64**, **65**, **190b** and **190d**, had high to very high hepatic clearance classifications; a likely reason for their very low *in vivo* activity.

7.5 Future Directions

Although imidazo[1,2-*b*]pyridazines **64**, **65**, **190b** and **190d** were found to be highly potent inhibitors of *Mtb in vitro*, they exhibited no *in vivo* activity, probably as a result of their metabolic fragility. As suggested in Chapter 6, the possible metabolic vulnerabilities within the structures of these molecules need to be addressed to extend their half-lives *in vivo*. These possible labile sites include the thioether (in **64** and **65**), the *N*-methylamine (in **190b** and **190d**), the methylene moiety, the methoxy moieties, the aromatic moieties, and the C=C bond in the imidazole ring. In Chapter 5, it was noted that 6-benzyloxy-imidazo[1,2-*b*]pyridazines showed comparable activity with the 6-benzylthio derivatives. Therefore the antimycobacterial activity of such imidazo[1,2-*b*]pyridazines is likely to be maintained if the readily oxidisable thioether is replaced with an ether linker. Additionally, replacement of the *N*-methylamine linker with an ether linker will remove the possibility of *N*-demethylation^{78,118,119}. However, it was found that the *N*-methylamine derivatives were generally more active against *Mtb* compared to the ether derivatives. Alternatively, the hydrogen atoms (some or all) on the *N*-methylamine moiety could be replaced

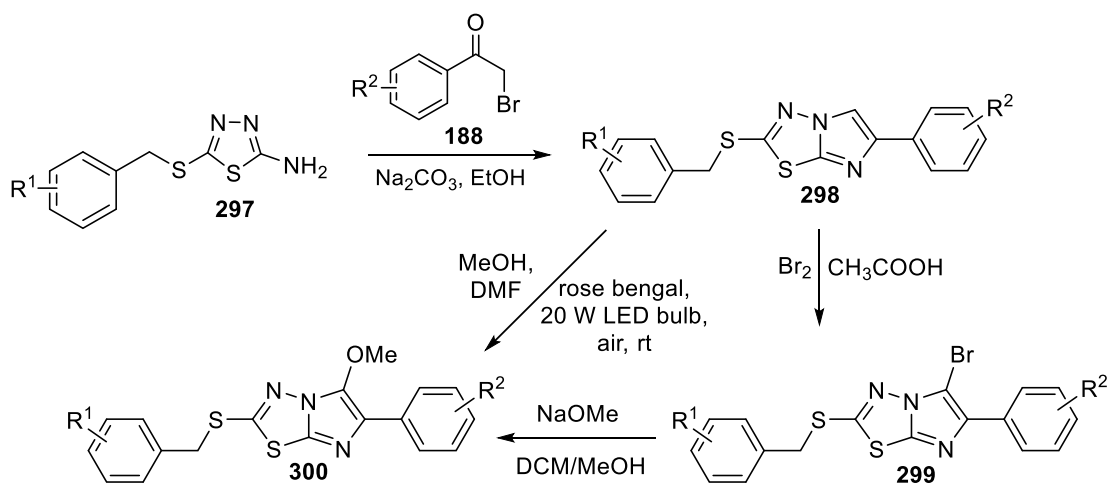
with deuterium isotopes. Deuteration of the *N*-methylamine moiety, in addition to the methylene, methoxy and/or aromatic moieties, is an attractive solution since deuterium has similar electron clouds and polar surface areas to hydrogen which can result in similar biochemical activities.¹²⁴ Not only is deuterium an ideal bioisostere, the carbon-deuterium bond is more stable than the carbon-hydrogen bond due to the deuterium kinetic isotope effect.^{124,125} This can result in a ~6-10 fold decrease in kinetic rates of metabolism when the rate determining step is bond cleavage.^{124,125} Notably, its likely not all hydrogen atoms will need replacing with the isotope, however, a library of imidazo[1,2-*b*]pyridazines with differing degrees of deuteration could be developed. SARs and comparisons between the hepatic clearances of the deuterated molecules as well as non-deuterated molecules could be formed in determining the most active and metabolically stable imidazo[1,2-*b*]pyridazine.

As noted in Chapter 5, 2-(2,4-difluorophenyl)imidazo[1,2-*b*]pyridazine **190d** was more metabolically stable than 2-(4-fluorophenyl)imidazo[1,2-*b*]pyridazine **190b**, presumably due to the additional fluoro group blocking metabolic arene oxidation.¹²¹ The introduction of more fluoro moieties on either of the aromatic substituents on the imidazo[1,2-*b*]pyridazine ring may also contribute to a higher metabolic stability. Furthermore, SARs could also be developed by introducing more fluoro groups on the C2 phenyl group as well as the C6 benzyl group.

Addressing the C=C bond metabolic soft spot in the imidazole ring could be challenging since alteration of the C2 and C3 substituents would drastically alter the *in vitro* activity of **64**, **65**, **190b** and **190d**. Since the methoxy group at C3 was deemed essential to the activity of the imidazo[1,2-*b*]pyridazine in Chapter 5, resorting to altering the substituents on the phenyl ring at C2 is likely a better solution. For example, a bromo group on the ortho position of the 2-phenyl ring could possibly block oxidants from the C=C bond. Since 2-(4-bromophenyl)imidazo[1,2-*b*]pyridazines were active in Chapter 5, the SARs of 2-(2,4-dibromophenyl)imidazo[1,2-*b*]pyridazines would be of interest.

The metabolic stability of the imidazo[2,1-*b*][1,3,4]thiadiazoles that were proposed for synthesis in Chapter 4 are unknown and could potentially have lower hepatic extraction ratios than the imidazo[1,2-*b*]pyridazines. Additionally, acquiring the SAR data from these molecules and how

their antimycobacterial activities compare to the imidazo[1,2-*b*]pyridazines is desirable. Further efforts in synthesising these compounds would therefore be required. Since the thiadiazole starting material was an insufficiently reactive bis-nucleophile to condense with phenylglyoxal monohydrate, an alternative and more electrophilic bis-electrophile could be utilised. A new synthetic pathway is proposed in Scheme 7.1. Divyaanka Iyer *et al.* have reported condensing 5-benzyl-1,3,4-thiadiazol-2-amine **297** with phenacyl bromide **188** in ethanol with sodium carbonate to produce 2-benzylthio-6-phenylimidazo[2,1-*b*][1,3,4]thiadiazole **298**.¹²⁶ Bromination at the C3 position producing 3-bromo **299** can be achieved by stirring imidazo[2,1-*b*][1,3,4]thiadiazole **298** with bromine and sodium acetate in acetic acid at room temperature for 30 minutes.^{126,127} Finally, utilising the conditions that were reported by Kayla J. Temple *et al.* a nucleophilic aromatic substitution at C5 could produce 2-benzylthio-5-methoxy-6-phenylimidazo[2,1-*b*][1,3,4]thiadiazole **300**.¹²⁸ However, if C5 of the imidazo[2,1-*b*][1,3,4]thiadiazole ring system is not activated enough to undergo this reaction, a photoredox-catalysed C-H alkoxylation, which has been successful with imidazo[1,2-*b*]pyridines,¹²⁹ can be attempted (Scheme 7.1).



Scheme 7.1: Proposed synthetic pathway for the synthesis of 2-benzylthio-5-methoxy-6-phenylimidazo[2,1-*b*][1,3,4]thiadiazoles (**300**)

Chapter 8

Experimental Procedures

8.1 General experimental procedures

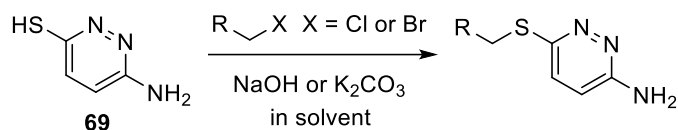
Experiments were analysed by thin-layer chromatography using aluminium backed silica sheets, visualised with UV light and, at times, with potassium permanganate dip (KMnO_4 , 3 g; K_2CO_3 , 20 g; 5 % NaOH, 5 mL; H_2O , 300 mL) to monitor reaction progress, for determination of compound purity and for enabling choice of appropriate solvent systems for column chromatography. Column chromatography was performed on (buffered and non-buffered) 230-400 mesh silica (particle size: 40-63 μm). Water sensitive reactions were carried out under a nitrogen atmosphere. DCM was distilled over calcium hydride, THF was distilled over sodium and benzophenone and DMF was distilled under vacuum onto 4 Å molecular sieves. Other commercial reagents were used as received. ^1H NMR and ^{13}C NMR spectroscopy and liquid chromatography-mass spectrometry (LC-MS) were used for structure confirmation and purity determination. ^1H NMR spectra were recorded on a Bruker Avance II NMR spectrometer (600MHz) using standard parameters and ^{13}C NMR spectra were recorded on the same instrument but at 150 MHz. Chemical shifts are reported in ppm using the solvent resonance as the internal lock and reference. For ^1H NMR and ^{13}C NMR spectroscopy, the CDCl_3 peak was calibrated to 7.26 ppm and 77.16 ppm respectively, while the $\text{DMSO-}d_6$ peak was calibrated to 2.50 ppm and 39.52 ppm respectively. Spectroscopic data is reported using the following format: (1) chemical shift (ppm), (2) multiplicity (s = singlet, d = doublet, t = triplet, q = quartet, dd = doublet of doublets, dt = doublet of triplets, td = triplet of doublets, tt = triplet of triplets, m = multiplet), (3) J coupling constant (Hz), (4) integration. COSY, HMQC, and HMBC NMR spectroscopy and high-resolution mass spectrometry (HRMS) were sometimes used in structure determination. HRMS was performed using either a PerkinElmer AxION DSA-ToF system (ESI or APCI), a Waters Synapt HDMS (ESI) or a Thermo Scientific Q Extractive FTMS (APCI). Melting points were determined in glass capillary tubes using a SANYO melting point apparatus and are uncorrected. X-ray crystallography was performed by Dr. Craig Forsyth at Monash University for structural determination of compounds **190c**, **191c**, **192c**, **190g** and **192g**.

Purity figures quoted are from LC-MS analysis. LC-MS analyses were performed at CSIRO, by Ms. Pamela M. Hoobin and/or co-workers Mrs. Megan Kruger and Mr. Andrey Mackay, on a Waters

Chapter 8

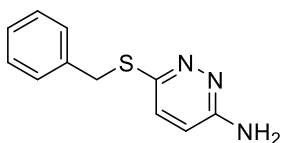
Acquity UPLC i-Class (Waters Corporation, Milford, MA, USA) with QDa performance mass detector with adjustment-free atmospheric pressure ionisation (API) electrospray (ES) interface. Positive and negative ions were recorded simultaneously with full scan analysis in m/z range 50 to 1000. High purity nitrogen (>95 %) nebulizing/desolvation gas was used for vaporisation with the pressure regulated at 650–700 kPa. The probe temperature was set at 600 °C, the source temperature at 120 °C, the cone voltage was 10 V whilst the capillary voltage was 0.8 kV for both positive and negative ion modes. The chromatographic conditions were as follows: column—Waters Acquity UPLC BEH C₁₈ (50 × 2.1 mm, 1.7 µm particle size); flow rate—0.4 mL/min; column temperature 30 °C; mobile phase A—100 % Milli-Q Water with 0.1 % formic acid; mobile phase B—100 % acetonitrile with 0.1 % formic acid; gradient—95 % A to 100 % B over 4.5 min, hold at 100 % B for 1 min, change to 95 % A over 0.5 min, then hold for 1 min. MS data were collected for the complete 7 min run. Spectral analysis was from 190 to 350 nm with chromatograms extracted using a wavelength of 254 nm.

8.2 General procedure for the syntheses of 6-(substituted)methylthio-3-amino-pyridazines



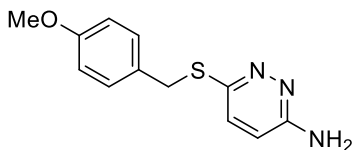
The halogenated alkyl species was added to either a stirred solution of 6-aminopyridazine-3-thiol (**69**) and sodium hydroxide in water⁷⁹ (or in a water/organic mixture) or a mixture of **69** with potassium carbonate in DMF at room temperature and allowed to stir overnight. If a precipitate formed, the solid was collected via vacuum filtration. Otherwise, the whole was extracted with ethyl acetate multiple times and the combined extract was washed with water, dried with sodium sulfate and concentrated under vacuum (unless stated otherwise). If purification was required, column chromatography and/or recrystallisation was applied.

The following compounds were synthesised according to the general procedure described above. Nuances including the amounts of substrates and reagents, reaction times, work-up variations, purifications, physical descriptions, yields, and characterisation data are described for each compound.

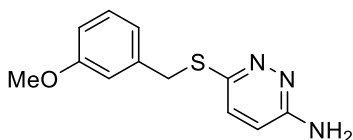


6-(Benzylthio)pyridazin-3-amine **81**.⁵³ Amounts: 6-aminopyridazine-3-thiol **69** (0.500 g, 3.93 mmol), benzyl bromide **70** (0.51 mL, 4.3 mmol), potassium carbonate (1.09 g, 7.86 mmol) and dry DMF (4 mL). Reaction time: 2.5 hours. Work-up: cold water (20 mL) was added to the reaction mixture whilst in an ice-bath, resulting in the precipitation of an orange-red solid. Purification: Recrystallisation from water. Physical description: yellow crystalline solid. Yield: 97 mg, 11 %. ¹H NMR (600 MHz, CDCl₃) δ 7.41 (d, *J* = 7.3 Hz, 2H), 7.28 (t, *J* = 7.5 Hz, 2H), 7.22 (t, *J* = 7.3 Hz, 1H), 7.05 (d, *J* = 9.1 Hz, 1 H), 6.61 (d, *J* = 9.1 Hz, 1H), 4.57 (s, 2H), 4.47 (s, 2H). ¹³C NMR (150 MHz, CDCl₃) δ 157.7, 152.3, 137.7, 129.2, 128.7, 128.6, 127.3, 115.4, 35.4.

Chapter 8

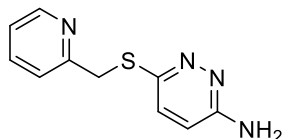


6-((4-Methoxybenzyl)thio)pyridazin-3-amine **82**.⁷⁹ Amounts: 6-aminopyridazine-3-thiol **69** (2.00 g, 15.7 mmol), 4-methoxybenzyl chloride **71** (2.35 mL, 17.3 mmol) and 0.5 M NaOH (80 mL). Reaction time: 16.5 hours. Work-up: a clump of red and white solids precipitated. The solvent was decanted and the red and white solid mixture was dissolved in DCM. The solution was dried with sodium sulfate and concentrated under vacuum. Purification: column chromatography (0-10 % MeOH/DCM, $R_f = 0.69$ (EtOAc)) and recrystallisation from toluene. Physical description: white crystals. Yield: 0.265 g, 7 %. ¹H NMR (600 MHz, DMSO-*d*₆) δ 7.27 (d, $J = 8.6$ Hz, 2H), 7.19 (d, $J = 9.2$ Hz, 1H), 6.84 (d, $J = 8.6$ Hz, 2H), 6.69 (d, $J = 9.2$ Hz, 1H), 6.26 (s, 2H), 4.29 (s, 2H), 3.71 (s, 3H). ¹³C NMR (150 MHz, DMSO-*d*₆) δ 158.9, 158.3, 149.4, 130.0, 129.7, 128.0, 115.0, 113.7, 55.0, 34.0.



6-((3-Methoxybenzyl)thio)pyridazin-3-amine **83**.⁷⁹ Amounts: 6-aminopyridazine-3-thiol **69** (0.509 g, 4.00 mmol), 3-methoxybenzyl chloride **72** (0.64 mL, 4.4 mmol) and 0.5 M NaOH (20 mL). Work-up: The reaction formed a red, gummy mass from which the aqueous phase was removed. The gummy mass was dissolved in DCM (10 mL), dried with magnesium sulfate and filtered. The organic layer within the filtrate was concentrated to obtain the crude product (1.175 g). Purification: Recrystallisation from toluene (8 mL) and left to stand overnight. Physical description: pink/orange crystalline solid. Yield: 0.447 g, 45 %. ¹H NMR (600 MHz, CDCl₃) δ 7.18 (t, $J = 7.9$ Hz, 1H), 7.02 (d, $J = 9.2$ Hz, 1H), 6.97 (d, $J = 7.6$ Hz, 1H), 6.94 (s, 1H), 6.77 (d, $J = 8.2$ Hz, 1H), 6.61 (d, $J = 9.2$ Hz, 1H), 4.82 (s, 2H), 4.43 (s, 2H), 3.77 (s, 3H). ¹³C NMR (150 MHz, CDCl₃) 159.7, 157.7, 152.3, 139.2, 129.6, 128.7, 121.5, 115.4, 114.6, 113.0, 55.1, 35.4.

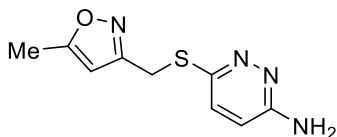
Chapter 8



6-((Pyridin-2-ylmethyl)thio)pyridazin-3-amine **84**. Amounts: 6-aminopyridazine-3-thiol **69** (0.229 g, 1.80 mmol), 2-(bromomethyl)pyridine hydrobromide **73** (0.500 g, 1.98 mmol) and 1.2 M NaOH (10 mL). Reaction time: 18 hours. Work-up: extraction process. Purification: not required. Physical description: yellow solid. Yield: 0.156 g, 40 %. ^1H NMR (600 MHz, CDCl_3) δ 8.54 (d, $J = 4.6$ Hz, 1H), 7.59 (td, $J = 7.7, 1.7$ Hz, 1H), 7.48 (d, $J = 7.7$ Hz, 1H), 7.14 (dd, $J = 6.8, 5.1$ Hz, 1H), 7.11 (d, $J = 9.2$ Hz, 1H), 6.62 (d, $J = 9.2$ Hz, 1H), 4.61 (s, 2H), 4.59 (s, 2H). ^{13}C NMR (150 MHz, $\text{DMSO}-d_6$) δ 158.0, 156.7, 148.2, 148.1, 135.9, 127.1, 122.1, 121.3, 114.2, 35.4.



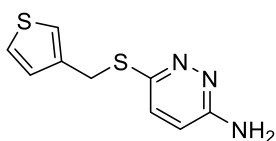
6-((Pyridin-4-ylmethyl)thio)pyridazin-3-amine **85**. Amounts: 6-aminopyridazine-3-thiol **69** (0.231 g, 1.82 mmol), 4-(bromomethyl)pyridine hydrobromide **74** (0.500 g, 1.98 mmol) and 1.0 M NaOH (10 mL). Reaction time: 19 hours. Work-up: vacuum filtration. Purification: not required. Physical description: light brown solid. Yield: 0.274 g, 70 %. ^1H NMR (600 MHz, $\text{DMSO}-d_6$) δ 8.46 (dd, $J = 6.0, 1.7$ Hz, 2H), 7.36 (dd, $J = 5.9, 1.6$ Hz, 2H), 7.22 (d, $J = 9.2$ Hz, 1H), 6.70 (d, $J = 9.2$ Hz, 1H), 6.30 (s, 2H), 4.37 (s, 2H). ^{13}C NMR (150 MHz, $\text{DMSO}-d_6$) δ 159.1, 149.6, 148.3, 147.6, 128.2, 124.0, 115.3, 33.0.



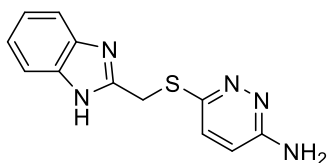
6-(((5-Methylisoxazol-3-yl)methyl)thio)pyridazin-3-amine **86**. Amounts: 6-aminopyridazine-3-thiol **69** (0.160 g, 1.25 mmol), 3-(bromomethyl)-5-methylisoxazole **75** (0.200 g, 1.14 mmol), 0.5

Chapter 8

M NaOH (5 mL), water (5 mL) and THF (1 mL). Reaction time: 16.5 hours. Work-up: vacuum filtration. Physical description: creamy white solid. Yield: 0.275 g, 95 %. ^1H NMR (600 MHz, CDCl_3) δ 7.12 (d, $J = 9.2$ Hz, 1H), 6.66 (d, $J = 9.2$ Hz, 1H), 6.04 (s, 1H), 4.66 (s, 2H), 4.45 (d, $J = 1.2$ Hz, 2H), 2.35 (d, $J = 1.1$ Hz, 3H). ^{13}C NMR (150 MHz, CDCl_3) δ 169.8, 161.8, 157.8, 151.4, 128.4, 115.4, 102.1, 25.2, 12.4.



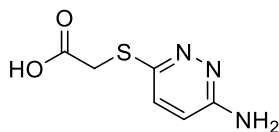
6-((Thiophen-3-ylmethyl)thio)pyridazin-3-amine **87**. Amounts: 6-aminopyridazine-3-thiol **69** (0.326 g, 2.56 mmol), 3-(bromomethyl)thiophene (0.31 mL, 2.8 mmol) **76**, 0.8 M NaOH (12 mL), water (8 mL), dioxane (2 mL) and THF (2 mL). Reaction time: 17 hours. Work-up: extraction process. Physical description: orange solid. Purification: column chromatography (ethyl acetate). Physical description: tan solid. Yield: 0.262 g, 47 %. ^1H NMR (600 MHz, CDCl_3) δ 7.24 (dd, $J = 4.9$, 3.0 Hz, 1H), 7.22 (d, $J = 2.8$ Hz, 1H), 7.10 (dd, $J = 4.9$, 1.3 Hz, 1H), 7.05 (d, $J = 9.1$ Hz, 1H), 6.62 (d, $J = 9.1$ Hz, 1H), 4.60 (s, 2H), 4.50 (s, 2H). ^{13}C NMR (150 MHz, CDCl_3) δ 157.5, 152.1, 137.8, 128.7, 128.36, 125.8, 123.2, 115.2, 29.8.



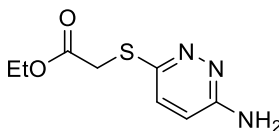
6-(((1H-Benzo[d]imidazol-2-yl)methyl)thio)pyridazin-3-amine **88**. Amounts: 6-aminopyridazine-3-thiol **69** (0.500 g, 3.93 mmol), 2-chloromethylbenzimidazole **77** (0.595 g, 3.57 mmol) and 0.8 M NaOH in THF/ H_2O (2 mL: 10 mL). Reaction time: 17 hours. Work-up: extraction process. Purification: not required. Physical description: yellow solid. Yield: 0.223 g, 24 %. ^1H NMR (600 MHz, $\text{DMSO}-d_6$) δ 12.36 (s, 1H), 7.53 (d, $J = 7.8$ Hz, 1H), 7.43 (d, $J = 7.7$ Hz, 1H), 7.31 (d, $J = 9.2$ Hz,

Chapter 8

1H), 7.19-7.08 (m, 2H), 6.73 (d, $J = 9.2$ Hz, 1H), 6.31 (s, 2H), 4.57 (s, 2H). ^{13}C NMR (150 MHz, DMSO- d_6) δ 159.1, 151.1, 148.7, 143.1, 134.4, 128.0, 122.0, 121.1, 118.4, 115.2, 111.2, 28.2.

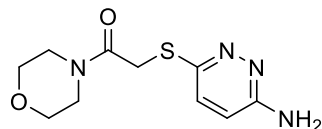


2-((6-Aminopyridazin-3-yl)thio)acetic acid **89**. Amounts: 6-aminopyridazine-3-thiol **69** (0.500 g, 3.93 mmol), ethyl bromoacetate **78** (0.48 mL, 4.3 mmol), and 1.0 M NaOH (10 mL). Reaction time: 18 hours. Work-up: 1 M HCl was added to the reaction mixture until pH 3 was reached resulting in precipitation and prompting vacuum filtration. Purification: not required. Physical description: a light blue/grey solid. Yield: 0.499 g, 69 %. ^1H NMR (600 MHz, DMSO- d_6) δ 7.25 (d, $J = 9.2$ Hz, 1H), 6.72 (d, $J = 9.2$ Hz, 1H), 6.26 (s, 2H), 3.90 (s, 2H). ^{13}C NMR (150 MHz, DMSO- d_6) δ 170.3, 158.9, 148.6, 127.5, 115.3, 32.8.

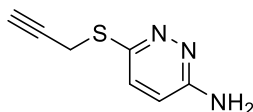


Ethyl 2-((6-aminopyridazin-3-yl)thio)acetate **90**. Amounts: 6-aminopyridazine-3-thiol **69** (0.500 g, 3.93 mmol), ethyl bromoacetate **78** (0.48 mL, 4.3 mmol), potassium carbonate (0.905 g, 6.55 mmol) and DMF (6 mL). Reaction time: 17.5 hours. Work-up: extraction process. Purification: not required. Physical description: honey coloured oil. Yield: 0.314 g, 37 %. ^1H NMR (600 MHz, CDCl_3) δ 7.15 (d, $J = 9.2$ Hz, 1H), 6.65 (d, $J = 9.2$ Hz, 1H), 4.66 (s, 2H), 4.20 (q, $J = 7.1$ Hz, 2H), 4.04 (s, 2H), 1.26 (t, $J = 7.1$ Hz, 4H). ^{13}C NMR (150 MHz, CDCl_3) δ 169.4, 157.7, 150.9, 128.3, 115.4, 61.9, 33.0, 14.3.

Chapter 8

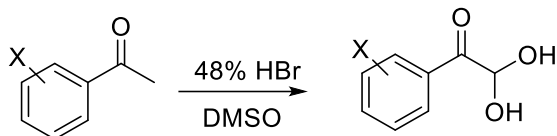


2-((6-Aminopyridazin-3-yl)thio)-1-morpholinoethan-1-one **91**. Amounts: 6-aminopyridazine-3-thiol **69** (0.500 g, 3.93 mmol), 4-(chloroacetyl)morpholine **79** (0.46 mL, 2.6 mmol) and 1.0 M NaOH (10 mL). Reaction time: ~30 seconds. Work-up: vacuum filtration. Physical description: white solid. Yield: 0.999 g, 68 %. ^1H NMR (600 MHz, CDCl_3) δ 7.17 (d, $J = 9.1$ Hz, 1H), 6.65 (d, $J = 9.1$ Hz, 1H), 4.58 (s, 2H), 4.21 (s, 2H), 3.69 (s, 2H), 3.66 (s, 2H) 3.63 (s, 4H). ^{13}C NMR (150 MHz, CDCl_3) δ 167.2, 157.6, 151.5, 128.4, 115.5, 66.9, 66.8, 46.8, 42.7, 33.0.



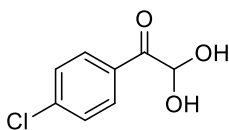
6-(Prop-2-yn-1-ylthio)pyridazin-3-amine **92**. Amounts: 6-aminopyridazine-3-thiol **69** (0.500 g, 3.93 mmol), propargyl bromide **80** (0.48 mL, 6.3 mmol), potassium carbonate (1.09 g, 7.86 mmol) and DMF (5.5 mL). Reaction time: 40 minutes. Work-up: extraction process. Physical description: black solid. Yield: 0.467 g, 72 %. ^1H NMR (600 MHz, CDCl_3) δ 7.15 (d, $J = 9.2$ Hz, 1H), 6.69 (d, $J = 9.2$ Hz, 1H), 4.84 (s, 2H), 3.97 (d, $J = 2.4$ Hz, 2H), 2.18 (t, $J = 2.4$ Hz, 1H). ^{13}C NMR (150 MHz, CDCl_3) δ 158.0, 150.9, 128.7, 115.4, 79.7, 71.2, 19.4.

8.3 General procedure for the syntheses of phenylglyoxal monohydrates⁵⁸



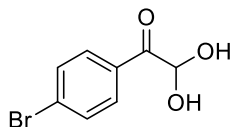
48% Aqueous HBr (3.4 mL, 30 mmol) was added dropwise to a stirred mixture of acetophenone (10.0 mmol) and DMSO (17 mL) at room temperature. The reaction mixture was stirred and heated to 55 °C for 17-26 hours. The whole was poured onto ice generally resulting in the formation of a precipitate. The precipitate was collected via vacuum filtration, washed with water and recrystallised from water affording the *title compound*. When no precipitation occurred, the reaction mixture was extracted with ethyl acetate multiple times and the combined extract was washed with water, dried with sodium sulfate and concentrated under vacuum. The residue was purified via column chromatography (50 % ethyl acetate/hexane) affording the *title compound*.

The following compounds were synthesised according to the general procedure described above. Nuances including reaction times, work-up variations, purifications, physical descriptions, yields, and characterisation data are described for each compound.

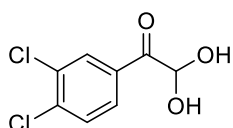


4'-Chlorophenylglyoxal monohydrate 105.⁶⁴ Reaction time: 24 hours. Work-up: vacuum filtration. Purification: recrystallisation. Physical description: white needles. Yield: 0.936 g, 50%. M.p 98-100 °C ¹H NMR (600 MHz, DMSO-*d*₆) δ 8.08 (d, *J* = 8.6 Hz, 2H), 7.59 (d, *J* = 8.6 Hz, 2H), 6.87 (d, *J* = 7.1 Hz, 2H), 5.63 (t, *J* = 7.1 Hz, 1H). ¹³C NMR (150 MHz, CDCl₃) δ 195.3, 138.2, 132.3, 131.4, 128.6, 89.7.

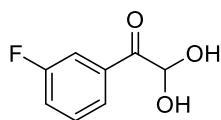
Chapter 8



4'-Bromophenylglyoxal monohydrate **106**.^{58,130} Reaction time: 26 hours. Work-up: vacuum filtration. Purification: recrystallisation. Physical description: white needles. Yield: 0.989 g, 43%. M.p 114-118 °C. ¹H NMR (600 MHz, DMSO-*d*₆) 8.00 (d, *J* = 8.5 Hz, 2H), 7.74 (d, *J* = 8.5 Hz, 2H), 6.86 (d, *J* = 7.0 Hz, 2H), 5.62 (t, *J* = 7.0 Hz, 1H). ¹³C NMR (150 MHz, CDCl₃) 195.5, 132.7, 131.6, 131.4, 127.4, 89.7.

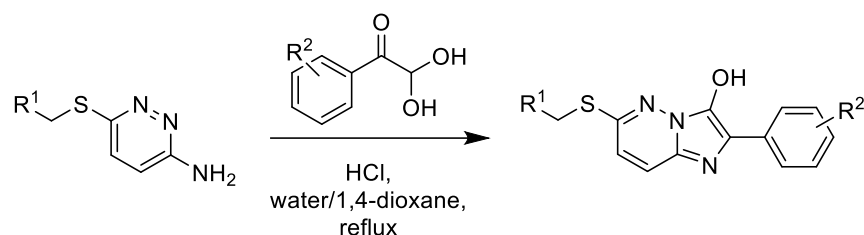


3',4'-Dichlorophenylglyoxal monohydrate **107**.¹³¹ Reaction time: 27 hours. Work-up: vacuum filtration. Purification: recrystallisation. Physical description: white needles. Yield: 0.257 g, 12%. M.p 70-74 °C. ¹H NMR (600 MHz, DMSO-*d*₆) 8.26 (d, *J* = 1.9 Hz, 1H), 8.00 (dd, *J* = 8.4, 2.0 Hz, 1H), 7.82 (d, *J* = 8.4 Hz, 1H), 7.02 (d, *J* = 6.9 Hz, 2H), 5.60 (t, *J* = 6.9 Hz, 1H). ¹³C NMR (150 MHz, CDCl₃) 194.3, 136.0, 133.7, 131.3, 131.3, 130.9, 129.4, 90.0.



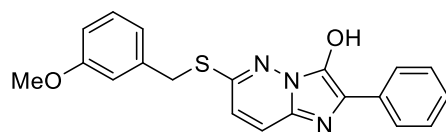
3'-Fluorophenylglyoxal monohydrate **108**.⁶² Reaction time: 17 hours. Work-up: extraction process. Purification: column chromatography. Physical description: white crystalline plates. Yield: 72 mg, 4%. ¹H NMR (600 MHz, DMSO-*d*₆) δ 7.91 (dt, *J* = 7.7, 1.2 Hz, 1H), 7.82 (ddd, *J* = 10.0, 2.7, 1.5 Hz, 1H), 7.58 (td, *J* = 8.0, 5.8 Hz, 1H), 7.49 (tdd, *J* = 8.4, 2.8, 1.0 Hz, 1H), 6.88 (d, *J* = 7.1 Hz, 2H), 5.64 (t, *J* = 7.1 Hz, 1H). ¹³C NMR (150 MHz, DMSO-*d*₆) δ 195.1, 161.8 (d, *J*_{C-F} = 243.0), 135.8 (d, *J*_{C-F} = 6.3 Hz) 130.6 (d, *J*_{C-F} = 7.7 Hz), 125.5 (d, *J*_{C-F} = 2.2 Hz), 120.1 (d, *J*_{C-F} = 20.9 Hz), 115.8 (d, *J*_{C-F} = 22.2 Hz), 89.6.

8.4 General procedure for the syntheses of imidazo[1,2-b]pyridazin-3-ols



Conc. HCl was added to a stirred solution of the pyridazin-3-amine and the phenylglyoxal monohydrate in 1,4-dioxane or aqueous 1,4-dioxane and the whole was heated at reflux overnight. The reaction mixture was cooled to ambient temperature and then further in an ice bath. Water was added and the resulting precipitate was collected via vacuum filtration and washed with water affording the *title compound* as an orange solid (unless stated otherwise).

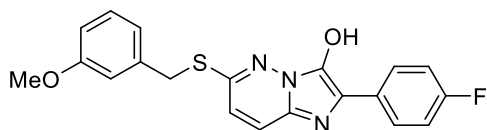
*The following compounds were synthesised according to the general procedure described above. Nuances including the amounts of substrates and reagents, reaction times, physical descriptions, yields, and characterisation data are described for each compound. Note: difficulties were encountered in obtaining ^{13}C NMR data for these molecules due to a lack of intensity of the peaks. As a reference, ^{13}C NMR data was obtained for 6-((3-methoxybenzyl)thio)-2-phenylimidazo[1,2-b]pyridazin-3-ol **120** by utilising 2D NMR spectroscopy to extract the peaks.*



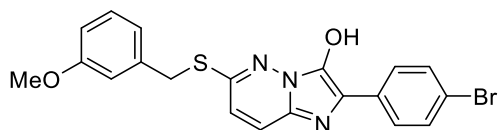
6-((3-Methoxybenzyl)thio)-2-phenylimidazo[1,2-b]pyridazin-3-ol **123**.⁷⁹ Amounts: 6-((3-Methoxybenzyl)thio)pyridazine-3-amine **83** (0.708 g, 2.86 mmol), phenylglyoxal monohydrate **113** (0.523 g, 3.44 mmol), conc. HCl (0.7 mL), 1,4-dioxane (7 mL) and water during work-up (35 mL). Reaction time: 17.5 hours. Yield: 0.901 g, 87 %. ^1H NMR (600 MHz, $\text{DMSO}-d_6$) δ 8.09 (d, $J = 7.7$ Hz, 2H), 7.87 (d, $J = 9.4$ Hz, 1H), 7.47 (t, $J = 7.6$ Hz, 2H), 7.29 (t, $J = 7.4$ Hz, 1H), 7.24 (t, $J = 7.69$ Hz, 1H), 7.13 (s, 1H), 7.12 (overlapping, 1H), 7.09 (d, $J = 7.6$ Hz, 1H), 6.82 (dd, $J = 8.2, 2.6$ Hz, 1H),

Chapter 8

4.53 (s, 2H), 3.74 (s, 3H). ^{13}C NMR (150 MHz, $\text{DMSO-}d_6$) δ 159.7, 154.5, 139.7, 139.1, 132.2, 130.4, 129.15, 129.0, 127.3, 125.4, 122.73, 121.9, 119.5, 117.9, 115.3, 113.4, 55.5, 34.2.

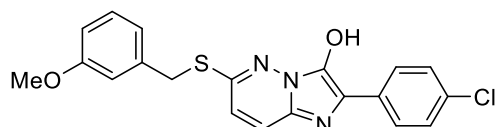


2-(4-Fluorophenyl)-6-((3-methoxybenzyl)thio)imidazo[1,2-b]pyridazin-3-ol **124**.⁷⁹ Amounts: 6-((3-Methoxybenzyl)thio)pyridazine-3-amine **83** (0.400 g, 1.62 mmol), 4'-fluorophenyglyoxal monohydrate **114** (0.275 g, 1.62 mmol), conc. HCl (0.4 mL), 1,4-dioxane (3 mL) and water during work-up (10 mL). Reaction time: 15.5 hours. Yield: 0.307 g, 74 %. ^1H NMR (600 MHz, $\text{DMSO-}d_6$) δ 8.11 (t, J = 6.4 Hz, 2H), 7.93 (d, J = 9.4 Hz, 1H), 7.35 (t, J = 8.7 Hz, 2H), 7.24 (overlapping, 2H), 7.13 (s, 1H), 7.09 (d, J = 7.5 Hz, 1H), 6.83 (d, J = 8.1 Hz, 1H), 4.54 (s, 2H), 3.73 (s, 3H).

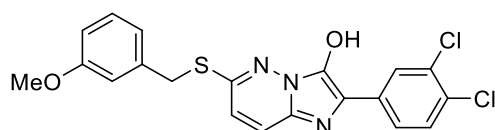


2-(4-Bromophenyl)-6-((3-methoxybenzyl)thio)imidazo[1,2-b]pyridazin-3-ol **125**. Amounts: 6-((3-Methoxybenzyl)thio)pyridazine-3-amine **83** (0.106 g, 0.430 mmol), 4'-bromophenyglyoxal monohydrate **106** (0.116 g, 0.500 mmol), conc. HCl (0.08 mL), 1,4-dioxane (2 mL) and water during work-up (15 mL). Reaction time: 20 hours. Yield: 0.131 g, 74 %. M.p. 190-200 °C (dec.). ^1H NMR (600 MHz, $\text{DMSO-}d_6$) δ 8.03 (d, J = 8.5 Hz, 2H), 7.84 (d, J = 9.4 Hz, 1H), 7.65 (d, J = 8.5 Hz, 2H), 7.23 (t, J = 7.9 Hz, 1H), 7.12 (s, 1H), 7.11 (d, J = 9.4 Hz, 1H), 7.08 (d, J = 7.6 Hz, 1H), 6.83 (dd, J = 8.2, 2.0 Hz, 1H), 4.52 (s, 2H), 3.74 (s, 3H).

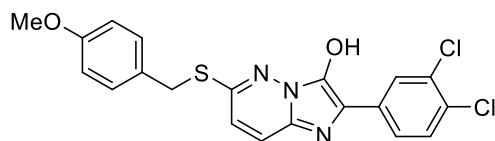
Chapter 8



2-(4-Chlorophenyl)-6-((3-methoxybenzyl)thio)imidazo[1,2-b]pyridazin-3-ol **126**. Amounts: 6-((3-Methoxybenzyl)thio)pyridazine-3-amine **83** (87 mg, 0.35 mmol), 4'-chlorophenyglyoxal monohydrate **105** (0.078 g, 0.42 mmol), conc HCl (0.08 mL), 1,4-dioxane (1.8 mL) and water during work-up (6 mL). Reaction time: 17.5 hours. Yield: 0.100 g, 72 %. M.p. 180-190 °C (dec.). ¹H NMR (600 MHz, DMSO-*d*₆) 8.11 (d, *J* = 8.3 Hz, 2H), 7.77 (d, *J* = 9.4 Hz, 1H), 7.49 (d, *J* = 8.2 Hz, 2H), 7.24 (t, *J* = 7.9 Hz, 1H), 7.12 (s, 1H), 7.08 (d, *J* = 7.6 Hz, 1H), 6.98 (d, *J* = 9.4 Hz, 1H), 6.82 (d, *J* = 5.6 Hz, 1H), 4.50 (s, 2H), 3.73 (s, 3H).



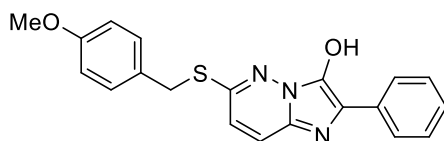
2-(3,4-Dichlorophenyl)-6-((3-methoxybenzyl)thio)imidazo[1,2-b]pyridazin-3-ol **127**. Amounts: 6-((3-Methoxybenzyl)thio)pyridazine-3-amine **83** (0.103 g, 0.420 mmol), 3',4'-dichlorophenyglyoxal monohydrate **107** (0.108 g, 0.490 mmol), conc. HCl (0.08 mL), 1,4-dioxane (2 mL) and water during work-up (6 mL). Reaction time: 17 hours. Yield: 0.123 g, 70%. M.p. 110-114 °C (dec.). ¹H NMR (600 MHz, DMSO-*d*₆) δ 8.25 (s, 1H), 8.04 (dd, *J* = 8.5, 2.0 Hz, 1H), 7.78 (d, *J* = 9.4 Hz, 1H), 7.68 (d, *J* = 8.5 Hz, 1H), 7.24 (t, *J* = 7.9 Hz, 1H), 7.12 (d, *J* = 2.4 Hz, 1H), 7.09 (d, *J* = 7.5 Hz, 1H), 7.02 (d, *J* = 9.4 Hz, 1H), 6.82 (dd, *J* = 8.2, 2.6 Hz, 1H), 4.51 (s, 2H), 3.74 (s, 3H).



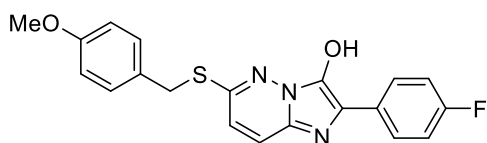
2-(3,4-Dichlorophenyl)-6-((4-methoxybenzyl)thio)imidazo[1,2-b]pyridazin-3-ol **128**. Amounts: 6-((4-Methoxybenzyl)thio)pyridazine-3-amine **82** (0.100 g, 0.404 mmol), 3',4'-dichlorophenyglyoxal monohydrate **107** (0.133 g, 0.602 mmol), conc. HCl (0.1 mL), 1,4-dioxane (2 mL) and water during

Chapter 8

work-up (10 mL). Reaction time: 16.5 hours. Yield: 0.162 g, 93 %. ^1H NMR (600 MHz, $\text{DMSO-}d_6$) δ 8.28 (d, $J = 2.0$ Hz, 1H), 8.05 (dd, $J = 8.5, 2.0$ Hz, 1H), 7.85 (d, $J = 9.4$ Hz, 1H), 7.70 (d, $J = 8.5$ Hz, 1H), 7.45 (d, $J = 8.7$ Hz, 2H), 7.13 (d, $J = 9.4$ Hz, 1H), 6.87 (d, $J = 8.7$ Hz, 2H), 4.48 (s, 2H), 3.71 (s, 3H).

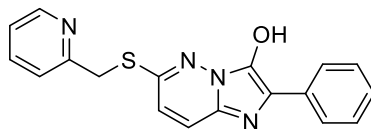


6-((4-Methoxybenzyl)thio)-2-phenylimidazo[1,2-b]pyridazin-3-ol **129**.⁷⁹ Amounts: 6-((4-Methoxybenzyl)thio)pyridazine-3-amine **82** (0.200 g, 0.809 mmol), phenylglyoxal monohydrate **113** (0.148 g, 0.970 mmol), conc. HCl (0.2 mL), 1,4-dioxane (3 mL) and water during work-up (none, a yellow precipitate formed after the reaction mixture was cooled to room temperature). Reaction time: 16.5 hours. Physical description: pale yellow solid. Yield: 0.192 g, 65 %. ^1H NMR (600 MHz, $\text{DMSO-}d_6$) δ 8.09 (dd, $J = 8.4, 1.2$ Hz, 2H), 7.96 (d, $J = 9.4$ Hz, 1H), 7.51 (t, $J = 7.9$ Hz, 2H), 7.46 (d, $J = 8.7$ Hz, 2H), 7.35 (t, $J = 7.4$ Hz, 1H), 7.29 (d, $J = 9.4$ Hz, 1H), 6.89 (d, $J = 8.7$ Hz, 2H), 4.53 (s, 2H), 3.72 (s, 3H).

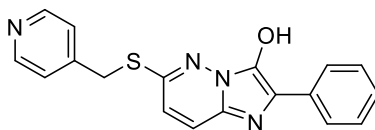


2-(4-Fluorophenyl)-6-((4-methoxybenzyl)thio)imidazo[1,2-b]pyridazin-3-ol **130**. Amounts: 6-((4-Methoxybenzyl)thio)pyridazine-3-amine **82** (0.128 g, 0.518 mmol), 4'-fluorophenyglyoxal monohydrate **114** (0.106 g, 0.621 mmol), conc. HCl (0.13 mL), 1,4-dioxane (2 mL) and water during work-up (13 mL). Reaction time: 17 hours. Yield: 0.131 g, 66 %. ^1H NMR (600 MHz, $\text{DMSO-}d_6$) δ 8.12 (dd, $J = 8.5, 5.6$ Hz, 2H), 7.79 (d, $J = 9.3$ Hz, 1H), 7.44 (d, $J = 8.2$ Hz, 2H), 7.30 (d, $J = 8.7$ Hz, 2H), 6.99 (d, $J = 9.3$ Hz, 1H), 6.88 (d, $J = 8.3$ Hz, 2H), 4.49 (s, 2H), 3.72 (s, 3H).

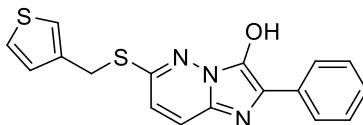
Chapter 8



*2-Phenyl-6-((pyridin-2-ylmethyl)thio)imidazo[1,2-*b*]pyridazin-3-ol* **131**. Amounts: 6-((Pyridin-2-ylmethyl)thio)pyridazin-3-amine **84** (0.175 g, 8.03 mmol), phenylglyoxal monohydrate **113** (0.147 g, 0.964 mmol), conc. HCl (0.2 mL), 20 % water/dioxane (5 mL) and water during work-up (10 mL). Reaction time: 19 hours. Yield: 0.230 g, 86 %. ^1H NMR (600 MHz, DMSO- d_6) δ 8.79 (d, $J = 5.4$ Hz, 1H), 8.30 (t, $J = 7.8$ Hz, 1H), 8.14 (d, $J = 8.0$ Hz, 1H), 8.10 (d, $J = 7.8$ Hz, 2H), 8.00 (d, $J = 9.4$ Hz, 1H), 7.75 (t, $J = 6.6$ Hz, 1H), 7.51 (t, $J = 7.7$ Hz, 2H), 7.41-7.32 (overlapping, 2H), 4.92 (s, 2H).



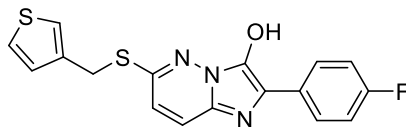
*2-Phenyl-6-((pyridin-4-ylmethyl)thio)imidazo[1,2-*b*]pyridazin-3-ol* **132**. Amounts: 6-((Pyridin-4-ylmethyl)thio)pyridazin-3-amine **85** (0.200 g, 0.916 mmol), phenylglyoxal monohydrate **113** (0.167 g, 1.10 mmol), conc. HCl (0.2 mL) and 20% water/1,4-dioxane (3.6 mL). Work-up: Water/THF (15mL/20 mL) was added to the reaction mixture and the azeotropic mixture was evaporated under vacuum revealing a brown solid. The brown solid was triturated with ethyl acetate (5 mL x 4). Residual solvent was removed under vacuum. Physical description: brown solid. 0.305 g, quantitative yield. ^1H NMR (600 MHz, DMSO- d_6) δ 8.85 (d, $J = 6.7$ Hz, 2H), 8.28 (d, $J = 6.7$ Hz, 2H), 8.11 (d, $J = 7.1$ Hz, 2H), 7.95 (d, $J = 9.4$ Hz, 1H), 7.49 (t, $J = 7.6$ Hz, 2H), 7.33 (t, $J = 7.4$ Hz, 1H), 7.29 (d, $J = 9.3$ Hz, 1H), 4.83 (s, 2H).



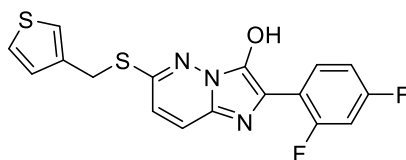
*2-Phenyl-6-((thiophen-3-ylmethyl)thio)imidazo[1,2-*b*]pyridazin-3-ol* **133**. Amounts: 6-((Thiophen-3-ylmethyl)thio)pyridazin-3-amine **87** (0.210 g, 0.940 mmol), phenylglyoxal monohydrate **113**

Chapter 8

(0.173 g, 1.13 mmol), conc. HCl (0.2 mL) and water during work-up (20 mL). Reaction time: 17.5 hours. Yield: 0.273 g, 86 %. ^1H NMR (600 MHz, $\text{DMSO-}d_6$) δ 8.08 (d, $J = 7.8$ Hz, 2H), 7.93 (d, $J = 9.4$ Hz, 1H), 7.60 (d, $J = 3.0$ Hz, 1H), 7.52-7.47 (overlapping, 3H), 7.33 (s, 1H), 7.25-7.20 (overlapping, 2H), 4.59 (s, 2H).

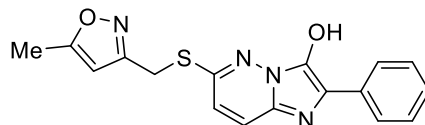


2-(4-Fluorophenyl)-6-((thiophen-3-ylmethyl)thio)imidazo[1,2-b]pyridazin-3-ol **134**. Amounts: 6-((Thiophen-3-ylmethyl)thio)pyridazin-3-amine **87** (0.293 g, 1.31 mmol), 4'-fluorophenylglyoxal monohydrate **114** (0.279 g, 1.57 mmol), conc. HCl (0.3 mL), 1,4-dioxane (5 mL) and water during workup (25 mL). Reaction time: 17 hours. Yield: 0.303 g, 62 %. ^1H NMR (600 MHz, $\text{DMSO-}d_6$) δ 8.08 (q, $J = 4.6$ Hz, 2H), 7.87 (t, $J = 6.1$ Hz, 1H), 7.56 (s, 1H), 7.47 (q, $J = 2.6$ Hz, 1H), 7.32 (t, $J = 8.7$ Hz, 2H), 7.21 (d, $J = 4.9$ Hz, 1H), 7.18 (t, $J = 7.3$ Hz, 1H), 4.56 (s, 2H).

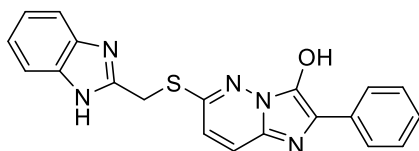


2-(2,4-Difluorophenyl)-6-((thiophen-3-ylmethyl)thio)imidazo[1,2-b]pyridazin-3-ol **135**. Amounts: 6-((Thiophen-3-ylmethyl)thio)pyridazin-3-amine **87** (0.250 g, 1.12 mmol), 2',4'-difluorophenylglyoxal monohydrate **115** (0.253 g, 1.34 mmol), conc. HCl (0.25 mL), 1,4-dioxane (3 mL) and water during workup (25 mL). Reaction time: 17 hours. Yield: 0.334 g, 76 %. ^1H NMR (600 MHz, $\text{DMSO-}d_6$) δ 8.03 (q, $J = 8.0$ Hz, 1H), 7.85 (d, $J = 9.4$ Hz, 1H), 7.57 (dd, $J = 2.9, 0.8$ Hz, 1H), 7.47 (dd, $J = 2.9, 1.9$ Hz, 1H), 7.37-7.34 (m, 1H), 7.23-7.20 (m, 2H), 7.14 (t, $J = 9.4$ Hz, 1H), 4.56 (s, 2H).

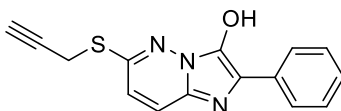
Chapter 8



6-(((5-Methylisoxazol-3-yl)methyl)thio)-2-phenylimidazo[1,2-b]pyridazin-3-ol **136**. Amounts: 6-(((5-Methylisoxazol-3-yl)methyl)thio)pyridazin-3-amine **86** (0.250 g, 1.12 mmol), phenylglyoxal monohydrate **113** (0.205 g, 1.35 mmol), conc. HCl (0.25 mL), 1,4-dioxane (4 mL) and water during work-up (20 mL). Reaction time: 17 hours. Yield: 0.212 g, 56 %. ^1H NMR (600 MHz, DMSO- d_6) δ 8.09 (d, $J = 8.5$ Hz, 2H), 7.87 (d, $J = 9.4$ Hz, 1H), 7.46 (t, $J = 7.6$ Hz, 2H), 7.27 (t, $J = 7.4$ Hz, 1H), 7.11 (d, $J = 9.3$ Hz, 1H), 6.34 (s, 1H), 4.56 (s, 2H), 2.36 (s, 3H).



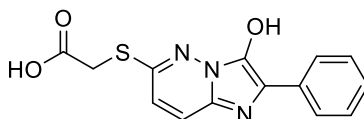
6-(((1H-Benzo[d]imidazol-2-yl)methyl)thio)-2-phenylimidazo[1,2-b]pyridazin-3-ol **137**. Amounts: of 6-(((1H-Benzo[d]imidazol-2-yl)methyl)thio)pyridazin-3-amine **88** (0.168 g, 0.654 mmol), phenylglyoxal monohydrate **113** (0.119 g, 0.785 mmol), conc. HCl (0.2 mL), 18 % water/1,4-dioxane (5.5 mL) and water during the work-up (20 mL). Reaction time: 16 hours. Physical description: red solid. Yield: 0.178 g, 73 %. ^1H NMR (600 MHz, DMSO- d_6) δ 8.09 (d, $J = 7.8$ Hz, 2H), 7.86 (d, $J = 9.4$ Hz, 1H), 7.74 (d, $J = 3.2$ Hz, 1H), 7.73 (d, $J = 3.1$ Hz, 1H), 7.49-7.39 (overlapping, 4H), 7.24 (t, $J = 7.4$ Hz, 1H), 7.14 (d, $J = 9.4$ Hz, 1H), 5.02 (s, 2H).



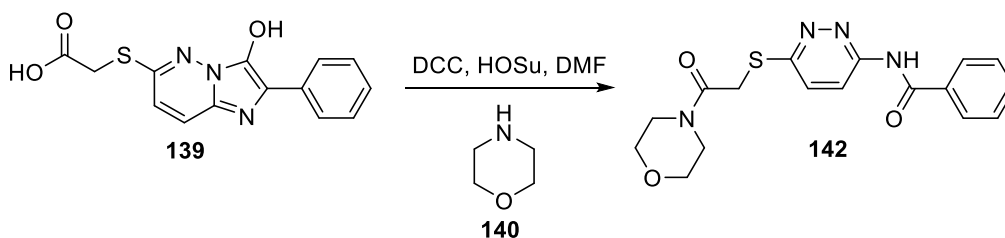
2-Phenyl-6-(prop-2-yn-1-ylthio)imidazo[1,2-b]pyridazin-3-ol **138**. Amounts: 6-(Prop-2-yn-1-ylthio)pyridazin-3-amine **92** (0.250 g, 1.51 mmol), phenylglyoxal monohydrate **113** (0.276 g, 1.82 mmol), conc. HCl (0.25 mL), 20 % water/1,4-dioxane (5 mL) and water during work-up (~20 mL). Reaction time: 20 hours. Physical description: brown solid. Yield: 0.342 g, 81 %. ^1H NMR (600

Chapter 8

MHz, DMSO- d_6) δ 8.08 (d, J = 7.8 Hz, 2H), 7.96 (d, J = 9.4 Hz, 1H), 7.48 (t, J = 7.6 Hz, 2H), 7.31 (t, J = 7.41 Hz, 1H), 7.23 (d, J = 9.4 Hz, 1H), 4.20 (d, J = 2.2 Hz, 2H), 3.25 (t, J = 2.2 Hz, 1H).



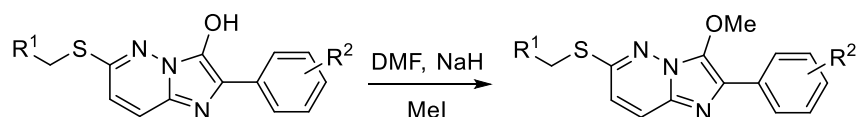
2-((3-Hydroxy-2-phenylimidazo[1,2-*b*]pyridazin-6-yl)thio)acetic acid **139**. Amounts: 2-((6-Aminopyridazin-3-yl)thio)acetic acid **89** (0.302 g, 1.62 mmol), phenylglyoxal monohydrate **113** (0.296 g, 1.94 mmol), conc. HCl (0.3 mL), 17 % water/1,4-dioxane (5.0 mL) and water during work-up (24 mL). Reaction time: 17 hours. Yield: 0.304 g, 62 %. ^1H NMR (600 MHz, DMSO- d_6) δ 8.08 (d, J = 8.2 Hz, 2H), 7.83 (d, J = 9.3 Hz, 1H), 7.44 (t, J = 7.6 Hz, 2H), 7.26 (t, J = 7.4 Hz, 1H), 7.07 (d, J = 9.3 Hz, 1H), 4.20 (s, 2H).



N-(6-((2-morpholino-2-oxoethyl)thio)pyridazin-3-yl)benzamide **142**. Morpholine **140** (69 mg, 0.796 mmol) was added to a stirred solution of 2-((3-Hydroxy-2-phenylimidazo[1,2-*b*]pyridazin-6-yl)thio)acetic acid **139** (0.200 g, 0.664 mmol), DCC (0.164 g, 0.796 mmol) and HOSu (0.092 g, 0.80 mmol) in DMF (3 mL) and the whole was stirred for 23 hours. A white precipitate, assumed to be DCU, was removed via vacuum filtration. Water was added to the filtrate and the mixture was extracted with ethyl acetate (x 3) and the combined organic phase was washed with water, dried with sodium sulfate and concentrated under vacuum. The residue was chromatographed and elution with 5-30 % ether/DCM and subsequently 4 % methanol/DCM afforded the *title compound* **142** (28 mg, 12 %). ^1H NMR (600 MHz, CDCl_3) δ 9.21 (s, 1H), 8.48 (d, J = 9.4 Hz, 1H), 7.95 (d, J = 7.7 Hz, 2H), 7.60 (t, J = 7.4 Hz, 1H), 7.51 (t, J = 7.6 Hz, 2H), 7.46 (d, J = 9.4 Hz, 1H), 4.24

(s, 2H), 3.71-3.70 (m, 4H), 3.64-3.69 (m, 4H). ^{13}C NMR (150 MHz, CDCl_3) δ 166.8, 166.5, 157.5, 153.6, 133.70, 133.1, 129.3, 128.3, 127.8, 119.6, 67.1, 66.9, 45.0, 42.9, 33.2. LCMS (ESI): $[\text{M}+\text{H}]^+$, found 359.09. $\text{C}_{17}\text{H}_{19}\text{N}_4\text{O}_3\text{S}^+$ 359.12. Purity: 96.2 %.

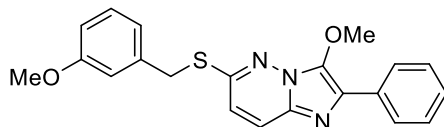
8.5 General procedure for the syntheses of 3-methoxyimidazo[1,2-*b*]pyridazines



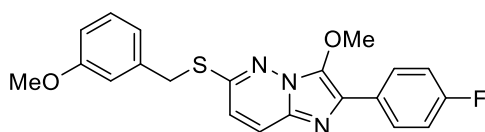
60 % Sodium hydride (dispersion in mineral oil) was triturated with hexane under nitrogen and the supernatant was removed via pipette. Residual hexane was removed by nitrogen flow. Dry DMF was added to the base under a nitrogen atmosphere and the mixture was cooled in an ice bath with stirring. Separately, a solution of the imidazo[1,2-*b*]pyridazin-3-ol in dry DMF was prepared. The substrate solution was added at 0 °C under a nitrogen atmosphere to the stirred base suspension or the suspension was added to the substrate solution, depending on the solubility of the substrate. The reaction mixture was warmed to room temperature (or higher, as specified) at which it was stirred for 10-40 minutes. Methyl iodide was added dropwise and the resulting mixture was stirred for a further 20-50 minutes. The reaction mixture was cooled in an ice bath and water was added. If a precipitate formed the solid was isolated via vacuum filtration. If no precipitate formed, the crude mixture was extracted with ethyl acetate multiple times. The combined extract was washed with water multiple times and dried with sodium sulfate. The solvent was removed *in vacuo* affording the crude 3-methoxyimidazo[1,2-*b*]pyridazine, which was purified by trituration or column chromatography.

The following compounds (except for 167 and 156) were synthesised according to the general procedure described above. Nuances including the amounts of substrates and reagents, reaction times, work-up variations, purifications, physical descriptions, yields, and characterisation data are described for each compound.

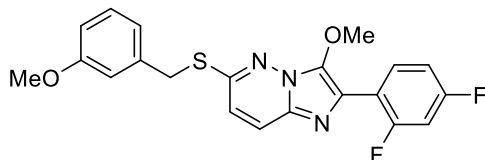
Chapter 8



3-Methoxy-6-((3-methoxybenzyl)thio)-2-phenylimidazo[1,2-b]pyridazine **64**.⁷⁹ Amounts: 2-Phenyl-6-((3-methoxybenzyl)thio)imidazo[1,2-b]pyridazin-3-ol **123** (0.450 g, 1.24 mmol), methyl iodide (0.23 mL, 3.7 mmol), 60% sodium hydride (0.102 g, 2.56 mmol) and dry DMF (8.0 mL). Deprotonation reaction time: 15 minutes. Methylation reaction time: 20 minutes. Temperature: RT. Work-up: extraction process. Purification: column chromatography (DCM). Physical description: golden brown waxy solid. Yield: 0.147 g, 31 %. ¹H NMR (600 MHz, CDCl₃) δ 8.12 (dd, *J* = 8.3, 1.3 Hz, 2H), 7.64 (d, *J* = 9.4 Hz, 1H), 7.46 (t, *J* = 7.8 Hz, 2H), 7.33 (t, *J* = 7.4 Hz, 1H), 7.25 (t, *J* = 7.6 Hz, 1H), 7.10-7.04 (overlapping, 2H), 6.82 (dd, *J* = 8.7, 2.1 Hz, 1H), 6.79 (d, *J* = 9.4 Hz, 1H), 4.47 (s, 2H), 4.11 (s, 3H), 3.80 (s, 3H). ¹³C NMR (150 MHz, CDCl₃) δ 159.9, 153.5, 139.4, 138.2, 133.2, 131.9, 129.8, 129.2, 128.8, 127.7, 126.3, 124.7, 121.5, 116.7, 114.9, 113.2, 61.0, 55.4, 35.0. HRMS (APCI): [M+H]⁺, found 378.1287. C₂₁H₂₀N₃O₂S⁺ requires 378.1271. Purity: 96.1 %.

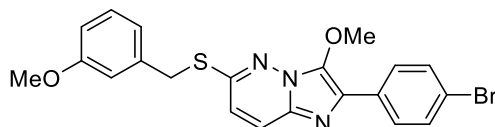


2-(4-Fluorophenyl)-3-methoxy-6-((3-methoxybenzyl)thio)imidazo[1,2-b]pyridazine **65**.⁷⁹ Amounts: 2-(4-Fluorophenyl)-6-((3-methoxybenzyl)thio)imidazo[1,2-b]pyridazin-3-ol **124** (0.648 g, 1.70 mmol), methyl iodide (0.21 mL, 3.4 mmol), 60% sodium hydride (0.204 g, 5.11 mmol), dry DMF (7 mL) and water during work-up (32 mL). Deprotonation reaction time: 30 minutes. Methylation reaction time: 35 minutes. Temperature: 24 °C. Work-up: vacuum filtration. Purification: not required. Physical description: pale yellow solid. Yield: 0.534 g, 79 %. ¹H NMR (600 MHz, CDCl₃) δ 8.10-8.08 (m, 2H), 7.62 (d, *J* = 9.3 Hz, 1H), 7.24 (t, *J* = 7.9 Hz, 1H), 7.14 (t, *J* = 8.7 Hz, 2H), 7.07 (d, *J* = 7.5 Hz, 1H), 7.05 (s, 1H), 6.82 (dd, *J* = 8.1, 2.0 Hz, 1H), 6.79 (d, *J* = 9.3 Hz, 1H), 4.46 (s, 2H), 4.09 (s, 3H), 3.80 (s, 3H). ¹³C NMR (150 MHz, CDCl₃) 162.5 (d, *J*_{C-F} = 95.7 Hz), 159.9, 153.6, 139.1, 138.1, 131.9, 129.8, 129.4 (d, *J*_{C-F} = 3.1 Hz), 128.4, 128.0 (d, *J*_{C-F} = 8.1 Hz), 124.6, 121.5, 116.8, 115.8 (d, *J*_{C-F} = 21.7 Hz), 114.9, 113.2, 61.0, 55.4, 35.0. HRMS (APCI): [M+H]⁺, found 396.1182. C₂₁H₁₉FN₃O₂S⁺ requires 396.1177. Purity: 99.0 %.



2-(2,4-Difluorophenyl)-3-methoxy-6-((3-methoxybenzyl)thio)imidazo[1,2-b]pyridazine **66.**

Amounts: Amounts: 2-(2,4-Difluorophenyl)-6-((3-methoxybenzyl)thio)imidazo[1,2-b]pyridazin-3-ol **261** (0.500 g, 1.25 mmol), methyl iodide (0.16 mL, 2.5 mmol), 60% sodium hydride (0.150 g, 3.75 mmol), dry DMF (6.5 mL), and water during work-up (22 mL). Deprotonation reaction time: 40 minutes. Methylation reaction time: 40 minutes. Temperature: 19.5 °C. Work-up: vacuum filtration. Purification: not required. Physical description: brown solid. Yield: 0.405 g, 78 %. M.p 99-100 °C. ¹H NMR (600 MHz, CDCl₃) 7.79 (q, *J* = 7.8 Hz, 1H), 7.65 (d, *J* = 9.4 Hz, 1H), 7.24 (t, *J* = 7.8 Hz, 1H), 7.06 (d, *J* = 6.06 Hz, 1H), 7.05 (s, 1H), 6.98 (td, *J* = 8.3, 2.5 Hz, 1H), 6.95-6.91 (m, 1H), 6.82 (dd, *J* = 8.0, 2.3 Hz, 1H), 6.81 (d, *J* = 9.4 Hz, 1H), 4.46 (s, 2H), 4.09 (s, 3H), 3.79 (s, 3H). ¹³C NMR (150 MHz, CDCl₃) δ 162.9 (dd, *J*_{C-F} = 248.4, 11.7 Hz), 160.0 (dd, *J*_{C-F} = 250.9, 11.4 Hz), 159.9, 153.81, 139.8, 138.0, 132.2, 131.8 (dd, *J*_{C-F} = 9.7, 5.2 Hz), 129.8, 124.9, 124.1, 121.5, 117.54 (dd, *J*_{C-F} = 14.3, 2.5 Hz), 116.9, 114.9, 113.2, 111.8 (dd, *J*_{C-F} = 29.9, 3.3 Hz), 104.5 (t, *J*_{C-F} = 25.5 Hz), 61.4 (d, *J*_{C-F} = 2.2 Hz), 55.4, 35.0. Purity: 96.7 %.

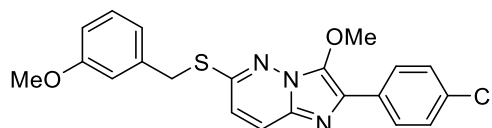


2-(4-Bromophenyl)-3-methoxy-6-((3-methoxybenzyl)thio)imidazo[1,2-b]pyridazine

144. Amounts: 2-(4-Bromophenyl)-6-((3-methoxybenzyl)thio)imidazo[1,2-b]pyridazin-3-ol **125** (0.182 g, 0.411 mmol), methyl iodide (77 μL, 1.2 mmol), 60% sodium hydride (0.033 g, 0.51 mmol) and dry DMF (4.5 mL). Deprotonation reaction time: 40 minutes. Methylation reaction time: 20 minutes. Temperature: 28 °C. Work-up: extraction process. Purification: not required. Physical description: dark red waxy solid. Yield: 0.146 g, 75 %. ¹H NMR (600 MHz, CDCl₃) δ 7.99 (d, *J* = 8.4 Hz, 2H), 7.62 (d, *J* = 9.4 Hz, 1H), 7.57 (d, *J* = 8.4 Hz, 2H), 7.26-7.23 (overlapping, 1H), 7.07-7.05 (overlapping, 2H), 6.81 (dd, *J* = 8.3, 2.2 Hz, 1H), 6.79 (d, *J* = 9.4 Hz, 1H), 4.46 (s, 2H), 4.10 (s, 3H),

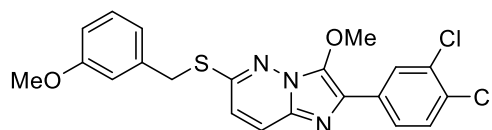
Chapter 8

3.80 (s, 3H). ^{13}C NMR (150 MHz, CDCl_3) δ 159.9, 153.8, 139.4, 138.0, 132.2, 132.0, 131.9, 129.8, 128.1, 127.8, 124.7, 121.7, 121.5, 117.0, 114.9, 113.2, 61.0, 55.4, 35.0. LCMS (ESI): $[\text{M}+\text{H}]^+$, found 458.10. $\text{C}_{21}\text{H}_{19}\text{BrN}_3\text{O}_2\text{S}^+$ requires 458.04. Purity: 95.0 %.



2-(4-Chlorophenyl)-3-methoxy-6-((3-methoxybenzyl)thio)imidazo[1,2-b]pyridazine **145.**

Amounts: 2-(4-Chlorophenyl)-6-((3-methoxybenzyl)thio)imidazo[1,2-b]pyridazin-3-ol **126** (0.084 g, 0.21 mmol), methyl iodide (39 μL , 0.63 mmol), 60% sodium hydride (0.098 g, 0.25 mmol) and dry DMF (3 mL). Deprotonation reaction time: 10 minutes. Methylation reaction time: 20 minutes. Temperature: 35 $^\circ\text{C}$. Work-up: extraction process. Purification: trituration (ether). Physical description: green solid. Yield: 36 mg, 42 %. ^1H NMR (600 MHz, CDCl_3) δ 8.05 (d, $J = 8.3$ Hz, 2H), 7.62 (d, $J = 9.4$ Hz, 1H), 7.42 (d, $J = 8.3$ Hz, 2H), 7.26-7.23 (overlapping, 1H), 7.07-7.05 (overlapping, 2H), 6.81 (dd, $J = 8.3, 2.6$ Hz, 1H), 6.79 (d, $J = 9.4$ Hz, 1H), 4.46 (s, 2H), 4.10 (s, 3H), 3.80 (s, 3H). ^{13}C NMR (150 MHz, CDCl_3) δ 159.9, 153.7, 139.4, 138.1, 133.4, 131.2, 131.8, 129.8, 129.0, 128.1, 127.5, 124.7, 121.5, 117.0, 114.9, 113.1, 61.0, 55.4, 35.0. LCMS (ESI): $[\text{M}+\text{H}]^+$, found 412.17. $\text{C}_{21}\text{H}_{19}\text{ClN}_3\text{O}_2\text{S}^+$ requires 412.09. Purity: 94.2 %.

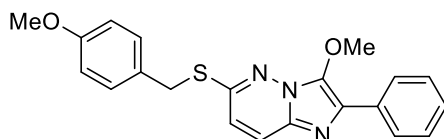


2-(3,4-Dichlorophenyl)-3-methoxy-6-((3-methoxybenzyl)thio)imidazo[1,2-b]pyridazine **146.**

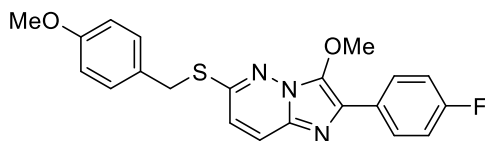
Amounts: 2-(3,4-Dichlorophenyl)-6-((3-methoxybenzyl)thio)imidazo[1,2-b]pyridazin-3-ol **127** (98 mg, 0.22 mmol), methyl iodide (41 μL , 0.66 mmol), 60% sodium hydride (9.5 mg, 0.24 mmol) and dry DMF (3 mL). Deprotonation reaction time: 10 minutes before. Methylation reaction time: 20 minutes. Temperature: 35 $^\circ\text{C}$. Work-up: extraction process. Purification: trituration (ether). Physical description: brown solid. Yield: 30 mg, 30 %. ^1H NMR (600 MHz, CDCl_3) δ 8.22 (d, $J = 2.0$

Chapter 8

Hz, 1H), 7.95 (dd, $J = 8.4, 2.0$ Hz, 1H), 7.62 (d, $J = 9.4$ Hz, 1H), 7.50 (d, $J = 8.4$ Hz, 1H), 7.25 (d, $J = 8.0$ Hz, 1H), 7.09-7.02 (overlapping, 2H), 6.84-6.78 (overlapping, 2H), 4.46 (s, 2H), 4.12 (s, 3H), 3.81 (s, 3H). ^{13}C NMR (150 MHz, CDCl_3) δ 160.0, 154.2, 139.6, 138.0, 133.4, 133.1, 132.10, 131.4, 130.8, 129.8, 127.9, 126.8, 125.3, 124.7, 121.5, 117.4, 114.9, 113.1, 61.1, 55.4, 35.1. LCMS (ESI): $[\text{M}+\text{H}]^+$, found 445.59. $\text{C}_{21}\text{H}_{18}\text{Cl}_2\text{N}_3\text{O}_2\text{S}^+$ requires 446.05. Purity: 97.6 %.



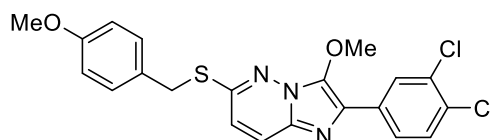
*3-Methoxy-6-((4-methoxybenzyl)thio)-2-phenylimidazo[1,2-*b*]pyridazine* **147.79** Amounts: 2-phenyl-6-((4-methoxybenzyl)thio)imidazo[1,2-*b*]pyridazin-3-ol **129** (0.142 g, 0.390 mmol), methyl iodide (73 μL , 1.2 mmol), 60% sodium hydride (39 mg, 0.98 mmol) and DMF (5 mL). Deprotonation reaction time: 35 minutes. Methylation reaction time: 30 minutes. Temperature: 20 $^\circ\text{C}$. Work-up: extraction process. Purification: not required. Physical description: green solid. Yield: 60 mg, 41 %. ^1H NMR (600 MHz, CDCl_3) δ 8.13 (d, $J = 7.5$ Hz, 2H), 7.63 (d, $J = 9.4$ Hz, 1H), 7.46 (t, $J = 7.7$ Hz, 2H), 7.41 (d, $J = 8.6$ Hz, 2H), 7.33 (t, $J = 7.4$ Hz, 1H), 6.87 (d, $J = 8.6$ Hz, 2H), 6.77 (d, $J = 9.4$ Hz, 1H), 4.45 (s, 2H), 4.14 (s, 3H), 3.79 (s, 3H). ^{13}C NMR (150 MHz, CDCl_3) δ 159.2, 153.7, 139.4, 133.3, 131.9, 130.4, 129.1, 128.8, 128.4, 127.7, 126.3, 124.6, 116.8, 114.2, 61.1, 55.5, 34.62. LCMS (ESI): $[\text{M}+\text{H}]^+$, found 441.38. $\text{C}_{23}\text{H}_{23}\text{F}_2\text{N}_4\text{OS}^+$ requires 441.16. Purity: 92.7 %.



*2-(4-Fluorophenyl)-3-methoxy-6-((4-methoxybenzyl)thio)imidazo[1,2-*b*]pyridazine* **148**. 2-(4-fluorophenyl)-6-((4-methoxybenzyl)thio)imidazo[1,2-*b*]pyridazin-3-ol **130** (0.200 g, 0.524 mmol), methyl iodide (98 μL , 1.6 mmol), 60% sodium hydride (55 mg, 1.3 mmol) and dry DMF (7 mL). Deprotonation reaction time: 40 minutes. Methylation reaction time: 30 minutes. Temperature: 24 $^\circ\text{C}$. Work-up: extraction process. Purification: not required. Physical description: golden brown

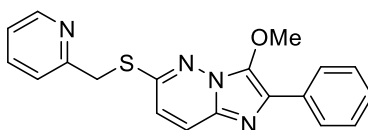
Chapter 8

solid. Yield: 0.161 g, 78 %. ^1H NMR (600 MHz, CDCl_3) δ 8.12-8.07 (m, 2H), 7.61 (d, $J = 9.4$ Hz, 1H), 7.40 (d, $J = 8.6$ Hz, 2H), 7.15 (t, $J = 8.7$ Hz, 2H), 6.87 (d, $J = 8.6$ Hz, 2H), 6.78 (d, $J = 9.4$ Hz, 1H), 4.45 (s, 2H), 4.13 (s, 3H), 3.79 (s, 3H). ^{13}C NMR (150 MHz, CDCl_3) δ 162.5 (d, $J_{\text{C-F}} = 245.1$ Hz), 159.2, 153.8, 139.1, 131.9, 130.4, 129.4 (d, $J_{\text{C-F}} = 3.1$ Hz), 128.4 (d, $J_{\text{C-F}} = 4.4$ Hz), 128.0 (d, $J_{\text{C-F}} = 7.6$ Hz), 124.6, 116.9, 115.9, 115.7, 114.2, 61.0, 55.5, 34.6. LCMS (ESI): $[\text{M}+\text{H}]^+$, found 396.17. $\text{C}_{21}\text{H}_{19}\text{FN}_3\text{O}_2\text{S}^+$ requires 396.12. Purity: 95.0 %.



2-(3,4-Dichlorophenyl)-3-methoxy-6-((4-methoxybenzyl)thio)imidazo[1,2-b]pyridazine **149.**

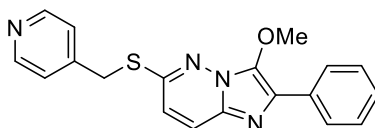
Amounts: *2-(3,4-Dichlorophenyl)-6-((4-methoxybenzyl)thio)imidazo[1,2-b]pyridazin-3-ol* **128** (0.128 g, 0.296 mmol), methyl iodide (55 μL , 0.89 mmol), 60% sodium hydride (0.024 g, 0.59 mmol), dry DMF (4 mL) and water during work-up (10 mL). Deprotonation reaction time: 15 minutes. Methylation reaction time: 20 minutes. Temperature: 34 $^\circ\text{C}$. Work-up: vacuum filtration. Purification: not required. Physical description: brown solid. Yield: 89 mg, 66 %. ^1H NMR (600 MHz, CDCl_3) δ 8.22 (d, $J = 2.0$ Hz, 1H), 7.95 (dd, $J = 8.4, 2.0$ Hz, 1H), 7.61 (d, $J = 9.4$ Hz, 1H), 7.51 (d, $J = 8.4$ Hz, 1H), 7.40 (d, $J = 8.5$ Hz, 2H), 6.87 (d, $J = 8.5$ Hz, 2H), 6.80 (d, $J = 9.4$ Hz, 1H), 4.44 (s, 2H), 4.15 (s, 3H), 3.79 (s, 3H). ^{13}C NMR (150 MHz, CDCl_3) δ 159.3, 154.3, 139.6, 133.4, 133.1, 132.1, 131.3, 130.8, 130.4, 128.2, 127.9, 126.7, 125.3, 124.7, 117.4, 114.2, 61.2, 55.5, 34.6. LCMS (ESI): $[\text{M}+\text{H}]^+$, found 445.92. $\text{C}_{21}\text{H}_{18}\text{Cl}_2\text{N}_3\text{O}_2\text{S}^+$ requires 446.05. Purity: 94.5 %.



3-Methoxy-2-phenyl-6-((pyridin-2-ylmethyl)thio)imidazo[1,2-b]pyridazine **151.** Amounts: *2-Phenyl-6-((pyridin-2-ylmethyl)thio)imidazo[1,2-b]pyridazin-3-ol* **131** (0.197 g, 0.590 mmol), methyl iodide (0.11 mL, 1.8 mmol) 60 % sodium hydride (0.072 g, 1.8 mmol) and dry DMF (4 mL).

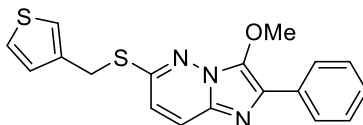
Chapter 8

The sodium hydride suspension was added to the substrate suspension. Deprotonation reaction time: 25 minutes. Methylation reaction time: 35 minutes. Temperature: 17 °C. Work-up: extraction process. Purification: column chromatography (0 - 1 % MeOH/DCM). Physical description: green solid. Yield: 0.108 g, 52 %. ¹H NMR (600 MHz, CDCl₃) δ 8.59 (d, *J* = 4.3 Hz, 1H), 8.11 (d, *J* = 7.4 Hz, 2H), 7.68-7.62 (overlapping, 2H), 7.58 (d, *J* = 7.8 Hz, 1H), 7.45 (t, *J* = 7.7 Hz, 2H), 7.32 (t, *J* = 7.4 Hz, 1H), 7.19 (dd, *J* = 7.3, 5.0 Hz, 1H), 6.83 (d, *J* = 9.4 Hz, 1H), 4.63 (s, 2H), 4.07 (s, 3H). ¹³C NMR (150 MHz, CDCl₃) δ 156.7, 153.2, 149.8, 139.4, 136.8, 133.2, 131.9, 129.2, 128.8, 127.8, 126.3, 124.7, 123.4, 122.5, 116.7, 61.0, 36.8. LCMS (ESI): [M+H]⁺, found 349.10. C₂₁H₁₉FN₃O₂S⁺ requires 349.11. Purity: 97.5 %.

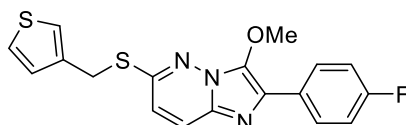


3-Methoxy-2-phenyl-6-((pyridin-4-ylmethyl)thio)imidazo[1,2-b]pyridazine **152**. Amounts: 2-Phenyl-6-((pyridin-4-ylmethyl)thio)imidazo[1,2-b]pyridazin-3-ol **132** (0.203 g, 0.608 mmol), methyl iodide (0.11 mL, 1.8 mmol), 60% sodium hydride (0.0728 g, 1.82 mmol) and dry DMF (6 mL). The sodium hydride suspension was added to the substrate suspension. Deprotonation reaction time: 35 minutes. Methylation reaction time: 25 minutes. Temperature: 17 °C. Work-up: ether (25mL) and water (10mL) were added to the mixture. The whole was extracted with ether (25 mL x 1, 15 ml x 3) and the combined organic layer was washed with water (10 mL x 7), dried with sodium sulfate and concentrated under vacuum. Purification: column chromatography (EtOAc). Physical description: yellow waxy solid. Yield: 57 mg, 27 %. ¹H NMR (600 MHz, CDCl₃) δ 8.58 (s (broad), 2H), 8.09 (dd, *J* = 8.5, 1.2 Hz, 2H), 7.71 (d, *J* = 9.4 Hz, 1H), 7.50-7.43 (overlapping, 4H), 7.33 (t, *J* = 7.4 Hz, 1H), 6.81 (d, *J* = 9.4 Hz, 1H), 4.44 (s, 2H), 3.99 (s, 3H).

Chapter 8



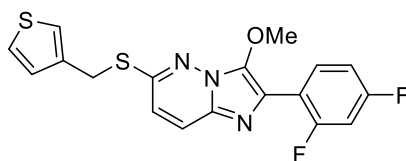
*3-Methoxy-2-phenyl-6-((thiophen-3-ylmethyl)thio)imidazo[1,2-*b*]pyridazine* **153**. Amounts: 2-Phenyl-6-((thiophen-3-ylmethyl)thio)imidazo[1,2-*b*]pyridazin-3-ol **133** (0.228 g, 0.663 mmol), DMF (6 mL), methyl iodide (0.12 mL, 2.0 mmol), 60 % sodium hydride (0.079 g, 2.0 mmol) and water during work-up (30 mL). Deprotonation reaction time: 25 minutes. Methylation reaction time: 30 minutes. Temperature: 19 °C. Work-up: vacuum filtration. Purification: not required. Physical description: brown solid. Yield: 0.126 g, 54 %. ¹H NMR (600 MHz, CDCl₃) δ 8.12 (d, *J* = 7.2 Hz, 2H), 7.64 (d, *J* = 9.4 Hz, 1H), 7.46 (t, *J* = 7.8 Hz, 2H), 7.36-7.31 (overlapping, 2H), 7.29 (dd, *J* = 5.0, 3.0 Hz, 1H), 7.18 (dd, *J* = 5.0, 1.3 Hz, 1H), 6.78 (d, *J* = 9.4 Hz, 1H) 4.51 (s, 2H), 4.12 (s, 3H). ¹³C NMR (150 MHz, CDCl₃) δ 153.4, 139.4, 136.8, 133.2, 131.9, 129.2, 128.8, 128.3, 127.8, 126.3 (overlapping), 124.7, 123.6, 116.8, 61.0, 29.6. LCMS (ESI): [M+H]⁺, found 354.11. C₁₈H₁₆N₃O₂S₂⁺ requires 354.07. Purity: 92.2 %.



*2-(4-Fluorophenyl)-3-methoxy-6-((thiophen-3-ylmethyl)thio)imidazo[1,2-*b*]pyridazine* **154**. Amounts: 2-(4-Fluorophenyl)-6-((thiophen-3-ylmethyl)thio)imidazo[1,2-*b*]pyridazin-3-ol **134** (0.303g, 0.848 mmol), methyl iodide (0.11 mL, 1.70 mmol), 60 % sodium hydride (0.091 g, 2.3 mmol), dry DMF (4 mL), and water during work-up (20 mL). Deprotonation reaction time: 30 minutes. Methylation reaction time: 35 minutes. Temperature: 16 °C. Work-up: vacuum filtration. Purification: not required. Physical description: brown solid. Yield: 0.244g, 74 %. ¹H NMR (600 MHz, CDCl₃) δ 8.11-8.08 (m, 2H), 7.63 (d, *J* = 9.3 Hz, 1H), 7.33 (s, 1H), 7.29 (dd, *J* = 4.9, 2.9 Hz, 1H), 7.17 (d, *J* = 4.9 Hz, 1H), 7.14 (t, *J* = 8.7 Hz, 2H), 6.79 (d, *J* = 9.3 Hz, 1H), 4.50 (s, 2H), 4.10 (s, 3H). ¹³C NMR (150 MHz, CDCl₃) δ 162.5 (d, *J*_{C-F} = 245.9 Hz) 153.4, 139.0, 136.8, 131.9, 129.3 (d, *J*_{C-F} = 3.1 Hz), 128.3 (d, *J*_{C-F} = 12.03 Hz), 128.0 (d, *J*_{C-F} = 7.8 Hz) 126.3, 124.6, 123.6, 116.8,

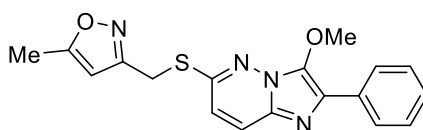
Chapter 8

115.8, 115.7, 61.0, 29.6. LCMS (ESI): $[M+H]^+$, found 372.18. $C_{21}H_{15}FN_3OS_2^+$ requires 372.06. Purity: 94.7 %.



2-(2,4-Difluorophenyl)-3-methoxy-6-((thiophen-3-ylmethyl)thio)imidazo[1,2-b]pyridazine **155.**

Amounts: 2-(2,4-Difluorophenyl)-6-((thiophen-3-ylmethyl)thio)imidazo[1,2-b]pyridazin-3-ol **135** (0.300 g, 0.799 mmol), methyl iodide (0.10 mL, 1.60 mmol), 60 % sodium hydride (0.096 g, 2.4 mmol), dry DMF (5 mL), and water during work-up (25 mL). Deprotonation reaction time: 30 minutes. Methylation reaction time: 35 minutes. Temperature: 17 °C. Work-up: vacuum filtration. Purification: not required. Physical description: brown solid. Yield: 0.143 g, 46 %. 1H NMR (600 MHz, $CDCl_3$) δ 7.80 (q, $J = 7.8$ Hz, 1H), 7.65 (d, $J = 9.4$ Hz, 1H), 7.33 (s, 1H), 7.30-7.28 (m, 1H), 7.17 (d, $J = 4.9$ Hz, 1H), 6.98 (td, $J = 8.2, 2.0$ Hz, 1H), 6.93 (td, $J = 9.2, 2.4$ Hz, 1H), 6.81 (d, $J = 9.4$ Hz, 1H), 4.50 (s, 2H), 4.10 (s, 3H). ^{13}C NMR (150 MHz, $CDCl_3$) δ 162.9 (dd, $J_{C-F} = 248.3, 11.7$ Hz) 160.1 (dd, $J_{C-F} = 251.0, 11.4$ Hz), 153.7, 139.8, 136.7, 132.21, 131.8 (dd, $J_{C-F} = 9.4, 4.8$ Hz), 128.3, 126.3, 124.9, 124.2, 123.7, 117.5 (dd, $J_{C-F} = 14.3, 3.5$ Hz), 117.0, 111.8 (dd, $J_{C-F} = 21.0, 3.3$ Hz), 104.5 (t, $J_{C-F} = 25.9$ Hz), 61.4 (d, $J_{C-F} = 2.4$ Hz), 29.6. LCMS (ESI): $[M+H]^+$, found 390.19. $C_{18}H_{14}F_2N_3OS_2^+$ requires 390.05. Purity: 92.6 %.

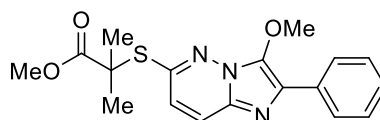


3-(((3-Methoxy-2-phenylimidazo[1,2-b]pyridazin-6-yl)thio)methyl)-5-methylisoxazole **156.**

Amounts: 6-(((5-Methylisoxazol-3-yl)methyl)thio)-2-phenylimidazo[1,2-b]pyridazin-3-ol **136** (0.180 g, 0.532 mmol), methyl iodide (99 μ L, 1.6 mmol), 60 % sodium hydride (0.065 g, 1.6 mmol) and dry DMF (8 mL). Deprotonation reaction time: 25 minutes. Methylation reaction time: 30 minutes. Temperature: 19 °C. Work-up: extraction process. Purification: column chromatography

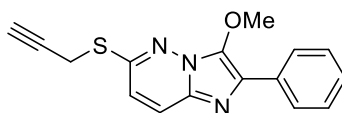
Chapter 8

(DCM). Physical description: golden waxy solid. Yield: 0.107 g, 57 %. M.p 80-84 °C. ^1H NMR (600 MHz, CDCl_3) δ 8.12 (d, $J = 7.9$ Hz, 2H), 7.67 (d, $J = 9.4$ Hz, 1H), 7.46 (t, $J = 7.7$ Hz, 2H), 7.33 (t, $J = 7.1$ Hz, 1H), 6.81 (d, $J = 9.4$ Hz, 1H), 6.12 (s, 1H), 4.47 (s, 2H), 4.14 (s, 3H), 2.39 (s, 3H). ^{13}C NMR (150 MHz, CDCl_3) δ 170.2, 160.8, 152.2, 139.5, 133.1, 131.9, 129.5, 128.8, 127.9, 126.3, 125.0, 116.3, 101.8, 61.1, 25.3, 12.5. LCMS (ESI): $[\text{M}+\text{H}]^+$, found 353.11 $\text{C}_{18}\text{H}_{17}\text{N}_4\text{O}_2\text{S}^+$ requires 353.11. Purity: 95.2 %.



Methyl 2-((3-methoxy-2-phenylimidazo[1,2-b]pyridazin-6-yl)thio)-2-methylpropanoate **158**.

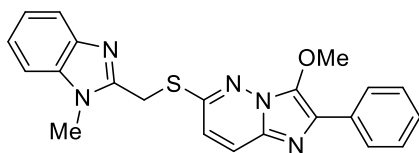
Amounts: 2-((3-Hydroxy-2-phenylimidazo[1,2-b]pyridazin-6-yl)thio)acetic acid **139** (0.329 g, 1.09 mmol), methyl iodide (0.41 mL, 6.6 mmol), 60 % sodium hydride (0.267 g, 6.55 mmol) and dry DMF (6 mL). Deprotonation reaction time: 30 minutes. Methylation reaction time: 45 minutes. Temperature: 30 °C. Work-up: extraction process. Purification: column chromatography (5 % ether/DCM). Physical description: green solid. Yield: 64 mg, 17 %. ^1H NMR (600 MHz, CDCl_3) δ 8.12 (d, $J = 7.4$ Hz, 2H), 7.67 (d, $J = 9.4$ Hz, 1H), 7.45 (t, $J = 7.8$ Hz, 2H), 7.32 (t, $J = 7.4$ Hz, 1H), 6.79 (d, $J = 9.4$ Hz, 1H), 4.12 (s, 3H), 3.79 (s, 3H), 1.76 (s, 6H). ^{13}C NMR (150 MHz, CDCl_3) δ 174.2, 152.0, 139.4, 133.1, 131.8, 129.7, 128.8, 127.8, 126.3, 124.9, 117.4, 61.3, 53.1, 51.6, 26.4. LCMS (ESI): $[\text{M}+\text{H}]^+$, found 358.07. $\text{C}_{18}\text{H}_{20}\text{N}_3\text{O}_3\text{S}^+$ requires 358.44. Purity: 95.7 %.



The above procedure was used to synthesise *3-Methoxy-2-phenyl-6-(prop-2-yn-1-ylthio)imidazo[1,2-b]pyridazine* **160**. Amounts: 2-Phenyl-6-(prop-2-yn-1-ylthio)imidazo[1,2-b]pyridazin-3-ol **138** (0.200 g, 0.711 mmol), methyl iodide (0.13 mL, 2.1 mmol), potassium carbonate (0.197 g, 1.43 mmol), dry DMF (3 mL) and water during work-up (15 mL). Deprotonation reaction time: 60 minutes. Methylation reaction time: 75 minutes. Temperature:

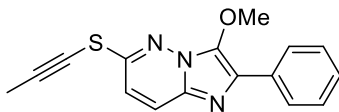
Chapter 8

20 °C. Purification: not required. Physical description: golden solid. Yield: 0.126 g, 60 %. ^1H NMR (600 MHz, CDCl_3) 8.13 (d, $J = 7.3$ Hz, 2H), 7.69 (d, $J = 9.3$ Hz, 1H), 7.46 (t, $J = 7.7$ Hz, 2H), 7.32 (t, $J = 7.3$ Hz, 1H), 6.82 (d, $J = 9.3$ Hz, 1H), 4.19 (s, 3H), 4.01 (d, $J = 2.5$ Hz, 2H), 2.21 (t, $J = 2.5$ Hz, 1H). δ ^{13}C NMR (150 MHz, CDCl_3) δ 151.8, 139.4, 133.1, 131.9, 129.47, 128.8, 127.8, 126.3, 124.9, 116.3, 79.0, 71.2, 61.1, 19.0. LCMS (ESI): $[\text{M}+\text{H}]^+$, found 296.24. $\text{C}_{16}\text{H}_{14}\text{N}_3\text{OS}^+$ requires 296.09. Purity: 90.0 %.

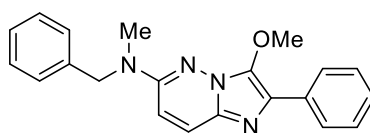


3-Methoxy-6-(((1-methyl-1H-benzo[d]imidazol-2-yl)methyl)thio)-2-phenylimidazo[1,2-b]pyridazine **171**. Amounts: Potassium carbonate (0.185 g, 1.34 mmol) was added to a stirred solution of 6-(((1H-benzo[d]imidazol-2-yl)methyl)thio)-2-phenylimidazo[1,2-b]pyridazin-3-ol **137** (0.200 g, 0.536 mmol) in dry DMF (3 mL) while under a nitrogen atmosphere and in an ice-bath. The reaction mixture was warmed to room temperature (20 °C) at which it was stirred for 75 minutes. Methyl iodide was added dropwise and the resulting mixture was stirred for a further 125 minutes. The reaction mixture was cooled in an ice bath and cold water (15 mL) was added resulting in the precipitation of a brown solid. The brown solid was chromatographed and elution with a mobile phase of 2.5 % methanol/DCM afforded the *title compound* **171** as a green solid (0.032 g, 15 %). ^1H NMR (600 MHz, CDCl_3) δ 8.11 (d, $J = 7.1$ Hz, 2H), 7.74 (d, $J = 7.7$ Hz, 1H), 7.69 (d, $J = 9.4$ Hz, 1H), 7.46 (t, $J = 7.8$ Hz, 2H), 7.35-7.25 (m, 4H), 6.86 (d, $J = 9.4$ Hz, 1H), 4.80 (s, 2H), 4.05 (s, 3H), 3.93 (s, 3H). ^{13}C NMR (150 MHz, CDCl_3) δ 152.4, 149.5, 142.6, 139.4, 136.2, 133.0, 131.9, 129.6, 128.9, 127.9, 126.3, 125.1, 123.2, 122.6, 119.9, 116.5, 109.4, 61.1, 30.5, 27.0. LCMS (ESI): $[\text{M}+\text{H}]^+$, found 402.26. $\text{C}_{22}\text{H}_{20}\text{N}_5\text{OS}^+$ requires 402.14. Purity: 91.5 %.

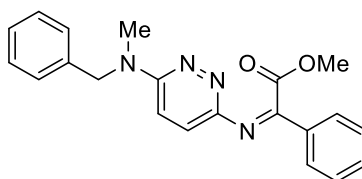
Chapter 8



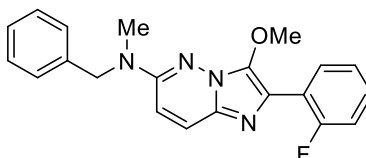
*3-Methoxy-2-phenyl-6-(prop-1-yn-1-ylthio)imidazo[1,2-*b*]pyridazine* **172**. Amounts: 2-Phenyl-6-(prop-2-yn-1-ylthio)imidazo[1,2-*b*]pyridazin-3-ol **138** (0.214 g, 0.760 mmol), methyl iodide (95 μ L, 1.52 mmol), 60 % sodium hydride (0.092 g, 2.3 mmol), DMF (4 mL) and water during work-up (20 mL). Deprotonation reaction time: 30 minutes. Methylation reaction time: 50 minutes. Temperature: 18 °C. Work-up: vacuum filtration. Purification: column chromatography (DCM). Physical description: green solid. Yield: 13 mg, 6 %. ^1H NMR (600 MHz, CDCl_3) δ 8.13 (d, $J = 7.3$ Hz, 2H), 7.79 (d, $J = 9.4$ Hz, 1H), 7.46 (t, $J = 7.7$ Hz, 2H), 7.33 (t, $J = 7.3$ Hz, 1H), 7.26 (d, $J = 9.3$ Hz, 1H), 4.15 (s, 3H), 2.14 (s, 3H). ^{13}C NMR (150 MHz, CDCl_3) δ 152.7, 139.3, 133.0, 131.9, 130.4, 128.9, 128.0, 126.4, 125.5, 114.6, 98.5, 61.1, 61.0, 5.5. HRMS (APCI): $[\text{M}+\text{H}]^+$, found 296.0855. $\text{C}_{16}\text{H}_{14}\text{N}_3\text{OS}^+$ requires 296.0853.



*3-Methoxy-6-(N-methylbenzylamino)-2-phenylimidazo[1,2-*b*]pyridazine* **18**.⁵⁴ Amounts: 6-(*N*-Methylbenzylamino)-2-phenylimidazo[1,2-*b*]pyridazin-3-ol **189a** (0.100 g, 0.303 mmol), methyl iodide (57 μ L, 0.91 mmol), 60 % sodium hydride (0.037 g, 0.91 mmol) and dry DMF (5 mL). *The sodium hydride suspension was added to the substrate suspension.* Deprotonation reaction time: 25 minutes. Methylation reaction time: 30 minutes. Temperature: 19 °C. Work-up: extraction process. Purification: column chromatography (10 % ether/DCM). Physical description: beige solid. Yield: 39 mg, 37 %. ^1H NMR (600 MHz, CDCl_3) δ 8.11 (d, $J = 7.2$ Hz, 2H), 7.60 (d, $J = 9.9$ Hz, 1H), 7.43 (t, $J = 7.9$ Hz, 2H), 7.34 (t, $J = 7.6$ Hz, 2H), 7.30-7.26 (overlapping, 4H), 6.67 (d, $J = 9.9$ Hz, 1H), 4.75 (s, 2H), 4.08 (s, 3H), 3.19 (s, 3H). ^{13}C NMR (150 MHz, CDCl_3) δ 154.2, 139.2, 137.9, 134.0, 130.8, 128.9, 128.7, 128.2, 127.5, 127.1, 127.1, 126.0, 125.9, 107.9, 60.4, 54.5, 37.2. LCMS (ESI): $[\text{M}+\text{H}]^+$, found 345.17. $\text{C}_{21}\text{H}_{21}\text{N}_4\text{O}^+$ requires 345.17. Purity: 97.4 %.



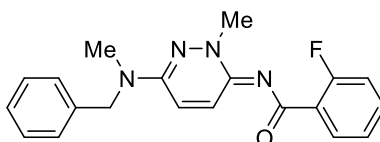
Earlier elution with the same mobile phase afforded methyl (Z)-2-((N-methylbenzylamino)pyridazin-3-yl)imino)-2-phenylacetate **191a**. Yield: 8 mg, 7 %. ^1H NMR (600 MHz, CDCl_3) δ 7.94 (d, J = 7.6 Hz, 2H), 7.51 (t, J = 7.3 Hz, 1H), 7.46 (t, J = 7.6 Hz, 2H), 7.32 (t, J = 7.5 Hz, 2H), 7.29-7.24 (overlapping, 4H), 6.85 (d, J = 9.5 Hz, 1H), 4.88 (s, 2H), 3.89 (s, 3H), 3.20 (s, 3H). ^{13}C NMR (150 MHz, CDCl_3) δ 165.9, 158.8, 158.6, 154.6, 137.7, 134.6, 131.9, 128.8, 128.8, 128.6, 127.5, 127.3, 126.0, 113.0, 53.8, 52.4, 36.8. LCMS (ESI): $[\text{M}+\text{H}]^+$, found 361.11. $\text{C}_{21}\text{H}_{21}\text{N}_4\text{O}_2^+$ requires 361.17. Purity: 58.9 % (degradation in the acidic aqueous mobile phase may have occurred).



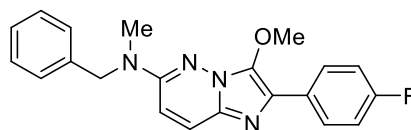
2-(2-Fluorophenyl)-3-methoxy-6-(N-methylbenzylamino)imidazo[1,2-b]pyridazine **190b**.⁵⁴
 Amounts: 2-(2-Fluorophenyl)-6-(N-methylbenzylamino)imidazo[1,2-b]pyridazin-3-ol **189b** (0.149 g, 0.431 mmol), methyl iodide (80 μL , 1.3 mmol), 60 % sodium hydride (0.053 g, 1.3 mmol), and dry DMF (4.5 mL). Deprotonation reaction time: 40 minutes. Methylation reaction time: 30 minutes. Temperature 18°C. The sodium hydride suspension was added to the substrate suspension. Work-up: extraction process. Purification: column chromatography (5-10 % ether/DCM). Physical description: light brown solid. Yield: 64 mg, 41 %. M.p 58-60 °C. ^1H NMR (600 MHz, CDCl_3) δ 7.81 (td, J = 7.6, 1.8 Hz, 1H), 7.62 (d, J = 9.9 Hz, 1H), 7.34 (t, J = 7.5 Hz, 2H), 7.32-7.26 (overlapping, 4H), 7.21 (td, J = 7.5, 1.2 Hz, 1H), 7.15 (ddd, J = 10.8, 8.2, 1.2 Hz, 1H), 6.69 (d, J = 9.9 Hz, 1H), 4.76 (s, 2H), 4.08 (s, 3H), 3.19 (s, 3H). ^{13}C NMR (150 MHz, CDCl_3) δ 160.0 (d, $J_{\text{C-F}}$ = 248.1 Hz), 154.2, 139.7, 137.8, 131.2, 130.8 (d, $J_{\text{C-F}}$ = 3.3 Hz), 129.1 (d, $J_{\text{C-F}}$ = 8.1 Hz), 128.9, 127.5,

Chapter 8

127.1, 126.3, 124.3 (d, $J_{C-F} = 3.6$ Hz), 123.9, 121.9 (d, $J_{C-F} = 13.9$ Hz), 116.1 (d, $J_{C-F} = 22.1$ Hz), 108.0, 60.8 (d, $J_{C-F} = 2.0$ Hz), 54.5, 37.2. HRMS (APCI): $[M+H]^+$, found 363.1626. $C_{21}H_{20}FN_4O^+$ requires 363.1616. Purity: 97.5 %.



Further elution with the same mobile phase afforded (*E*)-*N*-(6-(*N*-methylbenzylamino)-2-methylpyridazin-3(2*H*)-ylidene)-2-fluorobenzamide **192b**. Yield: 6.2 mg, 4 %. 1H NMR (600 MHz, $CDCl_3$) δ 8.59 (d, $J = 10.0$ Hz, 1H), 8.04 (t, $J = 7.7$ Hz, 1H), 7.36-7.35 (overlapping, 3H), 7.29 (t, $J = 7.2$ Hz, 1H), 7.20 (d, $J = 7.5$ Hz, 2H), 7.14 (t, $J = 7.6$ Hz, 1H), 7.11 (d, $J = 10.1$ Hz, 1H), 7.07 (t, $J = 9.6$ Hz, 1H), 4.64 (s, 2H), 3.99 (s, 3H), 3.07 (s, 3H). LCMS (ESI): $[M+H]^+$, found 351.10. $C_{20}H_{20}FN_4O^+$ requires 351.16. Purity: 93.8 %.

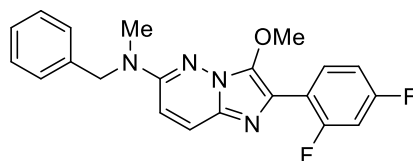


2-(4-Fluorophenyl)-3-methoxy-6-(*N*-methylbenzylamino)imidazo[1,2-*b*]pyridazine **190c**.⁵⁴

Amounts: 2-(4-Fluorophenyl)-6-(*N*-methylbenzylamino)imidazo[1,2-*b*]pyridazin-3-ol **189c** (0.150 g, 0.431 mmol), methyl iodide (54 μ L, 0.86 mmol), 60 % sodium hydride (0.052 g, 1.3 mmol) and dry DMF (4 mL). Deprotonation reaction time: 20 minutes. Methylation reaction time: 30 minutes. Temperature: 15 $^{\circ}C$. Work-up: extraction process. Purification: column chromatography (5 % ether/DCM). Physical description: light yellow solid. Yield: 75 mg, 48 %. Purity: 97.3 %. 1H NMR (600 MHz, $CDCl_3$) δ 8.07-8.04 (m, 2H), 7.59 (d, $J = 9.9$ Hz, 1H), 7.34 (t, $J = 7.6$ Hz, 2H), 7.30-7.26 (overlapping, 3H), 7.11 (t, $J = 8.7$ Hz, 2H), 6.68 (d, $J = 9.9$ Hz, 1H), 4.76 (s, 2H), 4.07 (s, 3H), 3.19 (s, 3H). ^{13}C NMR (150 MHz, $CDCl_3$) δ 162.1 (d, $J_{C-F} = 244.8$ Hz), 154.2, 138.9, 137.9, 130.7, 130.1 (d, $J_{C-F} = 3.2$ Hz), 128.9, 127.5, 127.5 (d, $J_{C-F} = 2.9$ Hz), 127.4, 127.1, 126.0, 115.6 (d, $J_{C-F} = 21$).

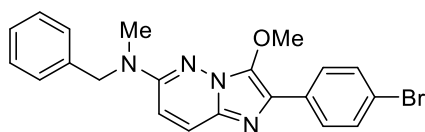
Chapter 8

1 Hz), 108.0, 60.4, 54.5, 37.2. HRMS (APCI): $[M+H]^+$, found 363.1618. $C_{21}H_{19}N_4O^+$ requires 362.1616. Purity: 97.3 %.



*2-(2,4-Difluorophenyl)-3-methoxy-6-(N-methylbenzylamino)imidazo[1,2-*b*]pyridazine* **190d**.

Amounts: 2-(2,4-Difluorophenyl)-6-(N-methylbenzylamino)imidazo[1,2-*b*]pyridazin-3-ol **189d** (0.150 g, 0.409 mmol), methyl iodide (51 μ L, 0.82 mmol), 60 % sodium hydride (0.049 g, 1.2 mmol), dry DMF (4 mL) and water during work-up (10 mL). Deprotonation reaction time: 25 minutes. Methylation reaction time: 30 minutes. Temperature: 18 °C. Work-up: vacuum filtration. Purification: not required. Physical description: brown solid. Yield: 94 mg, 60 %. 1H NMR (600 MHz, $CDCl_3$) δ 7.77 (q, $J = 7.9$ Hz, 1H), 7.61 (d, $J = 9.9$ Hz, 1H), 7.34 (t, $J = 7.4$ Hz, 2H), 7.28-7.26 (overlapping, 3H), 6.96 (td, $J = 8.4, 2.6$ Hz, 1H), 6.92-6.89 (m, 1H), 6.70 (d, $J = 9.9$ Hz, 1H), 4.76 (s, 2H), 4.07 (s, 3H), 3.19 (s, 3H). ^{13}C NMR (150 MHz, $CDCl_3$) δ 162.5 (dd, $J_{C-F} = 247.4, 11.4$ Hz), 160.0 (dd, $J_{C-F} = 250.7, 12.0$ Hz), 154.2, 139.5, 137.8, 131.6 (dd, $J_{C-F} = 9.5, 5.2$ Hz), 131.2, 128.9, 127.5, 127.0, 126.2, 123.2, 118.2 (dd, $J_{C-F} = 14.1, 3.0$ Hz), 111.6 (dd, $J_{C-F} = 21.2, 3.7$ Hz), 108.1, 104.4 (t, $J_{C-F} = 25.4$ Hz), 60.8 (d, $J_{C-F} = 2.0$ Hz), 54.5, 37.2. HRMS (APCI): $[M+H]^+$, found 381.1525. $C_{21}H_{19}F_2N_4O^+$ requires 381.1522. Purity: 97.0 %.

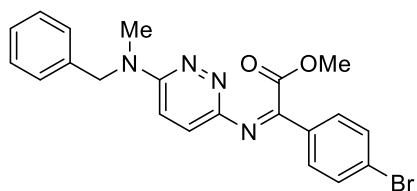


*2-(4-Bromophenyl)-3-methoxy-6-(N-methylbenzylamino)imidazo[1,2-*b*]pyridazine* **190e**.

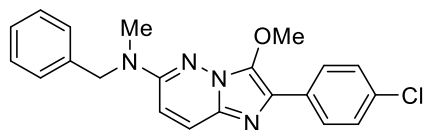
Amounts: 2-(4-Bromophenyl)-6-(N-methylbenzylamino)imidazo[1,2-*b*]pyridazin-3-ol **189e** (0.150 g, 0.366 mmol), methyl iodide (45 μ L, 0.73 mmol), 60 % sodium hydride (0.044 g, 1.1 mmol) and dry DMF (4 mL). Deprotonation reaction time: 30 minutes. Methylation reaction time: 30 minutes. Temperature: 15 °C. Work-up: extraction process. Purification: column chromatography

Chapter 8

(5 % ether/DCM). Physical description: golden solid. Yield: 48 mg, 31 %. ^1H NMR (600 MHz, CDCl_3) δ 7.97 (d, $J = 8.6$ Hz, 2H), 7.59 (d, $J = 9.9$ Hz, 1H), 7.54 (d, $J = 8.6$ Hz, 2H), 7.34 (t, $J = 7.6$ Hz, 2H), 7.28-7.26 (overlapping, 3H), 6.69 (d, $J = 9.9$ Hz, 1H), 4.76 (s, 2H), 4.07 (s, 3H), 3.19 (s, 3H). ^{13}C NMR (150 MHz, CDCl_3) δ 154.2, 139.3, 137.8, 133.0, 131.8, 130.9, 128.9, 127.6, 127.4, 127.1, 127.05, 126.0, 120.8, 108.2, 60.4, 54.5, 37.2. LCMS (ESI): $[\text{M}+\text{H}]^+$, found 425.16. $\text{C}_{21}\text{H}_{20}\text{BrN}_4\text{O}^+$ requires 425.08. Purity: 93.7 %.



Earlier elution with the the same mobile phase afforded methyl (Z)-2-((6-(N-methylbenzylamino)pyridazin-3-yl)imino)-2-(4-bromophenyl)acetate **191e**. Yield: 8 mg, 5 %. ^1H NMR (600 MHz, CDCl_3) δ 7.81 (d, $J = 8.6$ Hz, 2H), 7.59 (d, $J = 8.6$ Hz, 2H), 7.32 (t, $J = 7.5$ Hz, 2H), 7.28-7.24 (overlapping, 4H), 6.85 (d, $J =$ Hz, 1H), 4.88 (s, 2H), 3.88 (s, 3H), 3.20 (s, 3H). ^{13}C NMR (150 MHz, CDCl_3) δ 166.8, 158.8, 157.5, 154.4, 137.8, 133.7, 132.3, 130.3, 129.1, 127.7, 127.4, 127.0, 126.3, 113.2, 54.0, 52.7, 37.0. LCMS (ESI): $[\text{M}+\text{H}]^+$, found 441.02. $\text{C}_{21}\text{H}_{20}\text{BrN}_4\text{O}_2^+$ requires 341.07. Purity: 73.5 %.

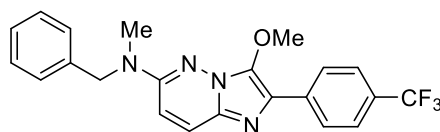


2-(4-Chlorophenyl)-3-methoxy-6-(N-methylbenzylamino)imidazo[1,2-b]pyridazine **190f**.⁵⁴

Amounts: 2-(4-Chlorophenyl)-6-(N-methylbenzylamino)imidazo[1,2-b]pyridazin-3-ol **189f** (0.150 g, 0.411 mmol), methyl iodide (51 μL , 0.82 mmol), 60 % sodium hydride (0.050 g, 1.23 mmol) and dry DMF (4 mL). Deprotonation reaction time: 25 minutes. Methylation reaction time: 20 minutes. Temperature: 15 $^\circ\text{C}$. Work-up: extraction process. Purification: column chromatography (5 % ether/DCM). Physical description: golden solid. Yield: 89 mg, 57 %. ^1H NMR (600 MHz, CDCl_3)

Chapter 8

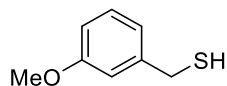
δ 8.03 (d, J = 8.6 Hz, 2H), 7.58 (d, J = 9.9 Hz, 1H), 7.39 (d, J = 8.6 Hz, 2H), 7.34 (t, J = 7.3 Hz, 2H), 7.28-7.26 (overlapping, 3H), 6.68 (d, J = 9.9 Hz, 1H), 4.75 (s, 2H), 4.07 (s, 3H), 3.19 (s, 3H). ^{13}C NMR (150 MHz, CDCl_3) δ 154.2, 139.2, 137.8, 132.6, 132.5, 130.9, 128.9, 128.9, 128.9, 127.5, 127.1, 127.0, 126.0, 108.2, 60.4, 54.5, 37.2. LCMS (ESI): $[\text{M}+\text{H}]^+$, found 379.15. $\text{C}_{21}\text{H}_{20}\text{ClN}_4\text{O}^+$ requires 379.13. Purity: 93.0 %.



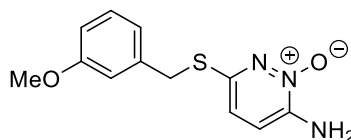
3-Methoxy-6-(N-methylbenzylamino)-2-(4-(trifluoromethyl)phenyl)imidazo[1,2-b]pyridazine

190g.⁵⁴ Amounts: 6-(N-Methylbenzylamino)-2-(4-(trifluoromethyl)phenyl)imidazo[1,2-b]pyridazin-3-ol **189g** (0.150 g, 0.377 mmol), methyl iodide (47 μL , 0.75 mmol), 60 % sodium hydride (0.045 g, 1.1 mmol) and dry DMF (2.5 mL). Deprotonation reaction time: 25 minutes. Methylation reaction time: 50 minutes. Temperature: 18 $^\circ\text{C}$. Work-up: extraction process. Purification: column chromatography (5 % ether/DCM). Physical description: yellow solid. Yield: 84 mg, 54 %. Purity: 93.4 %. ^1H NMR (600 MHz, CDCl_3) δ 8.21 (d, J = 8.2 Hz, 2H), 7.67 (d, J = 8.3 Hz, 2H), 7.61 (d, J = 9.9 Hz, 1H), 7.35 (t, J = 7.5 Hz, 2H), 7.29-7.24 (overlapping, 3H), 6.72 (d, J = 9.9 Hz, 1H), 4.76 (s, 2H), 4.10 (s, 3H), 3.20 (s, 3H). ^{13}C NMR (150 MHz, CDCl_3) δ 154.25, 139.89, 137.71, 137.49, 131.12, 128.94, 128.59 (q, $J_{\text{C-F}}$ = 32.3 Hz), 127.6, 127.0, 126.6, 126.2, 125.8, 125.6 (q, $J_{\text{C-F}}$ = 3.9 Hz), 124.6 (q, $J_{\text{C-F}}$ = 270.2 Hz), 108.7, 60.5, 54.5, 37.2. HRMS (APCI): $[\text{M}+\text{H}]^+$, found 413.1573. $\text{C}_{22}\text{H}_{19}\text{N}_4\text{OF}_3^+$ requires 412.1584. Purity: 93.4 %.

8.6 Procedures for the synthesis of 2-(2-Fluorophenyl)-3-methoxy-6-((3-methoxybenzyl)thio)imidazo[1,2-b]pyridazine **17**

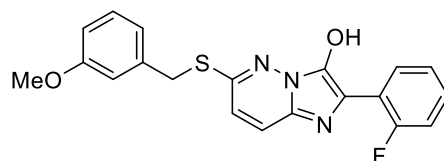


3-Methoxybenzyl thiol 182.⁷⁹ 3-Methoxybenzyl chloride **181** (2.00 g, 12.8 mmol) was added to a stirred solution of thiourea (0.69 mL, 13 mmol) in ethanol (10 mL) and the stirred mixture was heated at reflux for 20 hours. 2 M NaOH (10 mL) was added dropwise and the mixture was heated at reflux for a further 4 hours. 2 M HCl was added until pH 4 was reached and the whole was extracted with ethyl acetate (x 3). The combined organic layer was washed with water, dried with sodium sulfate and concentrated under vacuum affording the *title compound 182* as a clear colourless oil (1.28 g, 65 %). ¹H NMR (600 MHz, CDCl₃) δ 7.23 (t, *J* = 7.9 Hz, 1H), 6.91 (d, *J* = 8.3 Hz, 1H), 6.80 (s, 1H), (dd, *J* = 8.1, 2.4 Hz, 1H), (s, 3H), (d, *J* = 7.6 Hz, 2H), (t, *J* = 7.6 Hz 1H). ¹³C NMR (150 MHz, CDCl₃) δ 160.0, 142.8, 129.8, 120.5, 113.8, 112.7, 55.4, 29.1.

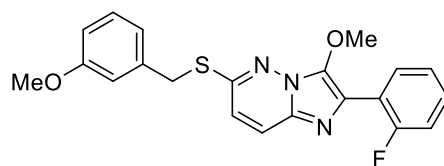


6-Amino-3-((3-methoxybenzyl)thio)pyridazine 1-oxide 184.⁷⁹ A mixture of 3-methoxybenzyl thiol **182** (0.473 g, 3.07 mmol), 6-amino-3-chloropyridazine 1-oxide **183** (0.372 g, 2.56 mmol) and 0.4 M NaOH aqueous solution (9.5 mL) was stirred at 115 °C for 16 hours in a sealed reaction vessel. After the reaction mixture was cooled to room temperature the reaction mixture was extracted with ethyl acetate (x 3) and the combined organic layer was washed with water, dried with sodium sulfate and concentrated under vacuum affording the *title compound 184* as a beige crystalline solid (0.481 g, 71 %). ¹H NMR (600 MHz, DMSO-*d*₆) δ 7.21 (t, *J* = 7.9 Hz, 1H), 7.15 (d, *J* = 8.7 Hz, 1H), 7.07 (d, *J* = 8.7 Hz, 1H), 6.97 (s, 1H), 6.95 (d, *J* = 7.6 Hz, 1H), 6.81 (dd, *J* = 8.1, 1.9 Hz, 1H), 6.77 (s, 2H), 4.27 (s, 2H), 3.72 (s, 3H). ¹³C NMR (150 MHz, DMSO-*d*₆) δ 159.2, 145.1, 144.1, 138.8, 129.5, 121.1, 119.1, 117.4, 114.6, 112.8, 55.0, 54.7.

Chapter 8



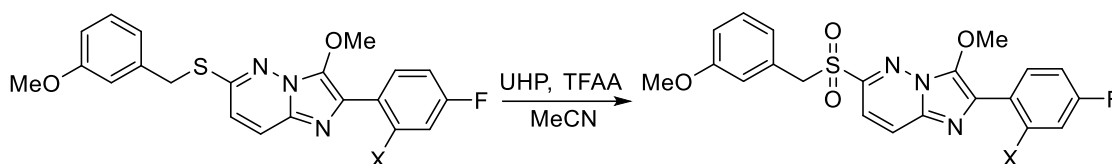
2-(2-Fluorophenyl)-6-((3-methoxybenzyl)thio)imidazo[1,2-b]pyridazin-3-ol **185**.⁷⁹ 6-Amino-3-((3-methoxybenzyl)thio)pyridazine 1-oxide **184** (0.565 g, 2.15 mmol) was added to a stirred solution of 2'-fluorophenacyl bromide **117** (0.331 mL, 3.36 mmol) in ethanol (7.5 mL) and the mixture was heated at reflux for 6 hours. Water (30 mL) was added while the reaction mixture was cooled in an ice-bath resulting in the precipitation of an orange solid. The solid was collected via vacuum filtration and washed with water and ether affording the *title compound* **190** as an orange solid (0.544 g, 66 %). ¹H NMR (600 MHz, DMSO-*d*₆) δ 8.06 (s, 1H), 7.78 (d, *J* = 9.4 Hz, 1H), 7.32 (s, 1H), 7.29-7.27 (overlapping, 2H), 7.23 (t, *J* = 7.9 Hz, 1H), 7.14 (s, 1H), 7.09 (d, *J* = 7.5 Hz, 1H), 7.00 (d, *J* = 9.4 Hz, 1H), 6.83 (d, *J* = 8.2 Hz, 1H), 4.49 (s, 2H), 3.74 (s, 3H).



The protocol under “8.5 General procedure for the syntheses of 3-methoxyimidazo[1,2-b]pyridazines” was utilised for the synthesis of 2-(2-fluorophenyl)-3-methoxy-6-((3-methoxybenzyl)thio)imidazo[1,2-b]pyridazine **17**. Amounts: 2-(2-Fluorophenyl)-6-((3-methoxybenzyl)thio)imidazo[1,2-b]pyridazin-3-ol **185** (0.199 g, 0.524 mmol), methyl iodide (98 μL, 1.6 mmol), 60% sodium hydride (0.023 g, 0.58 mmol) and dry DMF (3 mL). Deprotonation reaction time: 20 minutes. Methylation reaction time: 30 minutes. Temperature: 30 °C. Work-up: extraction process. Purification: trituration (ether). Physical description: red solid. Yield: 110 mg, 53 %. ¹H NMR (600 MHz, CDCl₃) δ 7.82 (tt, *J* = 7.6, 1.7 Hz, 1H), 7.66 (d, *J* = 9.4 Hz, 1H), 7.37-7.33 (m, 1H), 7.26-7.22 (overlapping, 2H), 7.18 (t, *J* = 9.4 Hz, 1H), 7.07 (overlapping, 2H), 6.81 (overlapping, 2H), 4.47 (s, 2H), 4.11 (s, 3H), 3.80 (s, 3H). ¹³C NMR (150 MHz, CDCl₃) δ 160.0 (d, *J*_{C-F} = 248.3 Hz), 159.9, 153.7, 139.9, 138.1, 132.2, 130.9 (d, *J*_{C-F} = 3.3 Hz), 129.8, 129.7 (d, *J*_{C-F} = 7.9 Hz), 124.9, 124.8, 124.4 (d, *J*_{C-F} = 3.2 Hz), 121.5, 121.2 (d, *J*_{C-F} = 13.7 Hz), 116.79, 116.2 (d, *J*_{C-F} =

21.92 Hz), 114.9, 113.2, 61.4 (d, $J_{C-F} = 2.2$ Hz), 55.4, 35.0. HRMS (APCI): $[M+H]^+$, found 396.1186. $C_{21}H_{19}FN_3O_2S^+$ requires 396.1177. Purity: 93.2 %.

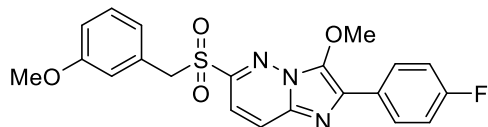
8.7 General procedure for the syntheses of 3-methoxy-6-((3-methoxybenzyl)sulfonyl)imidazo[1,2-b]pyridazines



Urea hydrogen peroxide was added to a stirred suspension of 3-methoxy-6-(3-methoxybenzylthio)imidazo[1,2-*b*]pyridazine in acetonitrile and stirred for 5 mins. Trifluoroacetic anhydride was added to the stirred suspension over a 2 minute period resulting in the formation of a solution. After 10-12 minutes 1 M sodium bisulfite was added to the reaction mixture. If a precipitate formed the solid was collected via vacuum filtration and washed with water. If no solid precipitated, the mixture was extracted with ethyl acetate, washed with water, dried with sodium sulfate and concentrated under vacuum. Purification of the residue was achieved using column chromatography and (where necessary) recrystallisation.

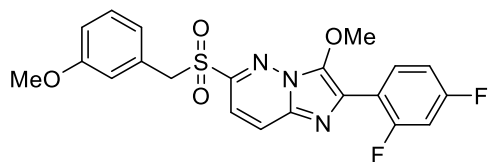
The following compounds were synthesised according to the general procedure described above. Nuances including the amounts of substrates and reagents, reaction times, work-up variations, purifications physical descriptions, yields, and characterisation data are described for each compound.

Chapter 8



2-(4-Fluorophenyl)-3-methoxy-6-((3-methoxybenzyl)sulfonyl)imidazo[1,2-b]pyridazine **174.**

Amounts: 2-(4-Fluorophenyl)-3-methoxy-6-((3-methoxybenzyl)thio)imidazo[1,2-b]pyridazine **65** (0.198 g, 0.499 mmol), UHP (0.376 g, 3.99 mmol), TFAA (0.42 mL, 3.0 mmol), MeCN (8 mL), and NaHSO₃ (10 mL). Reaction time: 12 minutes. Work-up: extraction process. Purification: column chromatography (DCM) and recrystallisation (DCM/ether, 0.5 mL/2.5 mL). Physical description: bright yellow solid. Yield: 12 mg, 6 %. ¹H NMR (600 MHz, CDCl₃) δ 8.19-8.17 (m, 2H), 7.90 (d, *J* = 9.3 Hz, 1H), 7.36 (d, *J* = 9.3 Hz, 1H), 7.21-7.16 (overlapping, 3H), 6.86-6.84 (overlapping, 2H), 6.81 (d, *J* = 7.5 Hz, 1H), 4.69 (s, 2H), 4.20 (s, 3H), 3.72 (s, 3H). ¹³C NMR (150 MHz, CDCl₃) δ 163.3 (d, *J*_{C-F} = 247.6 Hz), 160.0, 152.0, 139.4, 133.3, 132.7, 130.1, 128.8 (d, *J*_{C-F} = 8.5 Hz), 128.4 (d, *J*_{C-F} = 3.1 Hz), 128.0, 126.0, 123.5, 116.7, 116.1 (d, *J*_{C-F} = 21.7 Hz), 115.0, 113.3, 61.3, 60.2, 55.4. LCMS (ESI): [M+H]⁺, found 428.37. C₂₁H₁₉FN₃O₄S⁺ requires 428.11. Purity: 90.0 %.

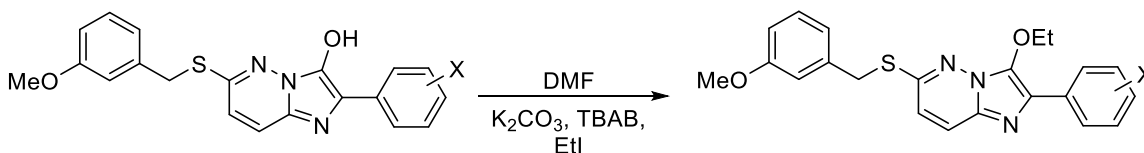


2-(2,4-Difluorophenyl)-3-methoxy-6-((3-methoxybenzyl)sulfonyl)imidazo[1,2-b]pyridazine **175.**

Amounts: 2-(2,4-Difluorophenyl)-3-methoxy-6-((3-methoxybenzyl)thio)imidazo[1,2-b]pyridazine **66** (0.350 g, 0.847 mmol), UHP (0.637 g, 6.77 mmol), TFAA (0.71 mL, 5.1 mmol), MeCN (10 mL), and NaHSO₃ (10 mL). Reaction time: 10 minutes. Work-up: vacuum filtration. Purification: column chromatography (DCM). Physical description: yellow solid. Yield: 45 mg, 12 %. M.p 166-168 °C. ¹H NMR (600 MHz, CDCl₃) δ 7.95 (d, *J* = 9.4 Hz, 1H), 7.86 (q, *J* = 7.8 Hz, 1H), 7.39 (d, *J* = 9.4 Hz, 1H), 7.19 (t, *J* = 8.0 Hz, 1H), 7.04 (td, *J* = 9.5, 2.4 Hz, 1H), 7.00-6.97 (m, 1H), 6.86-6.82 (overlapping, 3H), 4.70 (s, 2H), 4.18 (s, 3H), 3.73 (s, 3H). ¹³C NMR (150 MHz, CDCl₃) δ 163.3 (dd, *J*_{C-F} = 250.2, 12.8 Hz), 160.4 (d, *J*_{C-F} = 252.7, 12.0 Hz), 160.0, 152.4, 140.3, 132.8, 132.1 (dd, *J*_{C-F} = 9.8, 4.7 Hz), 130.1, 128.9, 127.9, 126.6, 123.5, 116.7 (dd, *J*_{C-F} = 14.0, 3.2 Hz), 116.7, 115.1, 113.3, 112.2 (dd, *J*_{C-F} = 14.0, 3.2 Hz), 115.1, 113.3, 112.2 (dd, *J*_{C-F} = 14.0, 3.2 Hz), 61.3, 60.2, 55.4.

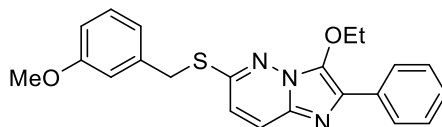
$f = 21.2, 3.5$ Hz), 104.8 (t, $J_{C-F} = 25.4$ Hz), 61.7 (d, $J_{C-F} = 2.7$ Hz), 60.1, 55.4. LCMS (ESI): $[M+H]^+$, found 446.13. $C_{21}H_{18}F_2N_3O_4S^+$ requires 446.33. Purity: 97.7 %.

8.8 General procedure for the syntheses of 3-ethoxy-imidazo[1,2-b]pyridazines



Ethyl iodide was added to a stirred solution of imidazo[1,2-b]pyridazin-3-ol, TBAB (or no TBAB) and K_2CO_3 in DMF under nitrogen and the whole was allowed to stir at room temperature overnight. Water (10 mL) was added and the mixture was extracted with ethyl acetate, washed with water, dried with sodium sulfate and concentrated under vacuum to afford the 3-ethoxy-imidazo[1,2-b]pyridazine.

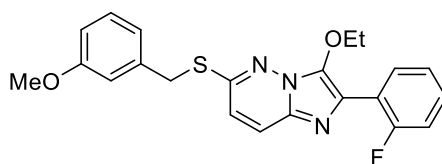
The following compounds were synthesised according to the general procedure described above. Nuances including the amounts of substrates and reagents, reaction times, physical descriptions, yields and characterisation data are described for each compound.



3-Ethoxy-6-((3-methoxybenzyl)thio)-2-phenylimidazo[1,2-b]pyridazine **216**.⁷⁹ Amounts: 6-((3-Methoxybenzyl)thio)-2-phenylimidazo[1,2-b]pyridazin-3-ol **123** (0.250 g, 0.689 mmol), ethyl iodide (0.75 mL, 9.4 mmol), TBAB (0.222 g, 0.689 mmol), K_2CO_3 (0.229 g, 1.65 mmol) and dry DMF (7 mL). Reaction time: 17.5 hours. Physical description: golden solid. Yield: 0.202 g, 75 %. M.p 54-58 °C. 1H NMR (600 MHz, $CDCl_3$) δ 8.14 (d, $J = 7.1$ Hz, 2H), 7.63 (d, $J = 9.4$ Hz, 1H), 7.48-7.42 (m,

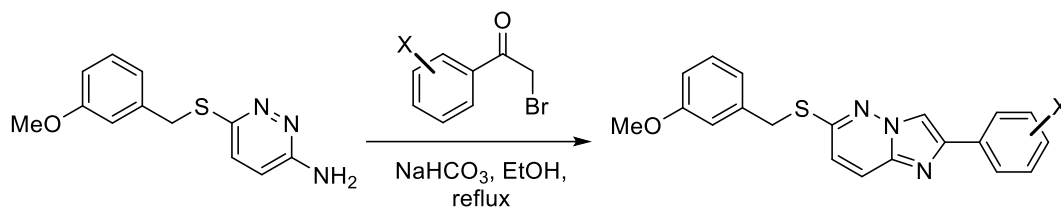
Chapter 8

2H), 7.32 (t, $J = 7.4$ Hz, 1H), 7.26-7.23 (overlapping, 1H), 7.09-7.03 (overlapping, 2H), 6.82 (dd, $J = 8.2, 1.6$ Hz, 1H), 6.78 (d, $J = 9.4$ Hz, 1H), 4.46 (s, 2H), 4.35 (q, $J = 7.1$ Hz, 2H), 3.80 (s, 3H), 1.46 (t, $J = 7.1$ Hz, 3H). ^{13}C NMR (150 MHz, CDCl_3) δ 160.0, 153.3, 138.4, 138.2, 133.4, 131.9, 129.8, 129.7, 128.8, 127.7, 126.3, 124.6, 121.4, 116.6, 114.8, 113.2, 70.0, 55.4, 34.9, 15.7. LCMS (ESI): $[\text{M}+\text{H}]^+$, found 392.33. $\text{C}_{22}\text{H}_{22}\text{N}_3\text{O}_2\text{S}^+$ requires 392.14. Purity: 91.5 %.



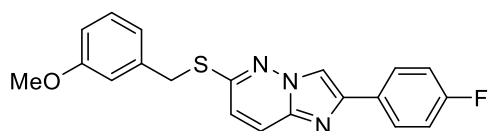
3-Ethoxy-2-(2-fluorophenyl)-6-((3-methoxybenzyl)thio)imidazo[1,2-b]pyridazine 217. Amounts: 2-(2-Fluorophenyl)-6-((3-methoxybenzyl)thio)imidazo[1,2-b]pyridazin-3-ol **185** (0.150 g, 0.393 mmol), ethyl iodide (0.43 mL, 5.5 mmol), K_2CO_3 (0.130 g, 9.43 mmol) and dry DMF (3 mL). Reaction time: 17 hours. Physical description: golden solid. Yield: 0.122 g, 76 %. ^1H NMR (600 MHz, CDCl_3) δ 7.83 (td, $J = 7.6, 1.8$ Hz, 1H), 7.65 (d, $J = 9.4$ Hz, 1H), 7.38-7.31 (m, 1H), 7.26-7.21 (overlapping, 2H), 7.17 (ddd, $J = 10.7, 8.2, 1.2$ Hz, 1H), 7.09-7.04 (overlapping, 2H), 6.81 (dd, $J = 8.0, 1.6$ Hz, 1H), 6.79 (d, $J = 9.4$ Hz, 1H), 4.46 (s, 2H), 4.32 (q, $J = 7.0$ Hz, 2H), 3.80 (s, 3H), 1.39 (t, $J = 7.1$ Hz, 3H). ^{13}C NMR (150 MHz, CDCl_3) δ 160.0 (d, $J_{\text{C-F}} = 249.4$ Hz), 159.9, 153.5, 139.1, 138.1, 132.2, 130.9 (d, $J_{\text{C-F}} = 3.5$ Hz), 129.8, 129.6 (d, $J_{\text{C-F}} = 8.1$ Hz), 125.5, 124.9, 124.3 (d, $J_{\text{C-F}} = 3.3$ Hz), 121.5, 121.3 (d, $J_{\text{C-F}} = 13.9$ Hz), 116.7, 116.2 (d, $J_{\text{C-F}} = 22.5$ Hz), 114.8, 113.2, 70.3 (d, $J_{\text{C-F}} = 1.9$ Hz), 55.4, 34.9, 15.6. LCMS (ESI): $[\text{M}+\text{H}]^+$, found 410.19. $\text{C}_{22}\text{H}_{21}\text{FN}_3\text{O}_2\text{S}^+$ requires 410.13. Purity: 93.2 %.

8.9 General procedure for the syntheses of 6-((3-methoxybenzyl)thio)imidazo[1,2-b]pyridazines



A stirred mixture of the phenacyl bromide, 6-((3-methoxybenzyl)thio)pyridazin-3-amine **76**, and ethanol was heated at reflux for 2.5 to 2.75 hours (stage 1). Sodium bicarbonate was added and heating at reflux was continued for 6 to 6.5 hours (stage 2). If a solid precipitated it was collected via vacuum filtration, washed with water, and subsequently recrystallised from water. If no solid precipitated, water was added to the crude mixture and the whole was extracted with ethyl acetate 3-4 times. The combined extract was washed with water, dried with sodium sulfate and concentrated under vacuum.

The following compounds were synthesised according to the general procedure described above. Nuances including the amounts of substrates and reagents, reaction times, work-up variations, purifications, physical descriptions, yields, and characterisation data are described for each compound.

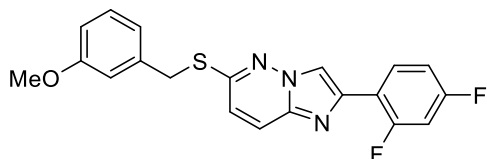


2-(4-Fluorophenyl)-6-((3-methoxybenzyl)thio)imidazo[1,2-b]pyridazine **220.**

Amounts: 6-((3-Methoxybenzyl)thio)pyridazin-3-amine **83** (0.254 g, 1.03 mmol), 4-fluorophenacyl bromide **218** (0.226 g, 1.04 mmol), ethanol (2.5 mL) and NaHCO₃ (0.119 g, 1.42 mmol). Stage 1 reaction time: 2.75 hours. Stage 2 reaction time: 3.75 hours. Work-up: extraction process. Purification: not required. Physical description: brown solid. Yield: 0.237 g, 64 %. ¹H NMR (600 MHz, CDCl₃) δ 8.12 (s, 1H), 7.92-7.90 (m, 2H), 7.71 (d, *J* = 9.4 Hz, 1H), 7.25 (t, *J* = 7.9 Hz, 1H), 7.14 (t, *J* = 8.7 Hz, 2H), 7.03 (d, *J* = 7.7 Hz, 1H), 7.00 (s, 1H), 6.84 (d, *J* = 9.4 Hz, 1H), 6.82 (dd, *J* =

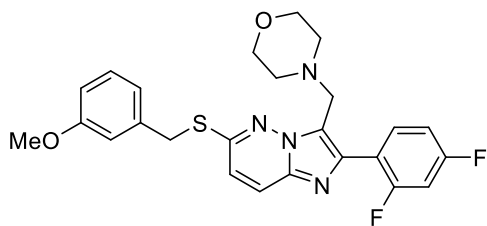
Chapter 8

8.3, 2.4 Hz, 1H), 4.41 (s, 2H), 3.80 (s, 3H). ^{13}C NMR (150 MHz, CDCl_3) δ 163.0 (d, $J_{\text{C-F}} = 246.2$ Hz), 159.2, 153.6, 144.1, 138.1, 138.0, 129.8, 129.8 (d, $J_{\text{C-F}} = 2.8$ Hz), 127.7 (d, $J_{\text{C-F}} = 7.8$ Hz), 124.2, 121.6, 118.3, 116.0 (d, $J_{\text{C-F}} = 21.6$ Hz), 115.0, 113.1, 112.6, 55.4, 35.0. LCMS (ESI): $[\text{M}+\text{H}]^+$, found 366.20. $\text{C}_{20}\text{H}_{16}\text{FN}_3\text{OS}^+$ requires 366.11. Purity: 93.6 %.



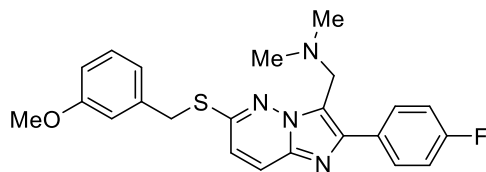
2-(2,4-Difluorophenyl)-6-((3-methoxybenzyl)thio)imidazo[1,2-b]pyridazine 221. Amounts: 6-((3-methoxybenzyl)thio)pyridazin-3-amine **83** (0.300 g, 1.21 mmol), 2',4'-difluorophenacyl bromide **219** (0.290 g, 1.23 mmol) and ethanol (3 mL). Water during purification (5 mL). Stage 1 reaction time: 2.5 hours. Stage 2 reaction time: 3.5 hours. Work-up: vacuum filtration. Purification: recrystallisation. Physical description: brown solid. Yield: 0.326 g, 74 %. ^1H NMR (600 MHz, CDCl_3) δ 8.30-8.26 (overlapping, 2H), 7.72 (d, $J = 9.4$ Hz, 1H), 7.25 (t, $J = 7.9$ Hz, 1H), 7.04-7.00 (overlapping, 3H), 6.95-6.91 (m, 1H), 6.86 (d, $J = 9.4$ Hz, 1H), 6.83 (dd, $J = 8.8, 2.4$ Hz, 1H), 4.42 (s, 2H), 3.80 (s, 3H). ^{13}C NMR (150 MHz, CDCl_3) δ 162.7 (dd, $J_{\text{C-F}} = 248.2, 11.9$ Hz), 160.3 (dd, $J_{\text{C-F}} = 250.4, 11.1$ Hz), 159.9, 153.8, 138.1, 137.8, 137.3, 129.8, 129.4 (dd, $J_{\text{C-F}} = 9.7, 5.4$ Hz), 124.2, 121.6, 118.6, 118.0 (dd, $J_{\text{C-F}} = 12.2, 4.6$ Hz), 116.2 (d, $J_{\text{C-F}} = 14.4$ Hz), 115.0, 113.3, 112.0 (dd, $J_{\text{C-F}} = 21.2, 3.3$ Hz), 104.3 (t, $J_{\text{C-F}} = 25.3$ Hz), 55.4, 35.0. $[\text{M}+\text{H}]^+$, found 384.22. $\text{C}_{20}\text{H}_{16}\text{F}_2\text{N}_3\text{OS}^+$ requires 384.10. Purity: 98.4 %.

8.10 Procedures for the syntheses of 3-Dialkylaminomethyl-imidazo[1,2-b]pyridazines

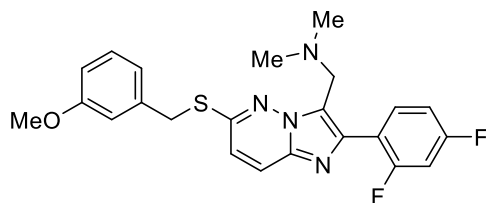


4-((2-(2,4-Difluorophenyl)-6-((3-methoxybenzyl)thio)imidazo[1,2-b]pyridazin-3-yl)methyl)morpholine **225**. Acetic acid (0.2 mL) was added to a stirred solution of 2-(2,4-difluorophenyl)-6-((3-methoxybenzyl)thio)imidazo[1,2-b]pyridazine **221** (0.050 g, 0.13 mmol), morpholine **140** (0.022 mL, 0.26 mmol), and formalin (0.2 mL) in methanol (2 mL) and the reaction mixture was heated at reflux for ~6 hours. Formalin (0.1 mL) was added and the mixture was heated at reflux for a further 17.5 hours. The mixture was cooled to <5 °C and water (9 mL) was added. The pH of the solution was adjusted to pH 13 using 1.3 M NaOH (~9 mL) and extracted with ethyl acetate 3 times. The combined extract was washed with water, dried with sodium sulfate and concentrated under vacuum affording the *title compound* **225** as a brown waxy solid (0.032 g, 51 %). ¹H NMR (600 MHz, CDCl₃) δ 7.79 (q, *J* = 7.8 Hz, 1H), 7.75 (d, *J* = 9.4 Hz, 1H), 7.26 (overlapping, 1H), 7.06 (d, *J* = 7.6 Hz, 1H), 7.02 (s, 1H), 6.98 (td, *J* = 8.2, 2.3 Hz, 1H), 6.94-6.91 (m, 1H), 6.89 (d, *J* = 9.4 Hz, 1H), 6.82 (dd, *J* = 8.3, 2.4 Hz, 1H), 4.45 (s, 2H), 4.01 (s, 2H), 3.80 (s, 3H), 3.50 (t, *J* = 4.4 Hz, 4H), 2.33 (t, *J* = 4.4 Hz, 4H). ¹³C NMR (150 MHz, CDCl₃) δ 163.1 (dd, *J*_{C-F} = 248.9, 11.7 Hz) 160.4 (dd, *J*_{C-F} = 249.2, 11.8 Hz), 160.0, 153.4, 138.6, 138.2, 137.3, 132.8 (dd, *J*_{C-F} = 9.5, 4.5 Hz), 129.9, 124.6, 123.5, 121.3, 119.1 (dd, *J*_{C-F} = 14.2, 3.7 Hz), 117.8, 114.9, 112.8, 111.6 (dd, *J*_{C-F} = 20.9, 3.3 Hz), 104.3 (t, *J*_{C-F} = 25.6 Hz), 67.0, 55.4, 53.2, 50.3 (dd, *J*_{C-F} = 3.8 Hz), 34.9. LCMS (ESI): [M+H]⁺, found 483.36. C₂₅H₂₅F₂N₄O₂S⁺ requires 483.17. Purity: 97.9 %.

Chapter 8



1-(2-(4-Fluorophenyl)-6-((3-methoxybenzyl)thio)imidazo[1,2-b]pyridazin-3-yl)-N,N-dimethylmethanamine **229**. Acetic acid (1 mL) was added to a stirred mixture of 33 % dimethylamine ethanol solution (0.46 mL, 2.6 mmol), formalin (0.5 mL) and 2-(4-fluorophenyl)-6-((3-methoxybenzyl)thio)imidazo[1,2-b]pyridazine **220** (0.237 g, 0.647 mmol) in methanol (5 mL) and the whole was stirred at room temperature (23 °C) for 1.5 hours. The reaction mixture was heated at reflux for 17.25 hours and cooled to room temperature. The mixture was extracted with ethyl acetate (x 3). The combined organic phase was washed with water (x 2), dried with sodium sulfate and concentrated under vacuum. The residual brown, viscous oil was chromatographed. Elution with 0-1 % methanol/DCM afforded the *title compound* **229** as a brown solid (49 mg, 18 %). M.p 104-107 °C. ¹H NMR (600 MHz, CDCl₃) δ 7.97-7.95 (m, 2H), 7.73 (d, *J* = 9.4 Hz, 1H), 7.25 (t, *J* = 7.9 Hz, 1H), 7.15 (t, *J* = 8.7 Hz, 2H), 7.07 (d, *J* = 7.6 Hz, 1H), 7.02 (s, 1H), 6.87 (d, *J* = 9.4 Hz, 1H), 6.83 (dd, *J* = 8.8, 2.4 Hz, 1H), 4.47 (s, 2H), 3.90 (s, 2H), 3.80 (s, 3H), 2.30 (s, 6H). ¹³C NMR (150 MHz, CDCl₃) δ 162.8 (d, *J*_{C-F} = 246.0 Hz), 160.0, 153.0, 143.5, 138.0, 137.0, 130.7 (d, *J*_{C-F} = 3.1 Hz), 130.1 (d, *J*_{C-F} = 7.8 Hz), 129.8, 124.3, 123.1, 121.4, 117.5, 115.6 (d, *J*_{C-F} = 21.0 Hz), 114.8, 113.1, 55.4, 50.93, 45.5, 35.1. LCMS (ESI): [M+H]⁺, found 423.40. C₂₃H₂₄FN₄OS⁺ requires 423.17. Purity: 95.0 %.

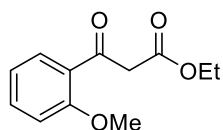


1-(2-(2,4-Difluorophenyl)-6-((3-methoxybenzyl)thio)imidazo[1,2-b]pyridazin-3-yl)-N,N-dimethylmethanamine **230**. Acetic acid (0.3 mL) was added to a stirred mixture of 33 % dimethylamine ethanol solution (0.1 mL, 0.6 mmol), formalin (0.2 mL) and 2-(2,4-difluorophenyl)-6-((3-methoxybenzyl)thio)imidazo[1,2-b]pyridazine **221** (0.108 g, 0.281 mmol) in methanol (4 mL) and

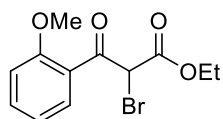
Chapter 8

the whole was heated at reflux for 3.5 hours. 33 % Dimethylamine ethanol solution (0.2 mL) and formalin (0.3 mL) were added and the mixture was heated at reflux for a further 2 hours. The mixture was cooled to room temperature over 30 minutes. 33 % Dimethylamine ethanol solution (0.5 mL), formalin (0.4 mL), acetic acid (0.5 mL) and methanol (2 mL) were added. The mixture was stirred at room temperature for 30 minutes and heated at reflux for 16.25 hours. The reaction mixture was cooled to room temperature and after 30 minutes 33 % dimethylamine ethanol solution (0.5 mL) and formalin (0.3 mL) were added. The resulting mixture was stirred at room temperature for 2 hours and heated at reflux for 5.75 hours. The mixture was cooled to room temperature. 33 % Dimethylamine ethanol solution (0.5 mL), formalin (0.5 mL) and acetic acid (0.5 mL) were added. The mixture was heated at reflux for 16 hours and cooled to room temperature. 5 % Sodium hydroxide solution was added to increase the pH from 4 to 7 resulting in the precipitation of a beige precipitate. Water (~20 mL) was added causing more solid to precipitate. The beige precipitate was collected via vacuum filtration and was washed with water and air-dried resulting in a brown waxy solid. The solid was dissolved in DCM (~10 mL), concentrated under vacuum, and the residue was chromatographed. Elution with ethyl acetate afforded **235** as an impure solid. The solid was dissolved in a mixture of ether (1 mL) and hexane (5 mL). A small amount of solvent was removed under nitrogen flow a solid began to precipitate. The suspension was placed in an ice-bath for 10 minutes and the supernatant solution was separated from the solid via pipette. The solution was concentrated under vacuum. The residual brown oil was dissolved in acetonitrile and washed with hexane. The acetonitrile phase was concentrated under vacuum affording the *title compound* **230** as a brown oil (13 mg, 10 %). ^1H NMR (600 MHz, CDCl_3) δ 7.77-7.73 (overlapping, 2H), 7.25 (t, $J = 7.9$ Hz, 1H), 7.07 (d, $J = 7.6$ Hz, 1H), 7.02 (s, 1H), 6.99 (td, $J = 8.3, 2.5$ Hz, 1H), 6.95-6.92 (m, 1H), 6.88 (d, $J = 9.5$ Hz, 1H), 6.83 (dd, $J = 8.3, 2.3$ Hz, 1H), 4.47 (s, 2H), 3.94 (s, 2H), 3.80 (s, 3H), 2.15 (s, 6H). ^{13}C NMR (150 MHz, CDCl_3) δ 163.1 (dd, $J_{\text{C-F}} = 237.2, 12.0$ Hz), 160.2 (dd, $J_{\text{C-F}} = 249.6, 11.7$ Hz), 160.0, 153.7, 138.5, 138.0, 137.5, 133.1 (dd, $J_{\text{C-F}} = 9.3, 4.8$ Hz), 129.8, 124.6, 124.1, 121.5, 119.0 (dd, $J_{\text{C-F}} = 14.0, 4.1$ Hz), 117.9, 114.9, 113.1, 111.8 (dd, $J_{\text{C-F}} = 21.0, 3$ Hz), 104.4 (t, $J_{\text{C-F}} = 25.7$ Hz), 55.4, 50.6 (d, $J_{\text{C-F}} = 4.2$ Hz), 45.4, 35.0. LCMS (ESI): $[\text{M}+\text{H}]^+$, found 441.38. $\text{C}_{23}\text{H}_{23}\text{F}_2\text{N}_4\text{OS}^+$ requires 441.16. Purity: 92.7 %.

8.11 Procedures for the synthesis of 9-Benzylthio-6H-chromeno[4',3':4,5]imidazo[1,2-b]pyridazin-6-one **234**



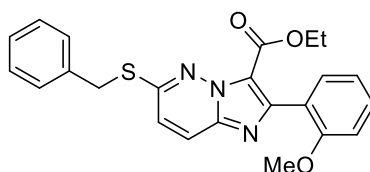
Ethyl 3-(2-methoxyphenyl)-3-oxopropanoate **236**.^{89,90} 60% sodium hydride (1.06 g, 0.0266 mol) was triturated in hexane (10 mL x 6) under a nitrogen atmosphere. The supernatant washings were removed via pipette. Residual hexane was removed by nitrogen flow. Dry THF (15 mL) was added to the washed sodium hydride under a nitrogen atmosphere and the resulting suspension was stirred and cooled in an ice-bath. 2'-Methoxyacetophenone **235** (1.8 mL, 0.013 mol) was added to the stirred suspension and the mixture was stirred for 35 minutes. The ice-bath was removed and the mixture was stirred for a further 35 minutes. The ice-bath was reapplied and diethyl carbonate (4.8 mL, 0.040 mol) was added dropwise with stirring. The mixture was warmed to room temperature at which it was stirred for 15 hours. The reaction mixture was quenched with saturated ammonium chloride (20 mL) and the whole was extracted with ethyl acetate (x 2). The combined organic phase was washed with water (x 6), dried with sodium sulfate, and concentrated under vacuum affording *the title compound* **236** as an orange oil (2.67 g, 90%). ¹H NMR (600 MHz, CDCl₃) δ 7.88 (dd, *J* = 7.8, 1.8 Hz, 1H), 7.52-7.49 (m, 1H), 7.02 (t, *J* = 7.5 Hz, 1H), 6.97 (d, *J* = 8.3 Hz, 1H), 4.18 (q, *J* = 7.1 Hz, 2H), 3.96 (s, 2H), 3.89 (s, 3H), 1.23 (t, *J* = 7.1 Hz, 3H).



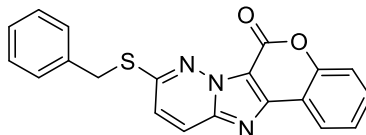
Ethyl 2-bromo-3-(2-methoxyphenyl)-3-oxopropanoate **237**.⁹⁰ *N*-bromosuccinimide (4.07 g, 22.8 mmol) was added to a stirred solution of 3-(2-methoxyphenyl)-3-oxo-propionic acid ethyl ester **236** (2.12 g, 9.52 mmol) in carbon tetrachloride (25 mL) under a nitrogen atmosphere and was stirred at room temperature for 1 hour and 10 minutes. Carbon tetrachloride (15 mL) was added to the mixture (to improve the dissolution of NBS) and stirring was continued for 3 hours and 30 minutes. The reaction mixture was concentrated under vacuum. Water (20 mL) was added to the

Chapter 8

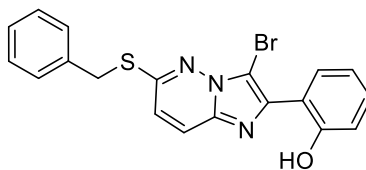
residue and the whole was extracted with DCM (x 2). The combined organic phase was washed with water (x 6), dried with sodium sulfate, and concentrated under vacuum. DCM (~20 mL) was added to the residue and the resulting mixture was washed sequentially with saturated sodium bicarbonate solution (x 2), water (x 6), and dried with sodium sulfate and concentrated under vacuum affording the *title compound* **237** as a dark brown oil (1.98 g, 69 %). ^1H NMR (600 MHz, CDCl_3) δ 7.91 (dd, $J = 7.8, 1.8$ Hz, 1H), 7.56-7.53 (m, 1H), 7.06 (t, $J = 7.5$ Hz, 1H), 6.98 (d, $J = 8.4$ Hz, 1H), 5.80 (s, 1H), 4.24 (q, $J = 7.2$ Hz, 2H), 3.91 (s, 3H), 1.24 (t, $J = 7.2$ Hz, 3H).



Ethyl 6-benzylthio-2-(2-methoxyphenyl)imidazo[1,2-b]pyridazine-3-carboxylate **238**. A stirred mixture of 3-amino-6-benzylthiopyridazine **81** (0.300 g, 1.38 mmol), 2-bromo-3-(2-methoxyphenyl)-3-oxopropionic acid ethyl ester **237** (0.464 g, 1.54 mmol), and ethanol (15 mL) was heated at reflux for 4 hours and 15 minutes. Sodium bicarbonate (0.174 g, 2.07 mmol) was added and the mixture was heated at reflux for 20 hours. The reaction mixture was concentrated under vacuum and the residue was extracted with ethyl acetate (x2). The combined organic phase was washed with water (x6), dried with sodium sulfate, and concentrated under vacuum. The residue was chromatographed. Elution with DCM afforded the *title compound* **238** as a yellow solid (0.175 g, 30 % impure). ^1H NMR (600 MHz, CDCl_3) δ 7.78 (d, $J = 9.4$ Hz, 1H), 7.58 (d, $J = 7.4$ Hz, 1H), 7.52 (d, $J = 7.5$ Hz, 2H) 7.40 (t, $J = 7.5$ Hz, 1H), 7.31 (t, $J = 7.5$ Hz, 2H), 7.26 (t, $J = 7.2$ Hz, 1H), 7.07 (t, $J = 7.4$ Hz, 1H), 6.97 (d, $J = 9.4$ Hz, 2H), 4.54 (s, 2H), 4.30 (q, $J = 7.1$ Hz, 2H), 3.78 (s, 3H), 1.17 (t, $J = 7.1$ Hz, 3H). ^{13}C NMR (150 MHz, CDCl_3) δ 160.1, 157.1, 154.4, 146.4, 138.8, 136.9, 130.9, 130.3, 129.6, 128.7, 127.6, 124.6, 123.7, 120.7, 119.7, 118.9, 110.7, 60.7, 55.5, 34.8, 14.1.



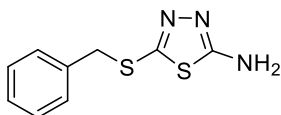
9-Benzylthio-6H-chromeno[4',3':4,5]imidazo[1,2-b]pyridazin-6-one **234**. Ethyl 6-benzylthio-2-(2-methoxyphenyl)imidazo[1,2-*b*]pyridazine-3-carboxylate **238** (0.175 g, 0.418 mmol) and a magnetic stirred bar was placed in a round bottom flask and heated under vacuum at 40 °C for 1.75 hours. The flask was cooled in an ice-bath. DCM (5 mL) was added to dissolve the substrate. Boron tribromide (1 M in DCM, 0.84 mmol) was added with stirring. The reaction was warmed to room temperature at which it was stirred for 2.5 hours. Ethanol (10 mL) was added and the mixture was heated at reflux for 1 hour. The mixture was concentrated under vacuum and the residue was chromatographed. Elution with 20 % ether/hexane to DCM afforded the *title compound* **234** as a white solid (0.0246 g, 16 %). ¹H NMR (600 MHz, CDCl₃) δ 8.25 (d, *J* = 7.7 Hz, 1H), 7.90 (d, *J* = 9.5 Hz, 1H), 7.68 (d, *J* = 7.7 Hz, 2H), 7.57 (t, *J* = 7.8 Hz, 1H), 7.51 (d, *J* = 8.3 Hz, 1H), 7.41 (t, *J* = 7.5 Hz, 1H), 7.32 (t, *J* = 7.7 Hz, 2H), 7.26-7.23 (overlapping, 1H), 7.18 (d, *J* = 9.5 Hz, 1H), 4.58 (s, 2H). ¹³C NMR (150 MHz, CDCl₃) δ 155.8, 153.3, 152.8, 147.8, 143.5, 136.5, 131.0, 130.1, 128.7, 127.7, 124.9, 124.5, 123.3, 123.2, 117.6, 116.6, 113.0, 35.0. LCMS (ESI): [M+H]⁺, found 360.29. C₂₀H₁₄N₃O₂S⁺ requires 360.08. Purity: 90.7 %.



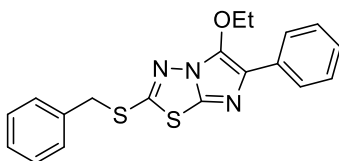
Earlier elution with the same mobile phase afforded 2-(6-Benzylthio-3-bromoimidazo[1,2-b]pyridazin-2-yl)phenol **239**, as a beige solid, which was triturated with hexane/ether (2 mL : 2 mL, x 1) and hexane (x 1). Residual solvent was removed under vacuum affording **239** as a white solid (18 mg, 8 %). ¹H NMR (600 MHz, CDCl₃) δ 12.13 (s, 1H), 8.39 (d, *J* = 7.8 Hz, 1H), 7.66 (d, *J* = 9.3 Hz, 1H), 7.56 (d, *J* = 7.5 Hz, 2H), 7.34 (t, *J* = 7.5 Hz, 2H), 7.31-7.26 (overlapping, 2H), 7.06 (d, *J* = 8.2 Hz, 1H), 6.98-6.94 (overlapping, 2H), 4.54 (s, 2H). ¹³C NMR (150 MHz, CDCl₃) δ 157.8, 155.2,

140.5, 136.6, 136.0, 130.6, 129.5, 128.8, 127.8, 127.0, 123.2, 119.1, 119.0, 117.9, 115.6, 97.0, 34.9. LCMS (ESI): $[M+H]^+$, found 414.23. $C_{19}H_{15}BrN_3O_2S^+$ requires 414.01. Purity: 85.6 %.

8.12 Procedures for attempted syntheses of imidazo[2,1-b][1,3,4]thia(oxa)diazoles



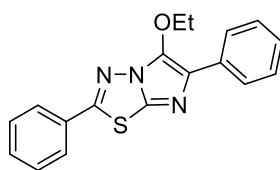
5-Benzylthio-1,3,4-thiadiazol-2-amine 262. A solution of potassium hydroxide (0.0783 g, 1.40 mmol) in water (2 mL) was added to a stirred suspension of 5-amino-1,3,4-thiadiazole-2-thiol (0.105 g, 0.788 mmol) in water (2 mL). After the amine dissolved, the mixture was cooled in an ice bath. Benzyl bromide (89 μ L, 0.751 mmol) was added drop wise while maintaining the temperature at 0-5 $^{\circ}$ C. The mixture was stirred at room temperature for 19 hours. The yellow precipitate was collected by vacuum filtration. Recrystallisation from ethyl acetate afforded the *title compound 262* as a yellow solid (0.065 g, 37 %). M.p. 155 - 157 $^{\circ}$ C. 1H NMR (600 MHz, $CDCl_3$) δ 7.35 (d, J = 7.6 Hz, 2H), 7.32 (t, J = 7.3 Hz, 2H), 7.28 (t, J = 6.9 Hz, 1H), 5.07 (s, 2H), 4.36 (s, 2H). ^{13}C NMR (150 MHz, $CDCl_3$) δ 168.5, 154.3, 136.4, 129.3, 128.9, 127.9, 39.9.



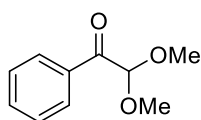
2-Benzylthio-5-ethoxy-6-phenylimidazo[2,1-b][1,3,4]thiadiazole 259. Conc. HCl (0.18 mL) was added to a stirred solution of 5-benzylthio-1,3,4-thiadiazol-2-amine **262** (0.200 g, 0.896 mmol) and phenylglyoxal monohydrate **113** (0.122 g, 0.907 mmol) in ethanol (2 mL). The resulting mixture was heated at reflux for 24 hours and was concentrated under vacuum. The crude material was triturated with ethyl acetate and the solid was removed by vacuum filtration. The filtrate was concentrated under vacuum revealing a yellow oil. The yellow oil was triturated in ethyl acetate forming an immiscible brown oil on the bottom of the flask. The supernatant was

Chapter 8

removed via pipette and the brown oil was chromatographed. Elution with 10 % ethyl acetate/hexane afforded the *title compound* **259** as a yellow solid (5 mg, 2 %). *R_f* (10% EtOAc/Hexane) 0.19. ¹H NMR (600 MHz, CDCl₃) δ 7.95 (d, *J* = 7.0 Hz, 2H), 7.42-7.38 (overlapping, 4H), 7.34 (t, *J* = 7.3 Hz, 2H), 7.30 (t, *J* = 7.3 Hz, 1H), 7.24 (t, *J* = 7.4 Hz, 1H), 4.46 (s, 2H), 4.33 (q, *J* = 7.1 Hz, 2H), 1.46 (t, *J* = 7.1 Hz, 3H). ¹³C NMR (150 MHz, CDCl₃) δ 159.3, 138.2, 137.9, 135.3, 133.8, 129.3, 129.0, 128.7, 128.3, 128.3, 126.7, 125.3, 71.1, 38.9, 15.5. HRMS (APCI): [M+H], found 368.0915. C₁₉H₁₈N₃OS₂⁺ requires 368.0886.



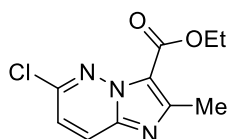
5-Ethoxy-2,6-diphenylimidazo[2,1-b][1,3,4]thiadiazole **260**. Conc. HCl (0.12 mL) was added to a stirred solution of 5-phenyl-1,3,4-thiadiazol-2-amine (0.203 g, 0.611 mmol) and phenylglyoxal monohydrate **113** (0.0935 g, 0.615 mmol) in ethanol (3 mL) and the resulting mixture was heated at reflux for 41 hours. The solvent was removed under vacuum and the crude mixture was purified by column chromatography (10-100 % ethyl acetate/hexane) affording the *title compound* **260** as a yellow solid (6.5 mg, 3 %). *R_f* (20% EtOAc/Hexane) 0.50. ¹H NMR (600 MHz, CDCl₃) δ 8.02 (d, *J* = 6.8 Hz, 2H), 7.91 (d, *J* = 6.2 Hz, 2H), 7.53-7.51 (overlapping, 3H), 7.42 (t, *J* = 7.7 Hz, 2H), 7.27-7.24 (overlapping, 1H), 4.44 (q, *J* = 7.1 Hz, 2H), 1.51 (t, *J* = 7.1 Hz, 3H). HRMS (APCI): [M+H], found 322.1015. C₁₈H₁₆N₃OS⁺ requires 322.1009.



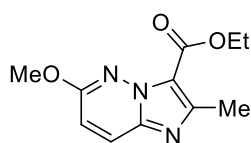
2,2-Dimethoxy-1-phenylethan-1-one **263**.¹³² Trimethylsilyl chloride (0.29 mL, 2.3 mmol) was added to a stirred solution of phenylglyoxal monohydrate **113** (0.152 g, 1.00 mmol) and methanol (2 mL) under a nitrogen atmosphere and the resulting mixture was stirred at room temperature for 48 hours. The solvent was removed under vacuum and the residue was purified by column chromatography (10 % EtOAc/hexane) affording the *title compound* **263** as a white solid (73 mg,

40 %). *R_f* (10% EtOAc/Hexane) 0.22. ¹H NMR (600 MHz, CDCl₃) 8.11 (d, *J* = 7.2 Hz, 2H), 7.57 (t, *J* = 7.8 Hz, 1H), 7.45 (t, *J* = 7.8 Hz, 2H), 5.22 (s, 1H), 3.47 (s, 6H).

8.13 Procedures for the syntheses of ethyl 2-methylimidazo[1,2-*b*]pyridazine-3-carboxylates **272** and **273**



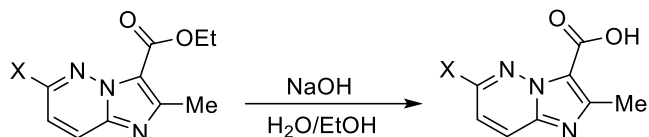
*Ethyl 6-chloro-2-methylimidazo[1,2-*b*]pyridazine-3-carboxylate* **272**. A stirred solution of 6-chloropyridazin-3-amine **210** (2.00 g, 15.4 mmol), ethyl-2-chloro-acetoacetate (1.9 mL, 0.015 mol) and ethanol (30 mL) was heated at reflux for 22 hours. The reaction mixture was cooled to room temperature and the solvent was removed under vacuum. The residual brown solid was chromatographed (10-20 % ether/DCM) affording the *title compound* **272** as a white solid (1.05 g, 28 %). ¹H NMR (600 MHz, DMSO-*d*₆) δ 8.22 (d, *J* = 9.5 Hz, 1H), 7.57 (d, *J* = 9.5 Hz, 1H), 4.36 (q, *J* = 7.1 Hz, 2H), 2.62 (s, 3H), 1.35 (t, *J* = 7.1 Hz, 3H). ¹³C NMR (150 MHz, CDCl₃) δ 159.4, 152.2, 147.4, 139.1, 126.2, 121.3, 117.5, 61.0, 16.8, 14.5.



*Ethyl 6-methoxy-2-methylimidazo[1,2-*b*]pyridazine-3-carboxylate* **273**. A stirred solution of 6-methoxypyridazin-3-amine **274** (0.500 g, 3.99 mmol), ethyl-2-chloro-acetoacetate (0.58 mL, 4.4 mmol) and ethanol (35 mL) was heated at reflux for 4.5 hours. Sodium bicarbonate (0.503 g, 5.99 mmol) was added and the reaction mixture was heated at reflux for 2.5 hours. The solvent was removed under vacuum and the residue was diluted with water and ethyl acetate with stirring. After dissolution was complete, the aqueous phase was extracted into ethyl acetate (x 3), and the combined extract washed with water, dried with sodium sulfate and concentrated under

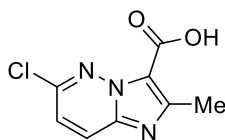
vacuum. The residual brown solid was recrystallised from a THF/H₂O (2 mL/10mL) mixture affording the *title compound 273* as a white solid (0.202 g, 47 %). ¹H NMR (600 MHz, CDCl₃) δ 7.75 (d, *J* = 9.6 Hz, 1H), 6.82 (d, *J* = 9.3 Hz, 1H), 4.44 (q, *J* = 7.1 Hz, 2H), 4.07 (s, 3H), 2.69 (s, 3H), 1.43 (t, *J* = 7.1 Hz, 3H). ¹³C NMR (150 MHz, CDCl₃) δ 160.1, 160.1, 150.6, 138.8, 126.7, 117.2, 113.9, 60.5, 55.0, 16.7, 14.6.

8.14 General procedure for the syntheses of 2-methylimidazo[1,2-*b*]pyridazine-3-carboxylic acids



An aqueous NaOH solution was added to a stirred solution of the ethyl ester in ethanol (10 mL) and the whole was heated at 60 °C overnight. The solvents were removed under vacuum. The residue was dissolved in water. Conc. HCl was added until pH 3-4 was reached, resulting in the precipitation of a white solid, which was collected by vacuum filtration.

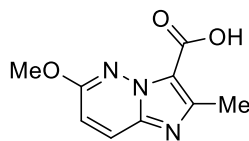
The following compounds were synthesised according to the general procedure described above. Nuances including the amounts of substrates and reagents, reaction times, purifications, physical descriptions, yields and characterisation data are described for each compound.



*6-Chloro-2-methylimidazo[1,2-*b*]pyridazine-3-carboxylic acid 270.* Amounts: 0.5 M NaOH solution (5 mL), ethyl 6-chloro-2-methylimidazo[1,2-*b*]pyridazine-3-carboxylate **272** (0.200 g, 0.835 mmol), ethanol (10 mL), water during work-up/purification (10 mL), and 1 M HCl until pH 4 was reached. Reaction time: 17 hours. Yield: 0.101 g, 57 %. ¹H NMR (600 MHz, DMSO-*d*₆) δ 13.23 (s, 1H), 8.22 (d, *J* = 9.4 Hz, 1H), 7.55 (d, *J* = 9.5 Hz, 1H), 2.62 (s, 3H). ¹³C NMR (150 MHz,

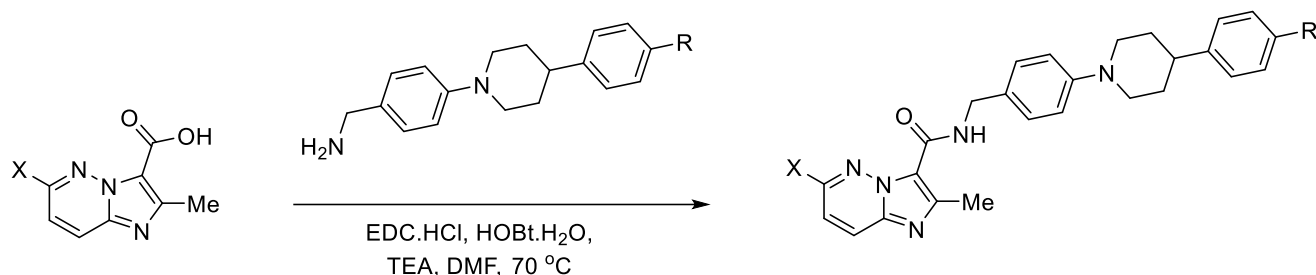
Chapter 8

DMSO- d_6) δ 160.0, 151.1, 146.4, 138.9, 127.0, 121.5, 116.9, 16.3. HRMS (ESI): $[M+H]^+$, found 212.0223. $C_8H_7ClN_3O_3^+$ requires 212.0222.



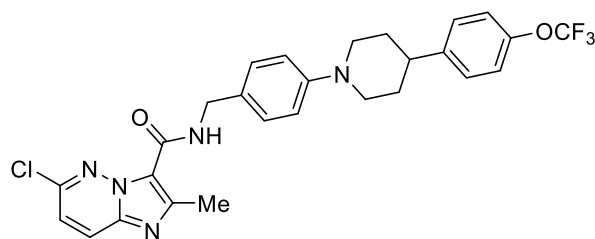
*6-Methoxy-2-methylimidazo[1,2-*b*]pyridazine-3-carboxylic acid* **271**. Amounts: 0.8 M NaOH solution (10 mL), ethyl 6-methoxy-2-methylimidazo[1,2-*b*]pyridazine-3-carboxylate **273** (0.620 g, 2.59 mmol), ethanol (20 mL), water during work-up/purification (4 mL), and 2 M HCl until pH 3 was reached. Reaction time: 17.5 hours. Yield: 0.432 g, 81 %. 1H NMR (600 MHz, DMSO- d_6) δ 8.00 (d, $J = 9.6$ Hz, 1H), 7.04 (d, $J = 9.6$ Hz, 1H), 3.96 (s, 3H), 2.55 (s, 3H). ^{13}C NMR (150 MHz, DMSO- d_6) δ 160.3, 159.6, 140.1, 138.1, 127.1, 116.7, 114.0, 54.6, 16.2.

8.15 General procedure for the syntheses of 2-methyl-N-(4-(4-phenylpiperidin-1-yl)benzyl)imidazo[1,2-b]pyridazine-3-carboxamides



EDC.HCl, HOBT.H₂O, TEA and the amine were added sequentially to a stirred solution of the carboxylic acid in DMF, and the whole was heated to 70 °C for 2 hours. The mixture was cooled to <5 °C and water was added, resulting in precipitation of a solid which was isolated by vacuum filtration. The solid was either recrystallized from or triturated with ethanol. The pure amide was isolated by vacuum filtration or by removal of the supernatant via pipette.

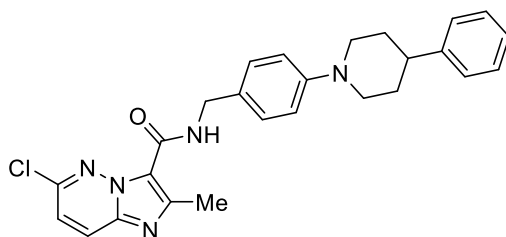
The following compounds were synthesised according to the general procedure described above. Nuances including the amounts of substrates and reagents, purifications, physical descriptions, yields, and characterisation data are described for each compound.



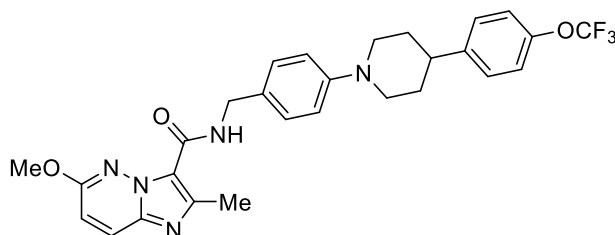
6-Chloro-2-methyl-N-(4-(4-(4-(trifluoromethoxy)phenyl)piperidin-1-yl)benzyl)imidazo[1,2-b]pyridazine-3-carboxamide **264**. Amounts: 6-Chloro-2-methylimidazo[1,2-b]pyridazine-3-carboxylic acid **270** (0.156 g, 0.736 mmol), (4-(4-(4-(trifluoromethoxy)phenyl)piperidin-1-yl)phenyl)methanamine **268** (0.232 g, 0.624 mmol), EDC.HCl (0.194 g, 1.00 mmol), HOBT.H₂O (0.062 g, 0.405 mmol), TEA (0.19 mL, 1.3 mmol), DMF (3 mL) and water during work-up (15 mL). Purification: Recrystallisation. Physical description: white solid. Yield: 71 mg, 20 %. ¹H NMR (600

Chapter 8

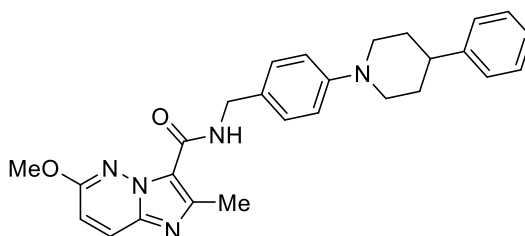
MHz, CDCl₃) δ 8.69 (s (broad), 1H), 7.94 (d, *J* = 9.4 Hz, 1H), 7.33 (d, *J* = 8.3 Hz, 2H), 7.26-7.25 (overlapping, 2H), 7.18-7.15 (overlapping, 3H), 6.99 (d, *J* = 8.3 Hz, 2H), 4.68 (d, *J* = 5.6 Hz, 2H), 3.81 (d, *J* = 12.2 Hz, 2H), 2.88 (s, 3H), 2.82 (t, *J* = 11.7 Hz, 2H), 2.66 (t, *J* = 11.9 Hz, 1H), 1.93 (d, *J* = 12.2 Hz, 2H), 1.90-1.84 (m, 2H). ¹³C NMR (150 MHz, CDCl₃) δ 159.2, 152.8, 151.2, 147.8, 146.2, 144.8, 137.5, 129.3, 128.7, 128.2, 127.0, 121.5, 121.2, 119.7, 119.0, 117.0, 50.6, 42.7, 42.0, 33.4, 16.8. LCMS (ESI): [M+H]⁺, found 544.29. C₂₇H₂₆ClF₃N₅O₂⁺ requires 544.17. Purity: 97.9 %.



6-Chloro-2-methyl-N-(4-(4-phenylpiperidin-1-yl)benzyl)imidazo[1,2-b]pyridazine-3-carboxamide **265**. Amounts: 6-Chloro-2-methylimidazo[1,2-b]pyridazine-3-carboxylic acid **270** (0.150 g, 0.709 mmol), (4-(4-phenylpiperidin-1-yl)phenyl)methanamine **269** (0.171 g, 0.641 mmol), EDC.HCl (0.184 g, 0.962 mmol), HOBT.H₂O (0.060 g, 0.39 mmol), TEA (0.18 mL, 1.3 mmol), DMF (2.5 mL), and water during work-up (13 mL). Purification: Recrystallisation. Physical description: beige solid. Yield: 0.116 g, 39 %. ¹H NMR (600 MHz, CDCl₃) 8.69 (s (broad), 1H), 7.94 (d, *J* = 9.4 Hz, 1H), 7.33-7.30 (overlapping, 4H), 7.26-7.24 (overlapping, 2H), 7.21 (t, *J* = 7.3 Hz, 1H). 7.17 (d, *J* = 9.3 Hz, 1H), 6.69 (d, *J* = 8.2 Hz, 2H), 4.68 (d, *J* = 5.6 Hz, 2H), 3.82 (d, *J* = 12.3 Hz, 2H), 2.88 (s, 3H), 2.82 (t, *J* = 11.3 Hz, 2H), 2.66 (tt, *J* = 12.2, 3.8 Hz, 1H), 1.95-1.89 (overlapping, 4H). δ ¹³C NMR (150 MHz, CDCl₃) δ 159.2, 152.8, 151.3, 146.2, 146.2, 137.5, 129.1, 128.7, 128.63, 127.0, 126.9, 126.4, 119.7, 118.9, 116.9, 50.7, 42.7, 42.6, 33.4, 16.8. LCMS (ESI): [M+H]⁺, found 460.32. C₂₆H₂₇ClN₅O⁺ requires 460.19. Purity: 98.2 %.



*6-Methoxy-2-methyl-N-(4-(4-(4-(trifluoromethoxy)phenyl)piperidin-1-yl)benzyl)imidazo[1,2-*b*]pyridazine-3-carboxamide* **266**. 6-Methoxy-2-methylimidazo[1,2-*b*]pyridazine-3-carboxylic acid **271** (0.150 g, 0.724 mmol), (4-(4-(4-(trifluoromethoxy)phenyl)piperidin-1-yl)phenyl)methanamine **268** (0.228 g, 0.652 mmol), EDC.HCl (0.189 g, 0.985 mmol), HOBT.H₂O (0.061 g, 0.40 mmol), TEA (0.81 mL, 1.3 mmol), DMF (2.5 mL) and water during work-up (11 mL). Purification: trituration. Physical description: beige solid. Yield: 0.202 g, 58 %. ¹H NMR (600 MHz, CDCl₃) δ 8.76 (s (broad), 1H), 7.81 (d, *J* = 9.4 Hz, 1H), 7.31 (d, *J* = 8.1 Hz, 2H), 7.27-7.25 (overlapping, 2H), 7.17 (d, *J* = 8.1 Hz, 2H), 6.96 (d, *J* = 8.0 Hz, 2H), 6.76 (d, *J* = 9.5 Hz, 1H), 4.61 (d, *J* = 4.7 Hz, 2H), 3.80 (d, *J* = 12.1 Hz, 2H), 3.65 (s, 3H), 2.83-2.79 (overlapping, 5H), 2.67 (t, *J* = 12.1 Hz, 1H), 1.95 (d, *J* = 11.9 Hz, 2H), 1.91-1.85 (m, 2H). ¹³C NMR (150 MHz, DMSO-*d*₆) δ 159.7, 159.5, 151.5, 150.1, 147.8, 144.7, 136.9, 129.3, 129.2, 128.2, 127.8, 121.5, 121.2, 118.6, 117.0, 112.3, 54.7, 50.7, 43.2, 42.0, 33.3, 16.4. LCMS (ESI): [M+H]⁺, found 540.35. C₂₈H₂₉F₃N₅O₃⁺ requires 540.22. Purity: 98.2 %.

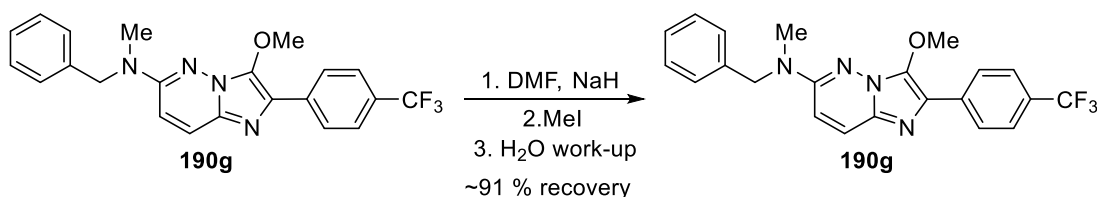


*6-Methoxy-2-methyl-N-(4-(4-phenylpiperidin-1-yl)benzyl)imidazo[1,2-*b*]pyridazine-3-carboxamide* **267**. Amounts: 6-Methoxy-2-methylimidazo[1,2-*b*]pyridazine-3-carboxylic acid **271** (0.085 g, 0.41 mmol), (4-(4-phenylpiperidin-1-yl)phenyl)methanamine **269** (0.120 g, 0.451 mmol), EDC.HCl (0.107 g, 0.556 mmol), HOBT.H₂O (0.0345 g, 0.226 mmol), TEA (0.10 mL, 0.74 mmol), DMF (2 mL) and water during work-up (10 mL). Purification: not required. Physical description: tan solid. Yield: 0.104 g, 56 %. ¹H NMR (600 MHz, CDCl₃) δ 8.75 (s (broad), 1H), 7.80 (d, *J* = 9.6 Hz, 1H), 7.33-7.30 (overlapping, 4H), 7.26-7.21 (overlapping, 3H), 6.97 (d, *J* = 8.2 Hz, 2H), 6.76 (d, *J* = 9.5 Hz, 1H), 4.61 (d, *J* = 4.6 Hz, 2H), 3.80 (d, *J* = 12.2 Hz, 2H), 3.64 (s, 3H), 2.83-2.79 (overlapping, 5H), 2.66 (t, *J* = 12.1 Hz, 1H), 1.98 (d, *J* = 12.4 Hz, 2H), 1.94-1.88 (m, 2H). ¹³C NMR (150 MHz, CDCl₃) δ 159.7, 159.50, 151.6, 150.1, 146.0, 136.9, 129.3, 120.0, 128.7, 127.7, 126.9, 126.5, 118.6, 116.9,

112.3, 54.7, 50.7, 43.2, 42.6, 33.3, 16.4. LCMS (ESI): $[M+H]^+$, found 456.41. $C_{27}H_{30}N_5O_2^+$ requires 456.24. Purity: 99.4 %.

8.16 Decomposition studies of 6-(N-methylbenzylamino)-2-phenylimidazo[1,2-b]pyridazines

Control experiment 1 - Testing if 3-methoxy **190g** decomposes under the conditions of its formation

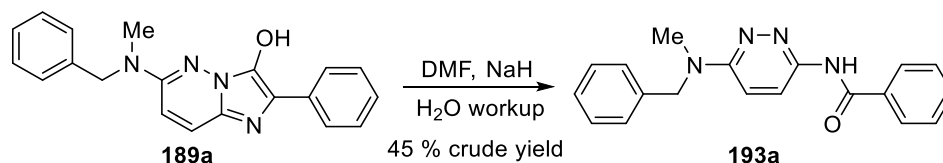


60 % Sodium hydride (in dispersion mineral oil) (0.014 g, 0.36 mmol) was triturated in hexane under nitrogen and the supernatant was removed via pipette. Residual hexane was removed under nitrogen flow. Dry DMF (0.5 mL) was added to the base under a nitrogen atmosphere and the mixture was cooled in an ice bath with stirring. Separately, a solution of the imidazo[1,2-*b*]pyridazine **190g** (0.075 g, 1.8 mmol) in dry DMF (2 mL) was prepared. The substrate solution was added at 0 °C under a nitrogen atmosphere to the stirred base suspension. The reaction mixture was warmed to room temperature (19 °C) at which it was stirred for 25 minutes. Methyl iodide was added dropwise and the resulting mixture was stirred for a further 50 minutes. The reaction mixture was cooled in an ice bath and water (12.5 mL) was added resulting in the formation of a beige precipitate which was collected via vacuum filtration. The filtrate was extracted with ethyl acetate (x 3). The combined organic layers were washed with water (x 5) and brine (x 1) and dried with sodium sulfate. The solvent was removed *in vacuo*. The beige residue and the solid were identified as 3-methoxyimidazo[1,2-*b*]pyridazine **190g** via ¹H NMR spectroscopy (~91 % recovery). Side-products **191g** and **192g** were present but at very low

Chapter 8

concentration, suggesting **190g** decomposing to form these side-products was not a significant reaction pathway.

*Control experiment 2 - Testing if 3-hydroxyimidazo[1,2-b]pyridazine **189a** decomposes to form side-product **193a** in the presence of DMF, sodium hydride and water*



60 % Sodium hydride (dispersion in mineral oil) (0.036 g, 0.91 mmol) was triturated in hexane under nitrogen and the supernatant was removed via pipette. Residual hexane was removed under nitrogen flow. Dry DMF (3 mL) was added to the base under a nitrogen atmosphere and the mixture was cooled in an ice bath with stirring. Separately, a solution of the imidazo[1,2-*b*]pyridazine **189a** (0.100 g, 0.303 mmol) in dry DMF (2 mL) was prepared. The substrate solution was added at 0 °C under a nitrogen atmosphere to the stirred base suspension. The reaction mixture was warmed to room temperature (17 °C) at which it was stirred for 40 minutes. Water (15 mL) was added and the whole was extracted with ethyl acetate (20 mL x 4). The combined organic phase was washed with water (20 mL x 7) and dried with sodium sulfate. The solvent was removed *in vacuo* affording the *title compound* **193a** as a black gum (0.043 g, 45 %). ¹H NMR (600 MHz, CDCl₃) δ 9.37 (s, 1H), 8.34 (d, *J* = 9.8 Hz, 1H), 7.97 (d, *J* = 7.4 Hz, 2H), 7.54 (t, *J* = 7.3 Hz, 1H), 7.46 (t, *J* = 7.6 Hz, 2H), 7.32 (t, *J* = 7.4 Hz, 2H), 7.27-7.23 (overlapping, 1H) 7.24 (d, *J* = 7.4 Hz, 2H), 6.91 (d, *J* = 9.8 Hz, 1H), 4.82 (s, 2H), 3.18 (s, 3H). ¹³C NMR (150 MHz, CDCl₃) δ 166.0, 158.1, 148.2, 137.7, 134.1, 132.3, 128.9, 128.8, 127.5, 127.4, 127.1, 122.0, 114.0, 53.8, 36.7. LCMS (APCI): [M+H]⁺, found 319.1553. C₁₉H₁₉N₄O⁺ requires 319.1554.

References

- (1) Tandon, R.; Nath, M. *Mini-Reviews Med. Chem.* **2017**, *17*, 549–570.
- (2) Zumla, A.; Nahid, P.; Cole, S. T. *Nat. Rev. Drug Discov.* **2013**, *12*, 388–404.
- (3) Jose, G.; Kumara, T. H. S.; Nagendrappa, G.; Sowmya, H. B. V; Sriram, D.; Yogeewari, P.; Sridevi, J. P.; Row, T. N. G.; Hosamani, A. A.; Sujan Ganapathy, P. S.; Chandrika, N.; Narendra, L. V. *Eur. J. Med. Chem.* **2015**, *89*, 616–627.
- (4) Hoagland, D. T.; Liu, J.; Lee, R. B.; Lee, R. E. *Adv. Drug Deliv. Rev.* **2016**, *102*, 55–72.
- (5) Koul, A.; Arnoult, E.; Lounis, N.; Guillemont, J.; Andries, K. *Nature* **2011**, *469*, 483–490.
- (6) Bocanegra-Garcia, V.; Garcia, A.; Palma-Nicolás, J. P.; Palos, I.; Rivera, G. In *Drug Development - A Case Study Based Insight into Modern Strategies*; Rundfeldt, C., Ed.; InTech: Shanghai, 2011; pp 207–242.
- (7) Dye, C.; Scheele, S.; Dolin, P.; Panthania, V.; Raviglione, M. C. *JAMA* **1999**, *282*, 677–686.
- (8) Moraski, G. C.; Miller, P. A.; Bailey, M. A.; Ollinger, J.; Parish, T.; Boshoff, H. I.; Cho, S.; Anderson, J. R.; Mulugeta, S.; Franzblau, S. G.; Miller, M. J. *ACS Infect. Dis.* **2016**, *1*, 85–90.
- (9) Villemagne, B.; Crauste, C.; Flipo, M.; Baulard, A. R.; Déprez, B.; Willand, N. *Eur. J. Med. Chem.* **2012**, *51*, 1–16.
- (10) Cole, S. T.; Riccardi, G. *Curr. Opin. Microbiol.* **2011**, *14*, 570–576.
- (11) Ballell, L.; Field, R. A.; Duncan, K.; Young, R. J. *Antimicrob. Agents Chemother.* **2005**, *49*, 2153–2163.
- (12) Sharma, S. K.; Mohan, A. *J. Indian Acad. Clin. Med.* **2004**, *5*, 109–113.
- (13) dos Santos Fernandes, G.; Jornada, Paula, D.; Souza, C.; Chin, C.; Pavan, F.; dos Santos, J. *Curr. Med. Chem.* **2015**, *22*, 3133–3161.
- (14) Zhang, Y. *Annu. Rev. Pharmacol.* **2005**, *45*, 529–564.
- (15) Banerjee, R.; Schechter, G. F.; Flood, J.; Porco, T. C. *Expert Rev. Anti Infect. Ther.* **2008**, *6*, 713–724.
- (16) Sarkar, S.; Suresh, M. R. *J. Pharm. Sci.* **2011**, *14*, 148–161.
- (17) Jain, S. K.; Lamichhane, G.; Nimmagadda, S.; Pomper, M. G.; Bishai, W. R. *Microbe* **2008**, *3*, 285–292.

References

- (18) The Drug Development Process
<https://www.fda.gov/ForPatients/Approvals/Drugs/default.htm> (accessed Mar 21, 2018).
- (19) Ashtekar, D. R.; Costa-periera, R.; Shrinivasan, T.; Iyer, R.; Vishvanathan, N.; Rittel, W. *Diagn. Microbiol. Infect. Dis.* **1991**, *14*, 465–471.
- (20) Barbachyn, M. R.; Hutchinson, D. K.; Brickner, S. J.; Cynamon, M. H.; Kilburn, J. O.; Klemens, S. P.; Glickman, S. E.; Grega, K. C.; Hendges, S. K.; Toops, D. S.; Ford, C. W.; Zurenko, G. E. *J. Med. Chem.* **1996**, *39*, 680–685.
- (21) newtdrugs.com.pdf www.newtdrugs.org (accessed Mar 22, 2018).
- (22) Cohen, J. *Science* **2013**, *339*, 130.
- (23) Andries, K.; Verhasselt, P.; Guillemont, J.; Neefs, J.; Winkler, H.; Gestel, J. Van; Timmerman, P.; Zhu, M.; Lee, E.; Williams, P.; Chaffoy, D. De; Huitric, E.; Hoffner, S.; Cambau, E.; Truffot-pernot, C.; Lounis, N.; Jarlier, V. *Science* **2005**, *307*, 223–228.
- (24) Huitric, E.; Verhasselt, P.; Andries, K.; Hoffner, S. E. **2007**, *51*, 4202–4204.
- (25) Sirturo product information for healthcare providers
<http://www.sirturo.com/sites/default/files/pdf/SIRTURO-product-guide.pdf> (accessed Feb 20, 2018).
- (26) Matsumoto, M.; Hashizume, H.; Tomishige, T.; Kawasaki, M.; Tsubouchi, H. *PLoS Med.* **2006**, *3*, 2131–2144.
- (27) Manjunatha, U. H.; Boshoff, H.; Dowd, C. S.; Zhang, L.; Albert, T. J.; Norton, J. E.; Daniels, L.; Dick, T.; Pang, S. S.; Barry, C. E. *PNAS* **2006**, *103*, 431–436.
- (28) Singh, R.; Manjunatha, U.; Boshoff, H. I. M.; Ha, Y. H.; Niyomrattanakit, P.; Ledwidge, R.; Dowd, C. S.; Lee, I. Y.; Kim, P.; Zhang, L.; Kang, S.; Keller, T. H.; Jiricek, J.; Barry, C. E. *Science* **2008**, *322*, 1392–1396.
- (29) Nuermberger, E.; Tyagi, S.; Tasneen, R.; Williams, K. N.; Almeida, D.; Rosenthal, I.; Grosset, J. H. *Antimicrob. Agents Chemother.* **2008**, *52*, 1522–1524.
- (30) Nuermberger, E.; Rosenthal, I.; Tyagi, S.; Williams, K. N.; Almeida, D.; Peloquin, C. A.; Bishai, W. R.; Grosset, J. H. *Antimicrob. Agents Chemother.* **2006**, *50*, 2621–2625.
- (31) Tasneen, R.; Tyagi, S.; Williams, K.; Grosset, J.; Nuermberger, E. *Antimicrob. Agents Chemother.* **2008**, *52*, 3664–3668.

References

- (32) Ginsberg, A. M. *Drugs* **2010**, *70*, 2201–2214.
- (33) Johns Hopkins University, Federal University of Rio de Janeiro. Study of daily rifapentine for pulmonary tuberculosis[Clinical Trials.gov identifier NCT00814671] US National Institutes of Health, ClinicalTrials.gov. <https://clinicaltrials.gov/> (accessed Mar 22, 2018).
- (34) Nikonenko, B. V.; Protopopova, M.; Samala, R.; Einck, L.; Nacy, C. A. *Antimicrob. Agents Chemother.* **2007**, *51*, 1563–1565.
- (35) Chen, P.; Gearhart, J.; Protopopova, M.; Einck, L.; Nacy, C. A. *J. Antimicrob. Chemother.* **2006**, *58*, 332–337.
- (36) Li, L.; Li, Z.; Liu, M.; Shen, W.; Wang, B.; Guo, H.; Lu, Y. *Molecules* **2016**, *21*, 49–62.
- (37) Pethe, K.; Bifani, P.; Jang, J.; Kang, S.; Park, S.; Ahn, S.; Jiricek, J.; Jung, J.; Jeon, H. K.; Cechetto, J.; Christophe, T.; Lee, H.; Kempf, M.; Jackson, M.; Lenaerts, A. J.; Pham, H.; Jones, V.; Seo, M. J.; Kim, Y. M.; Seo, M.; Seo, J. J.; Park, D.; Ko, Y.; Choi, I.; Kim, R.; Kim, S. Y.; Lim, S.; Yim, S.-A.; Nam, J.; Kang, H.; Kwon, H.; Oh, C.-T.; Cho, Y.; Jang, Y.; Kim, J.; Chua, A.; Tan, B. H.; Nanjundappa, M. B.; Rao, S. P. S.; Barnes, W. S.; Wintjens, R.; Walker, J. R.; Alonso, S.; Lee, S.; Kim, J.; Oh, S.; Oh, T.; Nehrbass, U.; Han, S.-J.; No, Z.; Lee, J.; Brodin, P.; Cho, S.-N.; Nam, K.; Kim, J. *Nat. Med.* **2013**, *19*, 1157–1160.
- (38) Kang, S.; Kim, R. Y.; Seo, M. J.; Lee, S.; Kim, Y. M.; Seo, M.; Seo, J. J.; Ko, Y.; Choi, I.; Jang, J.; Nam, J.; Park, S.; Kang, H.; Kim, H. J.; Kim, J.; Ahn, S.; Pethe, K.; Nam, K.; No, Z.; Kim, J. *J. Med. Chem.* **2014**, *57*, 5293–5305.
- (39) Abrahams, K. A.; Cox, J. A. G.; Spivey, V. L.; Loman, N. J.; Pallen, M. J.; Alemparte, C.; Remuin, M. J.; Constantinidou, C.; Ferna, R.; Barros, D.; Ballell, L.; Besra, G. S. *PLoS One* **2012**, *7*, 1–10.
- (40) Trumpower, B. L. *J. Biol. Chem.* **1990**, *265*, 11409–11412.
- (41) Crofts, A. R. *Annu. Rev. Physiol.* **2004**, *66*, 689–733.
- (42) Tang, J.; Wang, B.; Wu, T.; Wan, J.; Tu, Z.; Njire, M.; Wan, B.; Franzblauc, S. G.; Zhang, T.; Lu, X.; Ding, K. *ACS Med. Chem. Lett.* **2015**, *6*, 814–818.
- (43) Liu, Y.; Gao, Y.; Liu, J.; Tan, Y.; Liu, Z.; Chhotaray, C.; Jiang, H.; Lu, Z.; Chiwala, G.; Wang, S.; Makafe, G.; Islam, M. M.; Hameed, H. M. A.; Cai, X.; Wang, C.; Li, X.; Tan, S.; Zhang, T. *Nat. Commun.* **2019**, *10*, 524.

References

- (44) Ramachandran, S.; Panda, M.; Mukherjee, K.; Choudhury, N. R.; Tantry, S. J.; Kedari, C. K.; Ramachandran, V.; Sharma, S.; Ramya, V. K.; Guptha, S.; Sambandamurthy, V. K. *Bioorg. Med. Chem. Lett.* **2013**, *23*, 4996–5001.
- (45) Wu, Z.; Lu, Y.; Li, L.; Zhao, R.; Wang, B.; Lv, K.; Liu, M.; You, X. *ACS Med. Chem. Lett.* **2016**, *7*, 1130–1133.
- (46) No, Z.; Kim, J.; Brodin, P.; Seo, M. J.; Kim, Y. M.; Cechetto, J.; Jeon, H.; Genovesio, A.; Lee, S.; Kang, S.; Ewann, F. A.; Nam, J. Y.; Christophe, T.; Feninstein, D. P. C.; Heo, J.; Jiyeon, J. WO 2009/113606 A1, 2011.
- (47) de Araújo, R. V.; Santos, S. S.; Sanches, L. M.; Giarolla, J.; Seoud, O. El; Ferreira, E. I. *Mem. Inst. Oswaldo Cruz* **2020**, *115*, 1–20.
- (48) Chapman, T. M.; Osborne, S. A.; Bouloc, N.; Large, J. M.; Wallace, C.; Birchall, K.; Ansell, K. H.; Jones, H. M.; Taylor, D.; Clough, B.; Green, J. L.; Holder, A. A. *Bioorg. Med. Chem. Lett.* **2013**, *23*, 3064–3069.
- (49) Le Manach, C.; González Cabrera, D.; Douelle, F.; Nchinda, A. T.; Younis, Y.; Taylor, D.; Wiesner, L.; White, K. L.; Ryan, E.; March, C.; Duffy, S.; Avery, V. M.; Waterson, D.; Witty, M. J.; Wittlin, S.; Charman, S. A.; Street, L. J.; Chibale, K. *J. Med. Chem.* **2014**, *57*, 2789–2798.
- (50) Ali, A.; Cablewski, T.; Francis, C. L.; Ganguly, A. K.; Sargent, R. M.; Sawutz, D. G.; Winzenberg, K. N. *Bioorg. Med. Chem. Lett.* **2011**, *21*, 4160–4163.
- (51) Moraski, G. C.; Oliver, A. G.; Markley, L. D.; Cho, S.; Franzblau, S. G.; Miller, M. J. *Bioorg. Med. Chem. Lett.* **2014**, *24*, 3493–3498.
- (52) Barlin, G. B.; Davies, L. P.; Ngu, M. M. L. *Aust. J. Chem.* **1989**, *42*, 1749–1757.
- (53) Barlin, G. B.; Davies, L. P.; Ireland, S. J.; Ngu, M. M. L. *Aust. J. Chem.* **1989**, *42*, 1133–1146.
- (54) Barlin, G. B.; Davies, L. P.; Ireland, S. J.; Zhang, J. *Aust. J. Chem.* **1992**, *45*, 751–757.
- (55) Barlin, G. B. *J. Heterocycl. Chem.* **1998**, *35*, 1205–1217.
- (56) Dalvie, D. K.; Kalgutkar, A. S.; Khojasteh-Bakht, S. C.; Obach, R. S.; O'Donnell, J. P. *Chem. Res. Toxicol.* **2002**, *15*, 269–299.
- (57) Mandlik, V.; Bejugam, P. R.; Singh, S. In *Artificial Neural Network for Drug Design, Delivery and Disposition*; Puri, M., Pathak, Y., Sutariya, V. K., Tipparaju, S., Moreno, W.,

References

- Eds.; Elsevier Inc.: Pune, 2016; pp 123–139.
- (58) Floyd, M. B.; Du, M. T.; Fabio, P. F.; Jacob, L. A.; Johnson, B. D. *J. Org. Chem.* **1985**, *50*, 5022–5027.
- (59) Lu, Y.; Hendra, R.; Oakley, A. J.; Keller, P. A. *Tetrahedron Lett.* **2014**, *55*, 6212–6215.
- (60) Caron, S.; Do, N. M.; Sieser, J. E. *Tetrahedron Lett.* **2000**, *41*, 2299–2302.
- (61) Riley, H. A.; Gray, A. R. *Org. Synth.* **1943**, *2*, 509.
- (62) Wang, Q.; Xu, Y.; Yang, X.; Li, Y.; Li, X. *Chem. Commun.* **2017**, *53*, 9640–9643.
- (63) Karpov, S. V.; Grigor'Ev, A. A.; Kayukov, Y. S.; Karpova, I. V.; Nasakin, O. E.; Tafeenko, V. A. *J. Org. Chem.* **2016**, *81*, 6402–6408.
- (64) Lokhande, P. D.; Waghmare, S. R.; Gaikwad, H.; Hankare, P. P. *Indian J. Chem.* **2013**, *52*, 300–305.
- (65) Shen, M. G.; Shang, S. Bin; Song, Z. Q.; Wang, D.; Rao, X. P.; Gao, H.; Liu, H. *J. Chem. Res.* **2013**, *37*, 51–52.
- (66) Alayrac, C.; Berkenbusch, T.; Briet, B.; Ditrich, K.; Eckhardt, M.; Escher, I.; Gansäuer, A.; Glorius, F.; Göttlich, R.; Harcken, C.; Harmata, M.; Hashmi, A. S. K.; Kalesse, M.; Muñiz, K.; Oestreich, M.; Olpp, T.; Plietker, B.; Podlech, J.; Reiser, O.; Schall, A.; Witulski, B. *Science of Synthesis Houben-Weyl Methods of Molecular Transformations*; Brückner, R., Schaumann, E., Eds.; Thieme: Stuttgart, 2007.
- (67) Moine, E.; Dimier-Poisson, I.; Enguehard-Gueiffier, C.; Logé, C.; Pénichon, M.; Moiré, N.; Delehouzé, C.; Foll-Josselin, B.; Ruchaud, S.; Bach, S.; Gueiffier, A.; Debierre-Grockiego, F.; Denevault-Sabourin, C. *Eur. J. Med. Chem.* **2015**, *105*, 80–105.
- (68) Röhrig, U. F.; Majjigapu, S. R.; Grosdidier, A.; Bron, S.; Stroobant, V.; Pilotte, L.; Colau, D.; Vogel, P.; Van Den Eynde, B. J.; Zoete, V.; Michielin, O. *J. Med. Chem.* **2012**, *55*, 5270–5290.
- (69) Guildford, A. J.; Tometzki, M. A.; Turner, R. W. *Synth.* **1983**, *12*, 987–989.
- (70) Barlin, G. B. *Aust. J. Chem.* **1986**, *39*, 1803–1809.
- (71) Barlin, G. B.; Ireland, S. J. *Aust. J. Chem.* **1987**, *40*, 1491–1497.
- (72) Dračinský, M.; Pohl, R. In *Annual Reports on NMR Spectroscopy*; Webb, G., Ed.; Elsevier Ltd: Prague, 2014; pp 59–113.

References

- (73) Araya-Maturana, R.; Pessoa-Mahana, H.; Weiss-López, B. *Nat. Prod. Commun.* **2008**, *3*, 445–450.
- (74) Zhuang, J.; Wang, C.; Xie, F.; Zhang, W. *Tetrahedron* **2009**, *65*, 9797–9800.
- (75) Hjelmencrantz, A.; Berg, U. *J. Org. Chem.* **2002**, *67*, 3585–3594.
- (76) Itai, T.; Nakashima, T. *Chem. Pharm. Bull.* **1962**, *10*, 936–940.
- (77) Ibrahim, H.; Couderc, F.; Perio, P.; Collin, F.; Nepveu, F. *Rapid Commun. Mass Spectrom.* **2013**, *27*, 621–628.
- (78) Do Pham, D. D.; Kelso, G. F.; Yang, Y.; Hearn, M. T. W. *Green Chem.* **2012**, *14*, 1189–1195.
- (79) Barlin, G. B.; Davies, L. P.; Ireland, S. J.; Ngu, M. M. L. *Aust. J. Chem.* **1989**, *42*, 1735–1748.
- (80) Barlin, G. B.; Brown, D. J.; Kadunc, Z.; Petrič, A.; Stanovnik, B.; Tišler, M. *Aust. J. Chem.* **1983**, *36*, 1215–1220.
- (81) Barlin, G. B.; Davies, L. P.; Ireland, S. J.; Ngu, M. M. L.; Zhang, J. *Aust. J. Chem.* **1992**, *45*, 731–749.
- (82) Naresh, G.; Lakkaniga, R.; Kharbanda, A.; Yan, W. *Eur. J. Org. Chem.* **2019**, *2019*, 770–777.
- (83) Mondal, S.; Samanta, S.; Singsardar, M.; Hajra, A. *Org. Lett.* **2017**, *19*, 3751–3754.
- (84) Mondal, S.; Samanta, S.; Jana, S.; Hajra, A. *J. Org. Chem.* **2017**, *82*, 4504–4510.
- (85) Behr, A.; Becker, M.; Reyer, S. *Tetrahedron Lett.* **2010**, *51*, 2438–2441.
- (86) Khazi, I. A. M.; Gadad, A. K.; Lamani, R. S.; Bhongade, B. A. *Tetrahedron* **2011**, *67*, 3289–3316.
- (87) Zhang, W.; Lun, S.; Wang, S.-H.; Jiang, X.-W.; Yang, F.; Tang, J.; Manson, A. L.; Earl, A. M.; Gunosewoyo, H.; Bishai, W. R.; Yu, L. F. *J. Med. Chem.* **2018**, *61*, 791–803.
- (88) Liu, Y.; Hao, H.; Xie, H.; Lv, H.; Liu, C.; Wang, G. *J. Pharm. Sci.* **2009**, *98*, 4391–4401.
- (89) Buckman, B. O.; Nicholas, J. B.; Emayan, K.; Seiwert, S. D. US 2014/0200215 A1, 2014.
- (90) Pellicciari, R.; Moroni, F.; Gilbert, A. M. WO 2009/155402 A1, 2009.
- (91) Tang, J.; Wang, B.; Wu, T.; Wan, J.; Tu, Z.; Njire, M.; Wan, B.; Franzblau, S. G.; Zhang, T.; Lu, X.; Ding, K. *ACS Med. Chem. Lett.* **2015**, *6*, 814–818.
- (92) Langdon, S. R.; Ertl, P.; Brown, N. *Mol. Inform.* **2010**, *29*, 366–385.
- (93) Brown, N. In *Scaffold Hopping in Medicinal Chemistry*; Brown, N., Ed.; Wiley-VCH, 2014; pp 1–13.

References

- (94) Bhongade, B. A.; Talath, S.; Gadad, R. A.; Gadad, A. K. *J. Saudi Chem. Soc.* **2016**, *20*, S463–S475.
- (95) Hegde, V. S.; Kolavi, G. D.; Lamani, R. S.; Khazi, I. A. M. *J. Sulfur Chem.* **2006**, *27*, 553–569.
- (96) Palkar, M. B.; Noolvi, M. N.; Maddi, V. S.; Ghatole, M.; Nargund, L. G. *Med. Chem. Res.* **2012**, *21*, 1313–1321.
- (97) Anusha, S.; Baburajeev, C. P.; Mohan, C. D.; Mathai, J.; Rangappa, S.; Mohan, S.; Chandra; Paricharak, S.; Mervin, L.; Fuchs, J. E.; Mahedra, M.; Bender, A.; Basappa; Rangappa, K. S. *PLoS One* **2015**, *10*, 1–12.
- (98) Ramprasad, J.; Nayak, N.; Dalimba, U.; Yogeewari, P.; Sriram, D. *Bioorg. Med. Chem. Lett.* **2015**, *25*, 4169–4173.
- (99) Li, J.; Sha, Y. *Molecules* **2008**, *13*, 1111–1119.
- (100) Maes, B. U. W.; Lemièrre, G. L. F.; Dommissie, R.; Haemers, A. *J. Heterocycl. Chem.* **2001**, *38*, 1215–1218.
- (101) Stinear, T. P.; Jenkin, G. A.; Johnson, P. D. R.; Davies, J. K. *J. Bacteriol.* **2000**, *182*, 6322–6330.
- (102) Yang, F.; Njire, M. M.; Liu, J.; Wu, T.; Wang, B.; Liu, T.; Cao, Y.; Liu, Z.; Wan, J.; Tu, Z.; Tan, Y.; Tan, S.; Zhang, T. *PLoS One* **2015**, *10*, 1–13.
- (103) Zhang, T.; Li, S.-Y.; Nuermberger, E. L. *PLoS One* **2012**, *7*, e29774.
- (104) Surineni, G.; Gao, Y.; Hussain, M.; Liu, Z.; Lu, Z.; Chhotaray, C.; Islam, M. M.; Hameed, H. M. A.; Zhang, T. *Med. Chem. Commun.* **2019**, *10*, 49–60.
- (105) Zhang, W.; Lun, S.; Liu, L. L.; Xiao, S.; Duan, G.; Gunosewoyo, H.; Yang, F.; Tang, J.; Bishai, W. R.; Yu, L. F. *J. Med. Chem.* **2019**, *62*, 3575–3589.
- (106) Yang, B.; Du, S.; Lu, Y.; Jia, S.; Zhao, M.; Bai, J.; Li, P.; Wu, H. *J. Pharm. Pharmacol.* **2017**, *70*, 349–360.
- (107) Wager, T. T.; Chandrasekaran, R. Y.; Hou, X.; Troutman, M. D.; Verhoest, P. R.; Villalobos, A.; Will, Y. *ACS Chem. Neurosci.* **2010**, *1*, 420–434.
- (108) Veber, D. F.; Johnson, S. R.; Cheng, H. Y.; Smith, B. R.; Ward, K. W.; Kopple, K. D. *J. Med. Chem.* **2002**, *45*, 2615–2623.
- (109) Ritchie, T. J.; Macdonald, S. J. F. *Drug Discov. Today* **2009**, *14*, 1011–1020.

References

- (110) Lovering, F.; Bikker, J.; Humblet, C. *J. Med. Chem.* **2009**, *52*, 6752–6756.
- (111) Lombardo, F.; Shalaeva, M. Y.; Tupper, K. A.; Gao, F. *J. Med. Chem.* **2001**, *44*, 2490–2497.
- (112) Bevan, C. D.; Lloyd, R. S. *Anal. Chem.* **2000**, *72*, 1781–1787.
- (113) Ring, B. J.; Chien, J. Y.; Adkison, K. K.; Jones, H. M.; Rowland, M.; Jones, R. Do; Yates, J. W. T.; Ku, S.; Gibson, C. R.; He, H.; Vuppugalla, R.; Marathe, P.; Fischer, V.; Dutta, S.; Sinh, V. K.; Björnsson, T.; Lavé, T.; Poulin, P. *J. Pharm. Sci.* **2011**, *100*, 4090–4110.
- (114) Wilkinson, G. R.; Shand, D. G. *Clin. Pharmacol. Ther.* **1975**, *18*, 377–390.
- (115) Obach, R. S. *Drug Metab. Dispos.* **1999**, *27*, 1350–1359.
- (116) Rane, A.; Wilkinson, R.; Shand, D. . *J. Pharmacol. Exp. Ther.* **1976**, *200*, 420–424.
- (117) Roth, H. S.; Botham, R. C.; Schmid, S. C.; Fan, T. M.; Dirikolu, L.; Hergenrother, P. J. *J. Med. Chem.* **2015**, *58*, 4046–4065.
- (118) Smith, H. S. *Mayo Clin. Proc.* **2009**, *84*, 613–624.
- (119) Pellinen, P.; Honkakoski, P.; Stenbäck, F.; Niemitz, M.; Alhava, E.; Pelkonen, O.; Lang, M. A.; Pasanen, M. *Eur. J. Pharmacol. Environ. Toxicol.* **1994**, *270*, 35–43.
- (120) Gerber, J. G.; Rhodes, R. J.; Gal, J. *Chirality* **2004**, *16*, 36–44.
- (121) Purser, S.; Moore, P. R.; Swallow, S.; Gouverneur, V. *Chem. Soc. Rev.* **2008**, *37*, 320–330.
- (122) Kiani, Y. S.; Jabeen, I. *ACS Omega* **2020**, *5*, 179–188.
- (123) Broccatelli, F.; Aliagas, I.; Zheng, H. *ACS Med. Chem. Lett.* **2018**, *9*, 522–527.
- (124) Parcella, K.; Eastman, K.; Yeung, K. S.; Grant-Young, K. A.; Zhu, J.; Wang, T.; Zhang, Z.; Yin, Z.; Parker, D.; Mosure, K.; Fang, H.; Wang, Y. K.; Lemm, J.; Zhuo, X.; Hanumegowda, U.; Liu, M.; Rigat, K.; Donoso, M.; Tuttle, M.; Zvyaga, T.; Haarhoff, Z.; Meanwell, N. A.; Soars, M. G.; Roberts, S. B.; Kadow, J. F. *ACS Med. Chem. Lett.* **2017**, *8* (7), 771–774.
- (125) Murphy, R. B.; Wyatt, N. A.; Fraser, B. H.; Yepuri, N. R.; Holden, P. J.; Wotherspoon, A. T. L.; Darwish, T. A. *Anal. Chim. Acta* **2019**, *1064*, 65–70.
- (126) Kumar, S.; Gopalakrishnan, V.; Hegde, M.; Rana, V.; Dhepe, S. S.; Ramareddy, S. A.; Leoni, A.; Locatelli, A.; Morigi, R.; Rambaldi, M.; Srivastava, M.; Raghavan, S. C.; Karki, S. S. *Bioorg. Med. Chem. Lett.* **2014**, *24*, 4682–4688.
- (127) Kumar, S.; Hegde, M.; Gopalakrishnan, V.; Renuka, V. K.; Ramareddy, S. A.; De Clercq, E.; Schols, D.; Gudibabande Narasimhamurthy, A. K.; Raghavan, S. C.; Karki, S. S. *Eur. J. Med.*

References

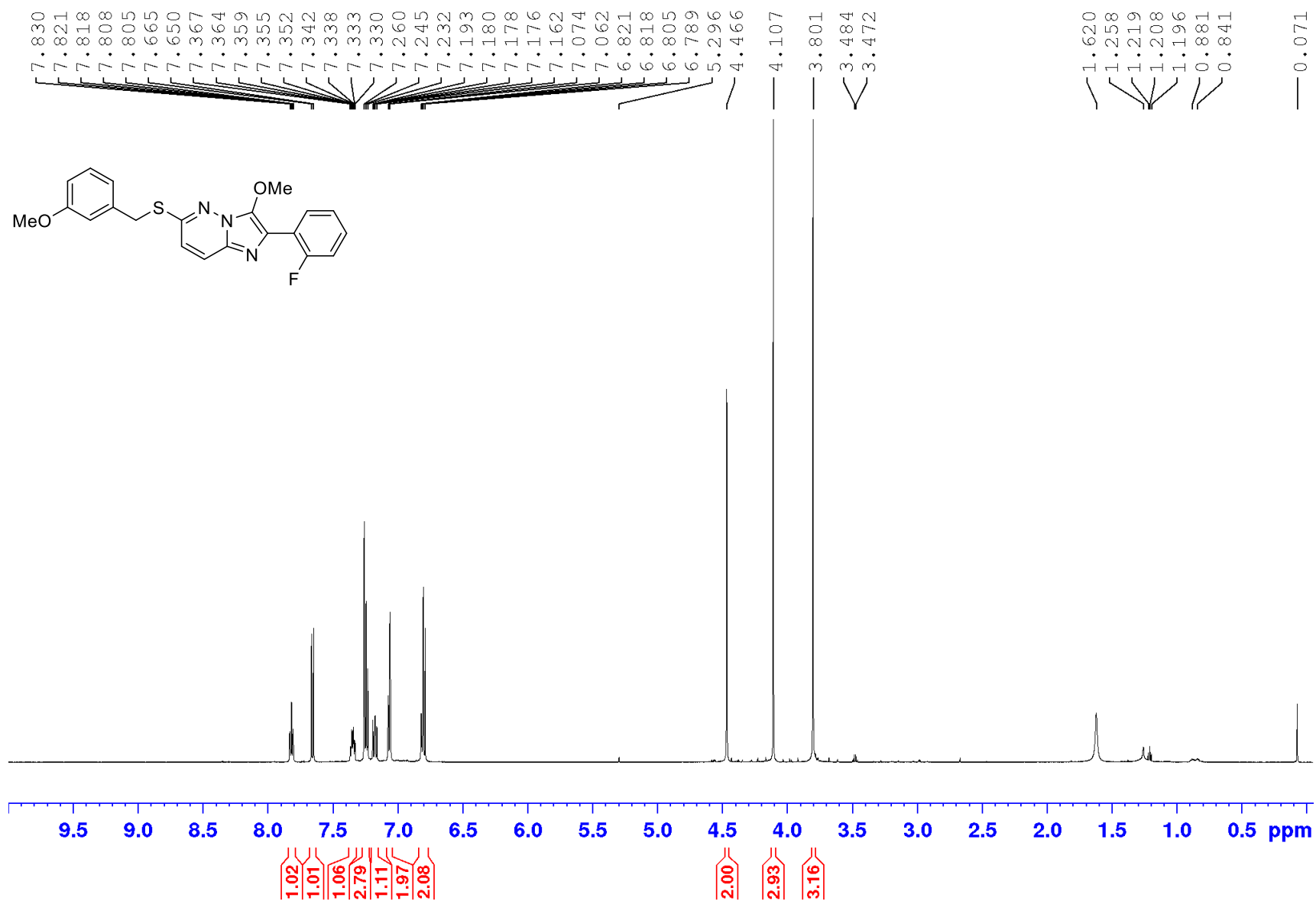
- Chem.* **2014**, *84*, 687–697.
- (128) Temple, K. J.; Duvernay, M. T.; Maeng, J. G.; Blobaum, A. L.; Stauffer, S. R.; Hamm, H. E.; Lindsley, C. W. *Bioorg. Med. Chem. Lett.* **2016**, *26*, 5481–5486.
- (129) Kibriya, G.; Samanta, S.; Jana, S.; Mondal, S.; Hajra, A. *J. Org. Chem.* **2017**, *82*, 13722–13727.
- (130) Baranac-Stojanović, M.; Marković, R.; Stojanović, M. *Tetrahedron* **2011**, *67*, 8000–8008.
- (131) Ma, G.-H.; Jiang, B.; Tu, X.-J.; Ning, Y.; Tu, S.-J.; Li, G. *Org. Lett.* **2014**, *16*, 4504–4507.
- (132) Ayala-Mata, F.; Barrera-Mendoza, C.; Jiménez-Vázquez, H. A.; Vargas-Díaz, E.; Zepeda, L. G. *Molecules* **2012**, *17*, 13864–13878.

Appendices

*Section 1: NMR spectra, LC-MS and HRMS
chromatograms/spectra for compounds tested against Mtb*

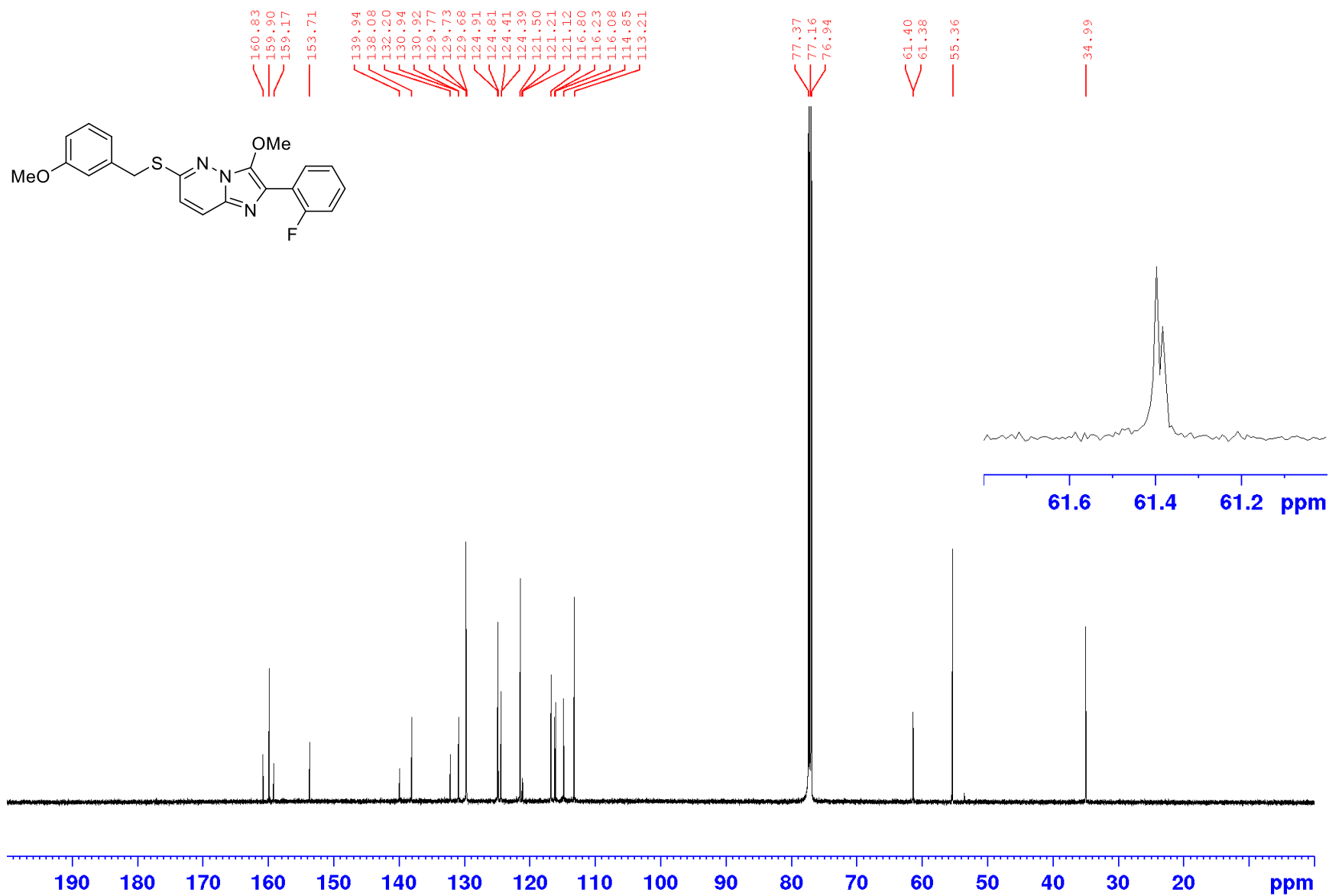
Appendices

¹H NMR spectrum of **17** (600 MHz; CDCl₃)



Appendices

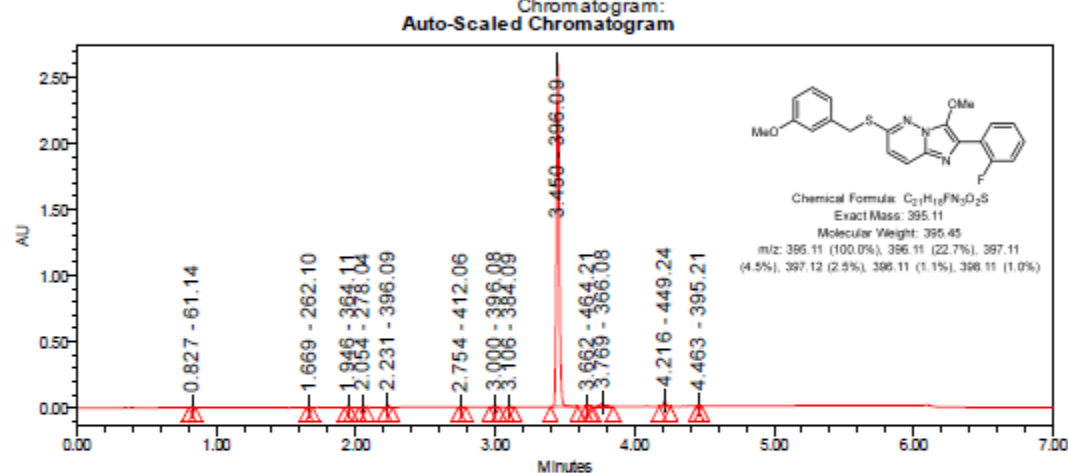
¹³C NMR spectrum of **17** (150 MHz; CDCl₃)



Appendices

LC-MS chromatogram of **17** [M+H]⁺

Instrument: Waters Acquity iClass
 PDA and QDa detectors
 Vial: 1:A,8
 Acquired By: System
 Injection #: 1
 Sample Set Name: MK_26_April2019
 Injection Volume: 0.30 ul
 Run Time: 7.0 Minutes
 Acquisition Method: 95% A1 to 100% B1
 Mobile Phase: A1: 100% H2O / 0.1% FA
 B1: 100% ACN / 0.1% FA
 Date Acquired: 26/04/2019 12:41:31 PM EST
 Date Processed: 26/04/2019 1:01:01 PM EST
 Extracted: PDA Spectrum PDA 254.0 nm
 Chromatogram:



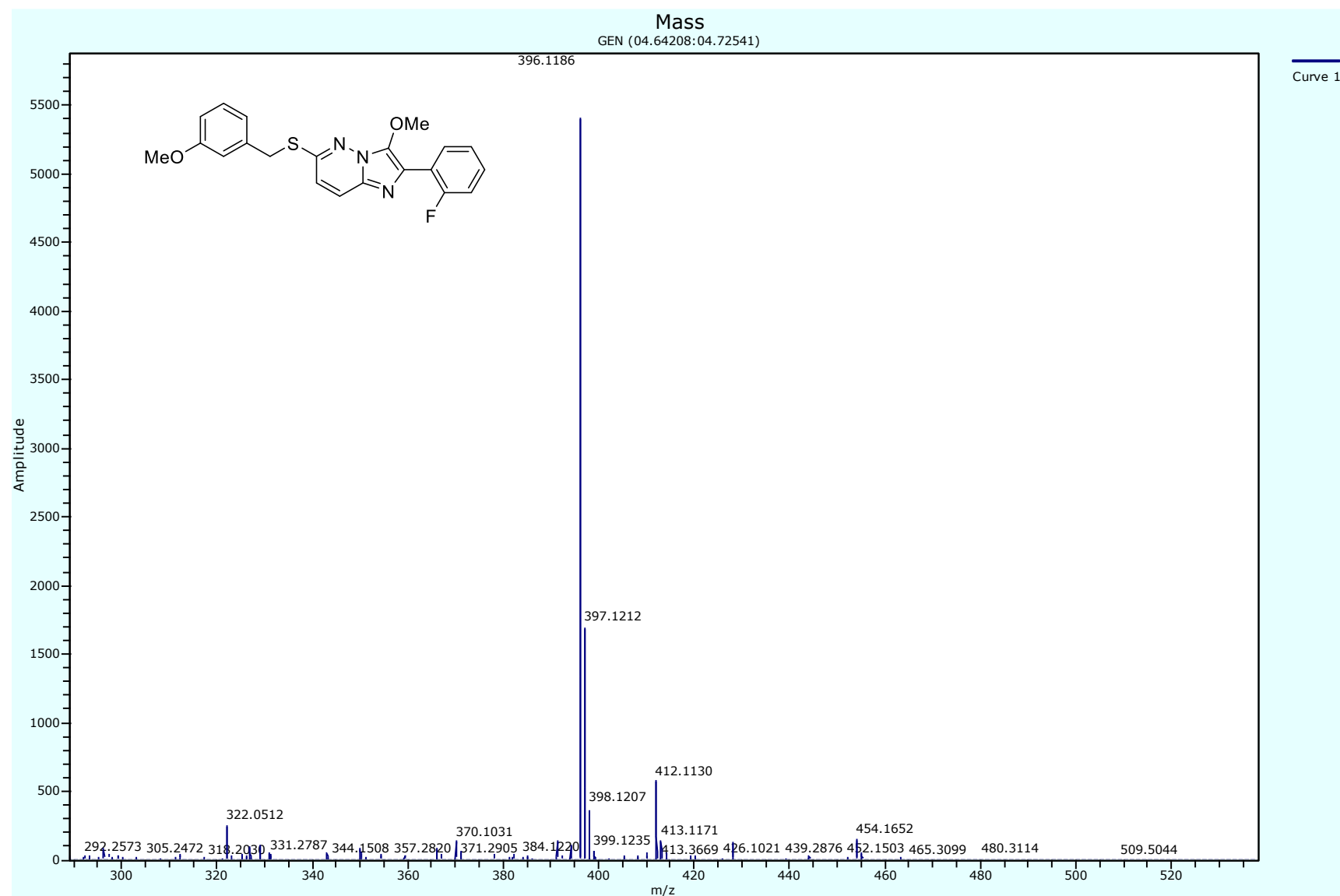
Peak Results

	RT	Area	% Area	Height	Base Peak (m/z)
1	0.827	10632	0.28	8380	61.14
2	1.669	6976	0.18	5689	262.10
3	1.946	8350	0.22	7694	364.11
4	2.054	9599	0.25	8725	278.04
5	2.231	23298	0.60	20853	396.09
6	2.754	4569	0.12	3502	412.06
7	3.000	15077	0.39	8397	396.08
8	3.106	6119	0.16	4455	384.09
9	3.450	3651052	94.62	2589535	396.09

	RT	Area	% Area	Height	Base Peak (m/z)
10	3.662	5555	0.14	4538	464.21
11	3.769	60443	1.57	24972	366.08
12	4.216	49902	1.29	41460	449.24
13	4.463	7049	0.18	6317	396.21

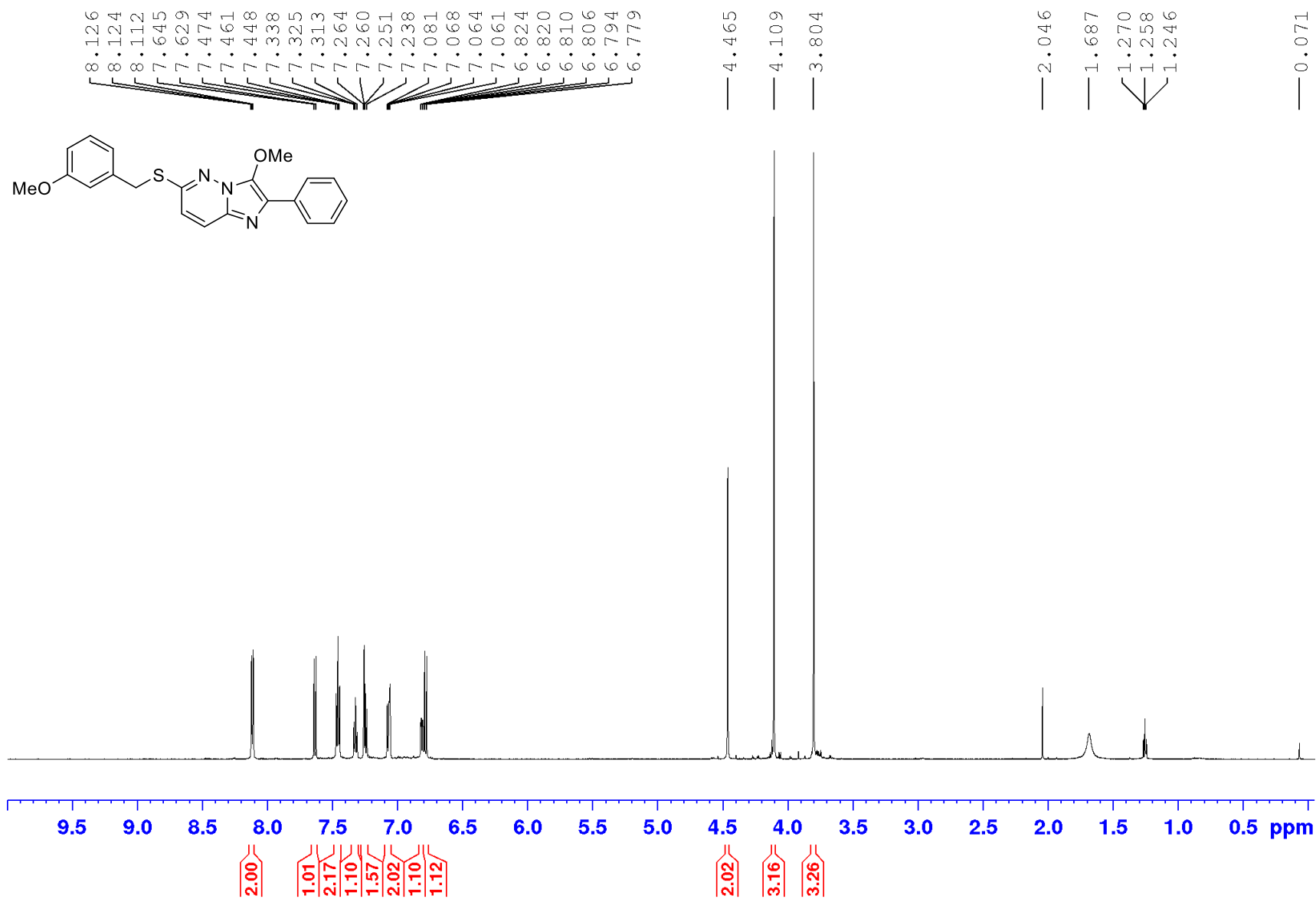
Appendices

HRMS (APCI) spectrum of **17** $[M+H]^+$



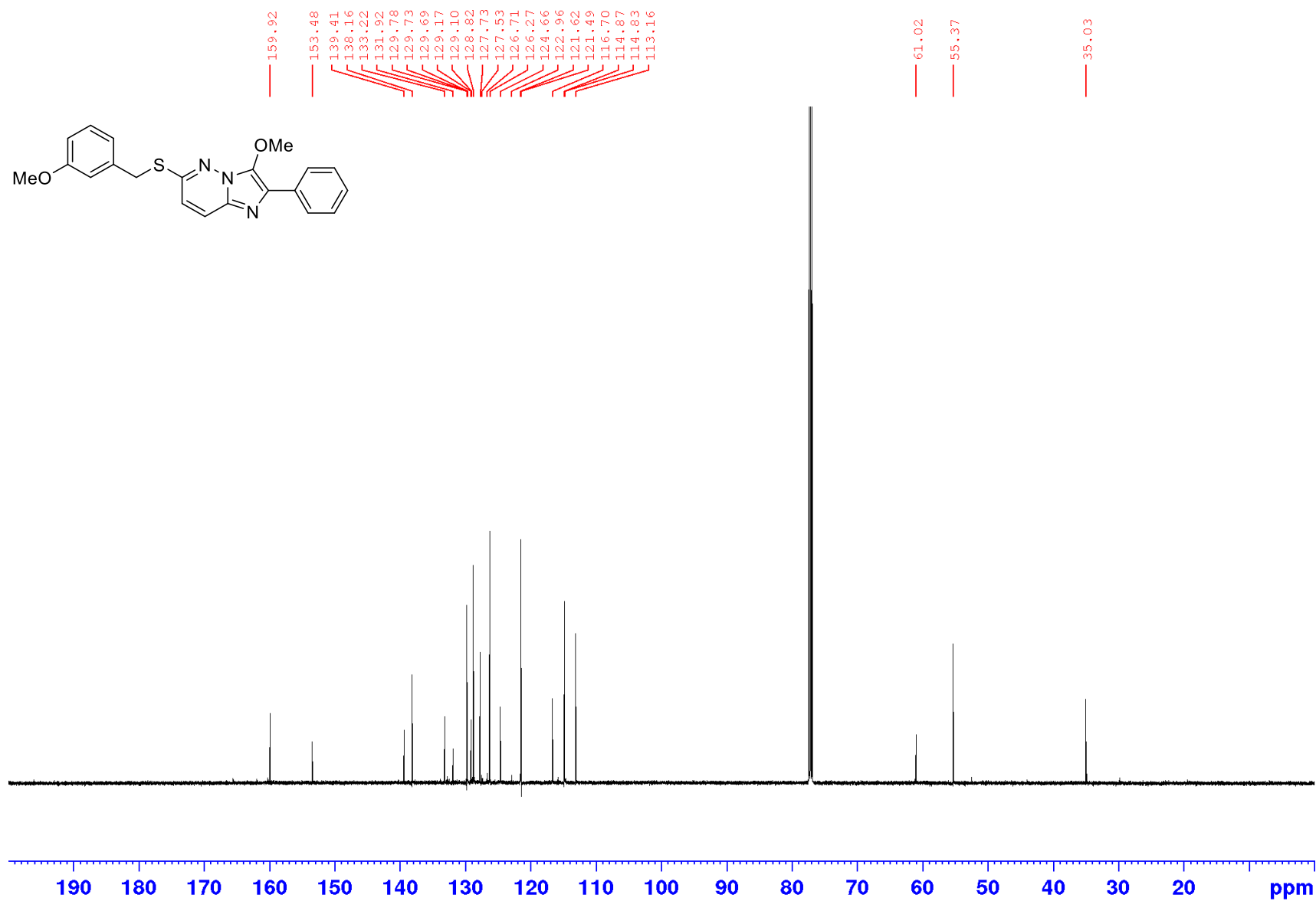
Appendices

¹H NMR spectrum of **64** (600 MHz; CDCl₃)



Appendices

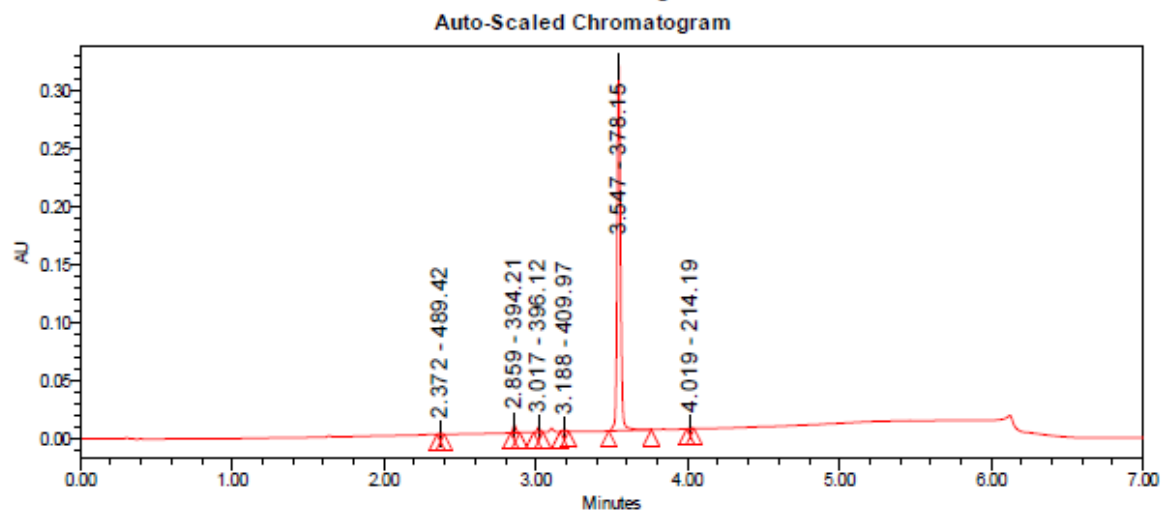
^{13}C NMR spectrum of **64** (150 MHz; CDCl_3)



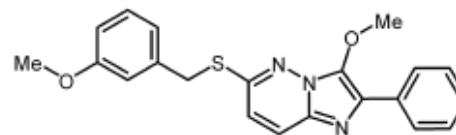
Appendices

LC-MS chromatogram of 64 [M+H]⁺

Vial:	1:A,5	Instrument:	Waters Acquity iClass PDA and QDa detectors
Injection #:	1	Acquired By:	System
Injection Volume:	0.10 ul	Sample Set Name:	MK_20_December2017
Run Time:	7.0 Minutes	Acquisition Method:	95% A1 to 100% B1 POSNEG
Date Acquired:	20/12/2017 10:56:43 AM EST	Mobile Phase:	A1: 100% H2O / 0.1% FA B1: 100% ACN / 0.1% FA
Date Processed:	20/12/2017 11:15:24 AM EST	Extracted Chromatogram:	PDA Spectrum PDA 254.0 nm



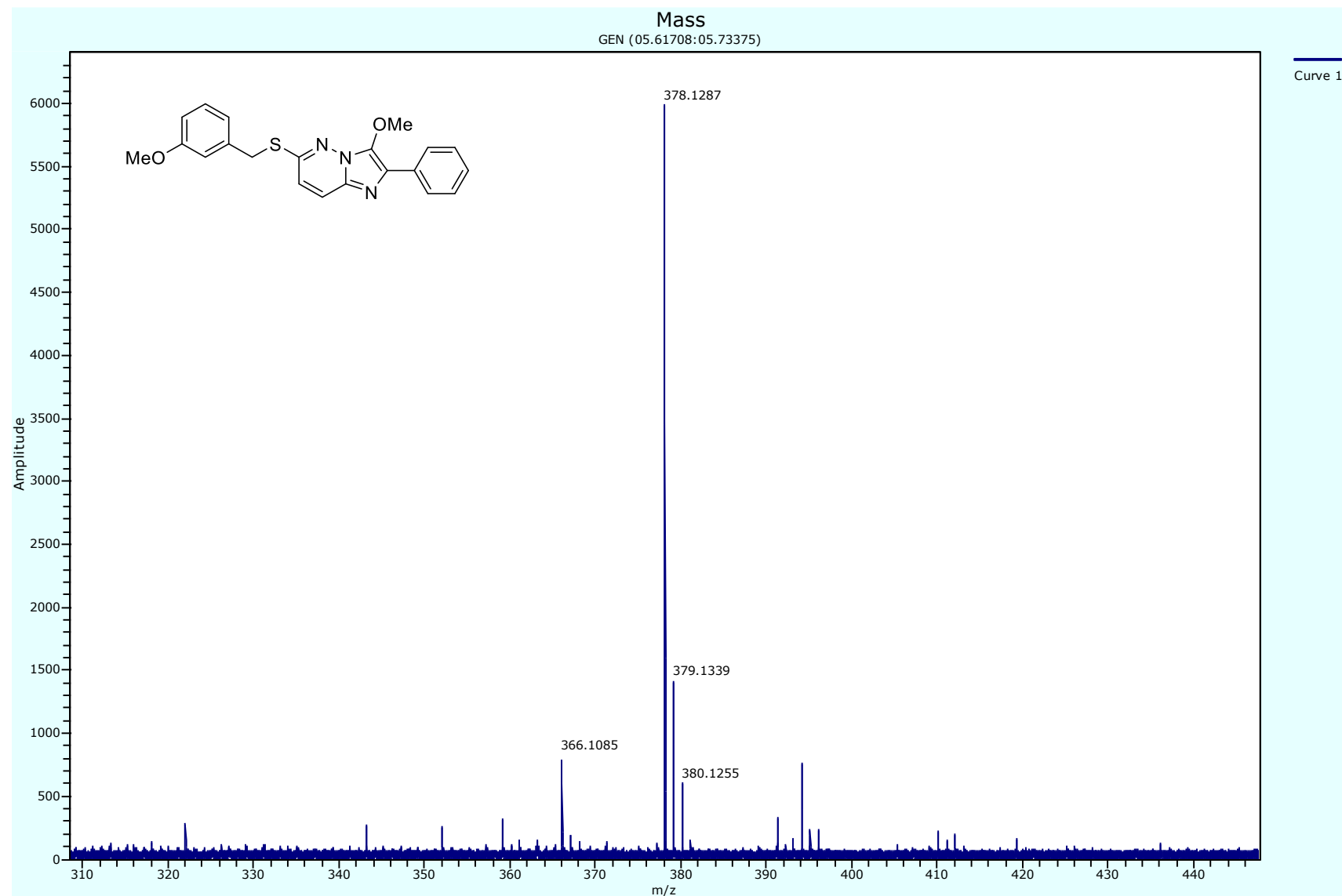
Peak Results					
	RT	Area	% Area	Height	Base Peak (m/z)
1	2.372	1123	0.22	773	489.42
2	2.859	8775	1.76	6578	394.21
3	3.017	5345	1.07	4110	396.12
4	3.188	2818	0.56	1866	409.97
5	3.547	479676	96.05	312825	378.15
6	4.019	1649	0.33	1258	214.19



Chemical Formula: C₂₁H₁₉N₃O₂S
 Exact Mass: 377.12
 Molecular Weight: 377.46
 m/z: 377.12 (100.0%), 378.12 (22.7%), 379.12 (4.5%),
 379.13 (2.5%), 378.12 (1.1%), 380.12 (1.0%)

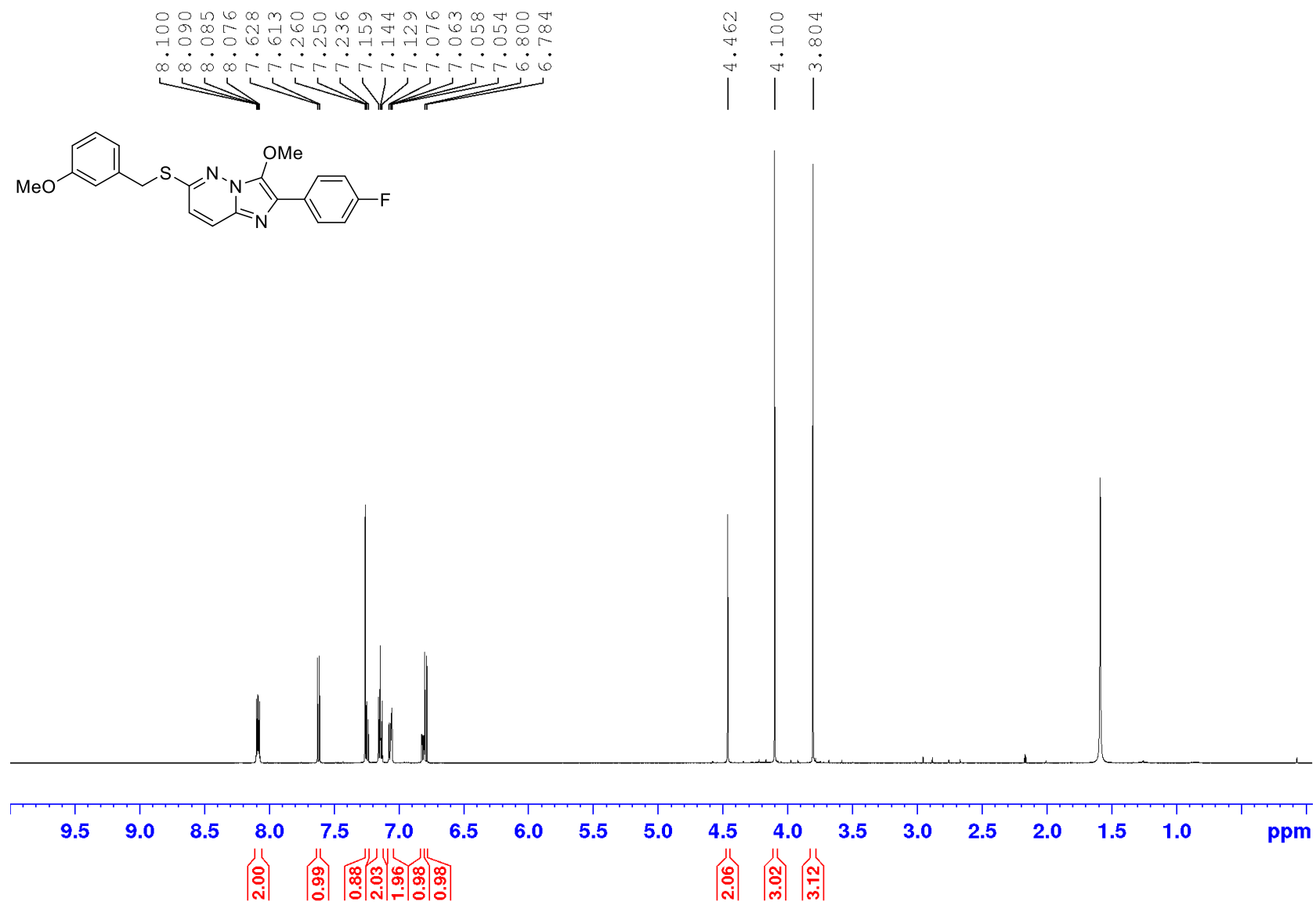
Appendices

HRMS (APCI) spectrum of **64** $[M+H]^+$



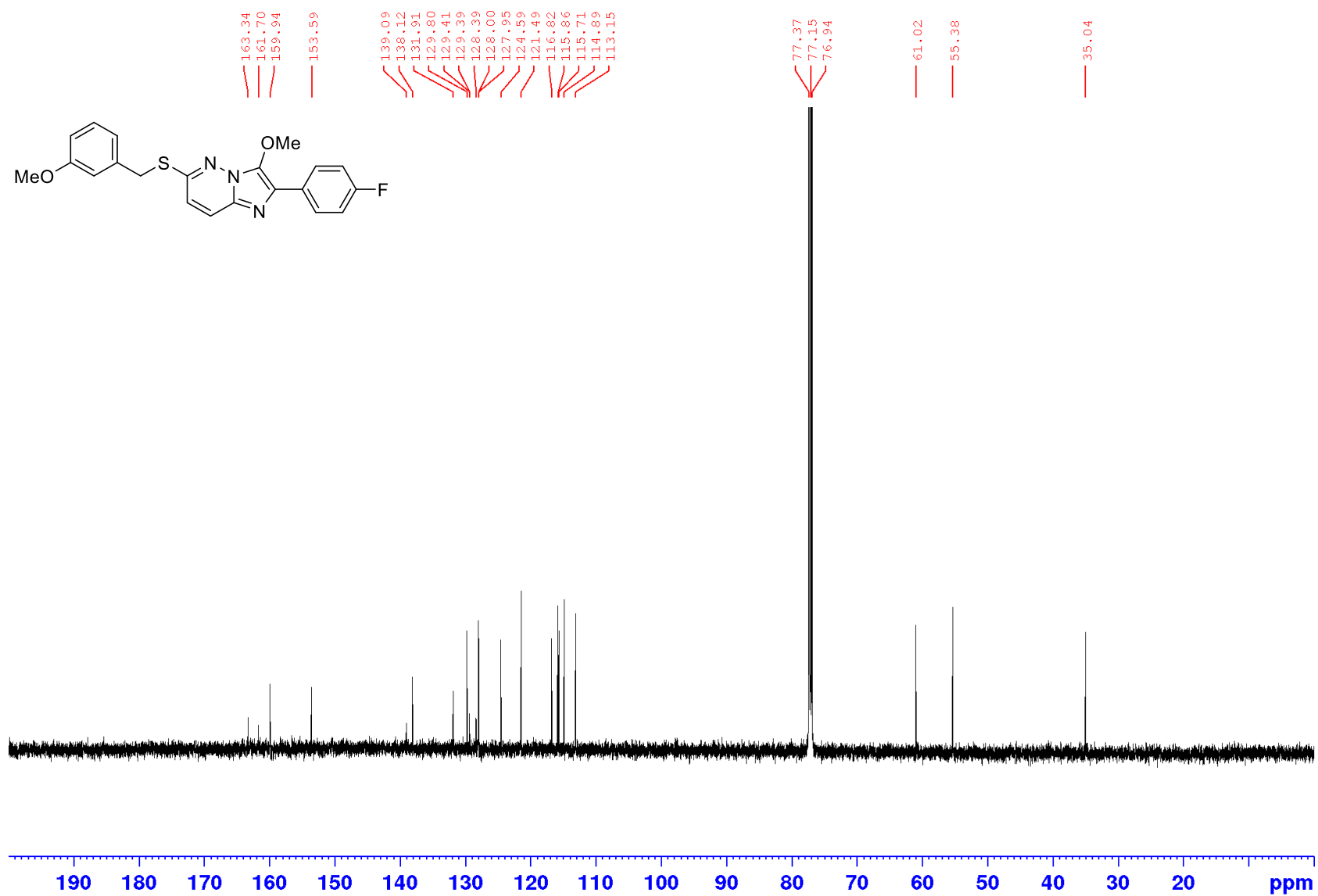
Appendices

¹H NMR spectrum of **65** (600 MHz; CDCl₃)



Appendices

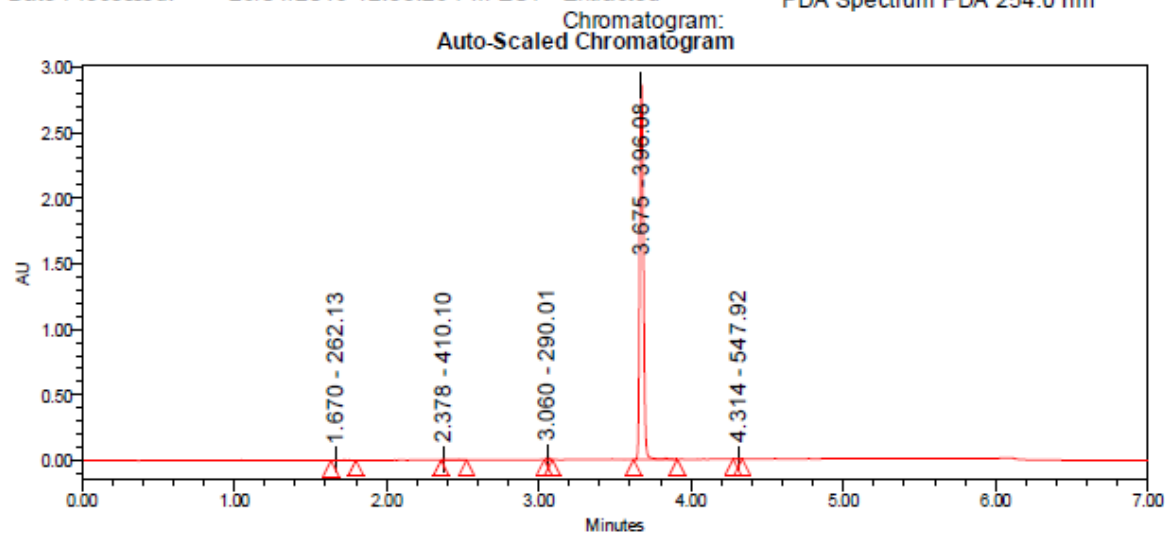
¹³C NMR spectrum of **65** (150 MHz; CDCl₃)



Appendices

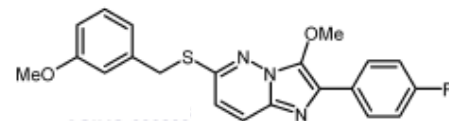
LC-MS chromatogram of 65 [M+H]⁺

Instrument: Waters Acquity iClass
 PDA and QDa detectors
 Vial: 1:A,7
 Acquired By: System
 Injection #: 1
 Sample Set Name: MK_26_April2019
 Injection Volume: 0.30 ul
 Run Time: 7.0 Minutes
 Acquisition Method: 95% A1 to 100% B1
 Mobile Phase: A1: 100% H2O / 0.1% FA
 B1: 100% ACN / 0.1% FA
 Date Acquired: 26/04/2019 12:24:31 PM EST
 Date Processed: 26/04/2019 12:38:26 PM EST
 Extracted: PDA Spectrum PDA 254.0 nm



Peak Results

	RT	Area	% Area	Height	Base Peak (m/z)
1	1.670	8793	0.18	2633	262.13
2	2.378	10927	0.22	4551	410.10
3	3.060	24859	0.51	19590	290.01
4	3.675	4842388	98.95	2885067	396.08
5	4.314	6795	0.14	5901	547.92



Chemical Formula: C₂₁H₁₈FN₃O₂S

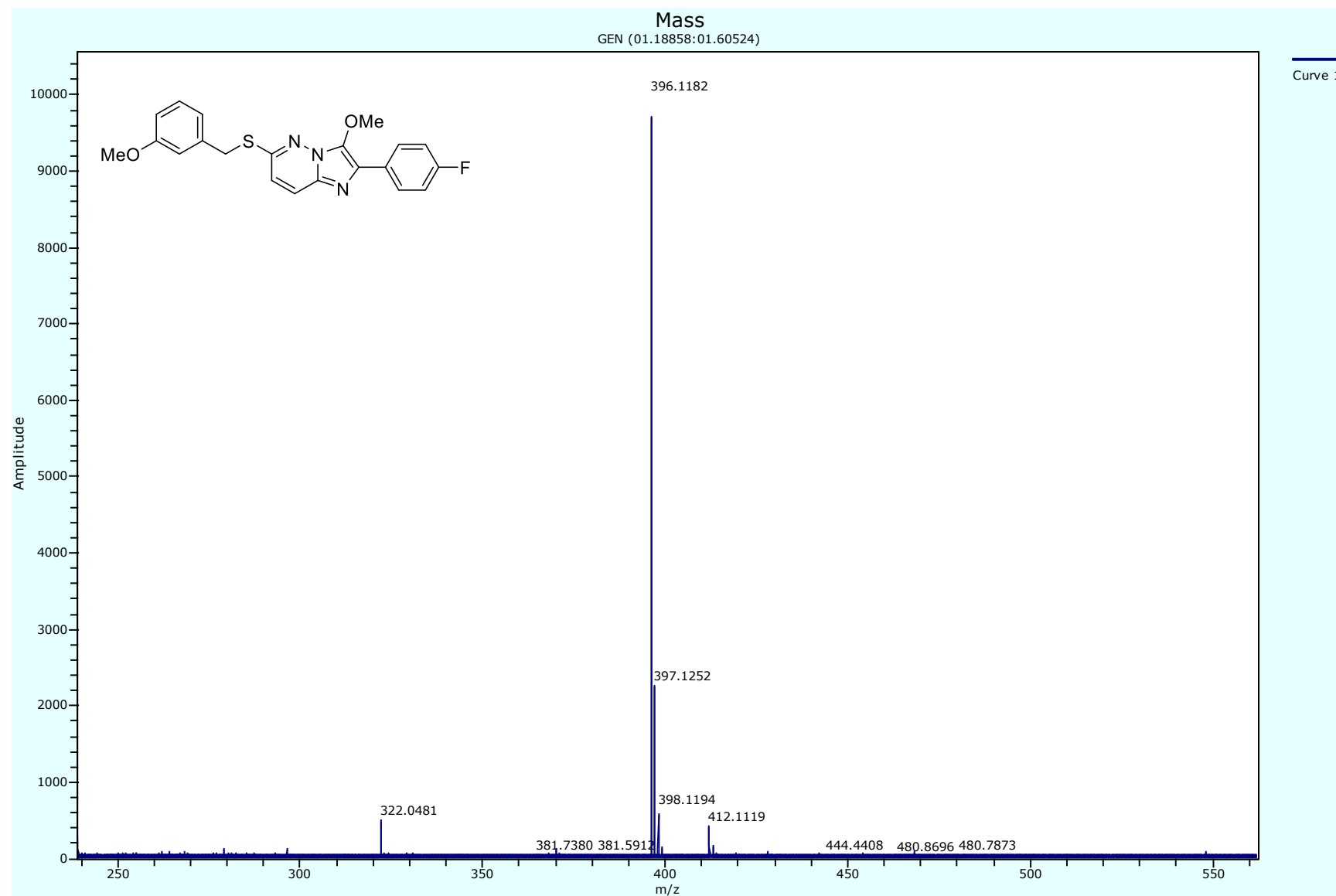
Exact Mass: 395.11

Molecular Weight: 395.45

m/z: 395.11 (100.0%), 396.11 (22.7%), 397.11 (4.5%),
 397.12 (2.5%), 396.11 (1.1%), 398.11 (1.0%)

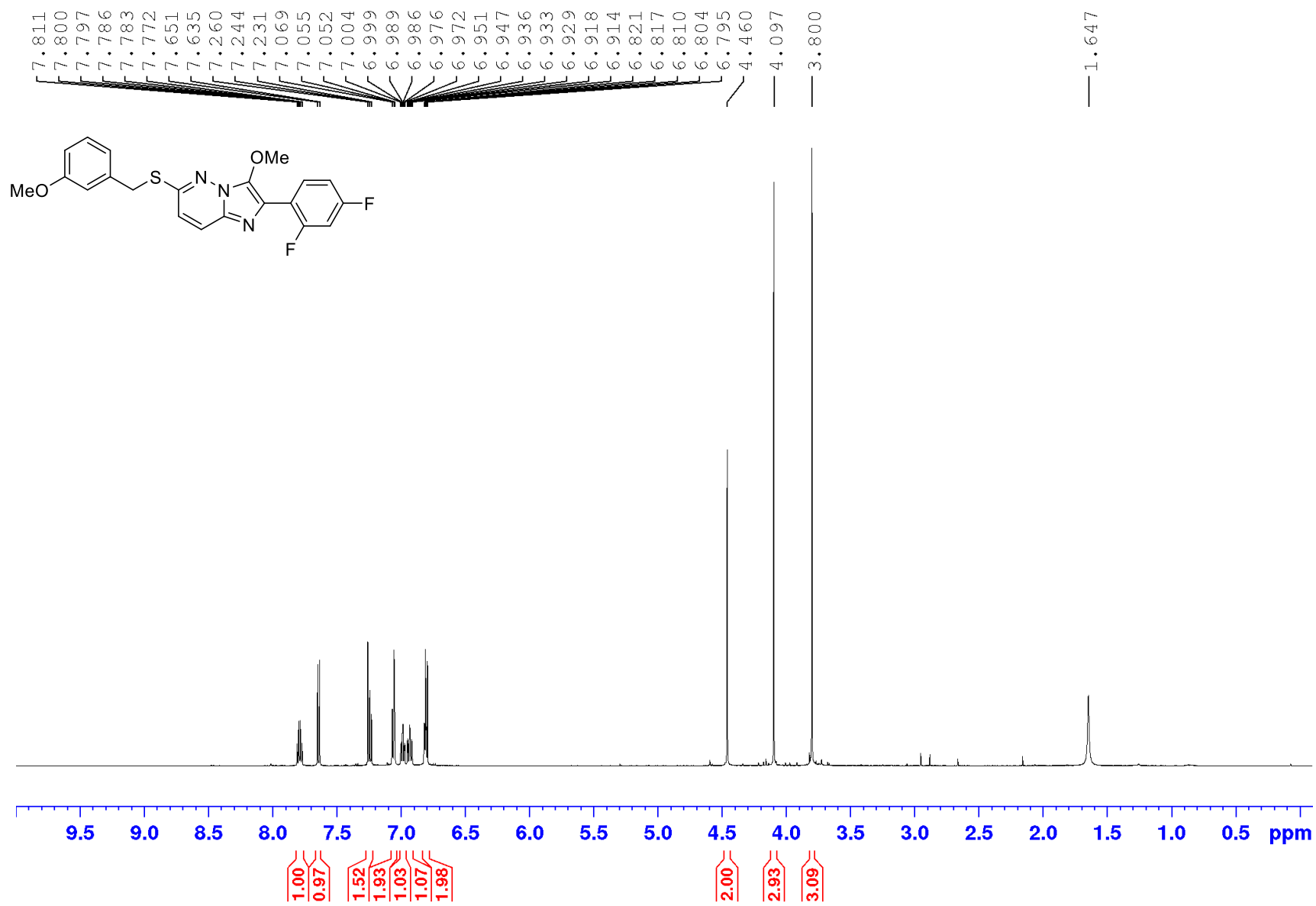
Appendices

HRMS (APCI) spectrum of **65** $[M+H]^+$



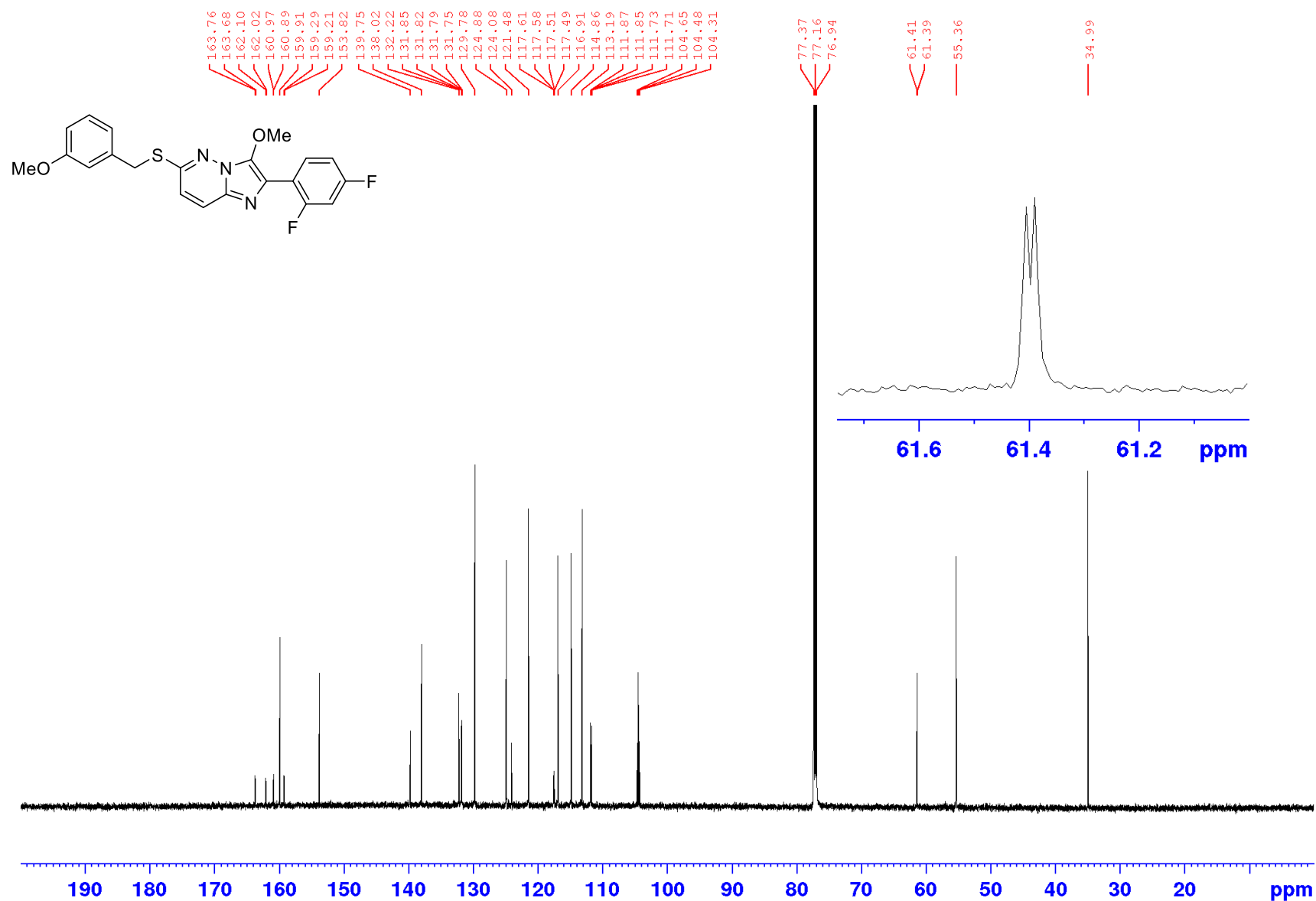
Appendices

¹H NMR spectrum of **66** (600 MHz; CDCl₃)



Appendices

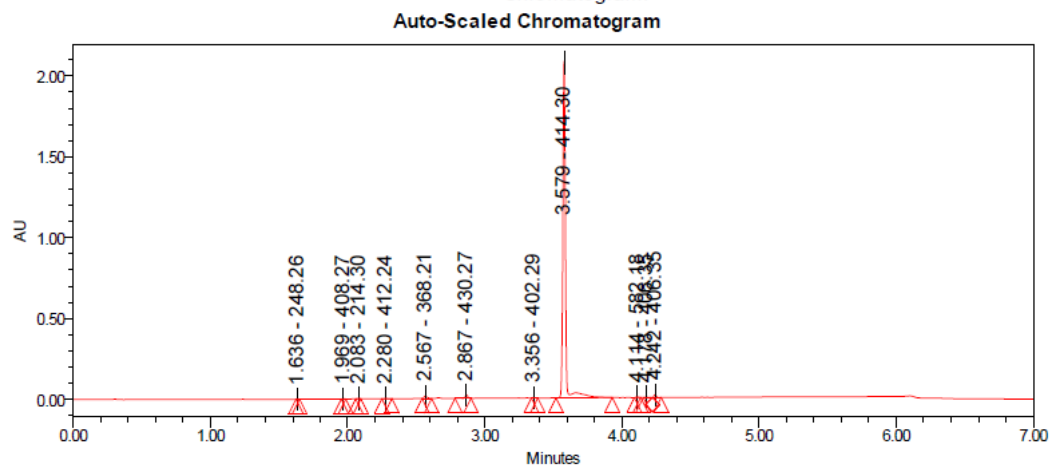
¹³C NMR spectrum of **66** (150 MHz; CDCl₃)



Appendices

LC-MS chromatogram of 66 [M+H]⁺

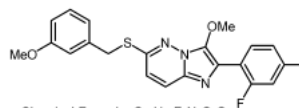
Instrument: Waters Acquity iClass
 PDA and QDa detectors
 Vial: 1:D,8
 Acquired By: System
 Injection #: 1
 Sample Set Name: MK_08_November2017
 Injection Volume: 0.20 ul
 Run Time: 7.0 Minutes
 Acquisition Method: 95% A1 to 100% B1 POSNEG
 Mobile Phase: A1: 100% H2O / 0.1% FA
 B1: 100% ACN / 0.1% FA
 Date Acquired: 8/11/2017 5:52:00 PM EST
 Date Processed: 8/11/2017 6:09:42 PM EST
 Extracted: PDA Spectrum PDA 254.0 nm
 Chromatogram:



Peak Results

	RT	Area	% Area	Height	Base Peak (m/z)
1	1.636	1927	0.07	2227	248.26
2	1.969	2336	0.08	2315	408.27
3	2.083	2496	0.09	2252	214.30
4	2.280	3156	0.11	1936	412.24
5	2.567	22197	0.76	15773	368.21
6	2.867	28915	1.00	21400	430.27
7	3.356	4397	0.15	4003	402.29
8	3.579	2808824	96.73	2091542	414.30
9	4.114	3871	0.13	3430	582.18

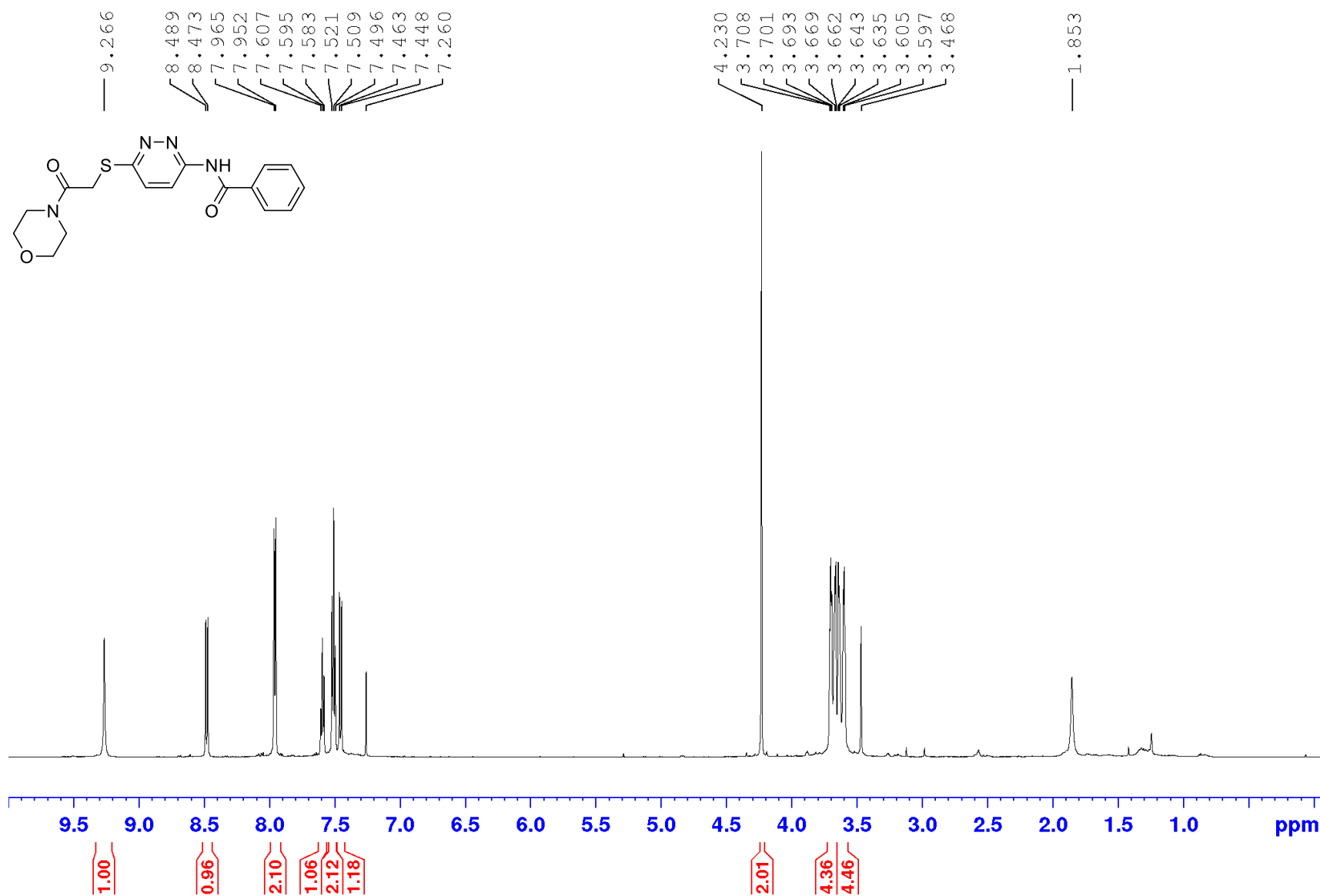
	RT	Area	% Area	Height	Base Peak (m/z)
10	4.178	5843	0.20	3565	406.35
11	4.242	19703	0.68	17136	406.35



Chemical Formula: C₂₁H₁₇F₂N₃O₂S
 Exact Mass: 413.1010
 Molecular Weight: 413.4428
 m/z: 413.1010 (100.0%), 414.1043 (22.7%),
 415.0968 (4.5%), 415.1077 (2.5%),
 414.0980 (1.1%), 416.1001 (1.0%)

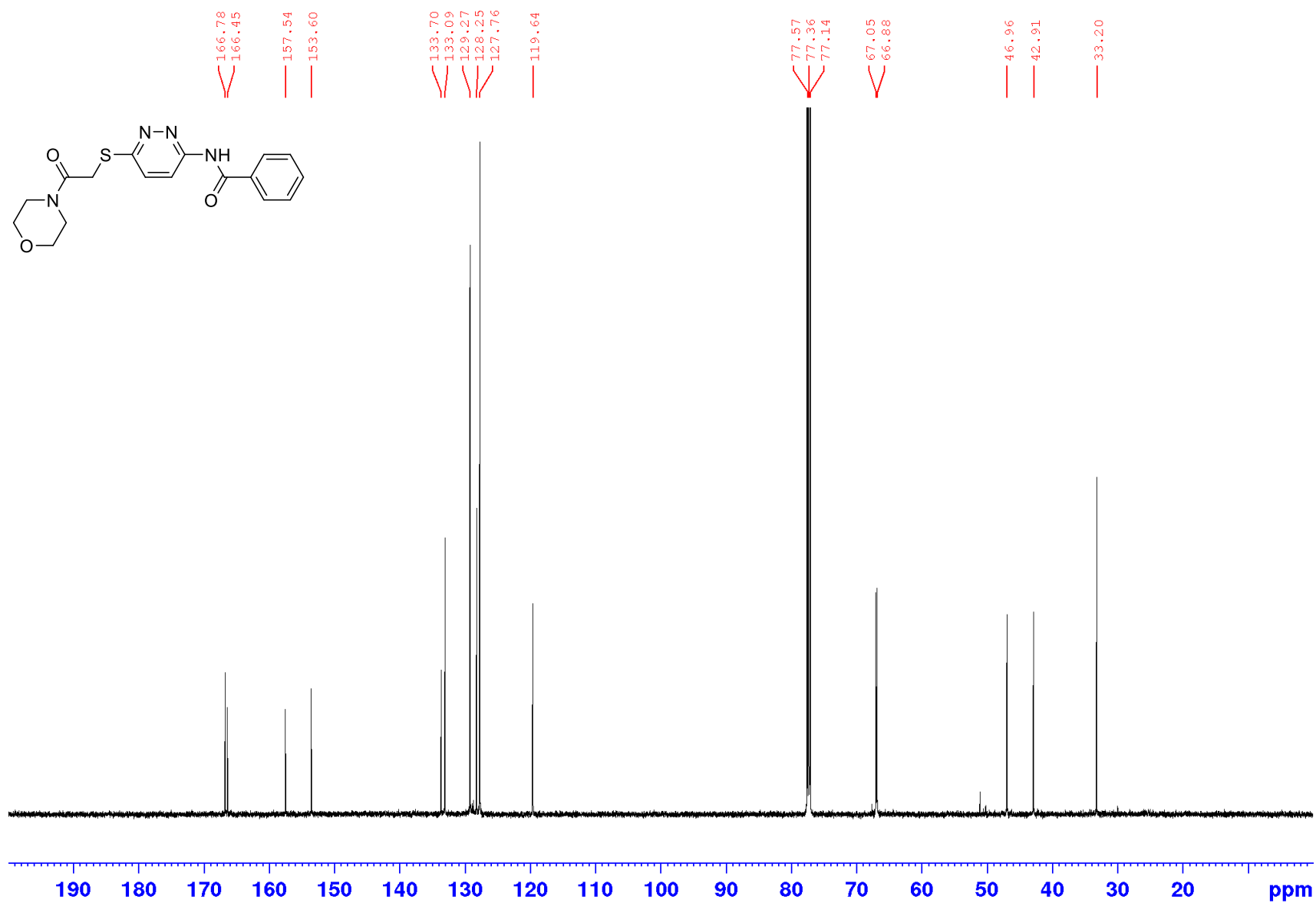
Appendices

¹H NMR spectrum of **142** (600 MHz; CDCl₃)



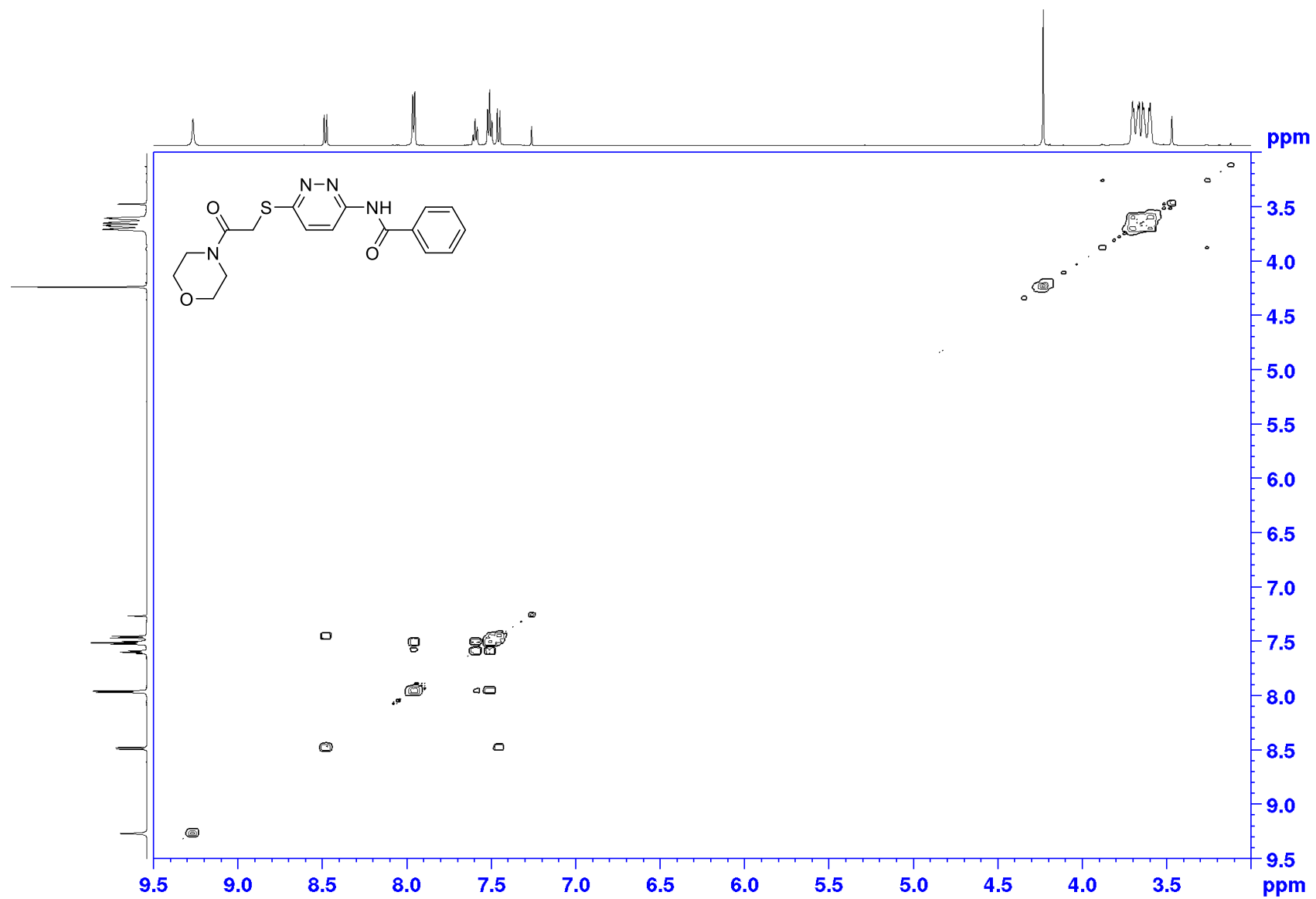
Appendices

^{13}C NMR spectrum of **142** (150 MHz; CDCl_3)



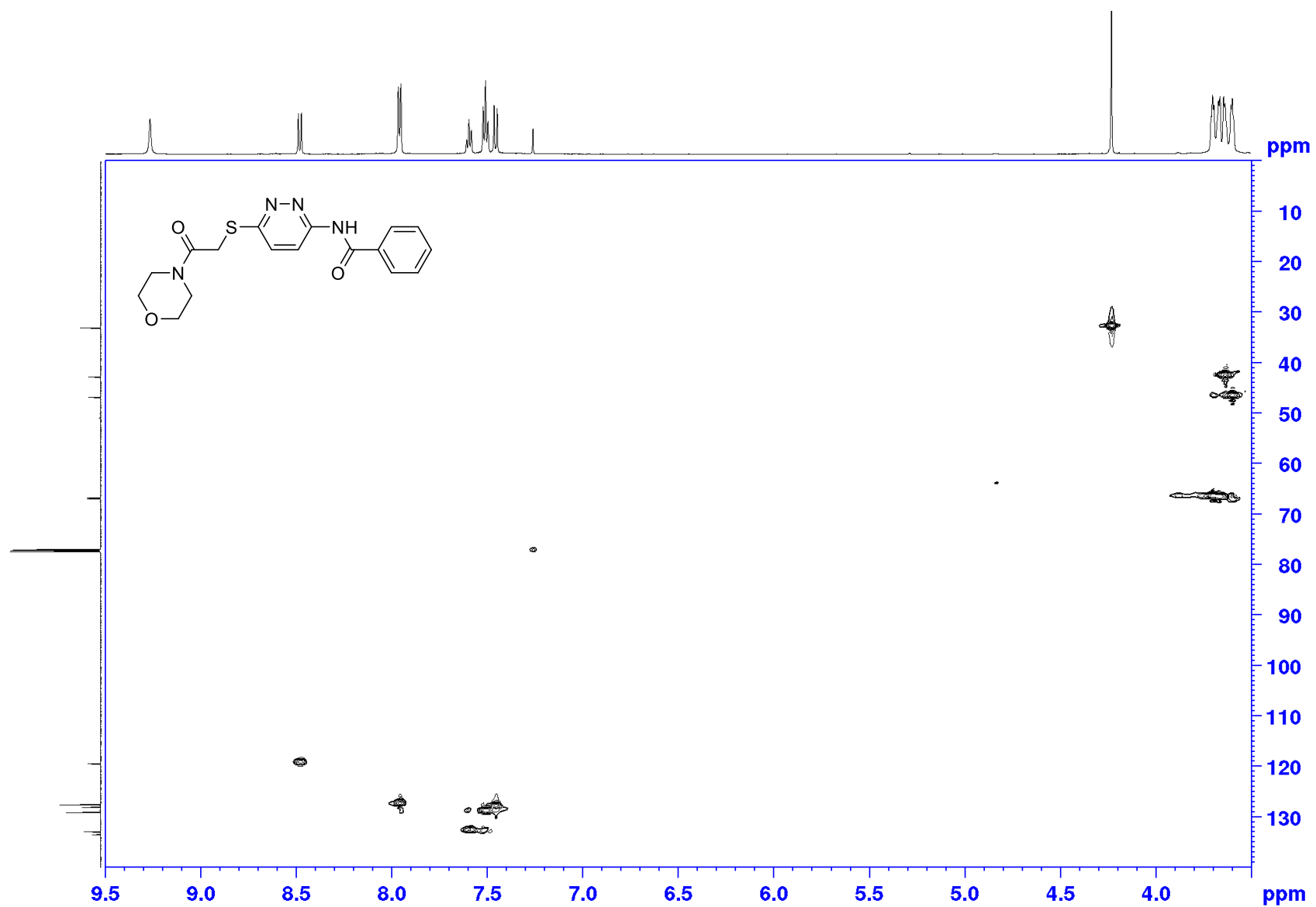
Appendices

COSY spectrum of **142** (600 x 600 MHz; CDCl₃)



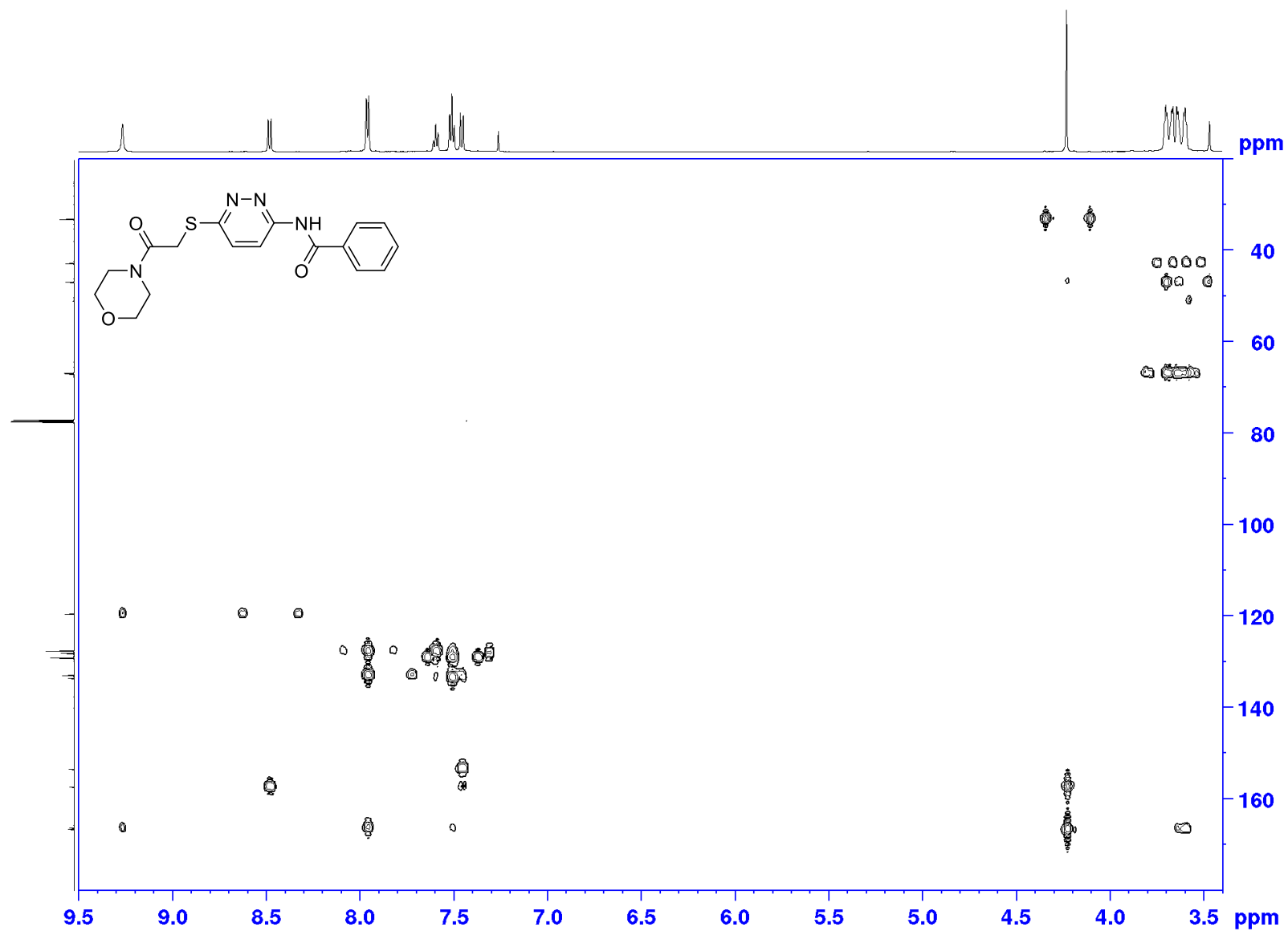
Appendices

HMQC spectrum of **142** (400 x 100 MHz; CDCl₃)



Appendices

HMBC spectrum of **142** (400 x 100 MHz; CDCl₃)

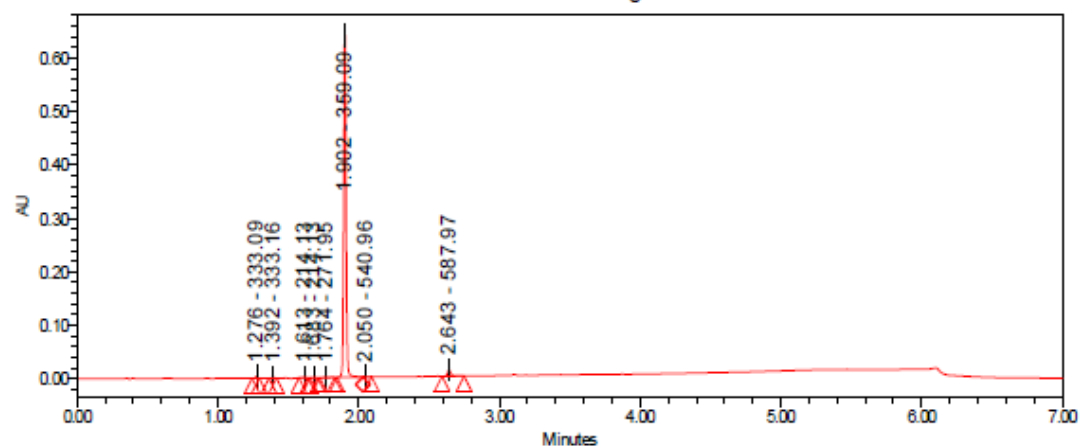


Appendices

LC-MS chromatogram of **142** [M+H]⁺

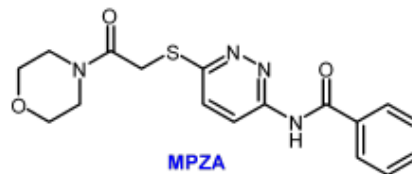
Sample Name:	CF MPZA	Instrument:	Waters Acquity iClass PDA and QDa detectors
Vial:	1:B,8	Acquired By:	System
Injection #:	1	Sample Set Name:	MK_26_April2019
Injection Volume:	0.30 ul	Acquisition Method:	95% A1 to 100% B1
Run Time:	7.0 Minutes	Mobile Phase:	A1: 100% H2O / 0.1% FA B1: 100% ACN / 0.1% FA
Date Acquired:	26/04/2019 1:57:54 PM EST	Extracted	PDA Spectrum PDA 254.0 nm
Date Processed:	26/04/2019 2:39:53 PM EST	Chromatogram:	

Auto-Scaled Chromatogram



Peak Results

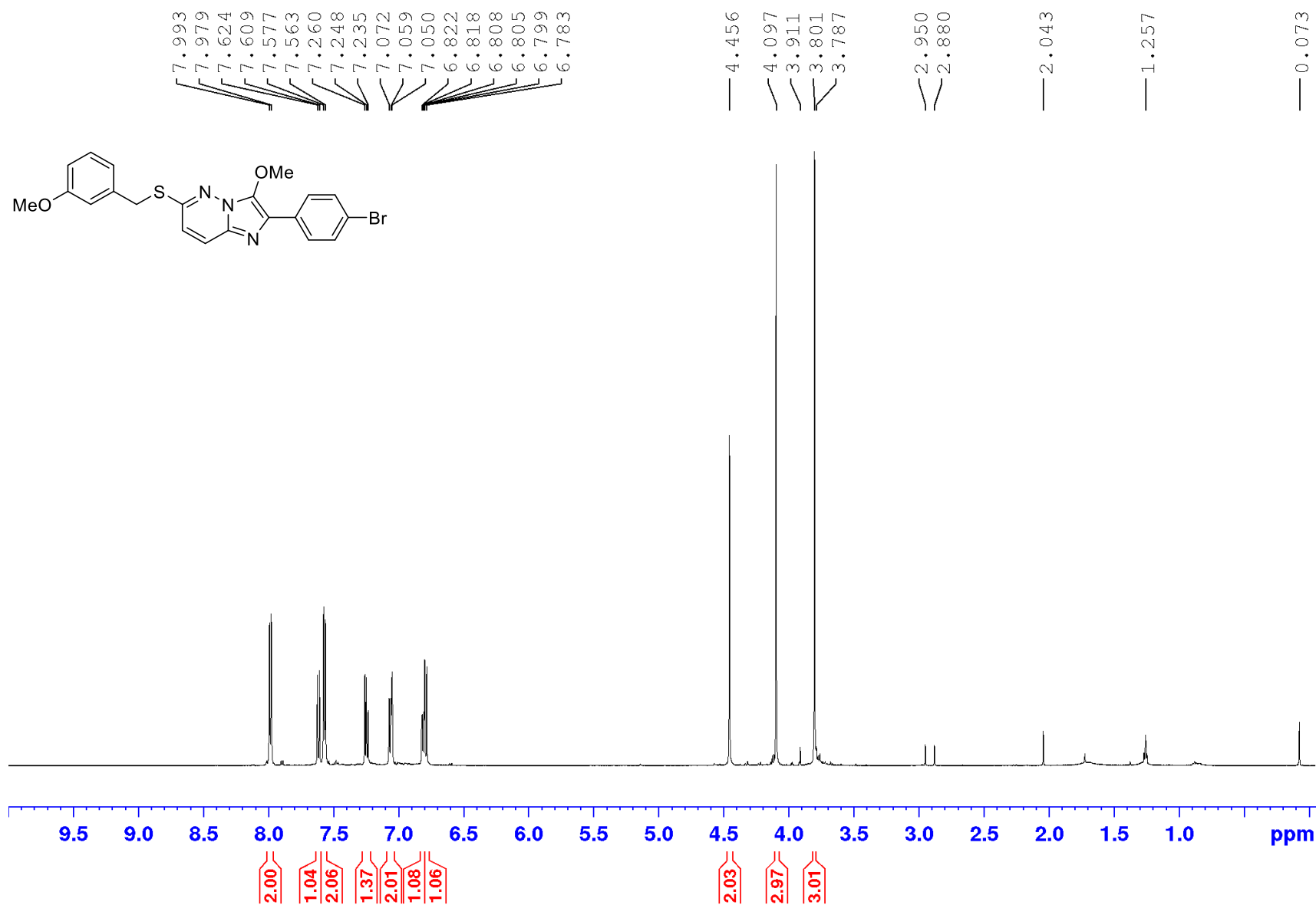
	RT	Area	% Area	Height	Base Peak (m/z)
1	1.276	3403	0.44	3353	333.09
2	1.392	1594	0.21	1517	333.16
3	1.613	1037	0.13	991	214.13
4	1.683	376	0.05	277	214.13
5	1.764	1422	0.18	947	271.95
6	1.902	746163	96.23	644298	359.09
7	2.050	1492	0.19	942	540.96
8	2.643	19942	2.57	11940	587.97



Chemical Formula: C₁₇H₁₈N₄O₃S
 Exact Mass: 358.11
 Molecular Weight: 358.42
 m/z: 358.11 (100.0%), 359.11 (18.4%),
 360.11 (4.5%), 360.12 (1.6%), 359.11 (1.5%)

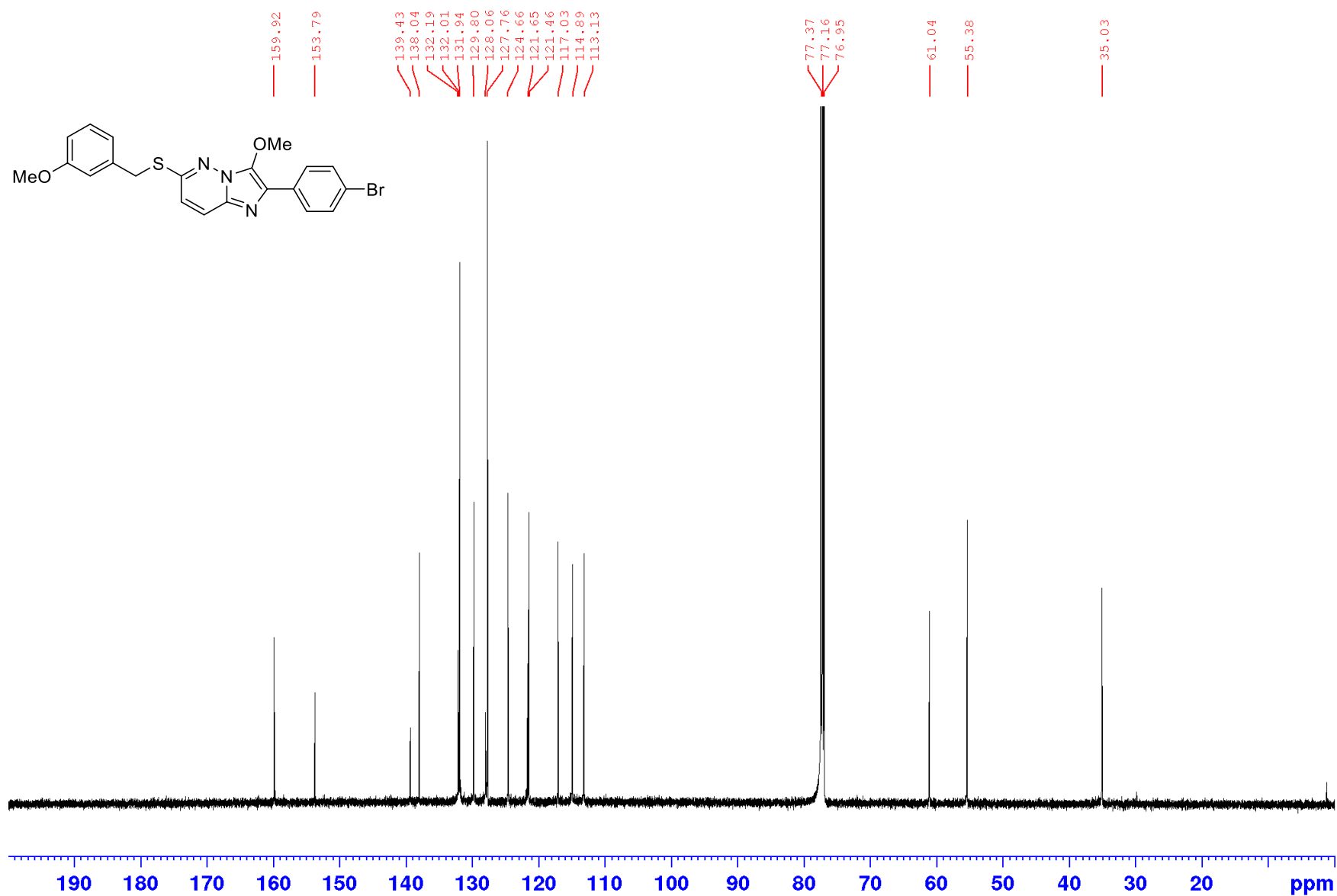
Appendices

¹H NMR spectrum of **144** (600 MHz; CDCl₃)



Appendices

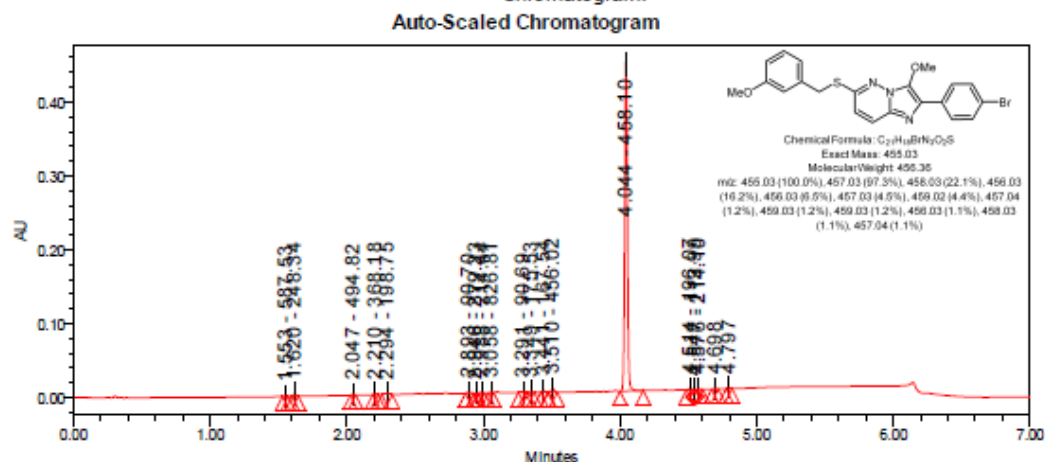
^{13}C NMR spectrum of **144** (150 MHz; CDCl_3)



Appendices

LC-MS chromatogram of **144** [M+H]⁺

<p>Vial: 1:C,6 Injection #: 1 Injection Volume: 0.20 ul Run Time: 7.0 Minutes Date Acquired: 30/01/2018 3:52:28 PM EST Date Processed: 30/01/2018 4:28:09 PM EST</p>	<p>Instrument: Waters Acquity iClass PDA and QDa detectors Acquired By: System Sample Set Name: KP_30_January2018 Acquisition Method: 95% A1 to 100% B1 POSNEG Mobile Phase: A1: 100% H2O / 0.1% FA B1: 100% ACN / 0.1% FA Extracted Chromatogram: PDA Spectrum PDA 254.0 nm</p>
---	---



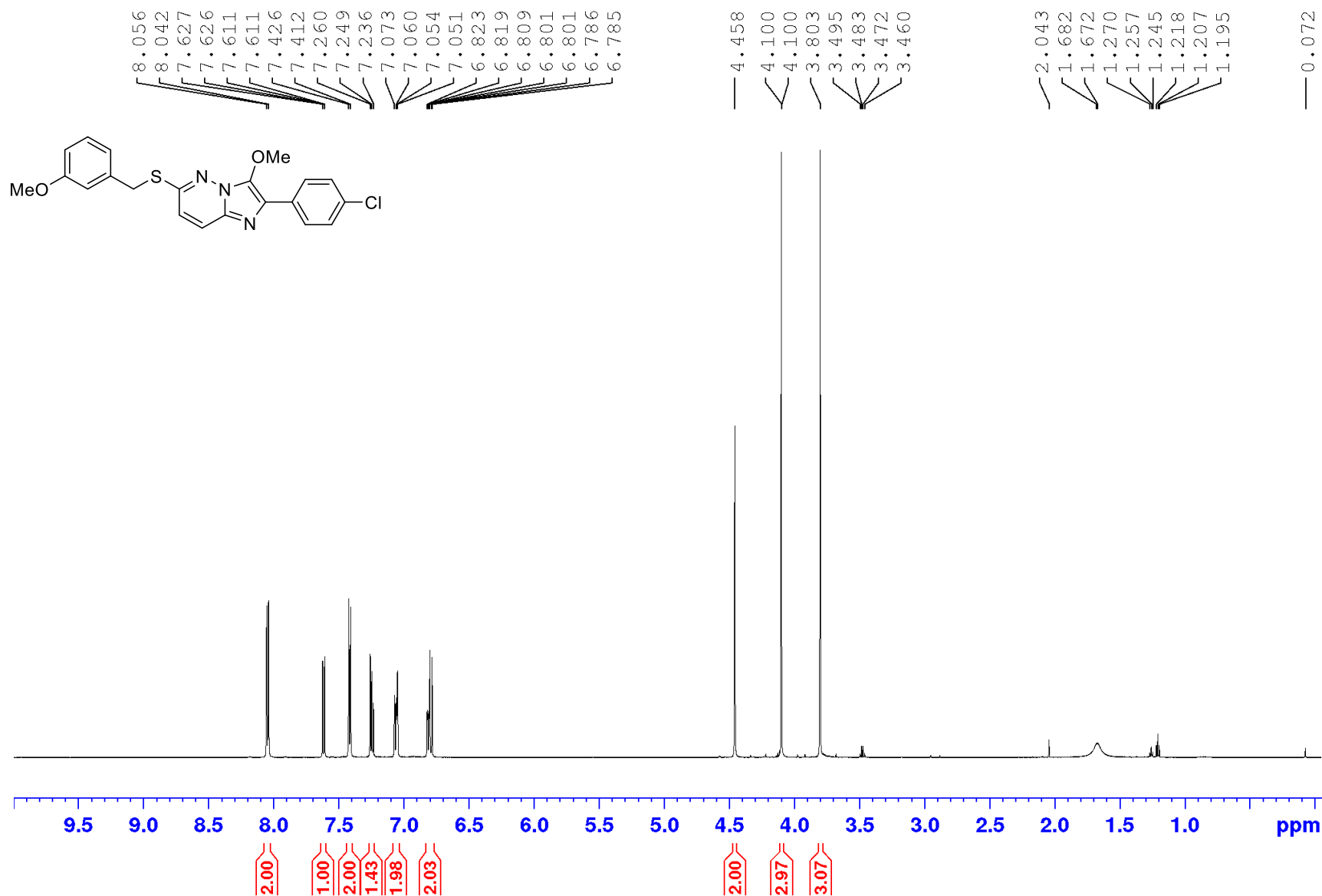
Peak Results

	RT	Area	% Area	Height	Base Peak (m/z)
1	1.553	593	0.09	398	587.53
2	1.620	4001	0.63	3360	248.34
3	2.047	1222	0.19	1096	494.82
4	2.210	1737	0.27	1559	368.18
5	2.294	2486	0.39	1053	198.75
6	2.893	1957	0.31	1320	90.70
7	2.946	152	0.02	185	279.23
8	2.988	1460	0.23	1126	214.44
9	3.058	907	0.14	766	826.81

	RT	Area	% Area	Height	Base Peak (m/z)
10	3.291	389	0.06	210	90.69
11	3.349	856	0.14	700	175.53
12	3.441	2680	0.42	1957	167.54
13	3.510	6284	0.99	4837	456.02
14	4.044	601381	95.01	445705	458.10
15	4.514	2827	0.45	1967	196.07
16	4.547	587	0.09	513	113.99
17	4.576	1071	0.17	840	214.10
18	4.698	652	0.10	503	

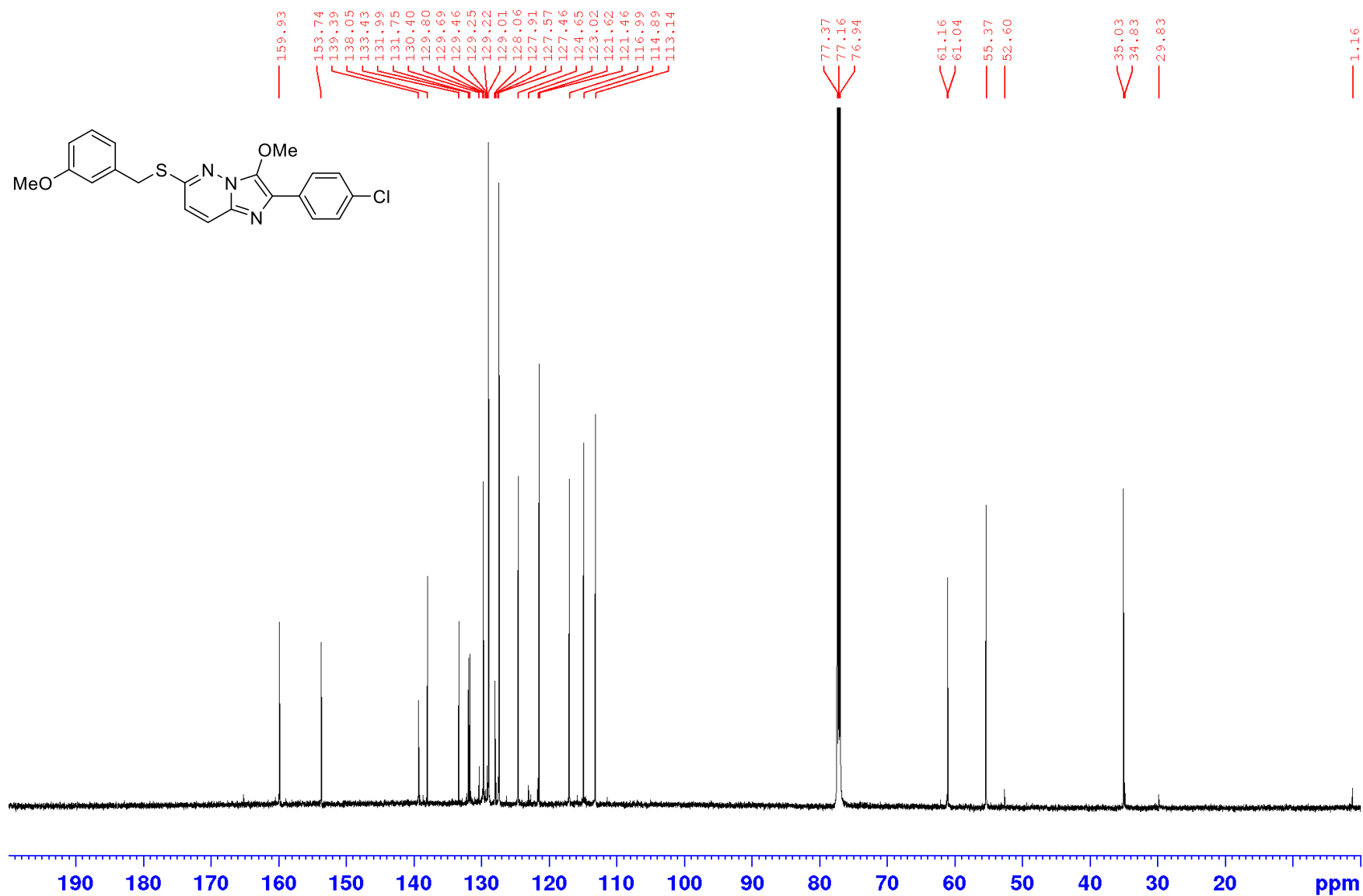
Appendices

¹H NMR spectrum of **145** (600 MHz; CDCl₃)



Appendices

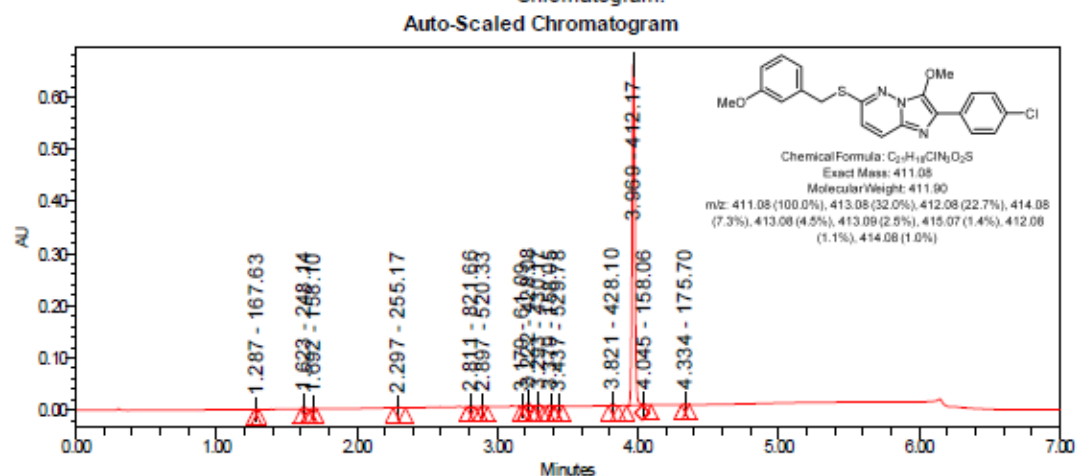
^{13}C NMR spectrum of **145** (150 MHz; CDCl_3)



Appendices

LC-MS chromatogram of **145** [M+H]⁺

Vial:	1:C,5	Instrument:	Waters Acquity iClass PDA and QDa detectors
Injection #:	1	Acquired By:	System
Injection Volume:	0.20 ul	Sample Set Name:	KP_30_January2018
Run Time:	7.0 Minutes	Acquisition Method:	95% A1 to 100% B1 POSNEG
Date Acquired:	30/01/2018 3:44:02 PM EST	Mobile Phase:	A1: 100% H2O / 0.1% FA B1: 100% ACN / 0.1% FA
Date Processed:	30/01/2018 4:26:15 PM EST	Extracted Chromatogram:	PDA Spectrum PDA 254.0 nm



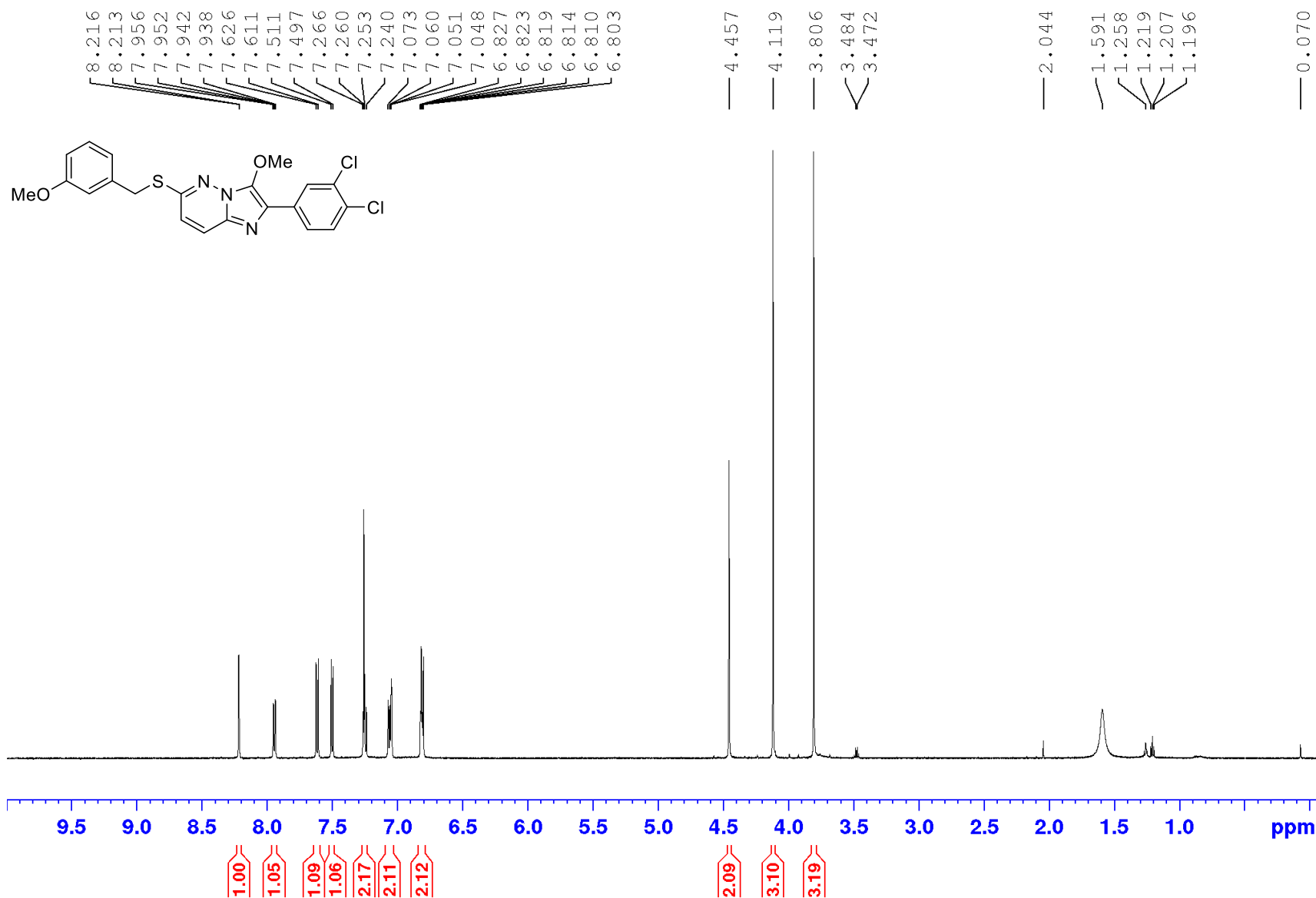
Peak Results

	RT	Area	% Area	Height	Base Peak (m/z)
1	1.287	737	0.08	730	167.63
2	1.623	7050	0.74	6004	248.14
3	1.682	1475	0.16	1361	158.10
4	2.297	2298	0.24	754	255.17
5	2.811	3870	0.41	2771	821.66
6	2.897	1882	0.20	1247	520.33
7	3.179	689	0.07	632	61.09
8	3.222	11018	1.16	8719	428.08
9	3.268	5930	0.62	4633	430.17

	RT	Area	% Area	Height	Base Peak (m/z)
10	3.379	3601	0.37	2778	158.05
11	3.437	2630	0.28	1783	529.78
12	3.821	6809	0.72	4802	428.10
13	3.969	895611	94.24	658811	412.17
14	4.045	4427	0.47	2425	158.06
15	4.334	2398	0.25	1755	175.70

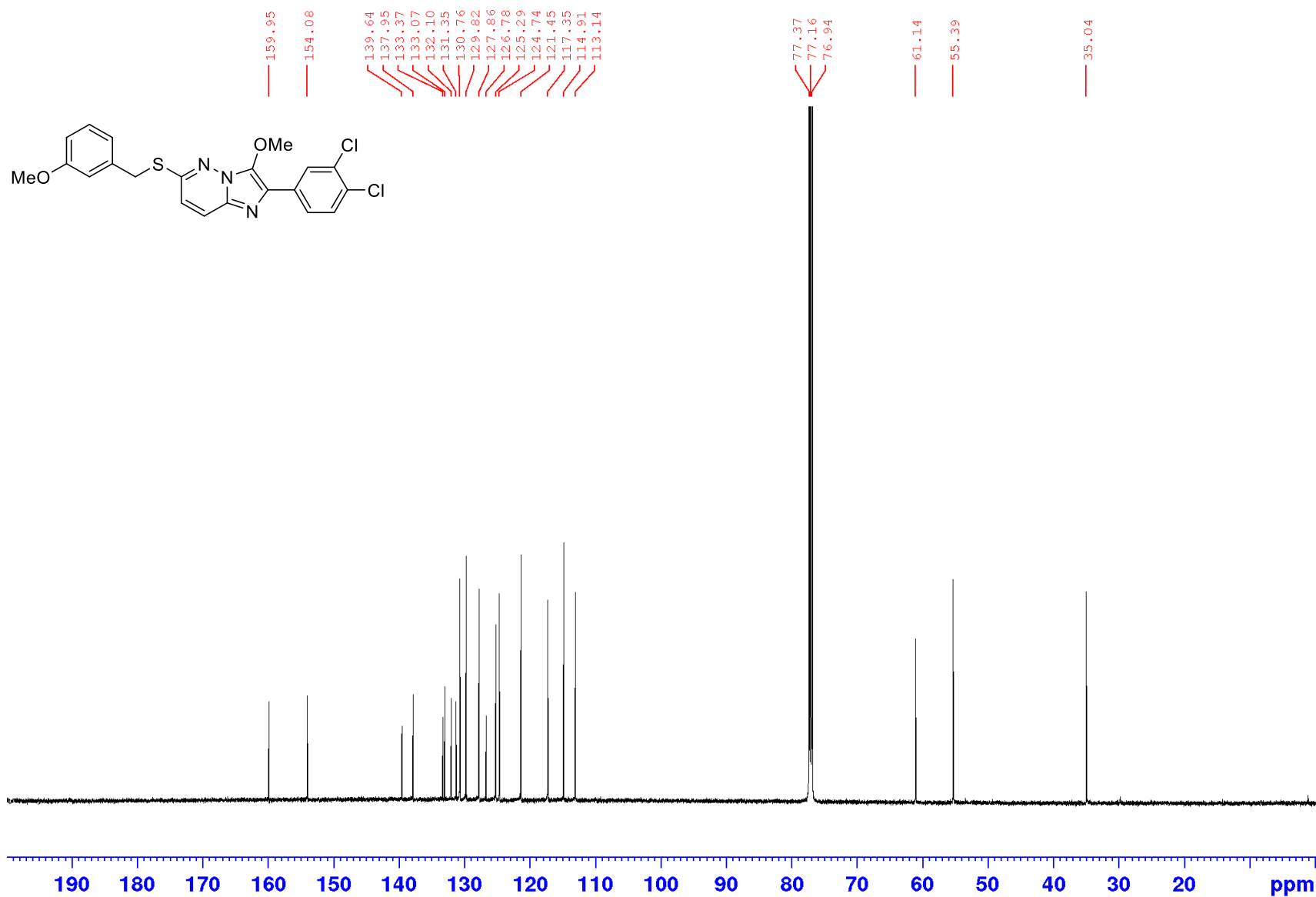
Appendices

¹H NMR spectrum of **146** (600 MHz; CDCl₃)



Appendices

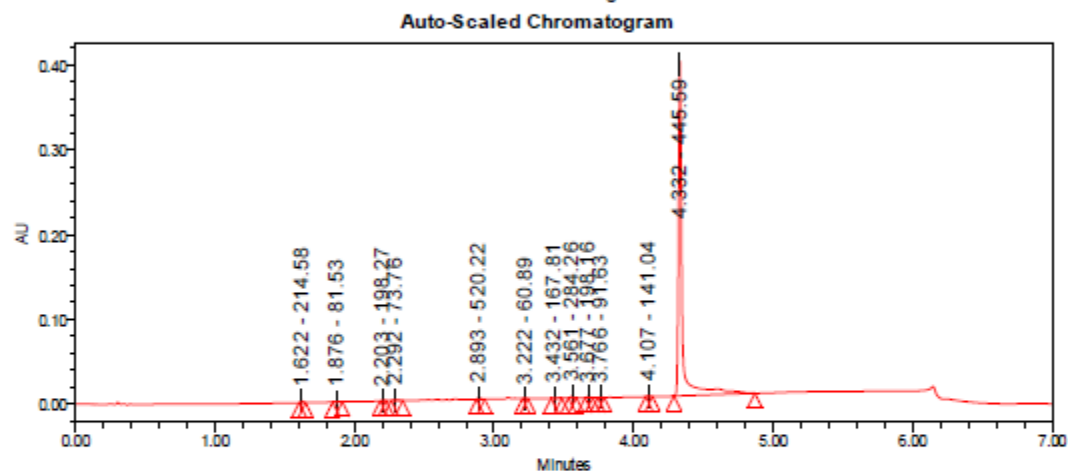
^{13}C NMR spectrum of **146** (150 MHz; CDCl_3)



Appendices

LC-MS chromatogram of **146** [M+H]⁺

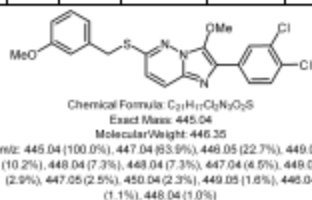
Vial:	1:C,4	Instrument:	Waters Acquity iClass PDA and QDa detectors
Injection #:	1	Acquired By:	System
Injection Volume:	0.20 ul	Sample Set Name:	KP_30_January2018
Run Time:	7.0 Minutes	Acquisition Method:	95% A1 to 100% B1 POSNEG
Date Acquired:	30/01/2018 3:35:35 PM EST	Mobile Phase:	A1: 100% H2O / 0.1% FA B1: 100% ACN / 0.1% FA
Date Processed:	30/01/2018 4:24:49 PM EST	Extracted Chromatogram:	PDA Spectrum PDA 254.0 nm



Peak Results

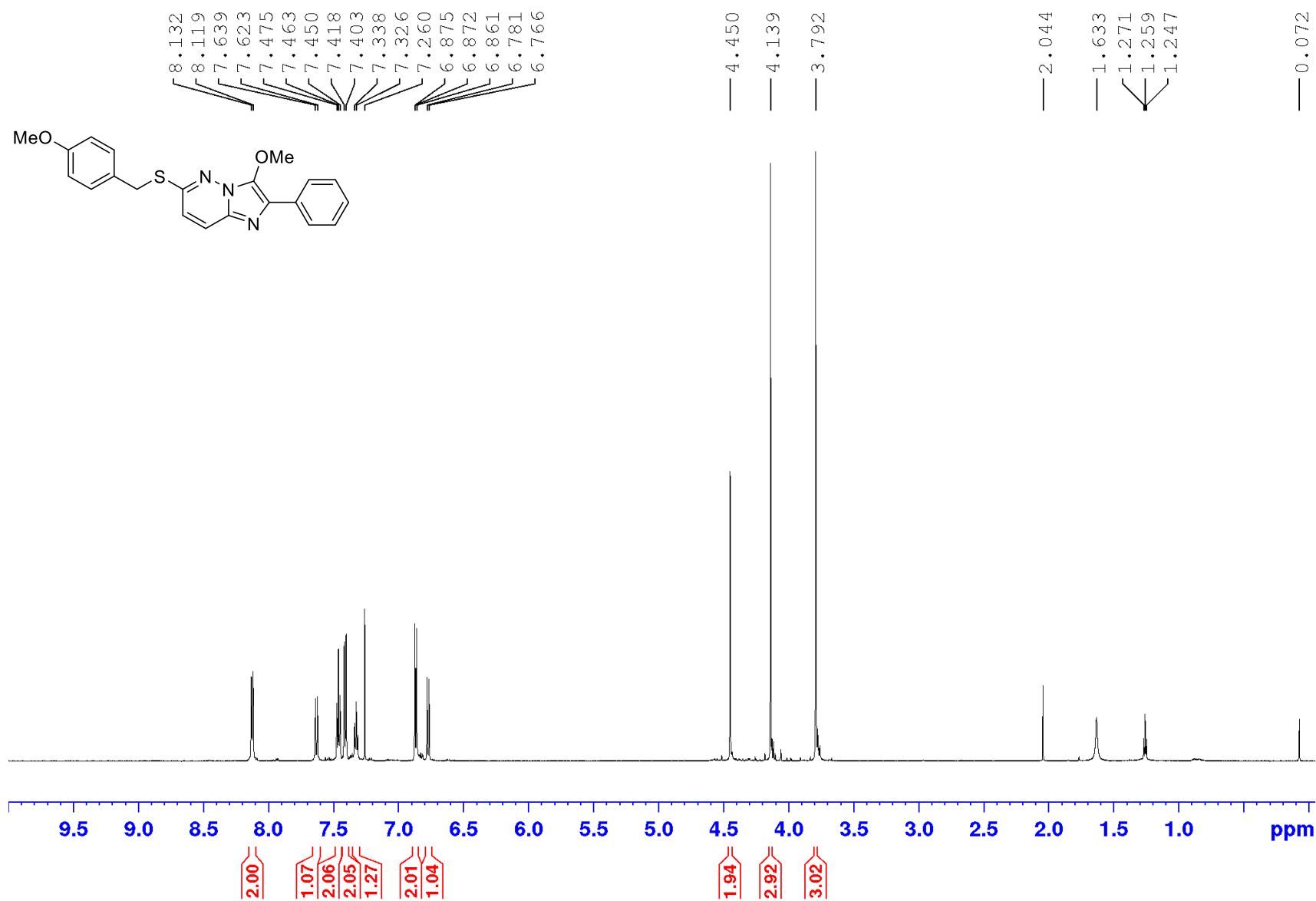
	RT	Area	% Area	Height	Base Peak (m/z)
1	1.622	2491	0.33	2106	214.58
2	1.876	983	0.13	432	81.53
3	2.203	535	0.07	360	198.27
4	2.292	1996	0.27	687	73.76
5	2.893	2719	0.36	1862	520.22
6	3.222	309	0.04	237	60.89
7	3.432	1129	0.15	512	167.81
8	3.561	3078	0.41	2058	284.26
9	3.677	2260	0.30	1564	198.16

	RT	Area	% Area	Height	Base Peak (m/z)
10	3.766	974	0.13	761	91.63
11	4.107	1335	0.18	1023	141.04
12	4.332	734860	97.63	394392	445.59



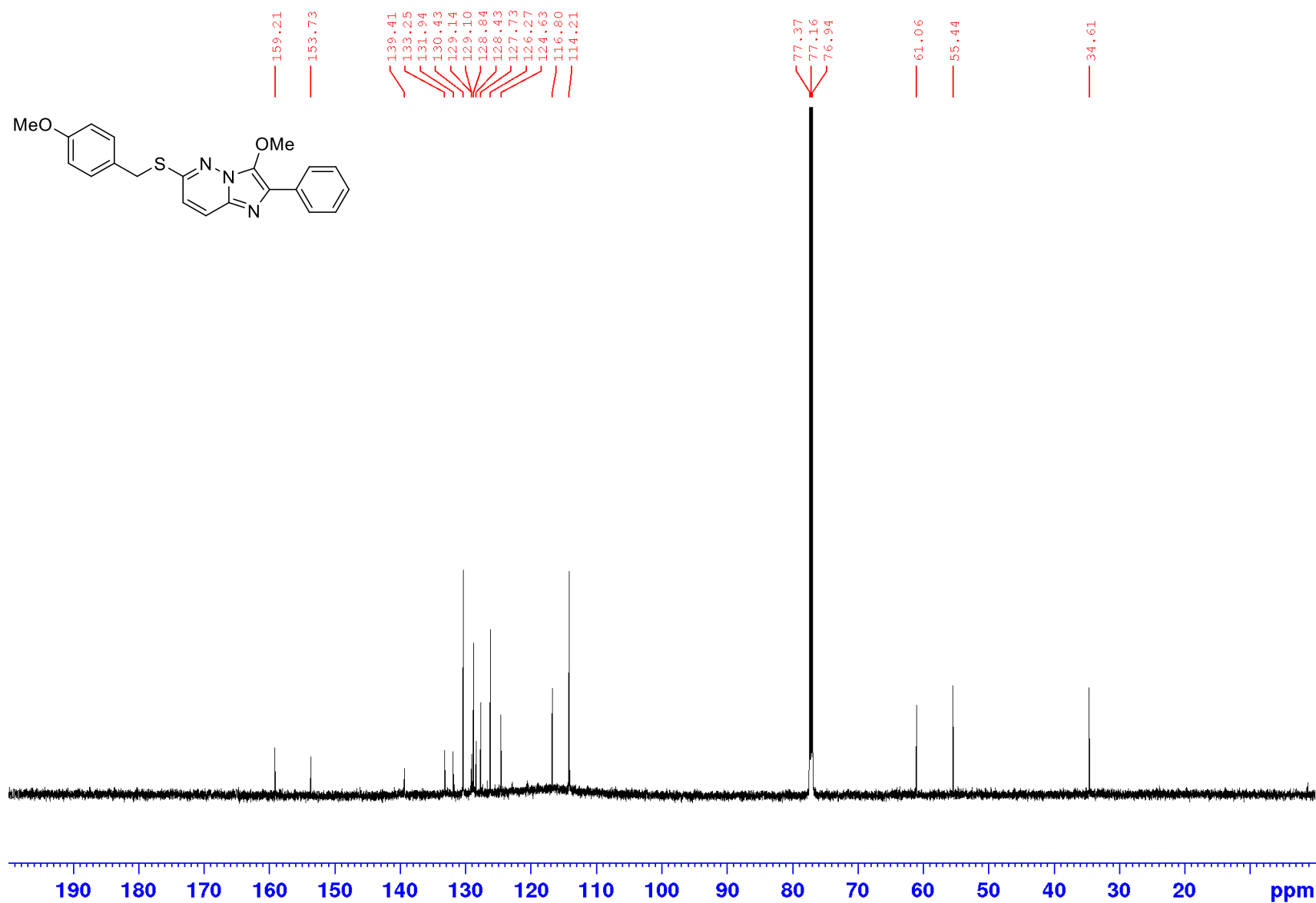
Appendices

¹H NMR spectrum of **147** (600 MHz; CDCl₃)



Appendices

^{13}C NMR spectrum of **147** (150 MHz; CDCl_3)

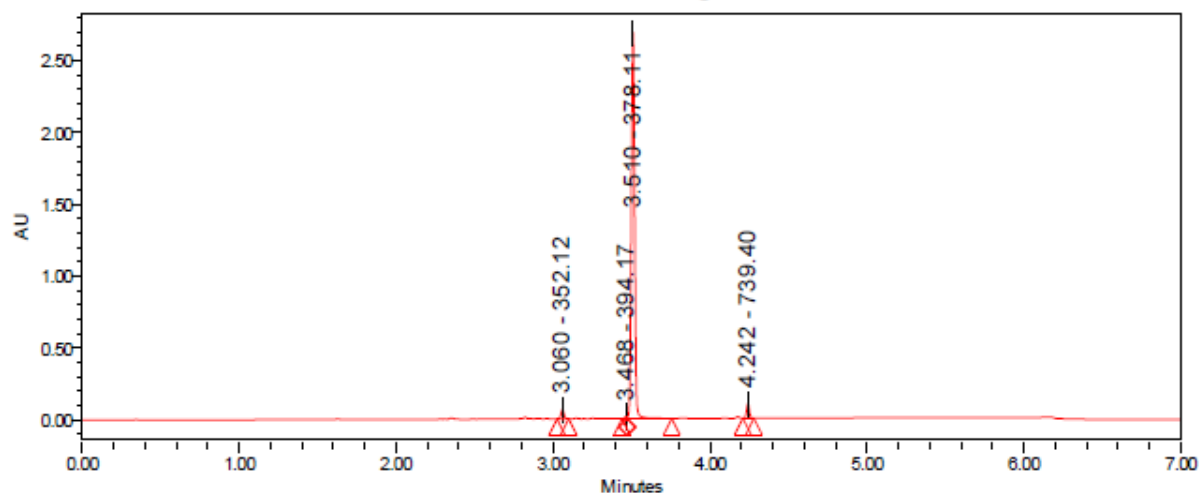


Appendices

LC-MS chromatogram of **147** [M+H]⁺

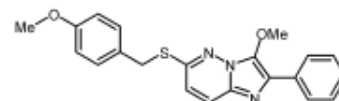
Sample Name:	R-IMPZ 12	Instrument:	Waters Acquity iClass PDA and QDa detectors
Vial:	1:A,6	Acquired By:	System
Injection #:	1	Sample Set Name:	PH_22_August2018
Injection Volume:	1.00 ul	Acquisition Method:	95% A1 to 100% B1 POSNEG
Run Time:	7.0 Minutes	Mobile Phase:	A1: 100% H2O / 0.1% FA B1: 100% ACN / 0.1% FA
Flowrate:	0.4 mL/min	Date Acquired:	23/08/2018 1:33:46 PM EST
Date Acquired:	23/08/2018 1:33:46 PM EST	Date Processed:	23/08/2018 1:42:12 PM EST
Date Processed:	23/08/2018 1:42:12 PM EST	Extracted Chromatogram:	PDA Spectrum PDA 254.0 nm

Auto-Scaled Chromatogram



Peak Results

	RT	Area	% Area	Height	Base Peak (m/z)
1	3.060	82139	1.92	62923	352.12
2	3.468	14636	0.34	13610	394.17
3	3.510	4046390	94.82	2686163	378.11
4	4.242	124068	2.91	101757	739.40

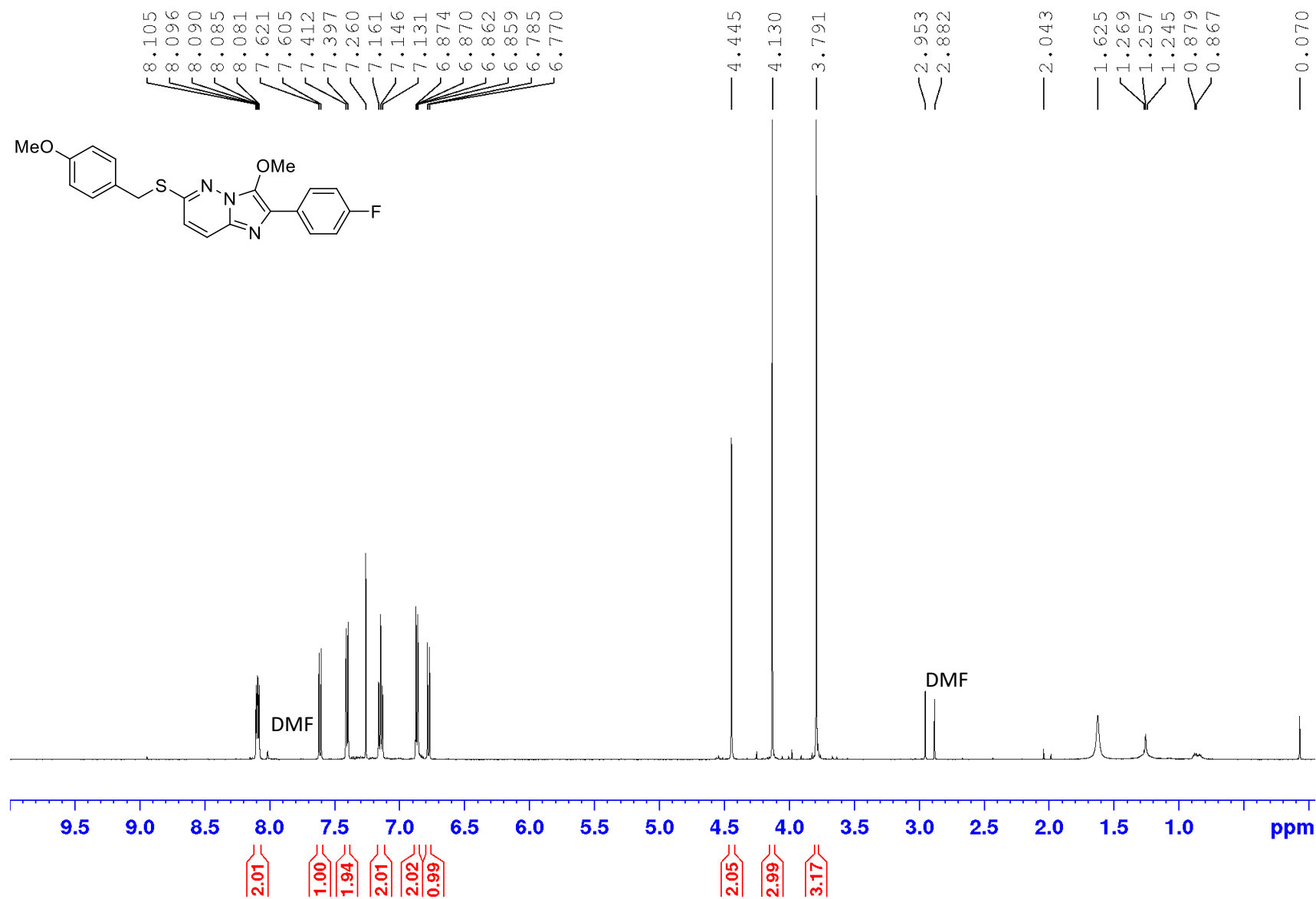


Chemical Formula: C₂₁H₁₉N₃O₂S
Exact Mass: 377.12
Molecular Weight: 377.46

m/z: 377.12 (100.0%), 378.12 (22.7%), 379.12 (4.5%), 379.13 (2.5%), 378.12 (1.1%), 380.12 (1.0%)

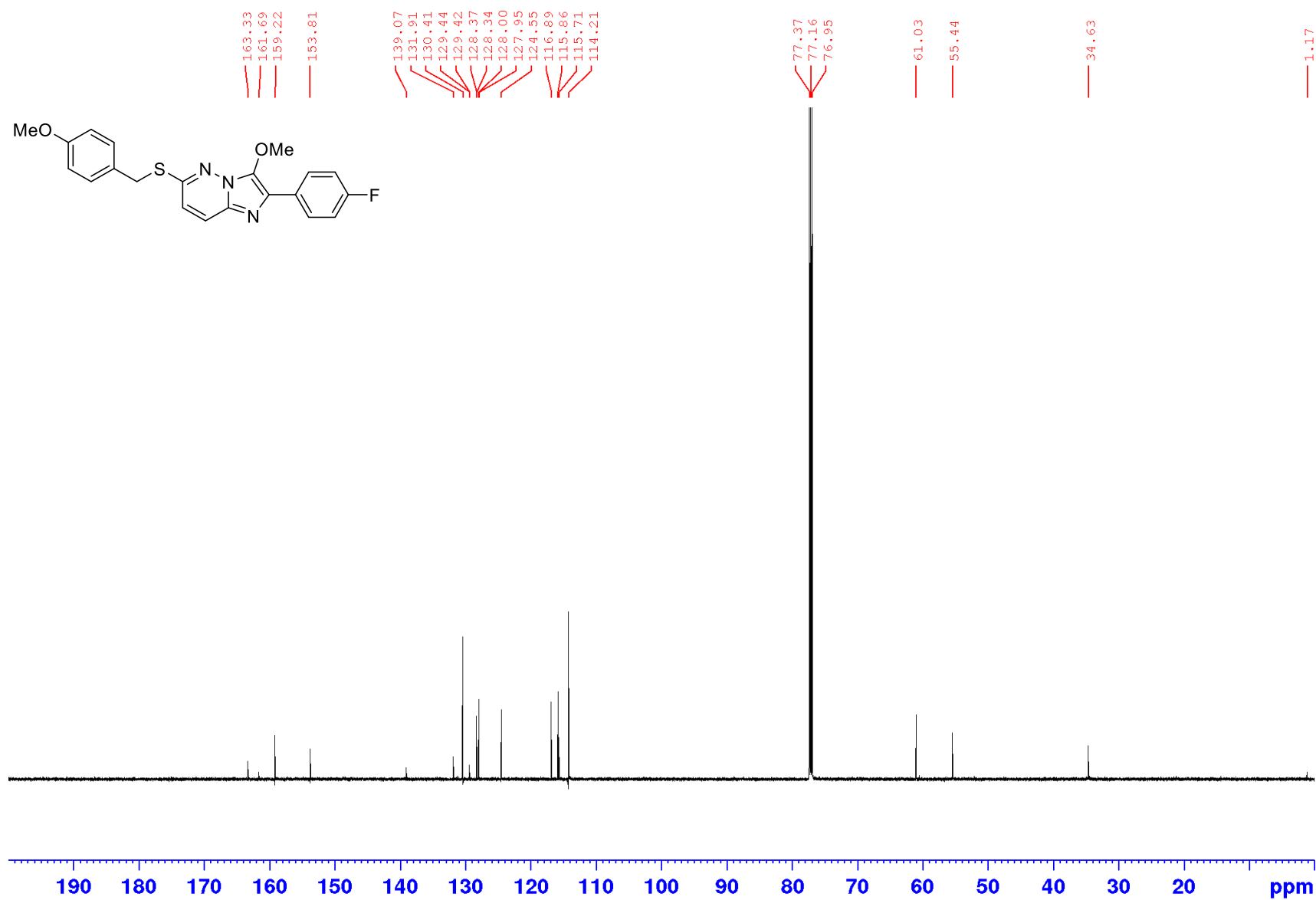
Appendices

¹H NMR spectrum of **148** (600 MHz; CDCl₃)



Appendices

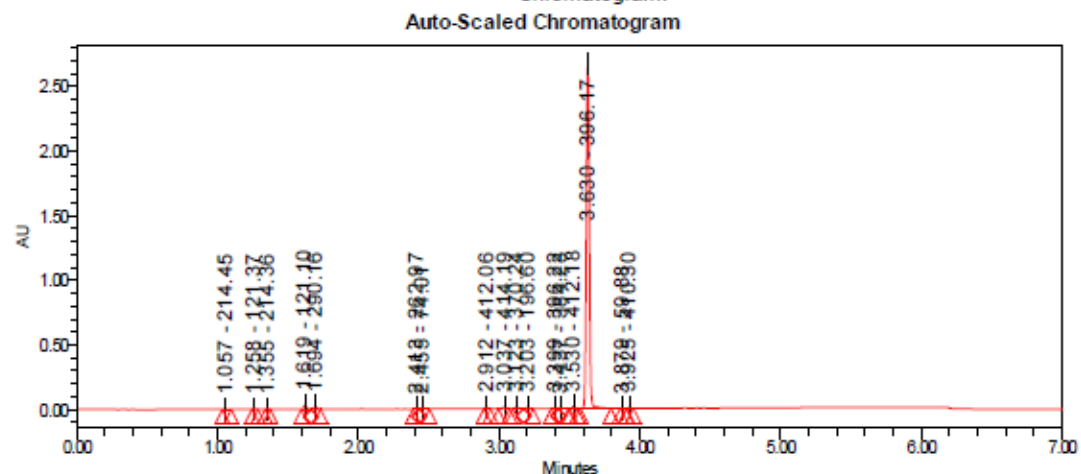
^{13}C NMR spectrum of **148** (150 MHz; CDCl_3)



Appendices

LC-MS chromatogram of **148** [M+H]⁺

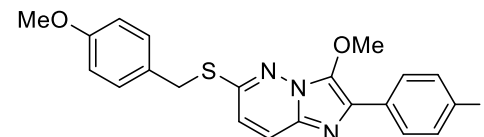
Sample Name:	IMPZ 14	Instrument:	Waters Acquity iClass PDA and QDa detectors
Vial:	1:A,8	Acquired By:	System
Injection #:	1	Sample Set Name:	MK_10_July2018
Injection Volume:	0.50 ul	Acquisition Method:	95% A1 to 100% B1 POSNEG
Run Time:	7.0 Minutes	Mobile Phase:	A1: 100% H2O / 0.1% FA B1: 100% ACN / 0.1% FA
Flowrate:	0.4 mL/min	Extracted	PDA Spectrum PDA 254.0 nm
Date Acquired:	10/07/2018 2:17:19 PM EST	Chromatogram:	
Date Processed:	10/07/2018 2:57:54 PM EST		



Peak Results

	RT	Area	% Area	Height	Base Peak (m/z)
1	1.057	3815	0.09	2481	214.45
2	1.258	4121	0.10	3667	121.37
3	1.355	1583	0.04	1530	214.36
4	1.619	45002	1.08	30466	121.10
5	1.694	27208	0.65	20025	290.18
6	2.413	9283	0.22	7418	262.97
7	2.455	12515	0.30	7227	74.01
8	2.912	9807	0.23	8442	412.06
9	3.037	18224	0.46	11052	414.19

	RT	Area	% Area	Height	Base Peak (m/z)
10	3.123	16224	0.39	11770	370.24
11	3.203	13236	0.32	8396	196.60
12	3.399	9218	0.22	7197	366.22
13	3.437	9345	0.22	5897	384.23
14	3.530	21172	0.51	16942	412.18
15	3.630	3964694	94.98	2676469	396.17
16	3.799	2102	0.05	1782	58.88
17	3.925	5674	0.14	4696	410.30



Chemical Formula: C₂₁H₁₈FN₃O₂S

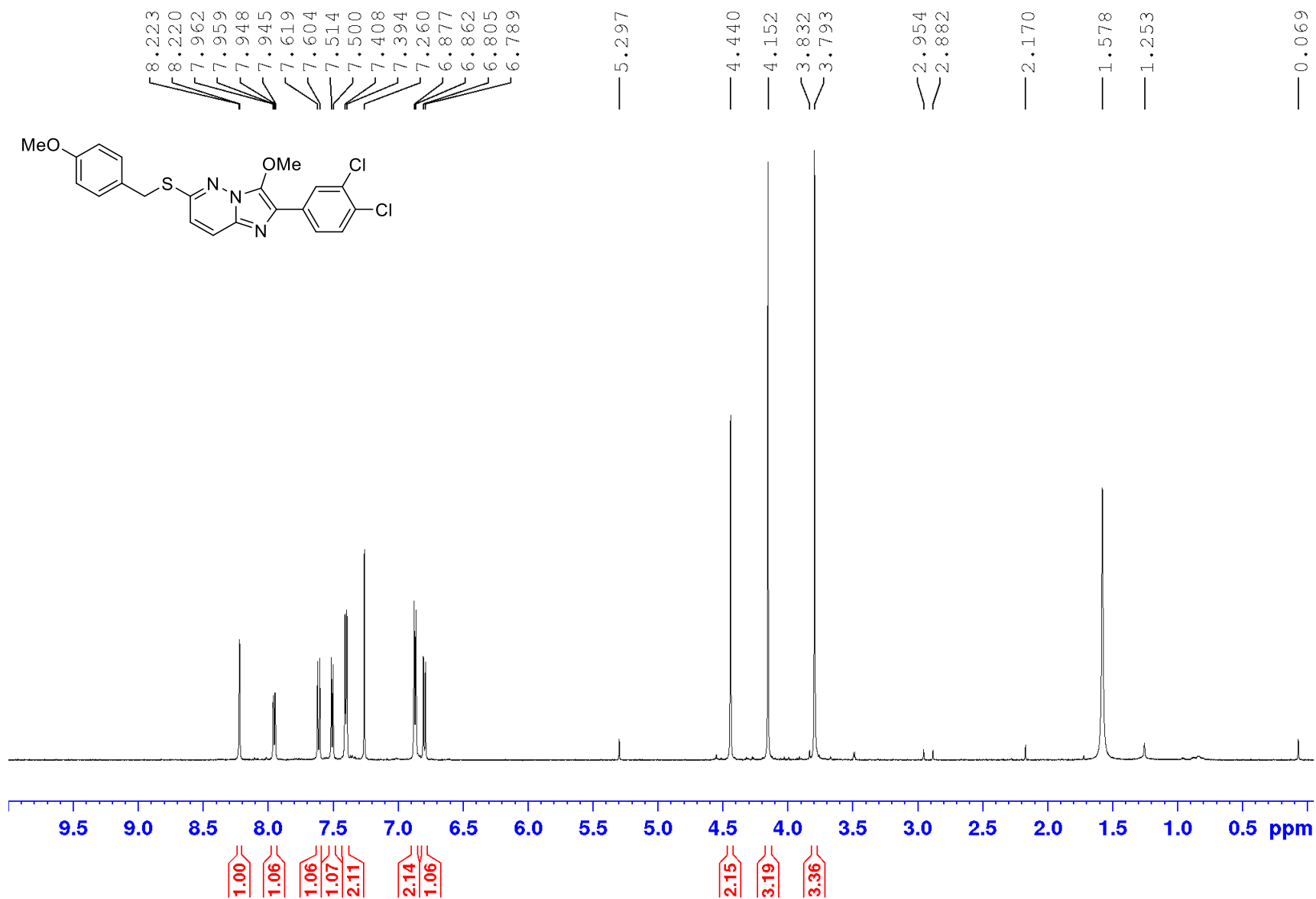
Exact Mass: 395.1104

Molecular Weight: 395.4524

m/z: 395.1104 (100.0%), 396.1137 (22.7%), 397.1062 (4.5%), 397.1171 (2.5%), 396.1074 (1.1%), 398.1095 (1.0%)

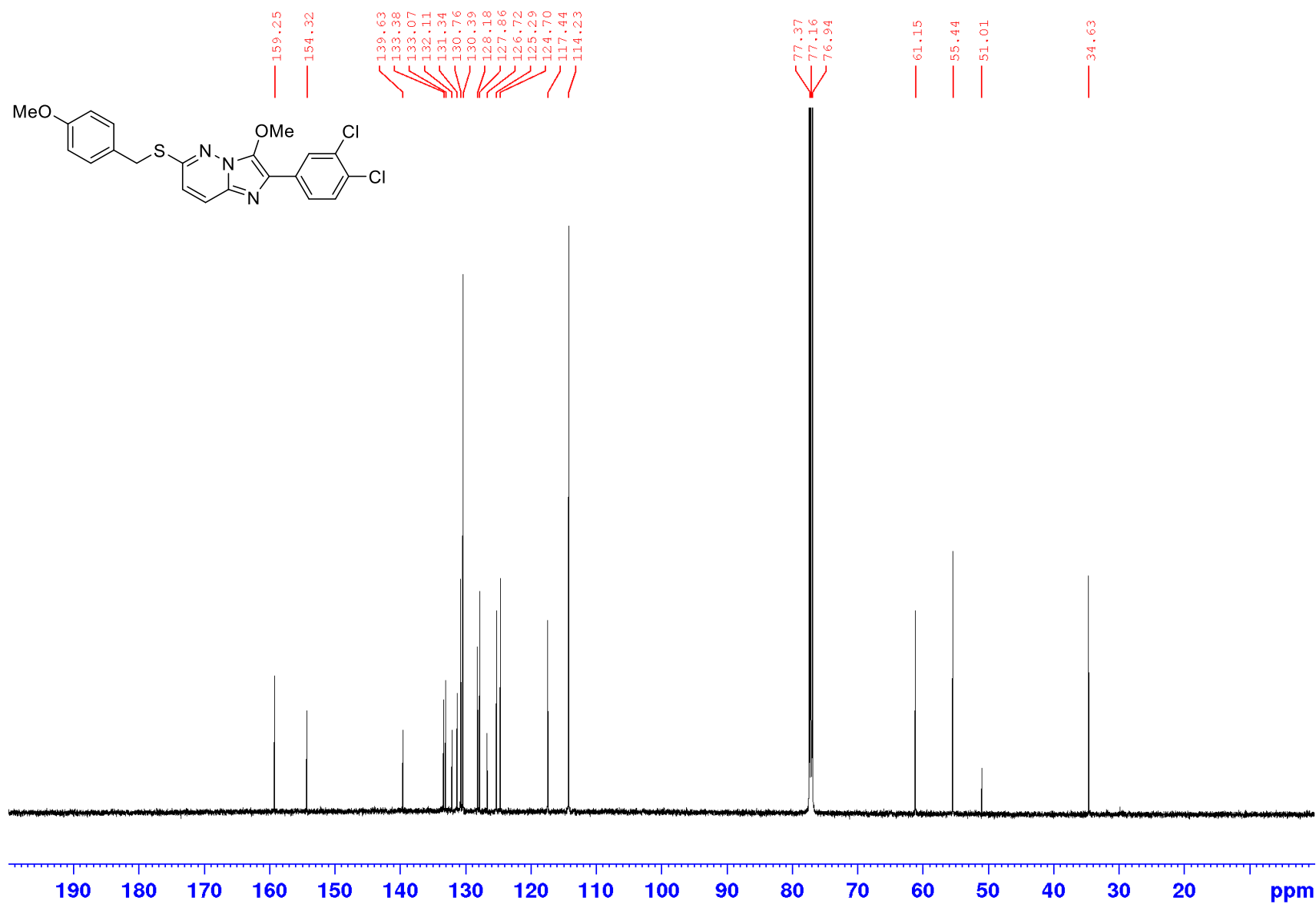
Appendices

¹H NMR spectrum of **149** (600 MHz; CDCl₃)



Appendices

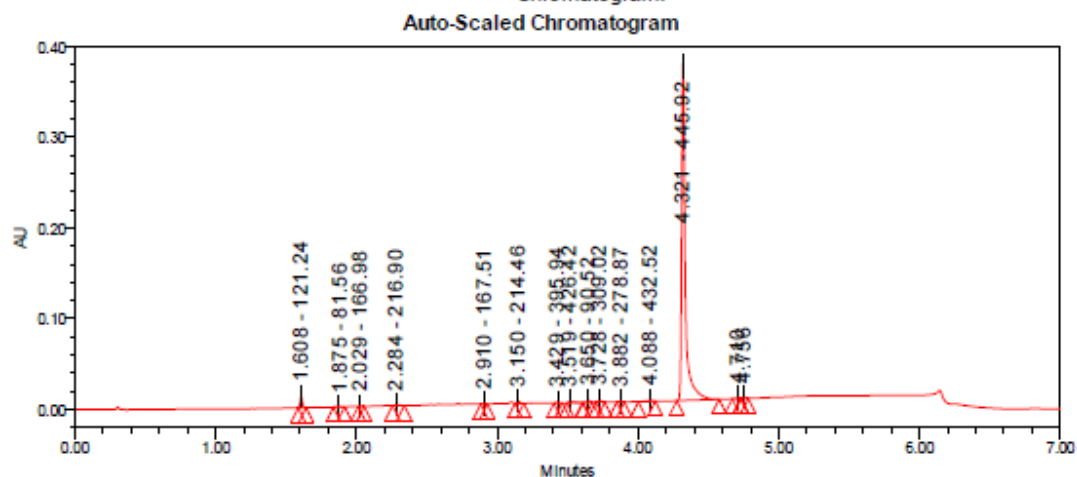
^{13}C NMR spectrum of **149** (150 MHz; CDCl_3)



Appendices

LC-MS chromatogram of **149** [M+H]⁺

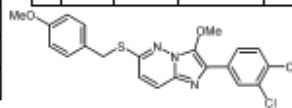
Vial:	1:C,2	Instrument:	Waters Acquity iClass PDA and QDa detectors
Injection #:	1	Acquired By:	System
Injection Volume:	0.20 ul	Sample Set Name:	KP_30_January2018
Run Time:	7.0 Minutes	Acquisition Method:	95% A1 to 100% B1 POSNEG
Date Acquired:	30/01/2018 3:18:41 PM EST	Mobile Phase:	A1: 100% H2O / 0.1% FA B1: 100% ACN / 0.1% FA
Date Processed:	30/01/2018 3:27:49 PM EST	Extracted Chromatogram:	PDA Spectrum PDA 254.0 nm



Peak Results

	RT	Area	% Area	Height	Base Peak (m/z)
1	1.608	13795	1.94	12002	121.24
2	1.875	899	0.13	387	81.56
3	2.029	569	0.08	494	166.98
4	2.284	2039	0.29	740	216.90
5	2.910	451	0.06	357	167.51
6	3.150	3335	0.47	2457	214.46
7	3.429	1434	0.20	1023	395.94
8	3.519	4020	0.57	1913	426.42
9	3.650	2788	0.39	1868	90.52

	RT	Area	% Area	Height	Base Peak (m/z)
10	3.728	3316	0.47	2516	309.02
11	3.882	568	0.08	358	278.87
12	4.088	2815	0.40	1319	432.52
13	4.321	671004	94.50	371685	445.92
14	4.710	1154	0.16	824	
15	4.756	1836	0.26	1477	



Chemical Formula: C₂₁H₁₇Cl₂N₂O₂S

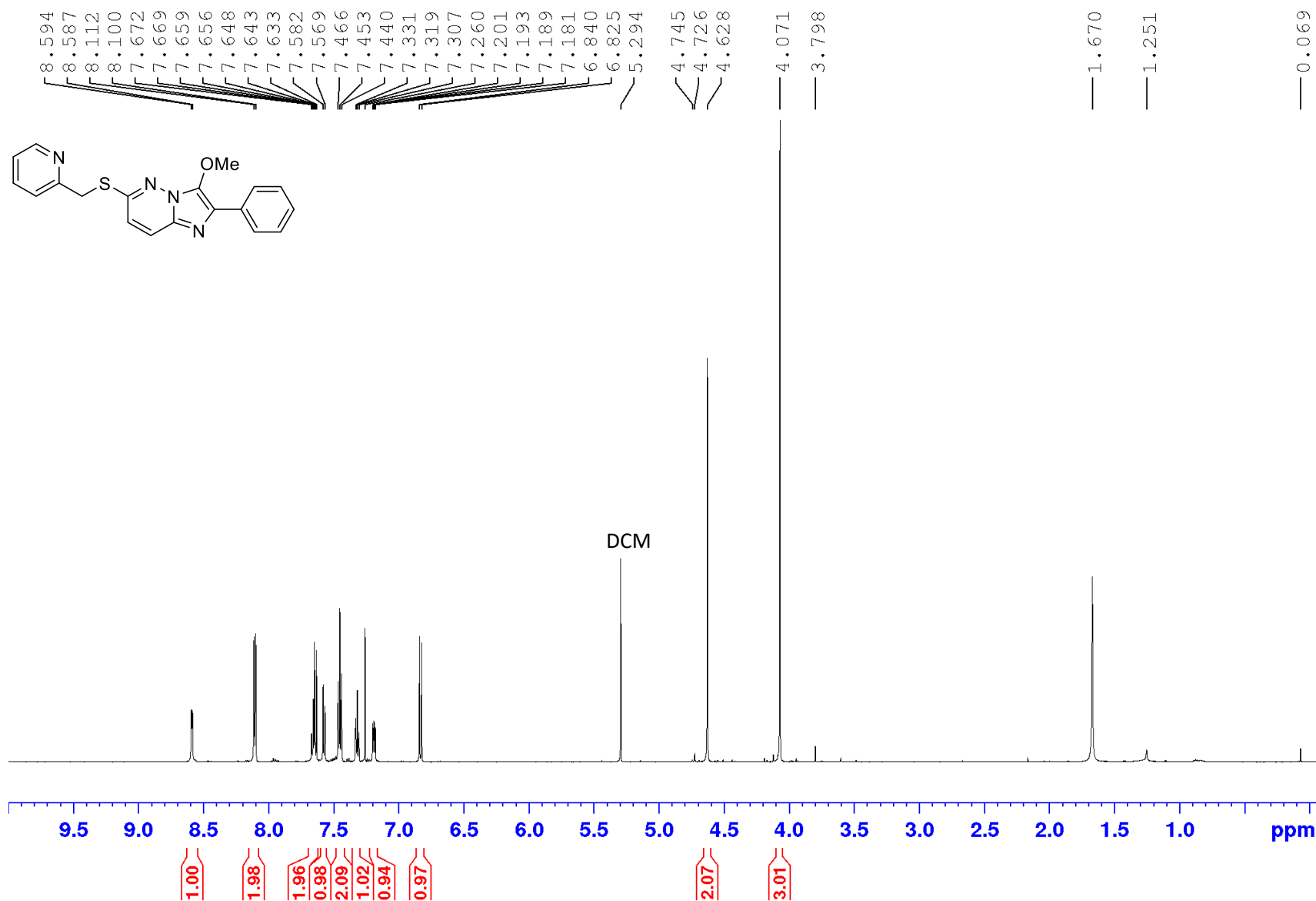
Exact Mass: 445.04

Molecular Weight: 446.35

m/z: 445.04 (100.0%), 447.04 (83.9%), 448.05 (22.7%), 449.04 (10.2%),
448.04 (7.3%), 448.04 (7.3%), 447.04 (4.0%), 448.03 (2.9%), 447.05
(2.5%), 450.04 (2.3%), 449.05 (1.8%), 448.04 (1.1%), 448.04 (1.0%)

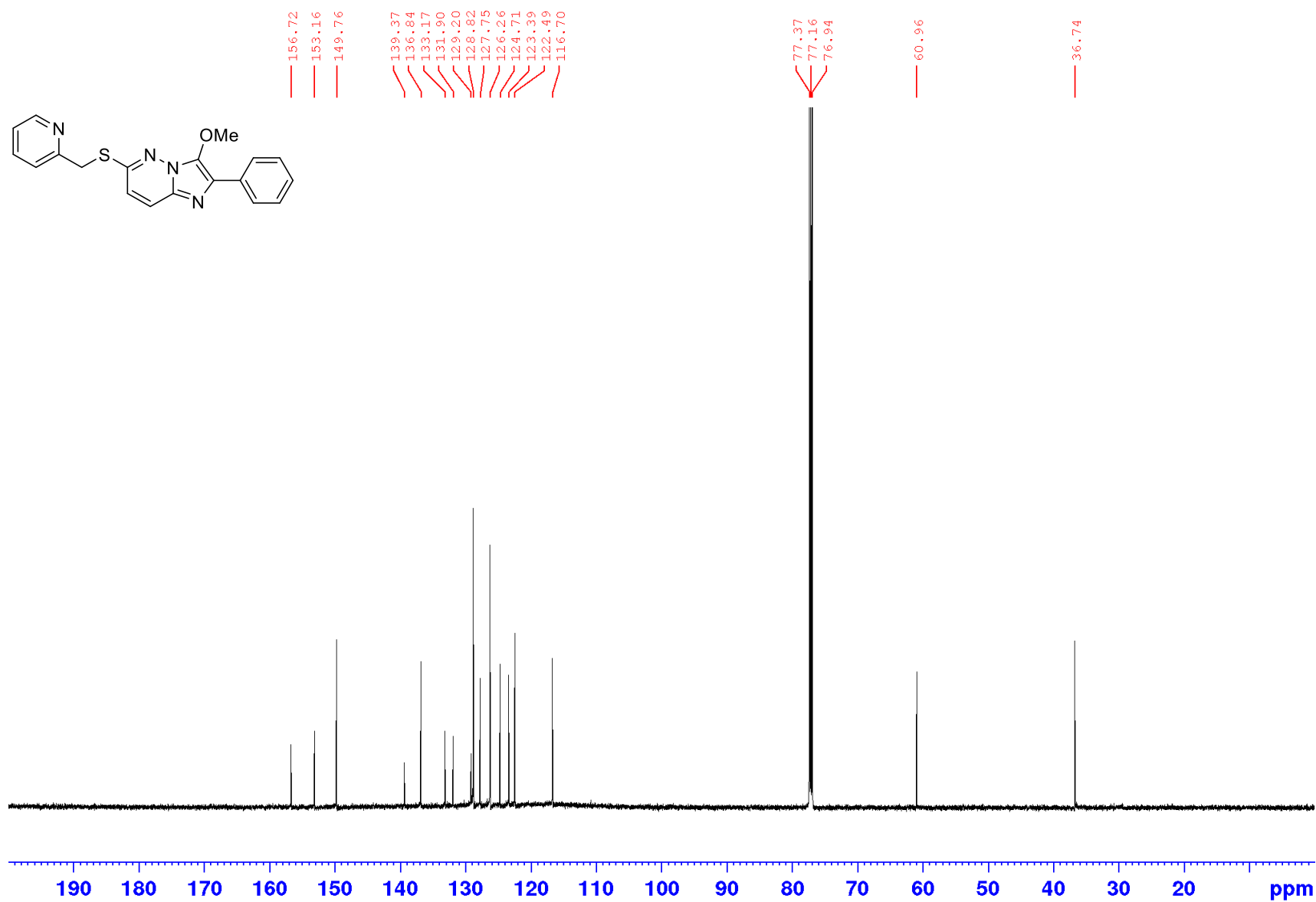
Appendices

¹H NMR spectrum of **151** (600 MHz; CDCl₃)



Appendices

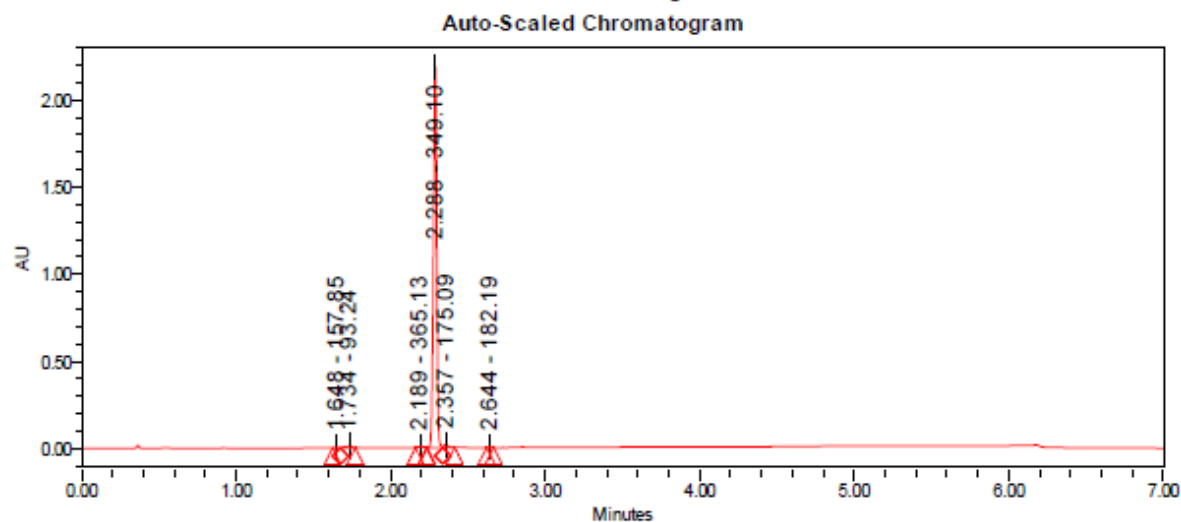
^{13}C NMR spectrum of **151** (150 MHz; CDCl_3)



Appendices

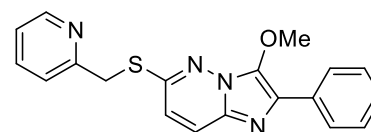
LC-MS chromatogram of **151** [M+H]⁺

Sample Name:	IMPZ 8	Instrument:	Waters Acquity iClass PDA and QDa detectors
Vial:	1:A,2	Acquired By:	System
Injection #:	1	Sample Set Name:	MK_10_July2018
Injection Volume:	0.50 ul	Acquisition Method:	95% A1 to 100% B1 POSNEG
Run Time:	7.0 Minutes	Mobile Phase:	A1: 100% H2O / 0.1% FA B1: 100% ACN / 0.1% FA
Flowrate:	0.4 mL/min	Extracted Chromatogram:	PDA Spectrum PDA 254.0 nm
Date Acquired:	10/07/2018 1:17:55 PM EST		
Date Processed:	10/07/2018 1:36:40 PM EST		



Peak Results

RT	Area	% Area	Height	Base Peak (m/z)	
1	1.648	4911	0.15	3893	157.85
2	1.734	29742	0.90	10196	93.24
3	2.189	15476	0.47	7307	365.13
4	2.288	3231546	97.48	2208838	349.10
5	2.357	30016	0.91	18552	175.09
6	2.644	3456	0.10	2783	182.19



Chemical Formula: C₁₉H₁₆N₄OS

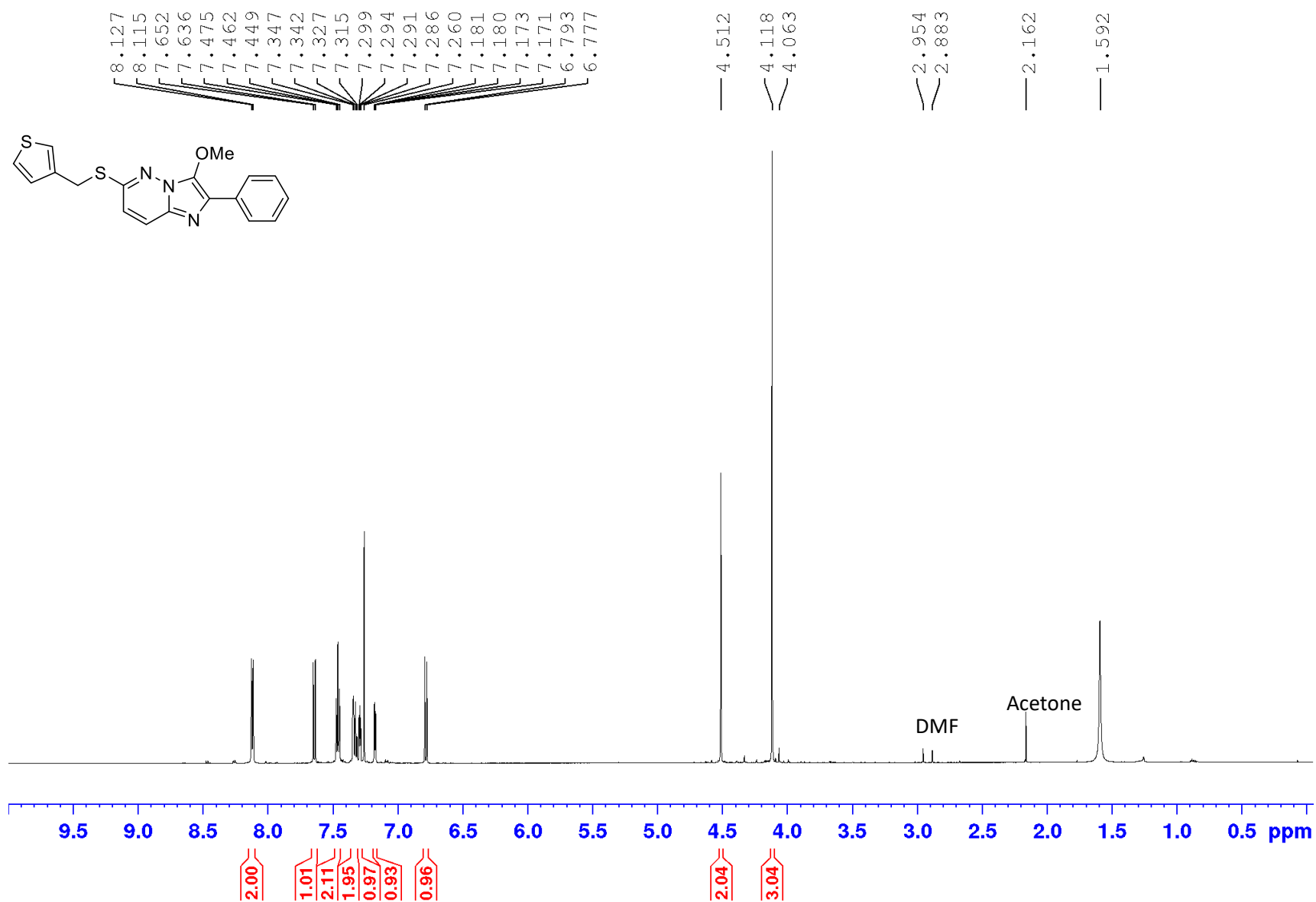
Exact Mass: 348.1045

Molecular Weight: 348.4240

m/z: 348.1045 (100.0%), 349.1078 (20.5%),
350.1003 (4.5%), 350.1112 (2.0%), 349.1015 (1.5%)

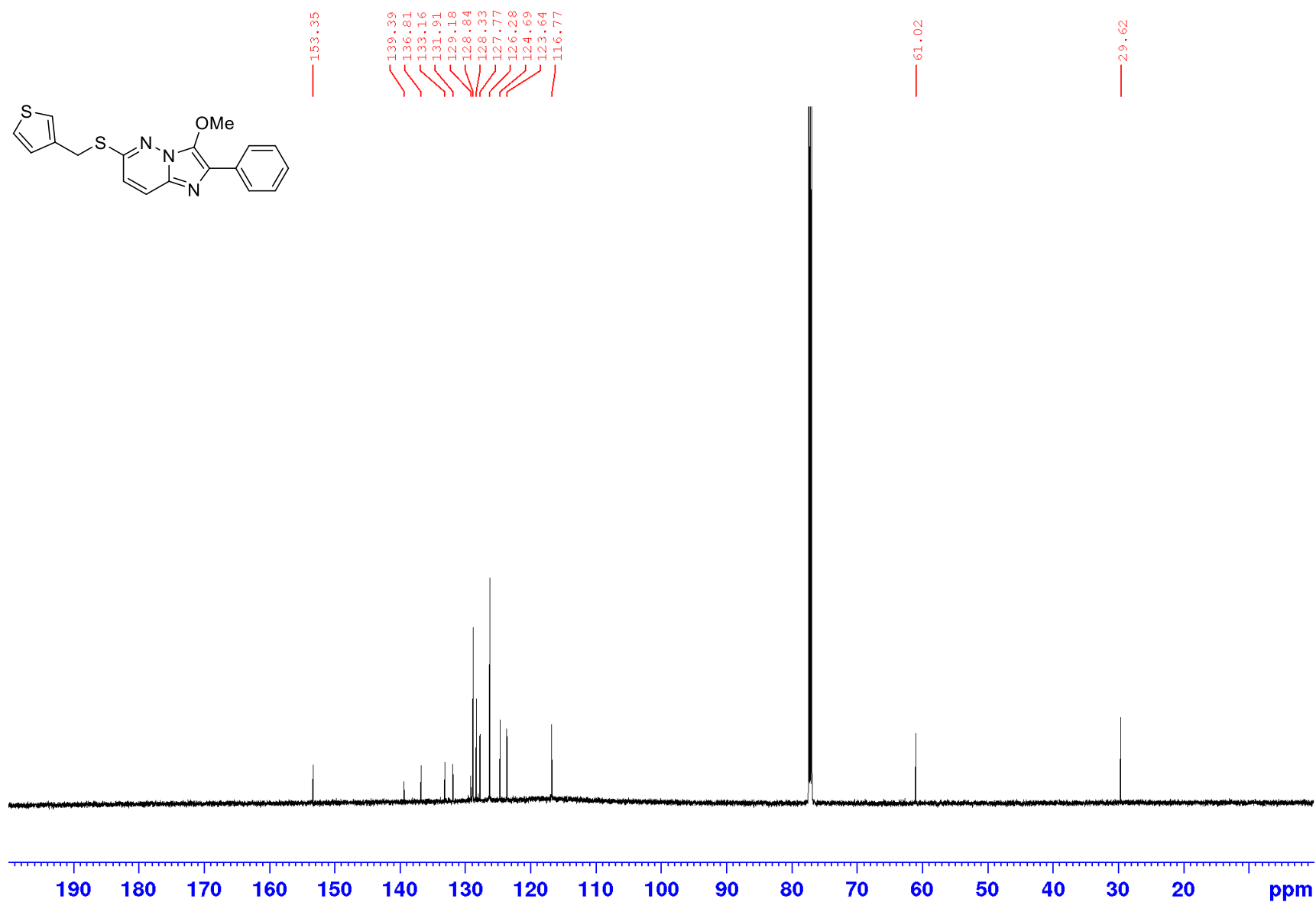
Appendices

¹H NMR spectrum of **153** (600 MHz; CDCl₃)



Appendices

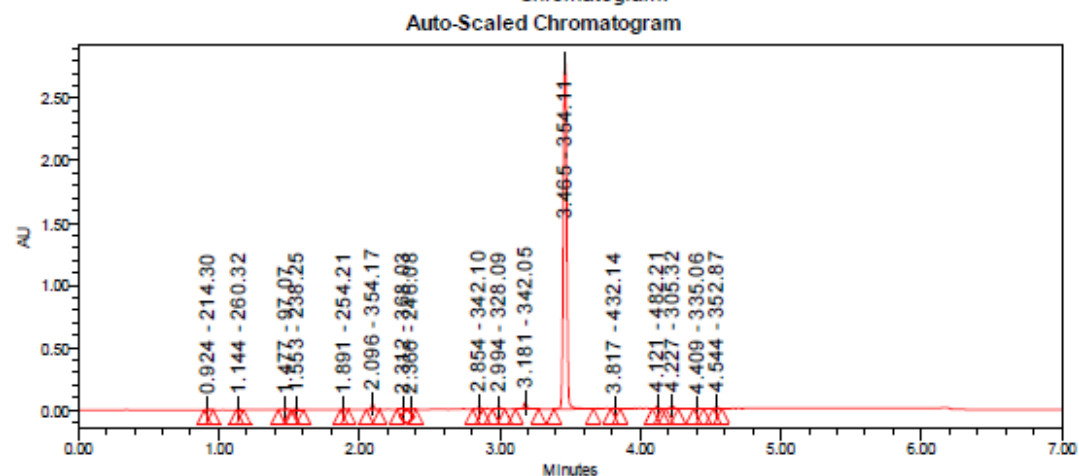
^{13}C NMR spectrum of **153** (150 MHz; CDCl_3)



Appendices

LC-MS chromatogram of **153** [M+H]⁺

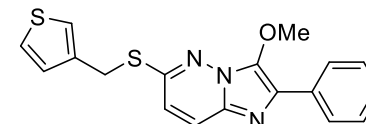
Sample Name:	IMPZ 13	Instrument:	Waters Acquity iClass PDA and QDa detectors
Vial:	1:A,7	Acquired By:	System
Injection #:	1	Sample Set Name:	MK_10_July2018
Injection Volume:	0.50 ul	Acquisition Method:	95% A1 to 100% B1 POSNEG
Run Time:	7.0 Minutes	Mobile Phase:	A1: 100% H2O / 0.1% FA B1: 100% ACN / 0.1% FA
Flowrate:	0.4 mL/min	Extracted Chromatogram:	PDA Spectrum PDA 254.0 nm
Date Acquired:	10/07/2018 2:08:51 PM EST		
Date Processed:	10/07/2018 2:55:50 PM EST		



Peak Results

	RT	Area	% Area	Height	Base Peak (m/z)
1	0.924	12267	0.24	8129	214.30
2	1.144	10513	0.21	9691	260.32
3	1.477	15019	0.30	8515	97.07
4	1.553	23880	0.47	17627	238.25
5	1.891	10027	0.20	8472	254.21
6	2.096	56307	1.11	45948	354.17
7	2.312	18886	0.37	13370	368.03
8	2.366	15198	0.30	9948	246.08
9	2.854	25788	0.51	18726	342.10

	RT	Area	% Area	Height	Base Peak (m/z)
10	2.994	27639	0.55	14872	328.09
11	3.181	85917	1.70	52876	342.05
12	3.465	4670928	92.17	2797413	354.11
13	3.817	12831	0.25	6857	432.14
14	4.121	21738	0.43	17887	482.21
15	4.227	36319	0.72	20342	305.32
16	4.409	7077	0.14	5010	335.06
17	4.544	17388	0.34	14225	352.87



Chemical Formula: C₁₈H₁₅N₃OS₂

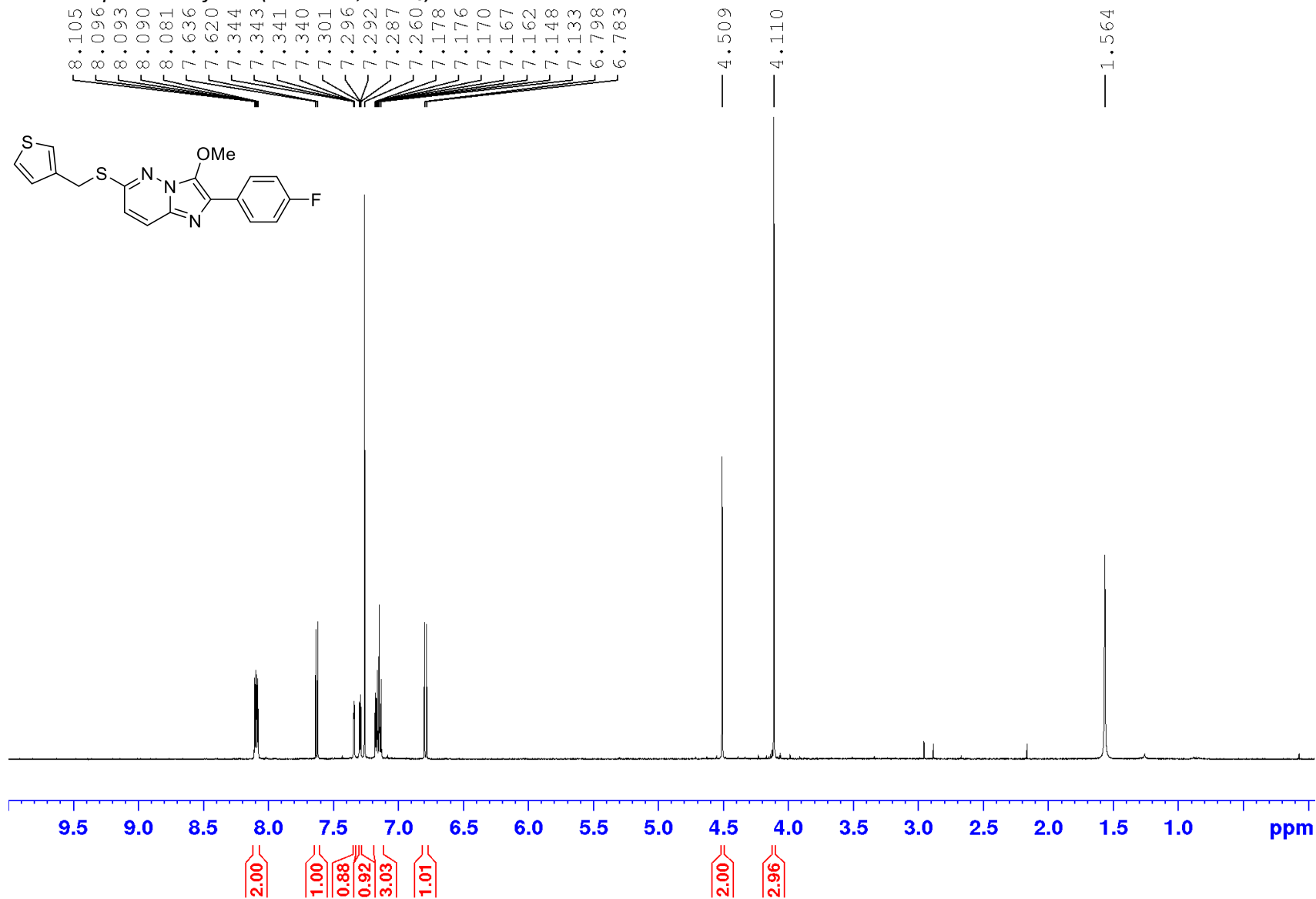
Exact Mass: 353.0657

Molecular Weight: 353.4580

m/z: 353.0657 (100.0%), 354.0690 (19.5%),
355.0614 (9.0%), 355.0724 (1.8%),
356.0648 (1.8%), 354.0650 (1.6%), 354.0627 (1.1%)

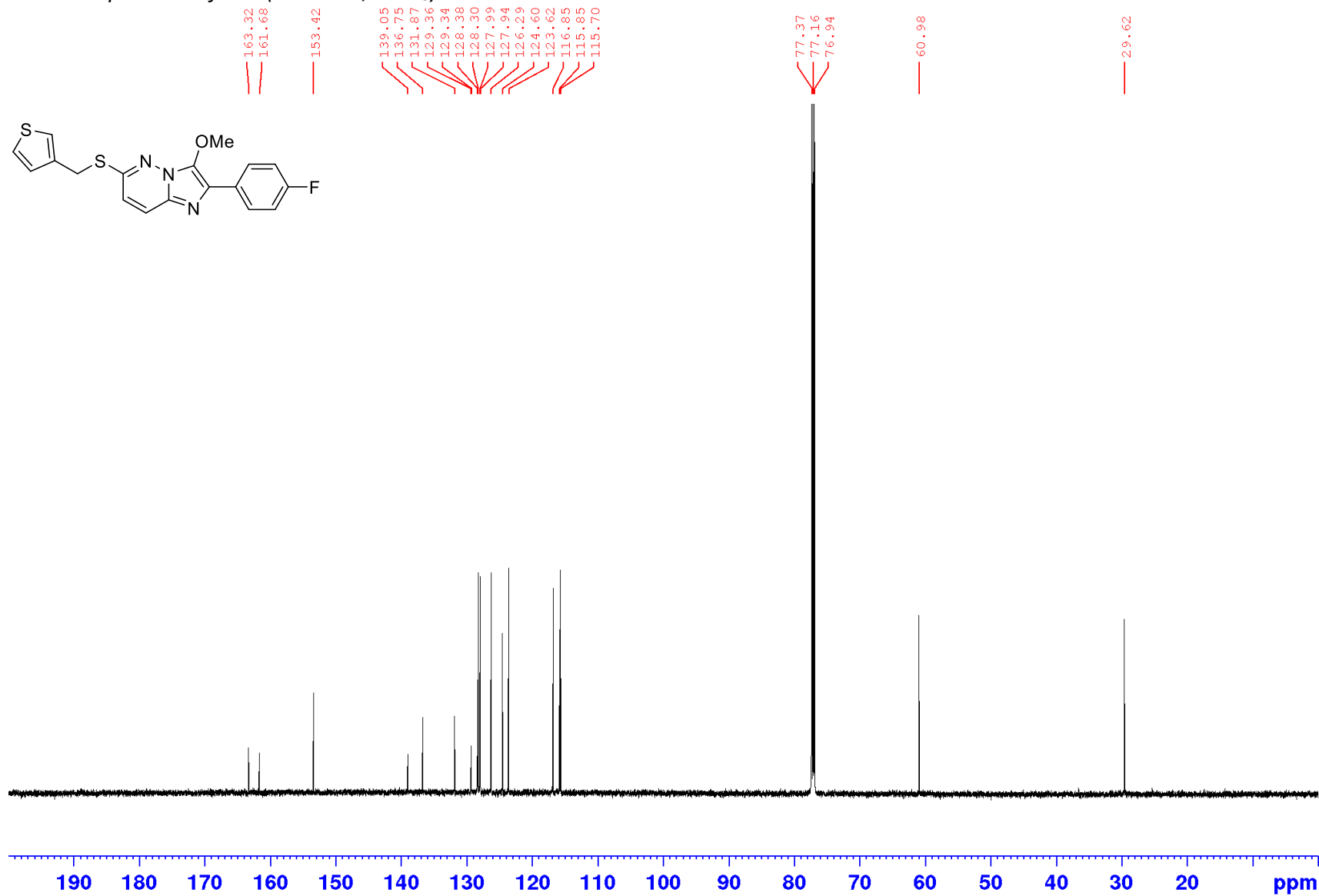
Appendices

¹H NMR spectrum of **154** (600 MHz; CDCl₃)



Appendices

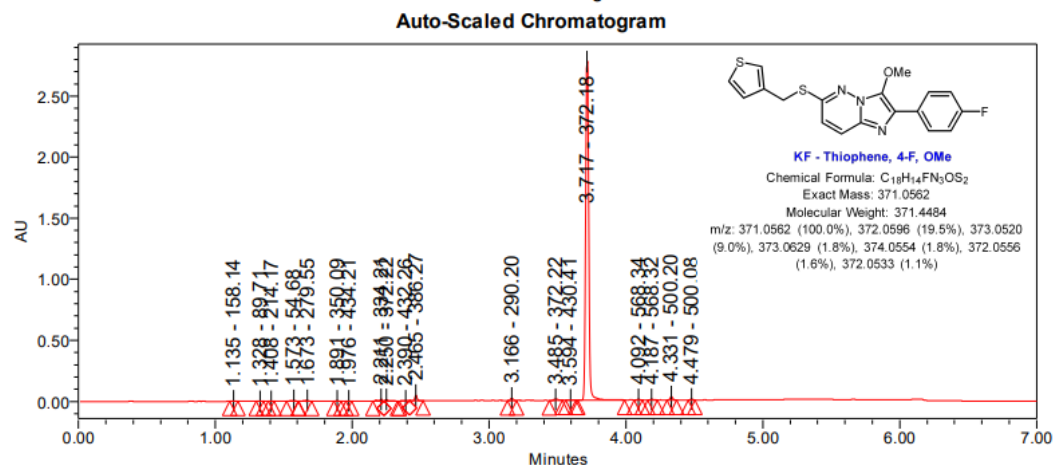
^{13}C NMR spectrum of **154** (150 MHz; CDCl_3)



Appendices

LC-MS chromatogram of **154** [M+H]⁺

Sample Name:	KF-Thiophene,4-F, OMe	Instrument:	Waters Acquity iClass PDA and QDa detectors
Vial:	1:C,3	Acquired By:	System
Injection #:	1	Sample Set Name:	MK_18_October_2019
Injection Volume:	1.00 ul	Acquisition Method:	95% A1 to 100% B1 POSNEG_Col2
Run Time:	7.0 Minutes	Mobile Phase:	A1: 100% H2O / 0.1% FA B1: 100% MeCN / 0.1% FA
Flowrate:	0.4 mL/min	Extracted Chromatogram:	PDA Spectrum PDA 254.0 nm
Date Acquired:	18/10/2019 3:49:53 PM EST		
Date Processed:	18/10/2019 4:03:21 PM EST		

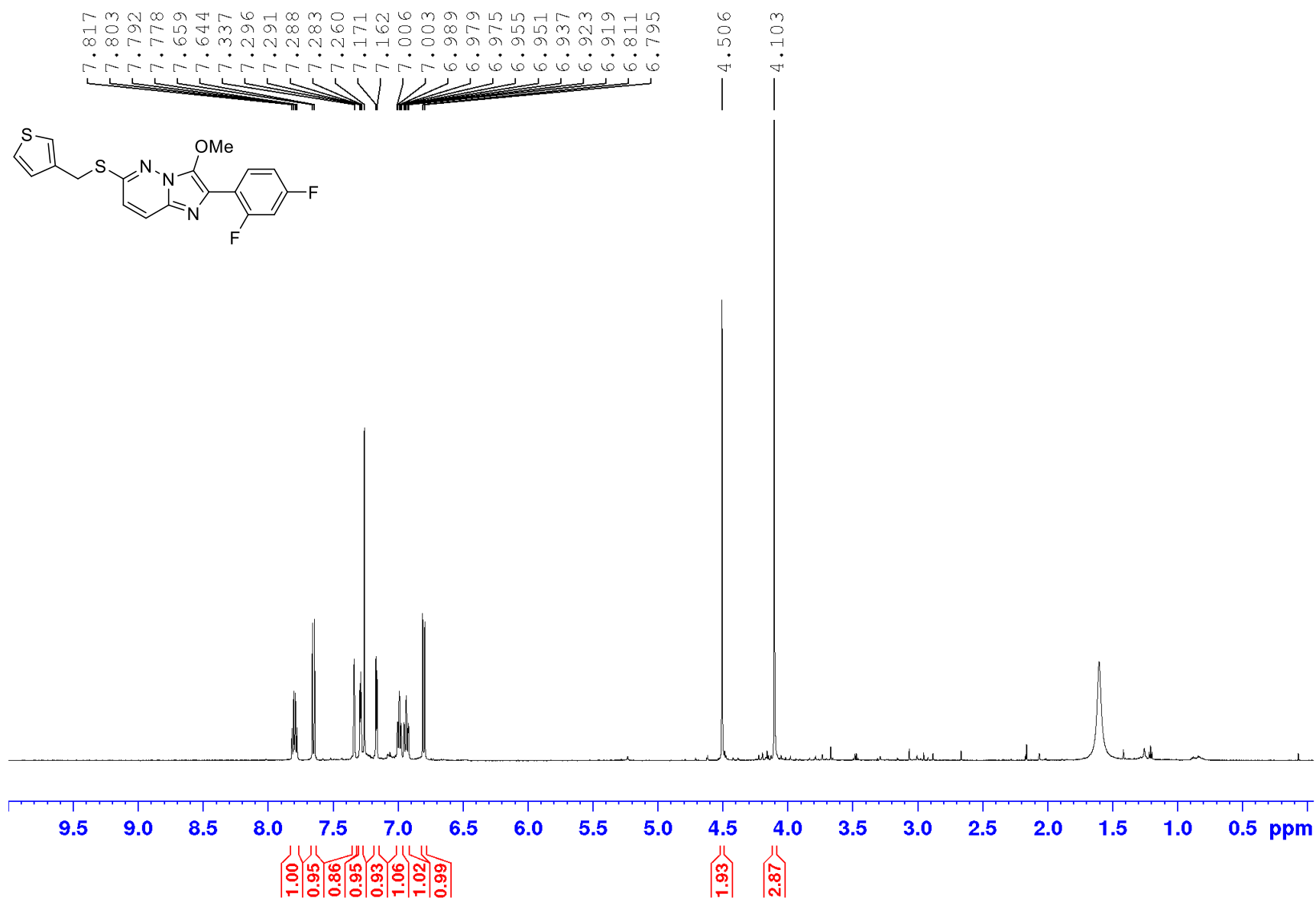


Peak Results

	RT	Area	% Area	Height	Base Peak (m/z)
1	1.135	2961	0.06	1798	158.14
2	1.328	875	0.02	549	89.71
3	1.408	660	0.01	577	214.17
4	1.573	12749	0.26	5780	54.68
5	1.673	11989	0.24	5005	279.55
6	1.891	3604	0.07	3111	350.09
7	1.976	1777	0.04	1502	434.21
8	2.211	27170	0.55	14122	334.21
9	2.250	18626	0.38	11902	372.22
10	2.390	4123	0.08	2007	432.26
11	2.465	58029	1.18	45803	386.27
12	3.166	26522	0.54	19243	290.20
13	3.485	23395	0.48	10689	372.22
14	3.594	7231	0.15	3560	430.41
15	3.717	4658860	94.66	2784818	372.18
16	4.092	8385	0.17	6691	568.34
17	4.187	9903	0.20	4998	568.32
18	4.331	37139	0.75	29073	500.20

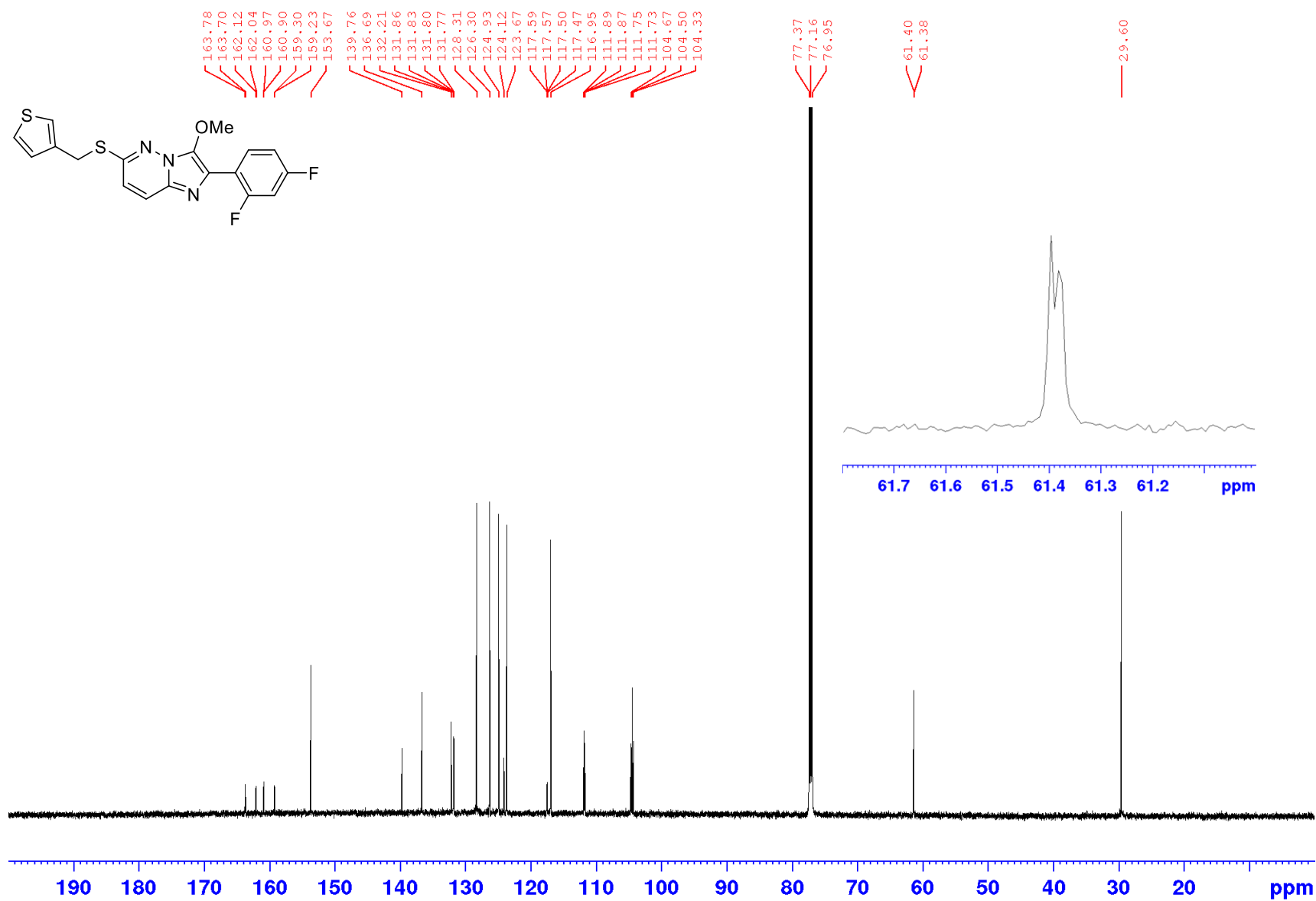
Appendices

¹H NMR spectrum of **155** (600 MHz; CDCl₃)



Appendices

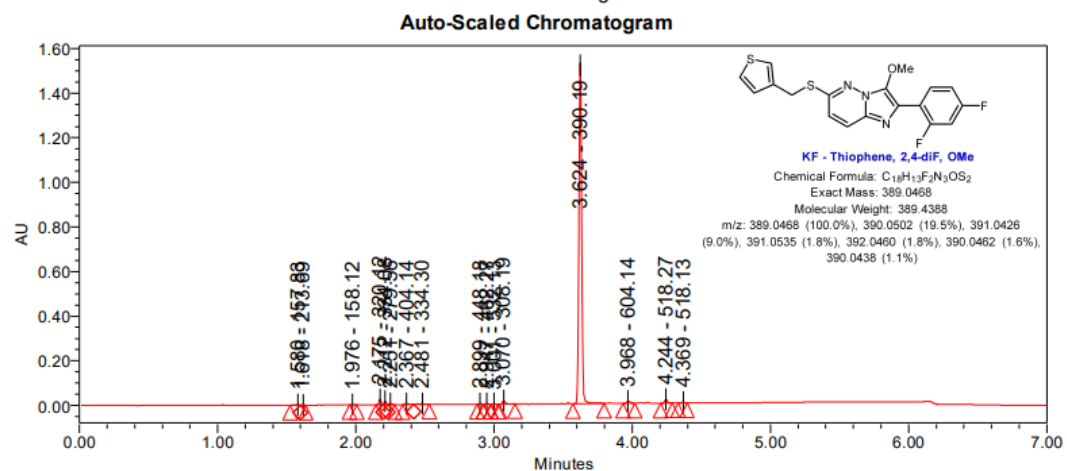
^{13}C NMR spectrum of **155** (150 MHz; CDCl_3)



Appendices

LC-MS chromatogram of 155 [M+H]⁺

Sample Name:	KF-Thiophene, 2,4-diF, OMe	Instrument:	Waters Acquity iClass PDA and QDa detectors
Vial:	1:C,5	Acquired By:	System
Injection #:	1	Sample Set Name:	MK_18_October_2019
Injection Volume:	0.30 ul	Acquisition Method:	95% A1 to 100% B1 POSNEG_Col2
Run Time:	7.0 Minutes	Mobile Phase:	A1: 100% H2O / 0.1% FA B1: 100% MeCN / 0.1% FA
Flowrate:	0.4 mL/min	Extracted Chromatogram:	PDA Spectrum PDA 254.0 nm
Date Acquired:	18/10/2019 4:41:59 PM EST		
Date Processed:	18/10/2019 4:53:36 PM EST		



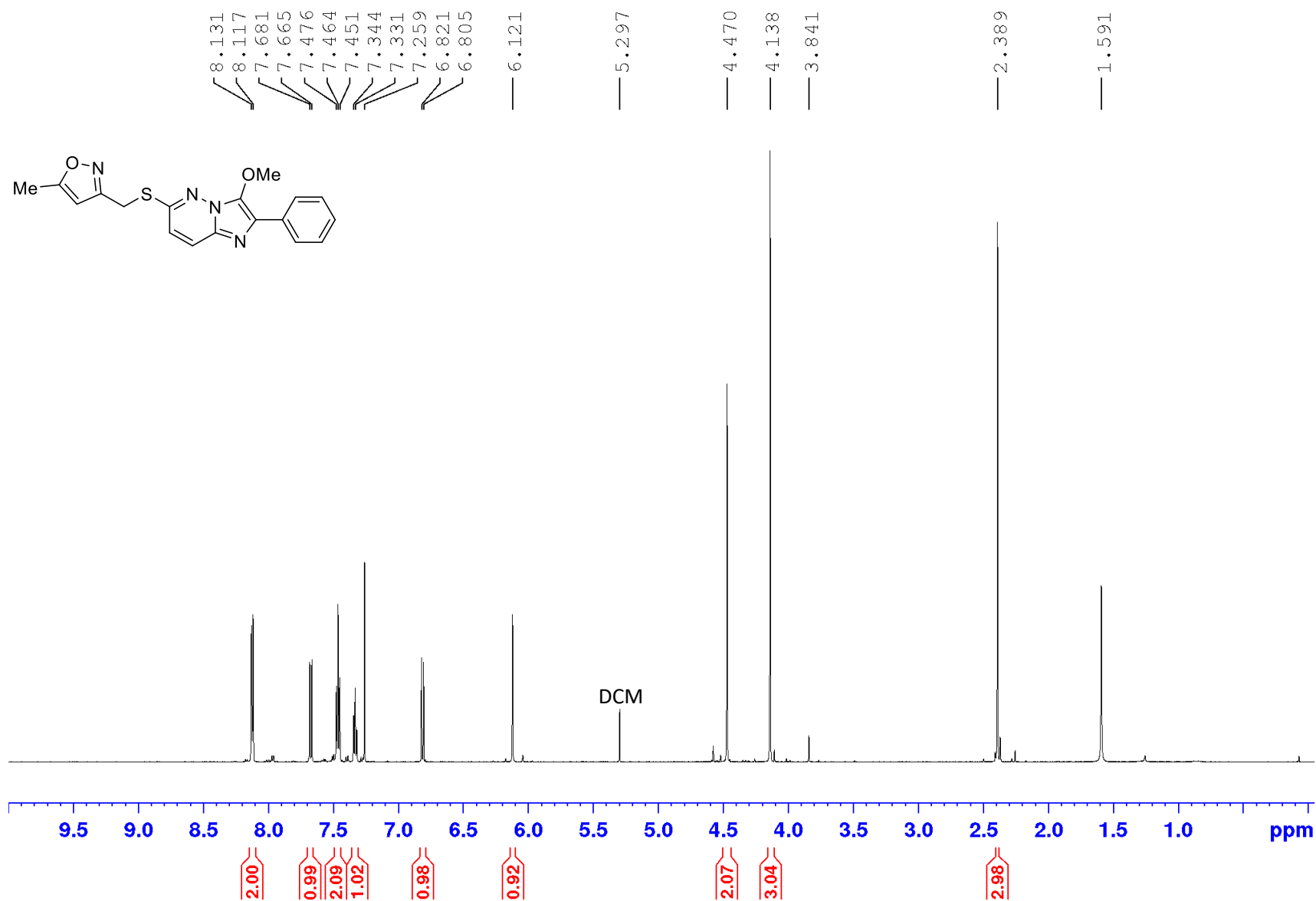
Peak Results

	RT	Area	%Area	Height	Base Peak (m/z)
1	1.580	5681	0.26	2912	157.83
2	1.618	1294	0.06	1126	213.69
3	1.976	1805	0.08	1430	158.12
4	2.175	27009	1.25	23417	320.12
5	2.212	18585	0.86	16248	334.08
6	2.251	7240	0.33	6059	279.56
7	2.367	8534	0.39	5618	404.14
8	2.481	12581	0.58	5033	334.30
9	2.899	3903	0.18	3265	448.18

	RT	Area	%Area	Height	Base Peak (m/z)
10	2.947	3658	0.17	3187	462.27
11	3.001	1695	0.08	1513	532.13
12	3.070	22058	1.02	14651	308.19
13	3.624	2006248	92.58	1520630	390.19
14	3.968	18502	0.85	9725	604.14
15	4.244	22711	1.05	17036	518.27
16	4.369	5546	0.26	4723	518.13

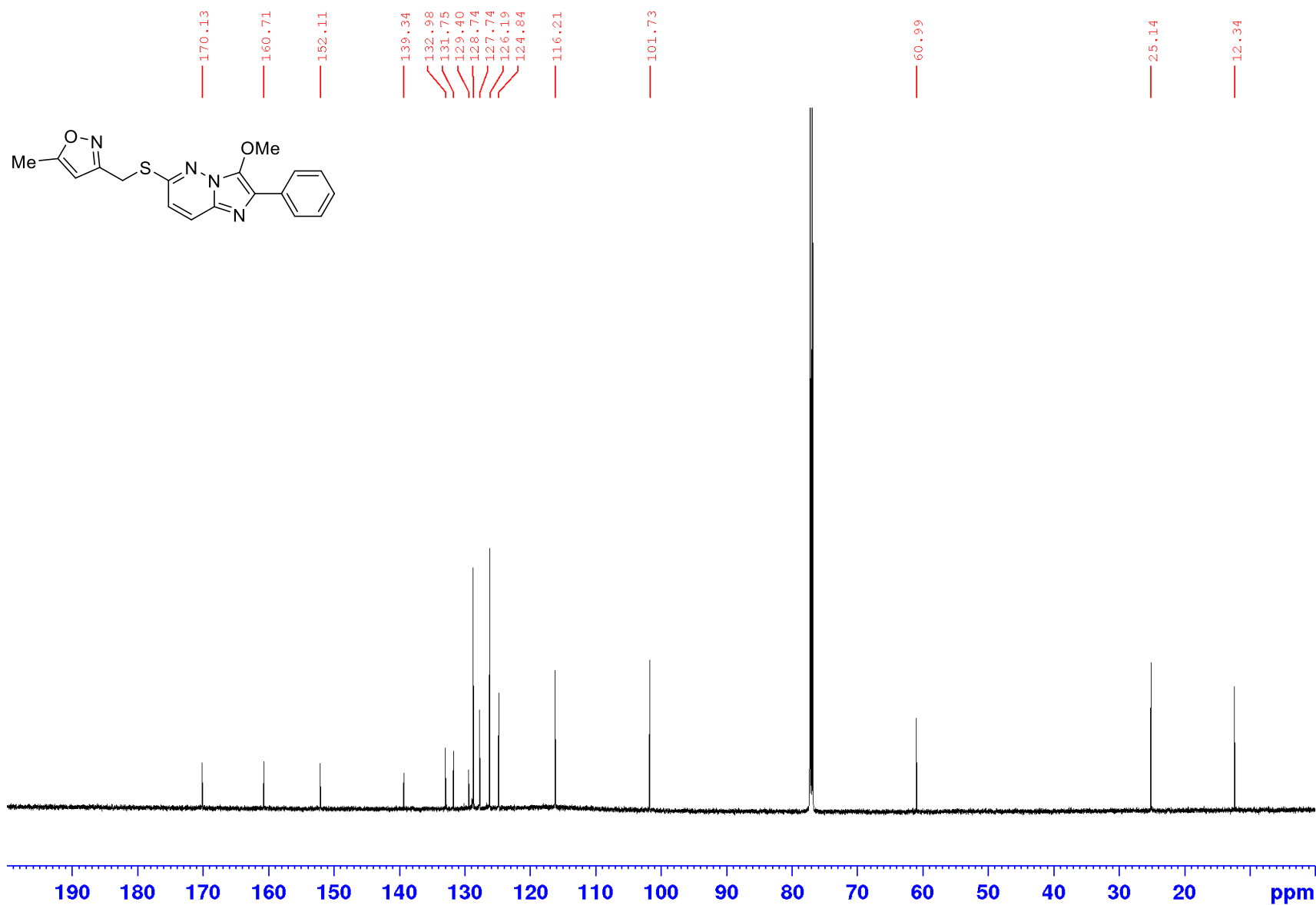
Appendices

¹H NMR spectrum of **156** (600 MHz; CDCl₃)



Appendices

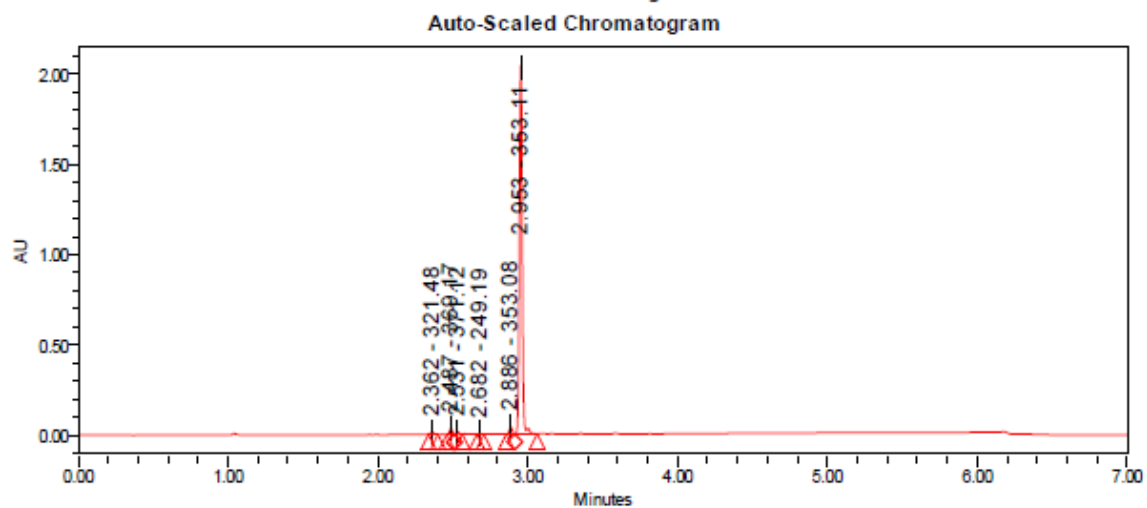
¹³C NMR spectrum of **156** (150 MHz; CDCl₃)



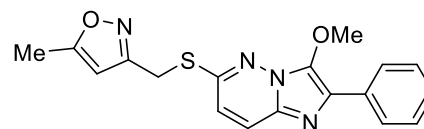
Appendices

LC-MS chromatogram of 156 [M+H]⁺

Sample Name:	IMPZ 10	Instrument:	Waters Acquity iClass PDA and QDa detectors
Vial:	1:A,4	Acquired By:	System
Injection #:	1	Sample Set Name:	MK_10_July2018
Injection Volume:	0.50 ul	Acquisition Method:	95% A1 to 100% B1 POSNEG
Run Time:	7.0 Minutes	Mobile Phase:	A1: 100% H2O / 0.1% FA B1: 100% ACN / 0.1% FA
Flowrate:	0.4 mL/min	Extracted Chromatogram:	PDA Spectrum PDA 254.0 nm
Date Acquired:	10/07/2018 1:34:56 PM EST		
Date Processed:	10/07/2018 1:50:38 PM EST		



Peak Results					
	RT	Area	% Area	Height	Base Peak (m/z)
1	2.362	17132	0.62	12322	321.48
2	2.487	40336	1.45	33300	369.17
3	2.531	18655	0.67	14270	371.12
4	2.682	6055	0.22	5130	249.19
5	2.886	49980	1.80	40159	353.08
6	2.953	2649262	95.25	2030055	353.11



Chemical Formula: C₁₈H₁₆N₄O₂S

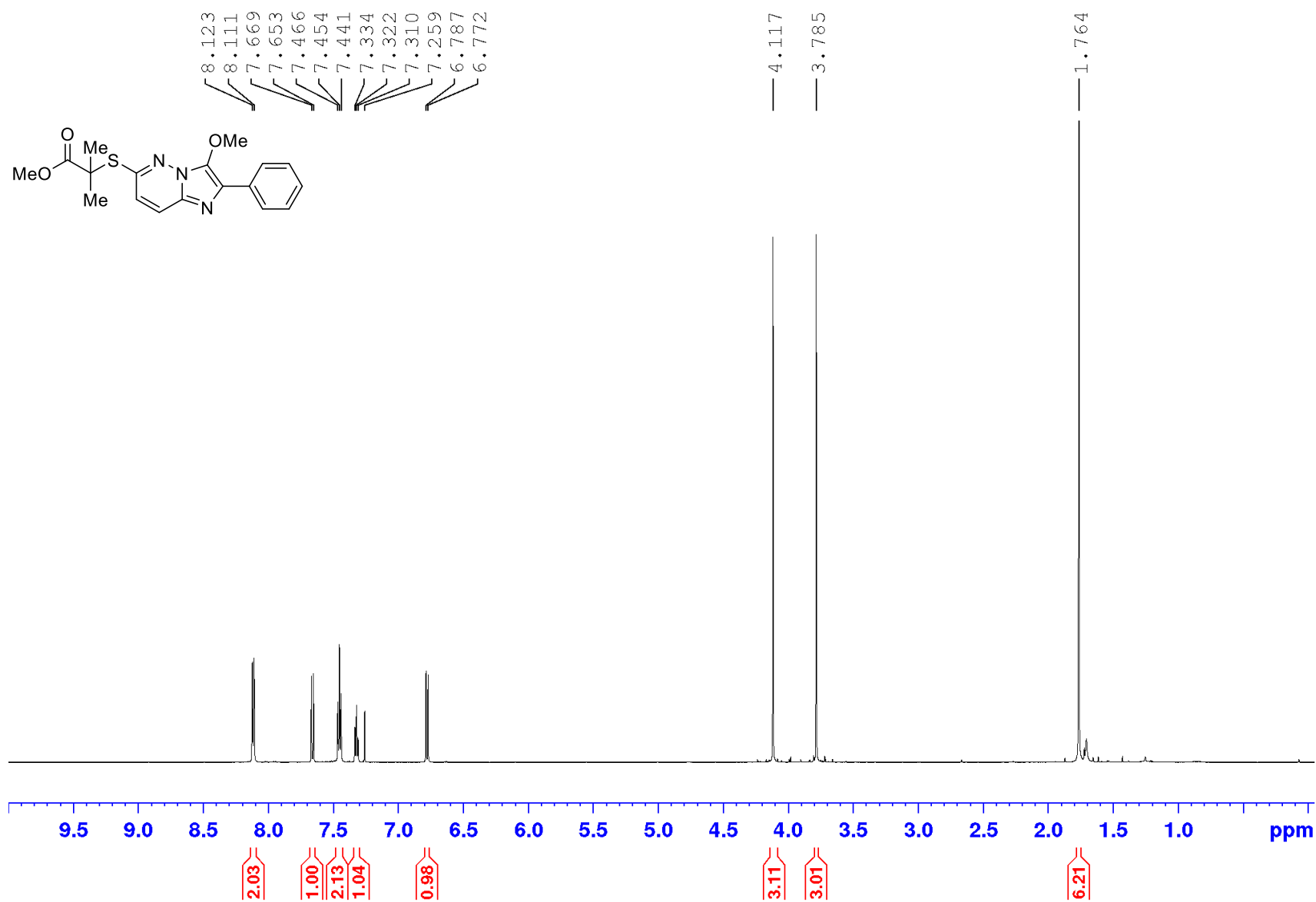
Exact Mass: 352.0994

Molecular Weight: 352.4120

m/z: 352.0994 (100.0%), 353.1028 (19.5%),
354.0952 (4.5%), 354.1061 (1.8%), 353.0964 (1.5%)

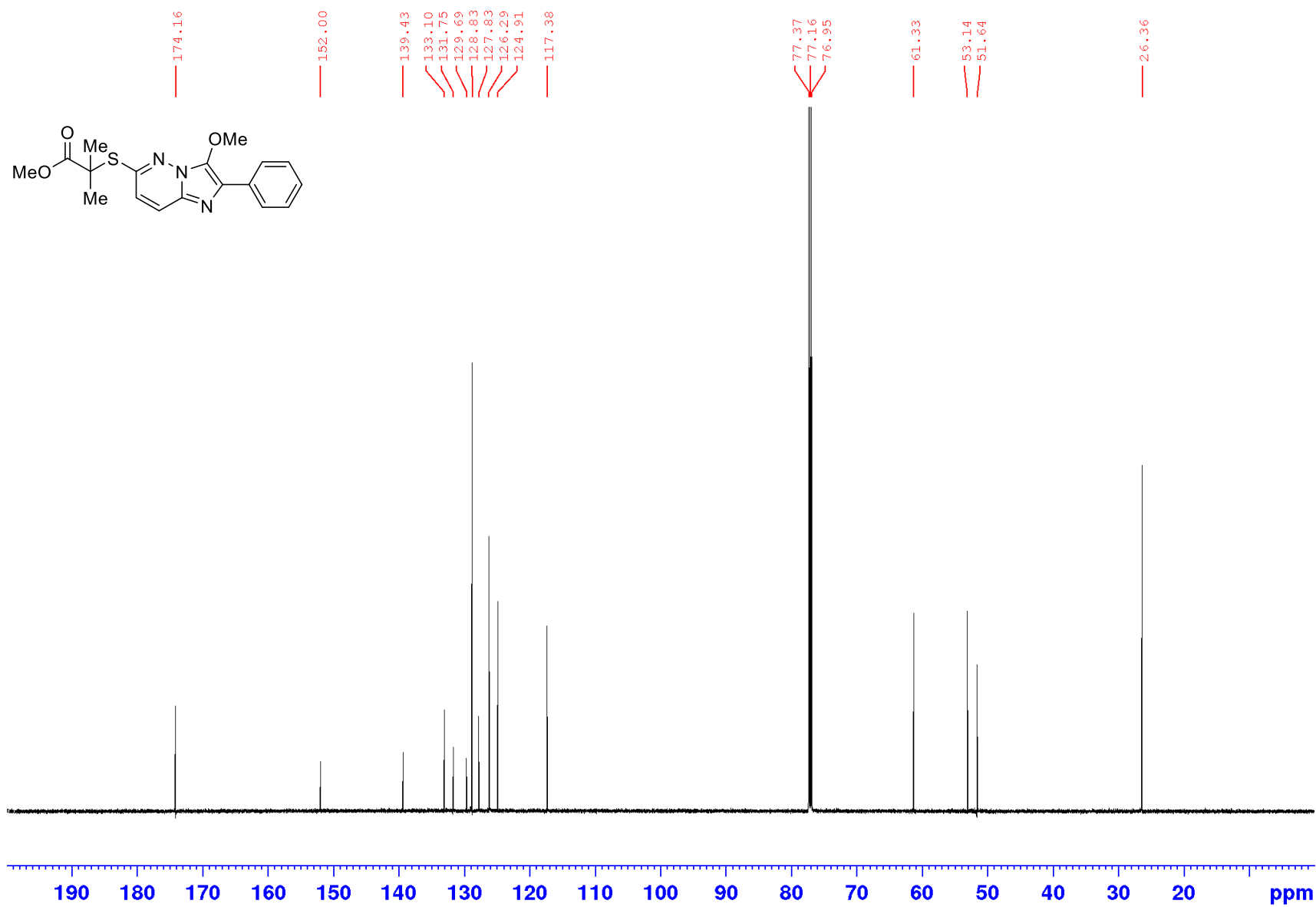
Appendices

¹H NMR spectrum of **158** (600 MHz; CDCl₃)



Appendices

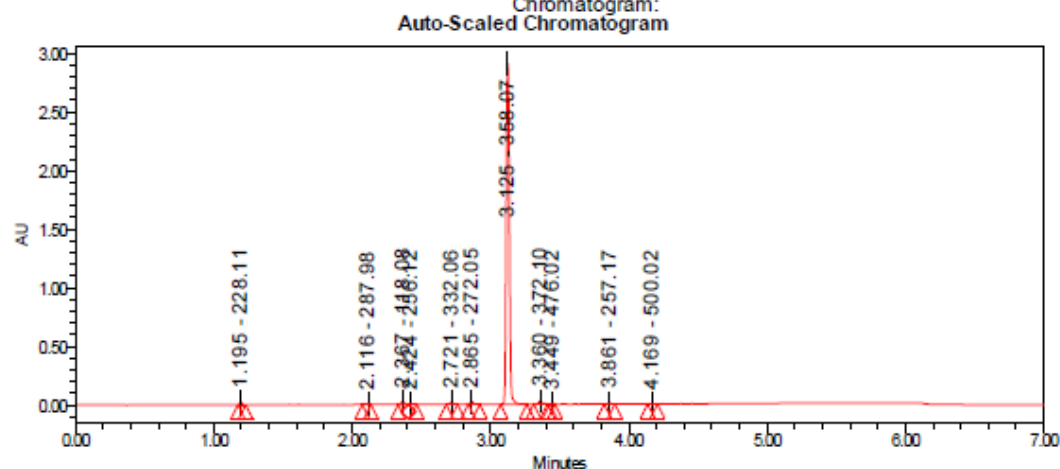
^{13}C NMR spectrum of **158** (150 MHz; CDCl_3)



Appendices

LC-MS chromatogram of **158** [M+H]⁺

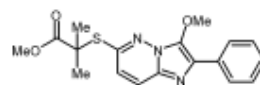
Sample Name:	CF TMIMPZ	Instrument:	Waters Acquity iClass PDA and QDa detectors
Vial:	1:B,4	Acquired By:	System
Injection #:	1	Sample Set Name:	MK_26_April2019
Injection Volume:	0.30 ul	Acquisition Method:	95% A1 to 100% B1
Run Time:	7.0 Minutes	Mobile Phase:	A1: 100% H2O / 0.1% FA B1: 100% ACN / 0.1% FA
Date Acquired:	26/04/2019 2:06:22 PM EST	Extracted	PDA Spectrum PDA 254.0 nm
Date Processed:	26/04/2019 2:41:22 PM EST	Chromatogram:	



Peak Results

	RT	Area	% Area	Height	Base Peak (m/z)
1	1.195	30639	0.62	28330	228.11
2	2.116	5090	0.10	4314	287.98
3	2.367	36693	0.75	27650	118.08
4	2.424	11445	0.23	8532	256.12
5	2.721	30201	0.61	17274	332.06
6	2.865	30278	0.61	24118	272.05
7	3.125	4712711	96.72	2933048	358.07
8	3.360	43818	0.89	27387	372.10
9	3.449	7439	0.15	7048	476.02

	RT	Area	% Area	Height	Base Peak (m/z)
10	3.861	11807	0.24	8848	257.17
11	4.169	3349	0.07	2716	500.02

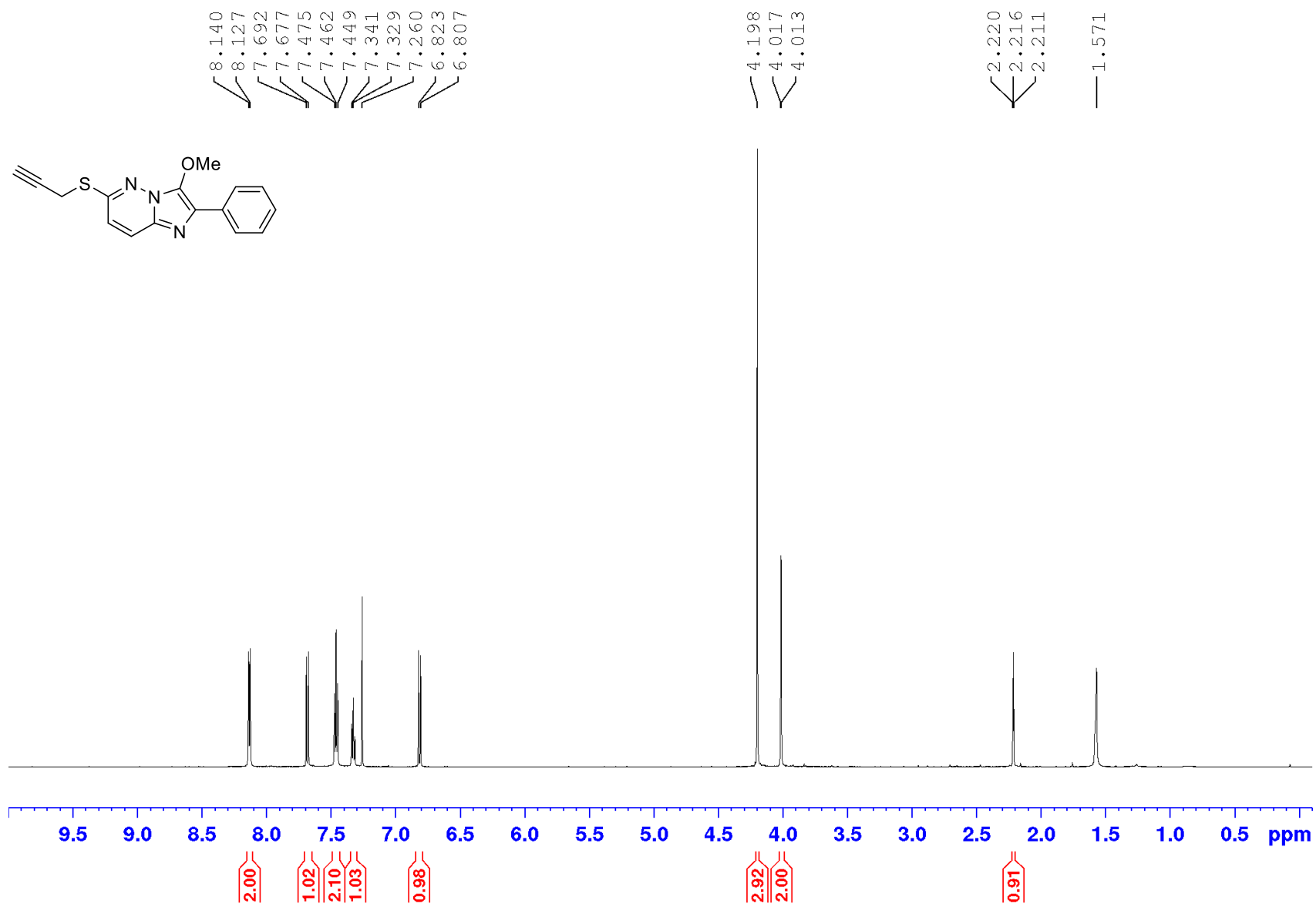


TMIMPZ

Chemical Formula: C₁₃H₁₃N₃O₃S
 Exact Mass: 357.11
 Molecular Weight: 357.43
 m/z: 357.11 (100.0%), 358.12 (19.6%), 359.11 (4.5%),
 359.12 (1.8%), 358.11 (1.1%)

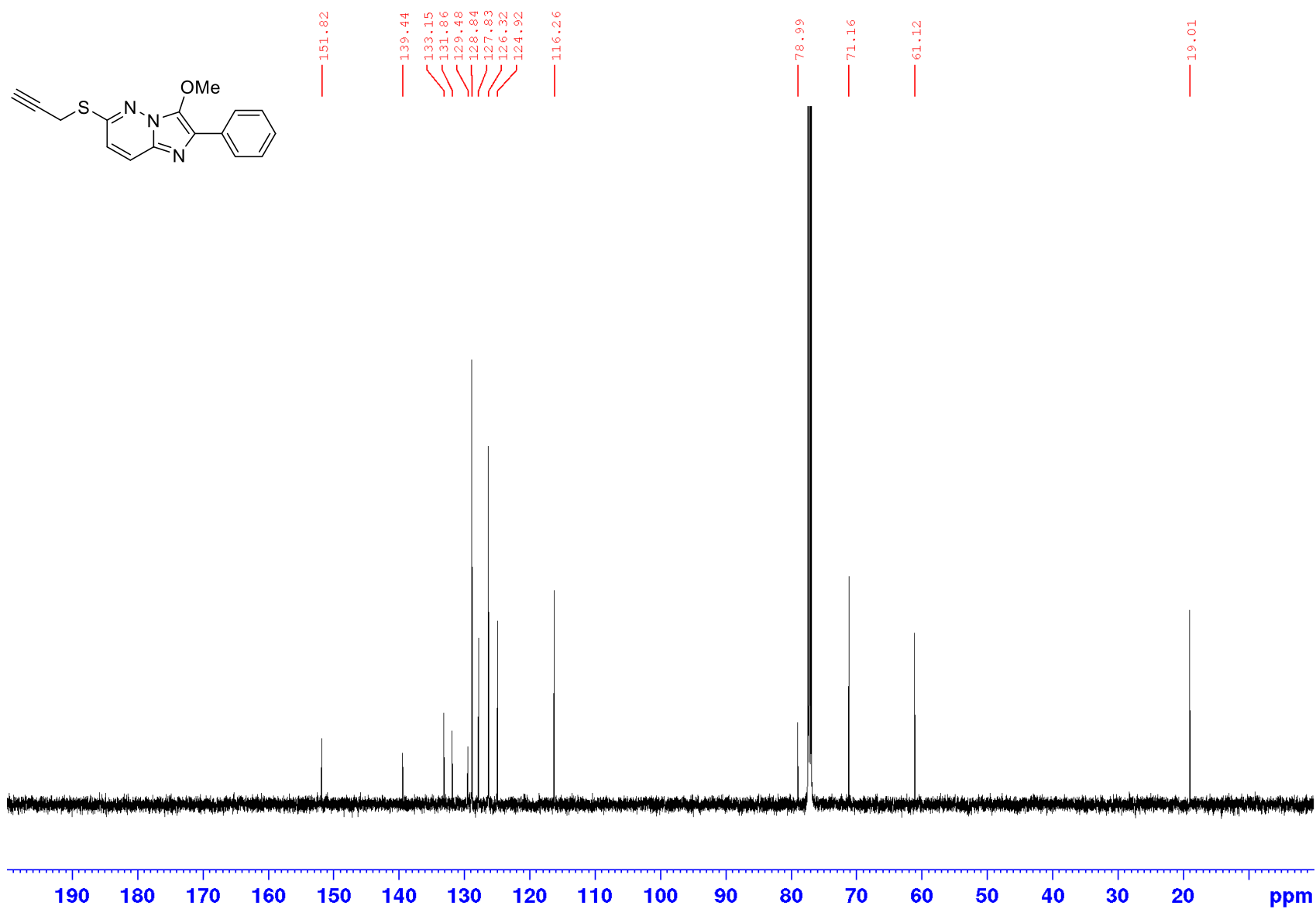
Appendices

¹H NMR spectrum of **160** (600 MHz; CDCl₃)



Appendices

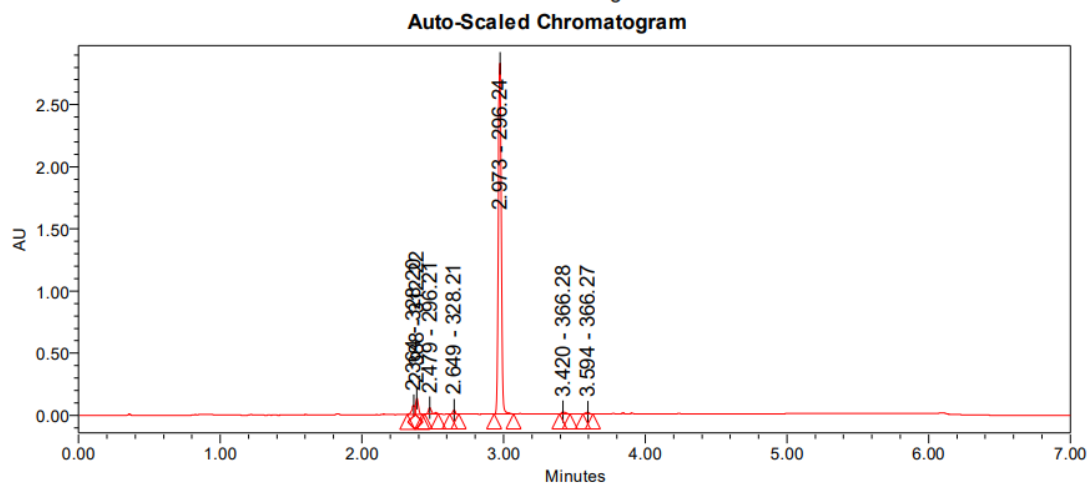
^{13}C NMR spectrum of **160** (150 MHz; CDCl_3)



Appendices

LC-MS chromatogram of **160** [M+H]⁺

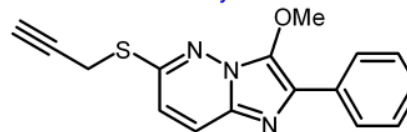
Sample Name:	CLF505-19-Alkyne	Instrument:	Waters Acquity iClass PDA and QDa detectors
Vial:	1:B,2	Acquired By:	System
Injection #:	1	Sample Set Name:	MK_24_January2020
Injection Volume:	1.00 ul	Acquisition Method:	95%A1_100%B1 POSNEGWaters
Run Time:	7.0 Minutes	Mobile Phase:	A1: 100% H2O / 0.1% FA B1: 100% ACN / 0.1% FA
Flowrate:	0.4 mL/min	Extracted Chromatogram:	PDA Spectrum PDA 254.0 nm
Date Acquired:	24/01/2020 11:06:42 AM EST		
Date Processed:	24/01/2020 11:37:25 AM EST		



Peak Results

	RT	Area	% Area	Height	Base Peak (m/z)
1	2.364	113084	2.35	71725	328.20
2	2.388	157521	3.27	129894	312.22
3	2.479	93203	1.94	50267	296.21
4	2.649	38594	0.80	31985	328.21
5	2.973	4351438	90.46	2823470	296.24
6	3.420	33947	0.71	16764	366.28
7	3.594	22336	0.46	12466	366.27

CLF505-19 - Alkyne



Chemical Formula: C₁₆H₁₃N₃OS

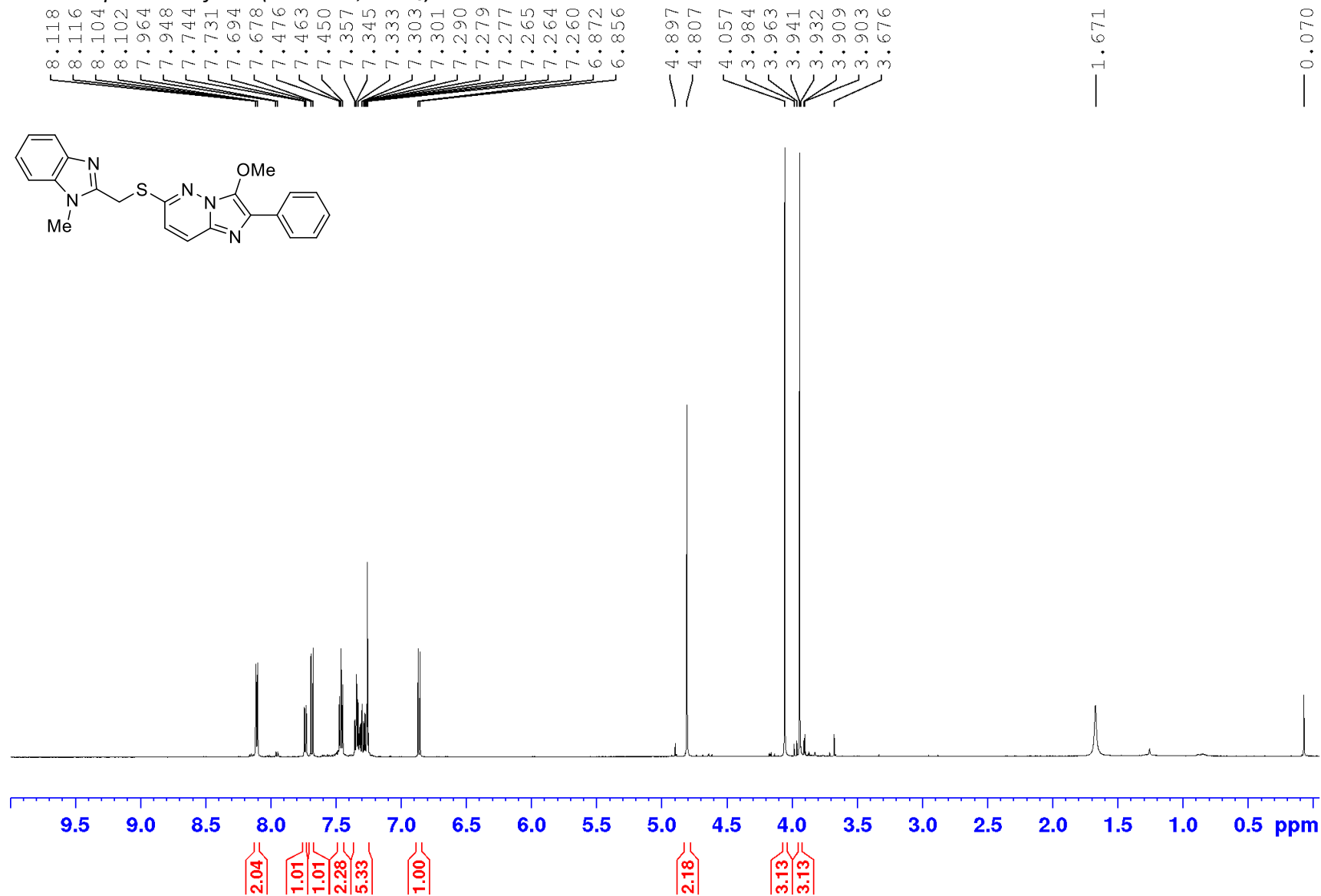
Exact Mass: 295.0779

Molecular Weight: 295.3600

m/z: 295.0779 (100.0%), 296.0813 (17.3%),
297.0737 (4.5%), 297.0846 (1.4%), 296.0750 (1.1%)

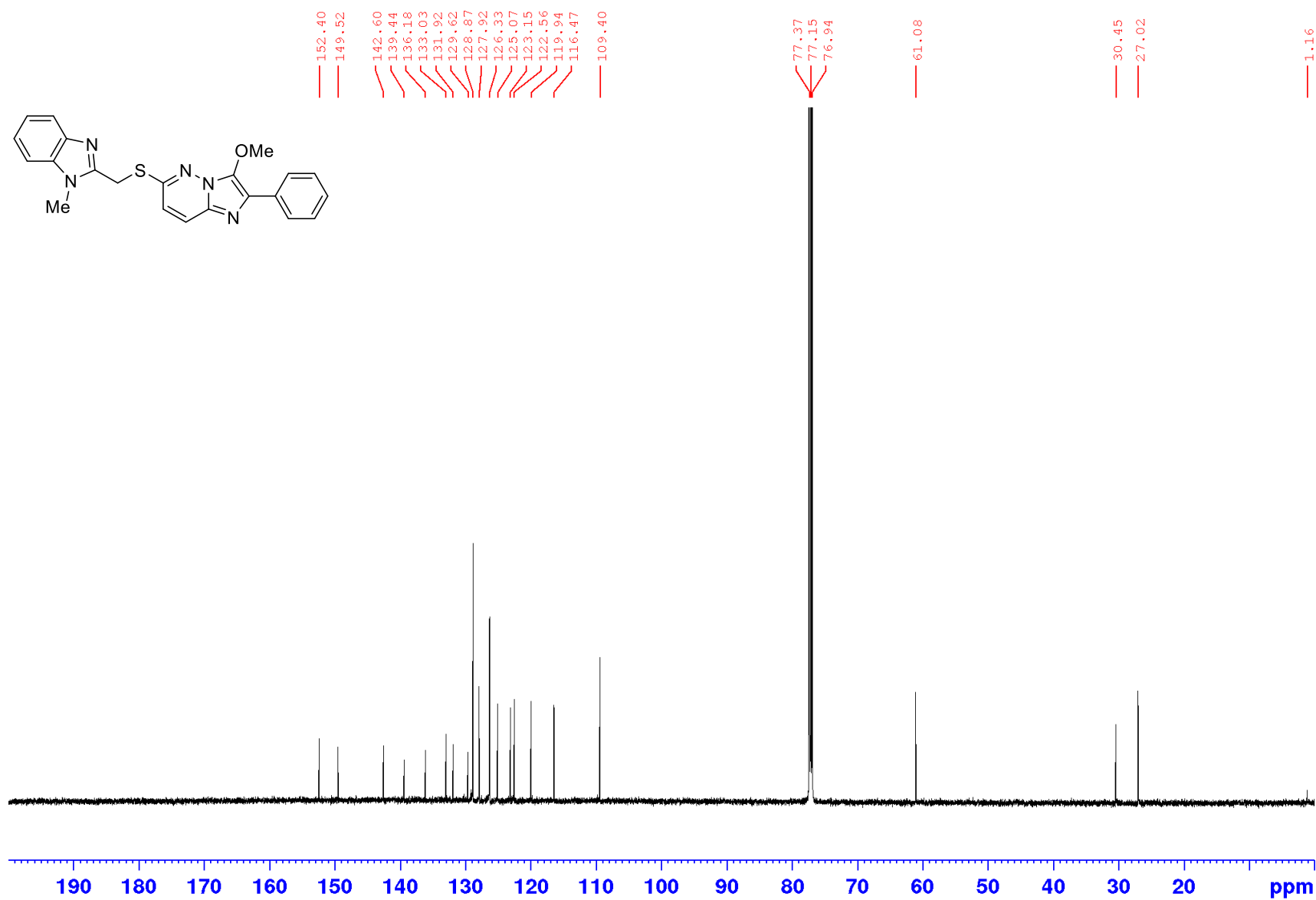
Appendices

¹H NMR spectrum of **171** (600 MHz; CDCl₃)



Appendices

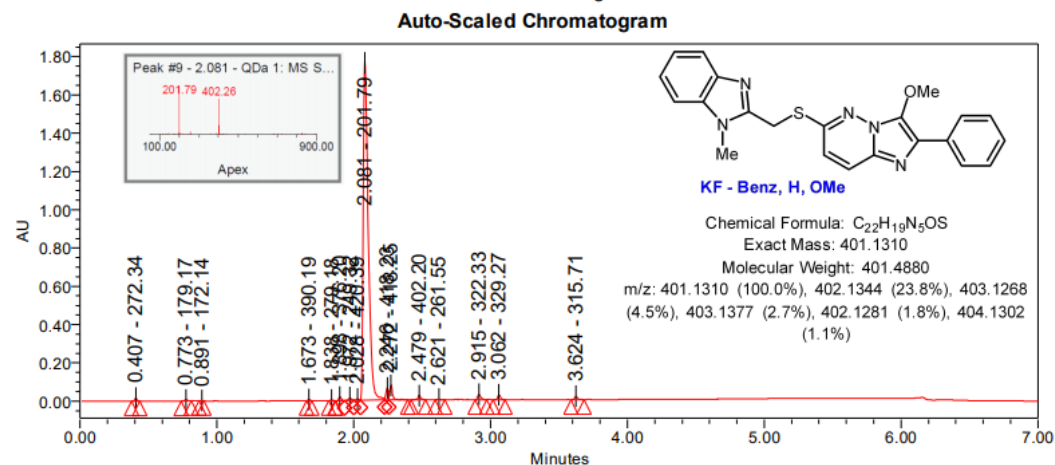
¹³C NMR spectrum of **171** (150 MHz; CDCl₃)



Appendices

LC-MS chromatogram of **171** [M+H]⁺

Sample Name:	KF-Benz, H, OMe	Instrument:	Waters Acquity iClass PDA and QDa detectors
Vial:	1:C,4	Acquired By:	System
Injection #:	1	Sample Set Name:	MK_18_October_2019
Injection Volume:	1.00 ul	Acquisition Method:	95% A1 to 100% B1 POSNEG_Col2
Run Time:	7.0 Minutes	Mobile Phase:	A1: 100% H2O / 0.1% FA B1: 100% MeCN / 0.1% FA
Flowrate:	0.4 mL/min	Extracted Chromatogram:	PDA Spectrum PDA 254.0 nm
Date Acquired:	18/10/2019 3:58:18 PM EST		
Date Processed:	18/10/2019 4:09:04 PM EST		



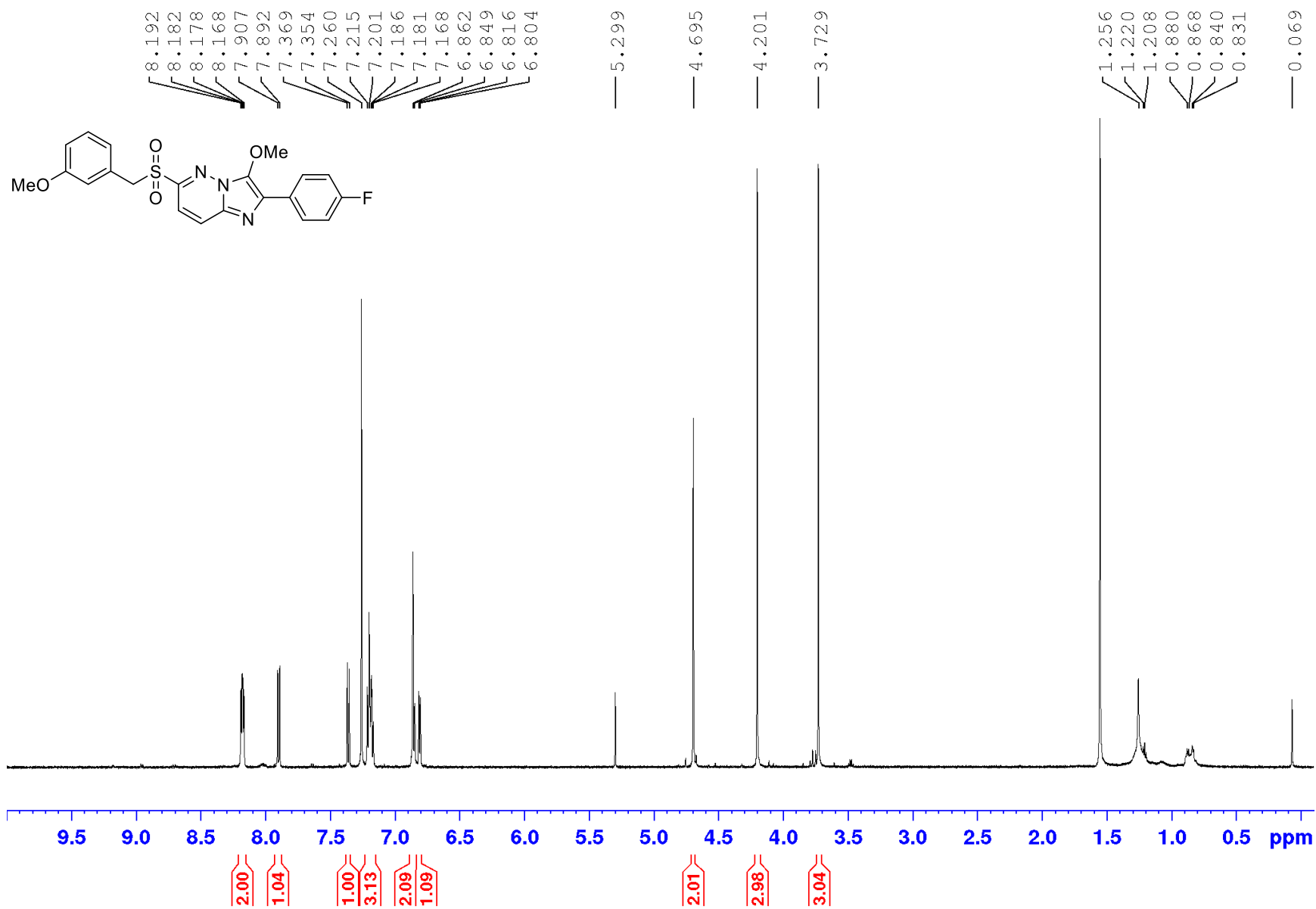
Peak Results

	RT	Area	% Area	Height	Base Peak (m/z)
1	0.407	16258	0.33	15514	272.34
2	0.773	7314	0.15	4921	179.17
3	0.891	1404	0.03	1444	172.14
4	1.673	5495	0.11	5279	390.19
5	1.838	2659	0.05	2362	279.18
6	1.898	22560	0.46	19241	376.20
7	1.972	22401	0.45	14496	249.32
8	2.028	10589	0.21	7628	420.39
9	2.081	4510424	91.45	1778324	201.79

	RT	Area	% Area	Height	Base Peak (m/z)
10	2.246	77782	1.58	62484	418.23
11	2.272	112628	2.28	75635	418.25
12	2.479	32664	0.66	21609	402.20
13	2.621	4576	0.09	3114	261.55
14	2.915	45810	0.93	28023	322.33
15	3.062	35292	0.72	25700	329.27
16	3.624	24320	0.49	17019	315.71

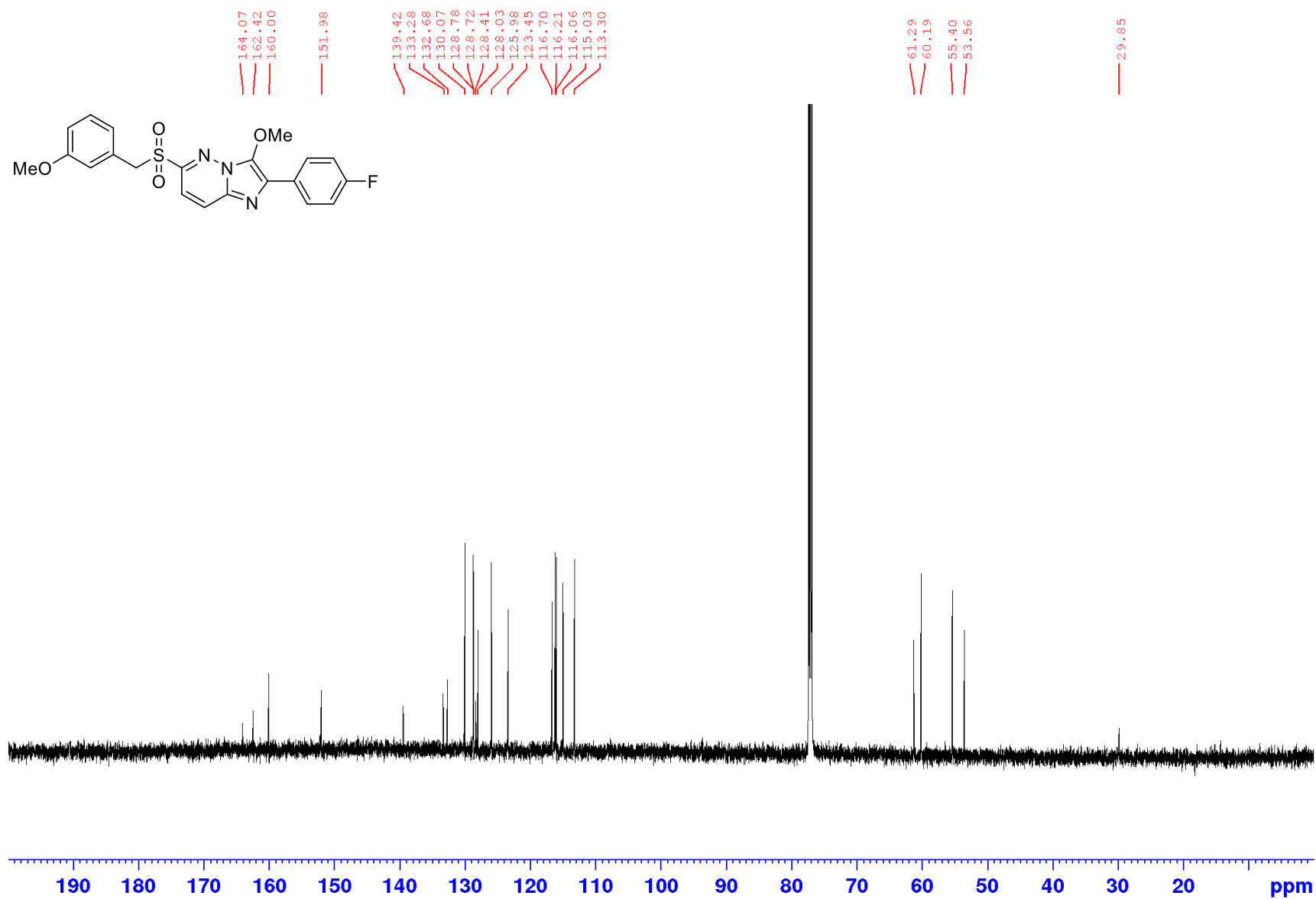
Appendices

¹H NMR spectrum of **174** (600 MHz; CDCl₃)



Appendices

¹³C NMR spectrum of **174** (150 MHz; CDCl₃)

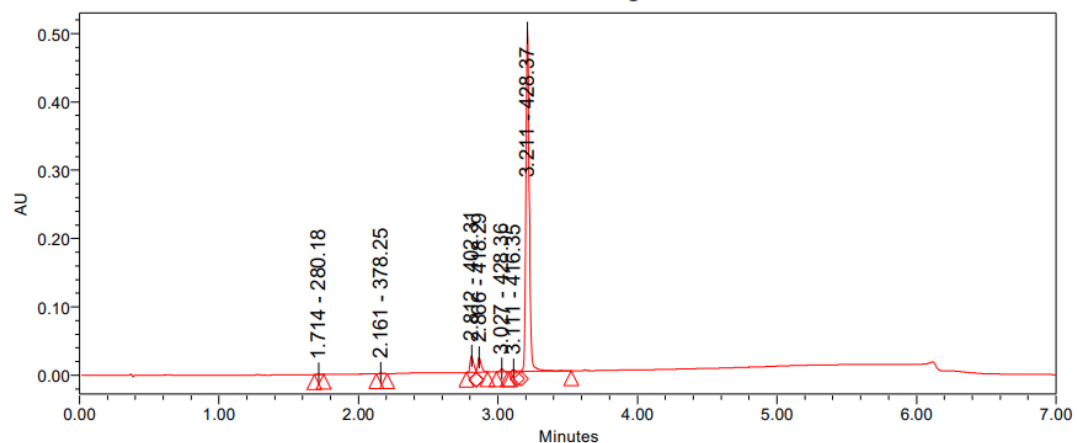


Appendices

LC-MS chromatogram of **174** [M+H]⁺

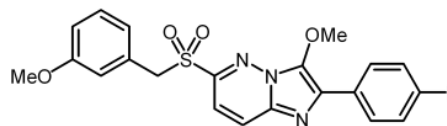
Sample Name:	KF Sulfone 4-F	Instrument:	Waters Acquity iClass PDA and QDa detectors
Vial:	1:C,8	Acquired By:	System
Injection #:	1	Sample Set Name:	MK_15_April2020
Injection Volume:	1.00 ul	Acquisition Method:	95% A1 to 100% B1 POSNEGWaters
Run Time:	7.0 Minutes	Mobile Phase:	A1: 100% H2O / 0.1% FA B1: 100% ACN / 0.1% FA
Date Acquired:	15/04/2020 3:51:11 PM EST	Extracted Chromatogram:	PDA Spectrum PDA 254.0 nm
Date Processed:	15/04/2020 4:04:22 PM EST		

Auto-Scaled Chromatogram



Peak Results

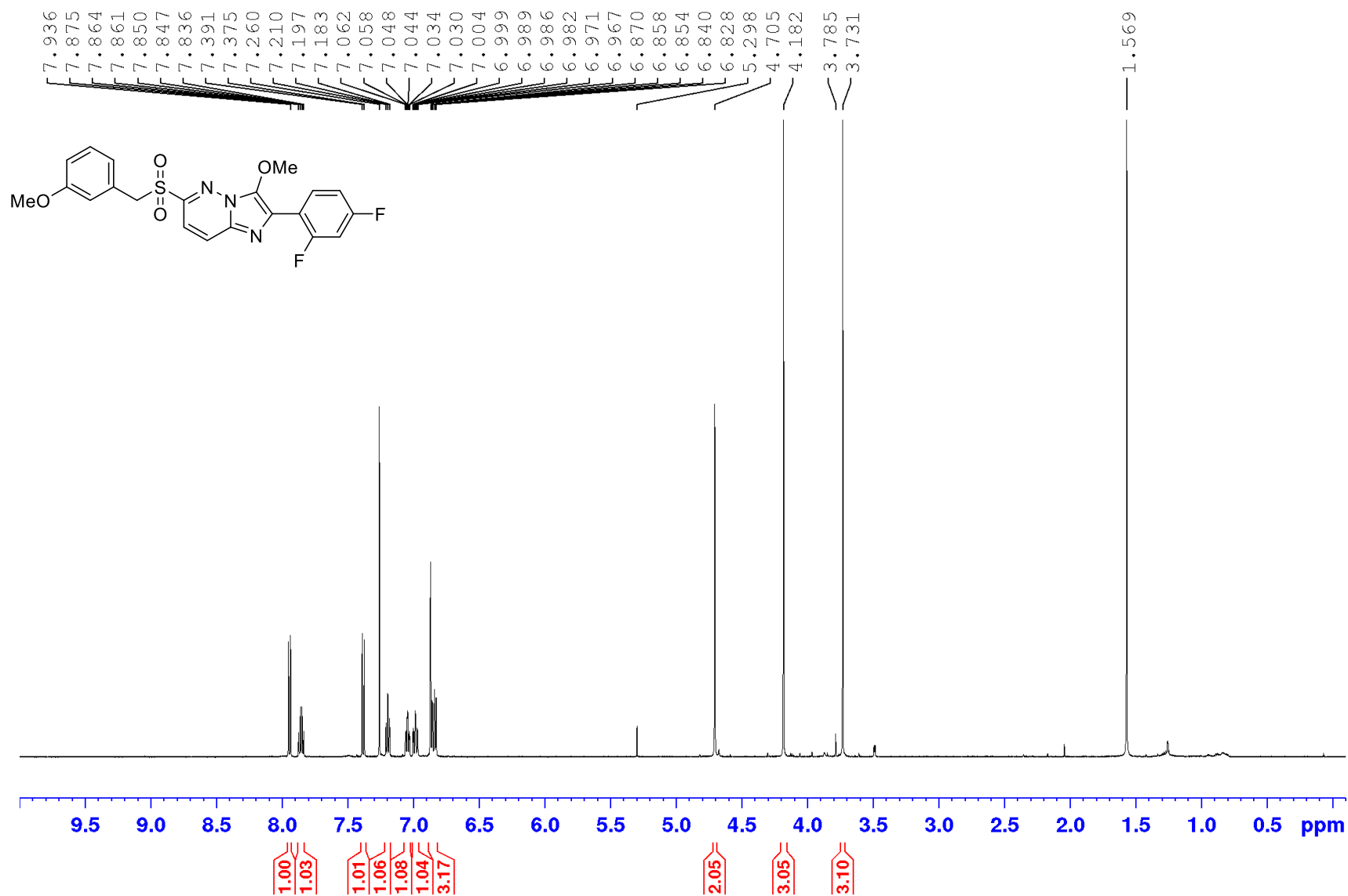
	RT	Area	% Area	Height	Base Peak (m/z)
1	1.714	1665	0.17	1178	280.18
2	2.161	2144	0.23	959	378.25
3	2.812	40990	4.31	24421	402.31
4	2.866	38013	3.99	21488	418.29
5	3.027	7259	0.76	4391	428.36
6	3.111	4698	0.49	2921	416.35
7	3.211	857094	90.04	499264	428.37



Chemical Formula: C₂₁H₁₈FN₃O₄S
 Exact Mass: 427.1002
 Molecular Weight: 427.4504
 m/z: 427.1002 (100.0%), 428.1036 (22.7%),
 429.0960 (4.5%), 429.1069 (2.5%),
 428.0972 (1.1%), 430.0994 (1.0%)

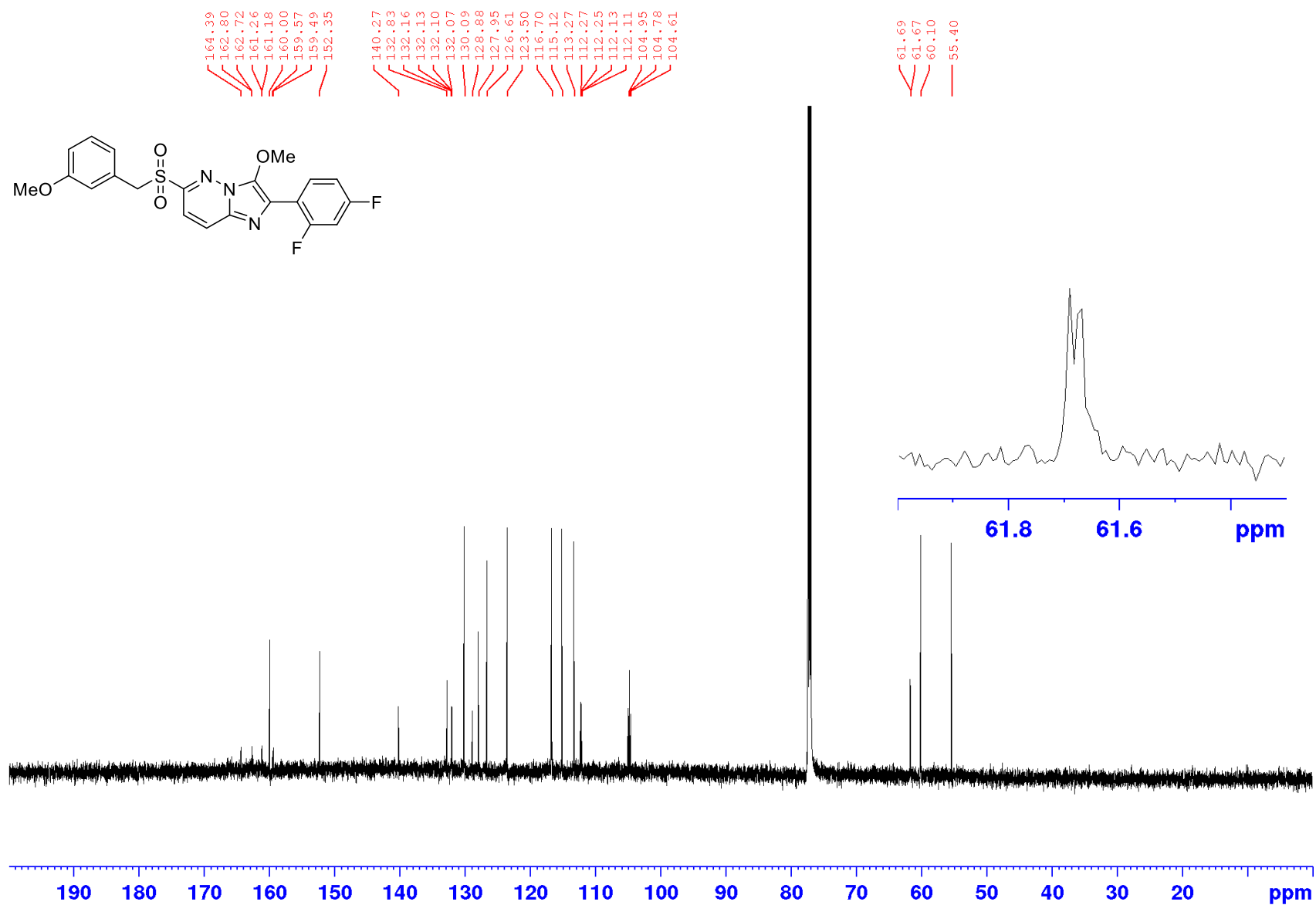
Appendices

¹H NMR spectrum of **175** (600 MHz; CDCl₃)



Appendices

¹³C NMR spectrum of **175** (150 MHz; CDCl₃)

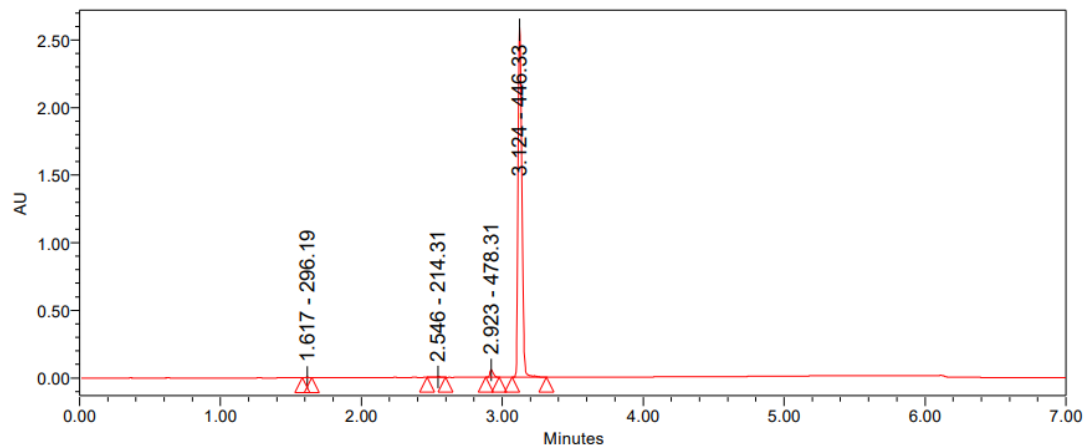


Appendices

LC-MS chromatogram of **175** [M+H]⁺

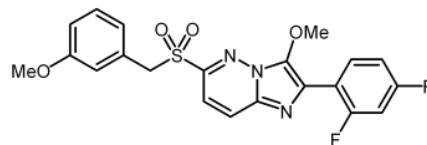
Sample Name: **KF Sulfone 2,4-diF** Instrument: Waters Acquity iClass
 PDA and QDa detectors
 Vial: 1:D,1 Acquired By: System
 Injection #: 1 Sample Set Name: MK_15_April2020
 Injection Volume: 1.00 ul
 Run Time: 7.0 Minutes Acquisition Method: 95% A1 to 100% B1 POSNEGWaters
 Mobile Phase: A1: 100% H2O / 0.1% FA
 B1: 100% ACN / 0.1% FA
 Date Acquired: 15/04/2020 3:59:41 PM EST
 Date Processed: 15/04/2020 4:10:05 PM EST
 Extracted Chromatogram: PDA Spectrum PDA 254.0 nm

Auto-Scaled Chromatogram



Peak Results

	RT	Area	% Area	Height	Base Peak (m/z)
1	1.617	6815	0.14	4385	296.19
2	2.546	11120	0.23	5404	214.31
3	2.923	95868	1.97	55358	478.31
4	3.124	4746080	97.66	2591679	446.33



Chemical Formula: C₂₁H₁₇F₂N₃O₄S

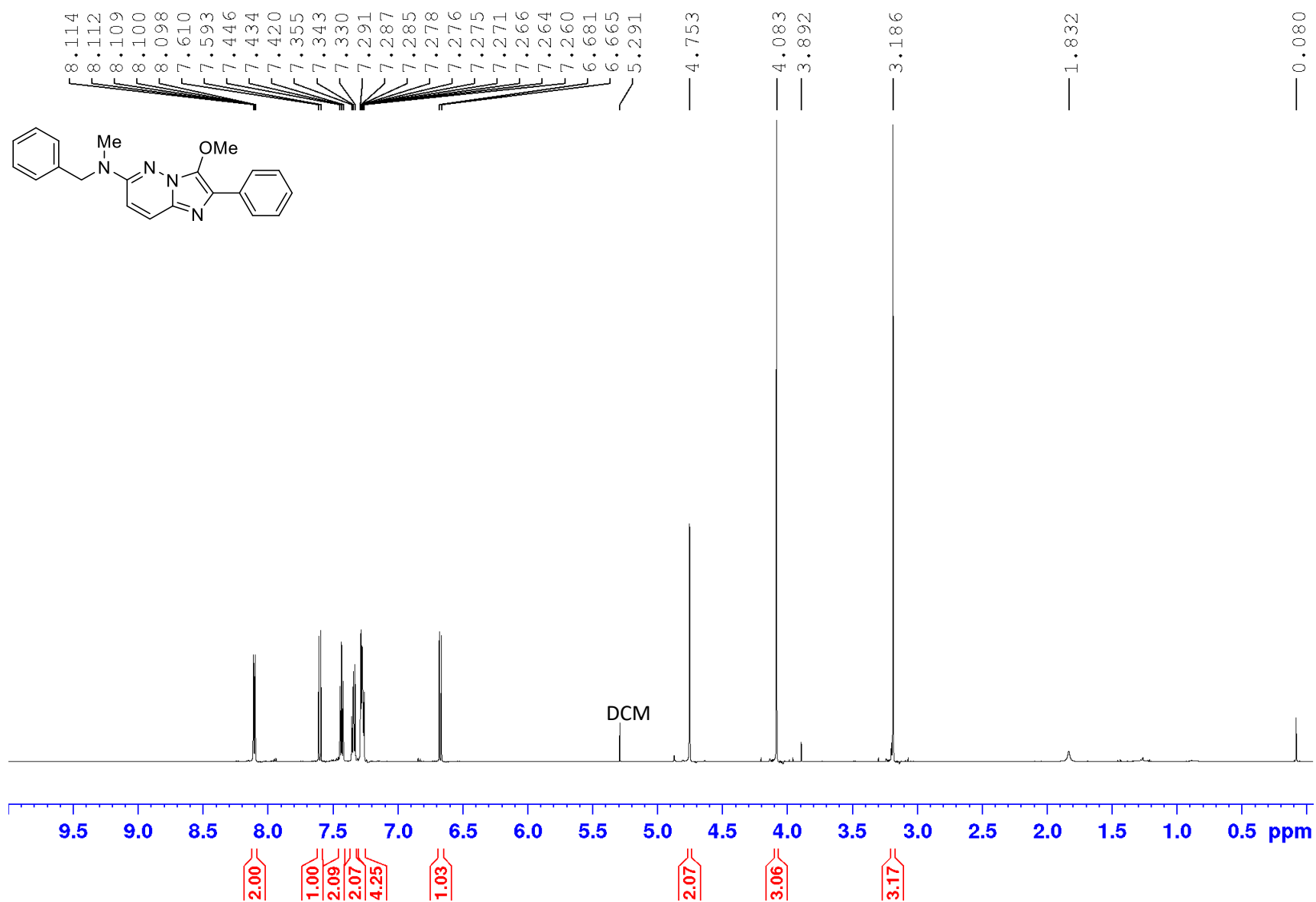
Exact Mass: 445.0908

Molecular Weight: 445.4408

m/z: 445.0908 (100.0%), 446.0941 (22.7%), 447.0866 (4.5%),
447.0975 (2.5%), 446.0878 (1.1%), 448.0899 (1.0%)

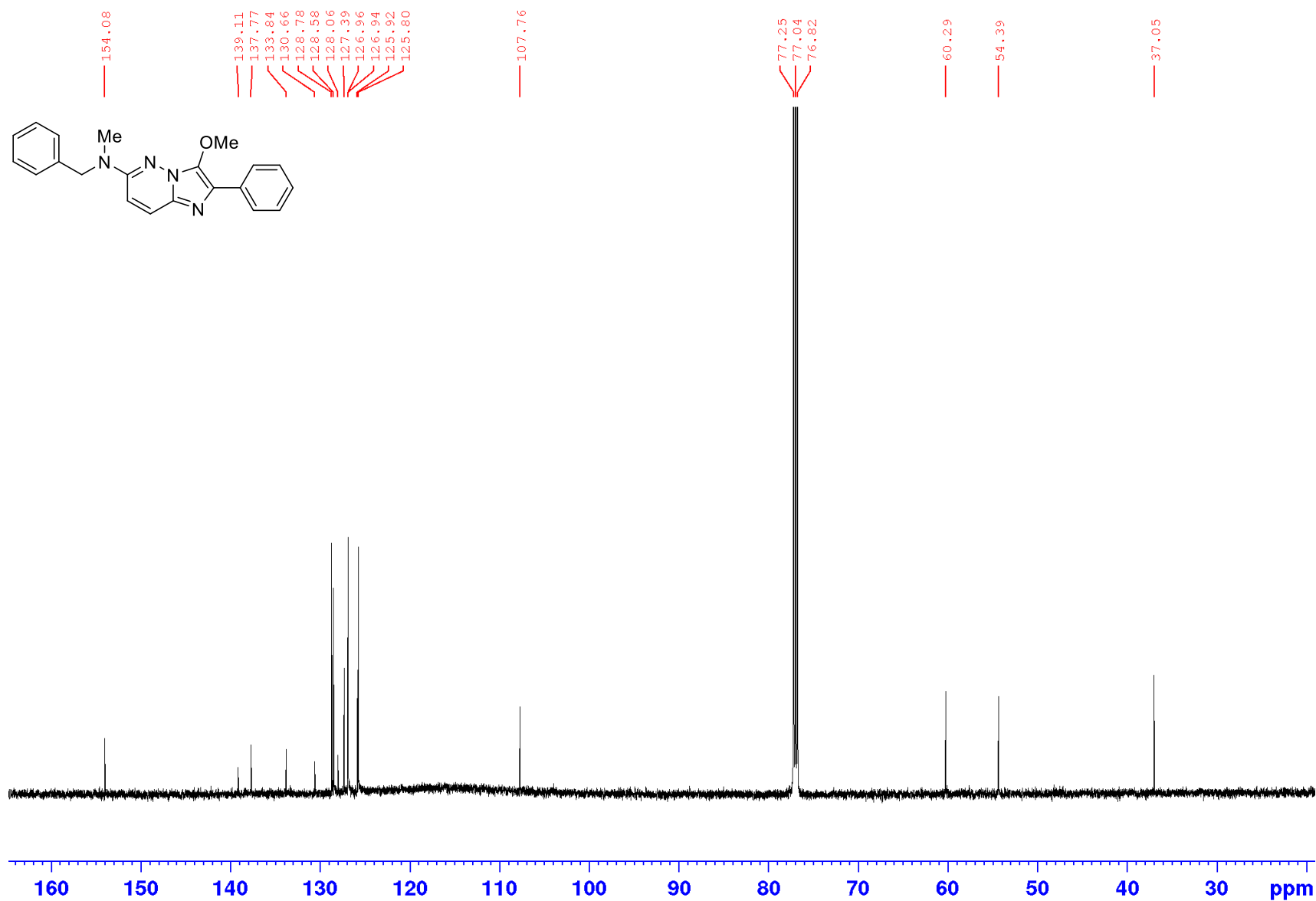
Appendices

¹H NMR spectrum of **18** (600 MHz; CDCl₃)



Appendices

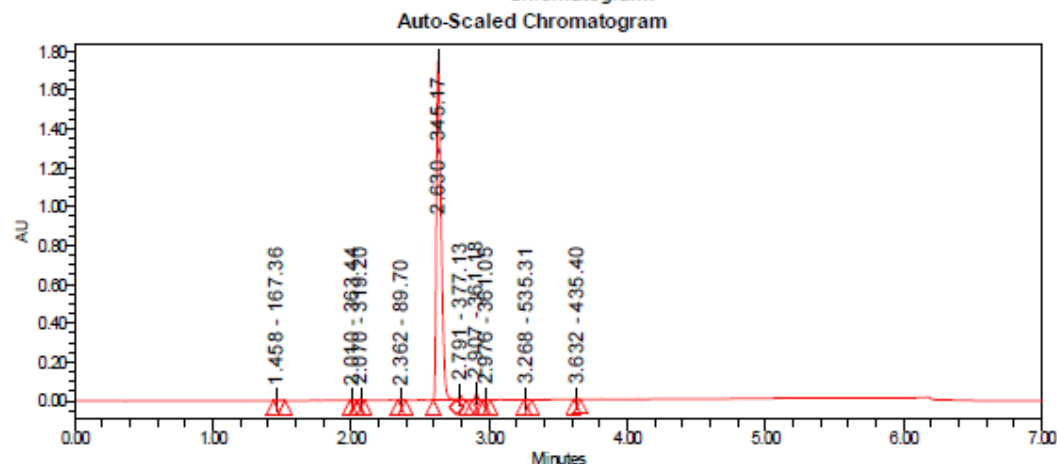
^{13}C NMR spectrum of **18** (150 MHz; CDCl_3)



Appendices

LC-MS chromatogram of **18** [M+H]⁺

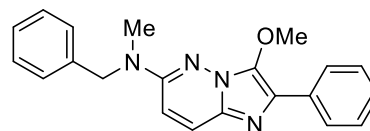
Sample Name:	IMPZ 15	Instrument:	Waters Acquity iClass PDA and QDa detectors
Vial:	1:B,1	Acquired By:	System
Injection #:	1	Sample Set Name:	MK_10_July2018
Injection Volume:	0.50 ul	Acquisition Method:	95% A1 to 100% B1 POSNEG
Run Time:	7.0 Minutes	Mobile Phase:	A1: 100% H2O / 0.1% FA B1: 100% ACN / 0.1% FA
Flowrate:	0.4 mL/min	Extracted Chromatogram:	PDA Spectrum PDA 254.0 nm
Date Acquired:	10/07/2018 2:25:50 PM EST		
Date Processed:	10/07/2018 3:02:02 PM EST		



Peak Results

	RT	Area	% Area	Height	Base Peak (m/z)
1	1.458	8647	0.20	4980	167.36
2	2.010	4842	0.11	4148	363.44
3	2.070	9441	0.22	7963	319.20
4	2.362	5128	0.12	3482	89.70
5	2.630	4139431	97.38	1744062	345.17
6	2.791	32745	0.77	24178	377.13
7	2.907	40499	0.96	31808	361.18
8	2.978	2357	0.06	2029	361.05
9	3.268	2488	0.06	1928	535.31

	RT	Area	% Area	Height	Base Peak (m/z)
10	3.632	5403	0.13	4066	435.40



Chemical Formula: C₂₁H₂₀N₄O

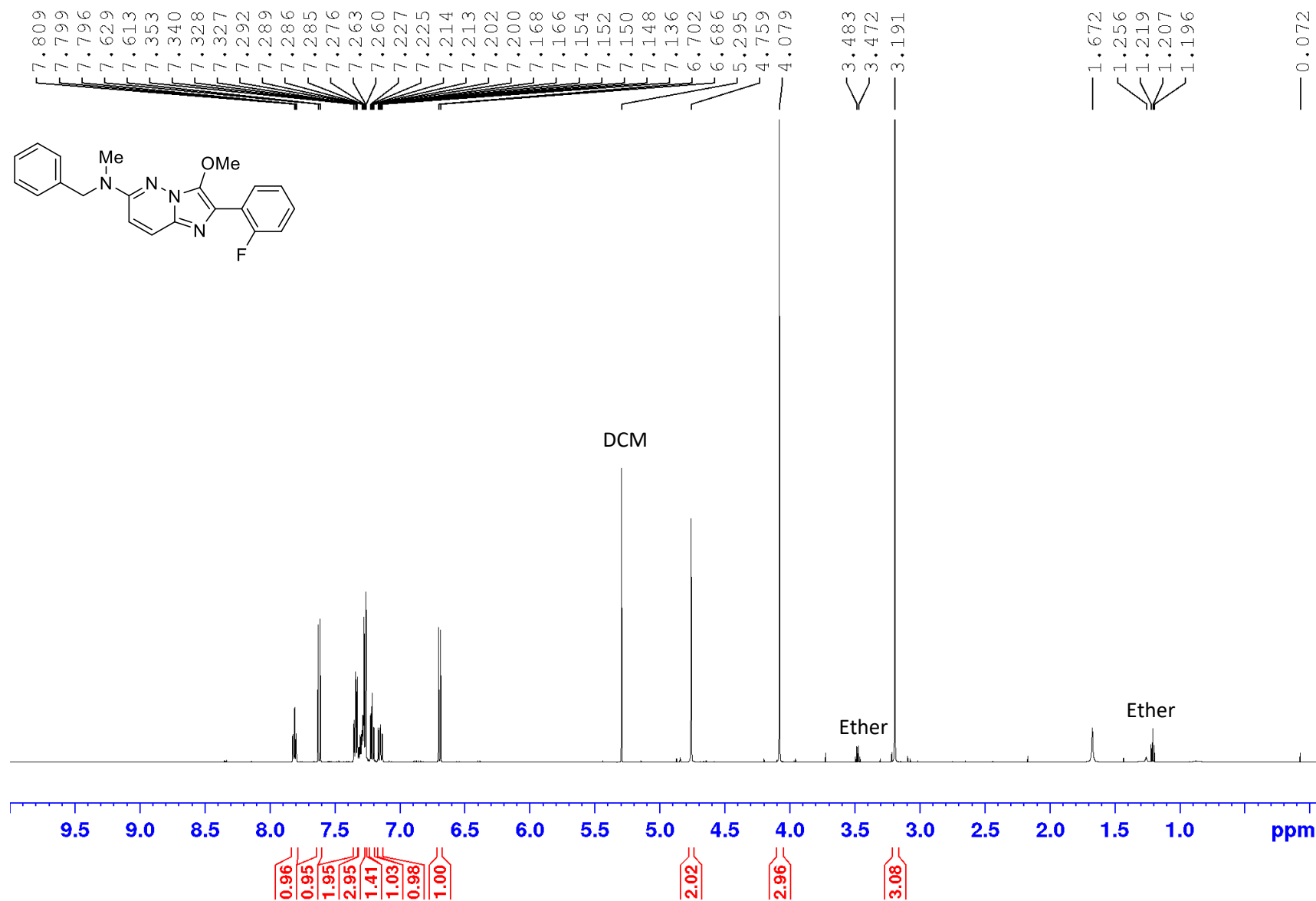
Exact Mass: 344.1637

Molecular Weight: 344.4180

m/z: 344.1637 (100.0%), 345.1671 (22.7%),
327346.1704 (2.5%), 345.1607 (1.5%)

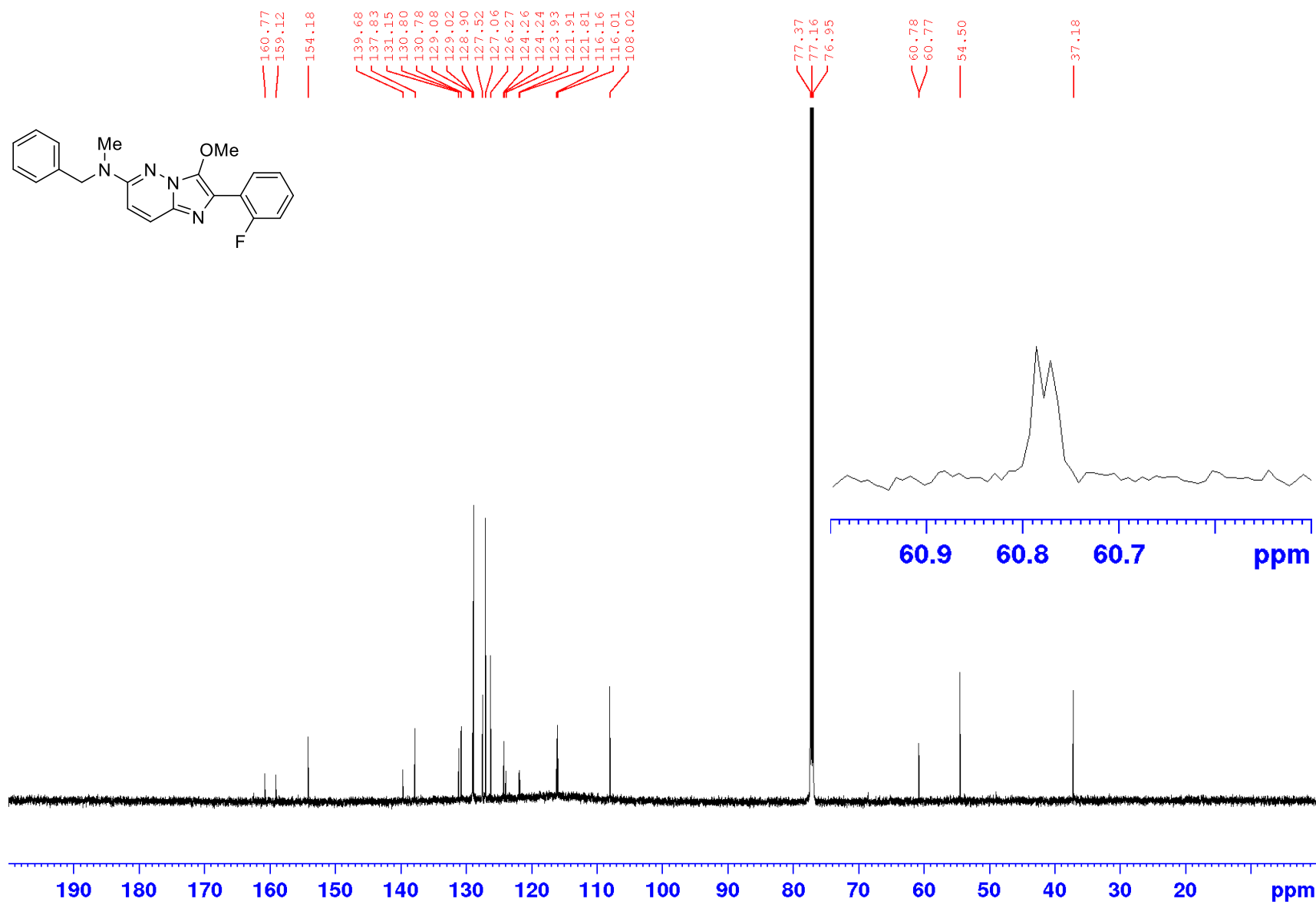
Appendices

¹H NMR spectrum of **190b** (600 MHz; CDCl₃)



Appendices

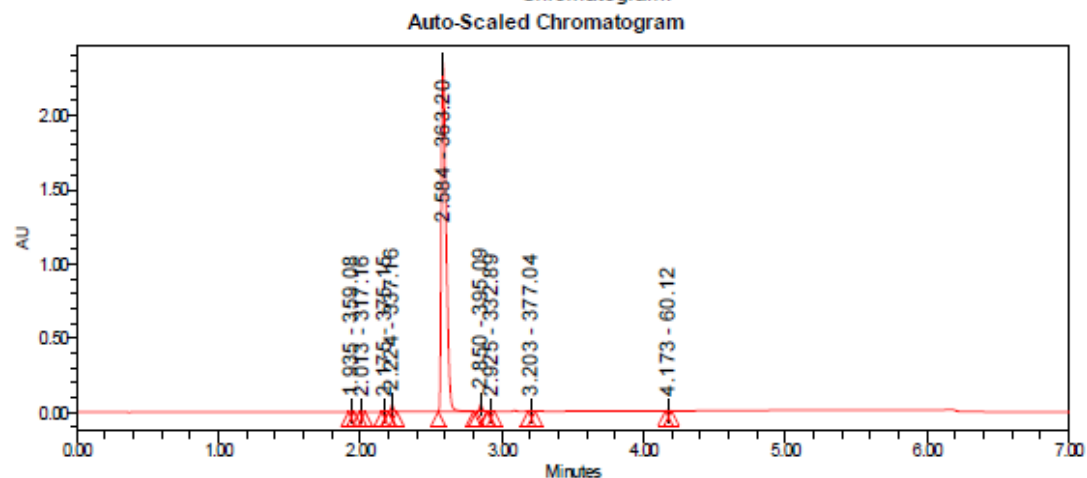
¹³C NMR spectrum of **190b** (150 MHz; CDCl₃)



Appendices

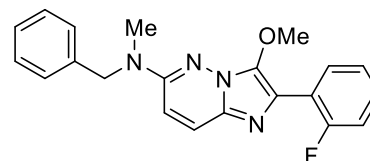
LC-MS chromatogram of **190b** [M+H]⁺

Sample Name:	IMPZ 16	Instrument:	Waters Acquity iClass PDA and QDa detectors
Vial:	1:B,2	Acquired By:	System
Injection #:	1	Sample Set Name:	MK_10_July2018
Injection Volume:	0.50 ul	Acquisition Method:	95% A1 to 100% B1 POSNEG
Run Time:	7.0 Minutes	Mobile Phase:	A1: 100% H2O / 0.1% FA B1: 100% ACN / 0.1% FA
Flowrate:	0.4 mL/min	Extracted	PDA Spectrum PDA 254.0 nm
Date Acquired:	10/07/2018 2:34:18 PM EST	Chromatogram:	
Date Processed:	10/07/2018 3:03:13 PM EST		



Peak Results

	RT	Area	% Area	Height	Base Peak (m/z)
1	1.895	2724	0.05	2384	369.08
2	2.013	3912	0.07	3586	317.16
3	2.175	5043	0.09	4457	375.15
4	2.224	55998	1.01	46483	337.16
5	2.584	5397866	97.50	2354648	363.20
6	2.850	60705	1.10	47457	365.09
7	2.925	3606	0.07	2872	332.89
8	3.203	4301	0.08	3618	377.04
9	4.173	2374	0.04	2004	60.12



Chemical Formula: C₂₁H₁₉FN₄O

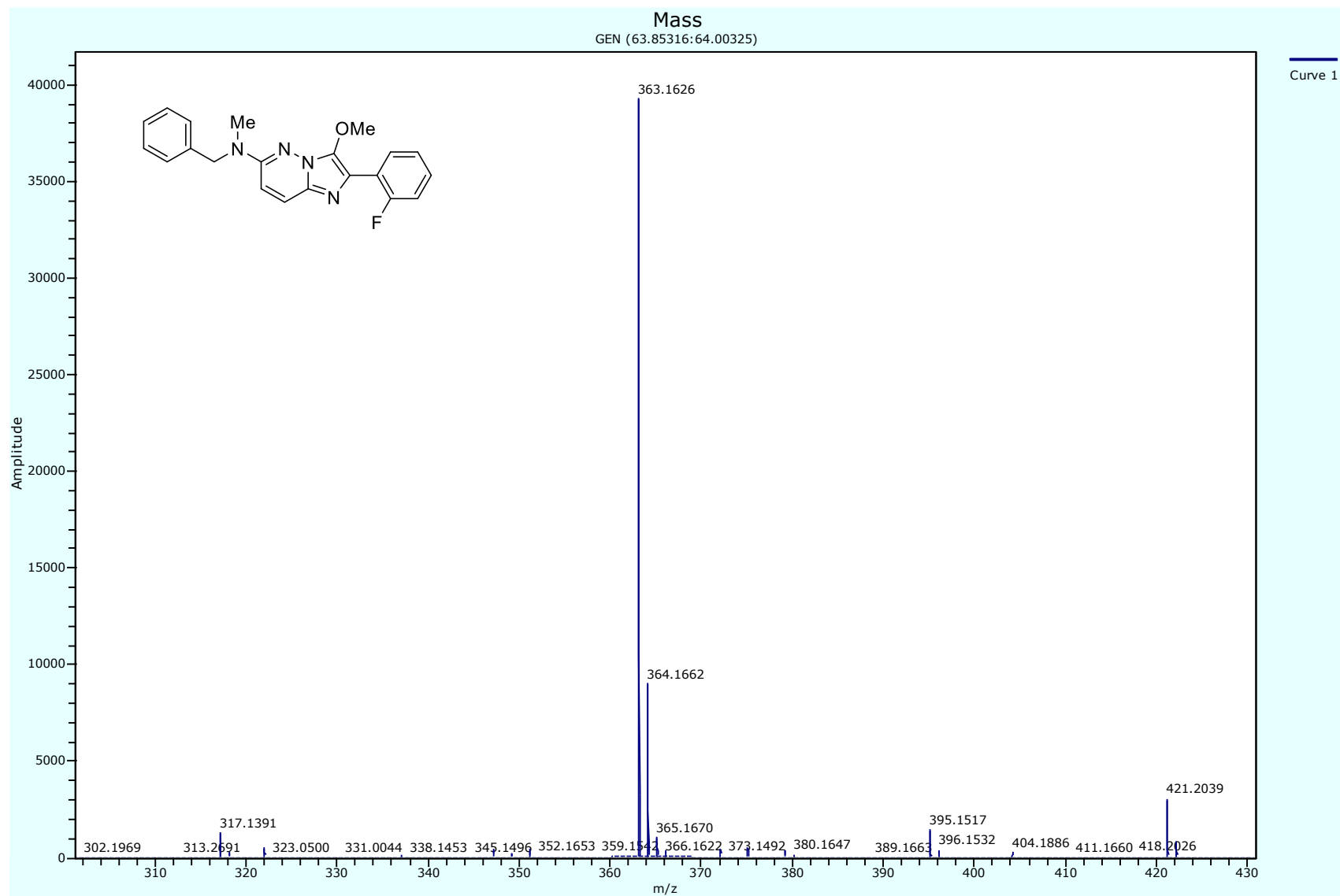
Exact Mass: 362.1543

Molecular Weight: 362.4084

m/z: 362.1543 (100.0%), 363.1576 (22.7%),
364.1610 (2.5%), 363.1513 (1.5%)

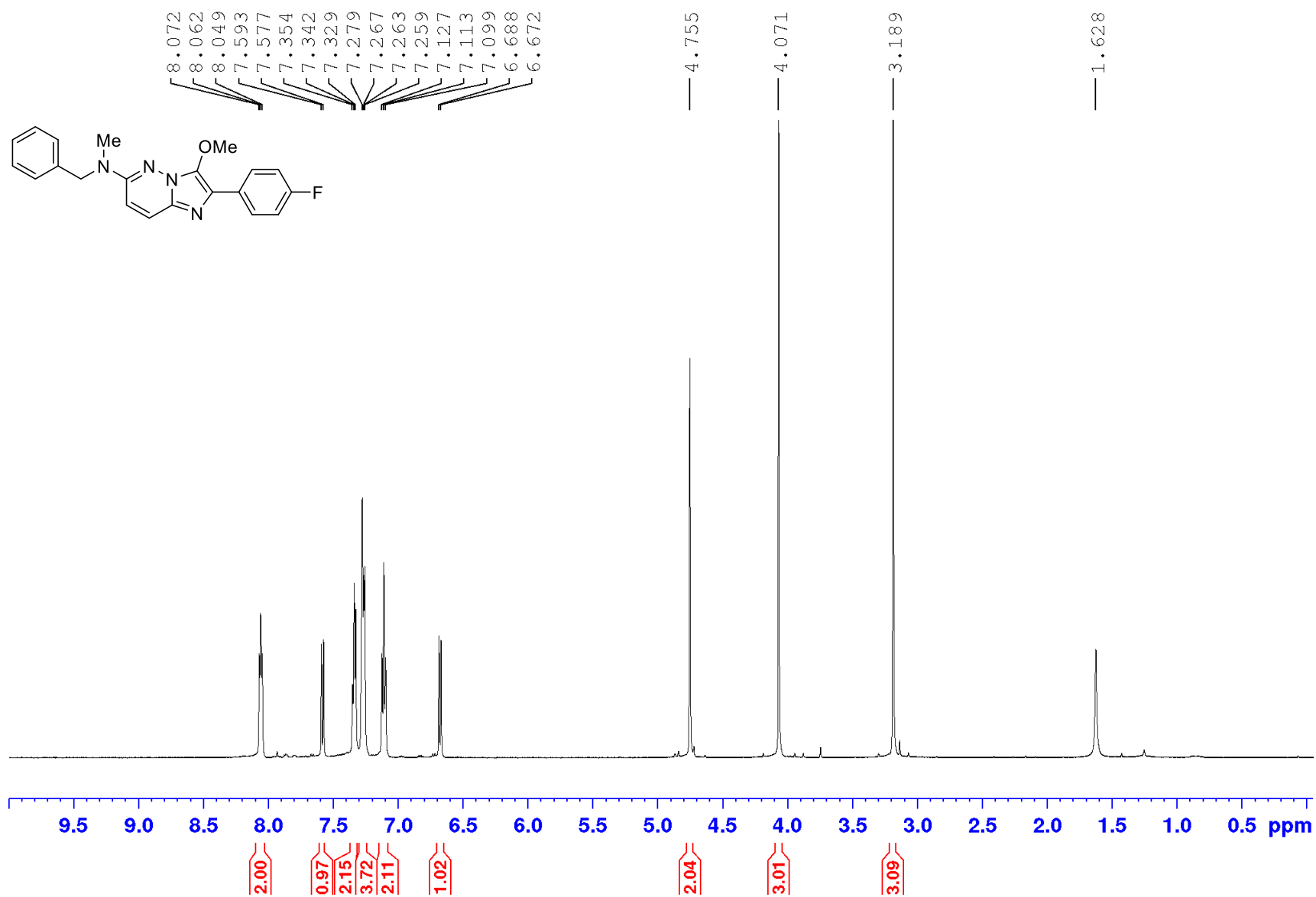
Appendices

HRMS (APCI) spectrum of **190b** $[M+H]^+$



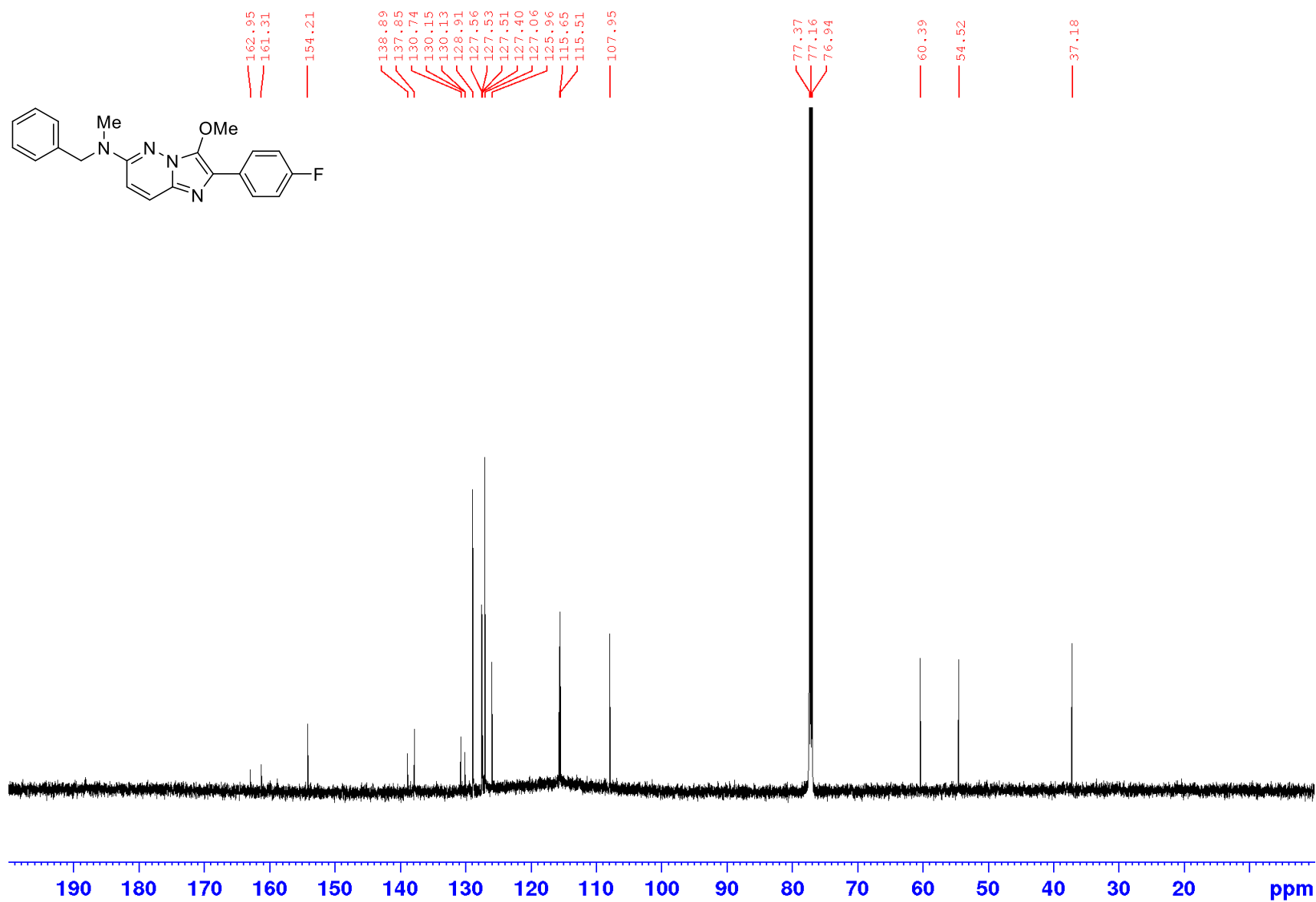
Appendices

¹H NMR spectrum of **190c** (600 MHz; CDCl₃)



Appendices

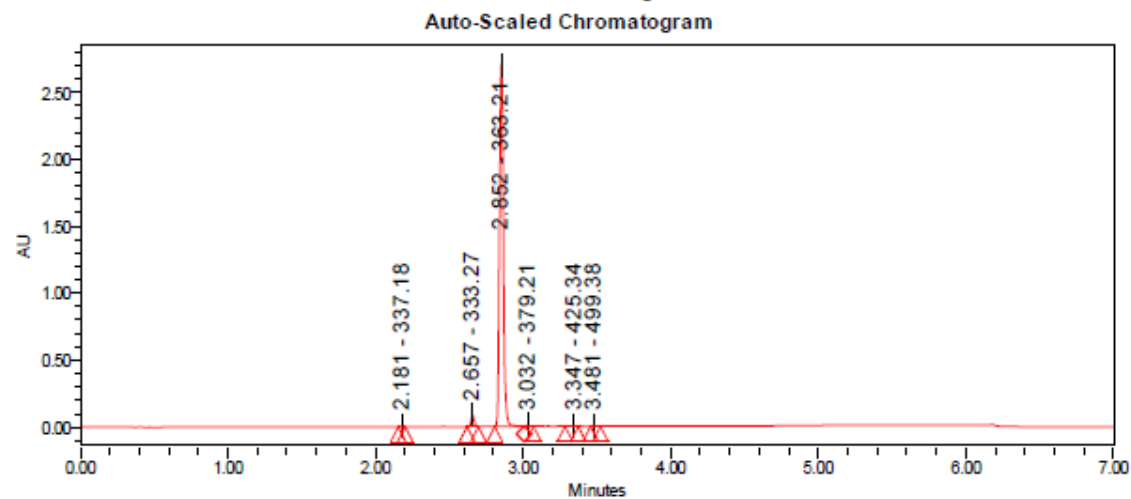
^{13}C NMR spectrum of **190c** (150 MHz; CDCl_3)



Appendices

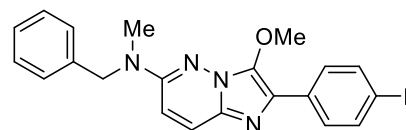
LC-MS chromatogram of **190c** [M+H]⁺

Sample Name:	IMPZ 19	Instrument:	Waters Acquity iClass PDA and QDa detectors
Vial:	1:B,5	Acquired By:	System
Injection #:	1	Sample Set Name:	MK_10_July2018
Injection Volume:	0.50 ul	Acquisition Method:	95% A1 to 100% B1 POSNEG
Run Time:	7.0 Minutes	Mobile Phase:	A1: 100% H2O / 0.1% FA B1: 100% ACN / 0.1% FA
Flowrate:	0.4 mL/min	Extracted Chromatogram:	PDA Spectrum PDA 254.0 nm
Date Acquired:	10/07/2018 3:08:17 PM EST		
Date Processed:	10/07/2018 3:19:28 PM EST		



Peak Results

	RT	Area	% Area	Height	Base Peak (m/z)
1	2.181	5452	0.11	4799	337.18
2	2.657	112483	2.20	85606	333.27
3	2.852	4964077	97.28	2714761	363.21
4	3.032	12568	0.25	8837	379.21
5	3.347	3769	0.07	1531	425.34
6	3.481	4424	0.09	3243	499.38

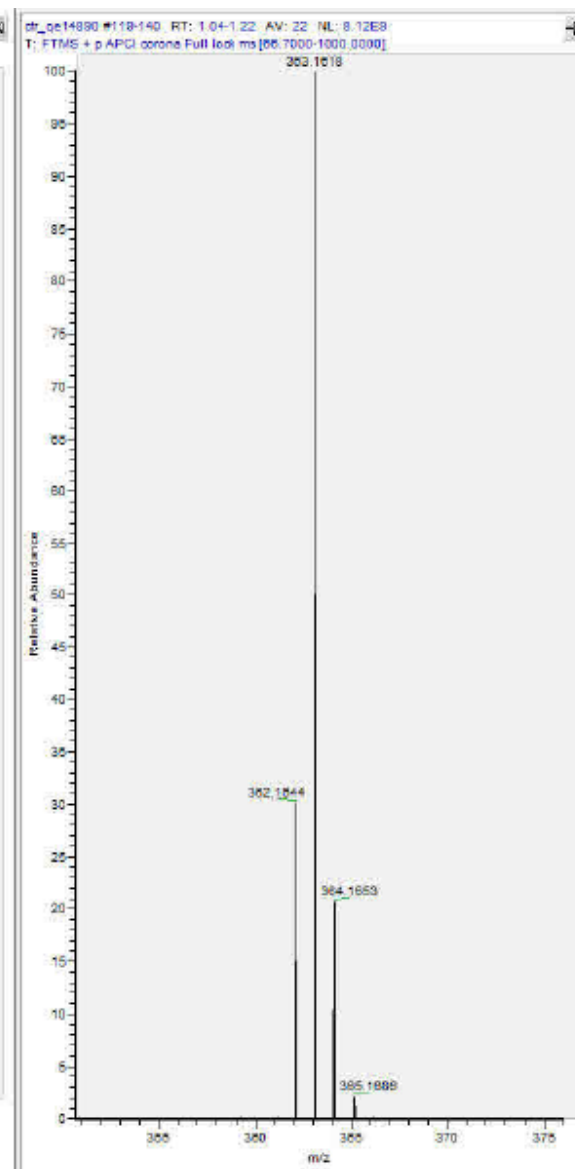
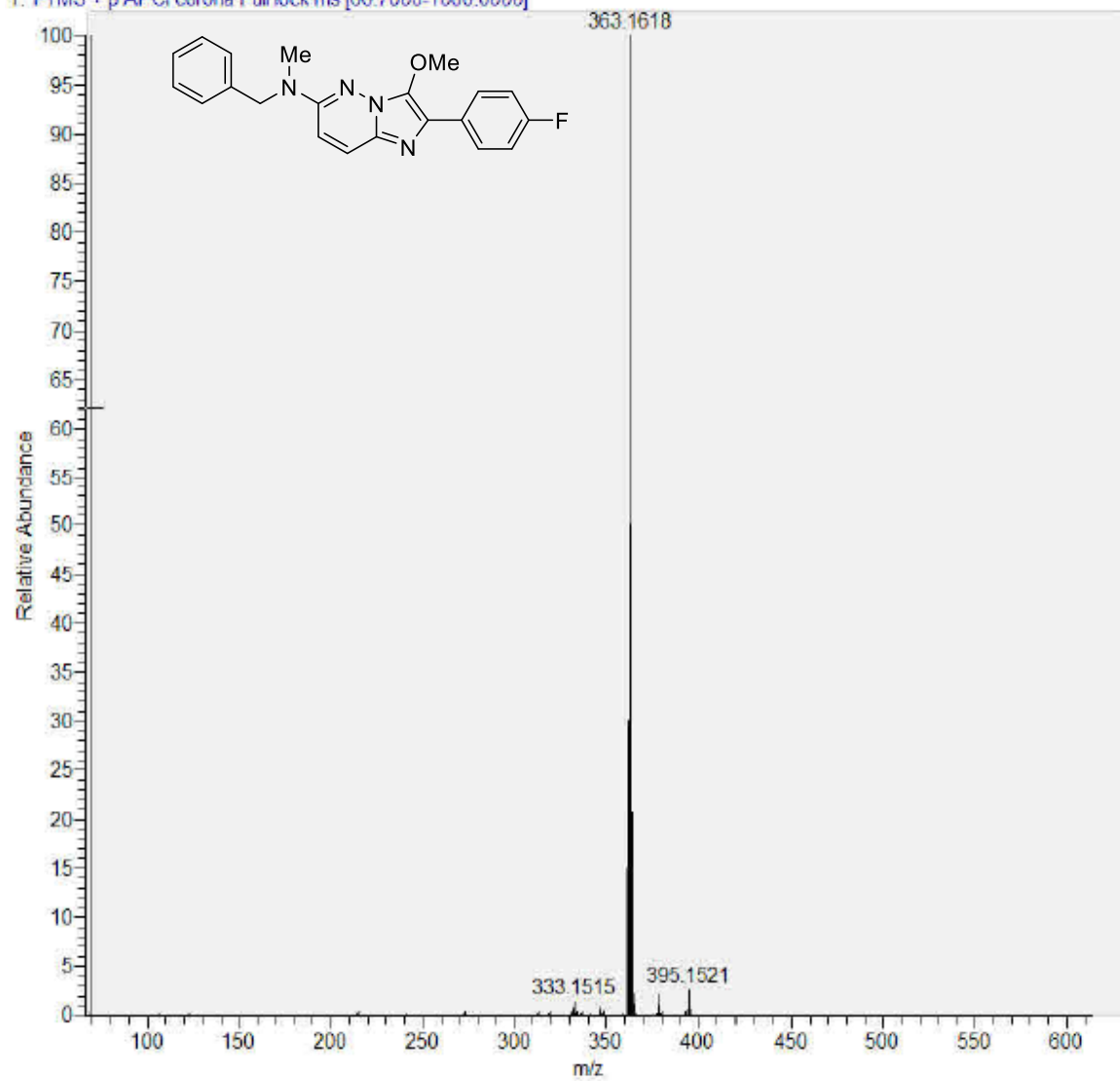


Chemical Formula: C₂₁H₁₉FN₄O
 Exact Mass: 362.1543
 Molecular Weight: 362.4084
 m/z: 362.1543 (100.0%), 363.1576 (22.7%),
 364.1610 (2.5%), 363.1513 (1.5%)

Appendices

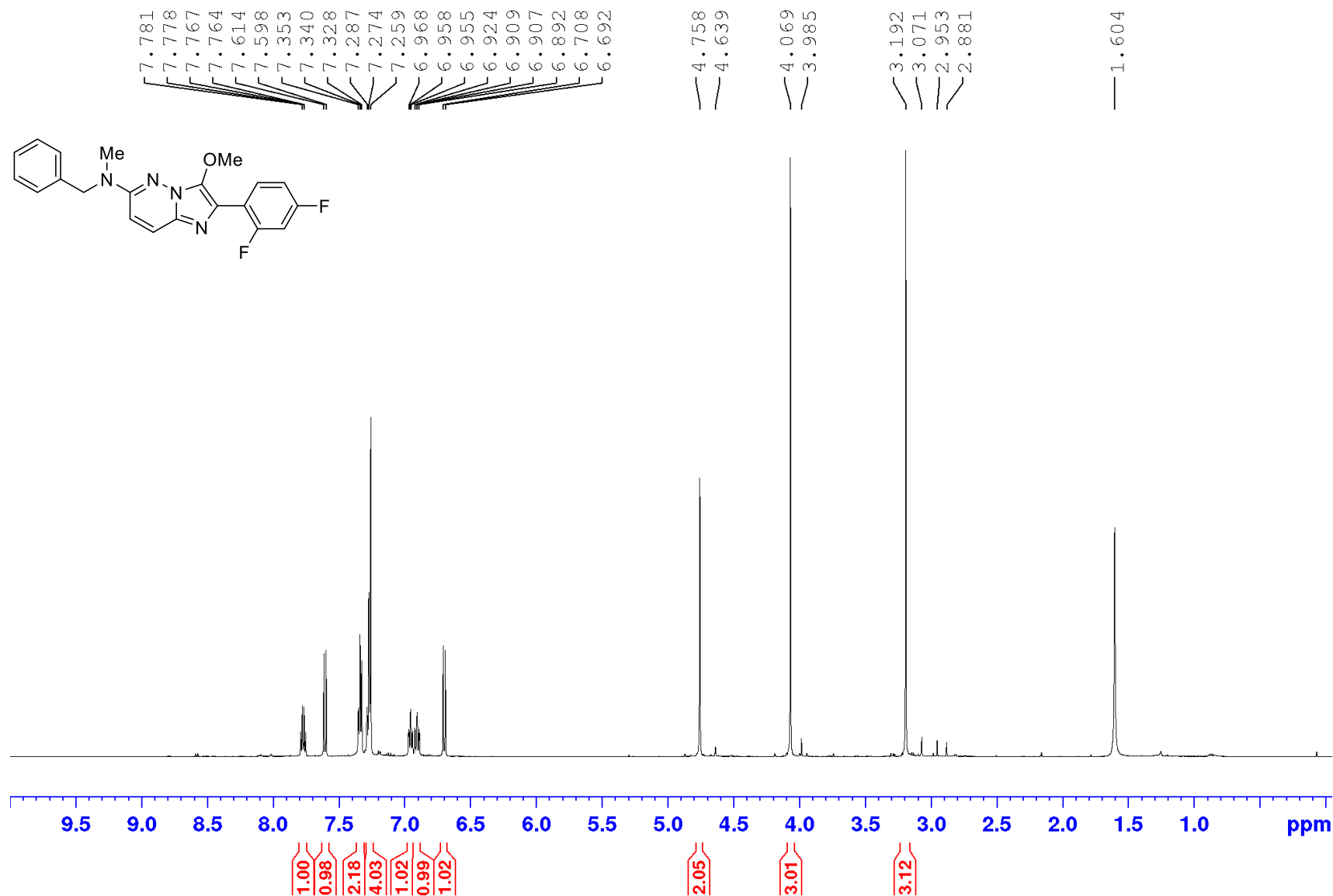
HRMS (APCI) spectrum of **190c** [M+H]⁺

cf: qe14890 #119-140 RT: 1.04-1.22 AV: 22 NL: 8.12E9
T: FTMS + p APCI corona Full lock ms [66.7000-1000.0000]



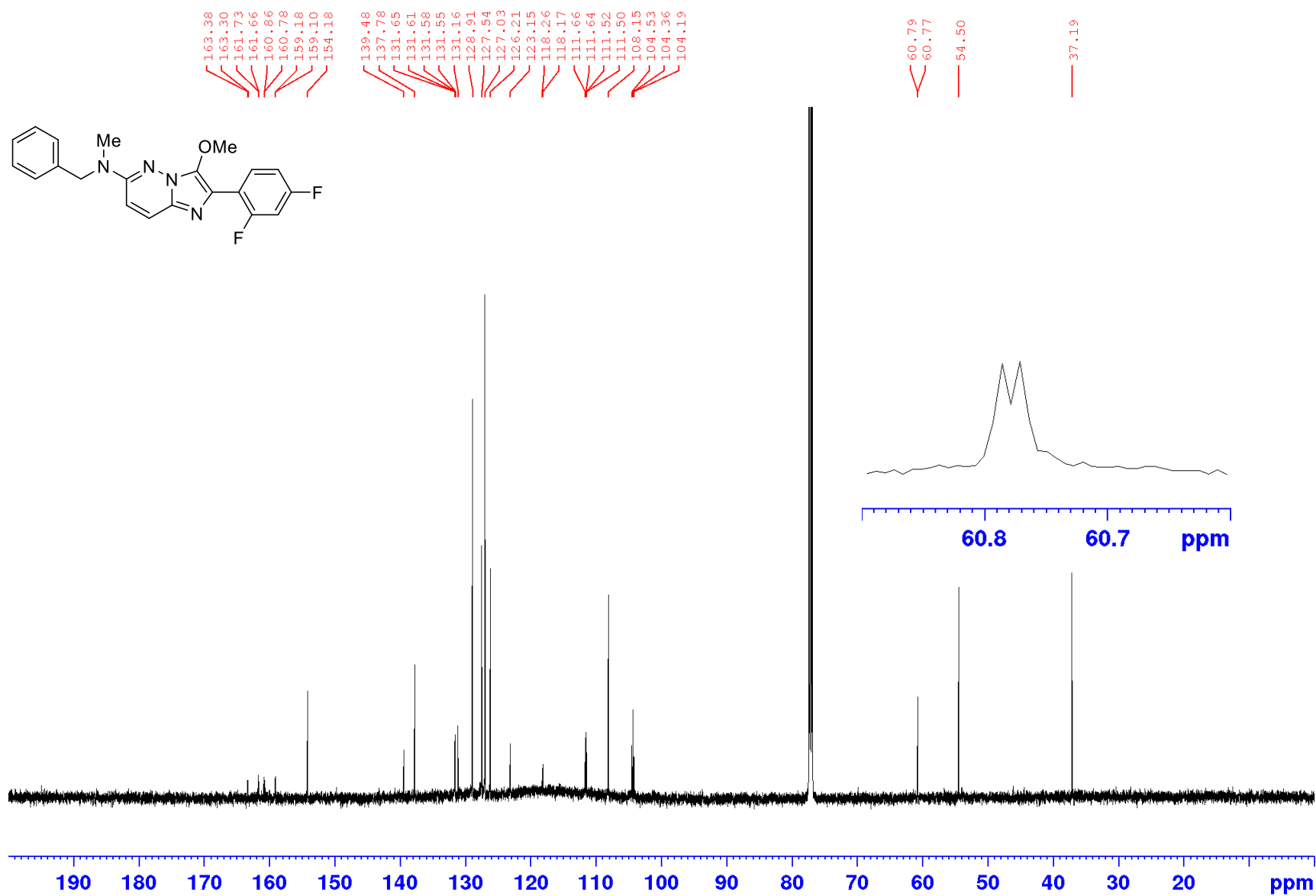
Appendices

¹H NMR spectrum of **190d** (600 MHz; CDCl₃)



Appendices

¹³C NMR spectrum of **190d** (150 MHz; CDCl₃)

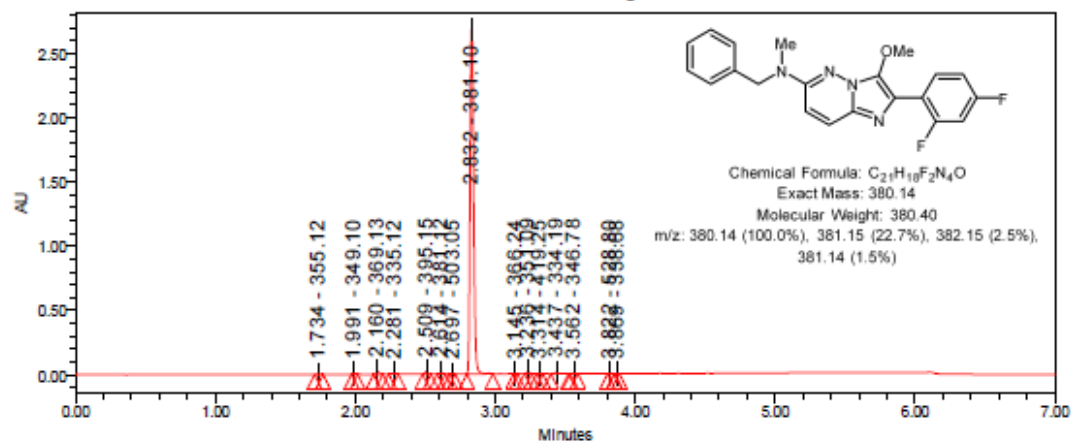


Appendices

LC-MS chromatogram of **190d** [M+H]⁺

<p>Vial: 1:B,3 Injection #: 1 Injection Volume: 1.00 ul Run Time: 7.0 Minutes Date Acquired: 8/05/2019 10:41:54 AM EST Date Processed: 8/05/2019 11:01:22 AM EST</p>	<p>Instrument: Waters Acquity iClass PDA and QDa detectors Acquired By: System Sample Set Name: PH_08_May2019 Acquisition Method: 95% A1 to 100% B1 Mobile Phase: A1: 100% H2O / 0.1% FA B1: 100% ACN / 0.1% FA Extracted Chromatogram: PDA Spectrum PDA 254.0 nm</p>
---	--

Auto-Scaled Chromatogram



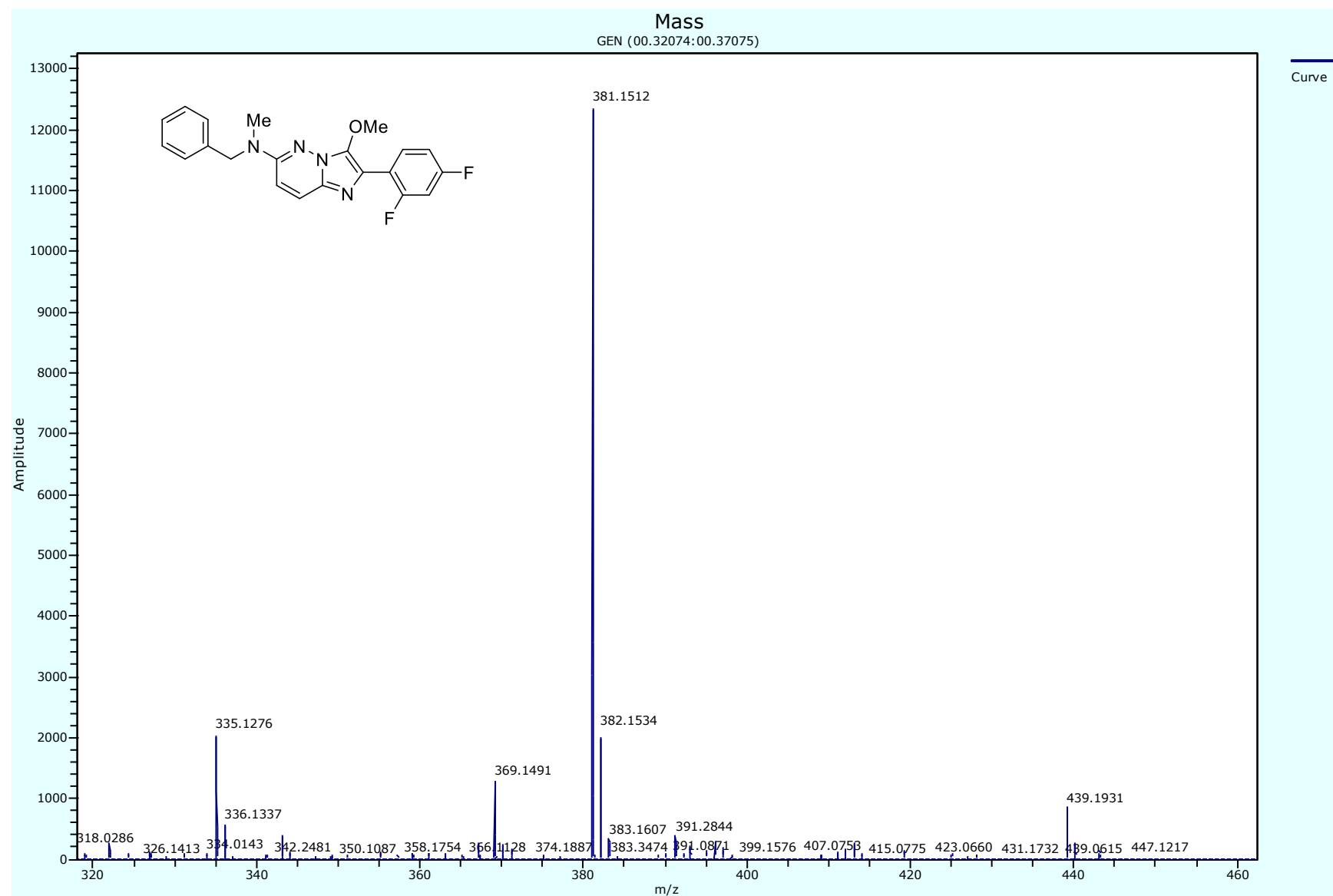
Peak Results

	RT	Area	% Area	Height	Base Peak (m/z)
1	1.734	5102	0.10	3509	355.12
2	1.991	5635	0.12	5324	349.10
3	2.160	30101	0.62	21431	369.13
4	2.281	11298	0.23	6617	335.12
5	2.509	26816	0.55	22450	395.15
6	2.614	13484	0.28	12125	381.12
7	2.697	1251	0.03	1066	503.05
8	2.832	4739195	97.02	2702407	381.10
9	3.145	792	0.02	853	366.24

	RT	Area	% Area	Height	Base Peak (m/z)
10	3.236	16912	0.35	14168	351.09
11	3.314	4155	0.09	3944	419.25
12	3.437	18052	0.37	11026	334.19
13	3.562	6657	0.14	5278	346.78
14	3.822	3613	0.07	2940	528.80
15	3.869	1661	0.03	1673	338.68

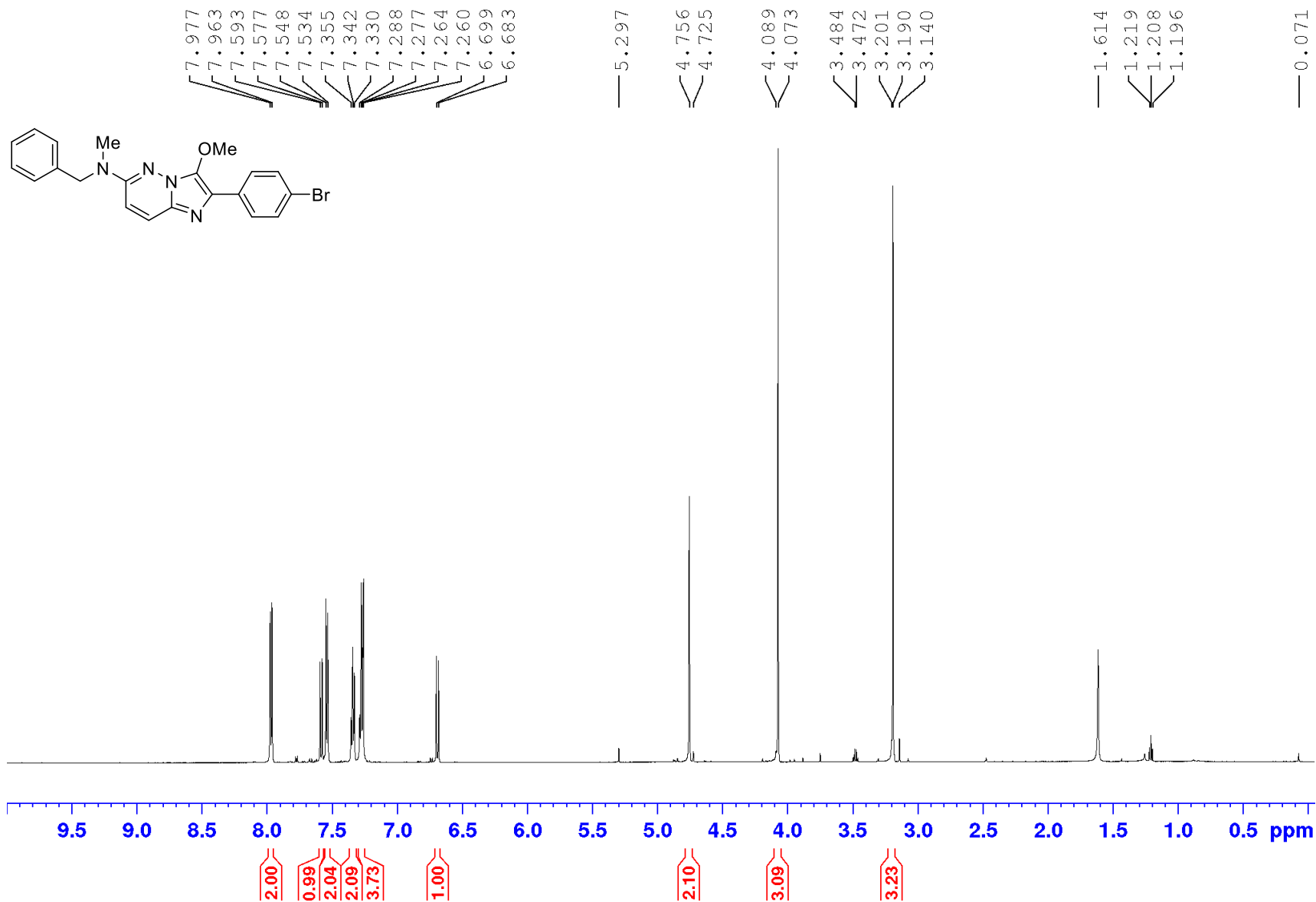
Appendices

HRMS (APCI) spectrum of **190d** $[M+H]^+$



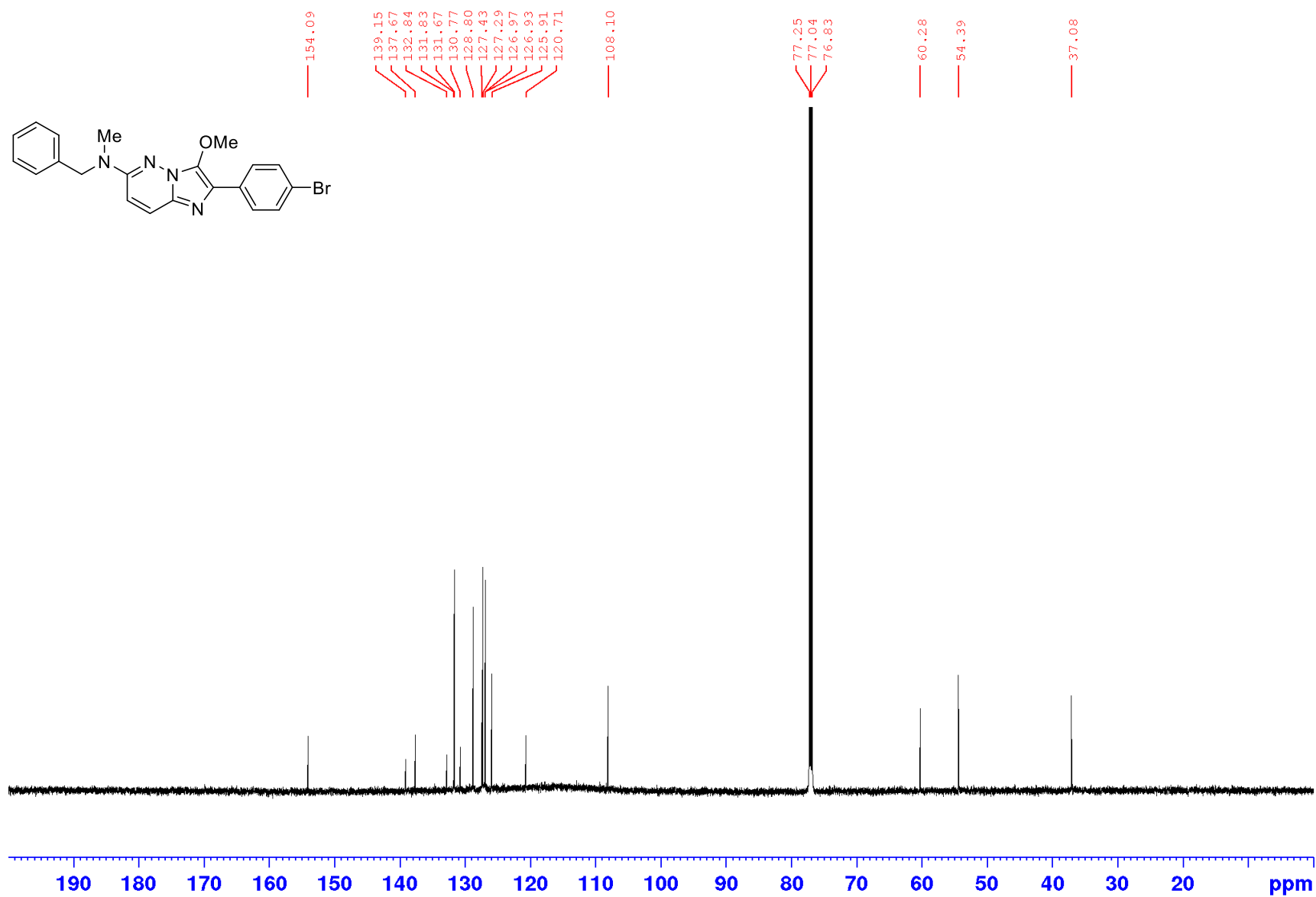
Appendices

¹H NMR spectrum of **190e** (600 MHz; CDCl₃)



Appendices

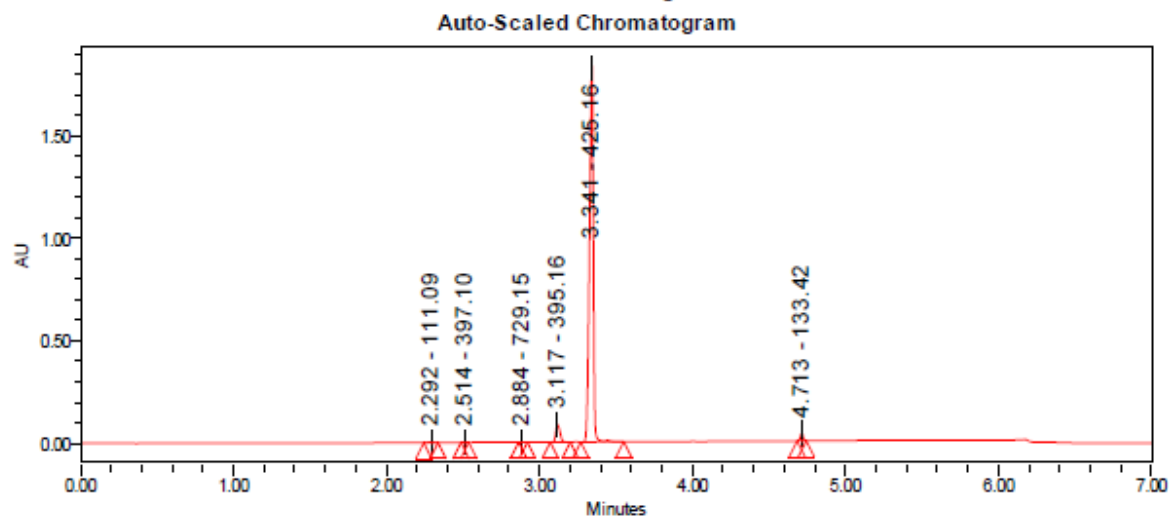
¹³C NMR spectrum of **190e** (150 MHz; CDCl₃)



Appendices

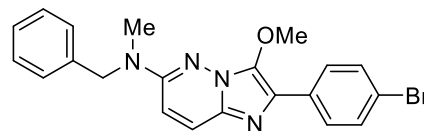
LC-MS chromatogram of **190e** [M+H]⁺

Sample Name:	IMPZ 18	Instrument:	Waters Acquity iClass PDA and QDa detectors
Vial:	1:B,4	Acquired By:	System
Injection #:	1	Sample Set Name:	MK_10_July2018
Injection Volume:	0.50 ul	Acquisition Method:	95% A1 to 100% B1 POSNEG
Run Time:	7.0 Minutes	Mobile Phase:	A1: 100% H2O / 0.1% FA B1: 100% ACN / 0.1% FA
Flowrate:	0.4 mL/min	Date Acquired:	10/07/2018 2:59:47 PM EST
Date Acquired:	10/07/2018 2:59:47 PM EST	Date Processed:	10/07/2018 3:17:26 PM EST
Date Processed:	10/07/2018 3:17:26 PM EST	Extracted Chromatogram:	PDA Spectrum PDA 254.0 nm



Peak Results

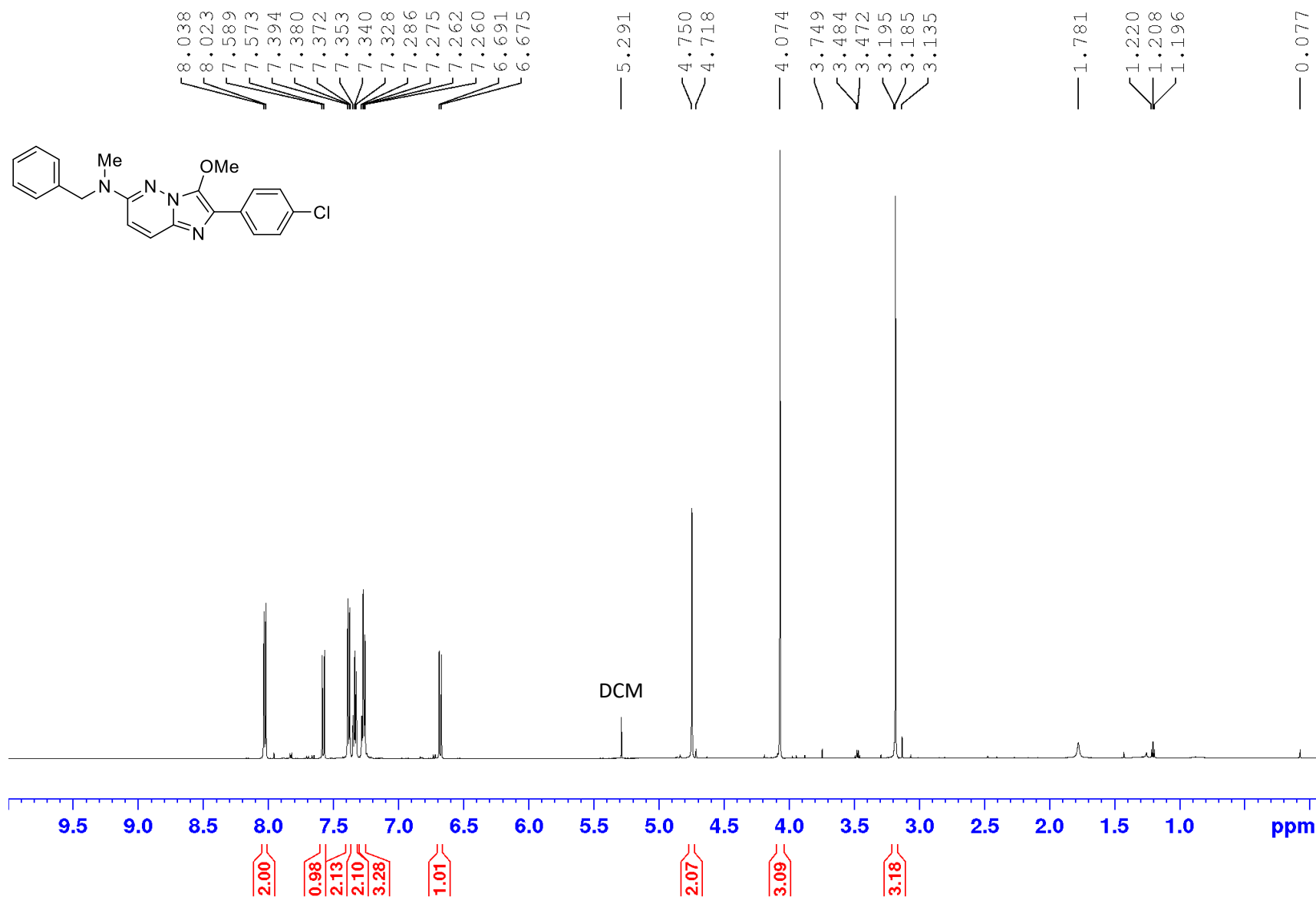
	RT	Area	% Area	Height	Base Peak (m/z)
1	2.292	4925	0.14	2683	111.09
2	2.514	3131	0.09	2514	397.10
3	2.884	1532	0.04	1265	729.15
4	3.117	161469	4.73	85165	395.16
5	3.341	3202195	93.71	1854833	425.16
6	4.713	43978	1.29	35811	133.42



Chemical Formula: C₂₁H₁₉BrN₄O
 Exact Mass: 422.0742
 Molecular Weight: 423.3140
 m/z: 422.0742 (100.0%), 424.0722 (97.3%),
 423.0776 (22.7%), 425.0755 (22.1%),
 424.0809 (2.5%), 426.0789 (2.4%),
 423.0713 (1.5%), 425.0692 (1.4%)

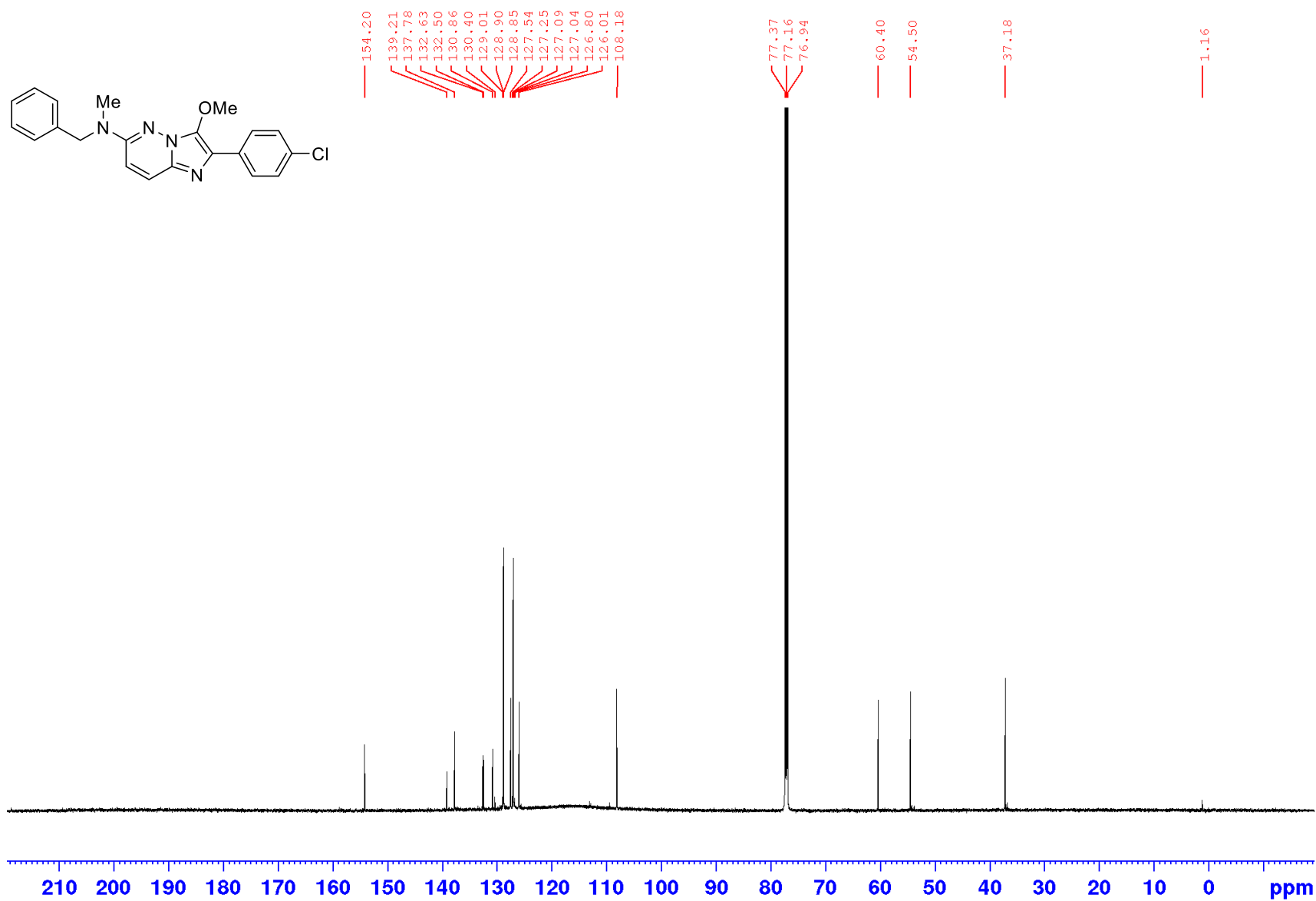
Appendices

¹H NMR spectrum of **190f** (600 MHz; CDCl₃)



Appendices

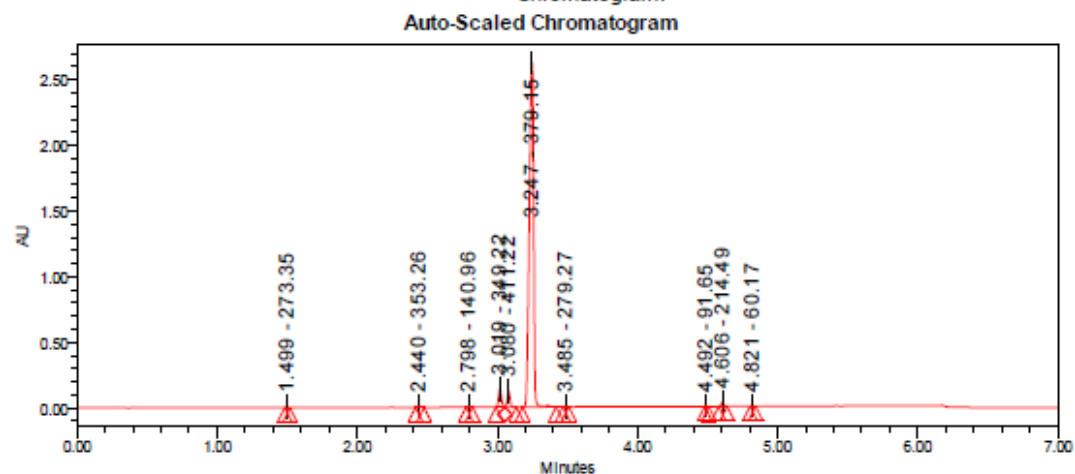
^{13}C NMR spectrum of **190f** (150 MHz; CDCl_3)



Appendices

LC-MS chromatogram of **190f** [M+H]⁺

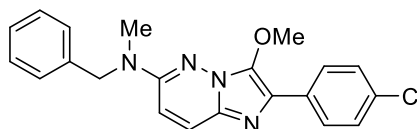
Sample Name:	IMPZ 17	Instrument:	Waters Acquity iClass PDA and QDa detectors
Vial:	1:B,3	Acquired By:	System
Injection #:	1	Sample Set Name:	MK_10_July2018
Injection Volume:	0.50 ul	Acquisition Method:	95% A1 to 100% B1 POSNEG
Run Time:	7.0 Minutes	Mobile Phase:	A1: 100% H2O / 0.1% FA B1: 100% ACN / 0.1% FA
Flowrate:	0.4 mL/min	Extracted Chromatogram:	PDA Spectrum PDA 254.0 nm
Date Acquired:	10/07/2018 2:42:47 PM EST		
Date Processed:	10/07/2018 3:05:19 PM EST		



Peak Results

	RT	Area	% Area	Height	Base Peak (m/z)
1	1.499	6394	0.11	6102	273.35
2	2.440	15253	0.25	12079	353.26
3	2.798	6367	0.11	4947	140.96
4	3.019	192600	3.21	139646	349.22
5	3.080	155052	2.59	121762	411.22
6	3.247	5569820	92.96	2629164	379.15
7	3.485	3460	0.06	2524	279.27
8	4.492	1338	0.02	1403	91.65
9	4.606	37955	0.63	30957	214.49

	RT	Area	% Area	Height	Base Peak (m/z)
10	4.821	3168	0.05	2792	60.17



Chemical Formula: C₂₁H₁₉ClN₄O

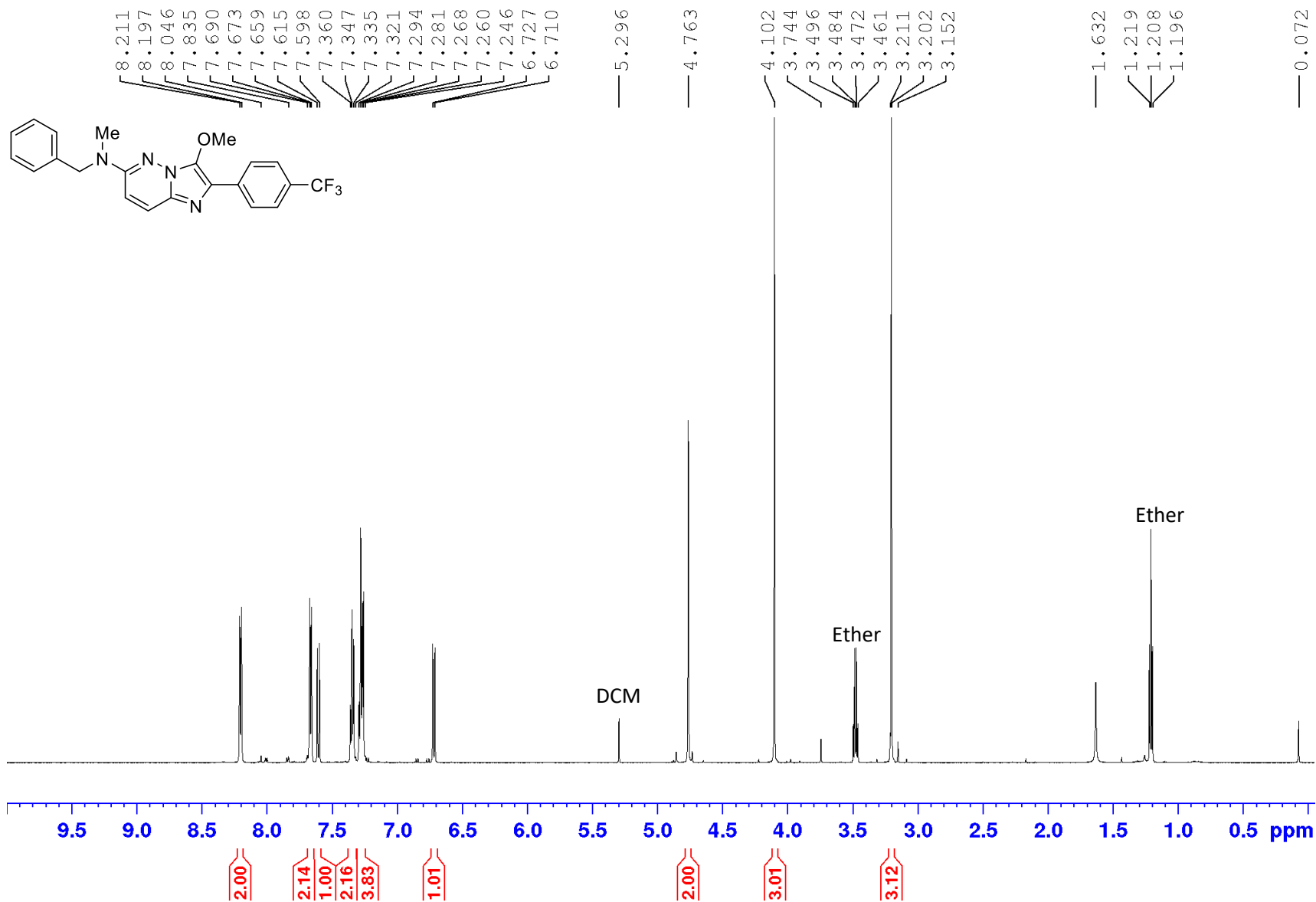
Exact Mass: 378.1247

Molecular Weight: 378.8600

m/z: 378.1247 (100.0%), 380.1218 (32.0%), 379.1281 (22.7%),
381.1251 (7.3%), 380.1314 (2.5%), 379.1218 (1.5%)

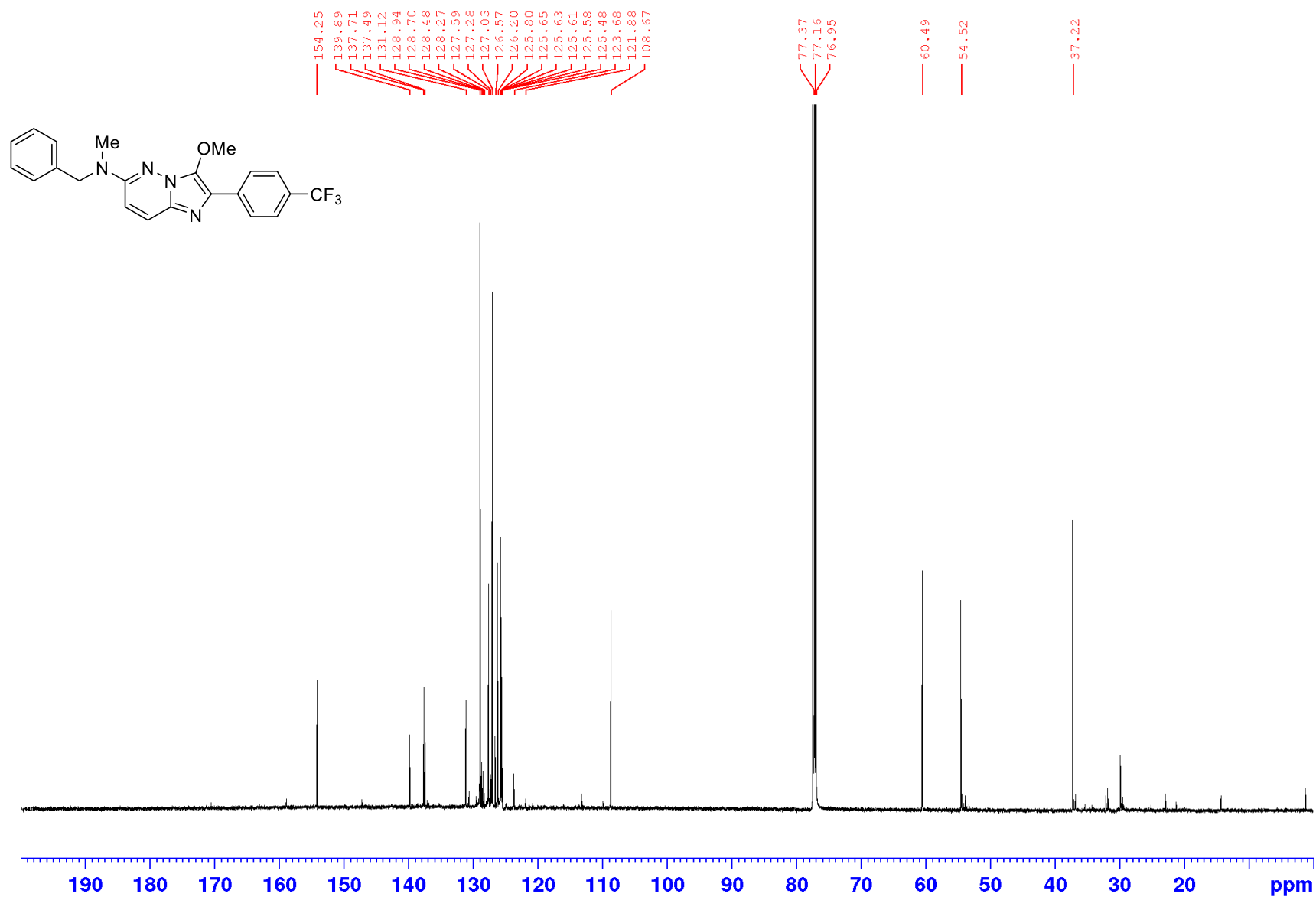
Appendices

¹H NMR spectrum of **190g** (600 MHz; CDCl₃)



Appendices

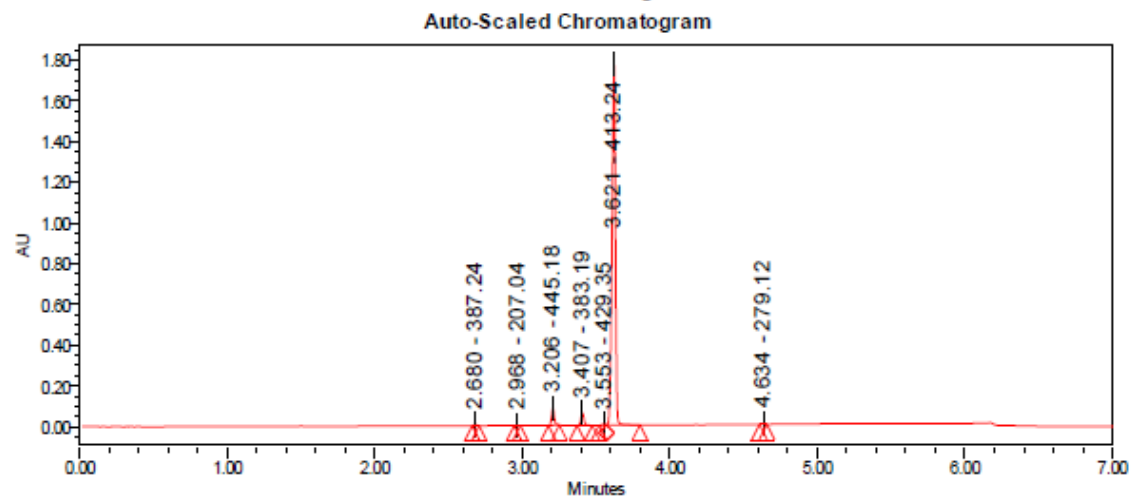
¹³C NMR spectrum of **190g** (150 MHz; CDCl₃)



Appendices

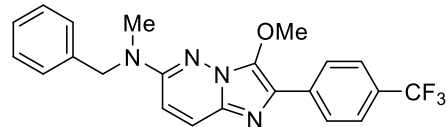
LC-MS chromatogram of **190g** [M+H]⁺

Sample Name:	IMPZ 21	Instrument:	Waters Acquity iClass PDA and QDA detectors
Vial:	1:B,7	Acquired By:	System
Injection #:	1	Sample Set Name:	MK_10_July2018
Injection Volume:	0.50 ul	Acquisition Method:	95% A1 to 100% B1 POSNEG
Run Time:	7.0 Minutes	Mobile Phase:	A1: 100% H2O / 0.1% FA B1: 100% ACN / 0.1% FA
Flowrate:	0.4 mL/min	Extracted Chromatogram:	PDA Spectrum PDA 254.0 nm
Date Acquired:	10/07/2018 3:33:41 PM EST		
Date Processed:	10/07/2018 3:45:56 PM EST		



Peak Results

	RT	Area	% Area	Height	Base Peak (m/z)
1	2.680	6597	0.22	5472	387.24
2	2.968	998	0.03	839	207.04
3	3.206	103684	3.38	83491	445.18
4	3.407	81818	2.67	61098	383.19
5	3.553	6212	0.20	4451	429.35
6	3.621	2860270	93.37	1777604	413.24
7	4.634	3902	0.13	3497	279.12



Chemical Formula: C₂₂H₁₉F₃N₄O

Exact Mass: 412.1511

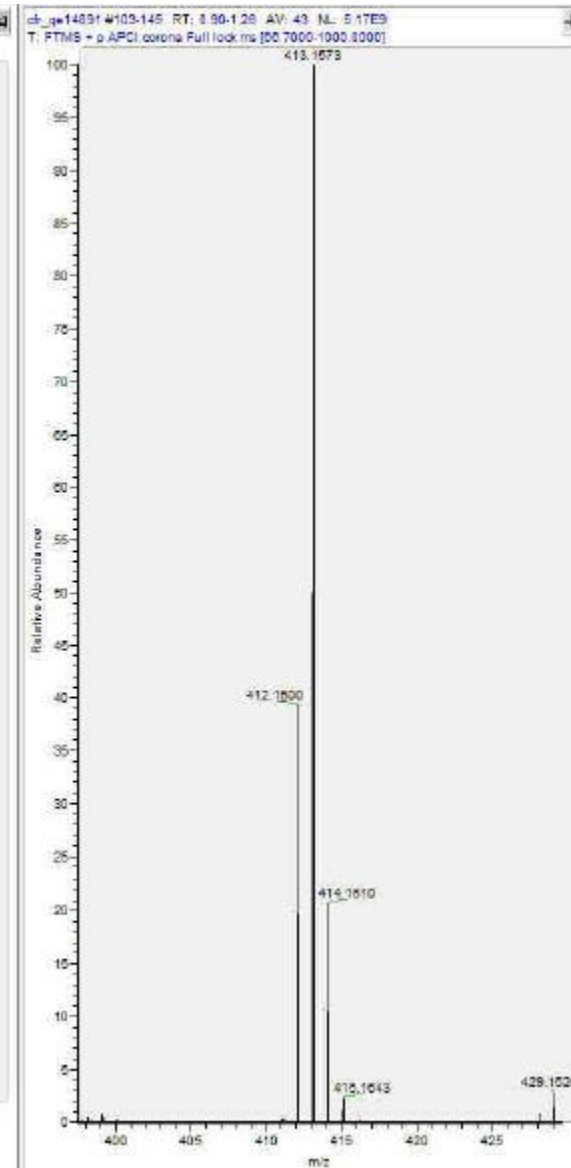
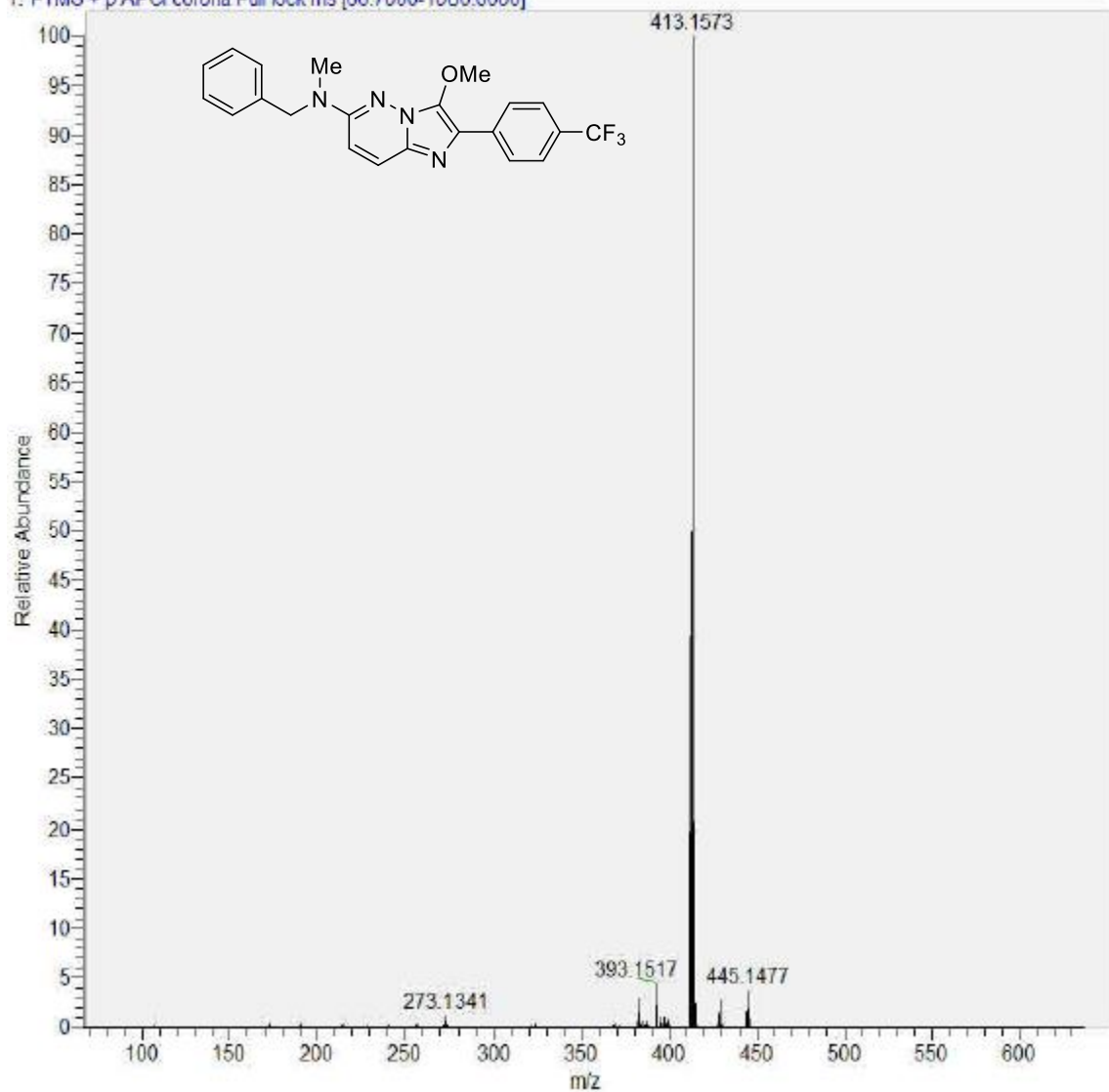
Molecular Weight: 412.4162

m/z: 412.1511 (100.0%), 413.1545 (23.8%),
414.1578 (2.7%), 413.1481 (1.5%)

Appendices

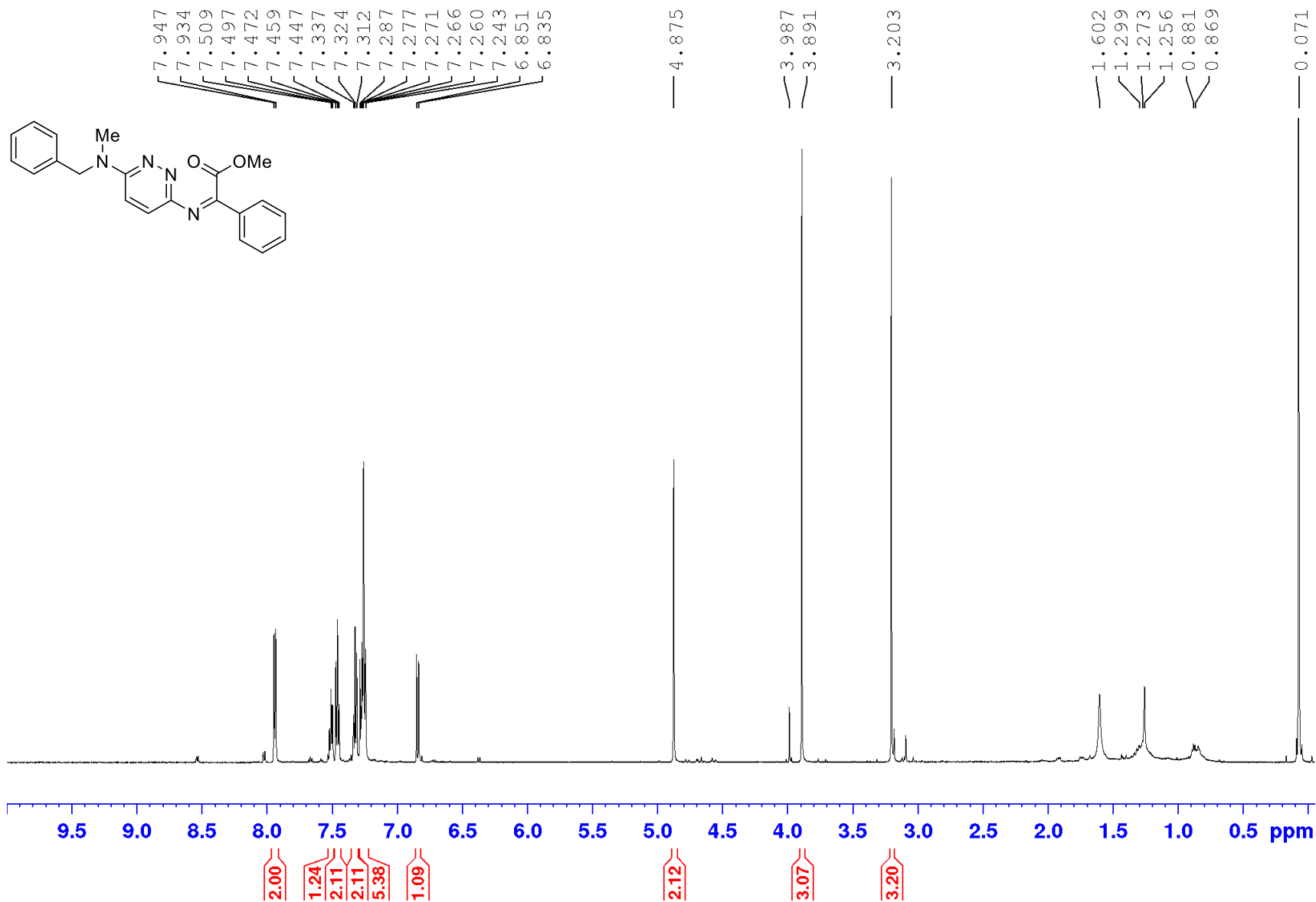
HRMS (APCI) of **190g** $[M+H]^+$

cf: qe14891 #103-145 RT: 0.90-1.26 AV: 43 NL: 5.17E9
T: FTMS + pAPCI corona Full lock ms [66.7000-1000.0000]



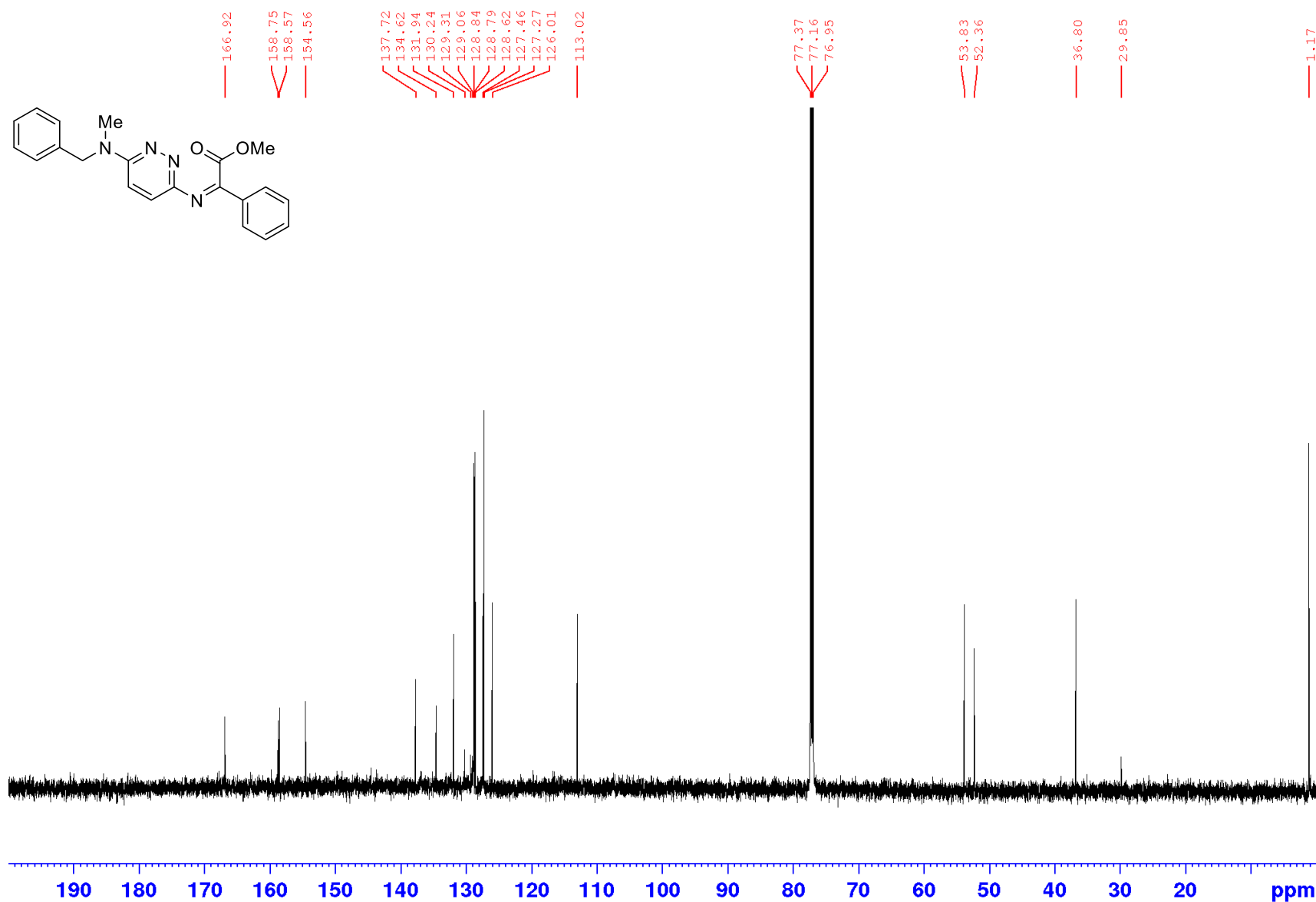
Appendices

¹H NMR spectrum of **191a** (600 MHz; CDCl₃) petrol present (0.8-1.7ppm)



Appendices

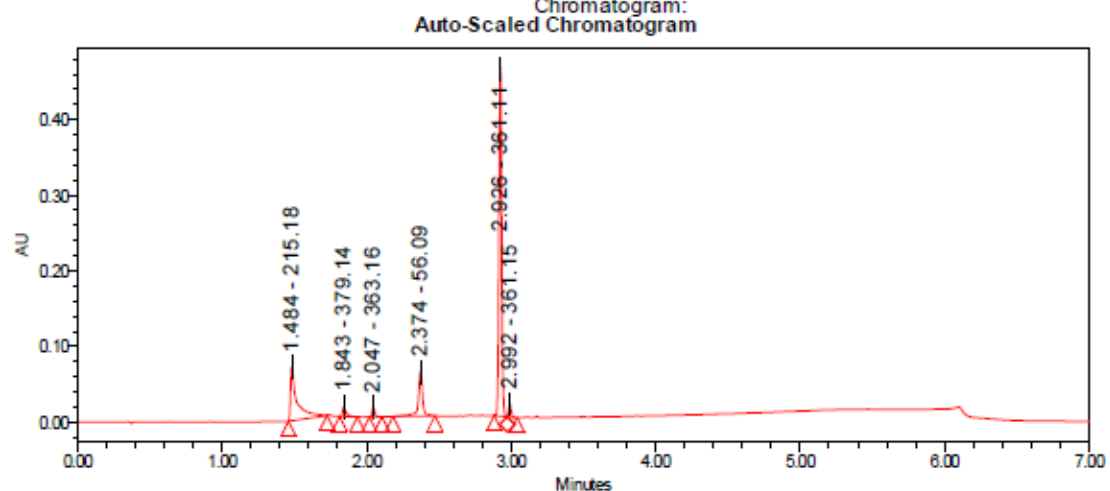
¹³C NMR spectrum of **191a** (150 MHz; CDCl₃) impurities present at low concentration



Appendices

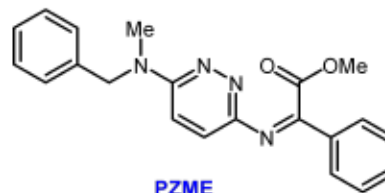
LC-MS chromatogram of **191a** $[M+H]^+$ degradation in the acidic aqueous mobile phase may have occurred

Sample Name:	CF PZME	Instrument:	Waters Acquity iClass PDA and QDa detectors
Vial:	1:B,7	Acquired By:	System
Injection #:	1	Sample Set Name:	MK_26_April2019
Injection Volume:	0.30 ul	Acquisition Method:	95% A1 to 100% B1
Run Time:	7.0 Minutes	Mobile Phase:	A1: 100% H2O / 0.1% FA B1: 100% ACN / 0.1% FA
Date Acquired:	26/04/2019 1:49:26 PM EST	Extracted Chromatogram:	PDA Spectrum PDA 254.0 nm
Date Processed:	26/04/2019 2:38:50 PM EST		



Peak Results

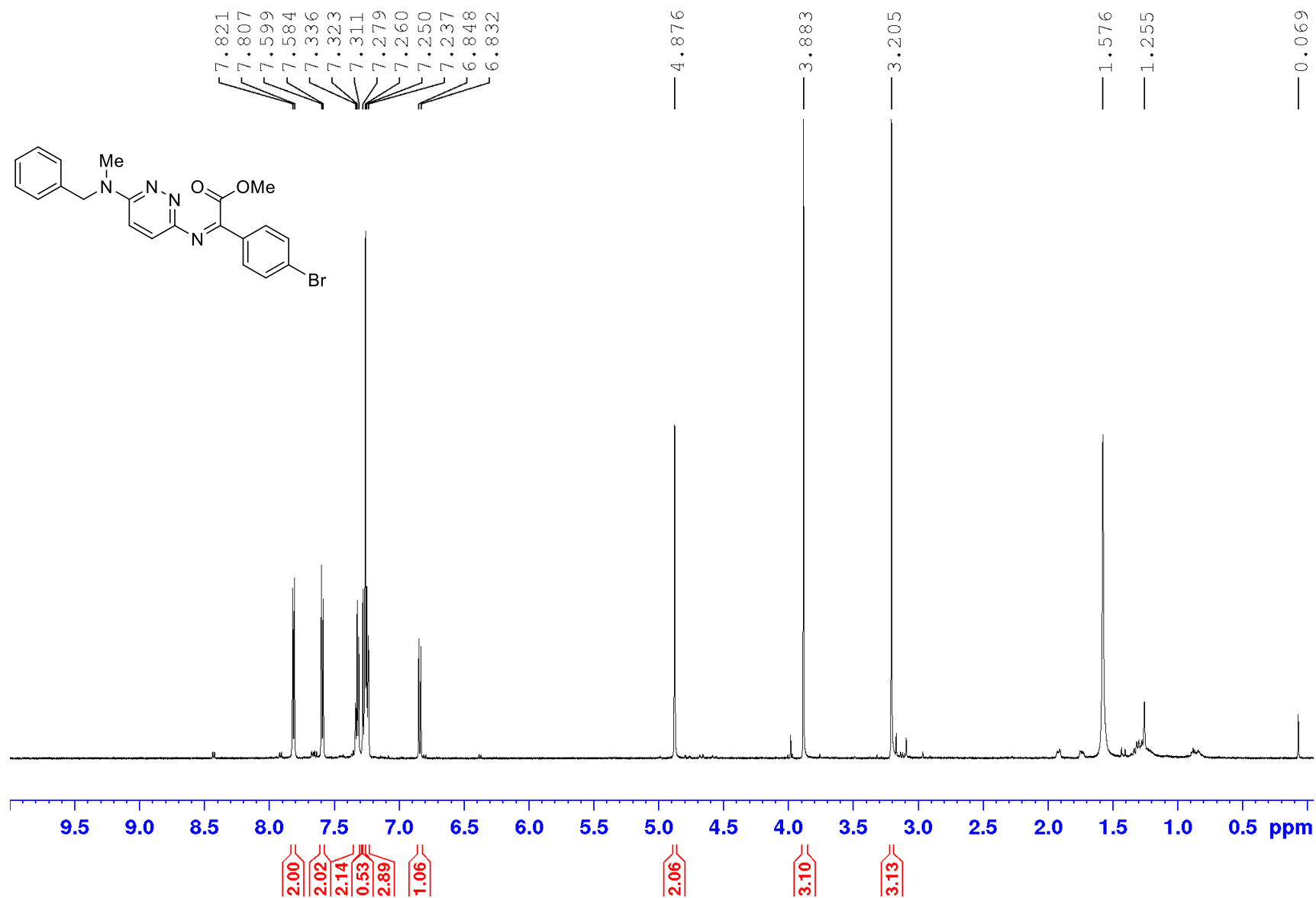
	RT	Area	% Area	Height	Base Peak (m/z)
1	1.484	227287	23.06	71772	215.18
2	1.843	21498	2.18	13196	379.14
3	2.047	16362	1.66	12908	363.16
4	2.374	119667	12.14	58563	56.09
5	2.926	580205	58.86	461224	361.11
6	2.992	20758	2.11	17144	361.15



Chemical Formula: $C_{21}H_{20}N_4O_2$
 Exact Mass: 360.16
 Molecular Weight: 360.42
 m/z: 360.16 (100.0%), 361.16 (22.7%),
 362.17 (2.5%), 361.16 (1.5%)

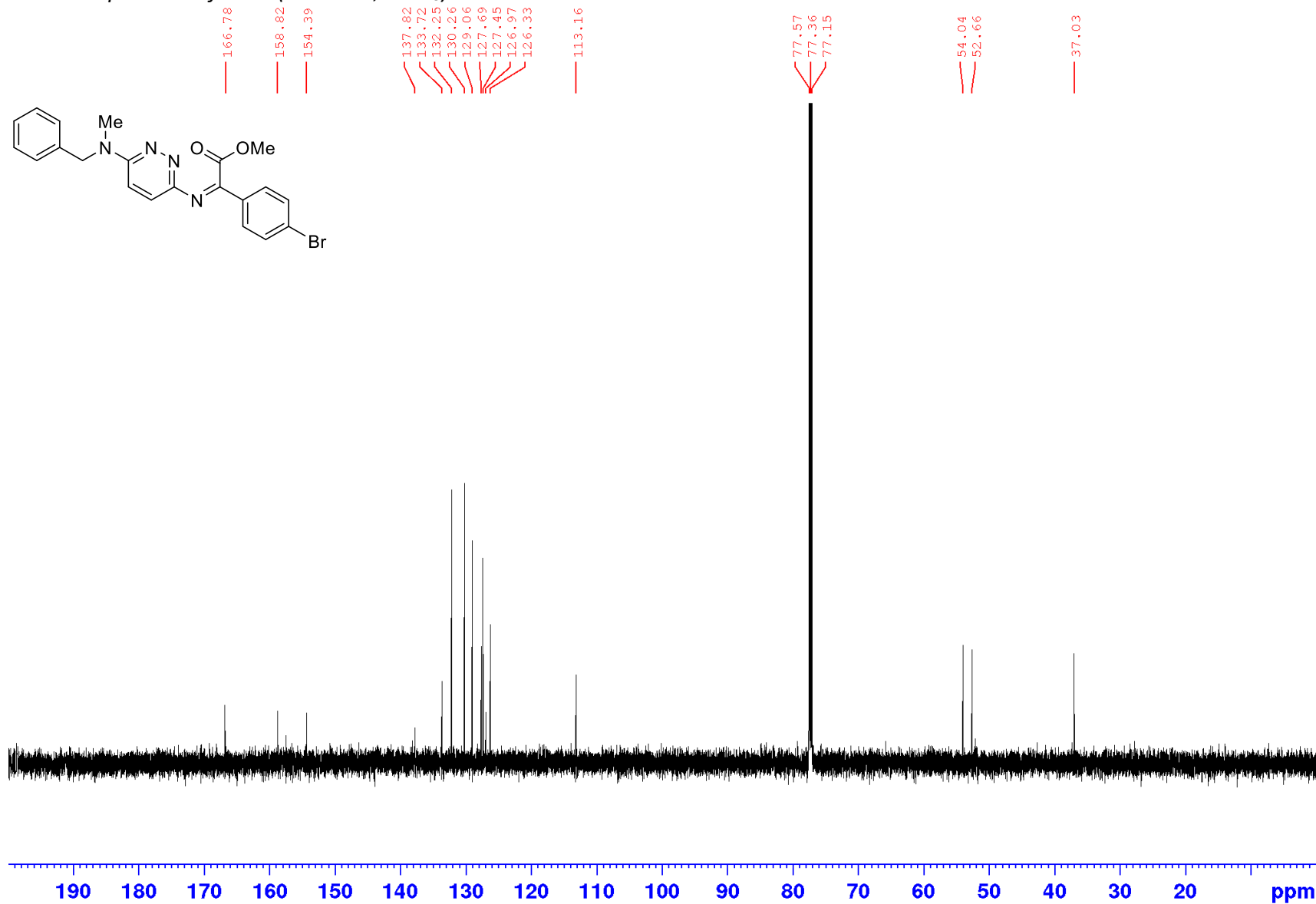
Appendices

¹H NMR spectrum of **191e** (600 MHz; CDCl₃) petrol present (0.8-1.7ppm)



Appendices

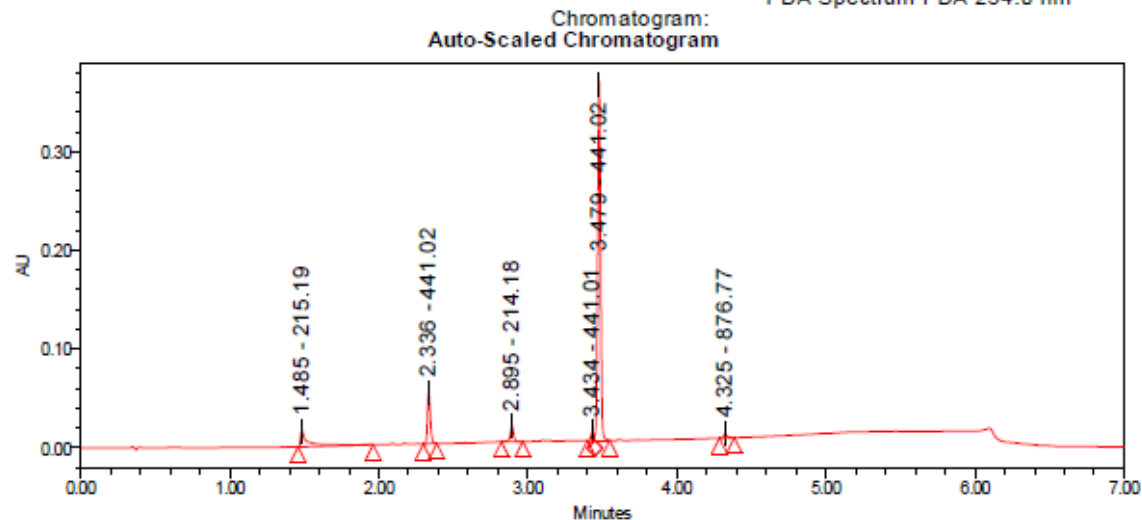
^{13}C NMR spectrum of **191e** (150 MHz; CDCl_3)



Appendices

LC-MS chromatogram of **191e** [M+H]⁺

Sample Name:	CF PZME4Br	Instrument:	Waters Acquity iClass PDA and QDa detectors
Vial:	1:B,6	Acquired By:	System
Injection #:	1	Sample Set Name:	MK_26_April2019
Injection Volume:	0.30 ul	Acquisition Method:	95% A1 to 100% B1
Run Time:	7.0 Minutes	Mobile Phase:	A1: 100% H2O / 0.1% FA B1: 100% ACN / 0.1% FA
Date Acquired:	26/04/2019 1:40:58 PM EST	Extracted	PDA Spectrum PDA 254.0 nm
Date Processed:	26/04/2019 2:08:19 PM EST	Chromatogram:	



Peak Results

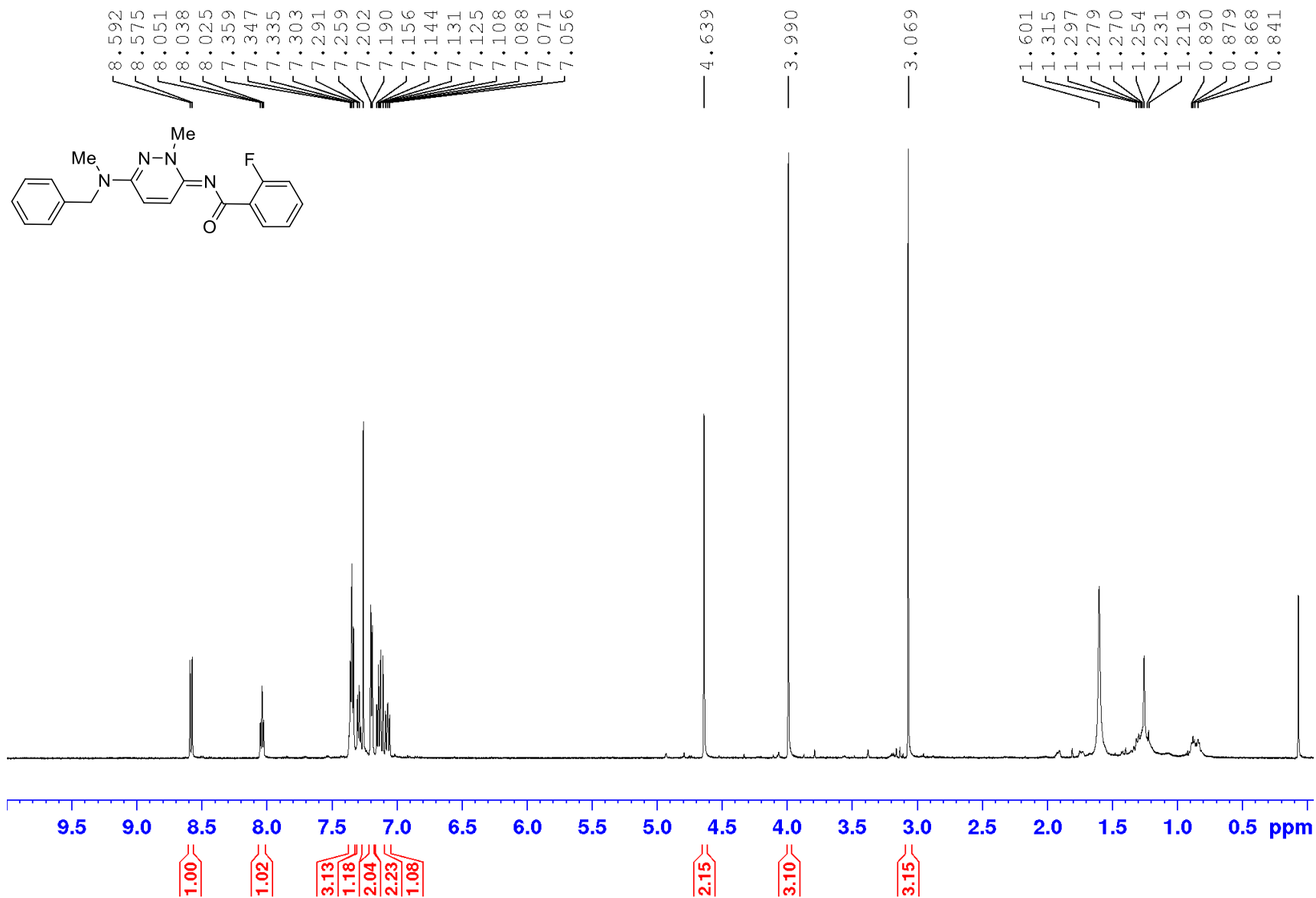
	RT	Area	% Area	Height	Base Peak (m/z)
1	1.485	66483	10.05	16352	215.19
2	2.336	68338	10.33	51653	441.02
3	2.895	24052	3.63	15049	214.18
4	3.434	10585	1.60	8402	441.01
5	3.479	486175	73.47	362929	441.02
6	4.325	6120	0.92	4300	876.77



Chemical Formula: C₂₁H₁₉BrN₄O₂
 Exact Mass: 438.07
 Molecular Weight: 439.31
 m/z: 438.07 (100.0%), 440.07 (97.3%), 441.07 (22.1%), 439.07 (16.2%), 439.07 (6.5%), 440.08 (2.3%), 439.07 (1.5%), 441.06 (1.4%).

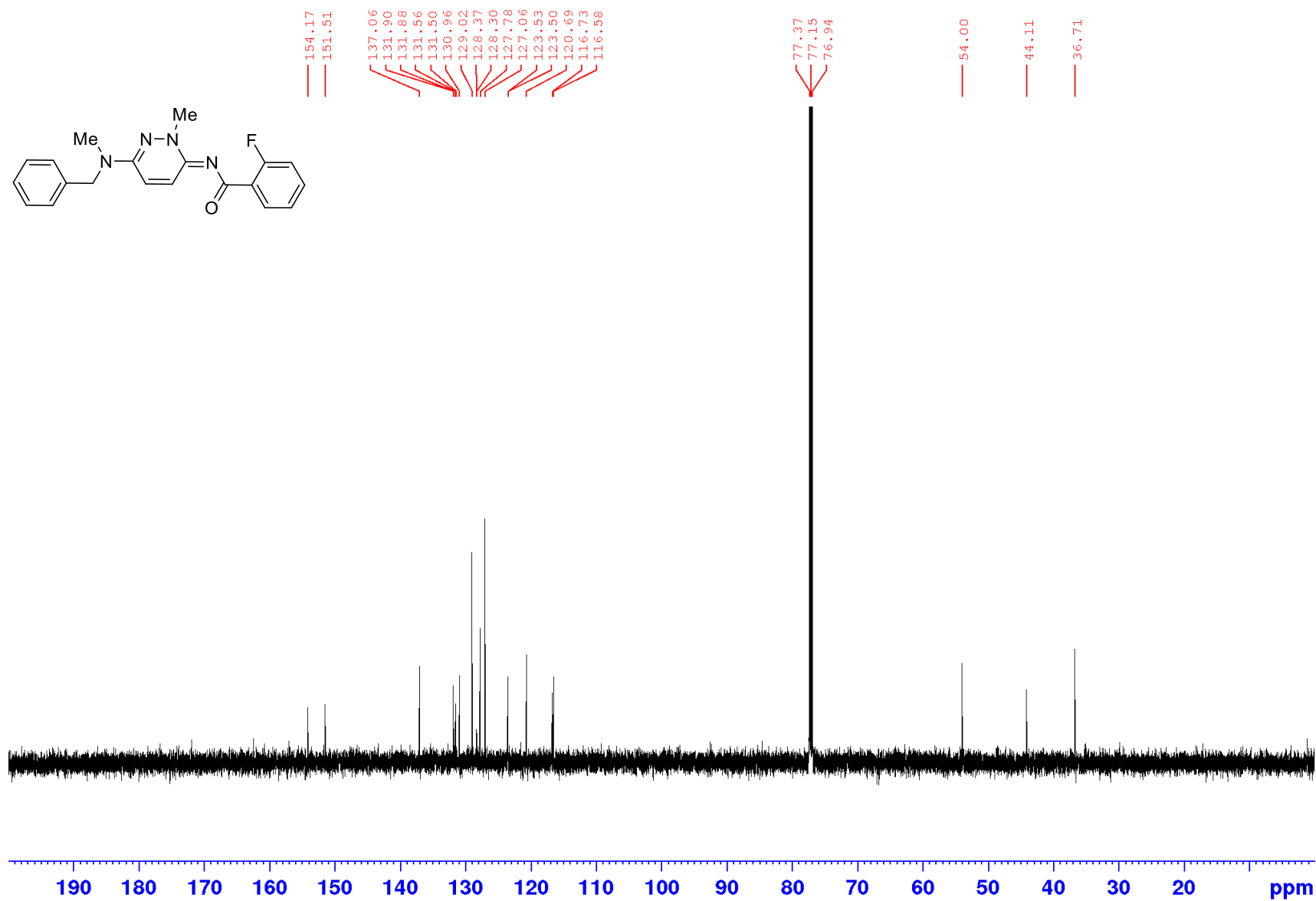
Appendices

¹H NMR spectrum of **192b** (600 MHz; CDCl₃) petrol present (0.8-1.7ppm)



Appendices

^{13}C NMR spectrum of **192b** (150 MHz; CDCl_3)

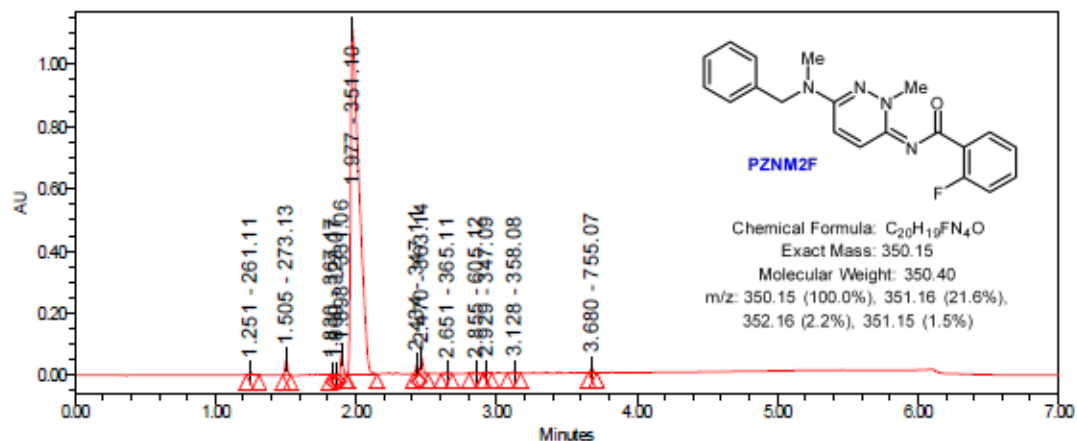


Appendices

LC-MS chromatogram of **192b** [M+H]⁺

Sample Name:	CF PZNM2F	Instrument:	Waters Acquity iClass PDA and QDa detectors
Vial:	1:B,5	Acquired By:	System
Injection #:	1	Sample Set Name:	MK_26_April2019
Injection Volume:	1.00 ul	Acquisition Method:	95% A1 to 100% B1
Run Time:	7.0 Minutes	Mobile Phase:	A1: 100% H2O / 0.1% FA B1: 100% ACN / 0.1% FA
Date Acquired:	26/04/2019 1:32:28 PM EST	Extracted Chromatogram:	PDA Spectrum PDA 254.0 nm
Date Processed:	26/04/2019 2:05:58 PM EST		

Auto-Scaled Chromatogram



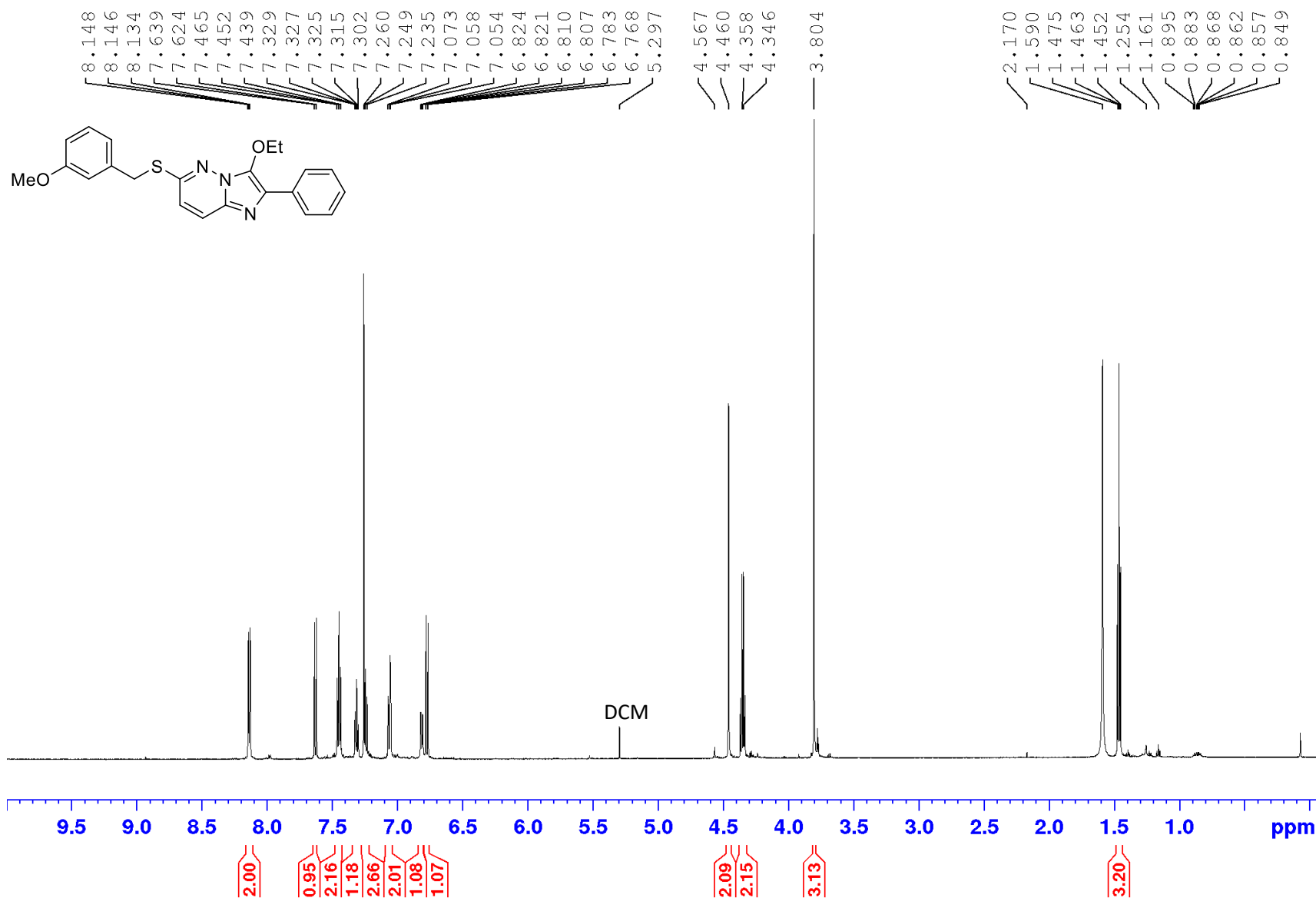
Peak Results

	RT	Area	% Area	Height	Base Peak (m/z)
1	1.251	12693	0.26	8948	261.11
2	1.505	56040	1.18	51080	273.13
3	1.830	3547	0.07	3518	367.17
4	1.880	3239	0.07	2703	323.07
5	1.898	75957	1.55	63913	331.08
6	1.977	4598939	93.82	1110813	351.10
7	2.434	32871	0.67	29187	347.11
8	2.470	60944	1.24	50865	363.14
9	2.651	6925	0.14	4668	365.11

	RT	Area	% Area	Height	Base Peak (m/z)
10	2.855	11299	0.23	4963	605.12
11	2.929	7577	0.15	6263	347.09
12	3.128	10084	0.21	5329	358.08
13	3.680	19951	0.41	16860	755.07

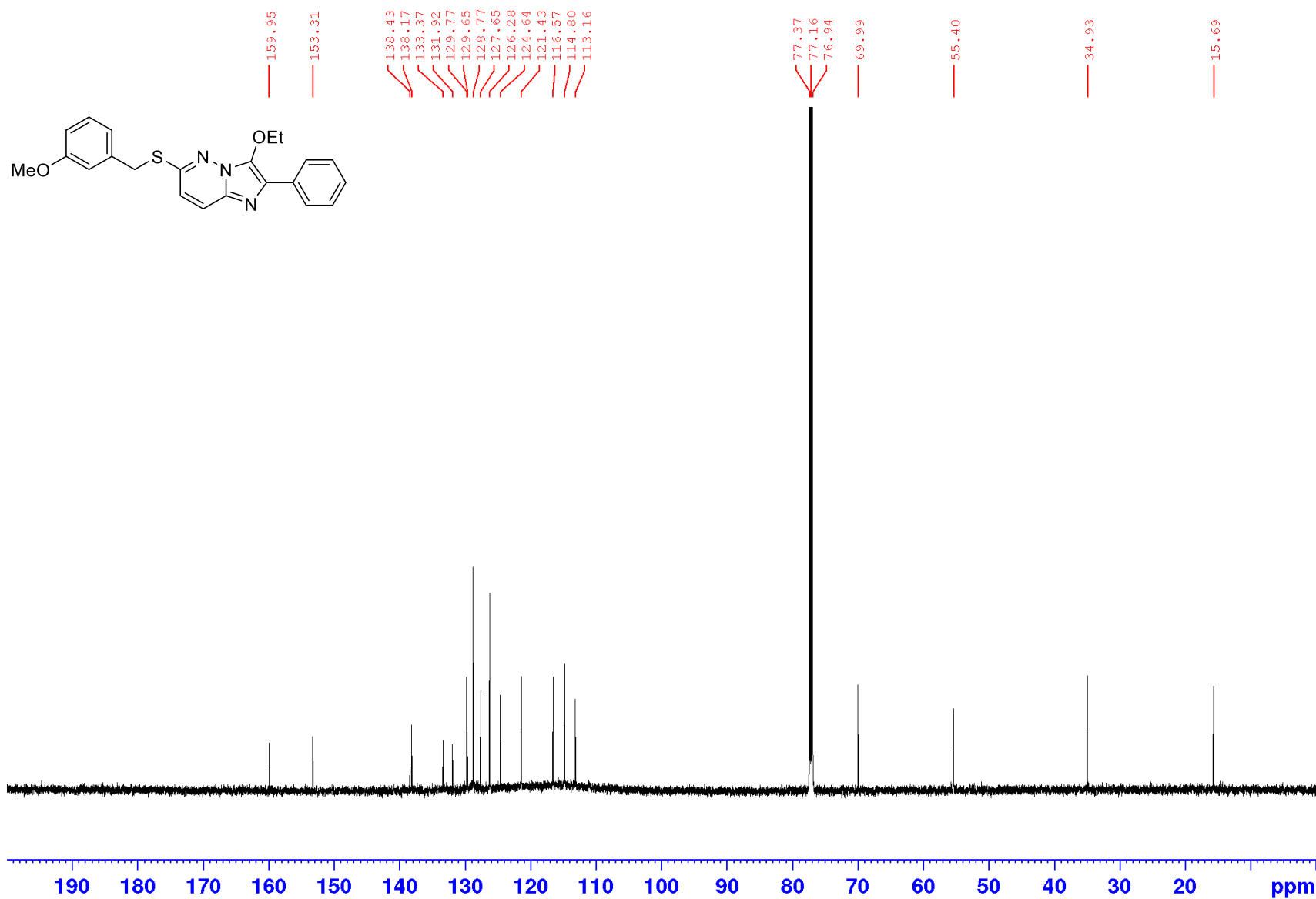
Appendices

¹H NMR spectrum of **216** (600 MHz; CDCl₃)



Appendices

¹³C NMR spectrum of **216** (150 MHz; CDCl₃)



Appendices

LC-MS chromatogram of **216** [M+H]⁺

Instrument: Waters Acquity iClass
PDA and QDa detectors

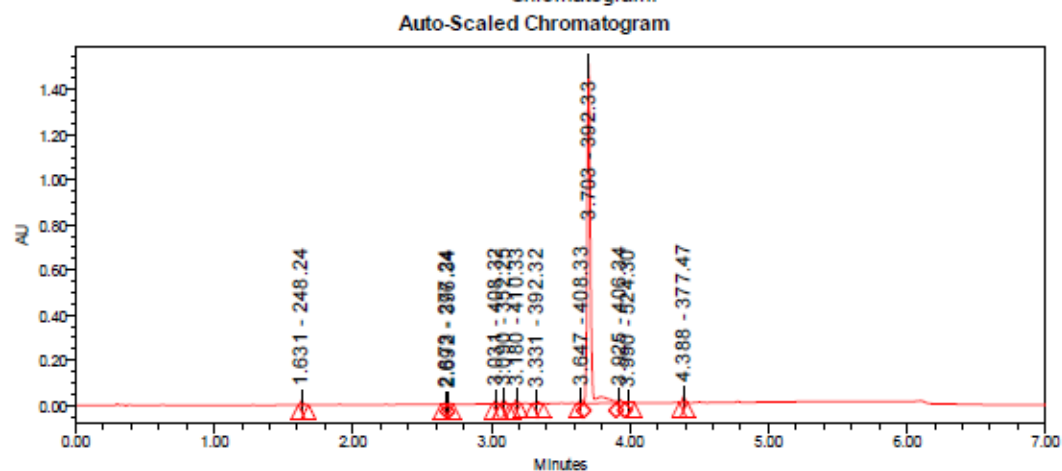
Vial: 1:C,3
Injection #: 1
Injection Volume: 0.50 ul
Run Time: 7.0 Minutes

Acquired By: System
Sample Set Name: MK_05_March2018_2

Acquisition Method: 95% A1 to 100% B1 POSNEG
Mobile Phase: A1: 100% H2O / 0.1% FA
B1: 100% ACN / 0.1% FA

Date Acquired: 5/03/2018 1:44:49 PM EST
Date Processed: 5/03/2018 1:52:57 PM EST

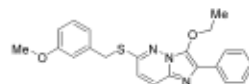
Extracted Chromatogram: PDA Spectrum PDA 254.0 nm



Peak Results

	RT	Area	% Area	Height	Base Peak (m/z)
1	1.631	24564	0.92	18849	248.24
2	2.673	10289	0.39	7672	277.24
3	2.692	8613	0.32	6069	396.34
4	3.031	18991	0.71	13949	408.32
5	3.090	24006	0.90	15665	362.25
6	3.180	23368	0.88	16156	410.33
7	3.331	17831	0.67	8789	392.32
8	3.647	22854	0.86	16251	408.33
9	3.703	2442796	91.48	1503167	392.33

	RT	Area	% Area	Height	Base Peak (m/z)
10	3.925	31562	1.18	16177	406.34
11	3.990	8747	0.33	4091	524.30
12	4.388	36806	1.38	27032	377.47



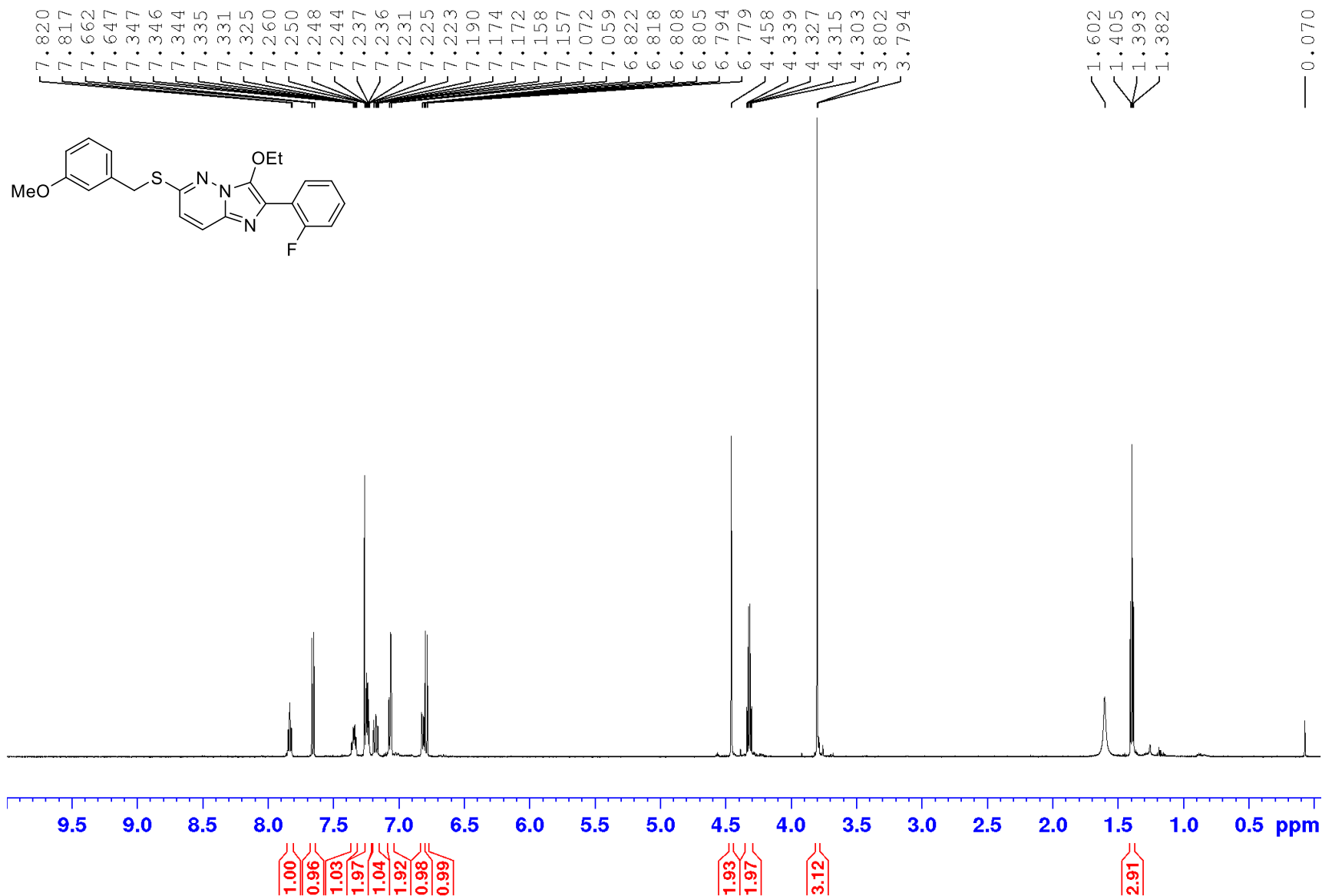
Chemical Formula: C₂₂H₂₁N₃O₂S

Exact Mass: 391.14

m/z: 391.14 (100.0%), 392.14 (23.8%), 393.13 (4.5%),
393.14 (2.7%), 392.13 (1.1%), 394.13 (1.1%)

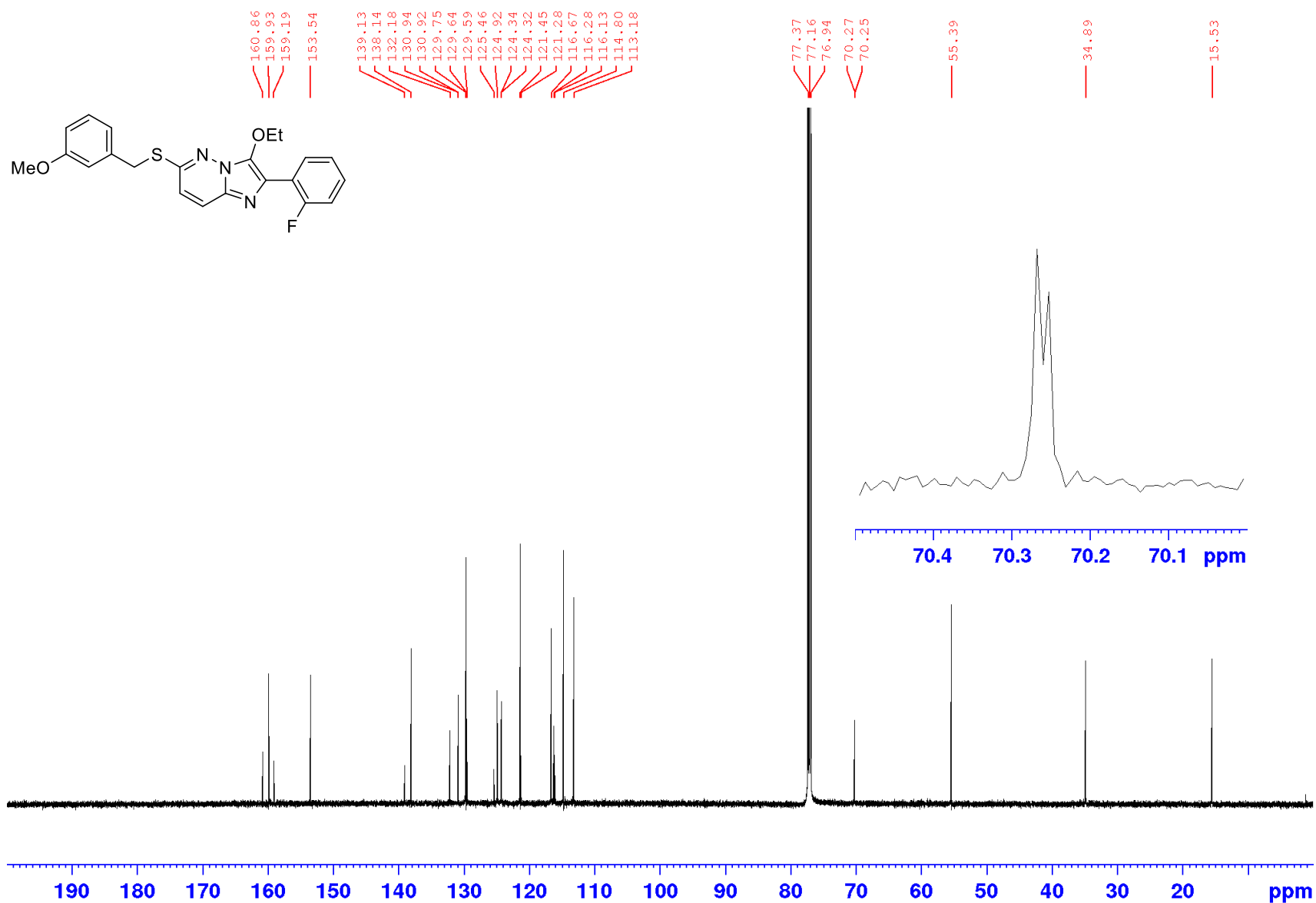
Appendices

¹H NMR spectrum of **217** (600 MHz; CDCl₃)



Appendices

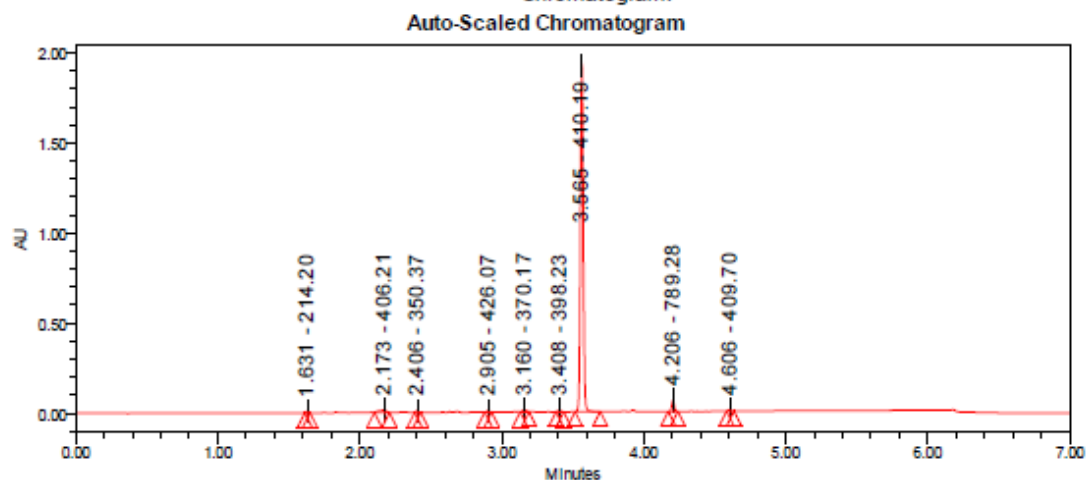
¹³C NMR spectrum of **217** (150 MHz; CDCl₃)



Appendices

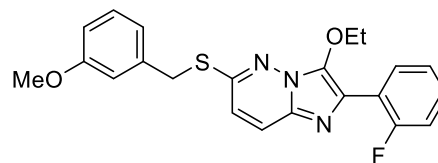
LC-MS chromatogram of **217** [M+H]⁺

Sample Name:	IMPZ 11	Instrument:	Waters Acquity iClass PDA and QDa detectors
Vial:	1:A,5	Acquired By:	System
Injection #:	1	Sample Set Name:	MK_10_July2018
Injection Volume:	0.50 ul	Acquisition Method:	95% A1 to 100% B1 POSNEG
Run Time:	7.0 Minutes	Mobile Phase:	A1: 100% H2O / 0.1% FA B1: 100% ACN / 0.1% FA
Flowrate:	0.4 mL/min	Extracted Chromatogram:	PDA Spectrum PDA 254.0 nm
Date Acquired:	10/07/2018 1:43:24 PM EST		
Date Processed:	10/07/2018 1:52:35 PM EST		



Peak Results

	RT	Area	% Area	Height	Base Peak (m/z)
1	1.631	9266	0.32	8475	214.20
2	2.173	49484	1.73	15006	406.21
3	2.406	10660	0.37	9569	360.37
4	2.905	9658	0.34	8136	426.07
5	3.160	19870	0.69	10185	370.17
6	3.408	11937	0.42	9032	398.23
7	3.565	2669990	93.15	1938036	410.19
8	4.206	74668	2.60	61664	789.28
9	4.606	10945	0.38	8785	409.70



Chemical Formula: C₂₂H₂₀FN₃O₂S

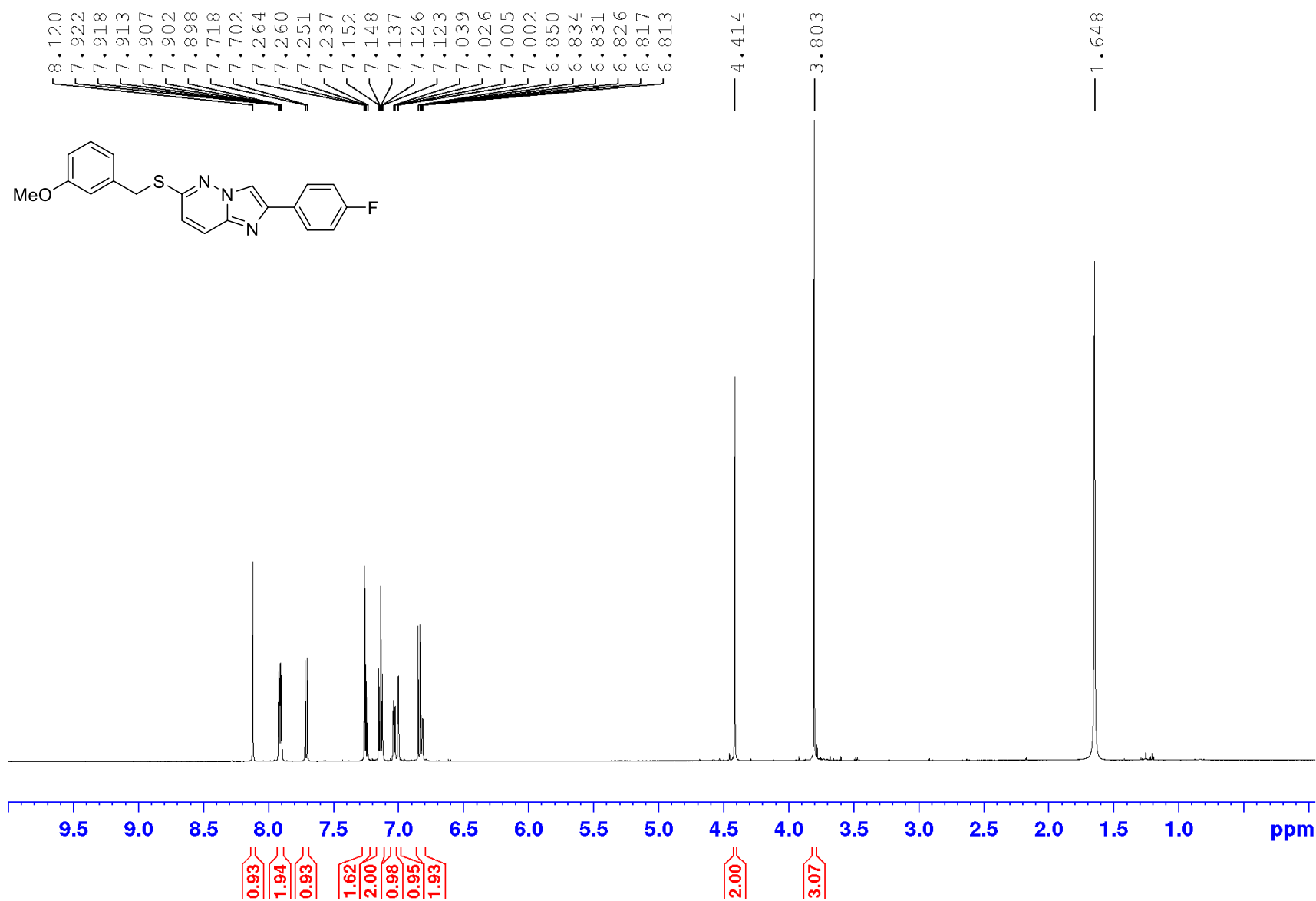
Exact Mass: 409.1260

Molecular Weight: 409.4794

m/z: 409.1260 (100.0%), 410.1294 (23.8%), 411.1218 (4.5%),
411.1327 (2.7%), 410.1231 (1.1%), 412.1252 (1.1%)

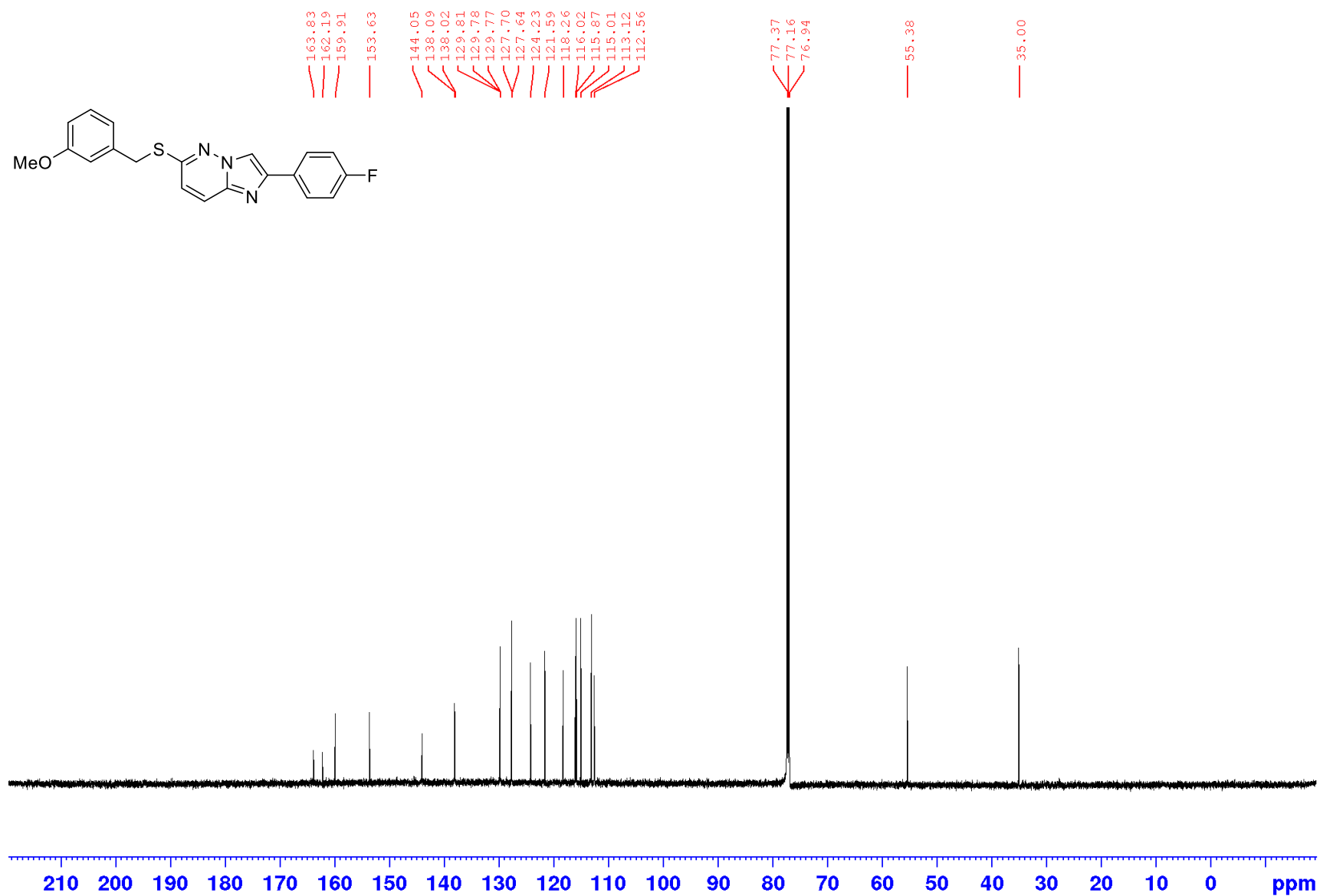
Appendices

¹H NMR spectrum of **220** (600 MHz; CDCl₃)



Appendices

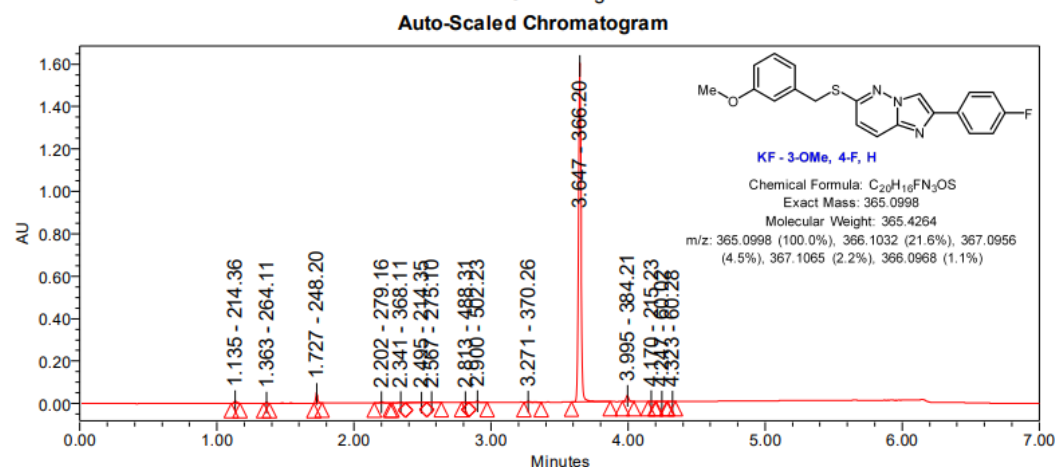
¹³C NMR spectrum of **220** (150 MHz; CDCl₃)



Appendices

LC-MS chromatogram of **220** [M+H]⁺

Sample Name:	KF-3-OMe, 4-F, H	Instrument:	Waters Acquity iClass PDA and QDa detectors
Vial:	1:C,6	Acquired By:	System
Injection #:	1	Sample Set Name:	MK_18_October_2019
Injection Volume:	0.30 ul	Acquisition Method:	95% A1 to 100% B1 POSNEG_Col2
Run Time:	7.0 Minutes	Mobile Phase:	A1: 100% H2O / 0.1% FA B1: 100% MeCN / 0.1% FA
Flowrate:	0.4 mL/min	Extracted Chromatogram:	PDA Spectrum PDA 254.0 nm
Date Acquired:	18/10/2019 4:33:32 PM EST		
Date Processed:	18/10/2019 4:44:09 PM EST		



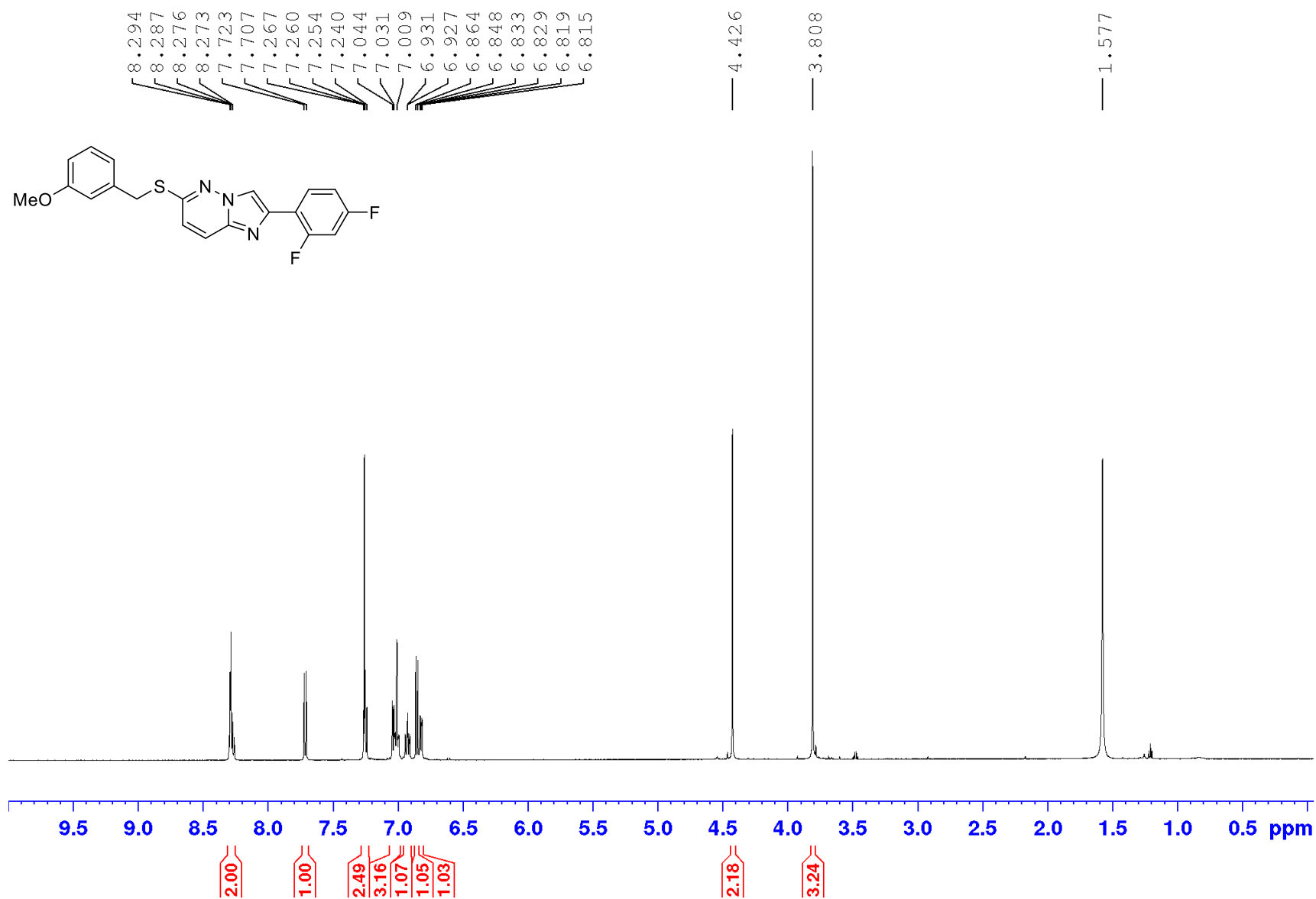
Peak Results

	RT	Area	% Area	Height	Base Peak (m/z)
1	1.135	13728	0.60	9548	214.36
2	1.363	3981	0.17	3782	264.11
3	1.727	49372	2.15	43549	248.20
4	2.202	7120	0.31	4228	279.16
5	2.341	4926	0.21	2912	368.11
6	2.495	4077	0.18	1055	214.35
7	2.567	3301	0.14	2145	275.10
8	2.813	2661	0.12	2097	488.31
9	2.900	9620	0.42	5649	502.23

	RT	Area	% Area	Height	Base Peak (m/z)
10	3.271	6390	0.28	3814	370.26
11	3.647	2146468	93.64	1592815	366.20
12	3.995	36798	1.61	27252	384.21
13	4.170	1783	0.08	1373	215.23
14	4.247	1523	0.07	710	60.02
15	4.323	618	0.03	500	60.28

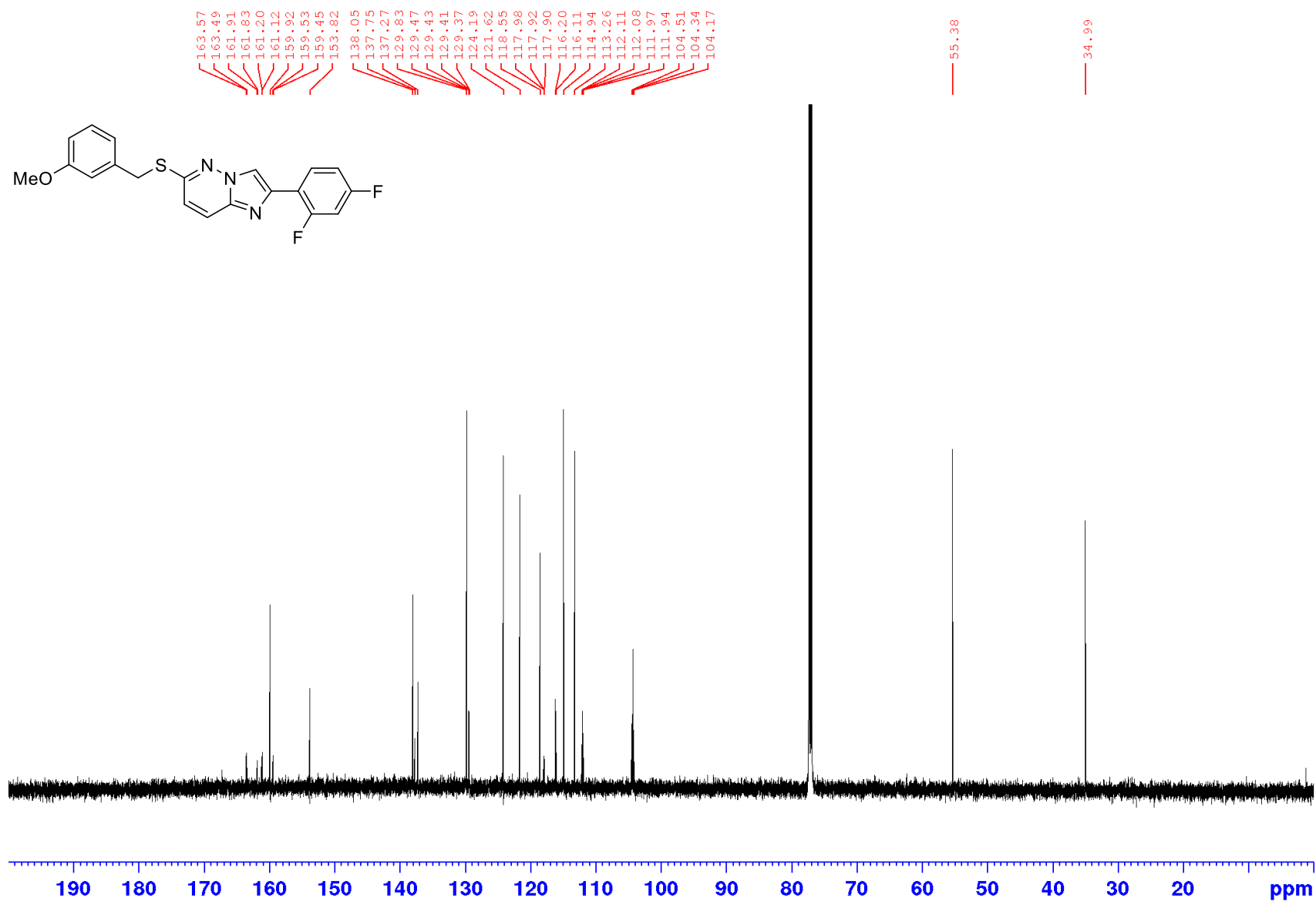
Appendices

¹H NMR spectrum of **221** (600 MHz; CDCl₃)



Appendices

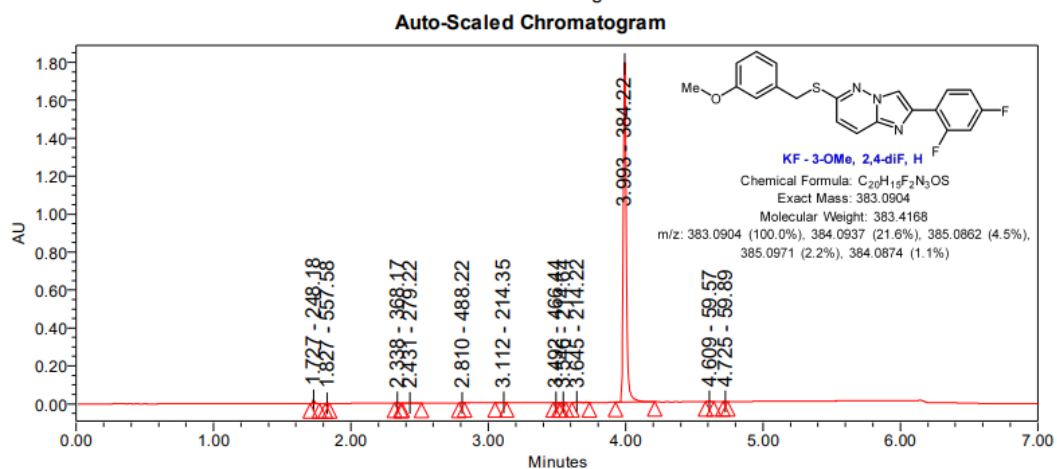
¹³C NMR spectrum of **221** (150 MHz; CDCl₃)



Appendices

LC-MS chromatogram of **221** [M+H]⁺

Sample Name:	KF-3-OMe, 2,4-diF, H	Instrument:	Waters Acquity iClass PDA and QDa detectors
Vial:	1:C,7	Acquired By:	System
Injection #:	1	Sample Set Name:	MK_18_October_2019
Injection Volume:	0.30 ul	Acquisition Method:	95% A1 to 100% B1 POSNEG_Col2
Run Time:	7.0 Minutes	Mobile Phase:	A1: 100% H2O / 0.1% FA B1: 100% MeCN / 0.1% FA
Flowrate:	0.4 mL/min	Extracted Chromatogram:	PDA Spectrum PDA 254.0 nm
Date Acquired:	18/10/2019 4:25:07 PM EST		
Date Processed:	18/10/2019 4:47:09 PM EST		



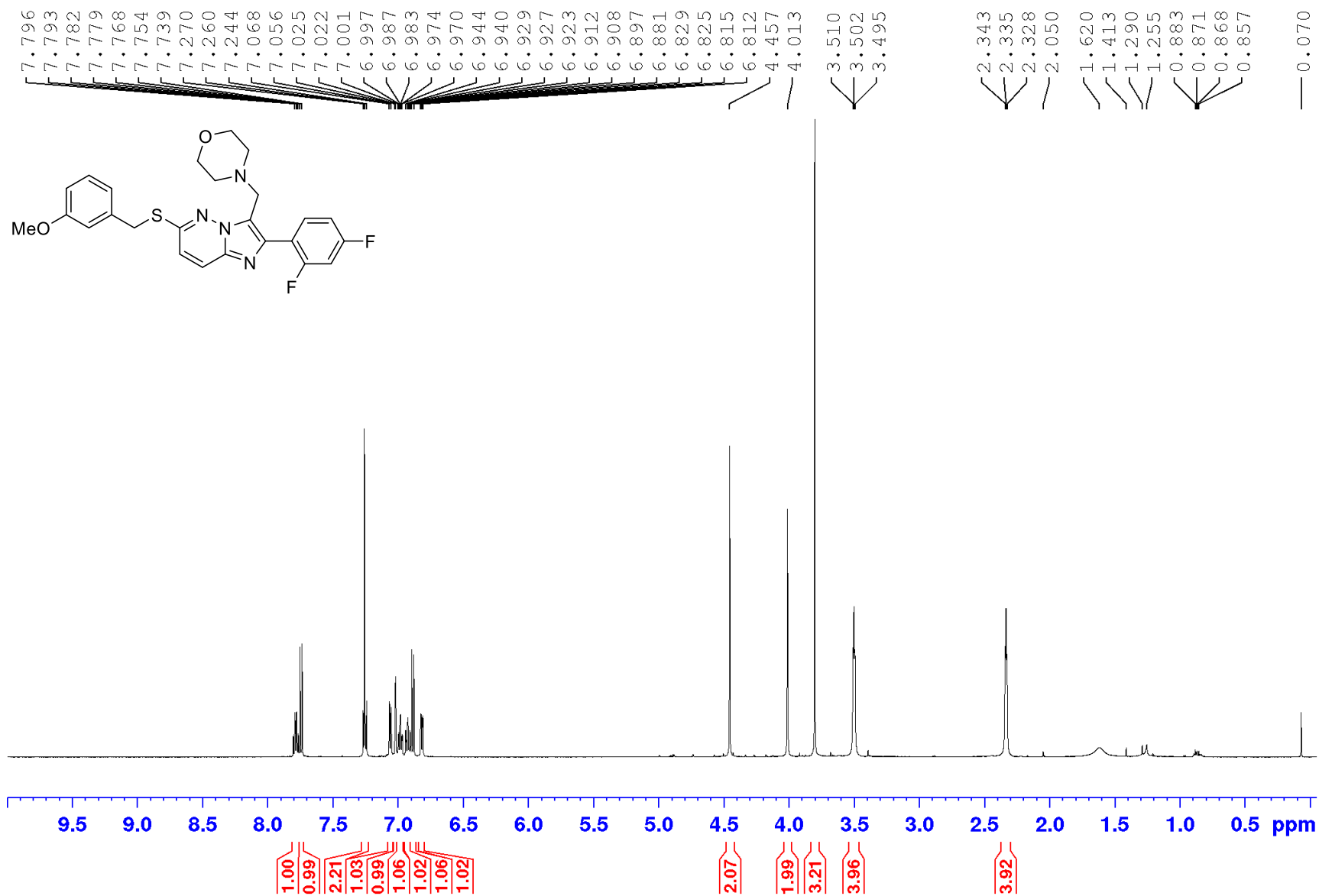
Peak Results

	RT	Area	% Area	Height	Base Peak (m/z)
1	1.727	18970	0.71	16769	248.18
2	1.827	689	0.03	727	557.58
3	2.338	3517	0.13	3130	368.17
4	2.431	3673	0.14	917	279.22
5	2.810	1185	0.04	1129	488.22
6	3.112	2408	0.09	935	214.35
7	3.492	1155	0.04	964	466.44
8	3.546	849	0.03	682	214.64
9	3.645	7082	0.26	2612	214.22

	RT	Area	% Area	Height	Base Peak (m/z)
10	3.993	2644664	98.40	1782694	384.22
11	4.609	2721	0.10	2116	59.57
12	4.725	641	0.02	591	59.89

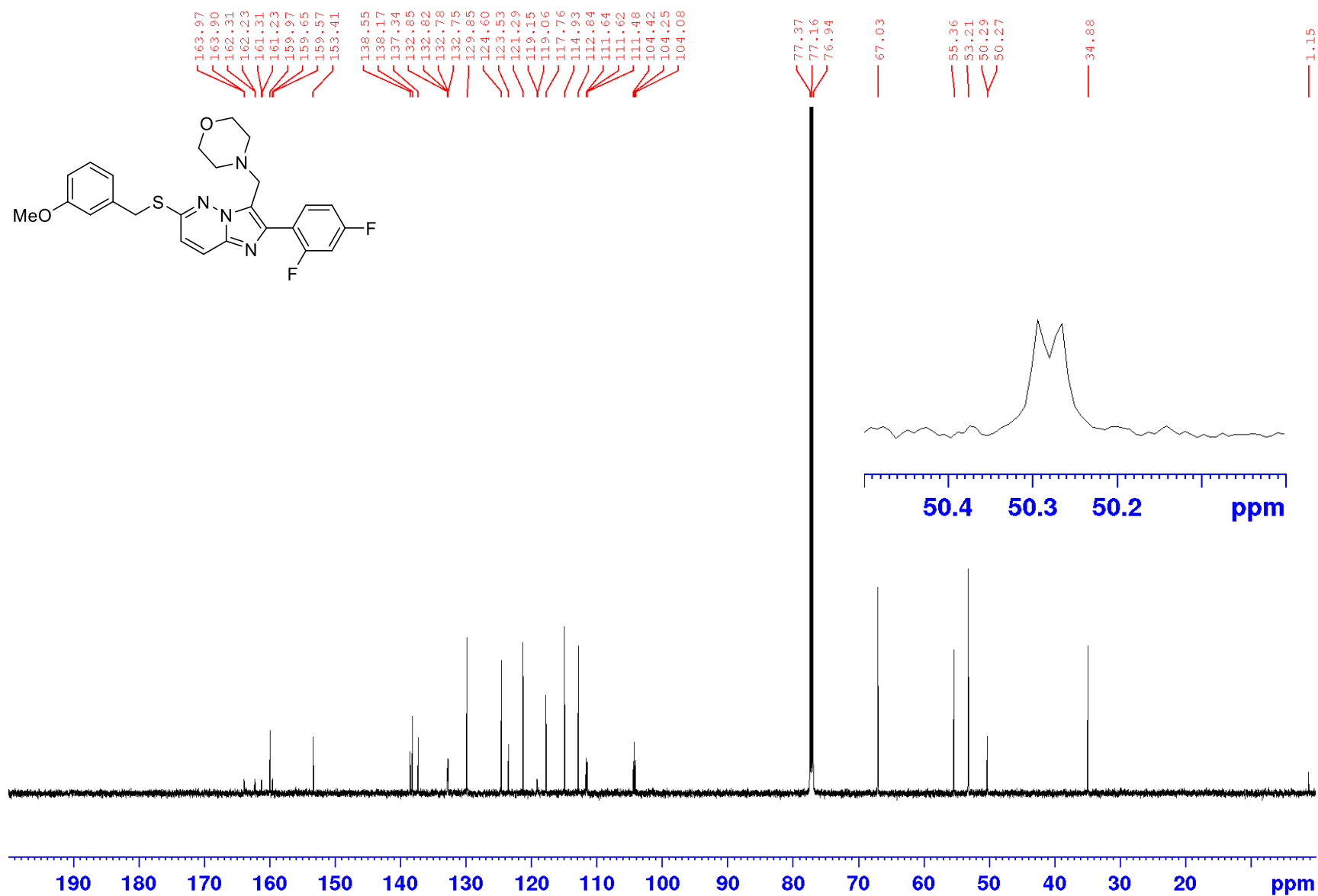
Appendices

¹H NMR spectrum of **225** (600 MHz; CDCl₃)



Appendices

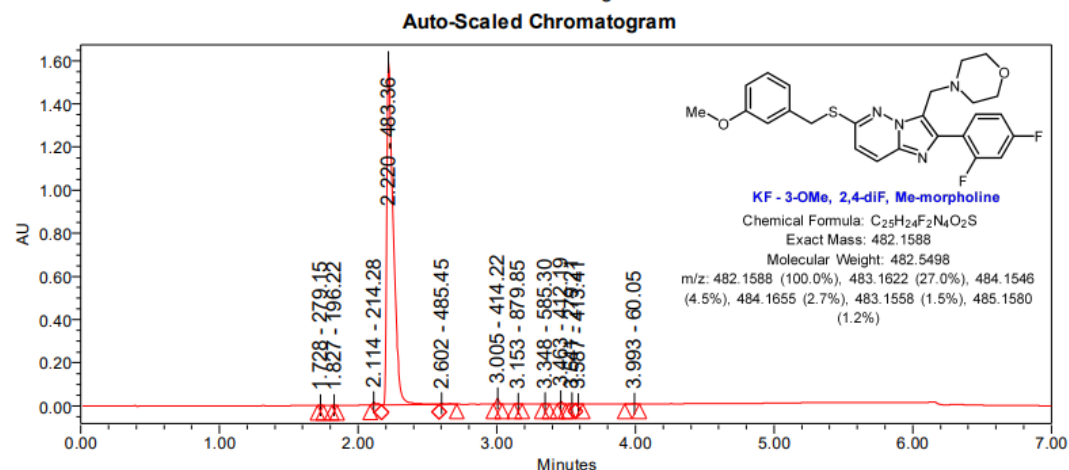
¹³C NMR spectrum of **225** (150 MHz; CDCl₃)



Appendices

LC-MS chromatogram of 225 [M+H]⁺

Sample Name:	KF-3-OMe,2,4-diF, Me-morpholine	Instrument:	Waters Acquity iClass PDA and QDa detectors
Vial:	1:C,2	Acquired By:	System
Injection #:	1	Sample Set Name:	MK_18_October_2019
Injection Volume:	1.00 ul	Acquisition Method:	95% A1 to 100% B1 POSNEG_Col2
Run Time:	7.0 Minutes	Mobile Phase:	A1: 100% H2O / 0.1% FA B1: 100% MeCN / 0.1% FA
Flowrate:	0.4 mL/min	Extracted Chromatogram:	PDA Spectrum PDA 254.0 nm
Date Acquired:	18/10/2019 3:41:26 PM EST		
Date Processed:	18/10/2019 4:00:13 PM EST		



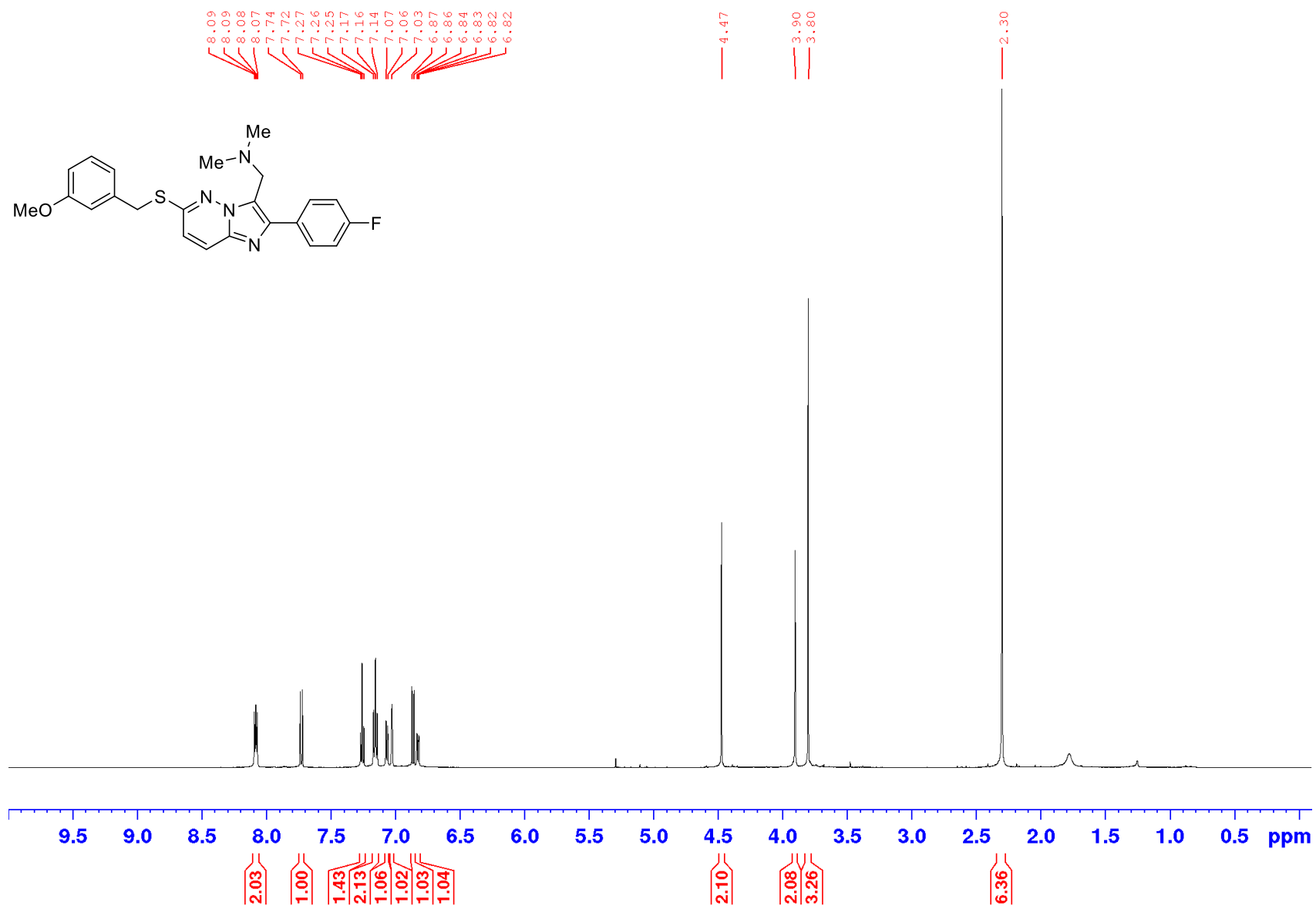
Peak Results

	RT	Area	% Area	Height	Base Peak (m/z)
1	1.728	2176	0.04	1953	279.15
2	1.827	987	0.02	937	196.22
3	2.114	27797	0.52	14445	214.28
4	2.220	5244141	97.87	1590043	483.36
5	2.602	16500	0.31	5104	485.45
6	3.005	33383	0.62	26508	414.22
7	3.153	4179	0.08	2868	879.85
8	3.348	4172	0.08	2987	585.30
9	3.463	15435	0.29	12431	412.19

	RT	Area	% Area	Height	Base Peak (m/z)
10	3.541	4121	0.08	3129	279.21
11	3.587	1168	0.02	847	413.41
12	3.993	3991	0.07	1774	60.05

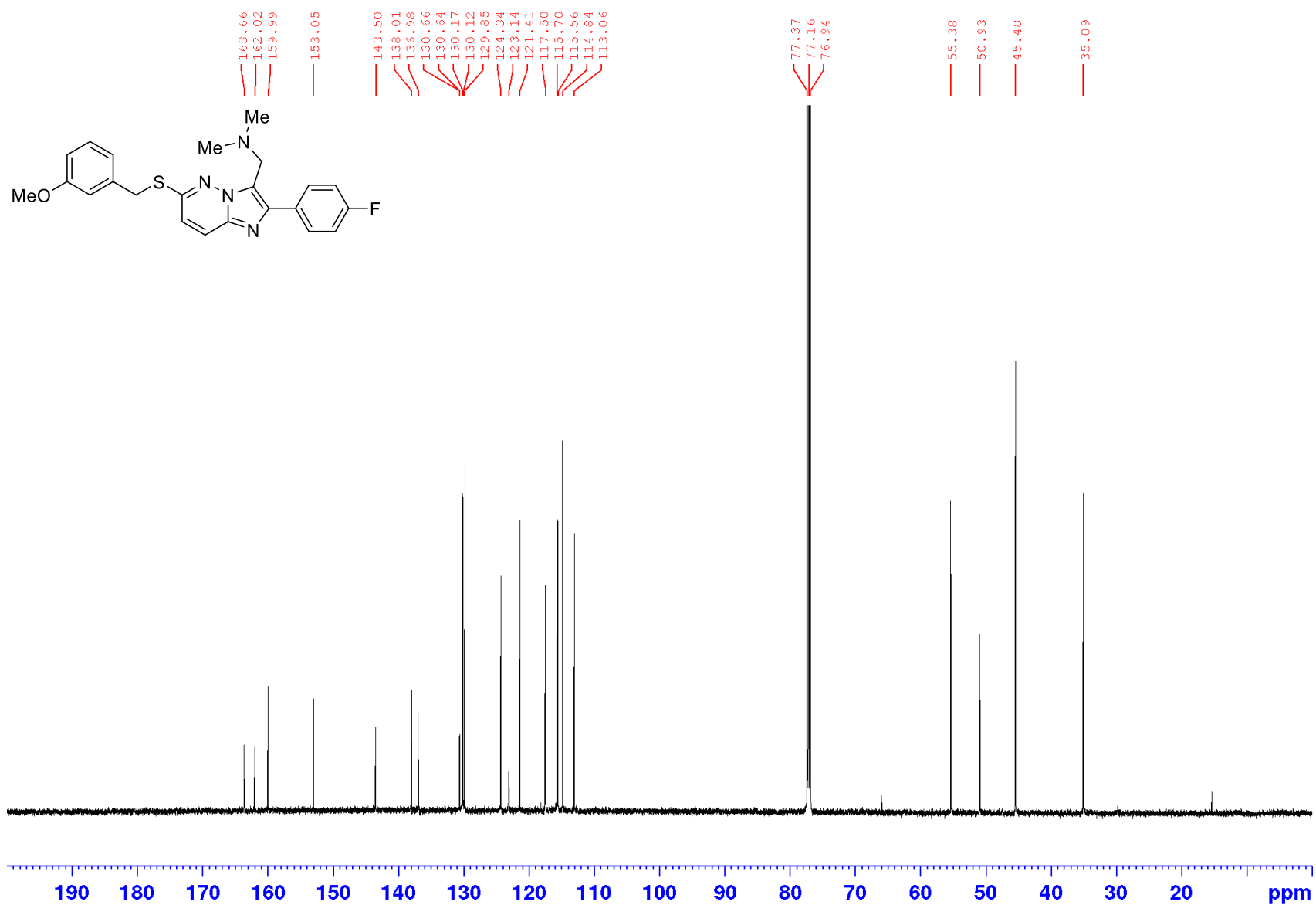
Appendices

¹H NMR spectrum of **229** (600 MHz; CDCl₃)



Appendices

¹³C NMR spectrum of **229** (150 MHz; CDCl₃)

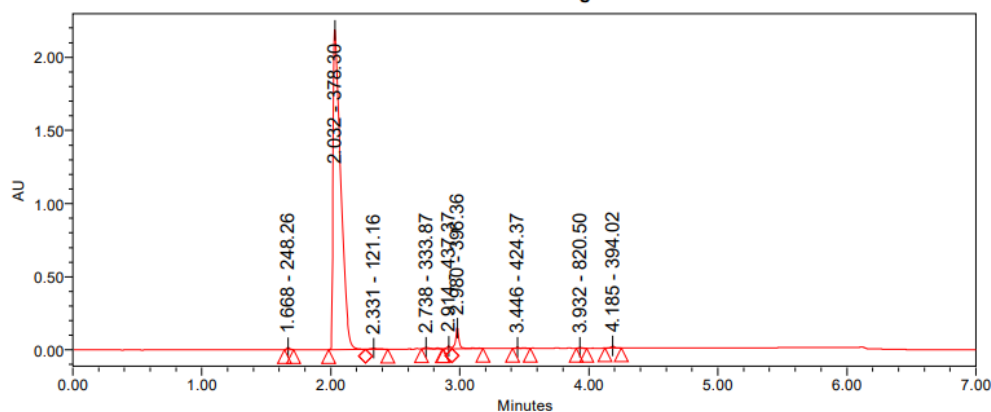


Appendices

LC-MS chromatogram of **229** [M+H]⁺

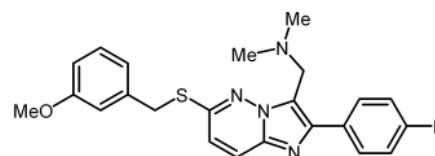
Sample Name: **KF Mannich 4-F** Instrument: Waters Acquity iClass
 Vial: 1:C,7 Acquired By: System
 Injection #: 1 Sample Set Name: MK_15_April2020
 Injection Volume: 1.00 ul
 Run Time: 7.0 Minutes Acquisition Method: 95% A1 to 100% B1 POSNEG Waters
 Mobile Phase: A1: 100% H2O / 0.1% FA
 B1: 100% ACN / 0.1% FA
 Date Acquired: 15/04/2020 3:42:43 PM EST
 Date Processed: 15/04/2020 4:02:57 PM EST Extracted PDA Spectrum PDA 254.0 nm

Chromatogram:
Auto-Scaled Chromatogram



Peak Results

	RT	Area	% Area	Height	Base Peak (m/z)
1	1.668	24140	0.26	14627	248.26
2	2.032	8923423	95.04	2202781	378.30
3	2.331	31879	0.34	7173	121.16
4	2.738	36900	0.39	10430	333.87
5	2.914	35210	0.38	16906	437.37
6	2.980	279949	2.98	140545	396.36
7	3.446	19994	0.21	9074	424.37
8	3.932	9163	0.10	5310	820.50
9	4.185	28144	0.30	14064	394.02



Chemical Formula: C₂₃H₂₃FN₄OS

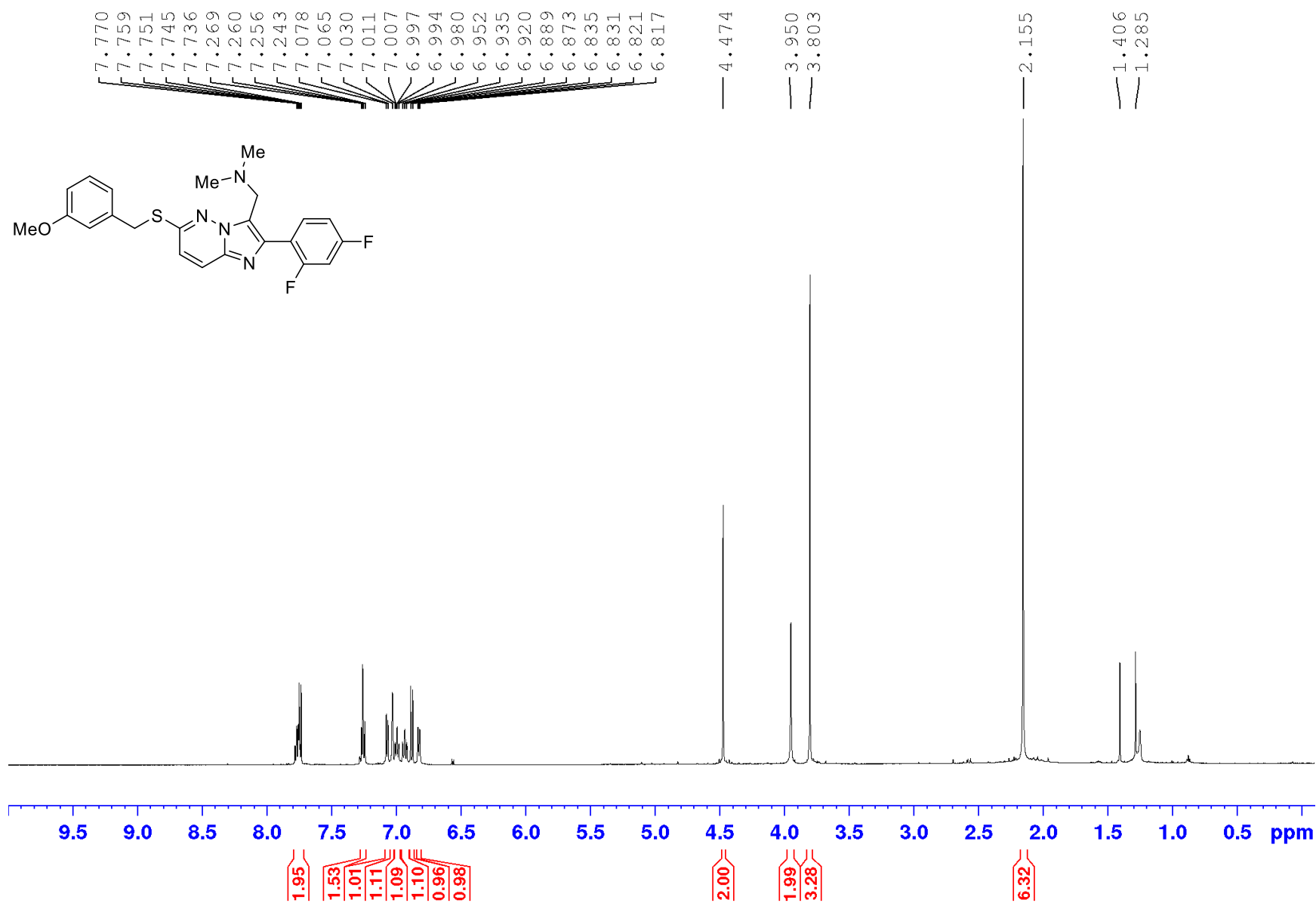
Exact Mass: 422.1577

Molecular Weight: 422.5224

m/z: 422.1577 (100.0%), 423.1610 (24.9%), 424.1535 (4.5%),
424.1644 (2.7%), 423.1547 (1.5%), 425.1568 (1.1%)

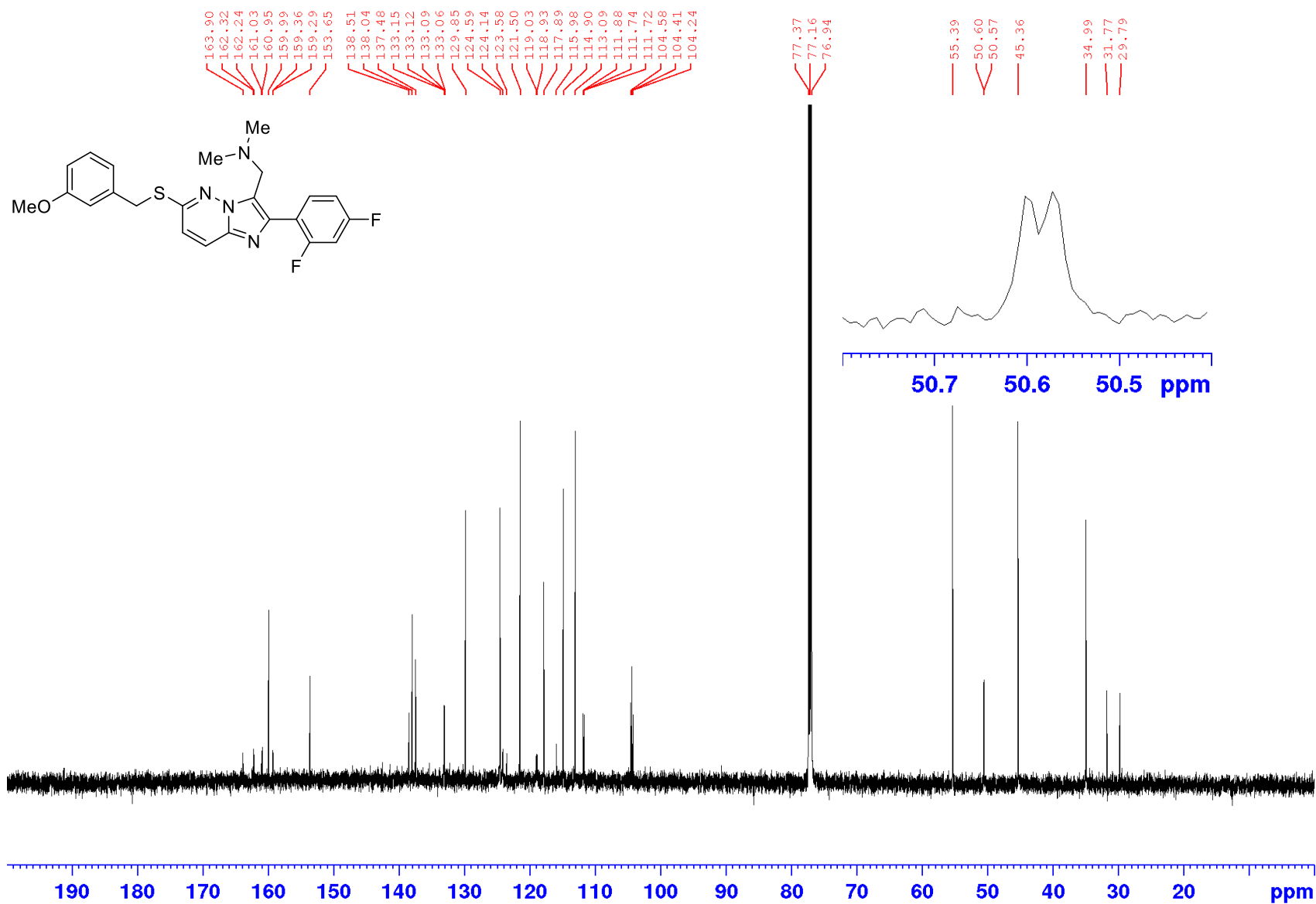
Appendices

¹H NMR spectrum of **230** (600 MHz; CDCl₃)



Appendices

^{13}C NMR spectrum of **230** (150 MHz; CDCl_3) petrol present (29.79 – 31.77 ppm)

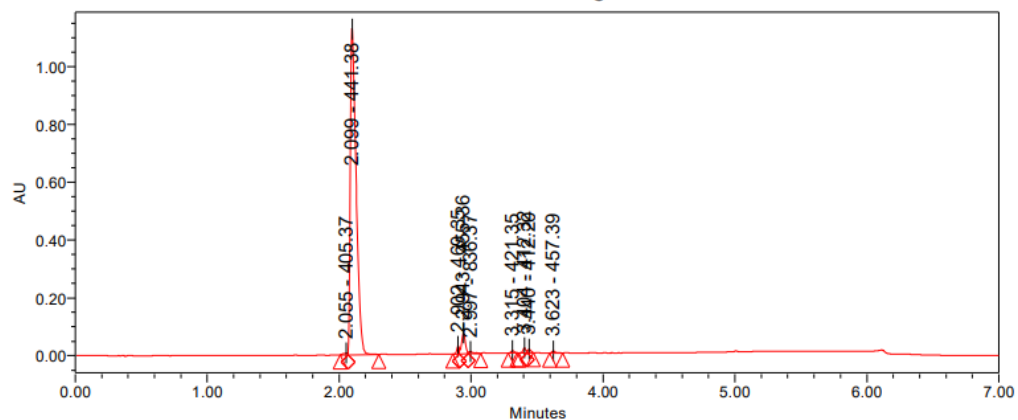


Appendices

LC-MS chromatogram of **230** [M+H]⁺

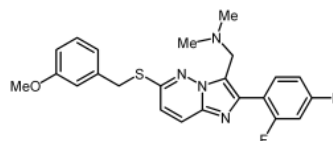
Sample Name: **KF Mannich 2,4-diF** Instrument: Waters Acquity iClass
 Vial: 1:C,6 Acquired By: System
 Injection #: 1 Sample Set Name: MK_15_April2020
 Injection Volume: 1.00 ul
 Run Time: 7.0 Minutes Acquisition Method: 95% A1 to 100% B1 POSNEG Waters
 Date Acquired: 15/04/2020 3:34:11 PM EST Mobile Phase: A1: 100% H₂O / 0.1% FA
 Date Processed: 15/04/2020 4:01:17 PM EST B1: 100% ACN / 0.1% FA
 Extracted Chromatogram: PDA Spectrum PDA 254.0 nm

Auto-Scaled Chromatogram



Peak Results

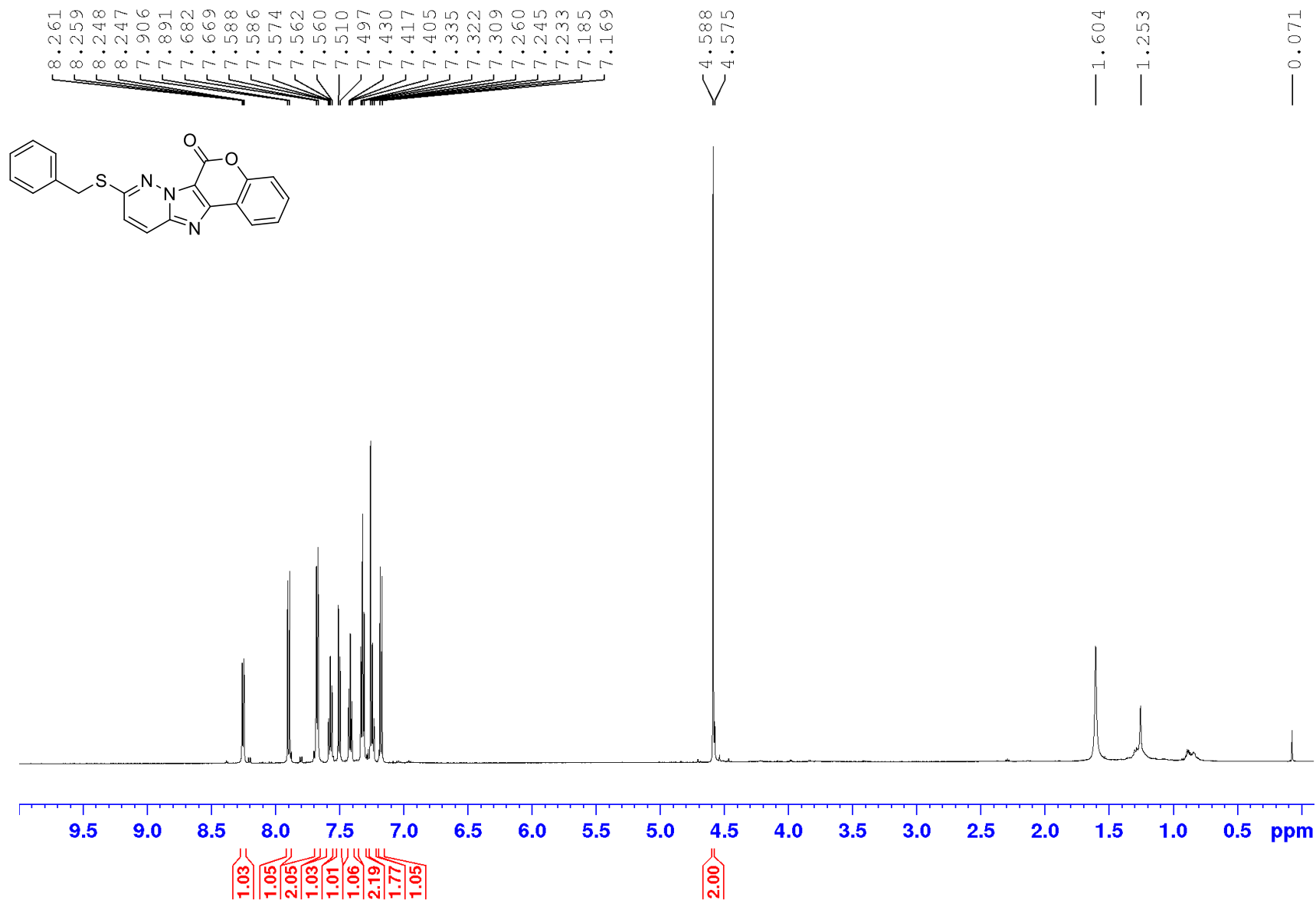
RT	Area	% Area	Height	Base Peak (m/z)
1 2.055	13813	0.38	6605	405.37
2 2.099	3389575	92.65	1138136	441.38
3 2.902	32585	0.89	26407	469.35
4 2.943	134458	3.68	71765	455.36
5 2.997	15466	0.42	7087	836.37
6 3.315	12778	0.35	7995	421.35
7 3.404	27597	0.75	16965	412.32
8 3.440	18612	0.51	12654	412.20
9 3.623	13776	0.38	7305	457.39



Chemical Formula: C₂₂H₂₂F₂N₄OS
 Exact Mass: 440.1482
 Molecular Weight: 440.5128
 m/z: 440.1482 (100.0%), 441.1516 (24.9%), 442.1440 (4.5%), 442.1549 (2.7%), 441.1453 (1.5%), 443.1474 (1.1%)

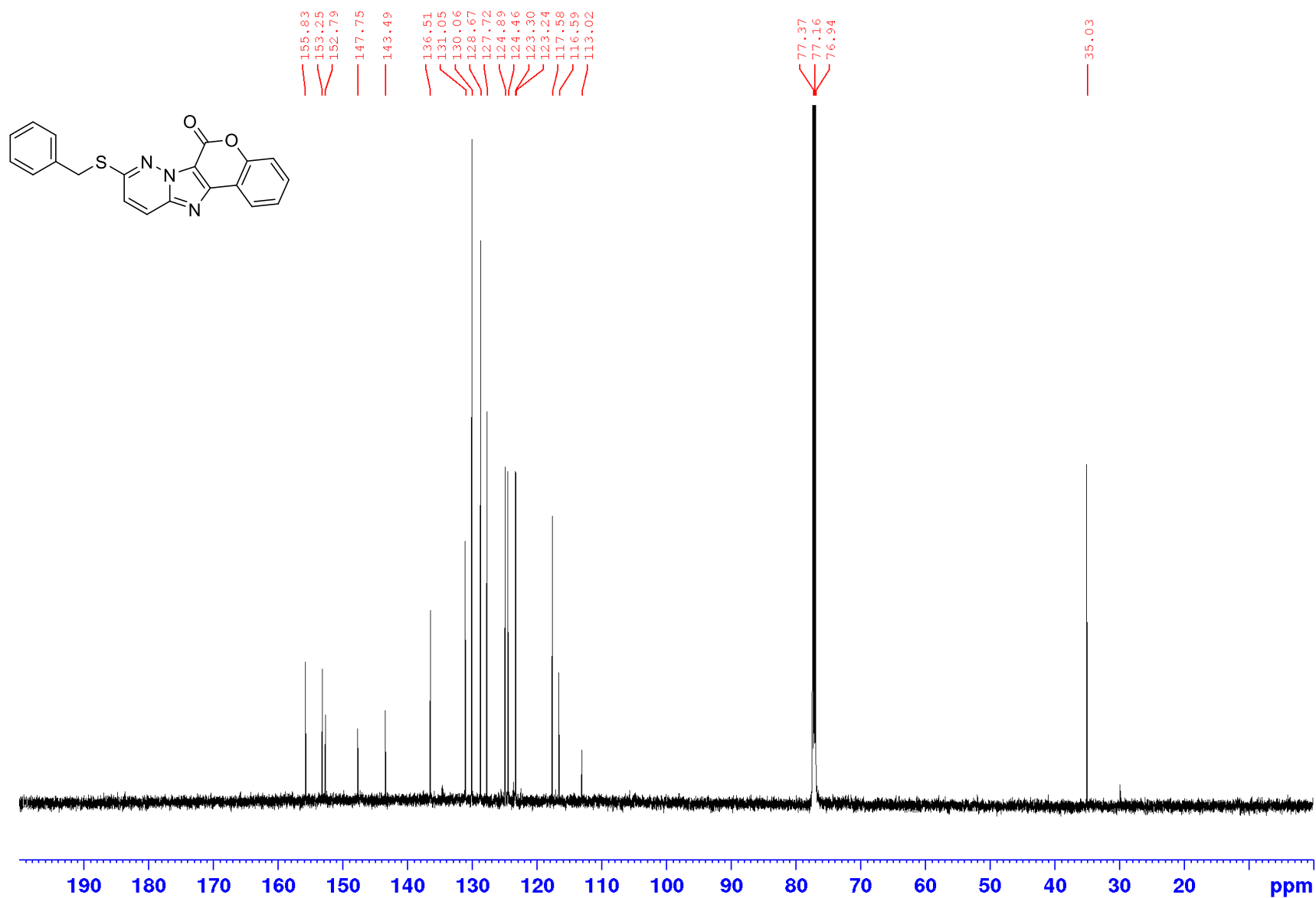
Appendices

¹H NMR spectrum of **234** (600 MHz; CDCl₃)



Appendices

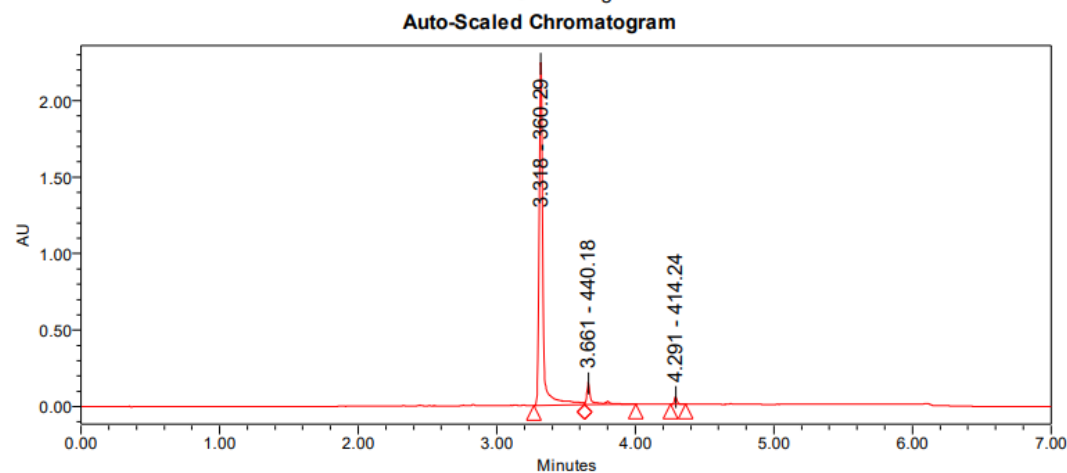
¹³C NMR spectrum of **234** (150 MHz; CDCl₃)



Appendices

LC-MS chromatogram of **234** [M+H]⁺

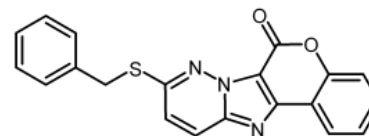
Sample Name:	CLF505-19-Lactone	Instrument:	Waters Acquity iClass PDA and QDa detectors
Vial:	1:B,4	Acquired By:	System
Injection #:	1	Sample Set Name:	MK_24_January2020
Injection Volume:	1.00 ul	Acquisition Method:	95%A1_100%B1 POSNEGWaters
Run Time:	7.0 Minutes	Mobile Phase:	A1: 100% H2O / 0.1% FA B1: 100% ACN / 0.1% FA
Flowrate:	0.4 mL/min	Extracted Chromatogram:	PDA Spectrum PDA 254.0 nm
Date Acquired:	24/01/2020 11:23:41 AM EST		
Date Processed:	24/01/2020 11:39:25 AM EST		



Peak Results

	RT	Area	% Area	Height	Base Peak (m/z)
1	3.318	4164214	90.72	2248897	360.29
2	3.661	356357	7.76	141887	440.18
3	4.291	69395	1.51	47679	414.24

CLF505-19 - Lactone



Chemical Formula: C₂₀H₁₃N₃O₂S

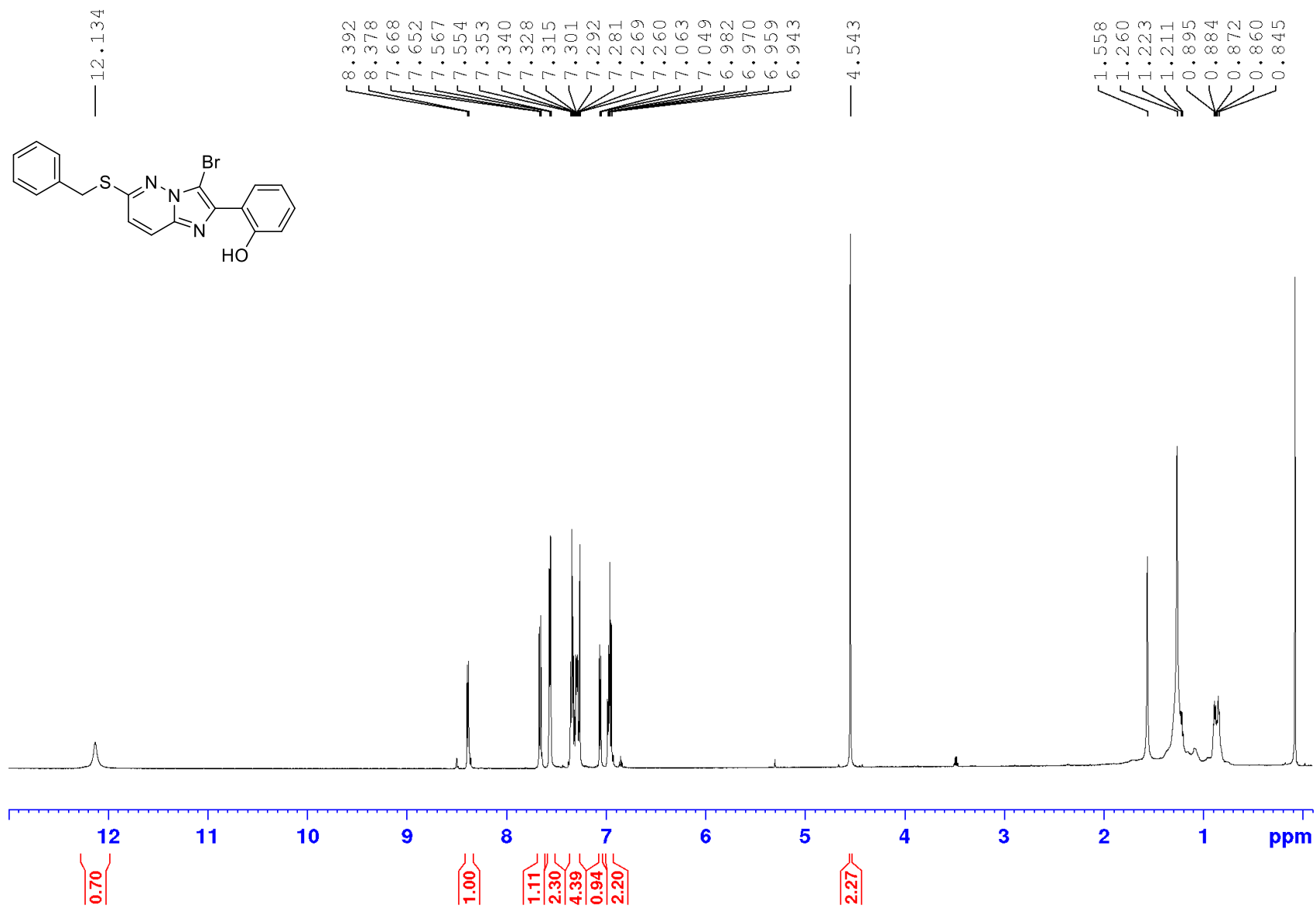
Exact Mass: 359.0728

Molecular Weight: 359.4030

m/z: 359.0728 (100.0%), 360.0762 (21.6%),
361.0686 (4.5%), 361.0796 (2.2%), 360.0699
(1.1%)

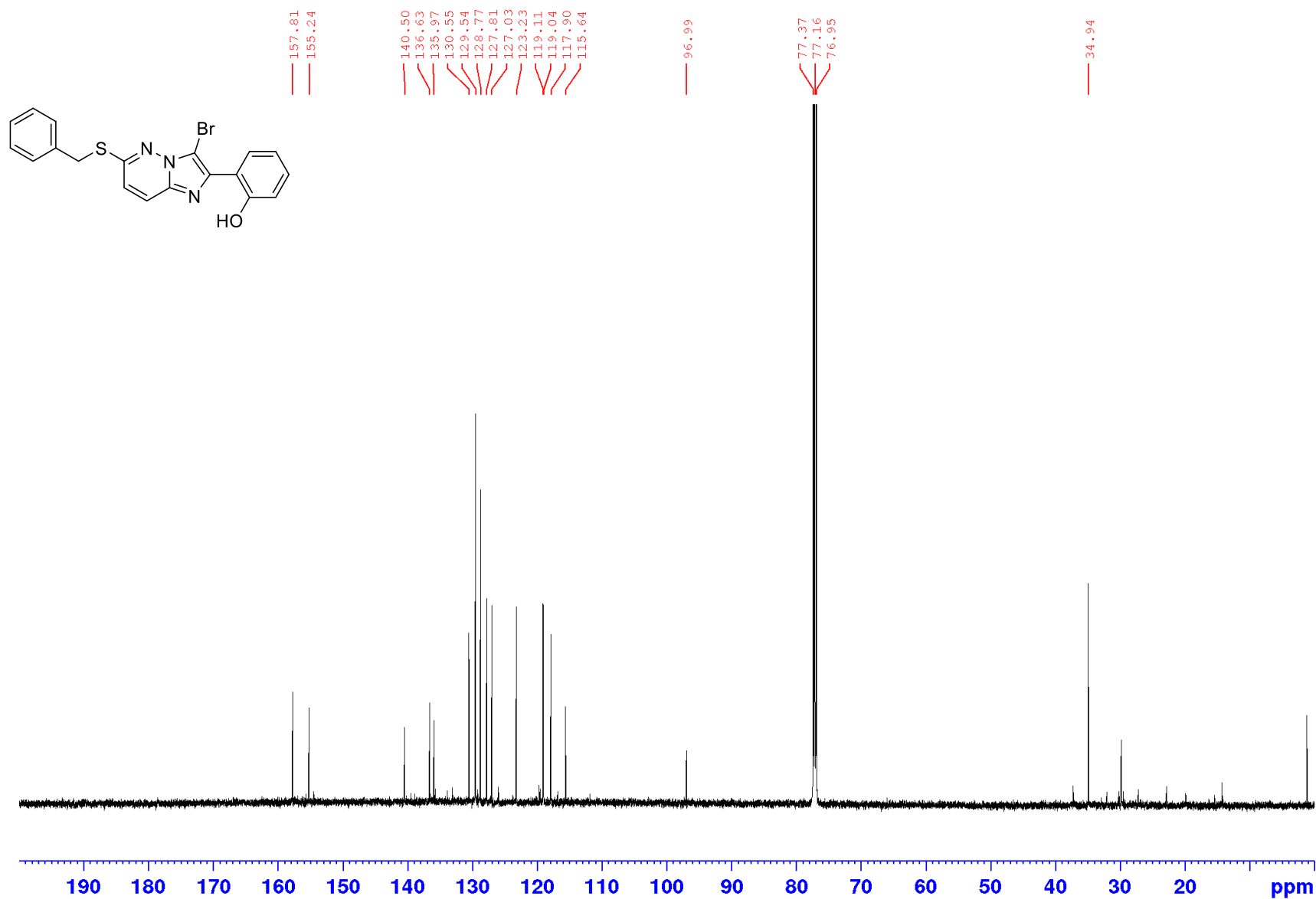
Appendices

¹H NMR spectrum of **239** (600 MHz; CDCl₃)



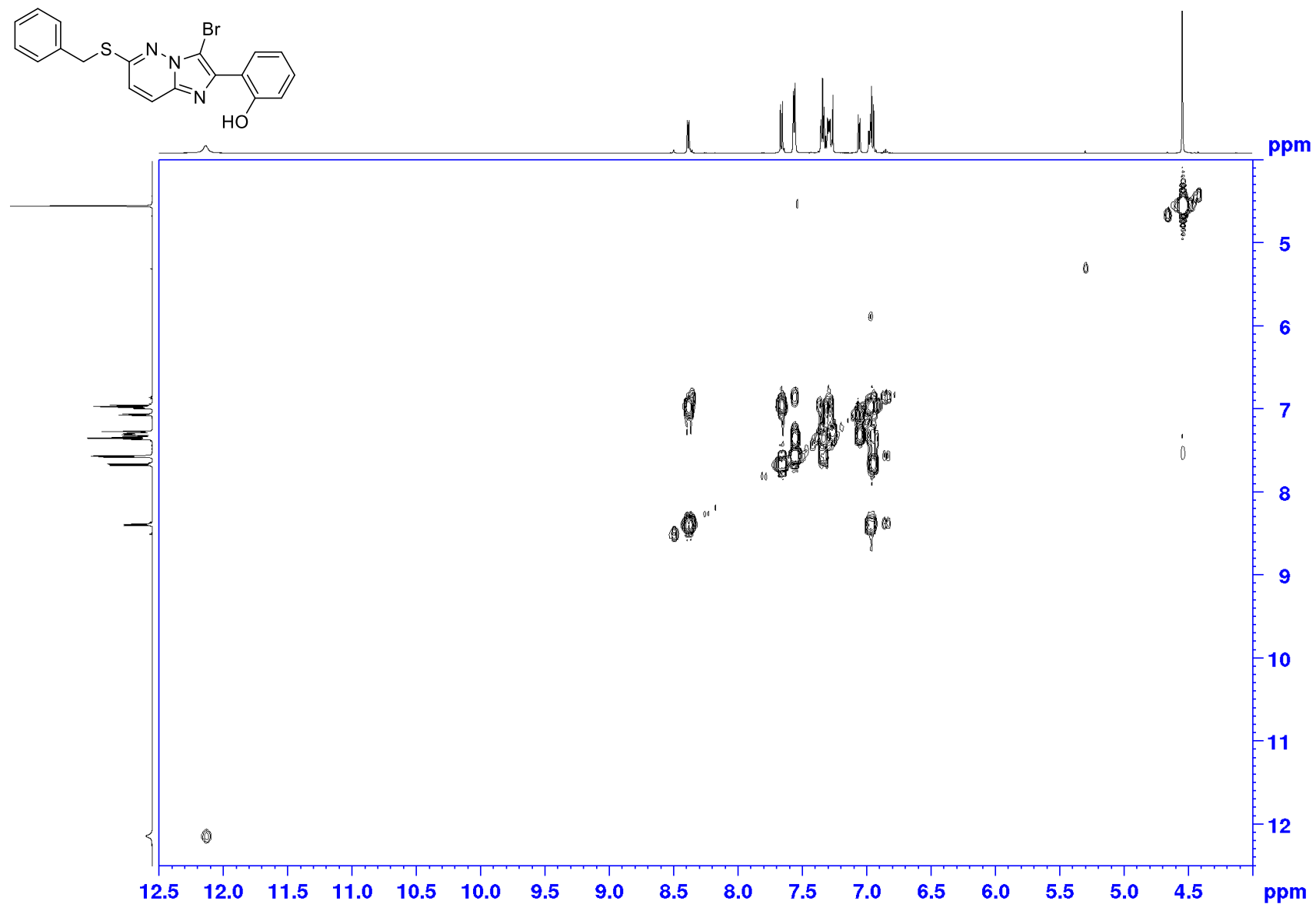
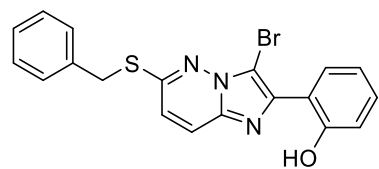
Appendices

¹³C NMR spectrum of **239** (150 MHz; CDCl₃)



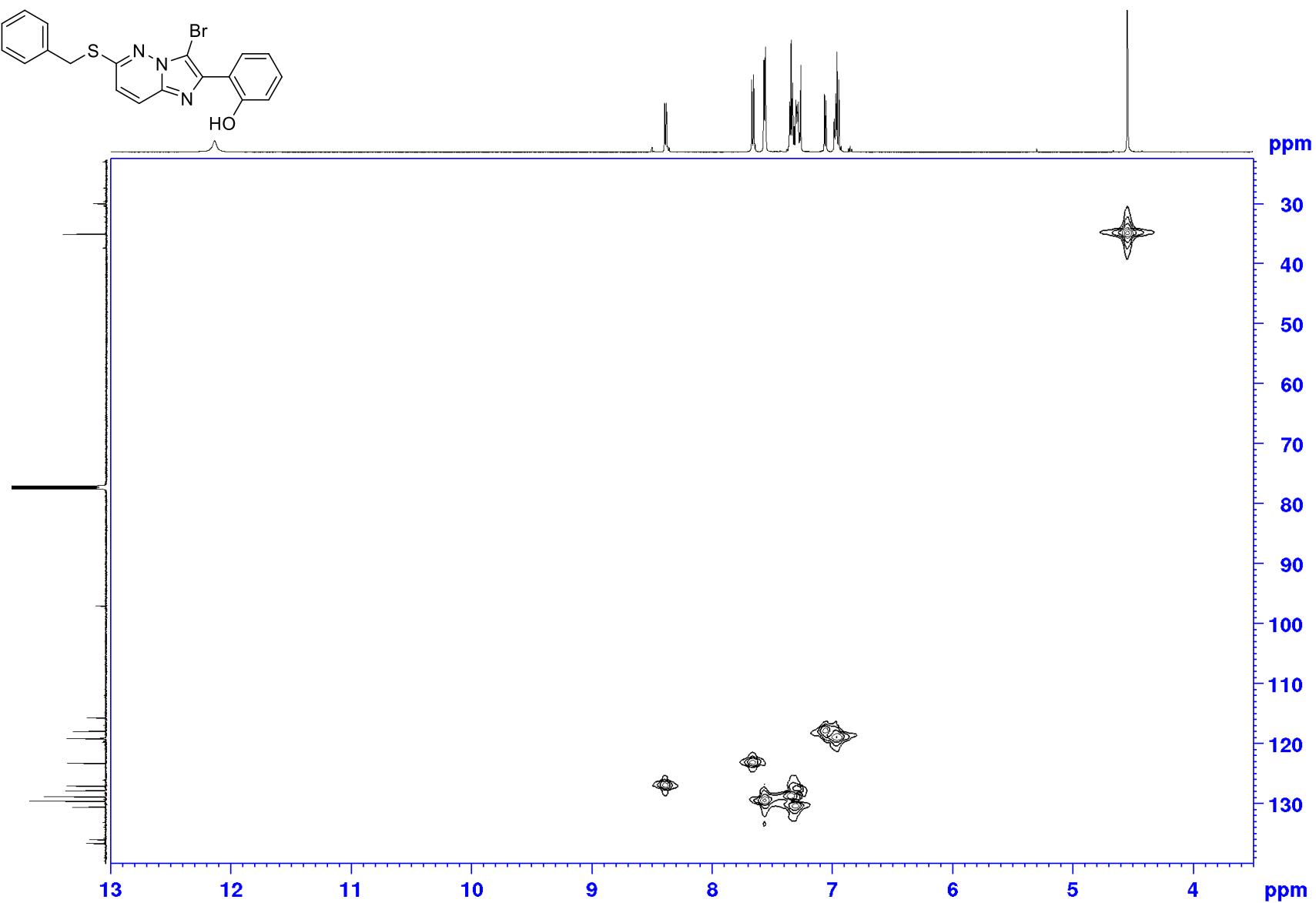
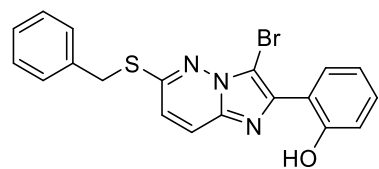
Appendices

COSY spectrum of **239** (600 x 600 MHz; CDCl₃)



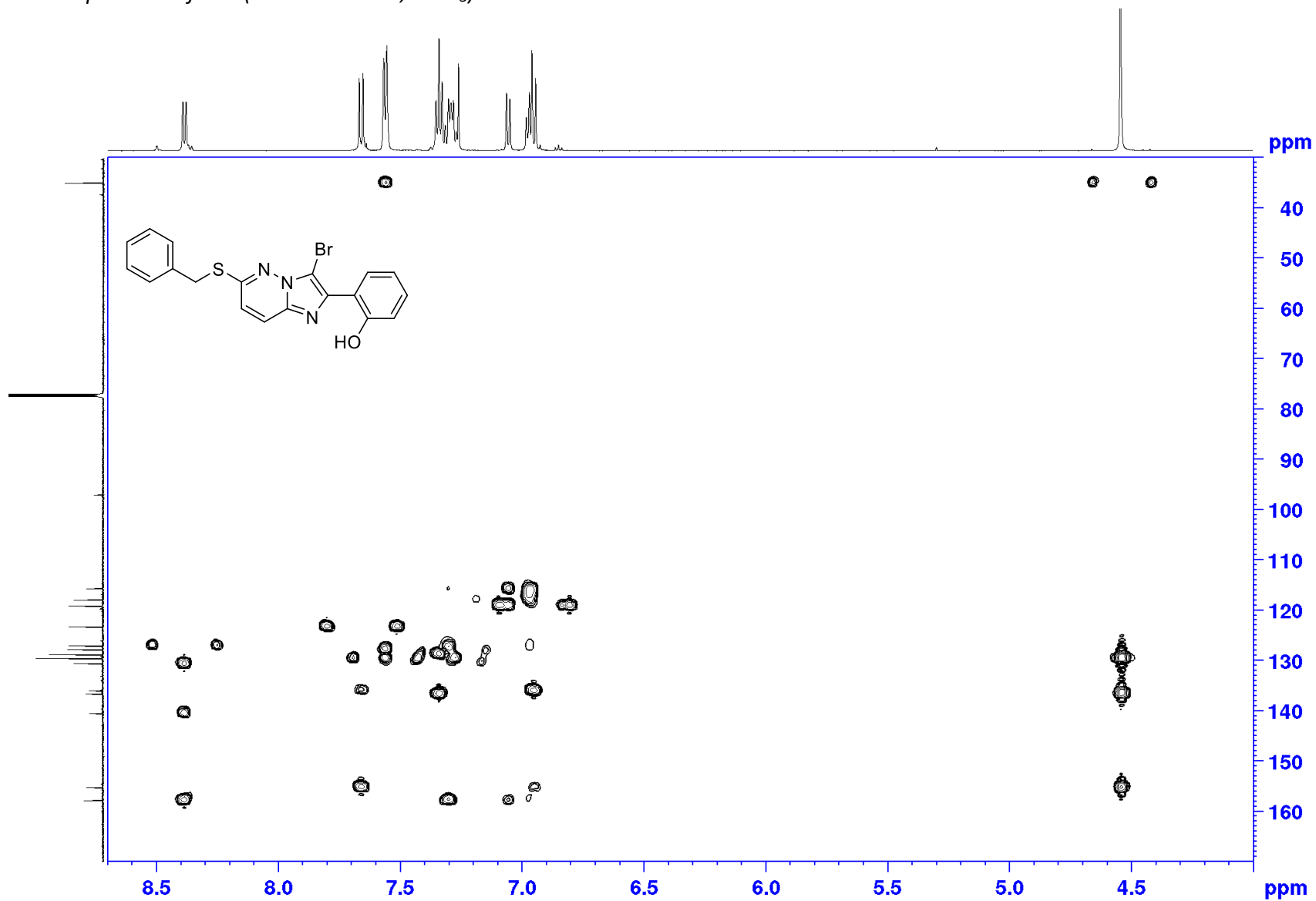
Appendices

HMQC spectrum of **239** (400 x 100 MHz; CDCl₃)



Appendices

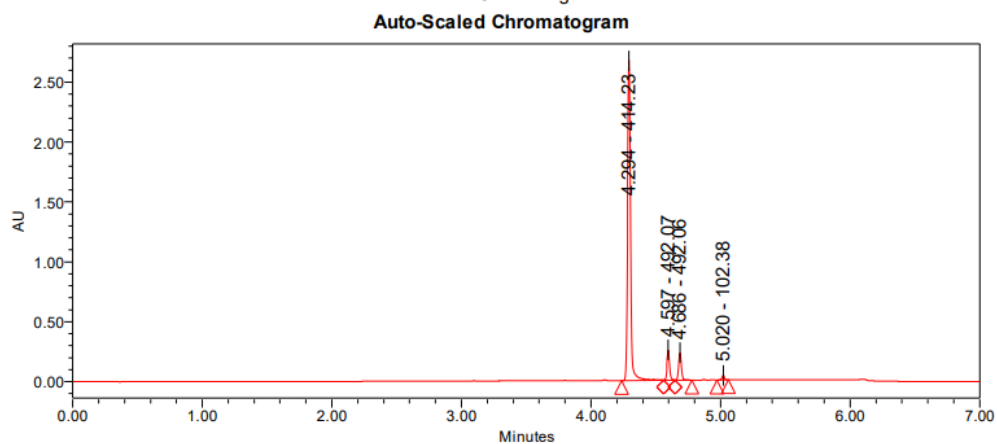
HMBC spectrum of **239** (400 x 100 MHz; CDCl₃)



Appendices

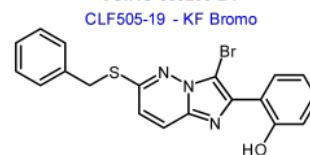
LC-MS chromatogram of **239** [M+H]⁺

Sample Name:	CLF505-19-KF Bromo	Instrument:	Waters Acquity iClass PDA and QDa detectors
Vial:	1:B,5	Acquired By:	System
Injection #:	1	Sample Set Name:	MK_24_January2020
Injection Volume:	1.00 ul	Acquisition Method:	95%A1_100%B1 POSNEGWaters
Run Time:	7.0 Minutes	Mobile Phase:	A1: 100% H2O / 0.1% FA B1: 100% ACN / 0.1% FA
Flowrate:	0.4 mL/min	Extracted Chromatogram:	PDA Spectrum PDA 254.0 nm
Date Acquired:	24/01/2020 11:32:09 AM EST		
Date Processed:	24/01/2020 11:40:43 AM EST		



Peak Results

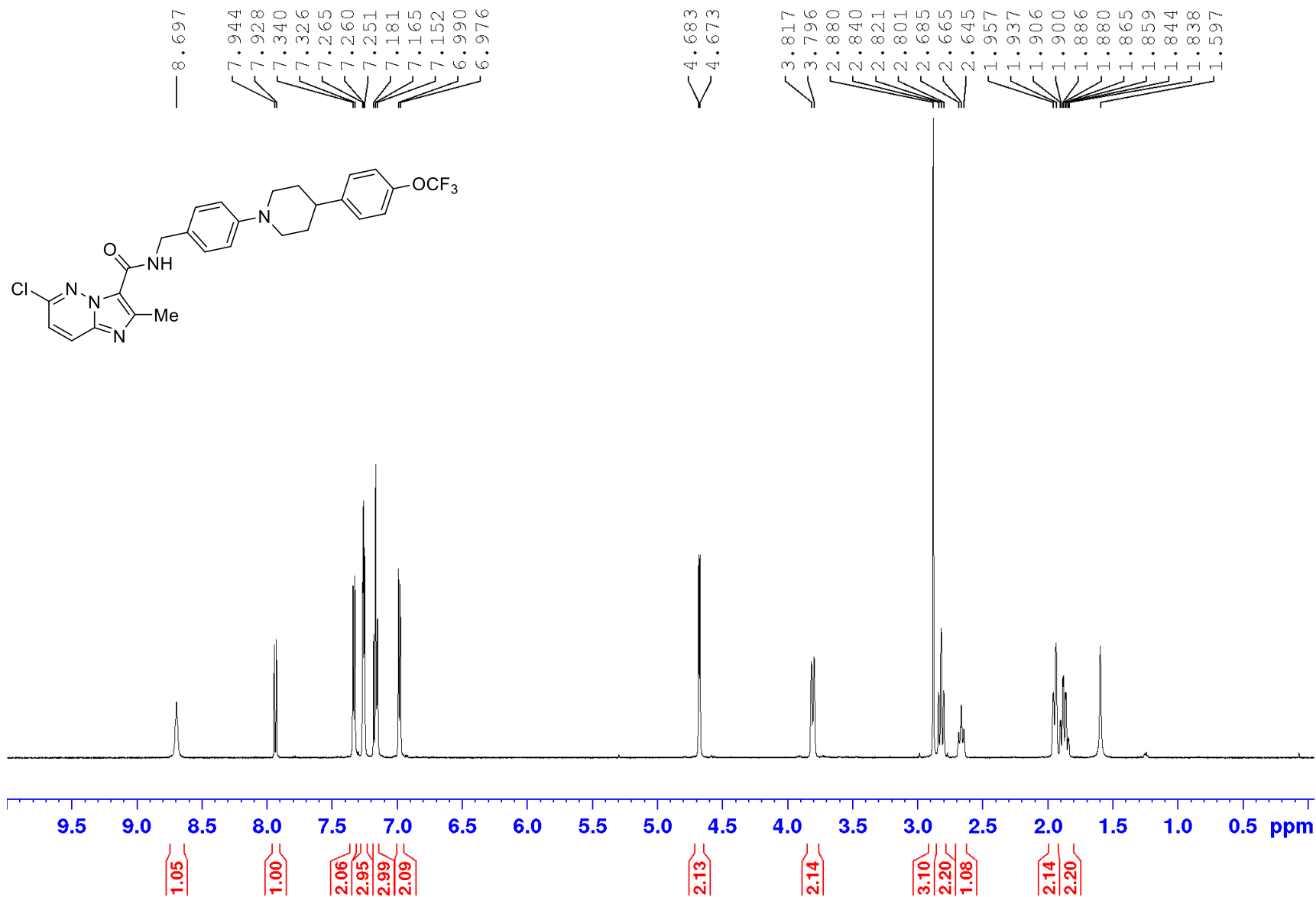
	RT	Area	% Area	Height	Base Peak (m/z)
1	4.294	4357026	85.64	2672150	414.23
2	4.597	355391	6.99	252054	492.07
3	4.686	322617	6.34	227731	492.06
4	5.020	52472	1.03	39303	102.38



Chemical Formula: C₁₉H₁₄BrN₃OS
 Exact Mass: 411.0041
 Molecular Weight: 412.3050
 m/z: 411.0041 (100.0%), 413.0020 (97.3%),
 414.0054 (20.0%), 412.0075 (16.2%),
 412.9999 (4.5%), 414.9978 (4.4%), 412.0075
 (4.3%), 415.0088 (1.2%), 412.0011 (1.1%),
 413.9991 (1.1%), 413.0108 (1.1%)

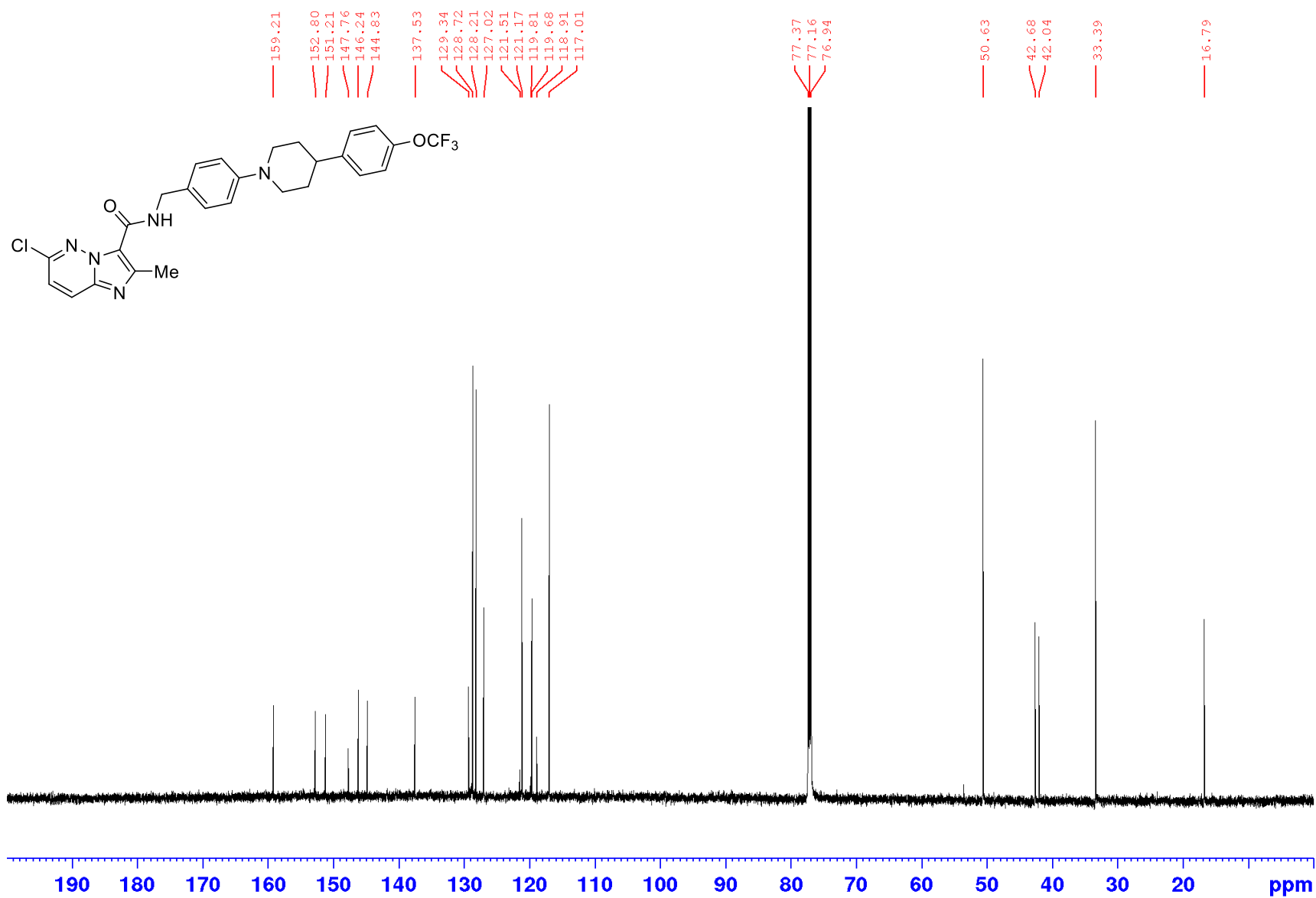
Appendices

¹H NMR spectrum of **264** (600 MHz; CDCl₃)



Appendices

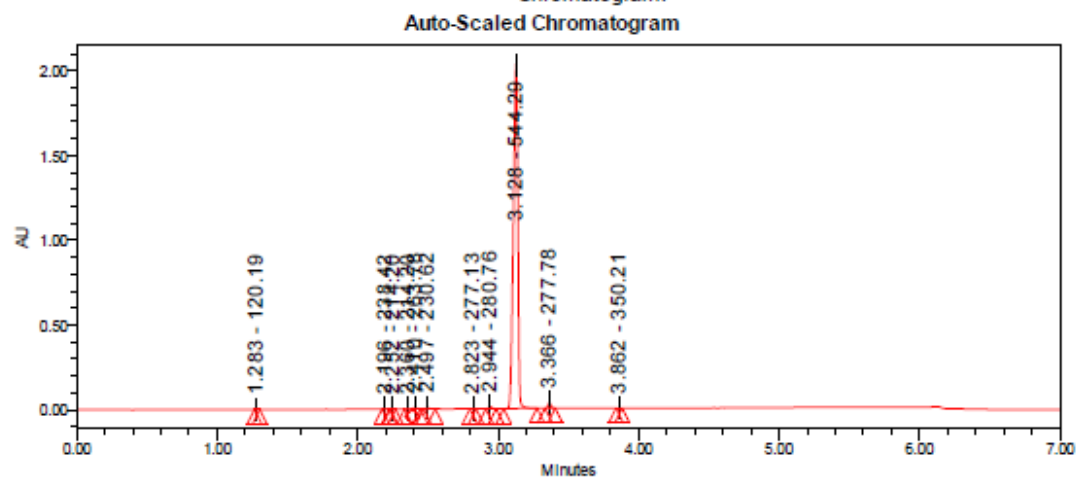
¹³C NMR spectrum of **264** (150 MHz; CDCl₃)



Appendices

LC-MS chromatogram of 264 [M+H]⁺

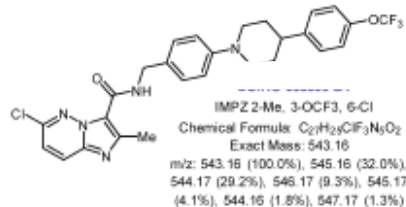
<p>Vial: 1:A,3 Injection #: 1 Injection Volume: 1.00 ul Run Time: 7.0 Minutes Flowrate: 0.4 mL/min Date Acquired: 5/06/2019 1:59:42 PM EST Date Processed: 5/06/2019 2:22:04 PM EST</p>	<p>Instrument: Waters Acquity iClass PDA and QDa detectors Acquired By: System Sample Set Name: PH_06_June_2019 Acquisition Method: 95% A1 to 100% B1 Mobile Phase: A1: 100% H2O / 0.1% FA B1: 100% ACN / 0.1% FA Extracted Chromatogram: PDA Spectrum PDA 254.0 nm</p>
---	--



Peak Results

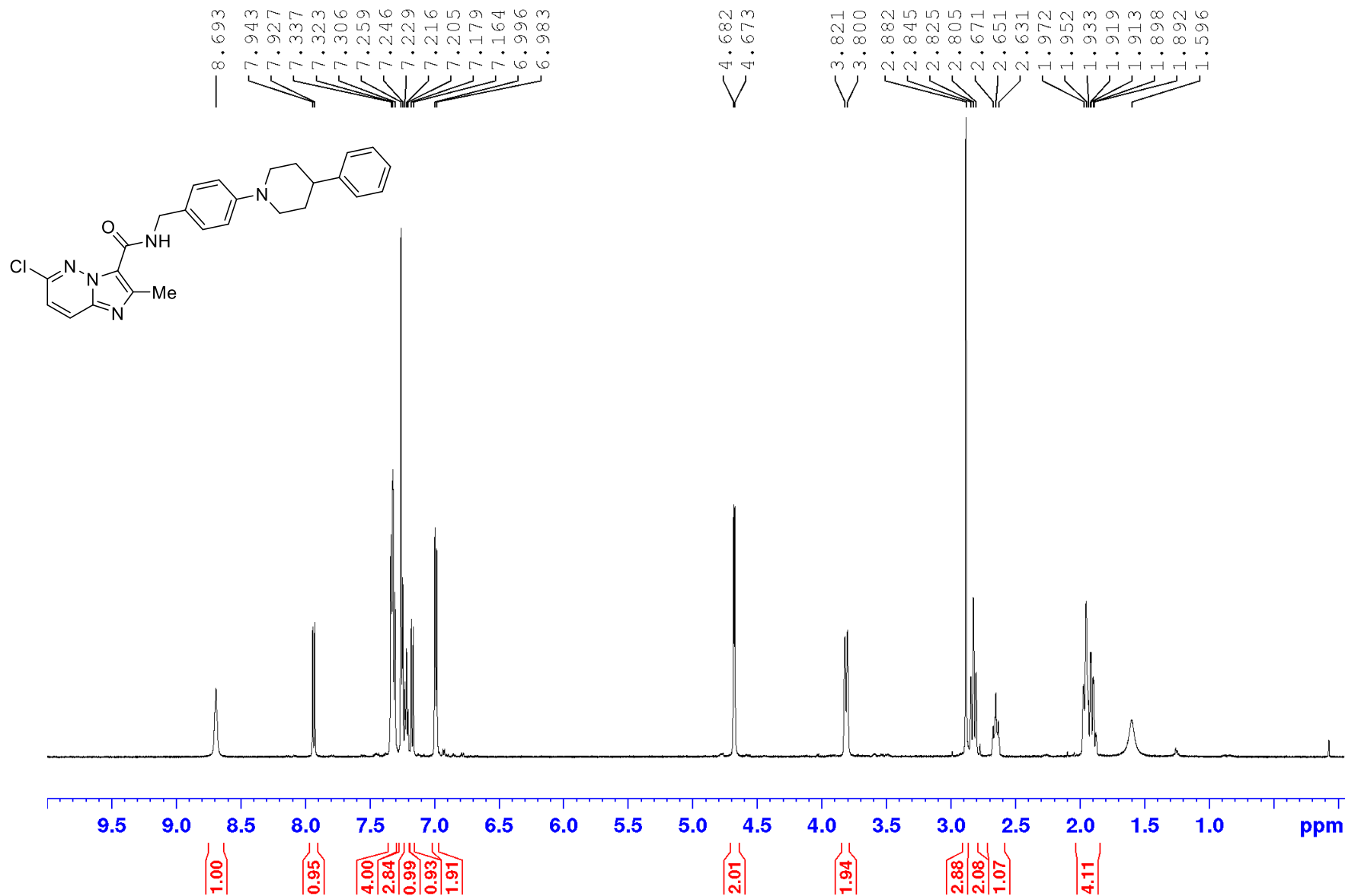
	RT	Area	% Area	Height	Base Peak (m/z)
1	1.283	2001	0.04	1796	120.19
2	2.196	2776	0.06	2102	238.42
3	2.252	967	0.02	842	214.20
4	2.360	1455	0.03	663	214.20
5	2.410	11594	0.25	8631	263.78
6	2.497	12617	0.28	7959	230.62
7	2.823	1930	0.04	1536	277.13
8	2.944	18506	0.40	12145	280.76
9	3.128	4487509	97.86	2048350	544.29

	RT	Area	% Area	Height	Base Peak (m/z)
10	3.366	44344	0.97	30783	277.78
11	3.862	1934	0.04	1609	350.21



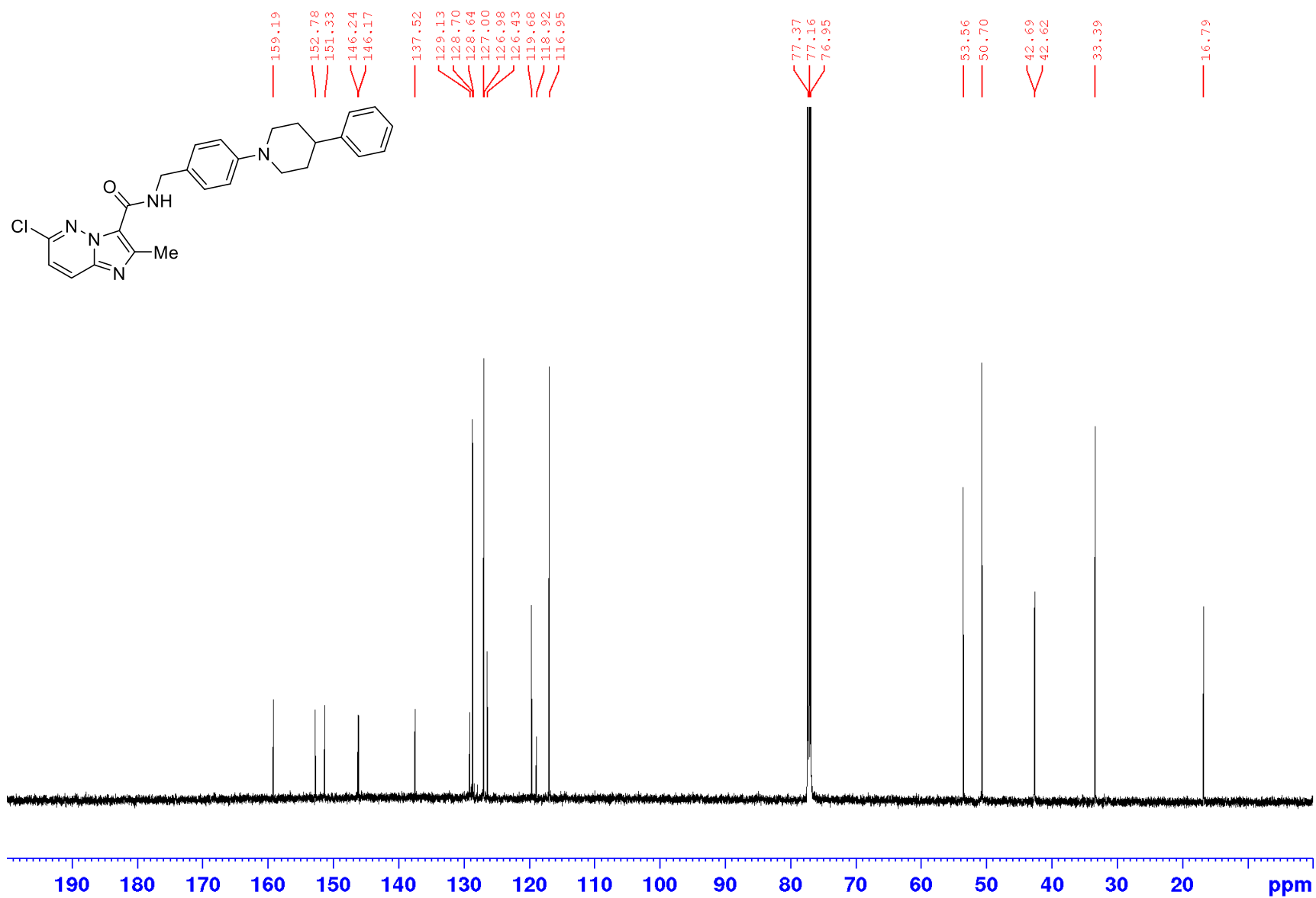
Appendices

¹H NMR spectrum of **265** (600 MHz; CDCl₃)



Appendices

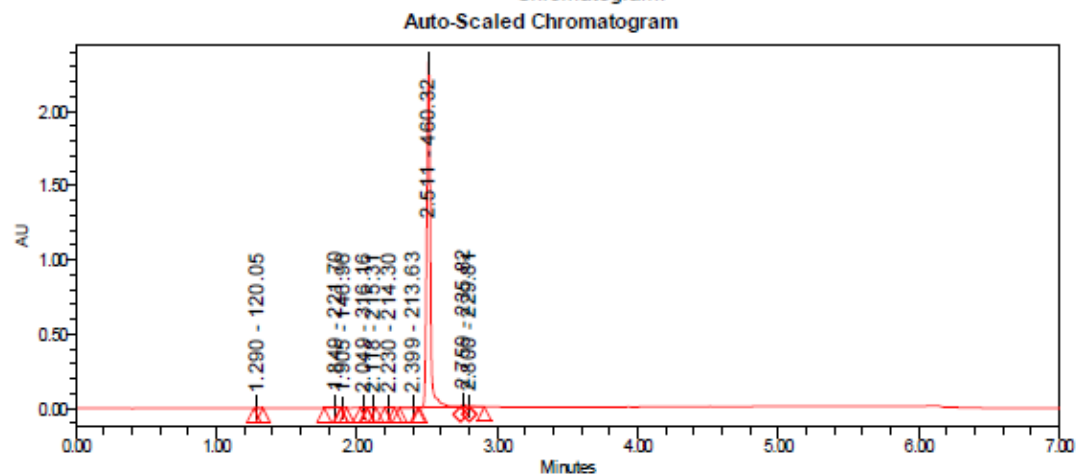
¹³C NMR spectrum of **265** (150 MHz; CDCl₃)



Appendices

LC-MS chromatogram of 265 [M+H]⁺

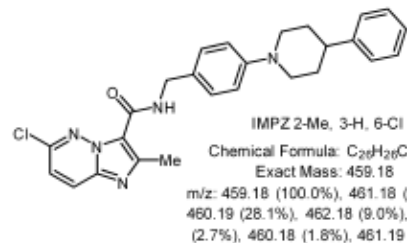
Vial:	1:A,2	Instrument:	Waters Acquity iClass PDA and QDa detectors
Injection #:	1	Acquired By:	System
Injection Volume:	1.00 ul	Sample Set Name:	PH_06_June_2019
Run Time:	7.0 Minutes	Acquisition Method:	95% A1 to 100% B1
Flowrate:	0.4 mL/min	Mobile Phase:	A1: 100% H2O / 0.1% FA B1: 100% ACN / 0.1% FA
Date Acquired:	5/06/2019 1:51:12 PM EST	Extracted Chromatogram:	PDA Spectrum PDA 254.0 nm
Date Processed:	5/06/2019 2:04:26 PM EST		



Peak Results

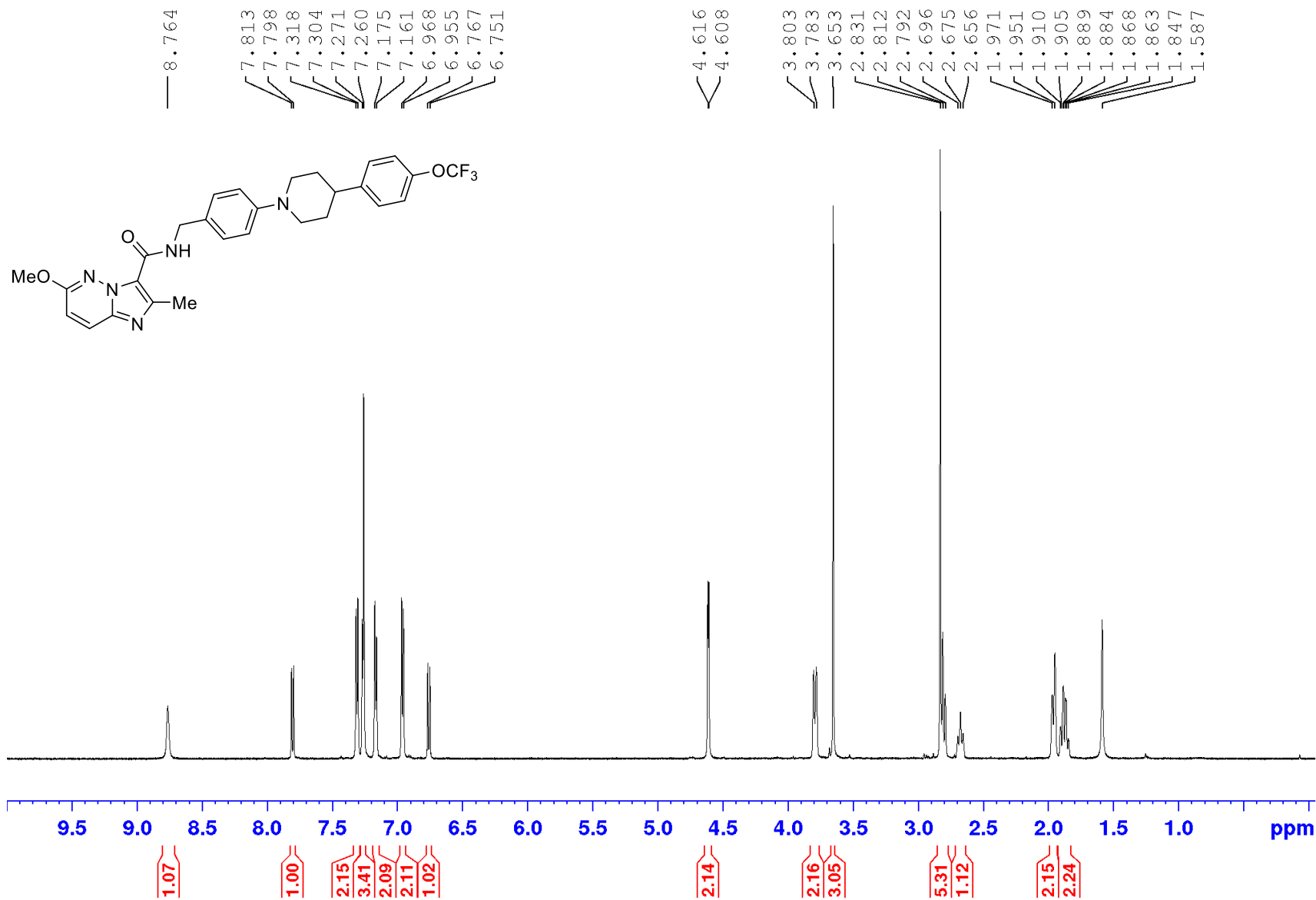
	RT	Area	% Area	Height	Base Peak (m/z)
1	1.290	5671	0.13	4517	120.05
2	1.849	14866	0.35	10644	221.70
3	1.905	657	0.02	641	146.96
4	2.049	3637	0.09	3364	316.16
5	2.118	874	0.02	543	215.31
6	2.230	1635	0.04	662	214.30
7	2.399	4665	0.11	1975	213.63
8	2.511	4175682	98.19	2325430	460.32
9	2.759	33752	0.79	17366	235.82

	RT	Area	% Area	Height	Base Peak (m/z)
10	2.800	10862	0.26	3206	229.81



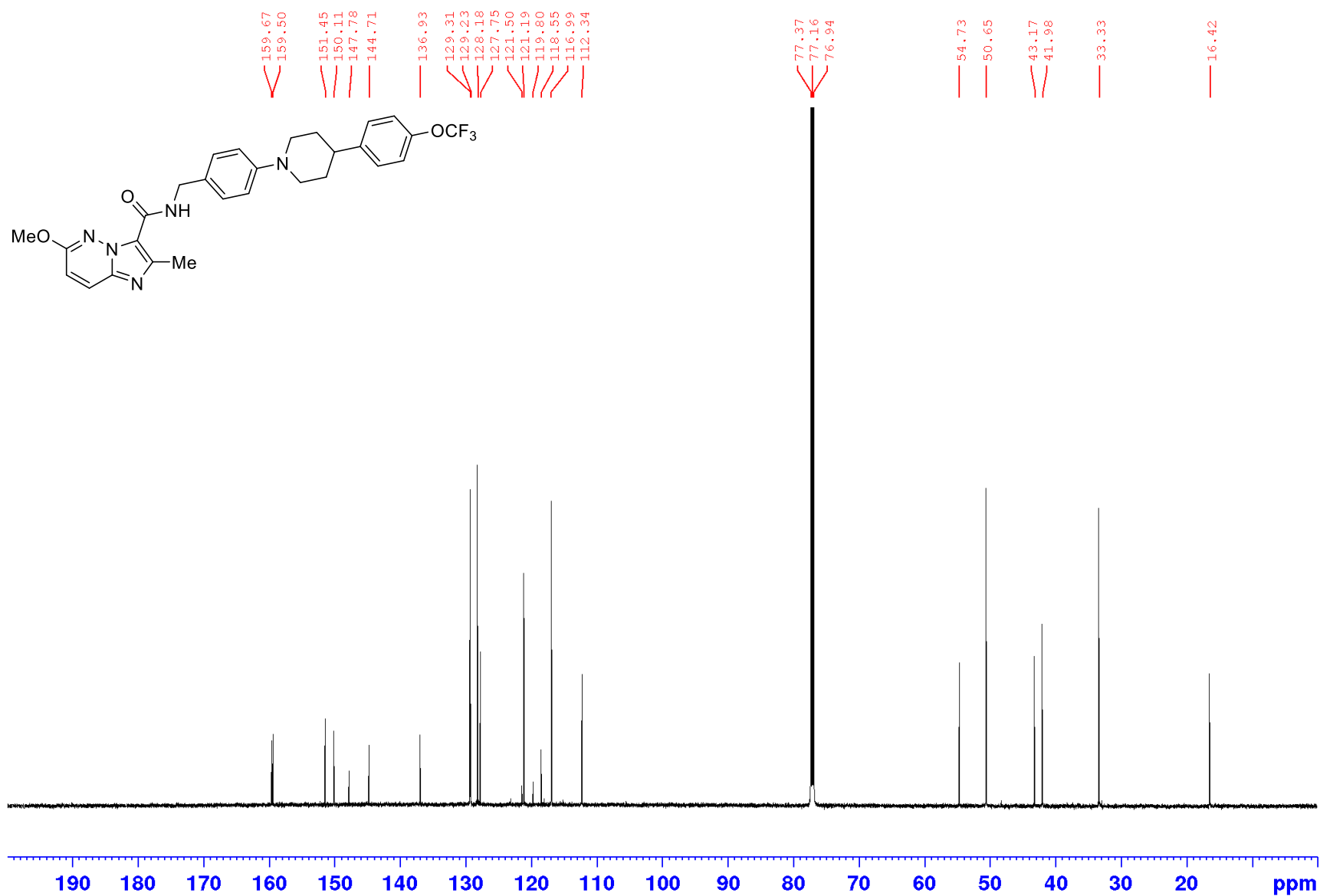
Appendices

¹H NMR spectrum of **266** (600 MHz; CDCl₃)



Appendices

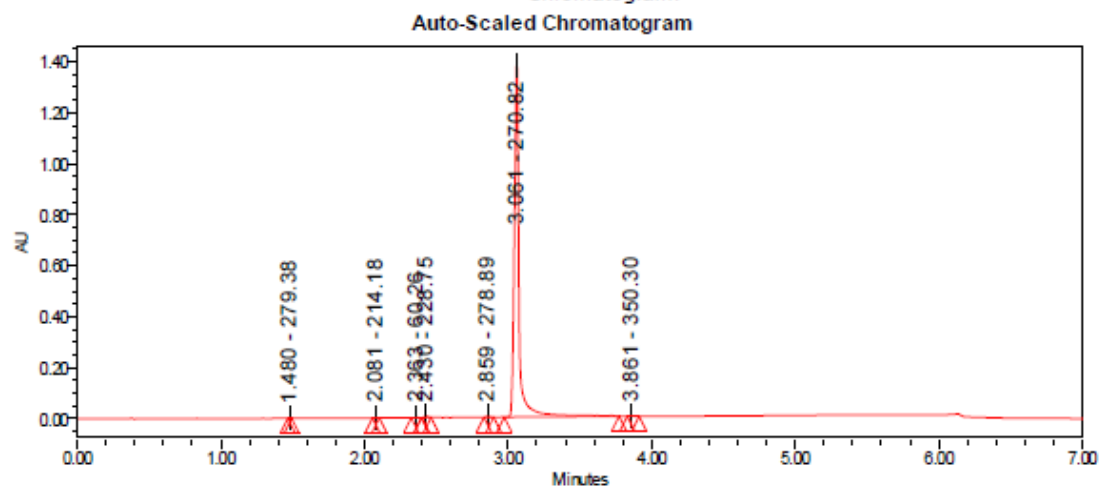
¹³C NMR spectrum of **266** (150 MHz; CDCl₃)



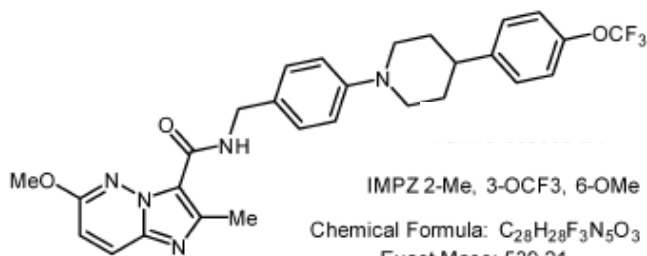
Appendices

LC-MS chromatogram of 266 [M+H]⁺

Vial:	1:A,5	Instrument:	Waters Acquity iClass
Injection #:	1		PDA and QDa detectors
Injection Volume:	1.00 ul	Acquired By:	System
Run Time:	7.0 Minutes	Sample Set Name:	PH_06_June_2019
Flowrate:	0.4 mL/min	Acquisition Method:	95% A1 to 100% B1
Date Acquired:	5/06/2019 2:16:42 PM EST	Mobile Phase:	A1: 100% H2O / 0.1% FA
Date Processed:	5/06/2019 2:27:41 PM EST		B1: 100% ACN / 0.1% FA
		Extracted Chromatogram:	PDA Spectrum PDA 254.0 nm



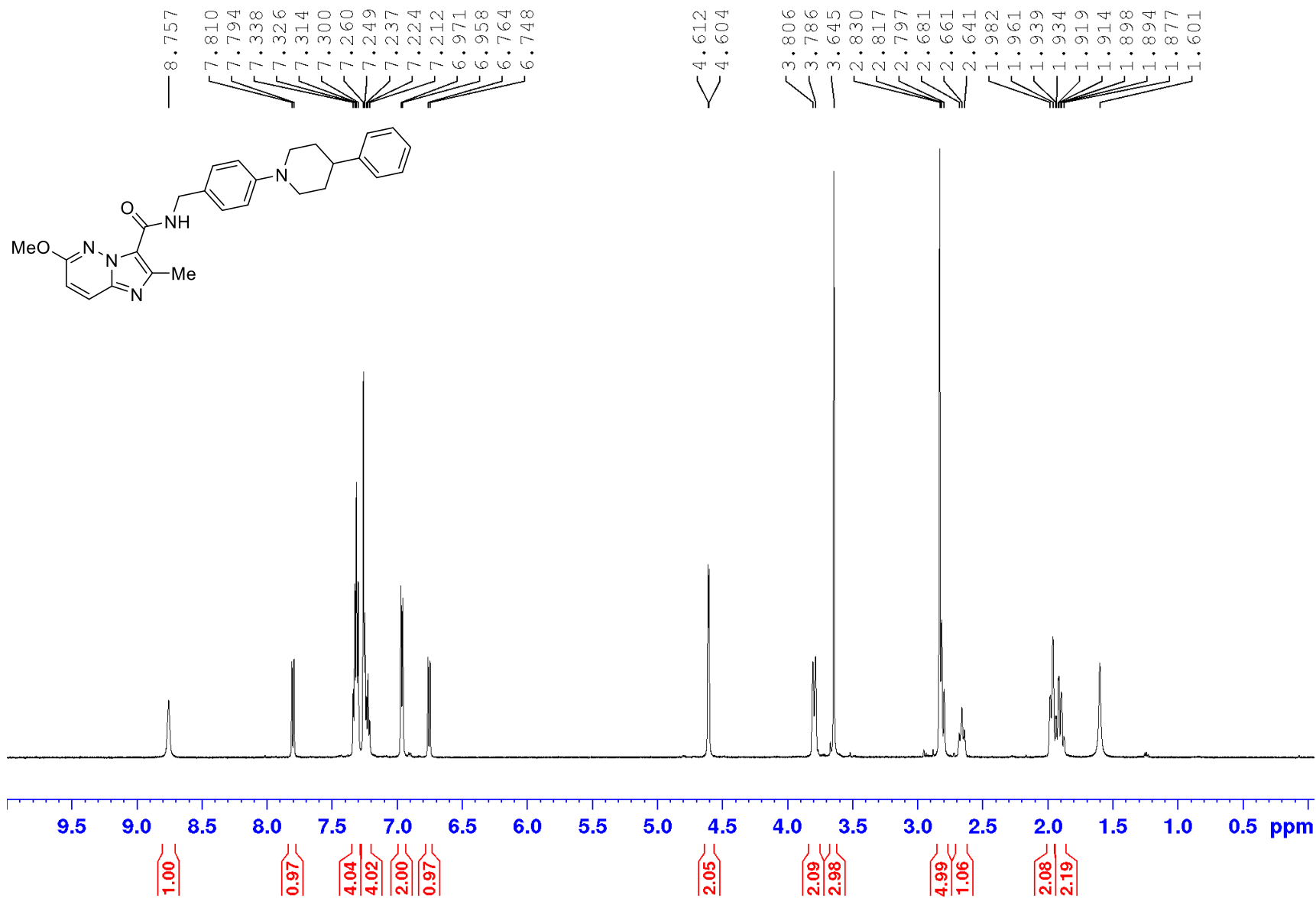
Peak Results					
RT	Area	% Area	Height	Base Peak (m/z)	
1	1480	360	0.01	395	279.38
2	2081	2132	0.07	1779	214.18
3	2363	1530	0.05	654	80.28
4	2430	8515	0.26	6459	228.75
5	2859	6172	0.19	4000	278.89
6	3061	3194883	99.32	1383971	270.82
7	3861	3101	0.10	2187	350.30



see MS for Peak #6
m/z: 539.21 (100.0%), 540.22 (30.3%), 541.22 (2.7%), 540.21 (1.8%), 541.22 (1.7%)

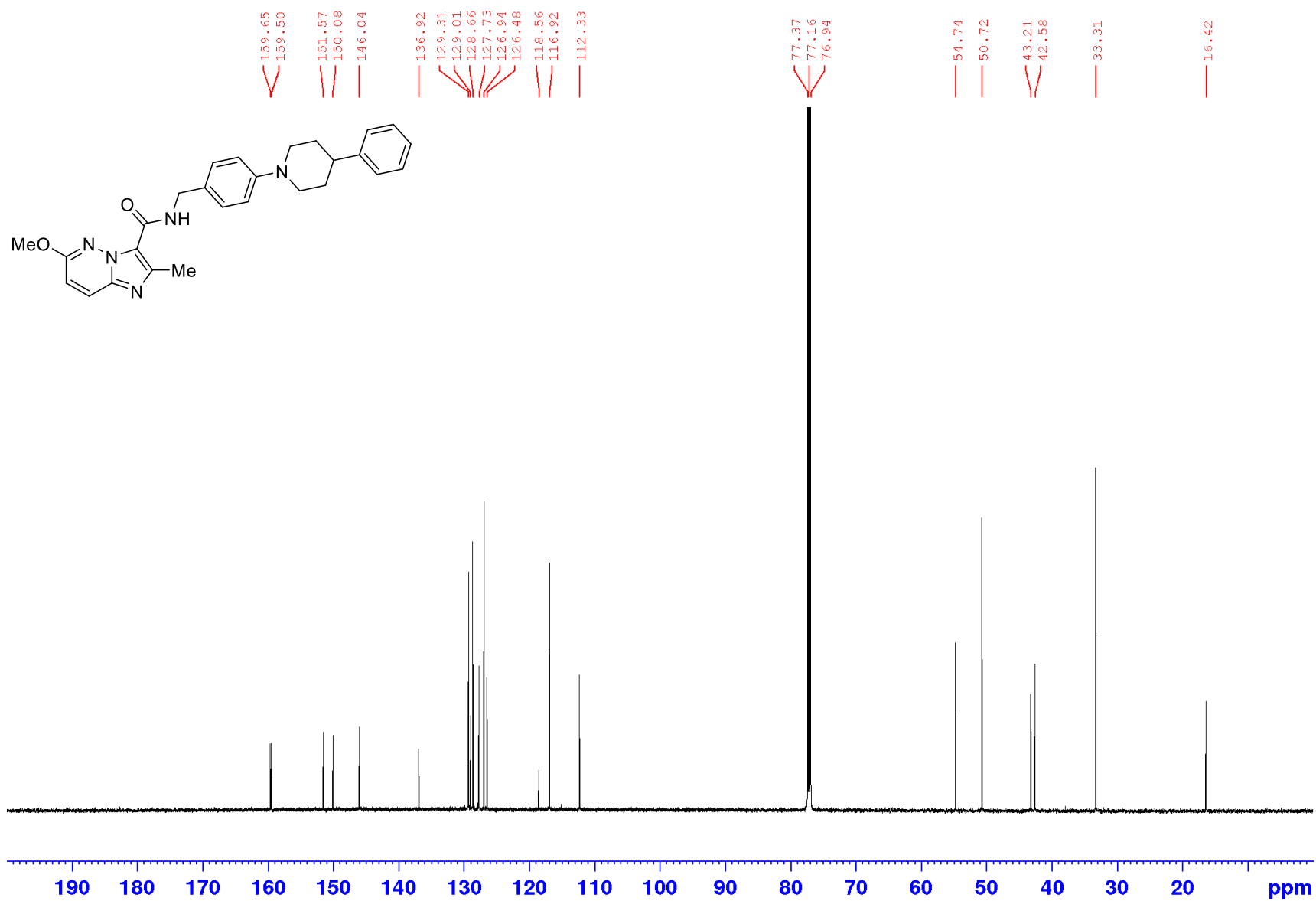
Appendices

¹H NMR spectrum of **267** (600 MHz; CDCl₃)



Appendices

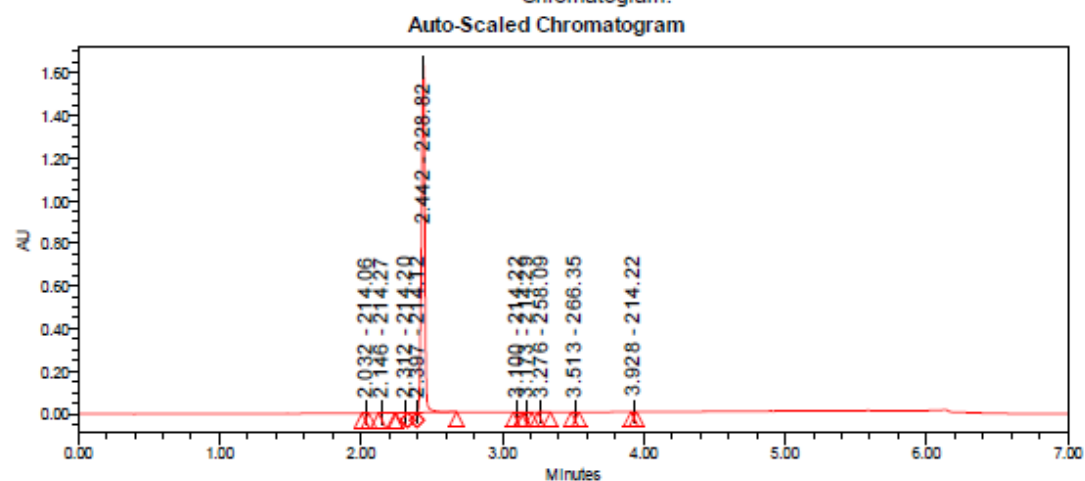
¹³C NMR spectrum of **267** (150 MHz; CDCl₃)



Appendices

LC-MS chromatogram of 267 [M+H]⁺

Vial:	1:A,4	Instrument:	Waters Acquity iClass
Injection #:	1		PDA and QDa detectors
Injection Volume:	1.00 ul	Acquired By:	System
Run Time:	7.0 Minutes	Sample Set Name:	PH_06_June_2019
Flowrate:	0.4 mL/min	Acquisition Method:	95% A1 to 100% B1
Date Acquired:	5/06/2019 2:08:12 PM EST	Mobile Phase:	A1: 100% H2O / 0.1% FA
Date Processed:	5/06/2019 2:25:01 PM EST		B1: 100% ACN / 0.1% FA
		Extracted Chromatogram:	PDA Spectrum PDA 254.0 nm



Peak Results

	RT	Area	% Area	Height	Base Peak (m/z)
1	2.032	826	0.03	620	214.06
2	2.146	2986	0.11	1012	214.27
3	2.312	1459	0.05	709	214.20
4	2.397	1440	0.05	1374	214.12
5	2.442	2671045	99.43	1638000	228.82
6	3.100	1089	0.04	765	214.22
7	3.173	1559	0.06	1038	214.29
8	3.276	3105	0.12	1877	258.09
9	3.513	2103	0.08	1576	266.35

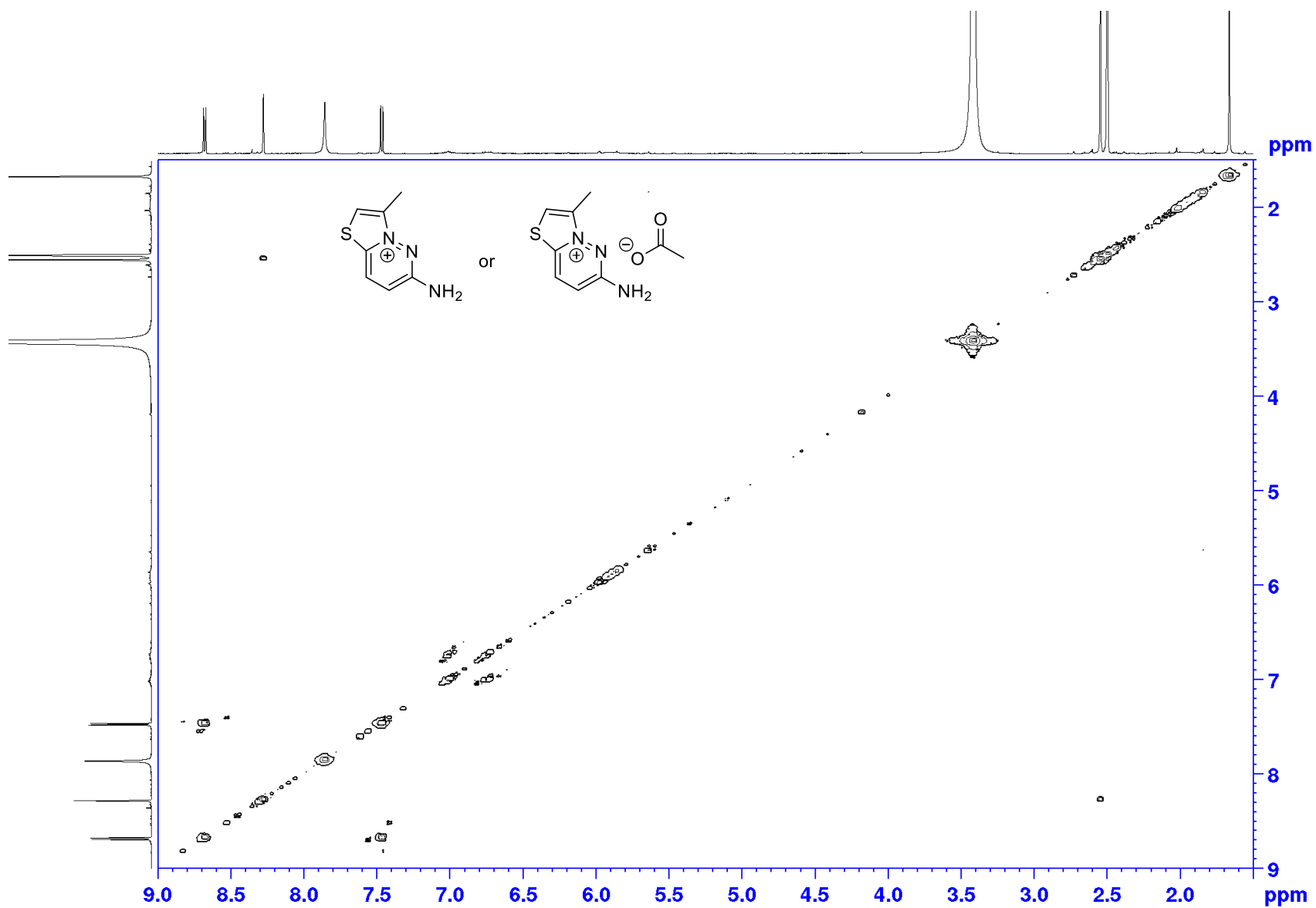
	RT	Area	% Area	Height	Base Peak (m/z)
10	3.928	712	0.03	591	214.22



Section 2: NMR and HRMS spectra for miscellaneous compounds

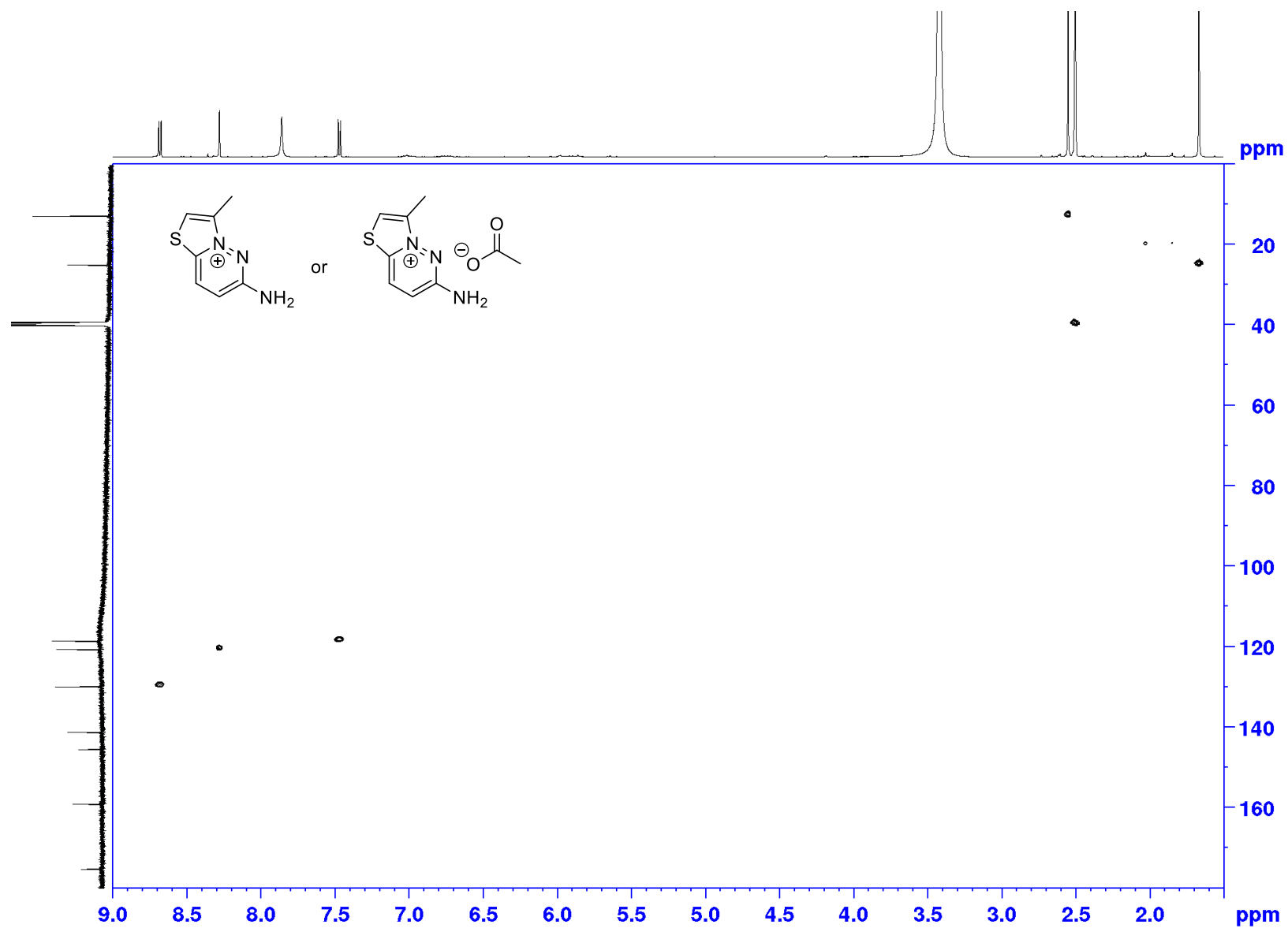
Appendices

COSY spectrum of **94** or **95** (600 x 600 MHz; DMSO-d₆)



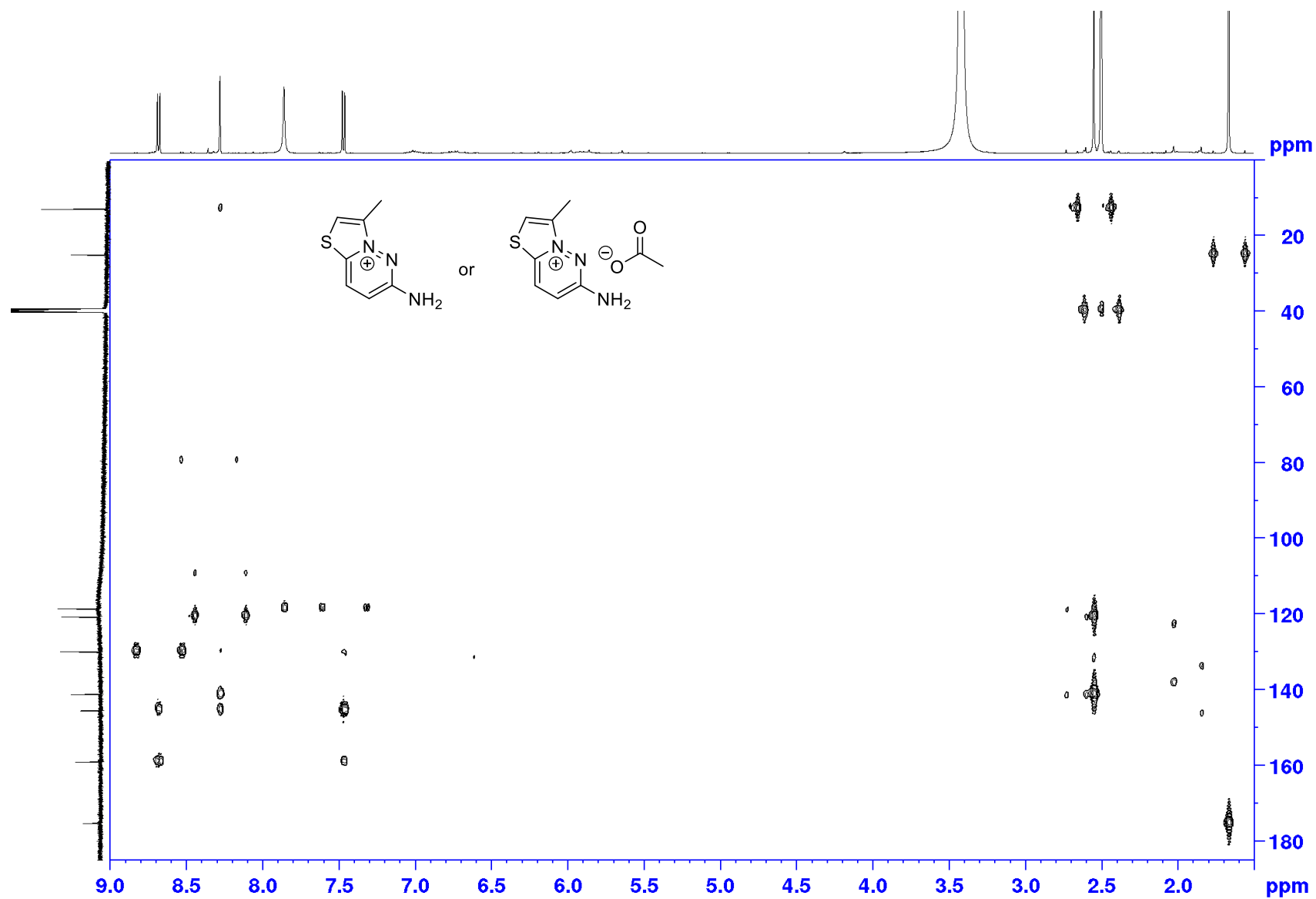
Appendices

HMQC spectrum of **94** or **95** (400 x 100 MHz; DMSO-d₆)



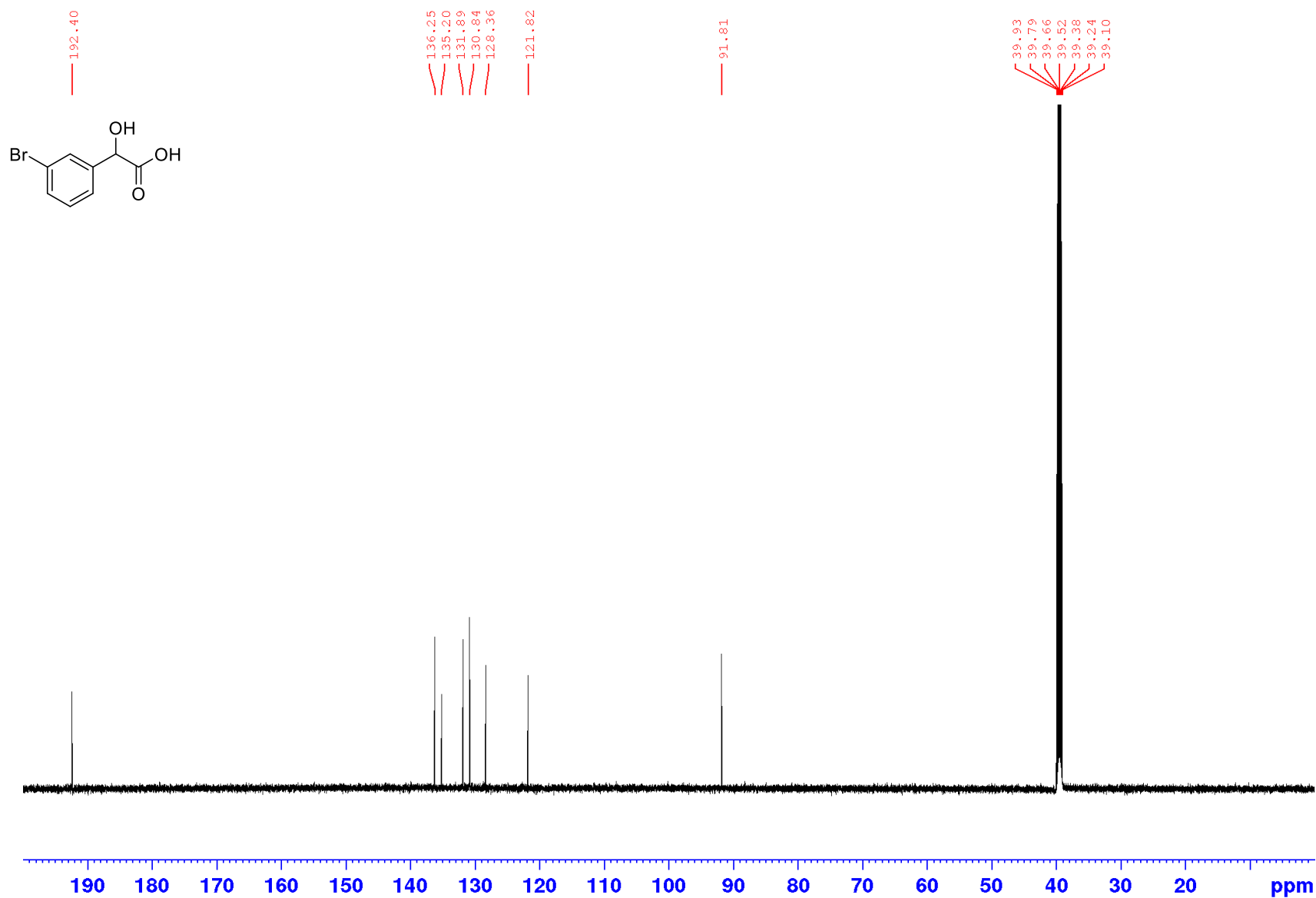
Appendices

HMNC spectrum of **94** or **95** (400 x 100 MHz; DMSO- d_6)



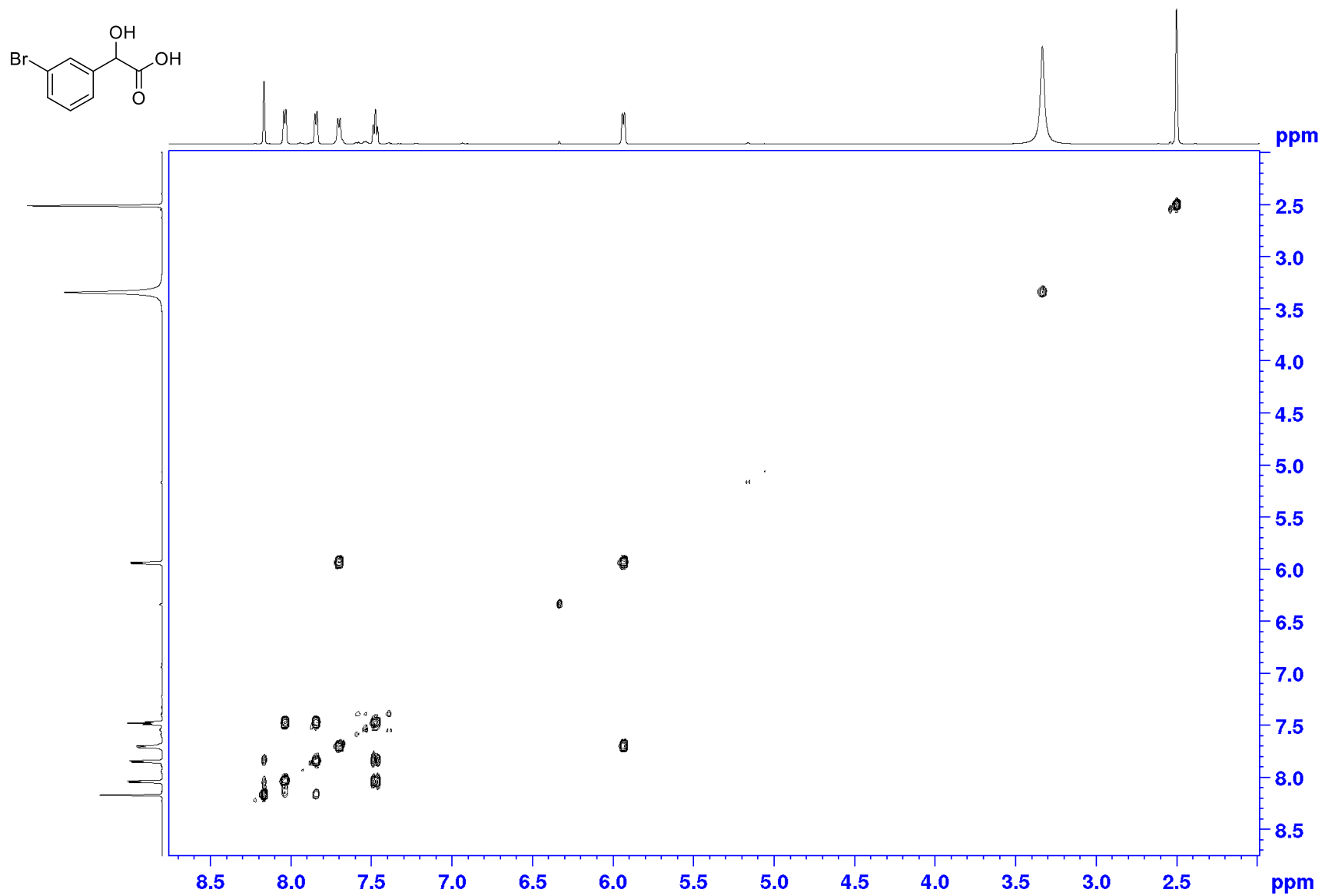
Appendices

^{13}C NMR spectrum of **116** (150 MHz; DMSO-d_6)



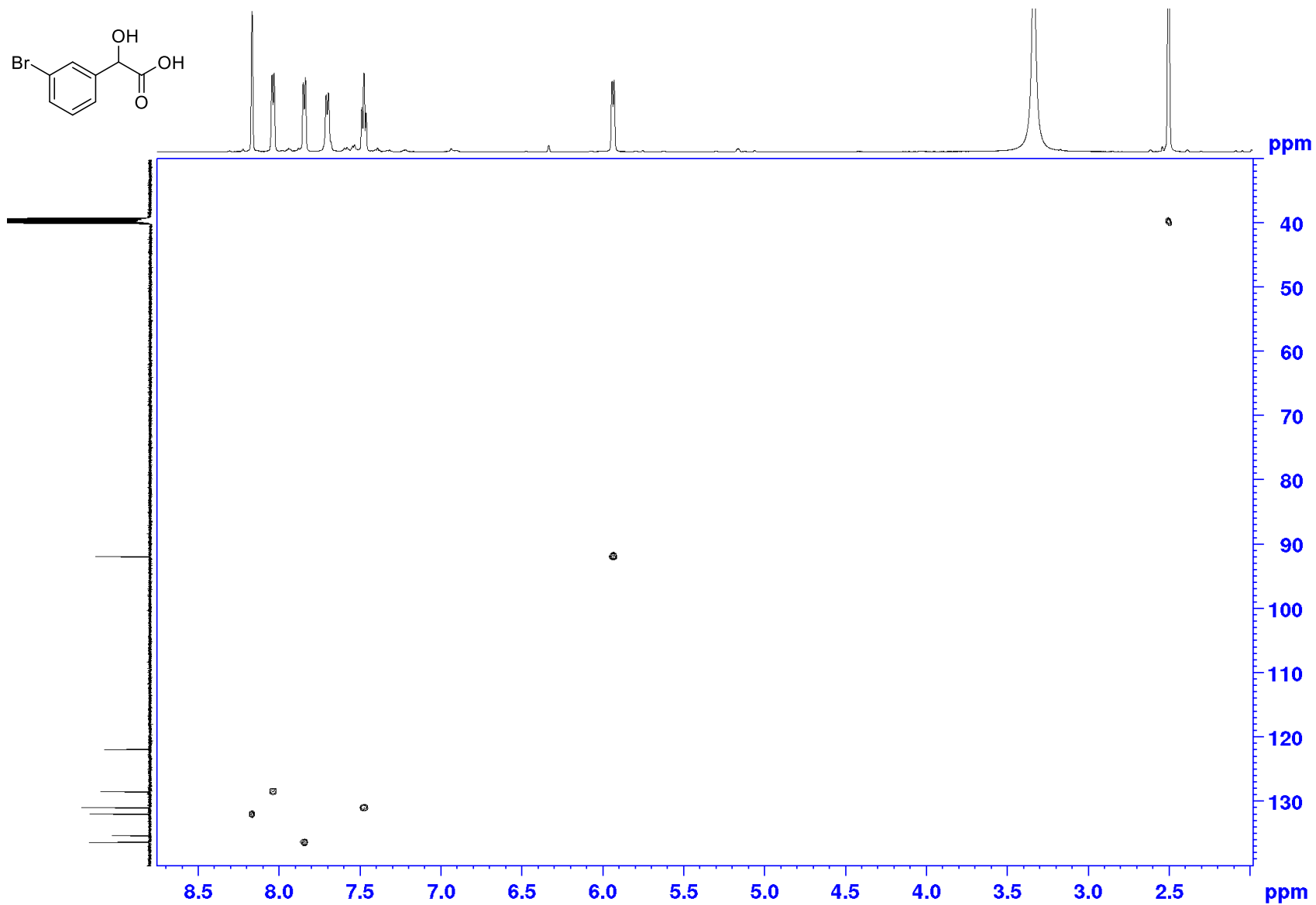
Appendices

COSY spectrum of **116** (600 x 600 MHz; DMSO- d_6)



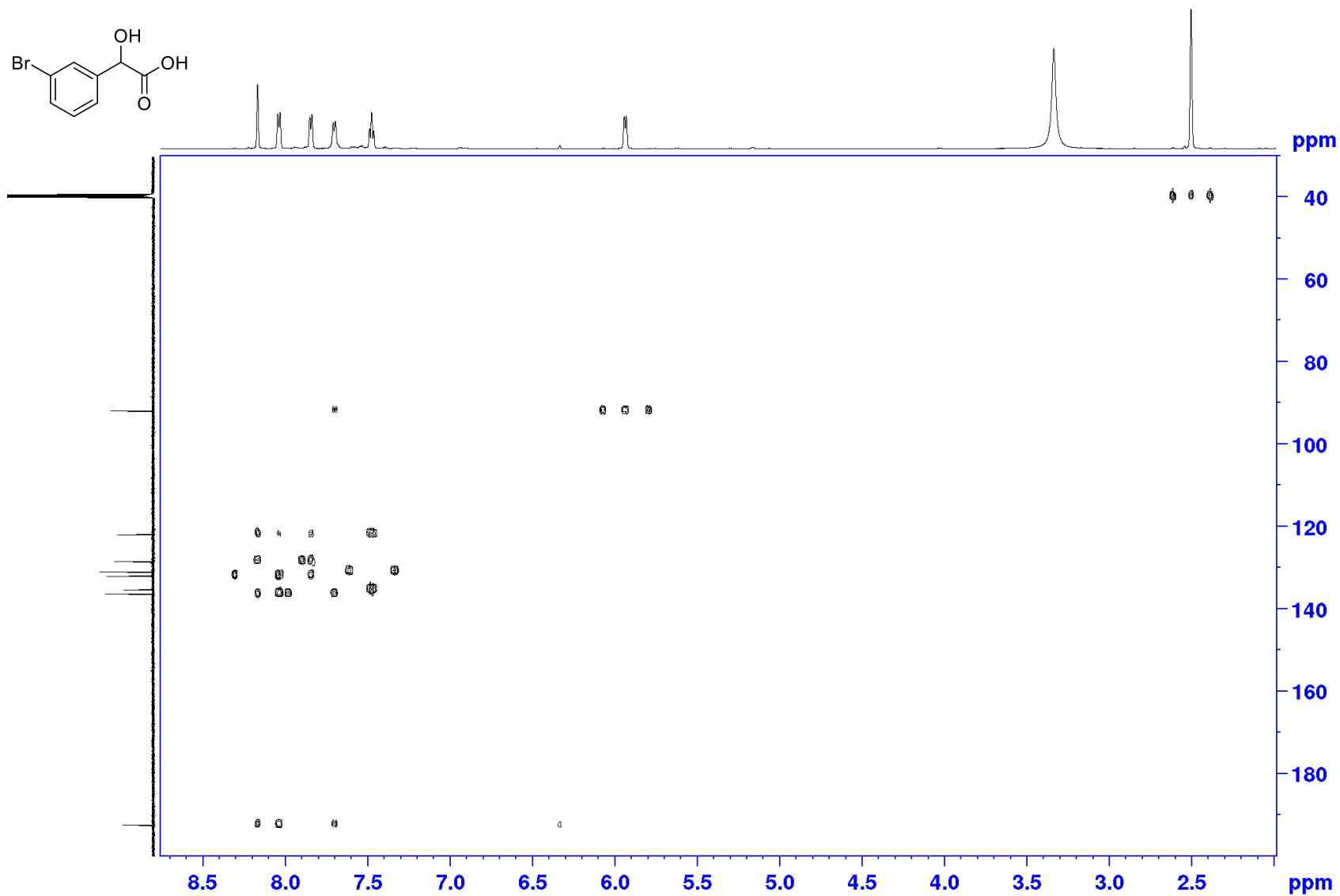
Appendices

HMQC spectrum of **116** (400 x 100 MHz; DMSO- d_6)



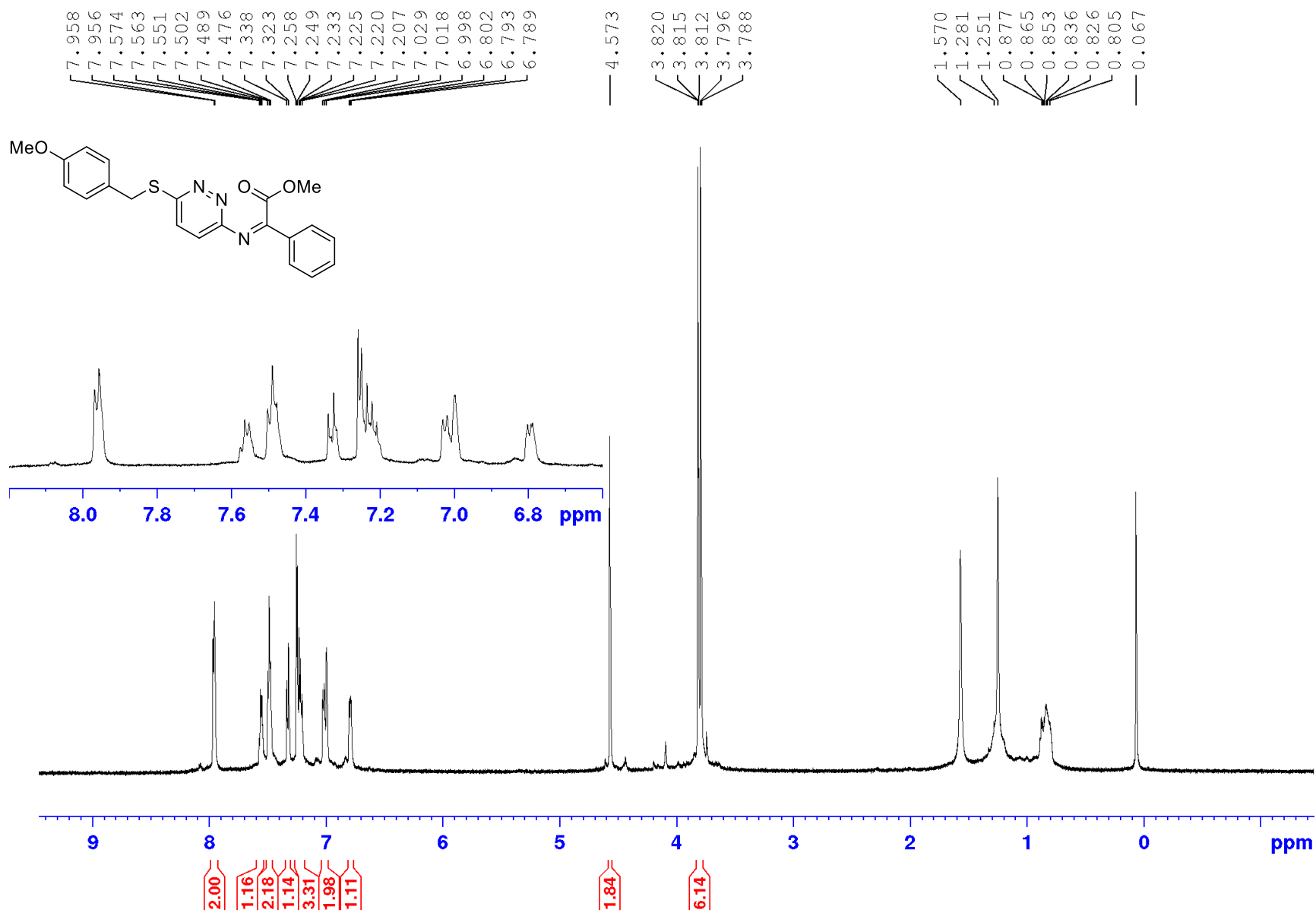
Appendices

HMBC spectrum of **116** (400 x 100 MHz; DMSO-d₆)



Appendices

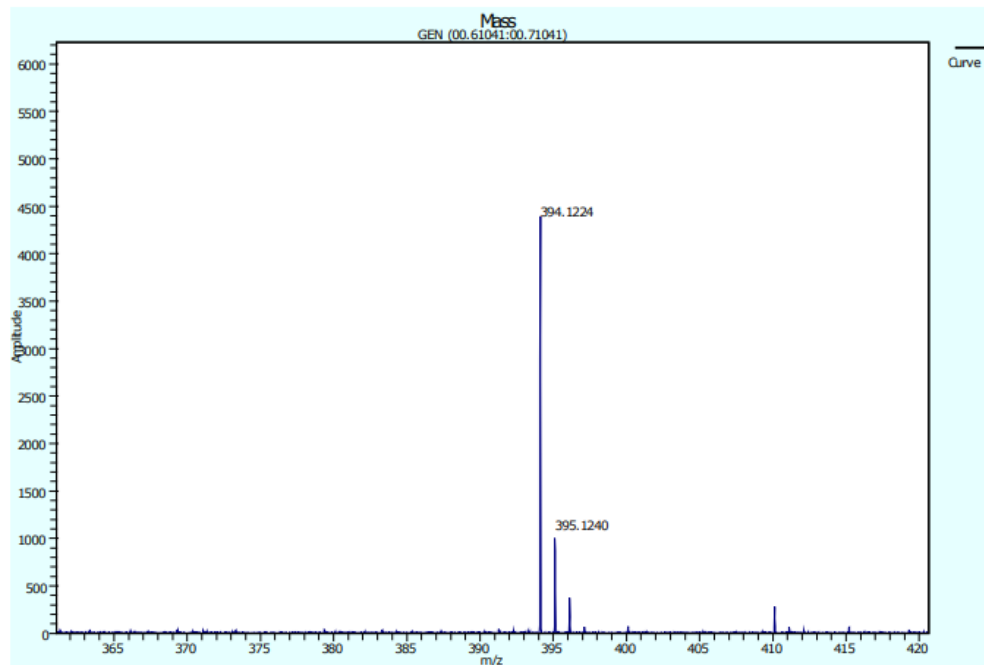
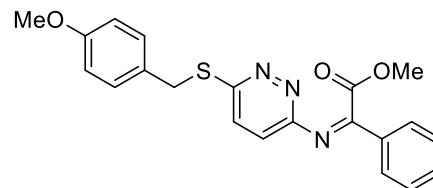
¹H NMR spectrum of **161** (600 MHz; CDCl₃)



Appendices

HRMS (APCI) spectrum of **161** $[M+H]^+$

Sample: 2.18 13-16
High Resolution Spectra
Positive ion, APCI

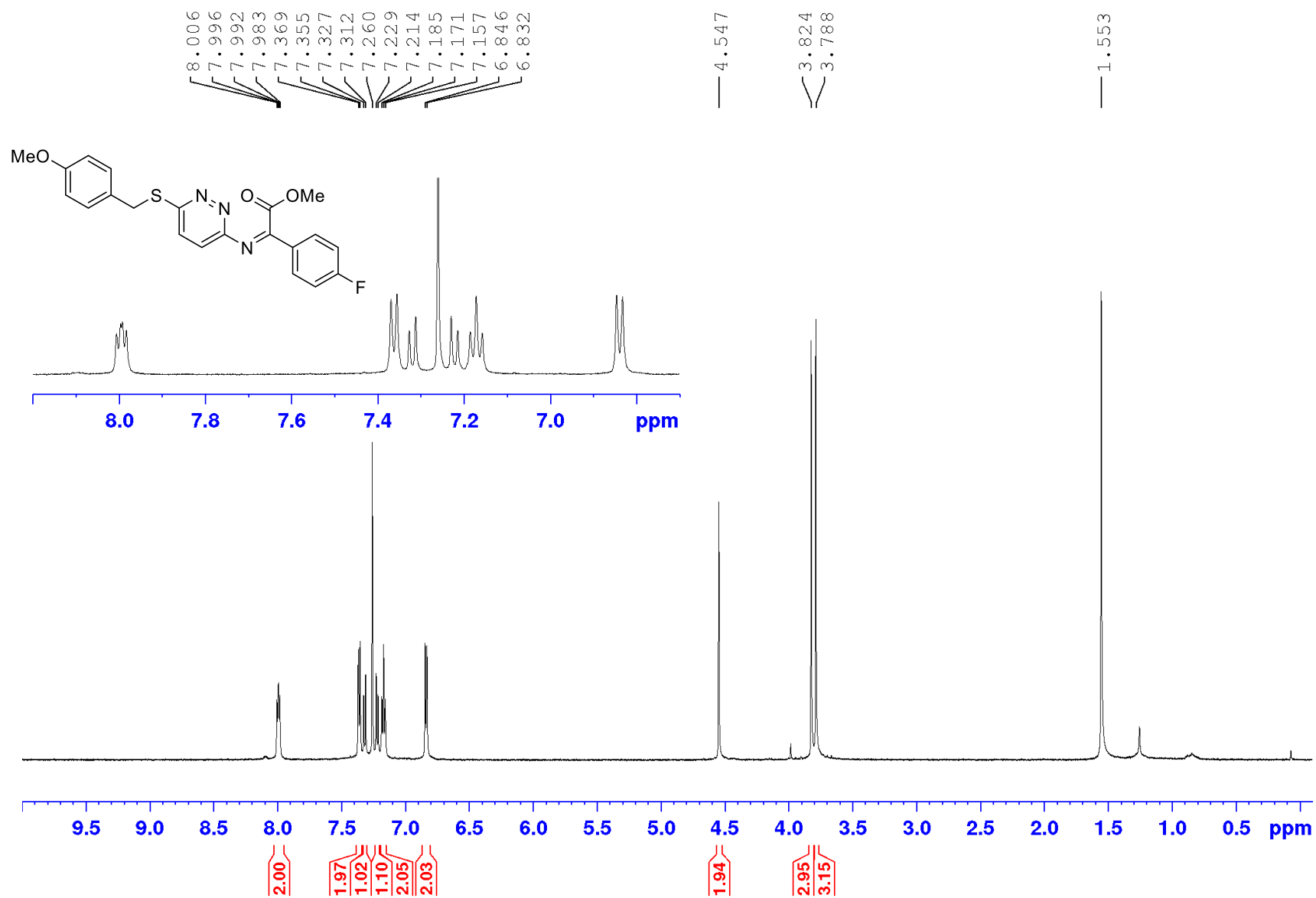


Accurate Mass Data

Observed Mass	Formula $[M+H]^+$	Calculated mass	Difference (ppm)
394.1224	C ₂₁ H ₂₀ N ₃ O ₃ S	394.1219	1.3

Appendices

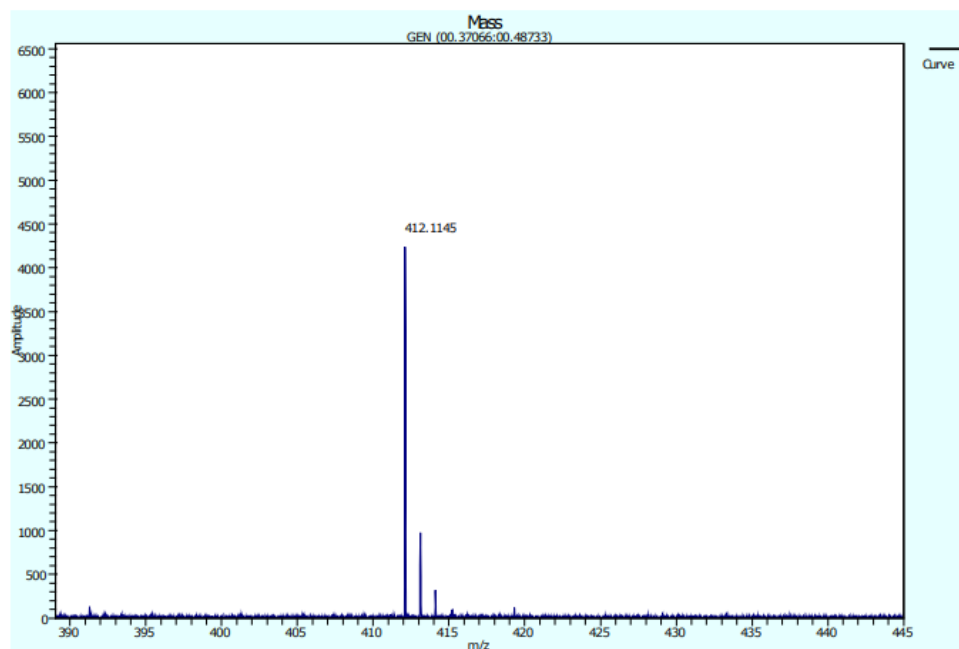
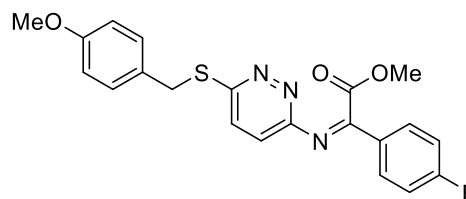
¹H NMR spectrum of **162** (600 MHz; CDCl₃)



Appendices

HRMS (APCI) spectrum of **162** $[M+H]^+$

Sample: 2.94 9-13
High Resolution Spectra
Positive ion, APCI

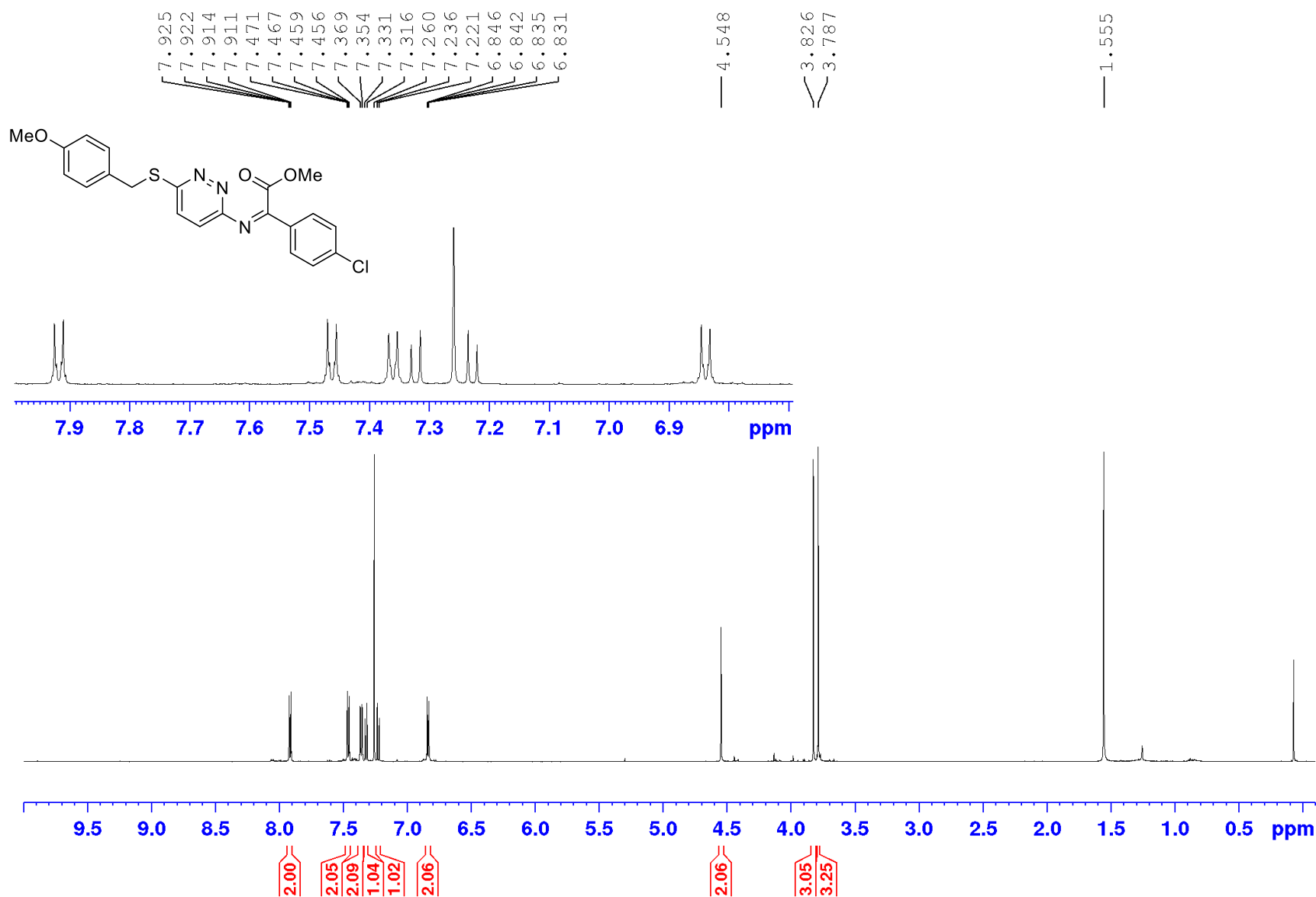


Accurate Mass Data

Observed Mass	Formula $[M+H]^+$	Calculated mass	Difference (ppm)
412.1145	C ₂₁ H ₁₉ N ₃ O ₃ SF	412.1126	4.6

Appendices

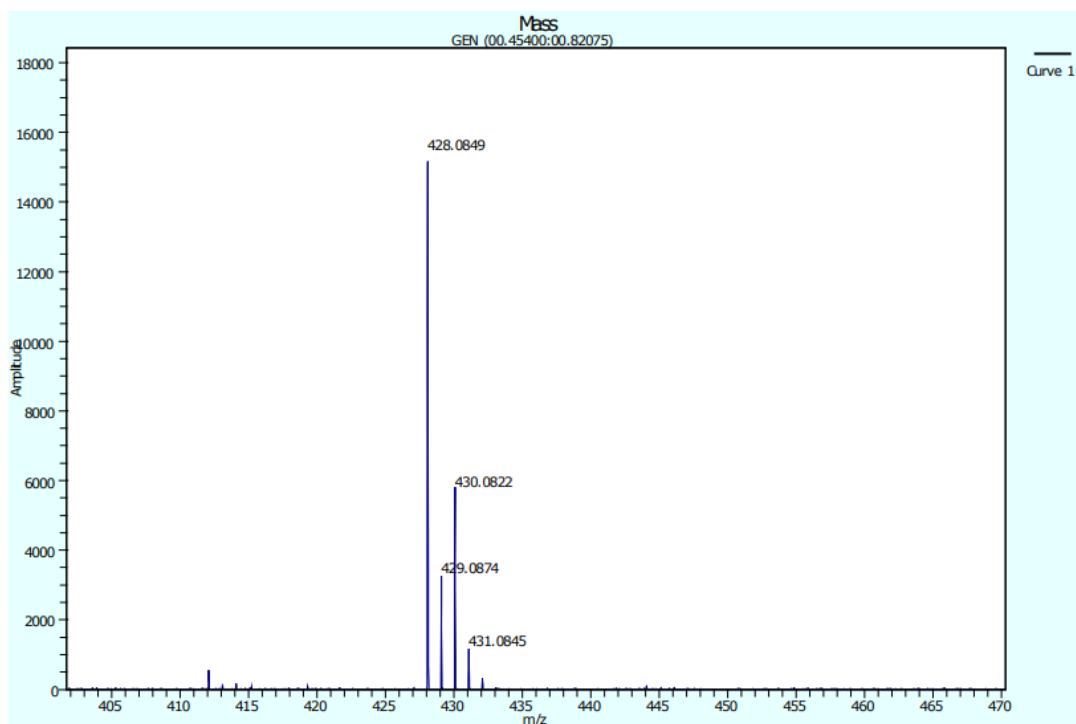
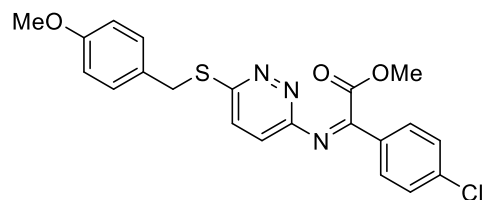
¹H NMR spectrum of **163** (600 MHz; CDCl₃)



Appendices

HRMS (APCI) spectrum of **163** $[M+H]^+$

Sample: 2.42 5-8
High Resolution Spectra
Positive ion, APCI

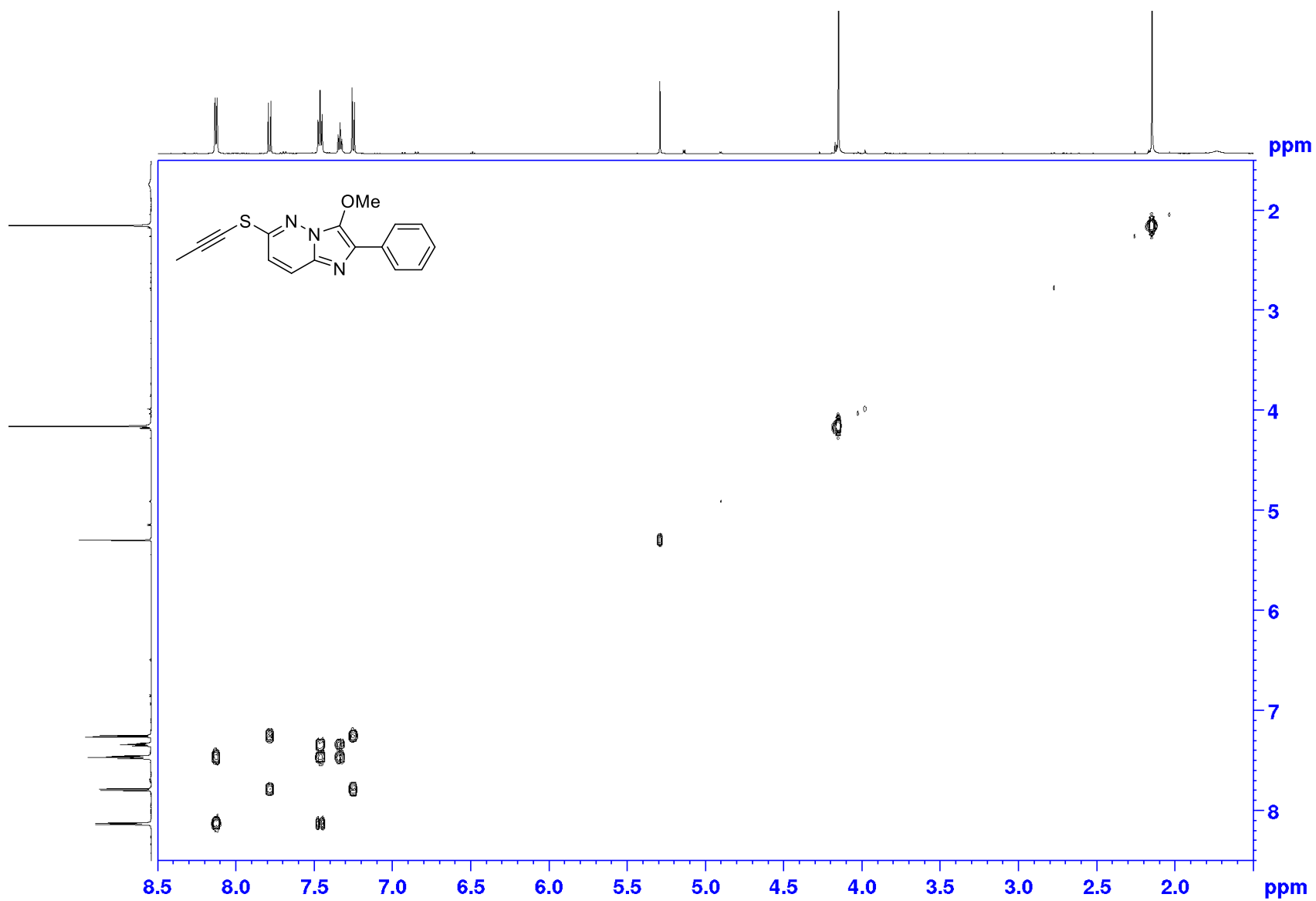


Accurate Mass Data

Observed Mass	Formula $[M+H]^+$	Calculated mass	Difference (ppm)
428.0849	C ₂₁ H ₁₉ N ₃ O ₃ SCl	428.0836	3.0

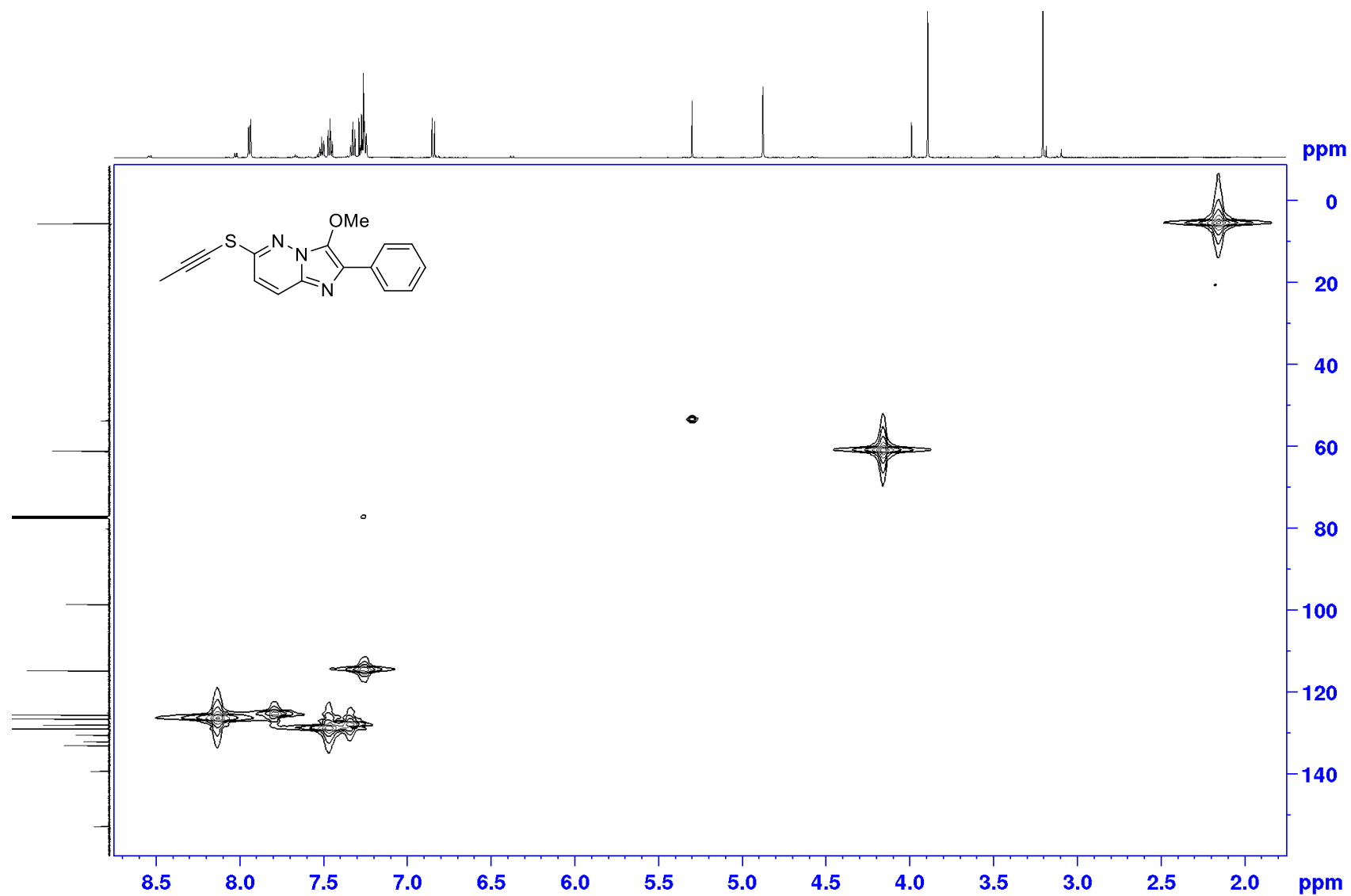
Appendices

COSY spectrum of **172** (600 x 600 MHz; CDCl₃)



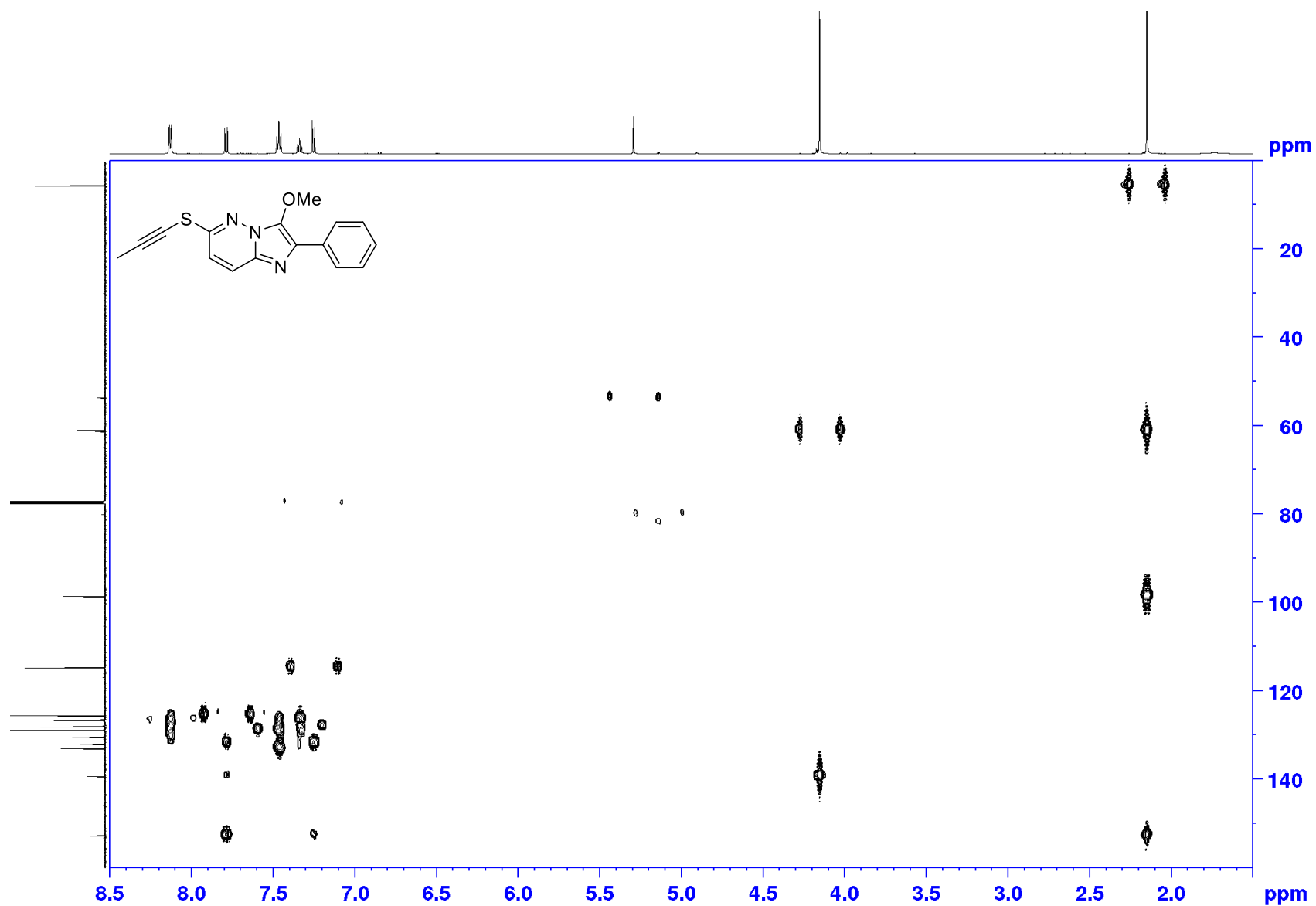
Appendices

HMQC spectrum of **172** (400 x 100 MHz; CDCl₃)



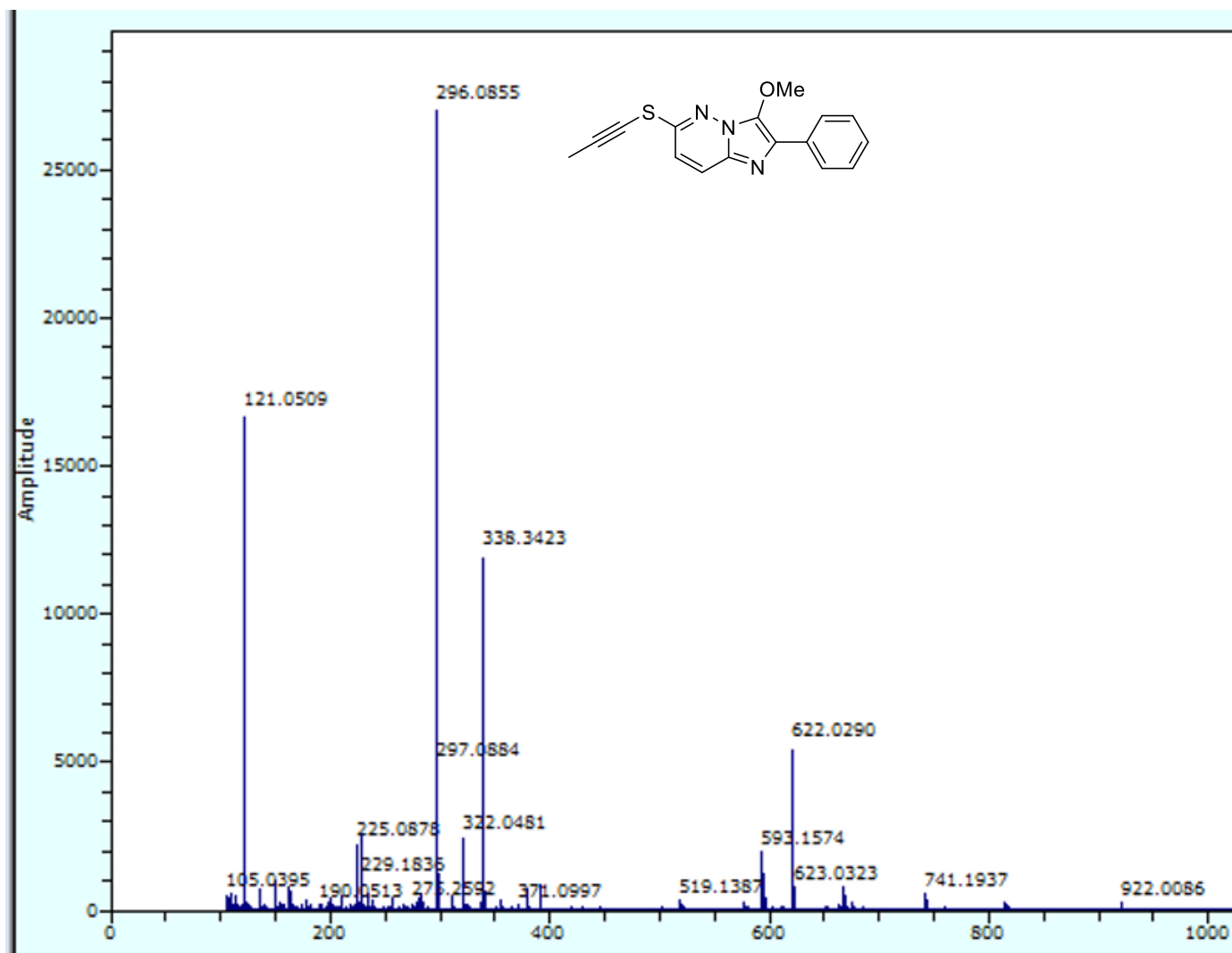
Appendices

HMBC spectrum of **172** (400 x 100 MHz; CDCl₃)



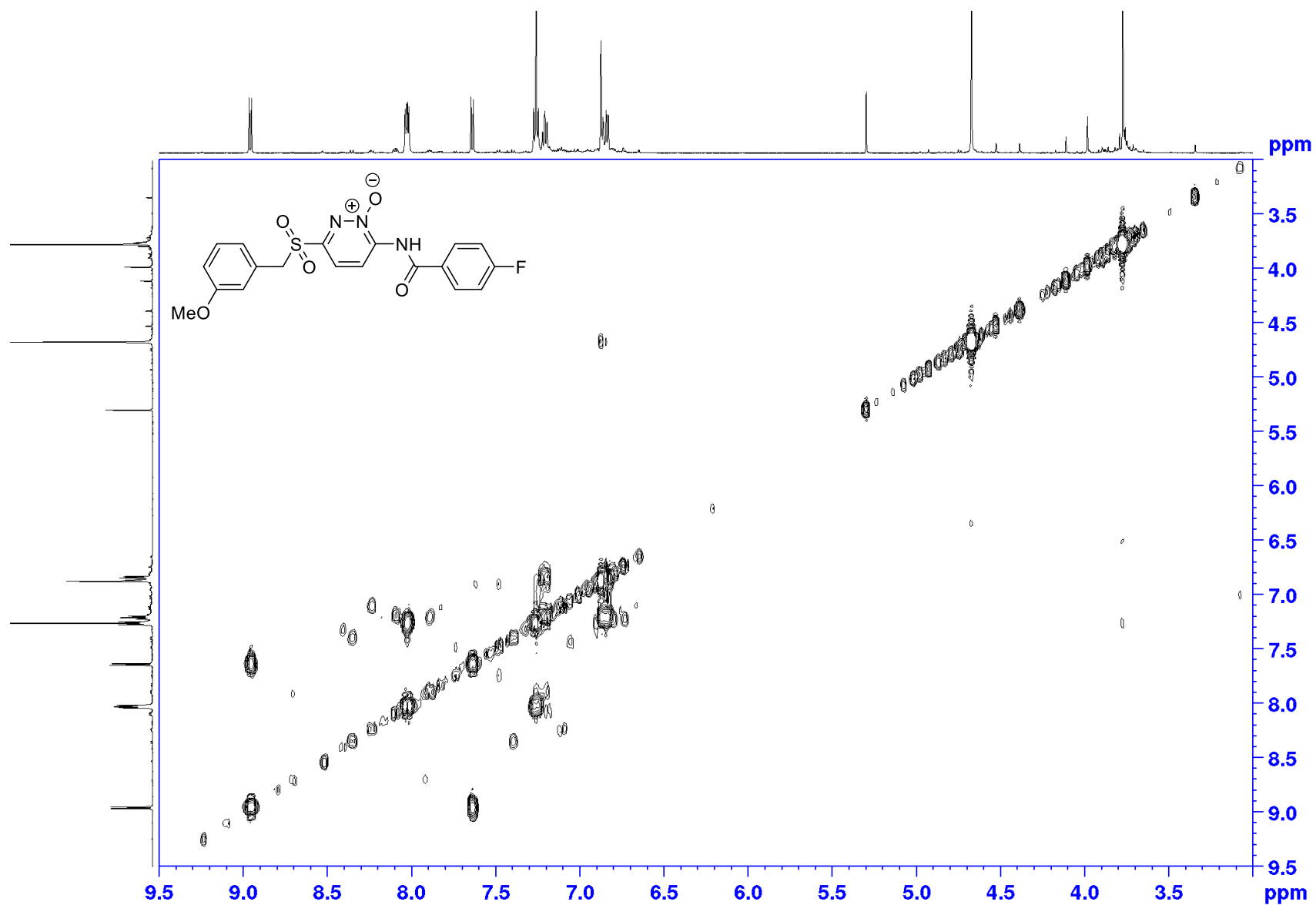
Appendices

HRMS (APCI) spectrum of **172** $[M+H]^+$ (calibrants masses are 121, 322, 622 and 922 Da)



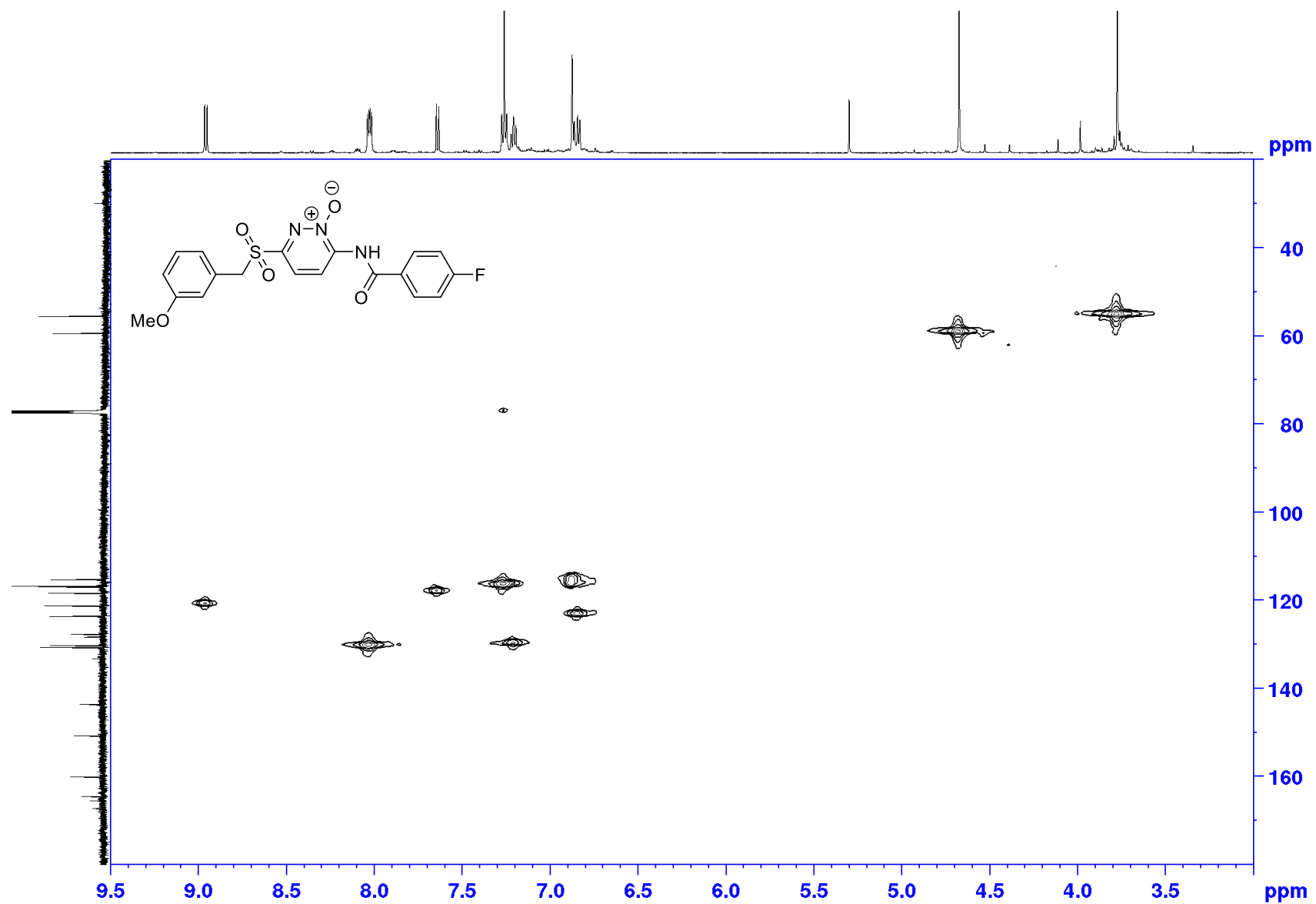
Appendices

COSY NMR spectrum of **177** (600 x 600 MHz; CDCl₃)



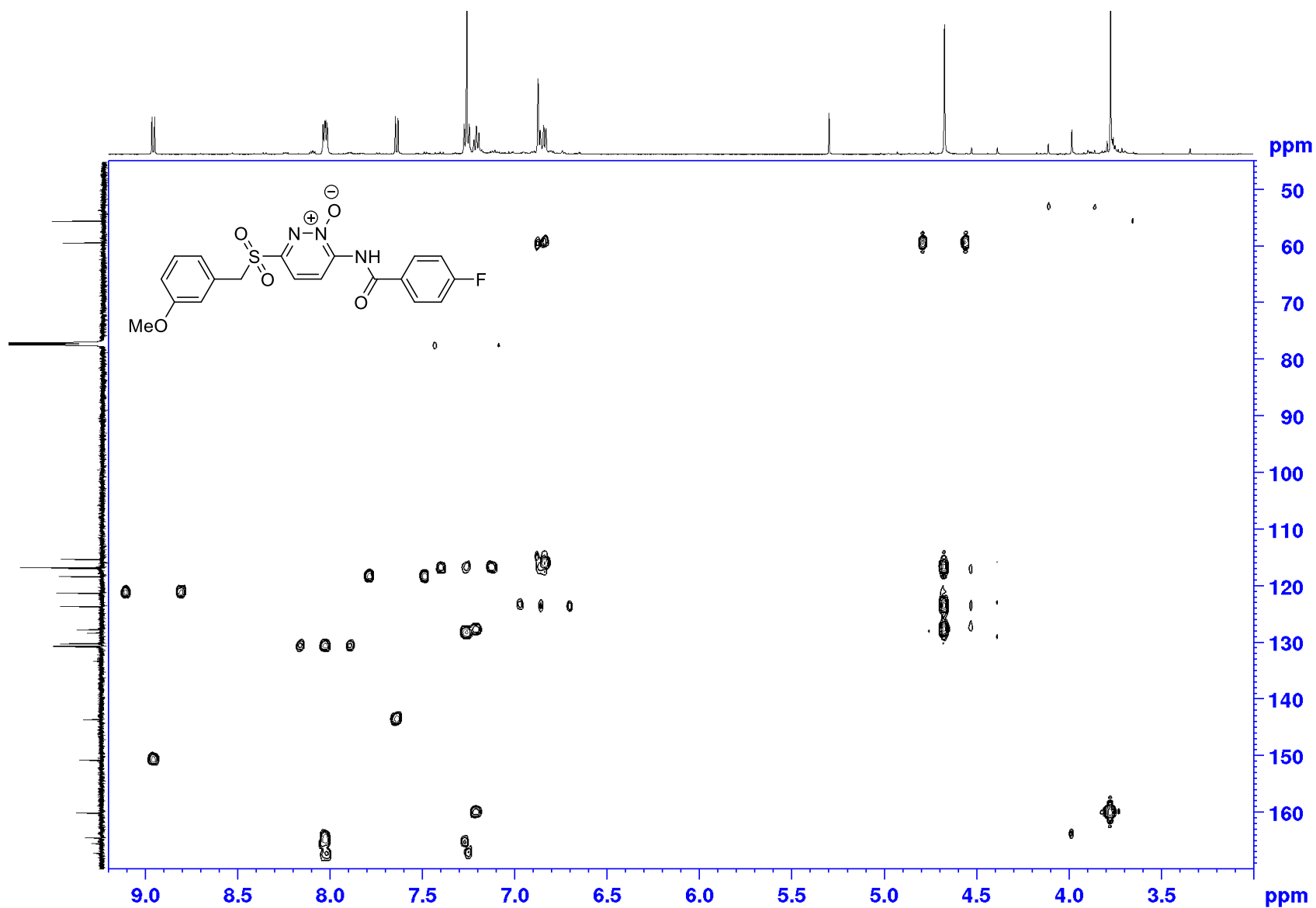
Appendices

HMQC NMR spectrum of **177** (400 x 100 MHz; CDCl₃)



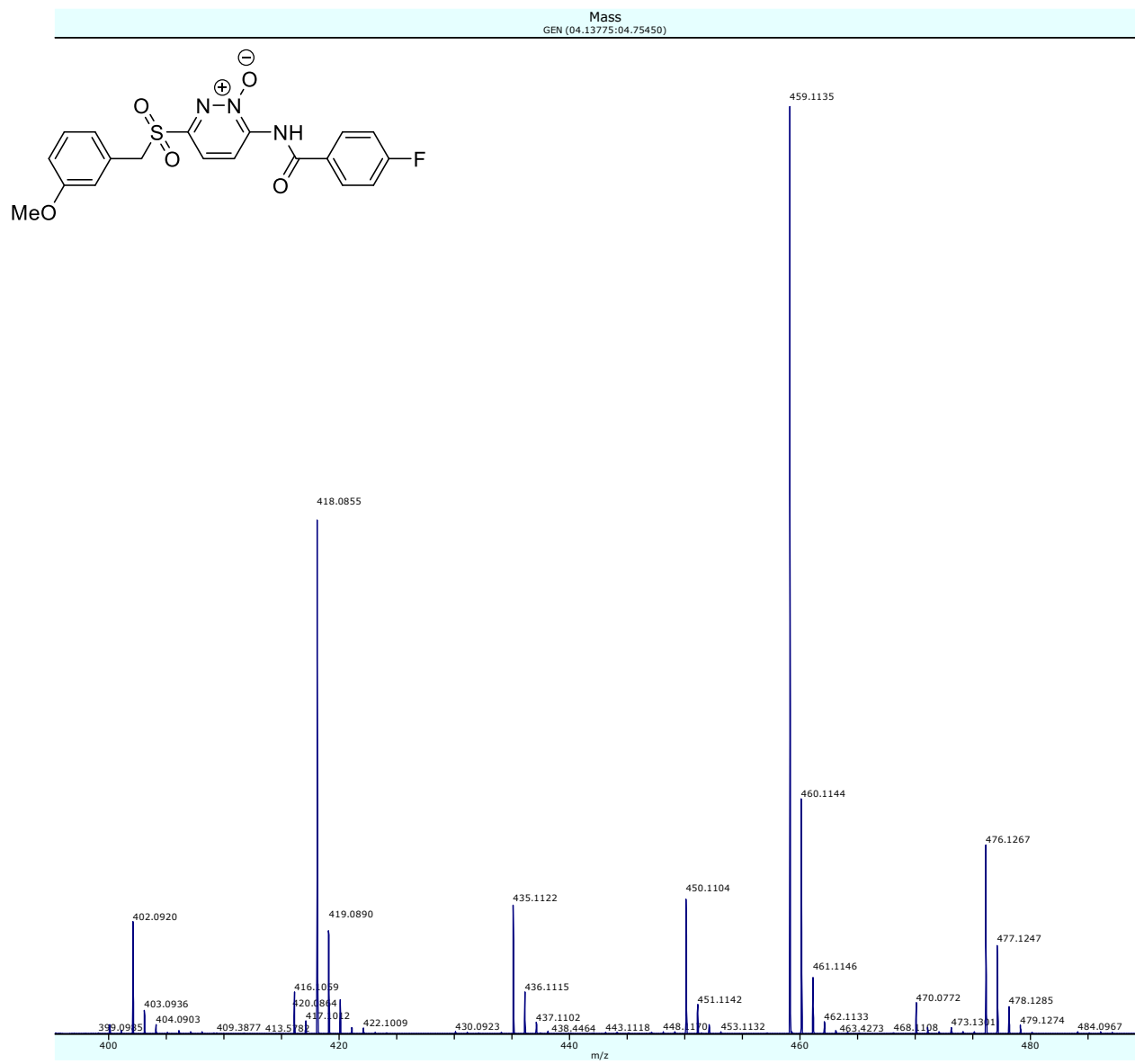
Appendices

HMBC NMR spectrum of **177** (400 x 100 MHz; CDCl₃)



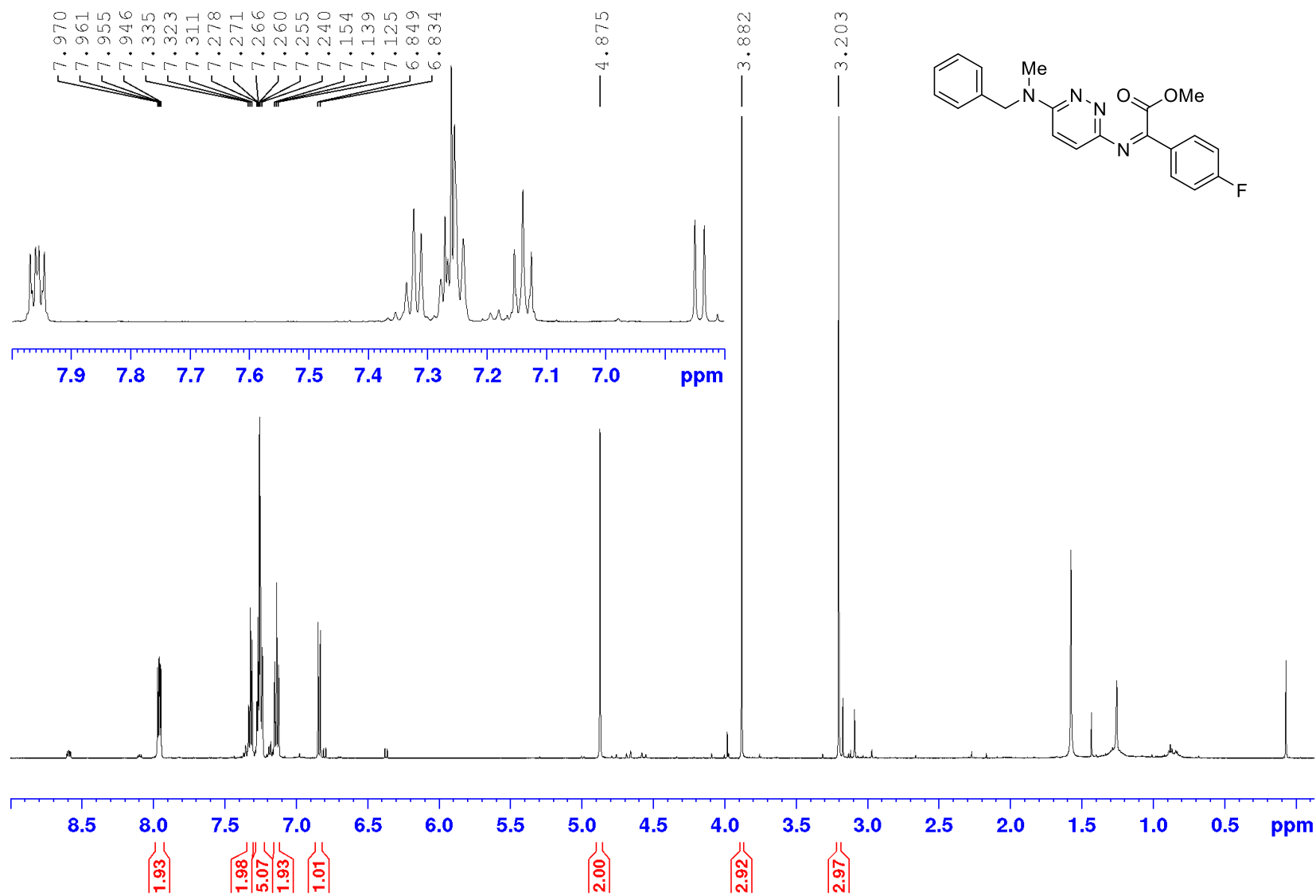
Appendices

HRMS (APCI) spectrum of **177** $[M+H]^+$



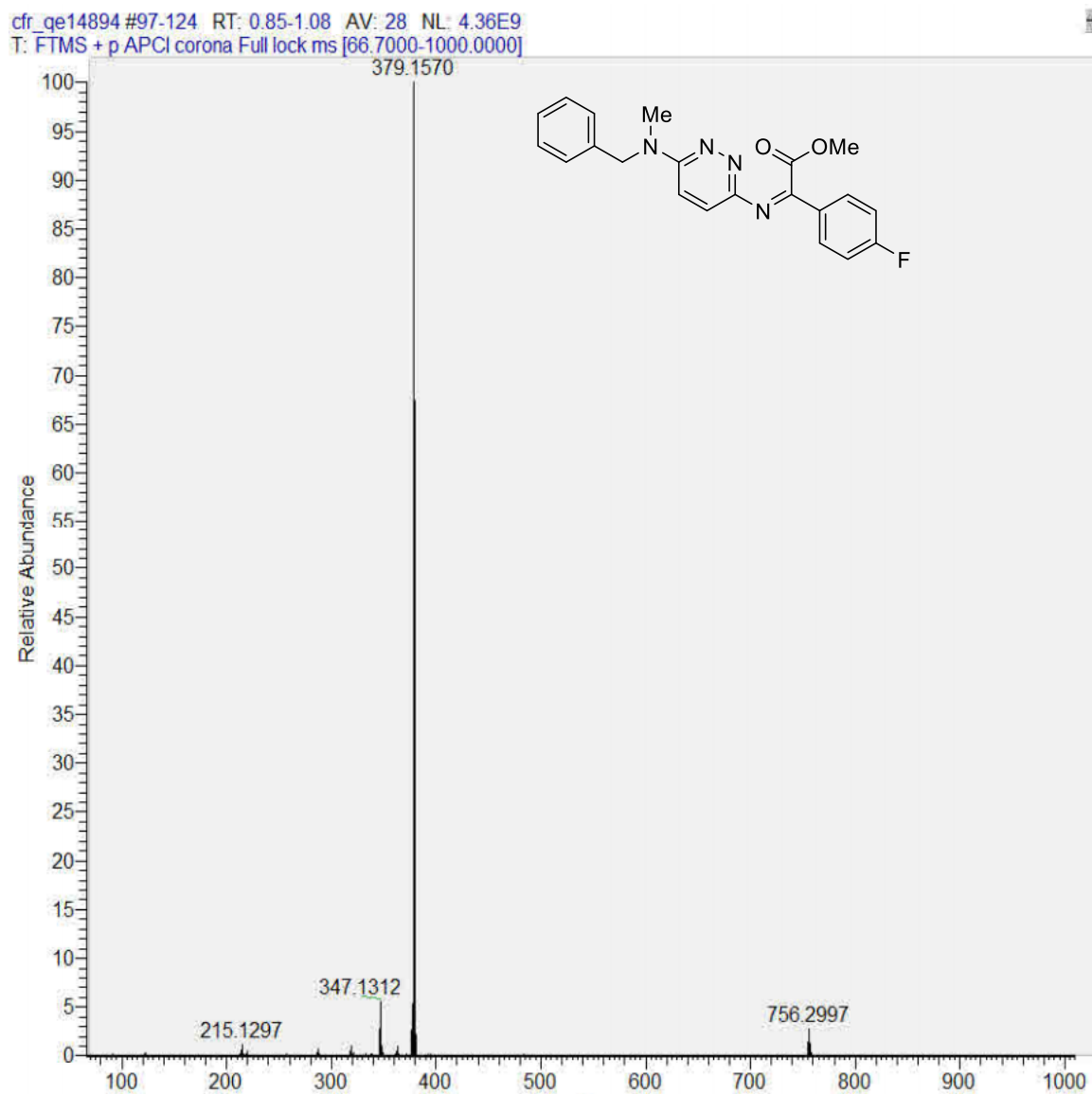
Appendices

¹H NMR spectrum of **191c** (600 MHz; CDCl₃)



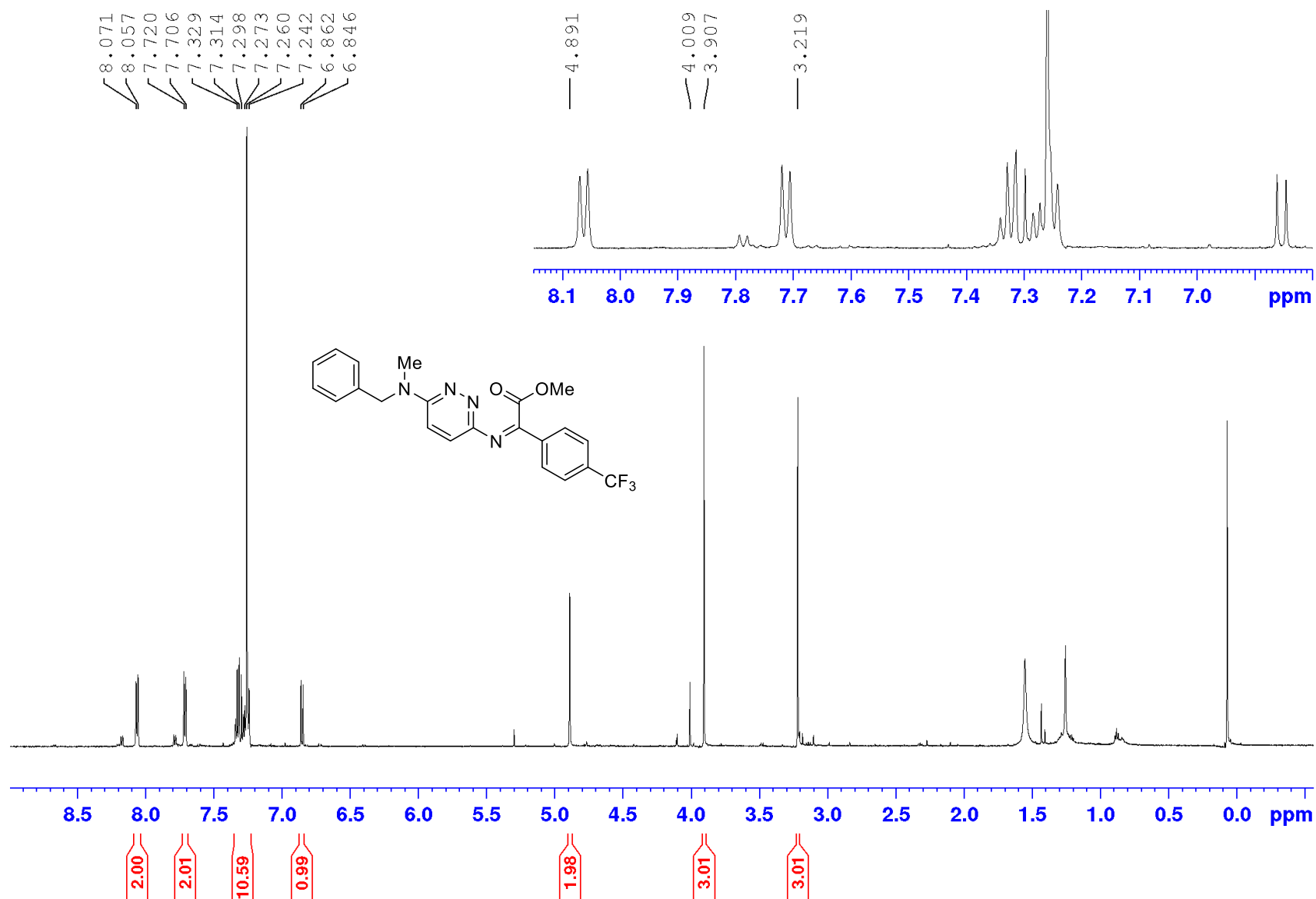
Appendices

HRMS (APCI) spectrum of **191c** $[M+H]^+$



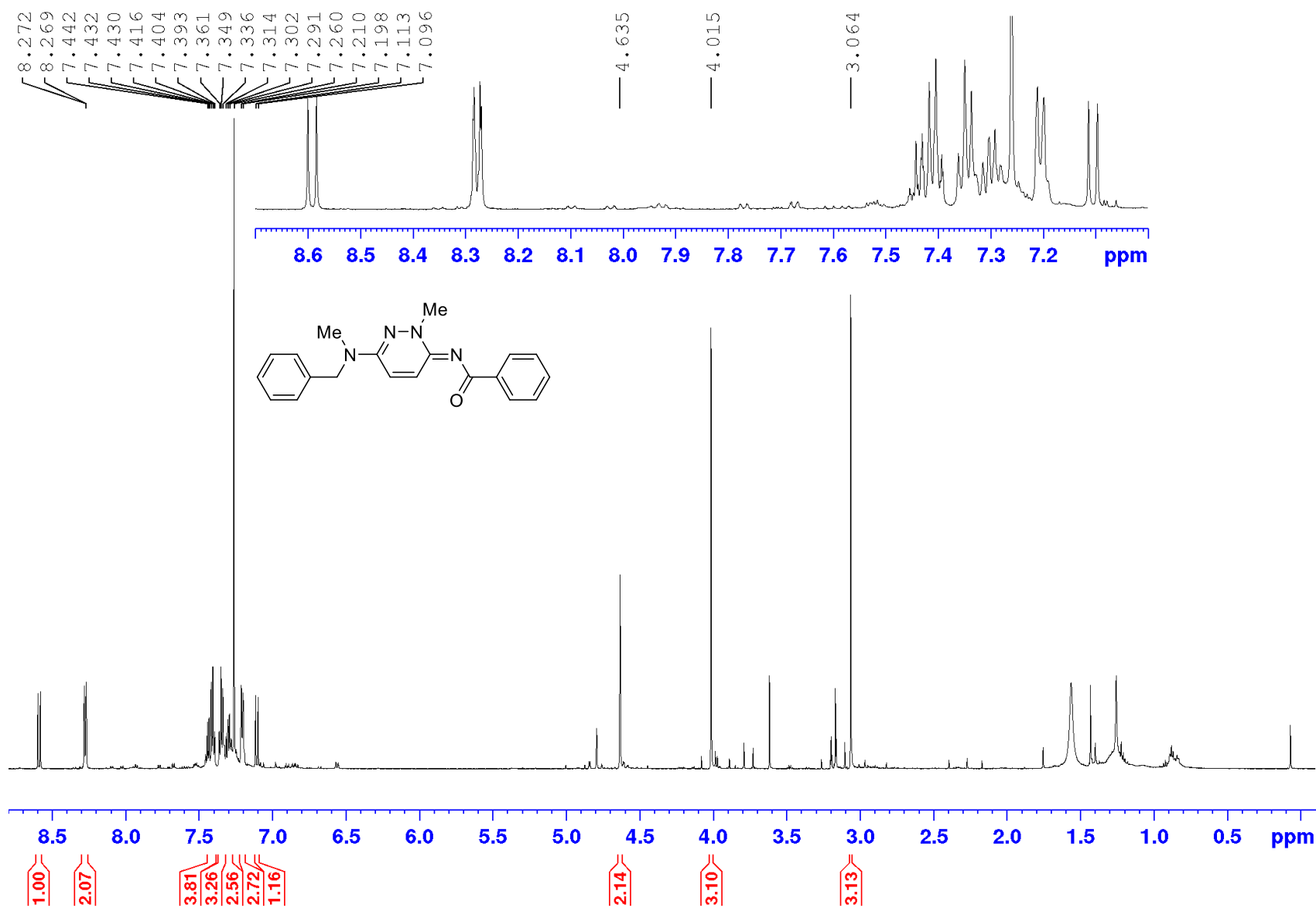
Appendices

¹H NMR spectrum of **191g** (600 MHz; CDCl₃)



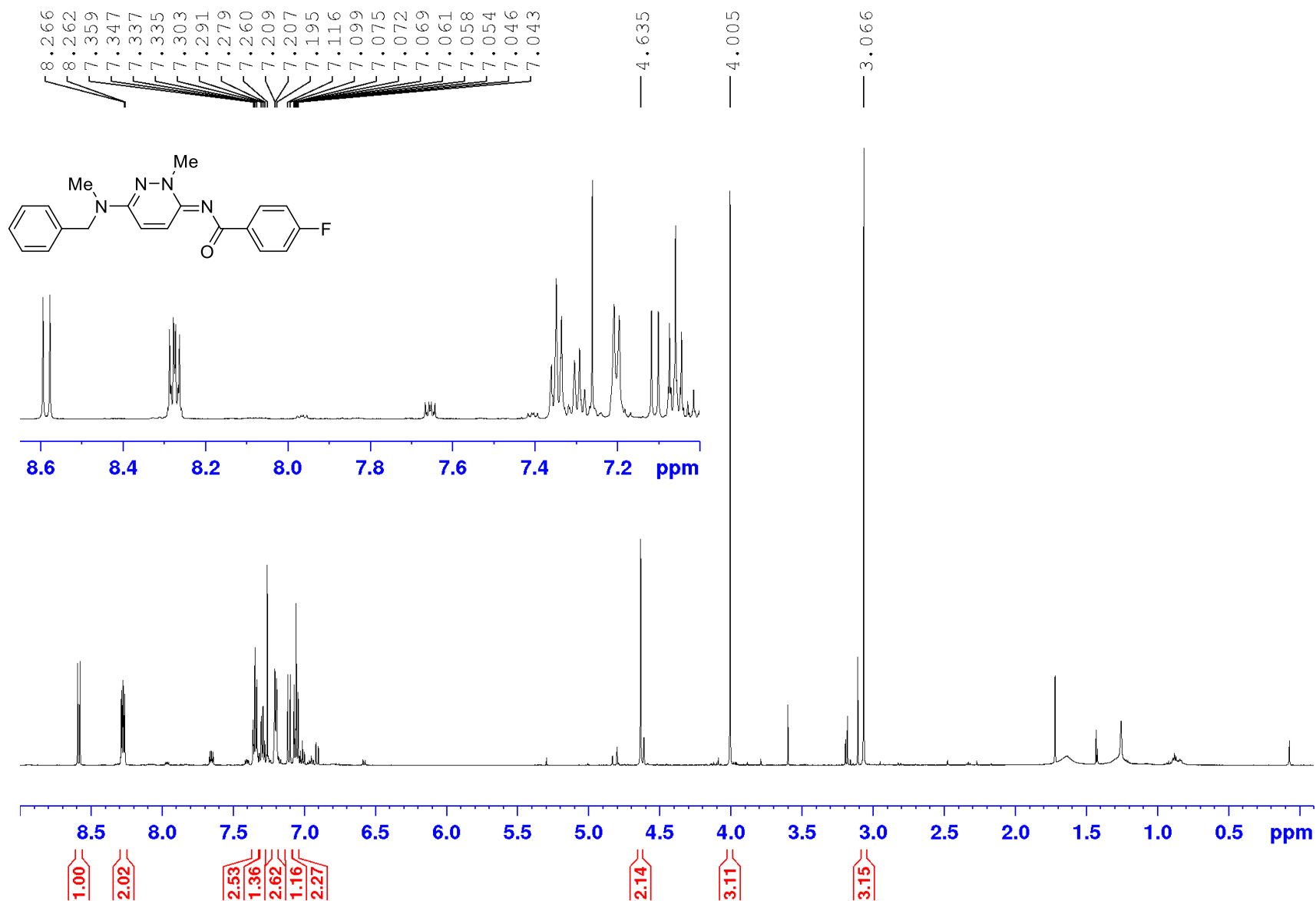
Appendices

¹H NMR spectrum of **192a** (600 MHz; CDCl₃)



Appendices

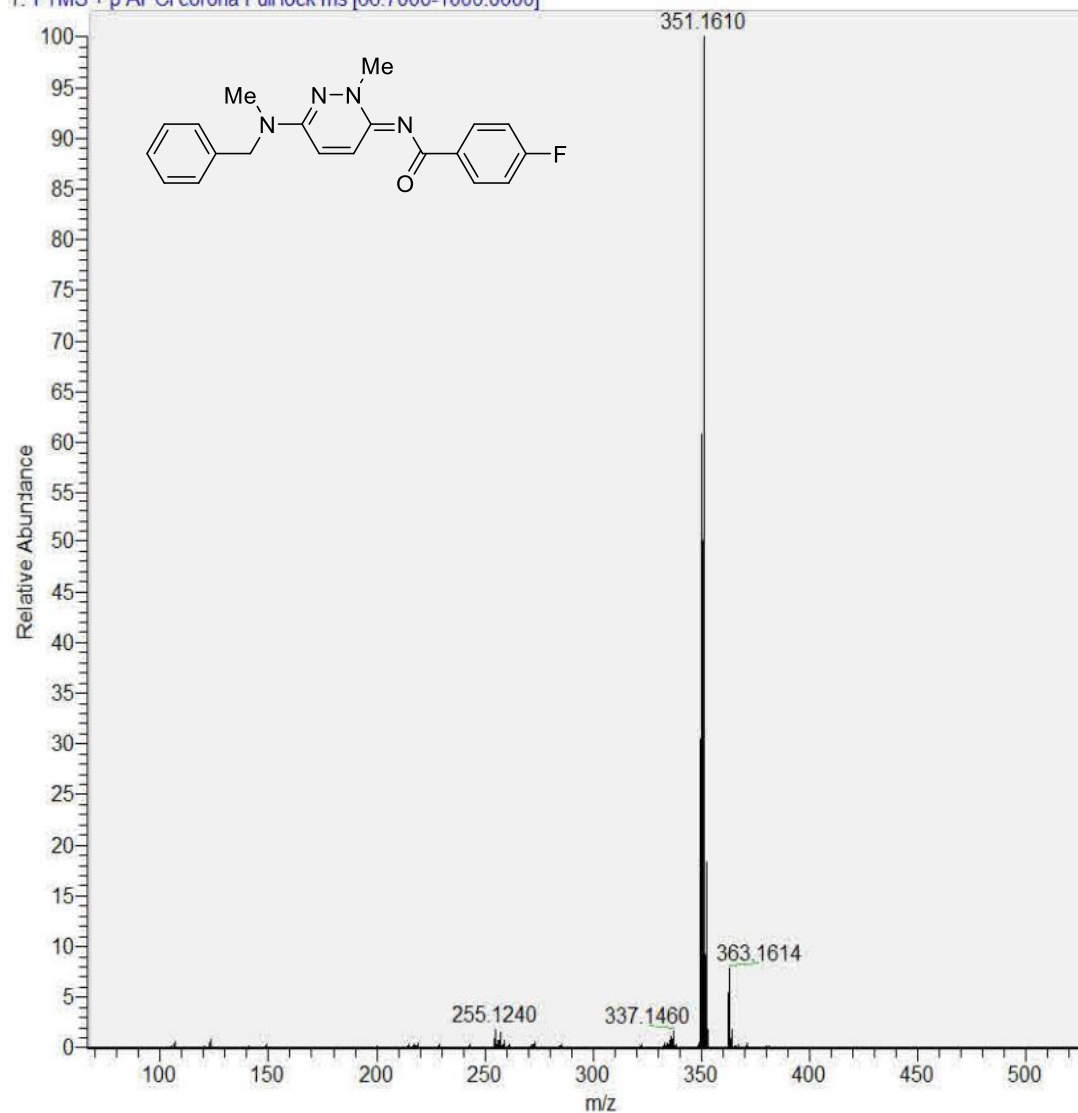
¹H NMR spectrum of **192c** (600 MHz; CDCl₃)



Appendices

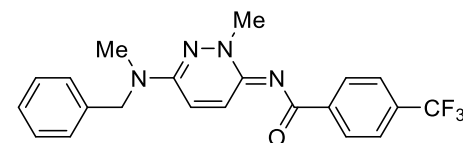
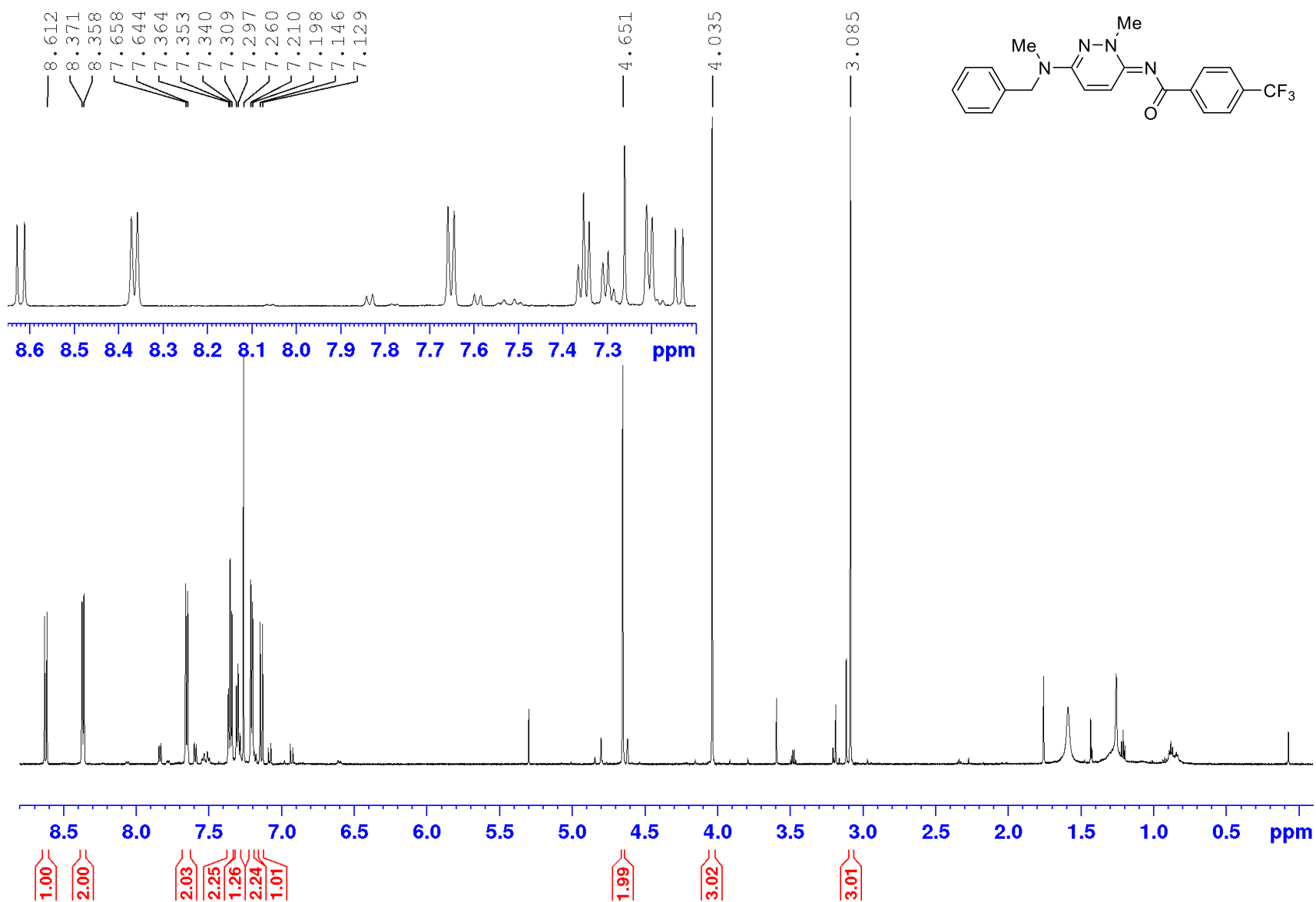
HRMS (APCI) spectrum of **192c** $[M+H]^+$

cf. _qe14892 #126-149 RT: 1.10-1.30 AV: 24 NL: 2.28E9
T: FTMS + p APCI corona Full lock ms [66.7000-1000.0000]



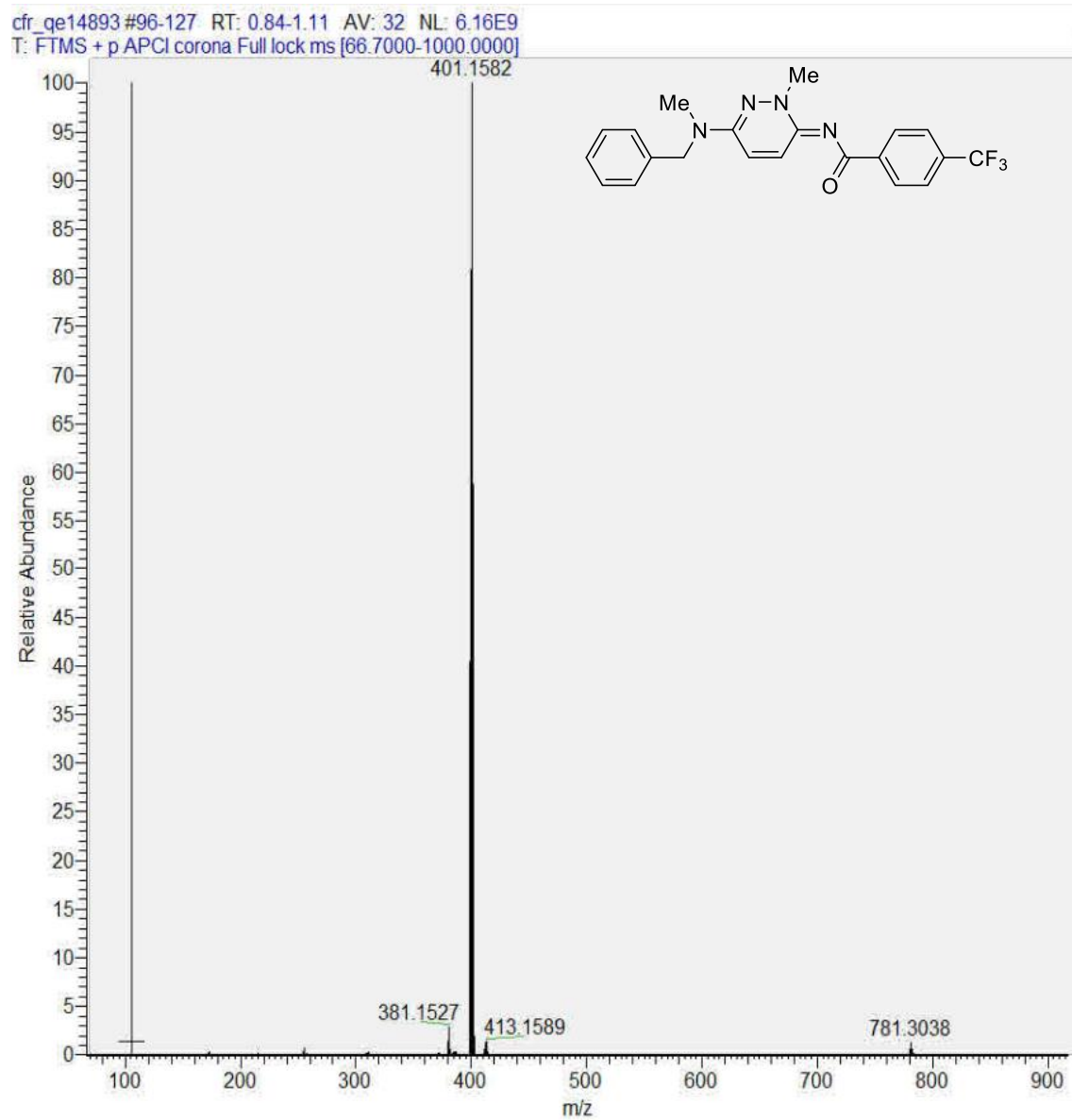
Appendices

¹H NMR spectrum of **192g** (600 MHz; CDCl₃)



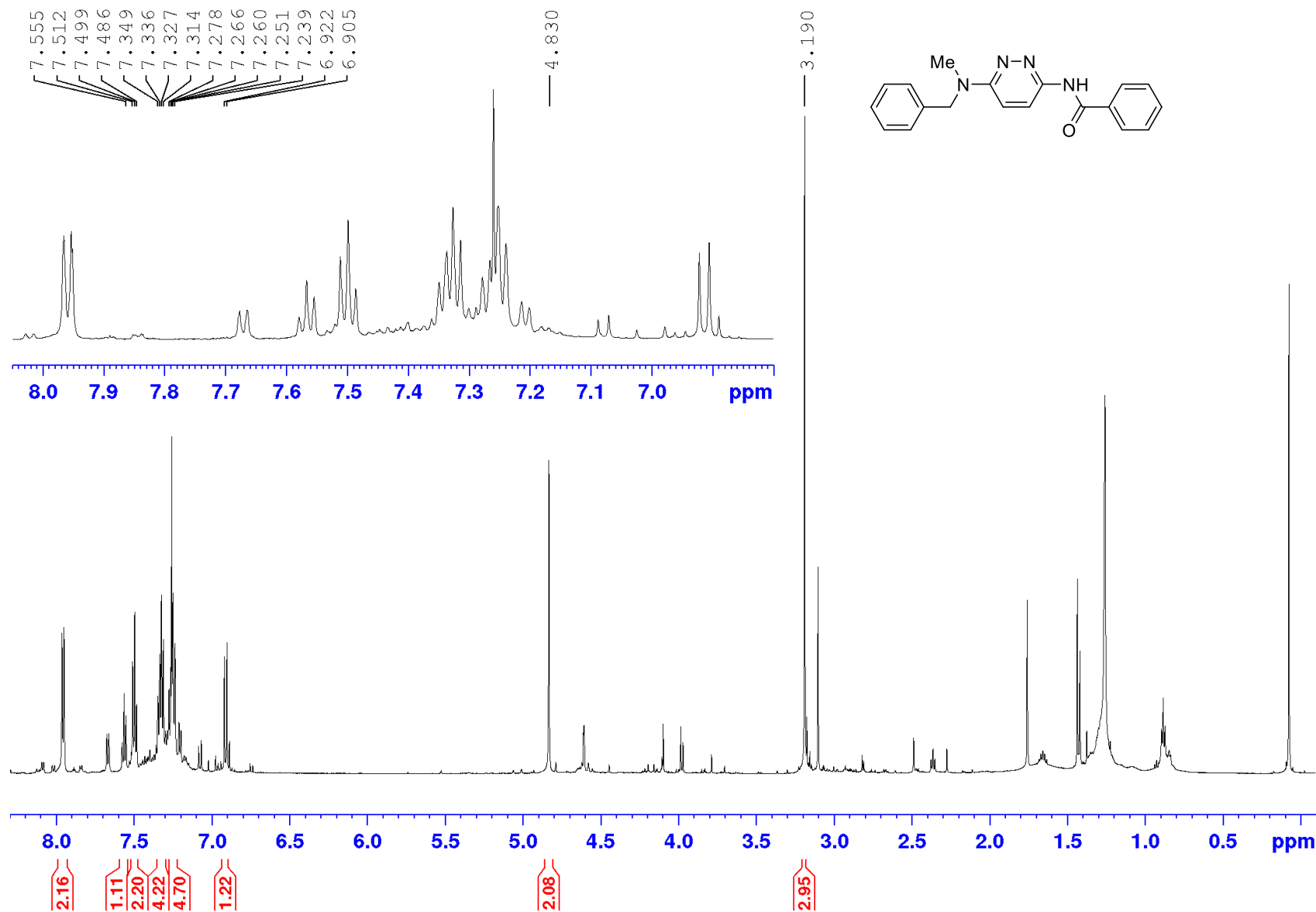
Appendices

HRMS (APCI) spectrum of **192g** $[M+H]^+$



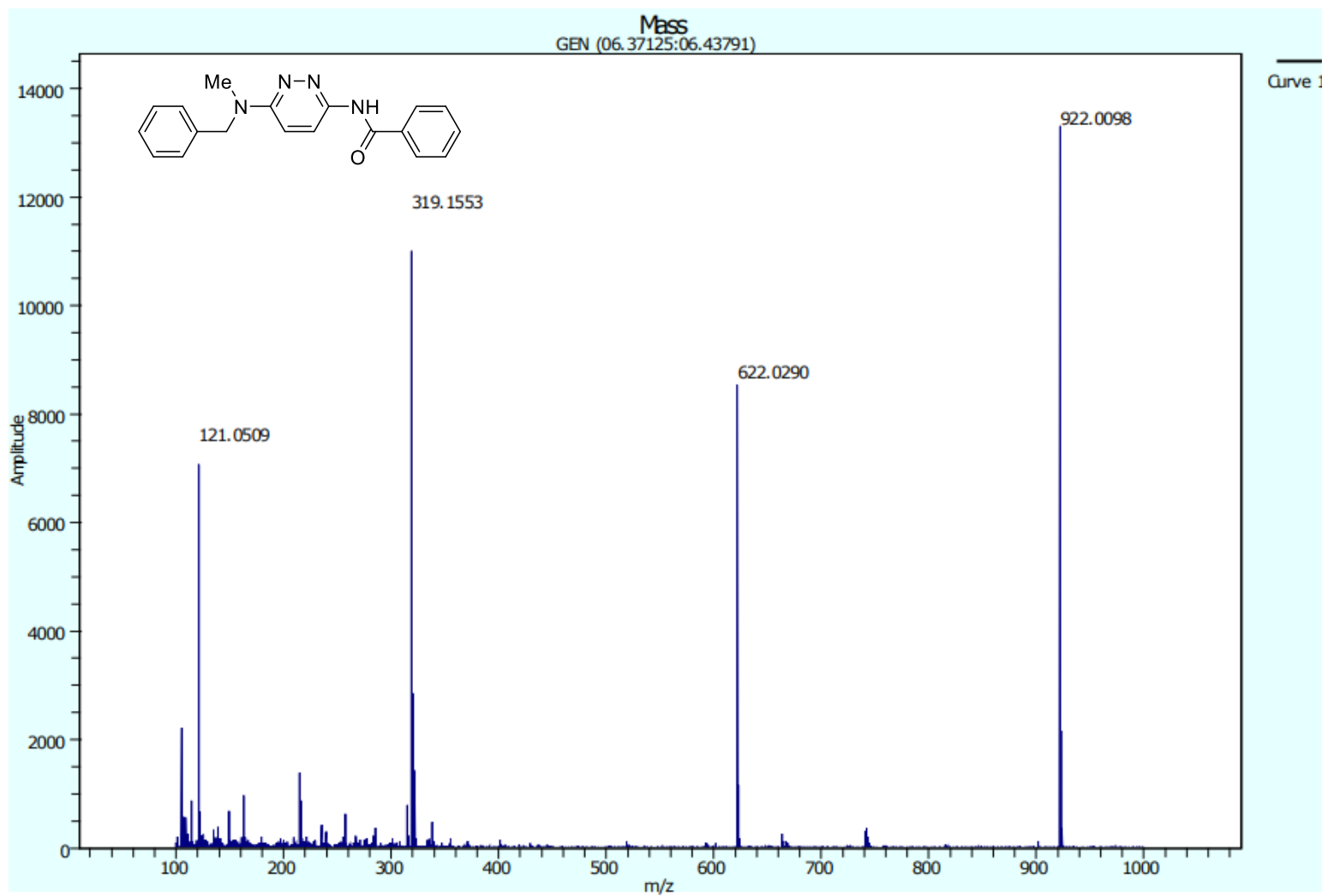
Appendices

¹H NMR spectrum of **193a** (600 MHz; CDCl₃)



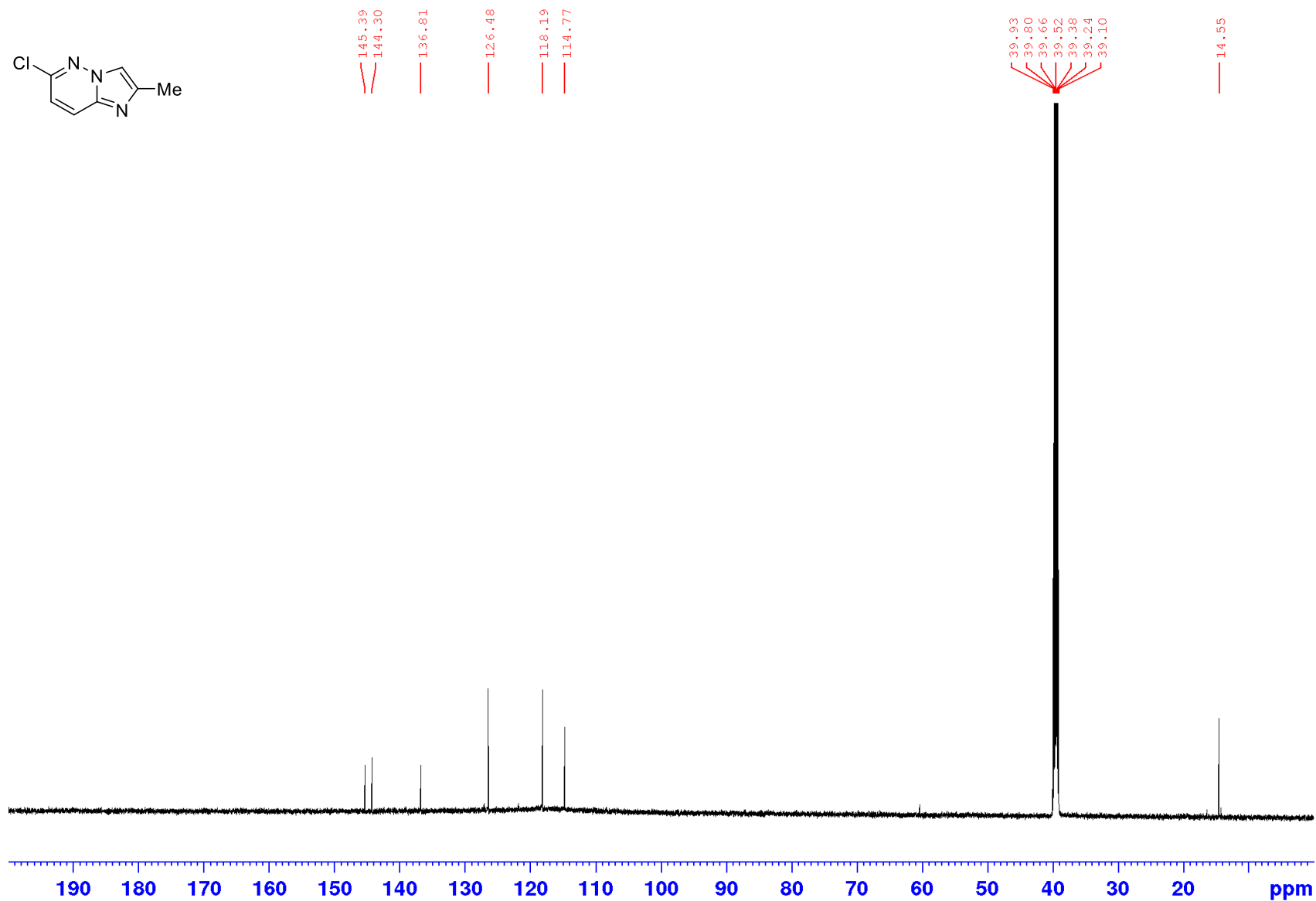
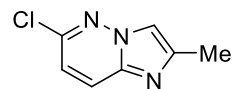
Appendices

HRMS (APCI) spectrum of **193a** $[M+H]^+$ (calibrant masses are 121, 322, 622 and 922 Da)



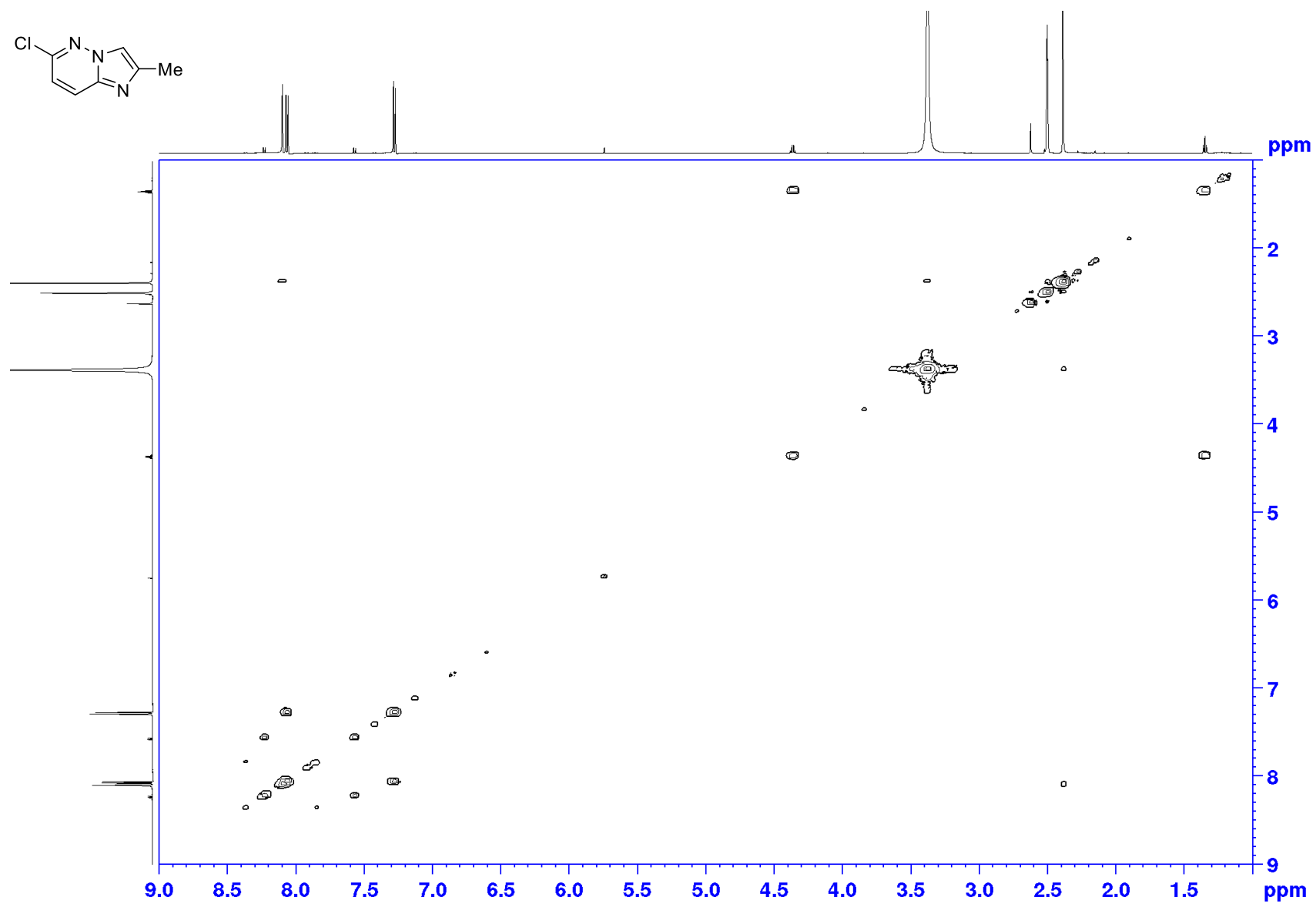
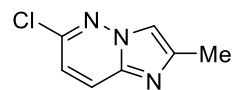
Appendices

¹³C NMR spectrum of **222** (150 MHz; DMSO-d₆)



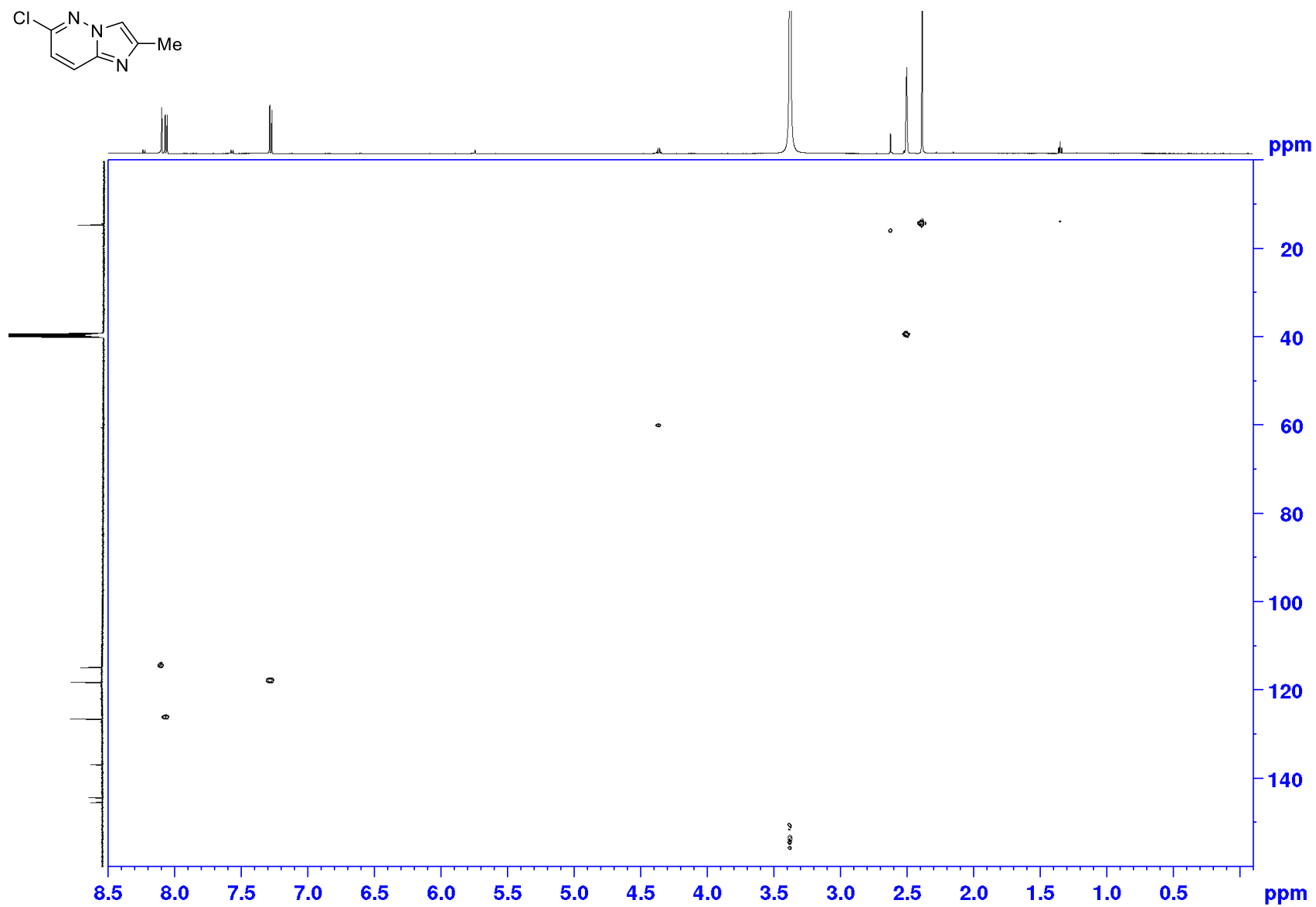
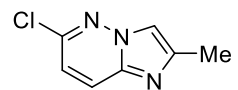
Appendices

COSY NMR spectrum of **222** (600 x 600 MHz; DMSO- d_6)



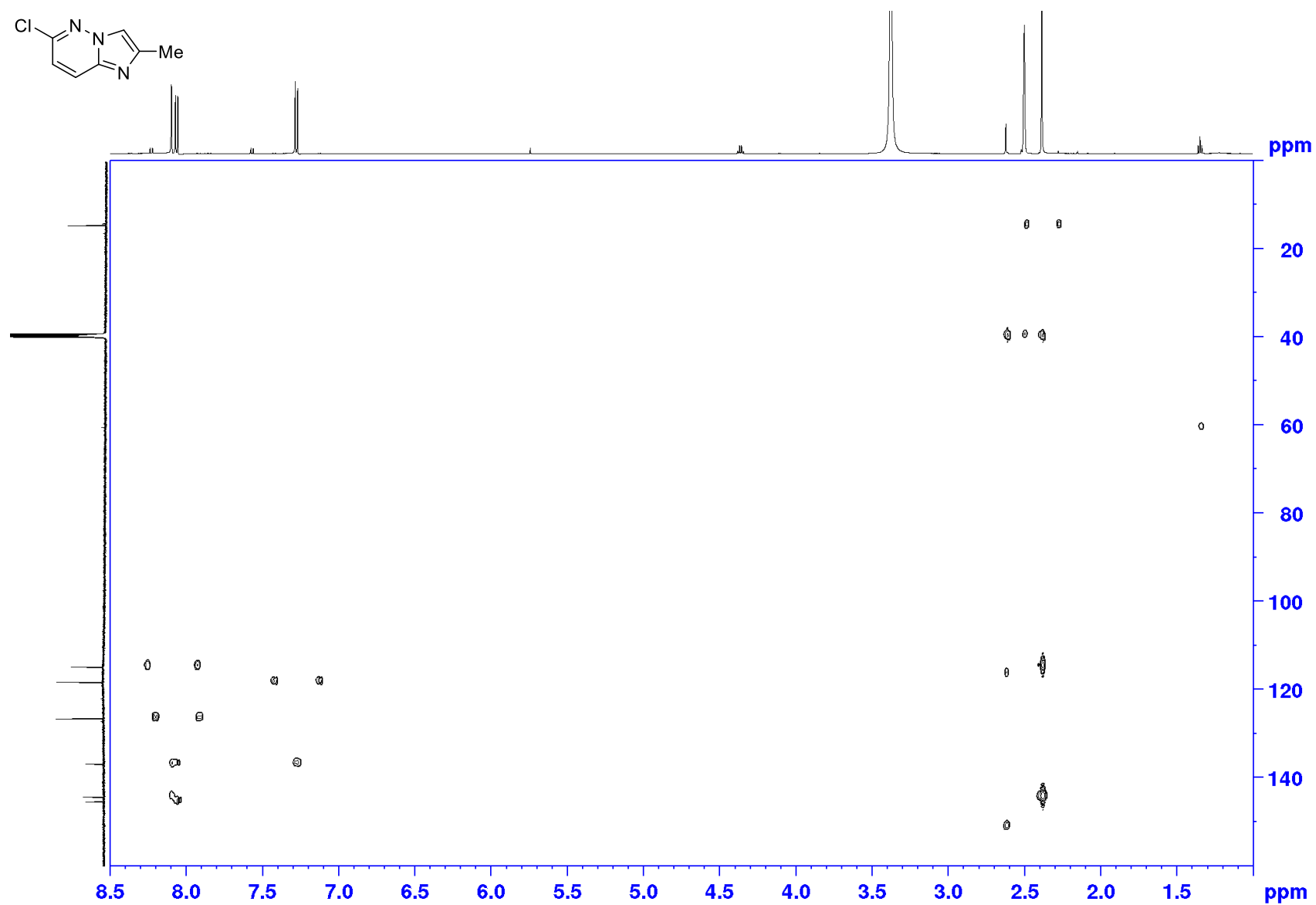
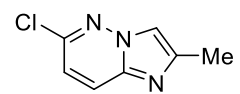
Appendices

HMQC NMR spectrum of **222** (400 x 100 MHz; DMSO-d₆)



Appendices

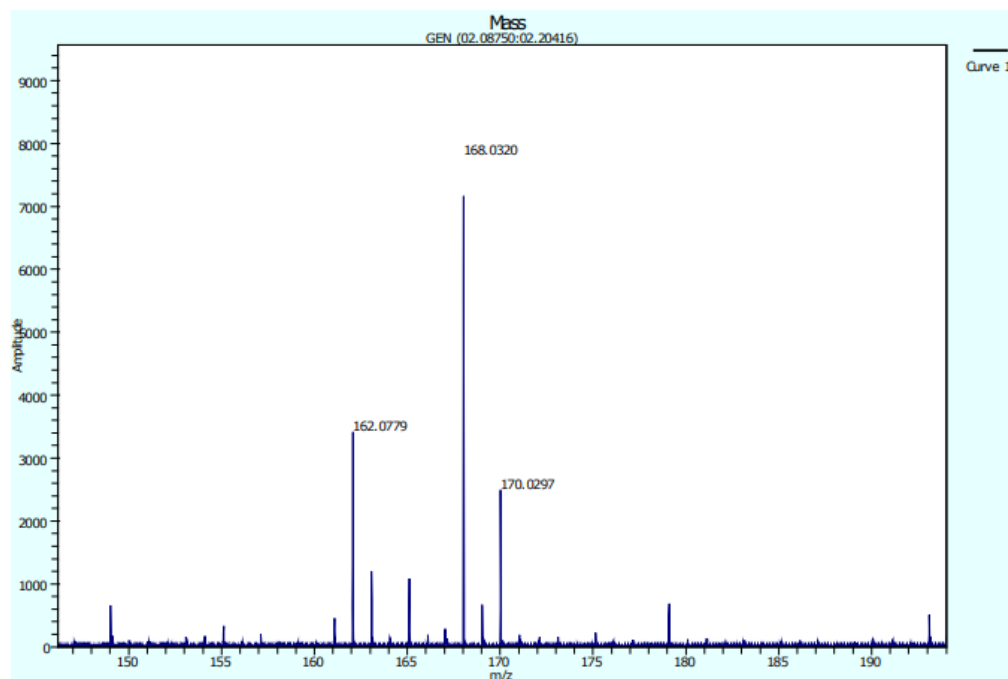
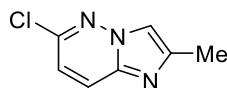
HMBC NMR spectrum of **222** (400 x 100 MHz; DMSO- d_6)



Appendices

HRMS (APCI) spectrum of **222** $[M+H]^+$

Sample: 3.84 110-114
High Resolution Spectra
Positive ion, APCI

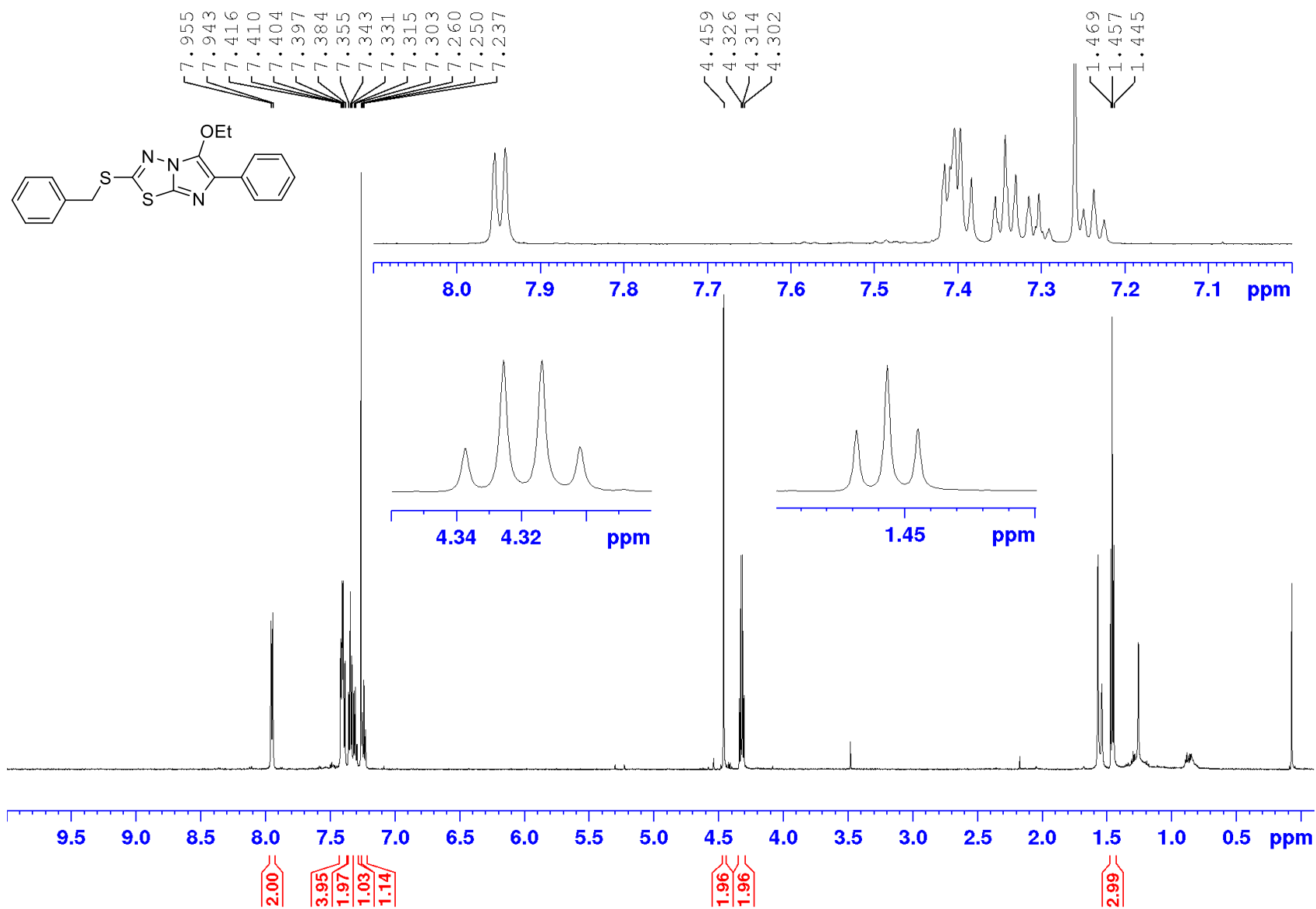


Accurate Mass Data

Observed Mass	Formula $[M+H]^+$	Calculated mass	Difference (ppm)
168.0320	C ₇ H ₇ ClN ₃	168.0323	-1.8

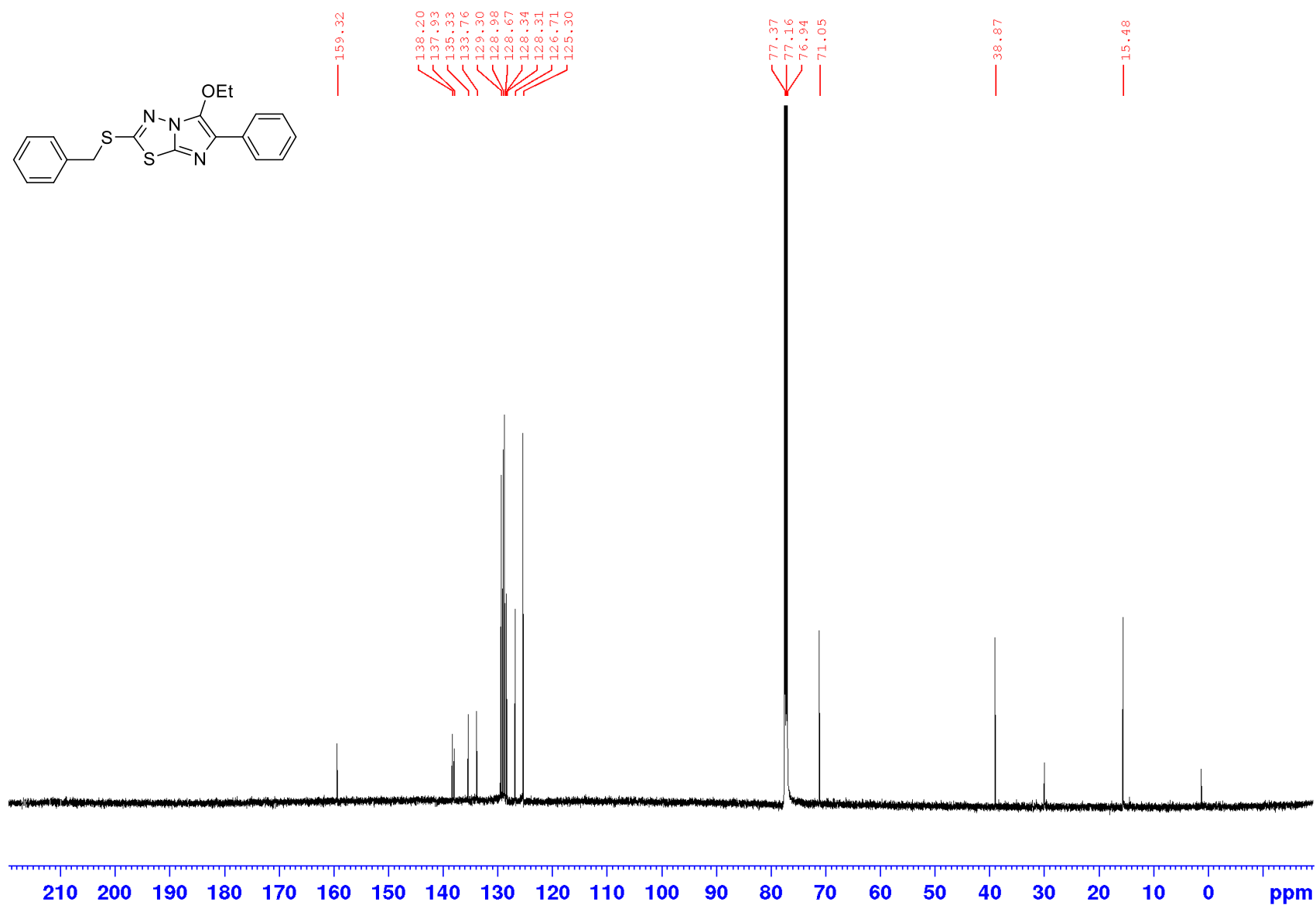
Appendices

¹H NMR spectrum of **259** (600 MHz; CDCl₃)



Appendices

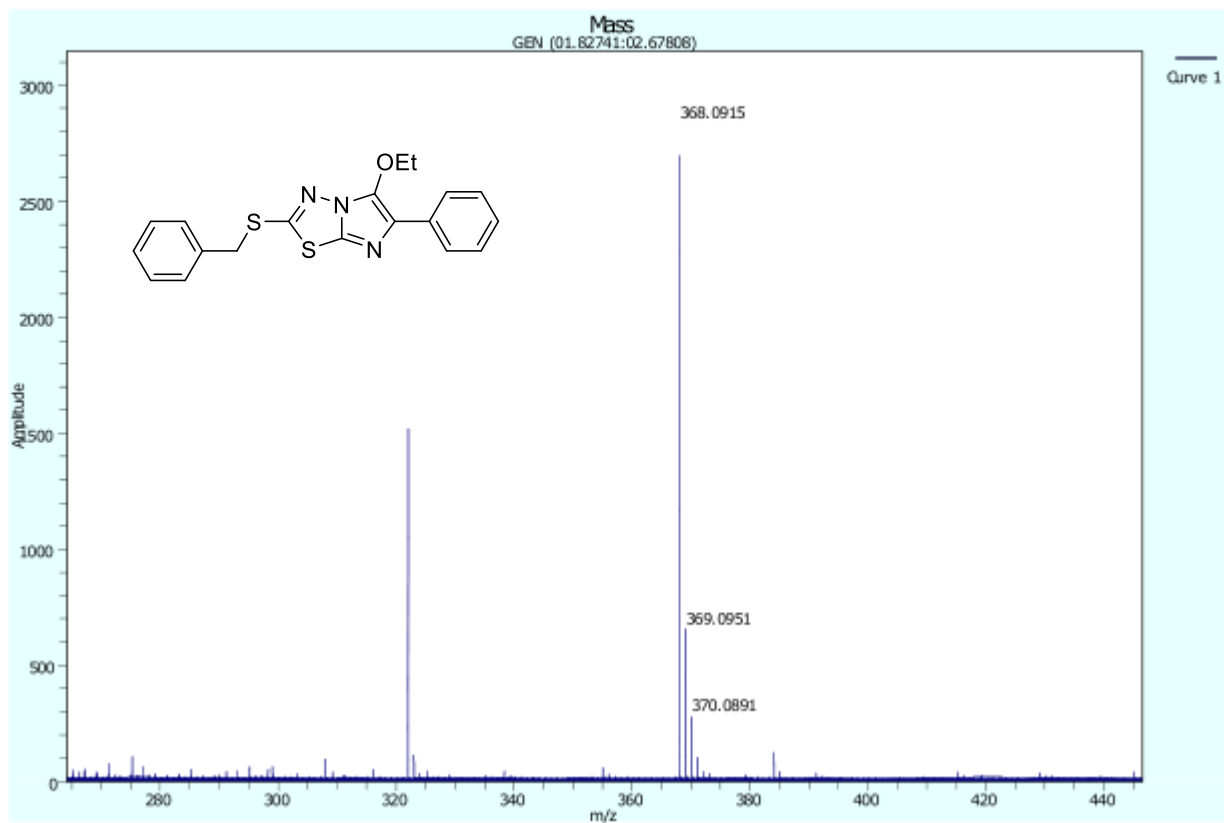
^{13}C NMR spectrum of **259** (150 MHz; CDCl_3)



Appendices

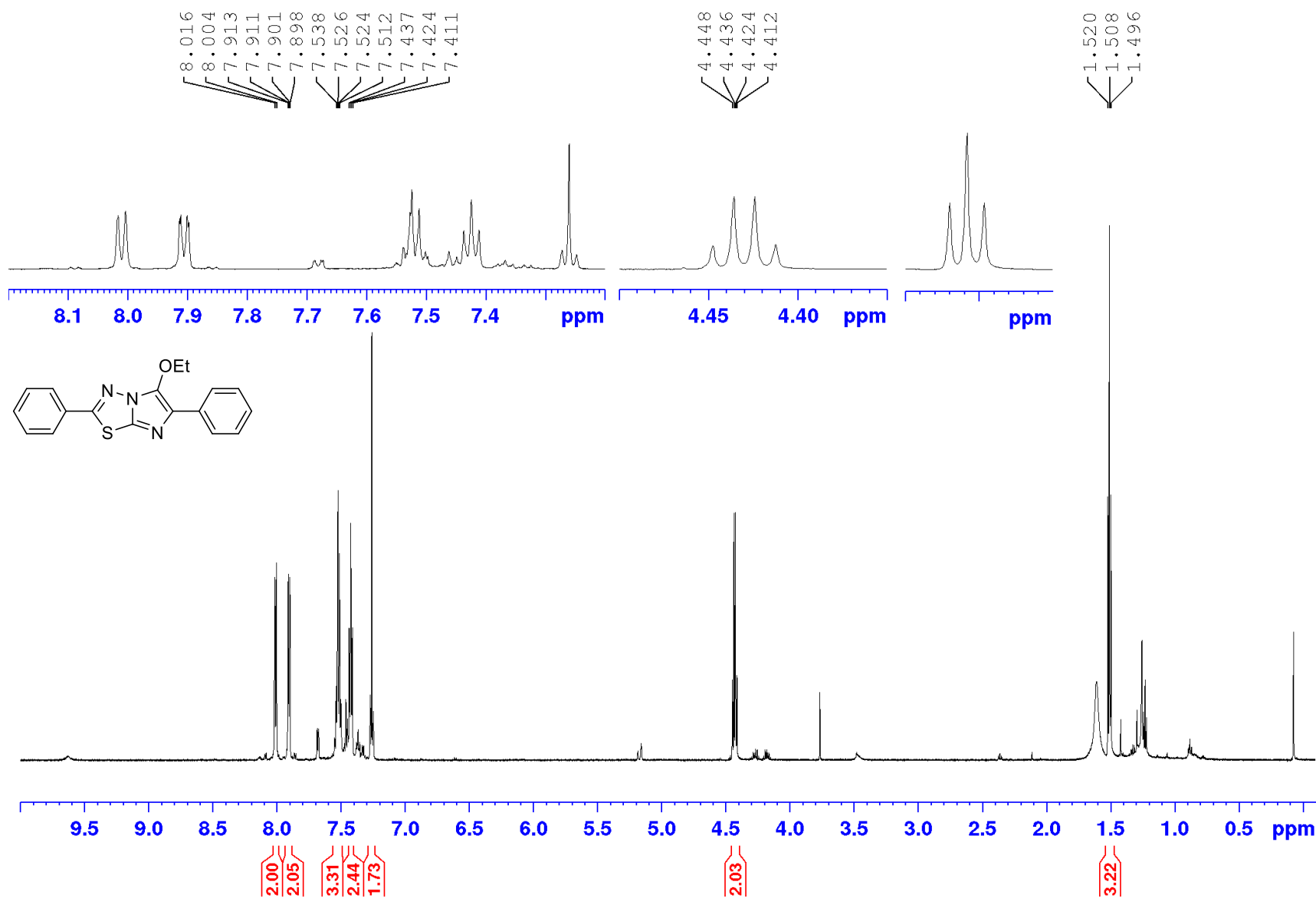
HRMS (APCI) spectrum of **259** $[M+H]^+$ (calibrants is 322 Da)

Sample: Bn-S-Ethoxy
High Resolution Spectra
Positive ion, APCI



Appendices

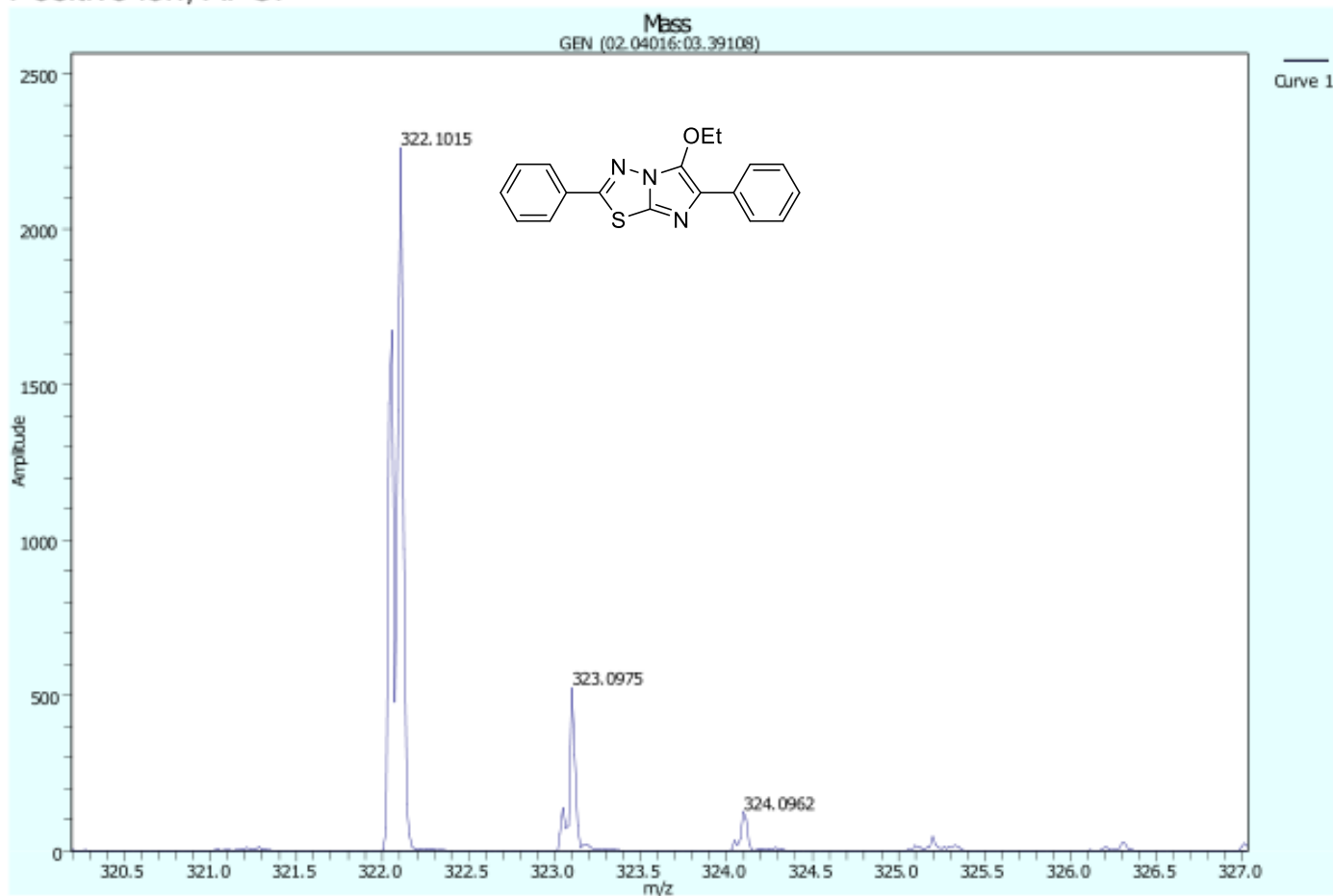
¹H NMR spectrum of **260** (600 MHz; CDCl₃)



Appendices

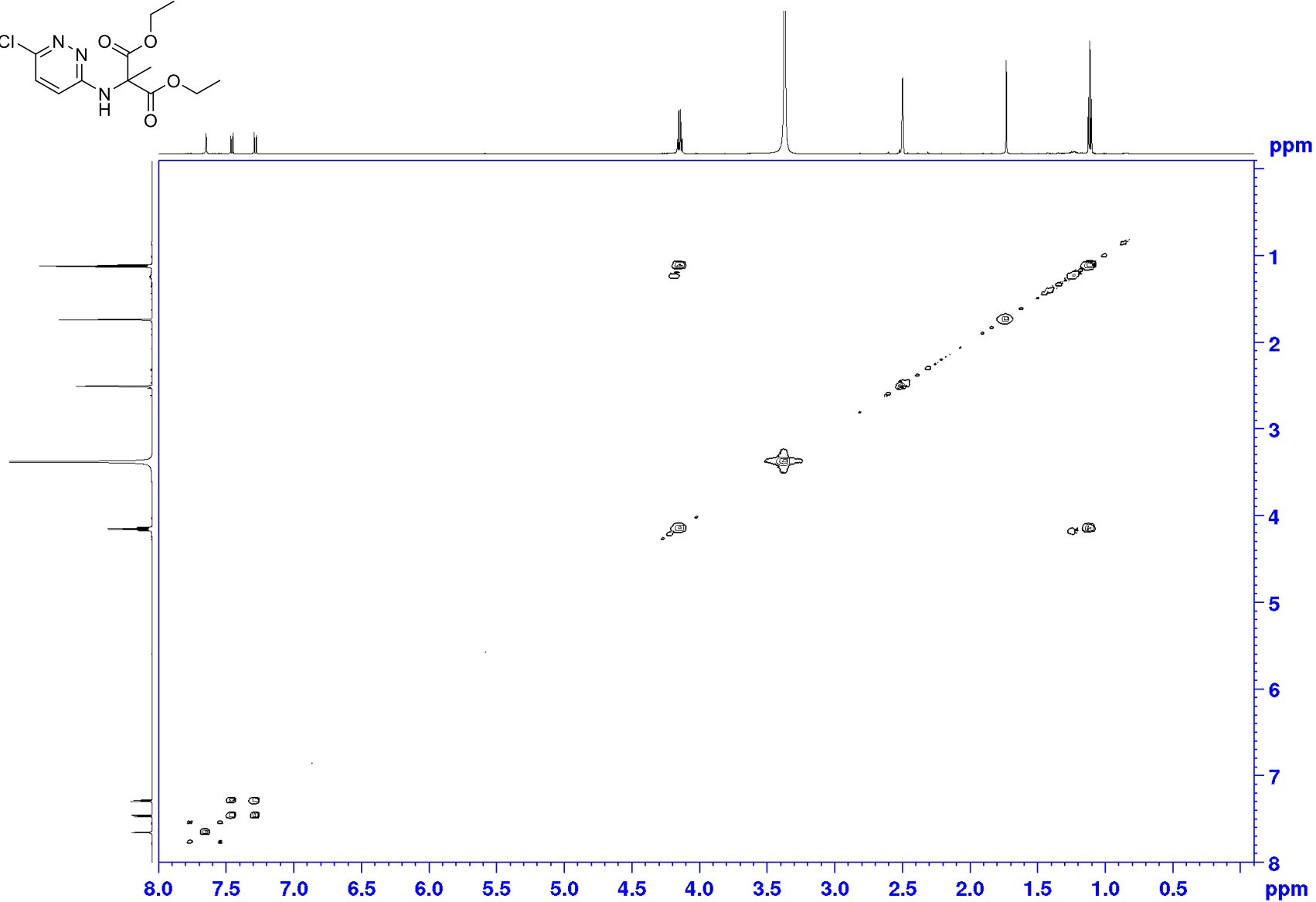
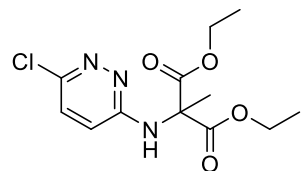
HRMS (APCI) spectrum of **260** $[M+H]^+$

Sample: Phenyl-ethoxy
High Resolution Spectra
Positive ion, APCI



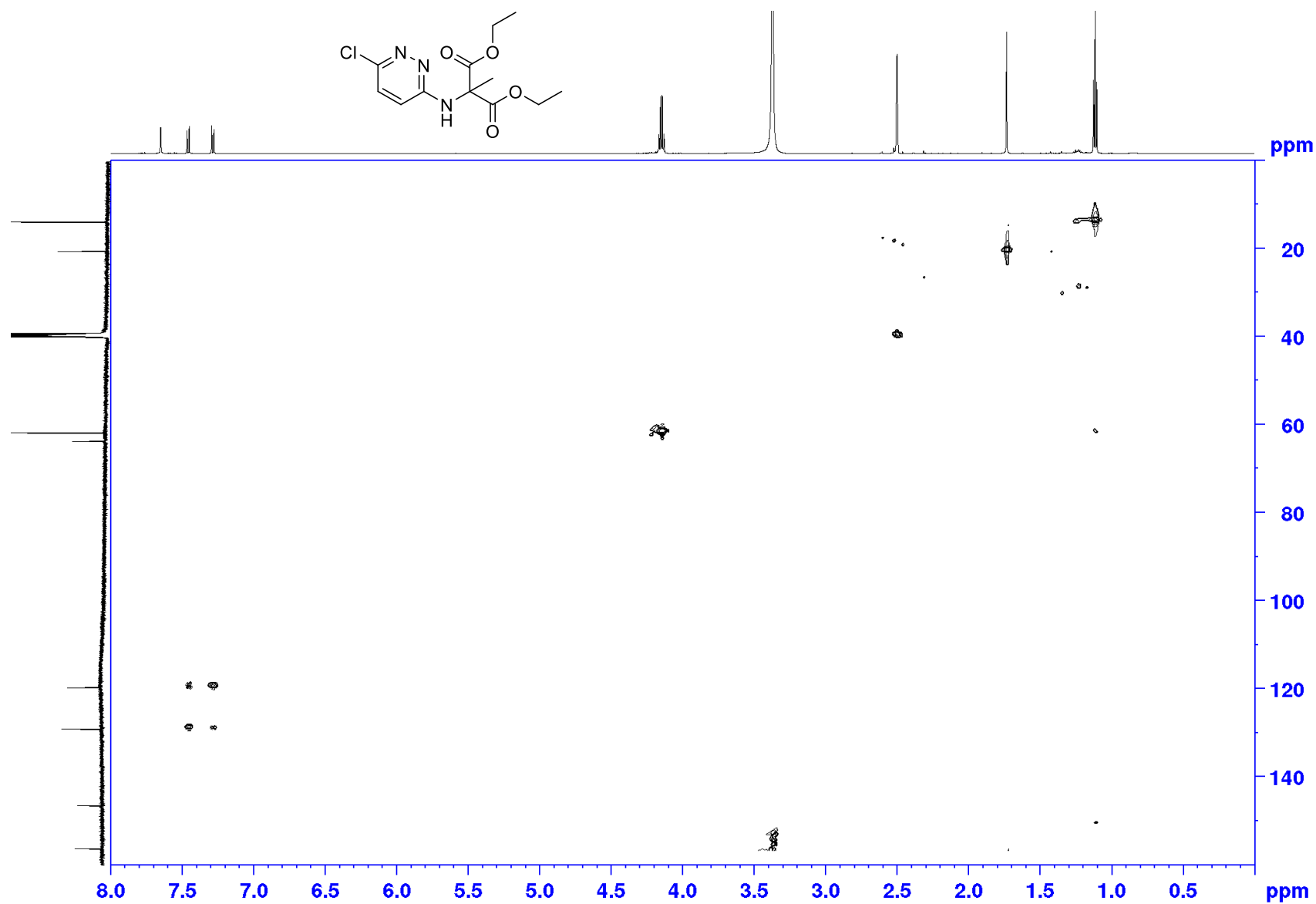
Appendices

COSY NMR spectrum of **276** (600 x 600 MHz; DMSO-d₆)



Appendices

HMQC NMR spectrum of **276** (400 x 100 MHz; DMSO-d₆)



Appendices

HMBC NMR spectrum of **276** (400 x 100 MHz; DMSO-d₆)

